frontiers | Research Topics

AIDS 40th year

Edited by
Linqi Zhang, Jiang Shibo, Tongqing Zhou, Zhiwei Chen, Xia Jin, Kai Deng, Wenyan Zhang, Supachai Rerks-ngarm and Anna Kramvis

Published in
Frontiers in Microbiology
Frontiers in Immunology

ISSN 1664-8714
ISBN 978-2-83252-176-2
DOI 10.3389/978-2-83252-176-2

About Frontiers

Frontiers is more than just an open access publisher of scholarly articles: it is a pioneering approach to the world of academia, radically improving the way scholarly research is managed. The grand vision of Frontiers is a world where all people have an equal opportunity to seek, share and generate knowledge. Frontiers provides immediate and permanent online open access to all its publications, but this alone is not enough to realize our grand goals.

Frontiers journal series

The Frontiers journal series is a multi-tier and interdisciplinary set of open-access, online journals, promising a paradigm shift from the current review, selection and dissemination processes in academic publishing. All Frontiers journals are driven by researchers for researchers; therefore, they constitute a service to the scholarly community. At the same time, the *Frontiers journal series* operates on a revolutionary invention, the tiered publishing system, initially addressing specific communities of scholars, and gradually climbing up to broader public understanding, thus serving the interests of the lay society, too.

Dedication to quality

Each Frontiers article is a landmark of the highest quality, thanks to genuinely collaborative interactions between authors and review editors, who include some of the world's best academicians. Research must be certified by peers before entering a stream of knowledge that may eventually reach the public - and shape society; therefore, Frontiers only applies the most rigorous and unbiased reviews. Frontiers revolutionizes research publishing by freely delivering the most outstanding research, evaluated with no bias from both the academic and social point of view. By applying the most advanced information technologies, Frontiers is catapulting scholarly publishing into a new generation.

What are Frontiers Research Topics?

Frontiers Research Topics are very popular trademarks of the *Frontiers journals series*: they are collections of at least ten articles, all centered on a particular subject. With their unique mix of varied contributions from Original Research to Review Articles, Frontiers Research Topics unify the most influential researchers, the latest key findings and historical advances in a hot research area.

Find out more on how to host your own Frontiers Research Topic or contribute to one as an author by contacting the Frontiers editorial office: frontiersin.org/about/contact

AIDS 40th year

Topic editors

Linqi Zhang — Tsinghua University, China
Jiang Shibo — Fudan University, China
Tongqing Zhou — National Institutes of Health (NIH), United States
Zhiwei Chen — The University of Hong Kong, Hong Kong, SAR China
Xia Jin — Fudan University, China
Kai Deng — Sun Yat-sen University, China
Wenyan Zhang — First Affiliated Hospital of Jilin University, China
Supachai Rerks-ngarm — Ministry of Public Health, Thailand
Anna Kramvis — University of the Witwatersrand, South Africa

Citation

Zhang, L., Shibo, J., Zhou, T., Chen, Z., Jin, X., Deng, K., Zhang, W., Rerks-ngarm, S., Kramvis, A., eds. (2023). *AIDS 40th year*. Lausanne: Frontiers Media SA.
doi: 10.3389/978-2-83252-176-2

Table of contents

frontiers | Frontiers in Microbiology

TYPE Editorial
PUBLISHED 31 March 2023
DOI 10.3389/fmicb.2023.1184684

OPEN ACCESS

EDITED AND REVIEWED BY
Axel Cloeckaert,
Institut National de recherche pour l'agriculture, l'alimentation et l'environnement (INRAE), France

*CORRESPONDENCE
Kai Deng
✉ dengkai6@mail.sysu.edu.cn
Linqi Zhang
✉ zhanglinqi@mail.tsinghua.edu.cn

SPECIALTY SECTION
This article was submitted to Virology, a section of the journal Frontiers in Microbiology

RECEIVED 12 March 2023
ACCEPTED 20 March 2023
PUBLISHED 31 March 2023

CITATION
Zhou J, Jiang S, Zhou T, Chen Z, Jin X, Zhang W, Rerks-ngarm S, Kramvis A, Deng K and Zhang L (2023) Editorial: AIDS 40th Year. *Front. Microbiol.* 14:1184684. doi: 10.3389/fmicb.2023.1184684

Editorial: AIDS 40th Year

Jiasheng Zhou[1], Shibo Jiang[2], Tongqing Zhou[3], Zhiwei Chen[4], Xia Jin[5], Wenyan Zhang[6], Supachai Rerks-ngarm[7], Anna Kramvis[8], Kai Deng[1]* and Linqi Zhang[9]*

[1]Key Laboratory of Tropical Diseases Control, Zhongshan School of Medicine, Sun Yat-sen University, Guangzhou, China, [2]Key Laboratory of Medical Molecular Virology (MOE/NHC/CAMS), School of Basic Medical Sciences, Institute of Infectious Disease and Biosecurity, Fudan University, Shanghai, China, [3]Vaccine Research Center, National Institute of Allergy and Infectious Diseases, National Institutes of Health (NIH), Bethesda, MD, United States, [4]School of Clinical Medicine, Li Ka Shing Faculty of Medicine, AIDS Institute, The University of Hong Kong, Hong Kong, Hong Kong SAR, China, [5]Shanghai Public Health Clinical Center, Fudan University, Shanghai, China, [6]The First Hospital of Jilin University, Institute of Virology and AIDS Research, Changchun, China, [7]Department of Disease Control, Ministry of Public Health, Bangkok, Thailand, [8]Hepatitis Virus Diversity Research Unit, Department of Internal Medicine, School of Clinical Medicine, Faculty of Health Sciences, University of the Witwatersrand, Johannesburg, South Africa, [9]Comprehensive AIDS Research Center, Global Health and Infectious Diseases, School of Medicine, Tsinghua University, Beijing, China

KEYWORDS

HIV-1, AIDS, virology, epidemiology, fungus

Editorial on the Research Topic
AIDS 40th Year

On June 1981, case reports from five AIDS patients in California, USA were published in *Morbidity and Mortality Weekly Report*, beginning the 40-year battle between humans and AIDS. In 1996, Dr. David Ho initiated highly effective antiretroviral therapy (HAART), which gradually prevented the rapid spread of HIV in humans and dramatically reduced the number of deaths from AIDS, globally. However, according to the report from the Joint United Nations Program on HIV/AIDS (UNAIDS) published in 2022, "Global AIDS Prevention Progress Report 2022: In Danger," up to 650,000 people still died from AIDS-associated diseases and approximately 1.5 million people were newly diagnosed as HIV-1 positive in 2021, even though the use of HAART had been established 25 years ago. While the indefatigable efforts from global scientists over the past 40 years have significantly reduced HIV-1 prevalence, a permanent cure for HIV-1 patients is still a long way off and a more comprehensive understanding of HIV-1 is urgently required. Here, 40 years since the discovery of HIV/AIDS, we discuss this topic as a special issue of Frontiers in Microbiology, to provide the scientific community with current understanding of HIV-1.

In total, 18 articles have been published in association with this topic. In this Editorial, we focus on four major areas as follows. First, from the perspective of epidemiology and virology, we explain the principles of viral transmission from different subtypes of viruses as well as their differences in virology and immunological response of the host; second, we highlight what is currently known about the host-HIV-1 interaction in terms of changes in host cell numbers and physiology during HIV-1 infections; third, we summarize the new findings on relationships between HIV-1 infections and other diseases; lastly, we briefly review the newly developed methods for detecting HIV-1/AIDS. Taken together, we hope that this collection of scientific articles provides new outlooks on studying HIV-1 and AIDS from different perspectives as well as providing comprehensive understanding of the specific phases of infection to identify and confirm viral mutations associated with drug resistance. In addition, the positive and negative responses of various host cells toward infection and

new strategies to reduce physiological discomfort resulting from primary and secondary infections are also discussed. Ultimately, it is our hope that these new research findings provide new avenues and guidelines to prevent the spread of the virus and stimulate the search for a cure for AIDS, eventually leading to the elimination of HIV-1.

It is critical to understand the epidemiology of AIDS and the spread of HIV-1. From 2010 to 2016, Li M. et al. conducted a seven-year horizontal epidemiological survey in Heilongjiang Province, China. By focusing on CRF01_AE, a main subtype of HIV-1, the study showed that sexual contact between men who have sex with men (MSM) was the major route of HIV-1 transmission. In addition, based on a study of the HIV-1 longitudinal genetic network in Guangxi, China, Chen Z. et al. highlight the role of antiretroviral therapy in preventing the spread of HIV-1. In the meanwhile, from population level studies, the authors noted that elderly male farmers, who were not educated in junior high schools, are at high risk of HIV infections. In a different study, Sivay et al. showed that the virus CRF63_02A6, the prevalent genetic variant of HIV-infected individuals in a major part of Siberia, probably originated from Novosibirsk, Russia, in 2005.

Although the virological aspect of HIV-1 has been studied for a relatively long time, given the evolution of virus-generated mutations, the characteristics of those new virus subtypes need to be clarified as an important reference for subsequent practices including disease prevention and control. In that regard, Li Y. et al. expressed HIV-1 CRF07 BC Gag antigen (p6Δ7 mutated or wild type) and screened the immunogenicity of the respective antigens in mice. They found that the single deleted amino acid within the P6 region of the Gag protein most likely resulted in enhanced immunogenicity of the mutated antigen. Meanwhile, by comparing the sequences of HIV-1 subtype B viruses from China and United States, Qian et al. verified two specific sites in the viruses from China, which contribute to the significant increase in viral mRNA transcription and Rev response element activity.

In the pathology of HIV infections, host related changes profoundly affect the development of AIDS. From the perspective of the relationship between host and HIV-1 virus, studies have reported that multiple cells types play diverse roles in the course of a HIV infection. Immune activation is the key factor leading to the impairment of immune reconstitution after long-term HAART. Double negative T cells (DN T) confer immunomodulation during HIV infections, but the relevant mechanism is still puzzling. In two articles within this special topic, different researchers studied the role of two different DN T cells in immune activation during HIV-1 infection. On one hand, Zhang et al. reported that $Foxp3^+$ $CD4^-$ $CD8^-$ T cells accumulated in untreated people living with HIV (PLWH), and the proportion of those cells was negatively correlated with $CD4^+$ T cell numbers and $CD4^+/CD8^+$ ratios, but positively correlated with immune activation and systemic inflammation in PLWH. On the other hand, Wang et al. found that, when compared with Immune Responders (IRs), Poor Immune Responders (PIRs) showed reduced percentages of $CD73^+$ $CD4^-$ $CD8^-$ T cells. The cell frequency was positively correlated with $CD4^+$ T cell numbers and $CD4^+/CD8^+$ ratios while negatively correlated with immune activation of PLWH. Those two types of cells played different roles in immune activation. From a microscopic perspective, the factors affecting $CD4^+$ T cell numbers may originate from $CD4^+$ T cells or surrounding cells. In $CD4^+$ T cells, Cai et al. observed that the down-regulation of TCF1 during HIV infection impairs T cell proliferation by destroying mitochondrial function. With the exception of $CD4^+$ T cells, Qian et al. noted that the proportion of $CD38^+$ $CD39^+$ NK cells in HIV-infected individuals was positively correlated with HIV viral load and negatively correlated with $CD4^+$ T cell numbers, with NK cells inhibiting the proliferation of $CD4^+$ T and $CD8^+$ T cells. In addition, based on the stemness and antiviral ability of HIV-1 specific $CD8^+$ T cells expressing CXCR5, Gao et al. summarize the functions of those $CD8^+$ T cells and propose strategies to translate the research findings into feasible strategies for HIV treatment and potential cure. Furthermore, in the context of an association between HIV-1 progression and non-infectious diseases, Qin et al. studied the relationship between HIV-1 and chronic kidney disease. The authors demonstrate that recovery of $CD4^+/CD8^+$ ratios was related to a lower incidence of chronic kidney disease (CKD) in HIV-1 infected patients receiving ART. Similarly, the treatment strategy based on non-nucleoside reverse transcriptase inhibitor (NNRTI) could be a better approach to restore $CD4^+/CD8^+$ ratios as well as reduce the risk of CKD.

Moving on to new strategies to eradicate HIV-1 infection, the "Shock and Kill" strategy has attracted much attention in recent years. Used in conjunction with latency reversing drugs to promote HIV-1 expression and virion production in latent cells, this strategy allows an infected individual to eliminate HIV-1 hiding within cells. Li Y. et al. synthesized a variety of compounds through the combinatorial strategy of computer-aided design and biological characterization. As a result, two agonists for TLR7/8 dual-receptors and one agonist specific for TLR8 were identified and shown to be highly efficacious in activating the latent reservoir of HIV-1 in cell lines and patient PBMCs. In particular, these agonists appeared to enhance the activity of NK and T cells.

In the late stages of a HIV infection, most HIV-infected people die from opportunistic infections due to their immune-deficient status, of which, a large proportion of deaths are caused by fungal infections. When investigating differences in lung microbiota of HIV-positive patients with different immune statuses, Chen J. et al. found that the diversity of bacteria in the lungs of HIV-positive patients was lower than that of HIV-negative patients, while the number of fungi was higher in HIV-positive patients. By studying fungal populations in the nose and mouth, Chen X. et al. discovered that invasive fungal diseases rarely developed in individuals with normal immune reconstitution, although these pathogenic filamentous fungi are readily detectable in the nose and mouth of such individuals. Meanwhile, Li Y. et al. elaborated on the neglected fungal species during HIV infections. In that context, the authors reviewed the latest progress in exploring the composition of fungal microbiota and common fungal diseases associated with HIV. The innate and adaptive antifungal immunity during HIV infections were also discussed. In addition, on the issue of intestinal microflora, Bragazzi et al. reviewed the impact of PrEP (pre-exposure prophylaxis) on the intestinal microflora of MSM.

Early diagnosis of HIV-1 infection and early initiation of HAART are very important to achieve better virus suppression and accelerated immune reconstruction. However, new

serological-based HIV-1 diagnostics and the potential for clinical application have yet to be approved. Nonetheless, Zhao et al. have developed a HIV-1 rapid recent-infection test strip (RRITS), which can distinguish HIV-1 near-term infection (RI) from long-term infection (LI) by recent infection testing algorithms (RITAs). This provides a feasible detection method for diagnosing the phase of a HIV-1 infection. In addition, identification of drug-resistant HIV-1 plays a key role in the follow-up drug treatment as well as prognosis. Li Y. et al. established a method to deep sequence the low-abundance HIV-1 drug resistance marker. This strategy is centered on NGS-based segmented amplification for detecting HIV-1 drug resistance mutations, whereby this approach can amplify the HIV-1 *pol* gene more accurately as well as economically to a threshold of 100 copies per ml.

In summary, this topic on "AIDS 40th Year" focuses on the epidemiological characteristics of HIV-1, viral differences between several HIV-1 subtypes, the consequences during pathogenesis of HIV-1 infection, the cure for HIV-1, the relationship between AIDS and other diseases, and related studies on current challenges. Collectively, findings from these studies can fill the existing gaps in certain areas of HIV/AIDS, however, more detailed studies are necessary to reduce the transmission of HIV-1, to prolong the lifespan of patients as well as to reduce patient discomfort. Finally, the development of a HIV-1 vaccine and achieving a complete cure for HIV-1 infections and AIDS still requires significant effort from researchers as well as all sectors of the community.

Author contributions

JZ wrote the manuscript. SJ, TZ, ZC, XJ, WZ, SR-n, AK, KD, and LZ edited the manuscript.

Conflict of interest

The authors declare that the research was conducted in the absence of any commercial or financial relationships that could be construed as a potential conflict of interest.

Publisher's note

frontiers in Microbiology

ORIGINAL RESEARCH
published: 10 February 2022
doi: 10.3389/fmicb.2022.827689

Association Between CD4/CD8 Ratio Recovery and Chronic Kidney Disease Among Human Immunodeficiency Virus-Infected Patients Receiving Antiretroviral Therapy: A 17-Year Observational Cohort Study

Fengxiang Qin[1,2†], Qing Lv[3†], Wen Hong[1†], Di Wei[3], Kui Huang[3], Ke Lan[3], Rongfeng Chen[1,2], Jie Liu[1,2], Bingyu Liang[1], Huayue Liang[1], Hao Liang[1,2], Shanfang Qin[3*], Li Ye[1,2*] and Junjun Jiang[1,2*]*

[1] Guangxi Key Laboratory of AIDS Prevention and Treatment, School of Public Health, Guangxi Medical University, Nanning, China, [2] Guangxi Collaborative Innovation Center for Biomedicine, Life Sciences Institute, Guangxi Medical University, Nanning, China, [3] Chest Hospital of Guangxi Zhuang Autonomous Region, Liuzhou, China

Background: CD4/CD8 ratio is considered as an emerging biomarker for human immunodeficiency virus (HIV)-related diseases. However, the relationship of CD4/CD8 ratio recovery and chronic kidney disease (CKD), and whether cumulative antiretroviral therapy (ART) is effective in the CD4/CD8 ratio recovery and in reducing CKD incidence among HIV patients remain unclear.

Methods: A 17-year observational cohort study was conducted on all HIV-infected patients receiving ART in Guangxi, China. Kaplan–Meier analysis was used to investigate the cumulative CKD incidence. Cox regression and propensity score matching (PSM) were used to evaluate the association between CD4/CD8 ratio recovery and CKD incidence, and the effect of ART regimens on CD4/CD8 ratio recovery and CKD incidence.

Results: A total of 59,268 eligible individuals contributing 285,143 person-years of follow-up, with an overall CKD incidence of 9.65%. After ART, patients who developed CKD showed higher mortality than those with normal kidney function (12.48 vs. 7.57%, $p < 0.001$). Patients whose CD4/CD8 ratio did not recover to 0.7 had a higher CKD incidence than the patients who recovered (aHR = 2.84, 95% CI 2.63–3.07), similar to the PSM analysis (aHR = 3.13, 95% CI 2.85–3.45). Compared with the PI-based and INSTI-based regimens, NNRTI-based regimen had a better CD4/CD8 ratio recovery rate

OPEN ACCESS

Edited by:
Linqi Zhang,
Tsinghua University, China

Reviewed by:
Adam M. Spivak,
The University of Utah, United States
Chao Qiu,
Fudan University, China

***Correspondence:**
Junjun Jiang
jiangjunjun@gxmu.edu.cn
Li Ye
yeli@gxmu.edu.cn
Shanfang Qin
2271976481@qq.com
Hao Liang
lianghao@gxmu.edu.cn

† These authors have contributed equally to this work and share first authorship

Specialty section:
This article was submitted to Infectious Agents and Disease, a section of the journal Frontiers in Microbiology

Received: *02 December 2021*
Accepted: *21 January 2022*
Published: *10 February 2022*

Citation:
Qin F, Lv Q, Hong W, Wei D, Huang K, Lan K, Chen R, Liu J, Liang B, Liang H, Liang H, Qin S, Ye L and Jiang J (2022) Association Between CD4/CD8 Ratio Recovery and Chronic Kidney Disease Among Human Immunodeficiency Virus-Infected Patients Receiving Antiretroviral Therapy: A 17-Year Observational Cohort Study. Front. Microbiol. 13:827689. doi: 10.3389/fmicb.2022.827689

(27.04, 16.16, and 29.66%, respectively) and a lower CKD incidence (17.43, 16.16, and 7.31%, respectively).

Conclusion: This large-scale real-world setting provide new evidence that the CD4/CD8 ratio recovery is associated with lower CKD incidence in HIV-infected patients receiving ART. NNRTI-based is a better choice for CD4/CD8 ratio recovery and reducing the risk of CKD.

Keywords: HIV, AIDS, CD4/CD8, chronic kidney disease, antiretroviral therapy

INTRODUCTION

Antiretroviral therapy (ART) has significantly decreased the mortality of human immunodeficiency virus (HIV)/acquired immune deficiency syndrome (AIDS) patients. As patients live longer, chronic non-communicable diseases (NCDs) have become a prominent public health problem. Previous studies have shown that diabetes, hypertension, and chronic kidney disease (CKD) are important NCDs among HIV patients (Kooij et al., 2017; Mathabire Rucker et al., 2018; Sutton et al., 2019). In China, the CKD prevalence among HIV patients is approximately 16.1–16.8% (Cheung et al., 2007; Cao et al., 2013), which is slightly higher than that in Japan (15.4%) (Yanagisawa et al., 2011) and the United States (15.5%) (Wyatt et al., 2007). The kidney plays an important role in drug metabolism and excretion, and its function or deficiency thereof is more evident in HIV-infected patients receiving long-term ART. It is worth noting that persistent kidney damage leads to an increased risk of death (Cristelli et al., 2017; Ekrikpo et al., 2018). The Guangxi Zhuang Autonomous Region, located in western China, suffers a high burden of HIV infection, with more than 110,000 HIV patients receiving ART in 2020. However, no reports were available on the incidence of CKD in this population in Guangxi.

Low CD4 cell counts and high viral loads have been considered as influencing factors for CKD in HIV-infected patients (Jose et al., 2018; Brito et al., 2019). CD4 cell count is the most important index used to evaluate the immune function of HIV-infected patients. In contrast to a persistent decrease in CD4 cell count, CD8 cell count is persistently high in HIV-infected patients. With ART, the CD4 cell count in most patients gradually normalizes, but their CD8 cell count remains at a high level (Geltzeiler et al., 2020). This ultimately leads to the CD4/CD8 ratio remaining low and difficult to recover to normal levels. A cohort study conducted in Hong Kong, China indicated that only 33% of HIV patients achieved a CD4/CD8 ratio $\geq$0.8 even though the CD4 cell count reached 500 cells/μL or higher after ART (Lee et al., 2017). Similarly, another study in Italy indicated that only 29% of HIV patients treated with ART who achieved viral suppression reached a CD4/CD8 ratio $\geq$1.0 (Mussini et al., 2015). Some previous studies have shown that the CD4/CD8 ratio is independently associated with mortality and morbidity of immune dysfunction, and metabolic syndrome (Sigel et al., 2017; Trickey et al., 2017; Han et al., 2018; Castilho et al., 2019; Gojak et al., 2019). Therefore, the CD4/CD8 ratio has been considered as an emerging biomarker for HIV-related diseases in recent years (Serrano-Villar and Deeks, 2015). The recovery of the CD4/CD8 ratio in HIV-infected patients in Guangxi after ART has not been reported so far; in particular, the relationship between the CD4/CD8 ratio and CKD remains unclear.

Cumulative ART significantly decreases the estimated glomerular filtration rate (eGFR) of HIV patients and increases the risk of developing CKD (Yombi et al., 2014; Mocroft et al., 2016). Additionally, it has been reported that antiretrovirals have a certain influence on the recovery of the CD4/CD8 ratio in HIV-infected patients (Herrera et al., 2020; Serrano-Villar et al., 2020). We suspect that there may be associations among ART regimens, CD4/CD8 ratio recovery, and the development of CKD in HIV patients. In this study, we retrospectively collected data on HIV patients receiving ART in Guangxi from the Chinese National Free Antiretroviral Treatment Program (NFATP) database to evaluate the incidence of CKD and the recovery of the CD4/CD8 ratio among HIV patients receiving ART who initially had a normal eGFR and to investigate the association of the CD4/CD8 ratio recovery and CKD among these patients with different ART regimens.

MATERIALS AND METHODS

Study Site and Participants

We retrospectively collected data from December 2003 through October 2020 for all HIV-infected adults reported to the NFATP at the initiation of ART in Guangxi, China. Patients who had a normal baseline eGFR ($\geq$90 mL/min per 1.73 m^2), available CD4/CD8 ratio measurements, treatment with ART, and triple treatment regimens [two nucleoside reverse transcriptase inhibitors (NRTIs) plus either a non-nucleoside reverse transcriptase inhibitor (NNRTI) (NNRTI-based), a protease inhibitor (PI) (PI-based), or an integrase strand transfer inhibitor (INSTI) (INSTI-based)] were included. Patients were excluded if they met the following criteria: (i) had no baseline CD4 cell count and/or CD8 cell count, (ii) did not have information to calculate baseline and follow-up eGFR, (iii) had a baseline eGFR $<$90 mL/min per 1.73 m^2, (iv) were followed up for less than 6 months, (v) had a baseline CD4/CD8 ratio $\geq$1.0, or (vi) were treated with regimens other than NNRTI-based, PI-based and INSTI-based regimens. This study was approved by the Human Research Ethics Committee of Guangxi Medical University (Ethical Review No. 2019-SB-102).

Definitions

Baseline was defined as various demographic data or clinical indicators from the most recent record prior to or following ART started. eGFRs were calculated by creatinine clearance as [(186 × serum creatinine)−(1.154 × age)−0.203] (for males) and [(186 × serum creatinine)−(1.154 × age) −(0.203 × 0.742]] (for females) (Simplified MRDR formula). CKD was defined as eGFR lower than 60 mL/min per 1.73 m^2 (Mocroft et al., 2016) and defined as the outcome event. A CD4/CD8 ratio ≥0.7 at two consecutive visits after long-term ART was defined as the CD4/CD8 ratio recovery in our study.

Statistics

Categorical variables were described as frequency while quantitative variables were expressed as the median ± interquartile range (IQR). A Kaplan–Meier graph was used to show the accumulative CKD incidence during the ART period, and statistical testing of differences was performed using the log-rank test. Multivariable Cox regression analysis was used to evaluate the association of CD4/CD8 ratio recovery and CKD incidence or ART regimen and CD4/CD8 ratio recovery or ART regimen combined with CD4/CD8 ratio recovery and CKD incidence. In addition, 1:1 propensity score matching (PSM) was used to match the characteristic variables between the CD4/CD8 ratio recovered and unrecovered groups, and 1:1:1 PSM was used to match the characteristic variables among the NNRTI-based, PI-based and INSTI-based groups. The forest plot was used to indicate the effect of the whole research population and the PSM population. Data were analyzed using the Statistical Package for the Social Sciences (SPSS) version 23.0 (SPSS Inc., Chicago, IL, United States), R studio (version 3.6.1; R studio, Boston, MA, United States) and GraphPad Prism version 8.2 (GraphPad Software, San Diego, CA, United States). A two-tailed statistical test with a *P*-value of 0.05 or less was considered statistically significant.

RESULTS

Demographic Characteristics of Eligible Human Immunodeficiency Virus Patients at Baseline

A total of 110,890 HIV patients who initiated ART between December 2003 and October 2020 in Guangxi, China, were screened for inclusion in the present study. Of those patients, 51,622 were excluded, detail in **Figure 1**. Ultimately, 59,268 patients met the inclusion criteria and were included in this study. These eligible patients contributed 285,143 person-years

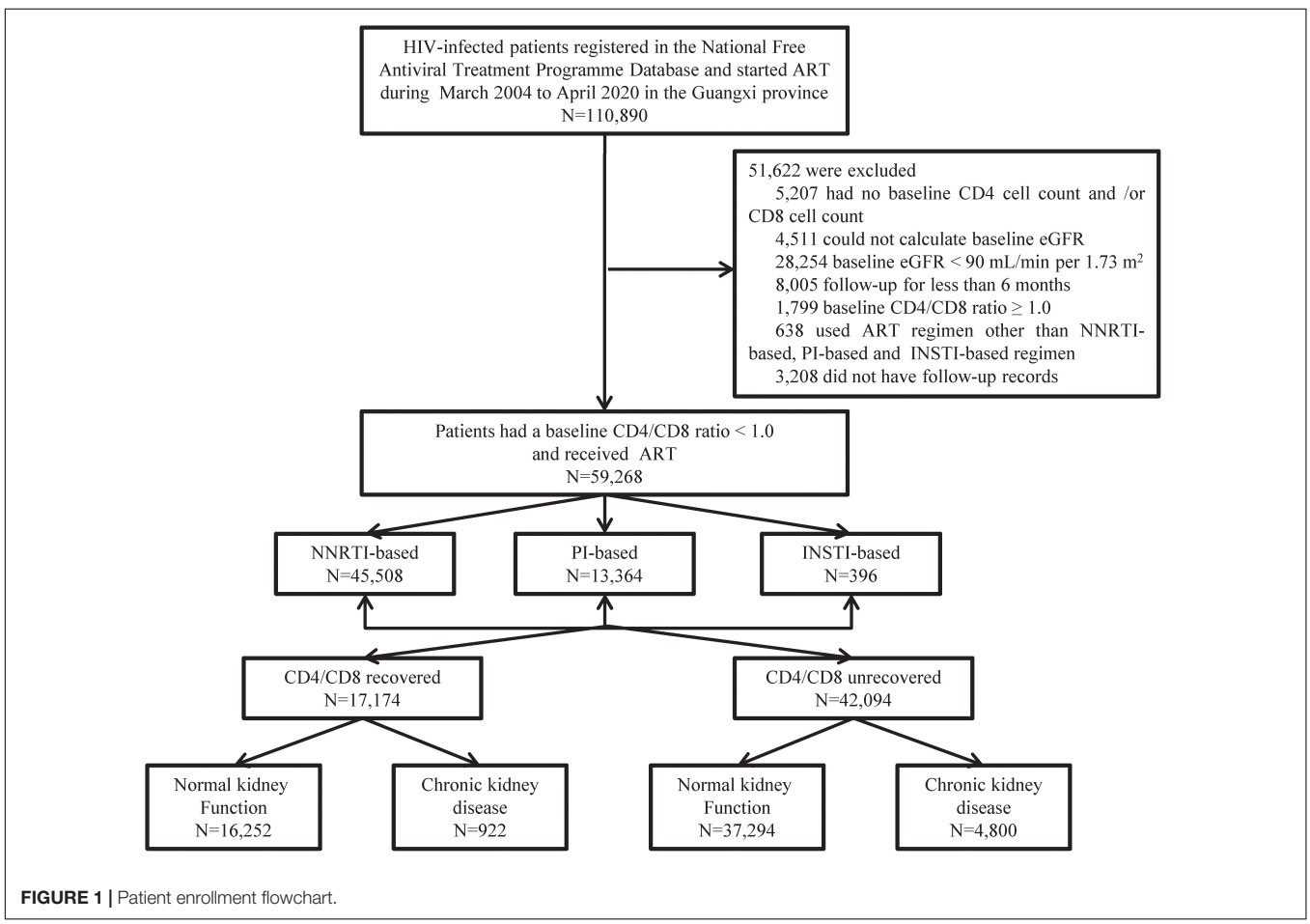

FIGURE 1 | Patient enrollment flowchart.

of follow-up, with a median of 4 person-years (IQR 2–7). **Table 1** shows that 64.63% patients were male, 63.49% were married or cohabiting, and most patients were diagnosed with HIV (63.71%) or started ART (65.79%) at 30–59 years of age. A total of 85.57% acquired HIV through heterosexual transmission, 45.65% had World Health Organization (WHO) HIV clinical stage I disease, 48.37% had a baseline body mass index (BMI) in the normal range (18.5–23.9 kg/m^2). 53.30% patients had a CD4 cell count <200 cells/μL, 47.02% had a CD8 cell count ≤760 cells/μL. And 68.96% patients had a baseline CD4/CD8 ratio <0.30.

TABLE 1 | Characteristics of HIV patients receiving ART [*n* (%)].

Variable	Study population (*n* = 59,268) (*n*, %)
Sex	
Male	38,304 (64.63)
Female	20,964 (35.37)
Marital status	
Single, divorced or widowed	21,482 (36.25)
Married or cohabitation	37,629 (63.49)
Unknown	157 (0.26)
Age at HIV diagnosis, year-old #	41.38 (31.57–54.34)
<30	12,235 (20.64)
30–59	37,758 (63.71)
≥60	9,275 (15.65)
Age at ART initiation, year-old #	42.12 (32.55–54.67)
<30	10,640 (17.95)
30–59	38,990 (65.79)
≥60	9,638 (16.26)
HIV transmission route	
Blood or plasma transfusion	3,820 (6.45)
Homosexual transmission	3,438 (5.80)
Heterosexual transmission	50,717 (85.57)
Other/unknown	1,293 (2.18)
WHO HIV disease stage	
I	27,055 (45.65)
II	9,206 (15.53)
III	10,264 (17.32)
IV	12,283 (20.72)
Unknown	460 (0.78)
Baseline body mass index, kg/m^2 #	20.32 (18.66–22.39)
<18.5	10,613 (17.91)
18.5–23.9	28,668 (48.37)
24–27.9	4,783 (8.07)
≥28	900 (1.52)
Unknown	14,304 (24.13)
Baseline CD4 cell count, cells/μL #	183.82 (51.39–309.71)
<200	31,590 (53.3)
200–349	16,845 (28.42)
350–499	7,427 (12.53)
≥500	3,406 (5.75)
Baseline CD8 cell count, cells/μL #	795.37 (509.96–1166.44)
≤760	27,869 (47.02)
761–1138	15,745 (26.57)
≥1138	15,654 (26.41)
Baseline CD4/CD8 #	0.20 (0.08–0.34)
<0.30	40,874 (68.96)
0.3–0.69	16,694 (28.17)
0.70–0.99	1,700 (2.87)

#Data are presented as medium [interquartile range (IQR)].

Kidney Function Was Related to Mortality in Human Immunodeficiency Virus Patients Receiving Antiretroviral Therapy

Of the 59,268 eligible patients, the incidence of CKD was 9.65% (5,722/59,268), and the overall mortality rate was 8.05% (4,770/59,268). The mortality in CKD patients was significantly higher than that in normal kidney function patients (12.48% vs. 7.57%, $P < 0.001$) (**Supplementary Table 1**).

CD4/CD8 Ratio Recovery Was Association With Chronic Kidney Disease Cumulative Incidence

In our study, CD4/CD8 ratio recovery in only 11.72% (6,947 of 59,268) of patients when the restoration cutoff point was defined as 1.0 (defined as "CD4/CD8 ratio normalized" in many other studies). In addition, 28.98% (17,174 of 59,268) of patients with a CD4/CD8 ratio recovery when the cutoff point was defined as 0.7 (**Supplementary Table 2**). Univariate Cox regression analysis showed that patients whose CD4/CD8 ratio did not recover to 0.7 (HR = 2.87, 95% CI 2.67–3.08) had a higher risk of developing CKD than those did not recover to 1.0 (HR = 1.33, 95% CI 1.22–1.46) (**Supplementary Table 2**). Therefore, we defined 0.7 as the CD4/CD8 ratio recovery cutoff point in this study for further analyses.

Kaplan–Meier analysis showed that patients with an unrecovered CD4/CD8 ratio had a significantly higher cumulative CKD incidence than the recovery patients over the 17-year follow-up period (log-rank test: $P < 0.001$, **Figure 2**). Cox regression also showed that unrecovered CD4/CD8 ratio patients had a higher risk for CKD than recovery patients (aHR = 2.84, 95% CI 2.63–3.06, $P < 0.001$) (**Supplementary Figure 1**, red line).

We used 1:1 PSM analysis to match variables between the recovered and unrecovered CD4/CD8 ratio groups to minimize potential biases. A caliper of 0.00001 was set to ensure that all characteristic variables and ART regimen were properly matched between the two groups. Finally, 12,112 CD4/CD8 ratio recovery patients and 12,112 CD4/CD8 ratio unrecovered patients were included. Chi-squared test was subsequently performed to evaluate the effectiveness of the PSM. The results showed that the matched variables no longer exhibited statistically significant differences between the two groups after matching (data not shown). Cox regression analysis showed that unrecovered CD4/CD8 ratio patients had a higher risk for CKD than recovery patients (aHR = 3.13, 95% CI 2.85–3.45, $P < 0.001$) (**Supplementary Figure 1**, blue line). The results before and after PSM showed a strong relationship between the CD4/CD8 ratio and CKD.

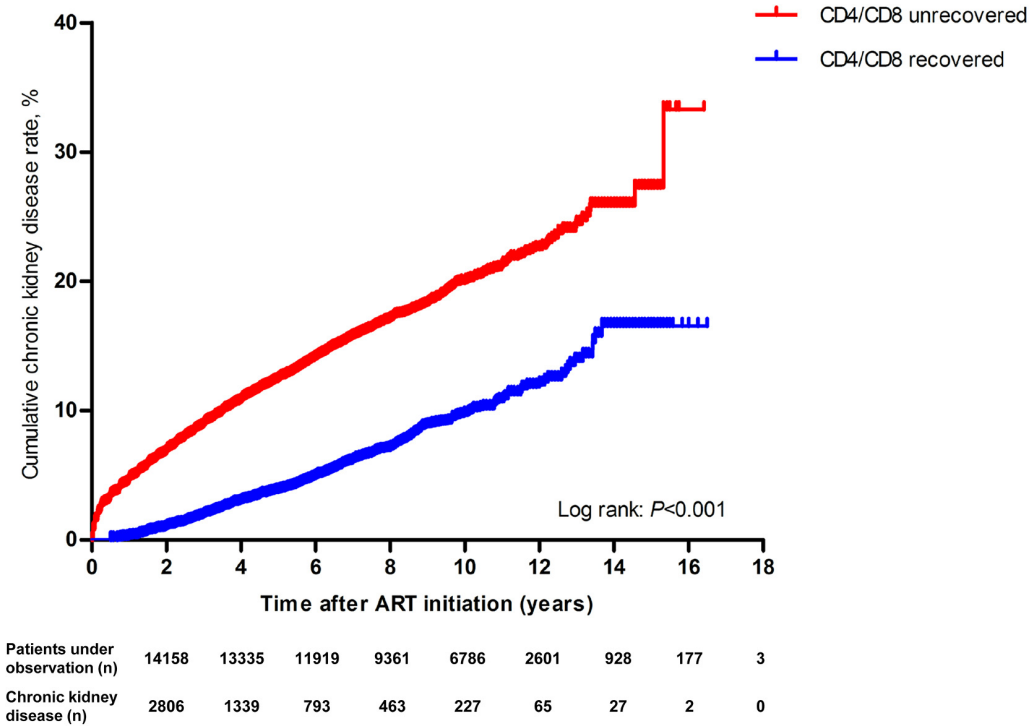

FIGURE 2 | Kaplan–Meier analysis of cumulative incidence of chronic kidney disease for HIV patients receiving ART, grouped by CD4/CD8 ratio recovery (The statistical significance was measured by log-rank test).

Relationship of Antiretroviral Therapy Regimen and CD4/CD8 Ratio Recovery or Chronic Kidney Disease Incidence

CD4/CD8 Ratio Recovery Among Different Antiretroviral Therapy Regimen Groups

In **Supplementary Table 3**, CD4/CD8 ratio recovery rate among the three ART regimen groups were significantly different, and the NNRTI-based group had the highest CD4/CD8 ratio recovery rate, followed by the PI-based and INSTI-based groups. While the CD8 also significantly decreased in the NNRTI-based group. However, the CD4 cell count showed highest increased in the PI-based group, followed by the NNRTI-based and INSTI-based groups. Moreover, median follow-up period and eGFR differences among the three ART regimen groups also showed statistically significance. **Table 2** showed the changes in the CD4/CD8 ratio and the CD4 or CD8 cell count at CD4/CD8 recovery between the NNRTI-based and PI-based groups were significantly different (the CD4 cell count at the CD4/CD8 ratio recovered NNRTI-based group was lower than that in the PI-based group, while the CD8 cell count was higher).

Antiretroviral Therapy Regimens Was Association With CD4/CD8 Ratio Recovery

Cox regression analysis showed that the patients treated with NNRTI-based (aHR = 0.58, 95% CI 0.52–0.65, $P < 0.001$) or PI-based (aHR = 0.61, 95% CI 0.54–0.68, $P < 0.001$) regimens had a lower risk for unrecovered CD4/CD8 ratios than patients treated with INSTI-based regimens in all participants (**Supplementary Figure 2**, red line).

Because the number of patients varies greatly among the three ART regimen groups and some demographic characteristics were significantly different among the ART regimen groups (data not shown), we used 1:1:1 PSM analysis to match variables among these three groups to minimize potential biases. First, a caliper of 0.00001 was set to ensure that all demographic variables were properly matched between the NNRTI-based and PI-based groups, 13,159 NNRTI-based and 13,159 PI-based patients were included. Then, 13,159 NNRTI-based patients were properly matched to INSTI-based patients, 372 NNRTI-based and 372 INSTI-based patients were included at a caliper of 0.00001; similarly, 380 PI-based and 380 INSTI-based patients were also included at a caliper of 0.0000005. Finally, the three ART regimen groups of matched subjects were integrated, and a final number of 1,098 patients (366 NNRTI-based, 366 PI-based and 366 INSTI-based) were included. Chi-squared test was subsequently performed to evaluate the effectiveness of the PSM. The results showed that these demographic variables no longer exhibited statistically significant differences between each pair of ART regimen groups after matching (data not shown).

Cox regression analysis showed that, compared with the INSTI-based regimen, the NNRTI-based (aHR = 0.56, 95% CI 0.47–0.67, $P < 0.001$) or PI-based (aHR = 0.61, 95% CI 0.52–0.72, $P < 0.001$) regimen had a lower risk for unrecovered CD4/CD8 ratios after PSM (**Supplementary Figure 2**, blue line).

TABLE 2 | CD4/CD8 ratio recovery among different ART regimen groups [Medium (IQR)].

Variable	NNRTI-based	PI-based	INSTI-based	*P**
Change in CD4/CD8 ratio	0.49 (0.36–0.63)	0.47 (0.34–0.61)	0.47 (0.36–0.61)	<0.001#
Time for CD4/CD8 ratio recovery, years	1.07 (0.49–2.89)	1.18 (0.49–3.00)	0.94 (0.30–1.97)	0.10
CD4 cell count at CD4/CD8 ratio recovery, cells/μL	502.24 (384.58–643.74)	550.13 (420.18–702.75)	552.50 (421.00–709.00)	<0.001#
CD8 cell count at CD4/CD8 ratio recovery, cells/μL	588.02 (441.47–766.23)	644.22 (480.77–841.77)	627.00 (515.50–831.00)	<0.001#

**P by non-parametric tests.*

#Pair wise comparison showed the difference was statistically significant only between the NNRTI-based and the PI-based group.

Antiretroviral Therapy Regimens Was Association With Chronic Kidney Disease Cumulative Incidence

As shown in **Figure 3**, after adjustment for a collection of predefined and forward-selection variables, Cox regression analysis indicated that the NNRTI-based (aHR = 0.33, 95% CI 0.25–0.42, $P < 0.001$) or PI-based (aHR = 0.71, 95% CI 0.55–0.91, $P = 0.01$) regimen had a lower incidence of CKD than that of INSTI-based regimen (**Figure 3**, red line). The PSM analysis also showed that the NNRTI-based (aHR = 0.26, 95% CI 0.16–0.44, $P < 0.001$) ART regimen had a lower incidence of CKD than that of INSTI-based regimen (**Figure 3**, blue line).

Stratified Analysis of Antiretroviral Therapy Regimens

Stratified analysis of different ART regimens was used to evaluate the relationship of CD4/CD8 ratio recovery and CKD in three subgroups of ART regimens using the Kaplan–Meier method. In all three ART regimen subgroups, the cumulative incidences of CKD in the CD4/CD8 ratio unrecovered group were significantly higher than those in the recovered group (**Figures 4A–C**). The largest difference in CKD incidence between the CD4/CD8 ratio recovered and unrecovered groups was found in the INSTI-based subgroup (**Figure 4A**). Additionally, the highest CKD incidence rate (7/100 person-years, 95% CI 5–8) was found among patients treated with the INSTI-based regimen and the CD4/CD8 ratio was unrecovered, and was significantly higher than the CD4/CD8 ratio recovery patients (**Supplementary Table 4**). Moreover, the stratified analysis after PSM also showed that in PI-based and INSTI-based ART regimen subgroups, the cumulative incidences of CKD in the CD4/CD8 ratio unrecovered group were significantly higher than those in the recovery group (**Figures 4D–F**). However, no significant difference was seen in the NNRTI-based group (log-rank test: $P = 0.22$, **Figure 4F**).

DISCUSSION

This is a real-world study with a 17-year observation period and a large sample size that was conducted on HIV-positive individuals in Guangxi, China to explore the relationship of the CD4/CD8 ratio recovery and CKD. The study indicated that the incidence of CKD was 9.65% in HIV patients with ART, which is lower than those (15.4–16.8%) in several previous studies (Cheung et al., 2007; Wyatt et al., 2007; Yanagisawa et al., 2011; Cao et al., 2013). The main reason for this difference is that the rates in previous studies were the overall incidence of CKD, whereas our study excluded HIV patients with an abnormal baseline eGFR, which leads to the relatively lower incidence of CKD. This is the first study to estimate the CKD incidence of 9.65% in Guangxi over a median ART period of 4 person-years. The incidence estimate is important, as it emphasizes a substantial burden of CKD among these patients. Our study also showed that patients with CKD had a higher risk of death, which is consistent with the results of previous research, indicating that kidney disease can significantly increase the risk of death in HIV-infected individuals (Sarfo et al., 2013; Mallipattu et al., 2014).

CD4 cell count has been considered as an influencing factor for NCDs in HIV-infected patients. With ART, the CD4 cell count in most patients gradually normalizes, but the CD8 cell count might remain at a high level, which leads to the CD4/CD8 ratio remaining low and difficult to recover to normal levels. In our study, the CD4 cell count did not necessarily raise to 500 cells/μL or above in patients whose CD4/CD8 ratio recovered to 0.7 (**Table 2**). Previous studies have showed that a low CD4/CD8 ratio in HIV-infected patients identifies greater immune defects, which might be at a higher risk of mortality, various infections, including kidney infection (Trickey et al., 2017). In recent years, growing evidence suggests that the CD4/CD8 ratio should be considered as an emerging biomarker for HIV-related diseases. Our study revealed that, among HIV patients with normal baseline kidney function, CD4/CD8 ratio recovery was strongly associated with the incidence of CKD, which was supported by the overall patient-wide Cox regression analysis and PSM analysis designed to reduce biases in the distribution of potentially confounding variables. Furthermore, our study found that patients whose CD4/CD8 ratio failed to recover to 0.7 may have poor immune function, leading to a higher risk of CKD. These findings have significant implications for the relationship between CD4/CD8 ratio and NCDs in HIV patients, and are an important complement to previous studies (Castilho et al., 2019; Gojak et al., 2019). In addition, we found that the median CD4 cell count in the NNRTI-based group was lower than that in PI-based or INSTI-based groups when CD4/CD8 ratio recovered, however, the incidence of CKD in NNRTI-based group was the lowest (**Supplementary Table 3**), indicating that although CD4 cell count of some participants did not return to normal level, the risk of CKD could be partially reduced as long as the CD4/CD8 ratio was restored. That is, the CD4/CD8 ratio may be a more important reflection for the CKD incidence of HIV-1 infected patients than the CD4 cell count alone.

Previous studies have reported that INSTI-based ART was associated with a greater increase in the CD4/CD8 ratio (Masia et al., 2016; Serrano-Villar et al., 2020). In the present study, we further explored whether there was a significant difference in the ART regimens between the recovered CD4/CD8 group and the

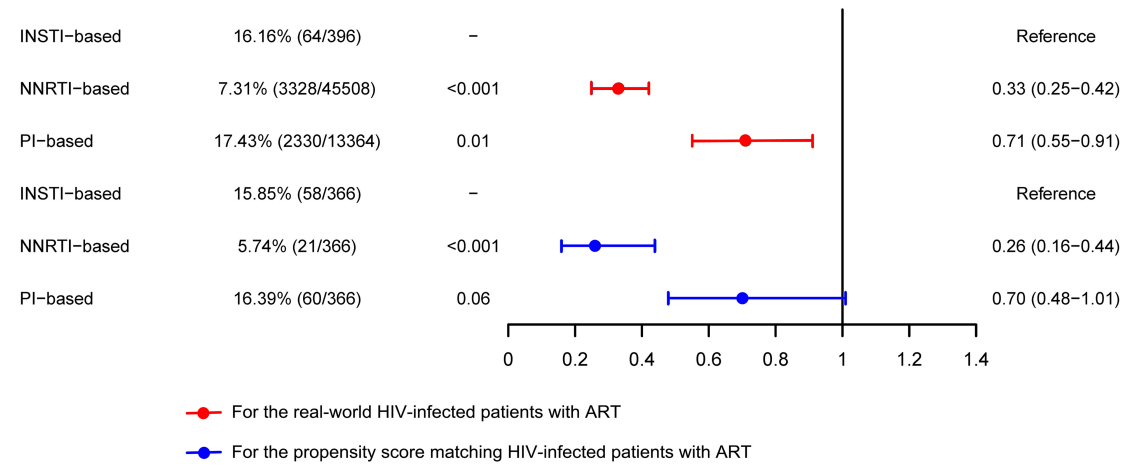

FIGURE 3 | Forest plots of multivariable Cox regression analysis of the effect of ART regimen on chronic kidney disease among HIV patients receiving ART. [*aHR, adjusted hazard ratio, adjusted by ART regimen, CD4/CD8 ratio recovery, sex, marital status, age at HIV diagnosis, age at ART initiation, HIV transmission route, WHO HIV disease stage, baseline BMI, baseline CD4 cell count, baseline CD8 cell count, baseline CD4/CD8 ratio, HBV infection, HCV infection, TB infection in the past year, and other opportunistic infections in the past 3 months (including thrush, hairy leukoplakia, esophageal candidiasis, PCP, toxoplasmic encephalitis, Cytomegalovirus infection, disseminated mycosis and extrapulmonary TB)].

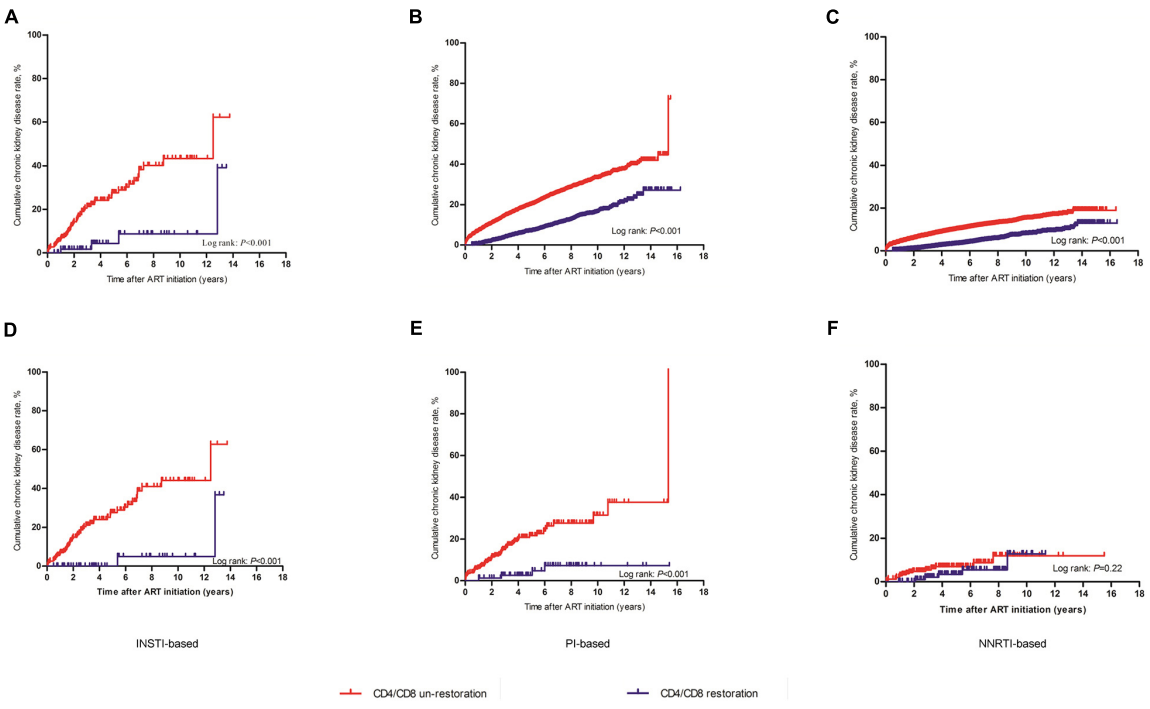

FIGURE 4 | Kaplan-Meier analysis of cumulative incidence of chronic kidney disease for HIV patients receiving ART, grouped by ART regimen. **(A)** The whole research patients treated with INSTI-based regimen. **(B)** The whole research patients treated with PI-based regimen. **(C)** The whole research patients treated with NNRTI-based regimen. **(D)** The PSM patients treated with INSTI-based regimen. **(E)** The PSM patients treated with PI-based regimen. **(F)** The PSM patients treated with NNRTI-based regimen. The statistical significance was measured by log-rank test.

non-recovered group. We found that the INSTI-based regimen had the lowest CD4/CD8 ratio recovery rate at a cutoff of 0.7, which is inconsistent with two previous studies, indicating the INSTI-based regimen had higher CD4/CD8 ratio normalization rates than NNRTI-based or PI-based regimens (Herrera et al., 2020; Serrano-Villar et al., 2020). Moreover, previous studies have showed the largest differences in CD4/CD8 ratio trajectories were driven by changes in the CD8 cell counts (Serrano-Villar et al., 2017, 2020). They found the adjusted mean CD8 cell counts was highest in PI-based regimen, and a higher rate of CD4/CD8 ratio normalization with efavirenz, which was driven by greater CD8 cell decline (Serrano-Villar et al., 2017, 2020). However, our study found that the median CD8 decreased only in the NNRTI-based regimen, and this regimen had the highest CD4/CD8 ratio recovery rate. The PI-based and INSTI-based regimens had relatively lower CD4/CD8 ratio recovery rate, and the median CD8 were almost unchanged. Different CD4/CD8 ratio cutoff values as well as different ART policies or treatment details in different countries may be the reasons for these inconsistent results.

Antiretroviral drugs have been shown to be associated with NCDs such as diabetes and obesity among HIV patients (Coetzee et al., 2019). Several studies have also confirmed an association of CKD incidence with PIs (Yombi et al., 2014; Mocroft et al., 2016). Our study showed that the association between CD4/CD8 ratio recovery and reduced CKD incidence was consistently observed in all three ART regimen groups. It is worth noting that the benefit of CD4/CD8 ratio recovery on CKD incidence was most significant in the INSTI-based group, this result was also confirmed by PSM analysis. This provides further support for the finding because the patients with the INSTI-based regimen in our study had the lowest CD4/CD8 ratio recovery rate. If CD4/CD8 ratio recovery is related with CKD incidence, patients with the least desirable CD4/CD8 recovery need to be focused. In particular, the CKD incidence in PI-based or INSTI-based regimens was significantly different between the CD4/CD8 ratio recovered and unrecovered groups, while there was no significant difference in NNRTI-based regimen. This suggests that patients using PI-based or INSTI-based regimens should pay more attention to CD4/CD8 ratio recovery to minimize the risk of CKD. In addition, PIs have been widely recognized as nephrotoxic, but there are few studies on whether INSTIs have side effects on the kidney (Yombi et al., 2014; Mocroft et al., 2016). In this sense, our study provides new clues that PI and INSTI may be nephrotoxic.

It should be noted that our study has some limitations. First, this was a retrospective cohort study, and we could not control some confounding factors, such as the use of medications other than the ART regimens, which might be associated with renal toxicity. Second, due to the lack of viral suppression data from the participants, it was not possible to determine whether patients' viral load was suppressed when the CD4/CD8 ratio recovered to 0.7. Despite these limitations, to the best of our knowledge, this is the first large cohort study in a real-world setting to investigate the relationship of CD4/CD8 ratio recovery and CKD incidence in HIV-infected patients receiving ART. The recovery of the CD4/CD8 ratio is better, and the incidence of CKD is lower in HIV patients treated with NNRTI-based regimens than in those treated with PI-based or INSTI-based regimens. These results highlight the importance of monitoring the CD4/CD8 ratio in patients receiving ART, especially with PI-based or INSTI-based regimens.

DATA AVAILABILITY STATEMENT

The original contributions presented in the study are included in the article/**Supplementary Material**, further inquiries can be directed to the corresponding author/s.

ETHICS STATEMENT

The studies involving human participants were reviewed and approved by the Human Research Ethics Committee of Guangxi Medical University. Written informed consent for participation was not required for this study in accordance with the National Legislation and the Institutional Requirements.

AUTHOR CONTRIBUTIONS

JJ, LY, SQ, and HaL conceived and designed the study. FQ, JJ, QL, and WH conducted the data analysis and literature review and drafted the manuscript. FQ, QL, WH, DW, KH, and KL involved in the study supervision, data collection, and interpretation of the data. FQ, RC, JL, BL, and HuL assisted with data management and data analysis. All authors contributed to the revision of the manuscript and approved the final version.

FUNDING

This study was supported by the National Natural Science Foundation of China (NSFC, 31860040, 31970167 and 81960602), Guangxi Bagui Scholar (to JJ), Guangxi Medical University Training Program for Distinguished Young Scholars (to JJ), Guangxi Science Fund for Distinguished Young Scholars (2018GXNSFFA281001), National Science and Technology Major Projects (2018ZX10715008-002), and Guangxi Key Research and Development Program (Guike AB18050022 and AB19245038).

ACKNOWLEDGMENTS

We would like to express our gratitude to all of staffs from the Chest Hospital of Guangxi Zhuang Autonomous Region, Guangxi, China, for their collecting and providing epidemiological data of local HIV/AIDS.

SUPPLEMENTARY MATERIAL

The Supplementary Material for this article can be found online at: https://www.frontiersin.org/articles/10.3389/fmicb.2022.827689/full#supplementary-material

REFERENCES

Brito, R. M., Nguyen, D. T., Johnson, J. R., Lai, E. J., Castro, R. E., Albert, A. M., et al. (2019). Chronic kidney disease in patients infected with human immunodeficiency virus (HIV) in an urban cohort. *PLoS One* 14:e0215575. doi: 10.1371/journal.pone.0215575

Cao, Y., Gong, M., Han, Y., Xie, J., Li, X., Zhang, L., et al. (2013). Prevalence and risk factors for chronic kidney disease among HIV-infected antiretroviral therapy-naive patients in mainland China: a multicenter cross-sectional study. *Nephrology (Carlton)* 18, 307–312. doi: 10.1111/nep.12031

Castilho, J. L., Turner, M., Shepherd, B. E., Koethe, J. R., Furukawa, S. S., Bofill, C. E., et al. (2019). CD4/CD8 ratio and CD4 nadir predict mortality following noncommunicable disease diagnosis in adults living with HIV. *AIDS Res. Hum. Retroviruses* 35, 960–967. doi: 10.1089/AID.2019.0064

Cheung, C. Y., Wong, K. M., Lee, M. P., Liu, Y. L., Kwok, H., Chung, R., et al. (2007). Prevalence of chronic kidney disease in Chinese HIV-infected patients. *Nephrol. Dial. Transplant.* 22, 3186–3190. doi: 10.1093/ndt/gfm350

Coetzee, L., Bogler, L., De Neve, J. W., Barnighausen, T., Geldsetzer, P., and Vollmer, S. (2019). HIV, antiretroviral therapy and non-communicable diseases in sub-Saharan Africa: empirical evidence from 44 countries over the period 2000 to 2016. *J. Int. AIDS Soc.* 22:e25364. doi: 10.1002/jia2.25364

Cristelli, M. P., Cofan, F., Rico, N., Trullas, J. C., Manzardo, C., Aguero, F., et al. (2017). Estimation of renal function by CKD-EPI versus MDRD in a cohort of HIV-infected patients: a cross-sectional analysis. *BMC Nephrol.* 18:58. doi: 10.1186/s12882-017-0470-4

Ekrikpo, U. E., Kengne, A. P., Bello, A. K., Effa, E. E., Noubiap, J. J., Salako, B. L., et al. (2018). Chronic kidney disease in the global adult HIV-infected population: a systematic review and meta-analysis. *PLoS One* 13:e0195443. doi: 10.1371/journal.pone.0195443

Geltzeiler, C. B., Xu, Y., Carchman, E., Ghouse, Y., Beczkiewicz, J., Son, J., et al. (2020). CD4/CD8 ratio as a novel marker for increased risk of high-grade anal dysplasia and anal cancer in HIV+ patients: a retrospective cohort study. *Dis. Colon. Rectum* 63, 1585–1592. doi: 10.1097/DCR.0000000000001763

Gojak, R., Hadziosmanovic, V., Baljic, R., Zecevic, L., Coric, J., and Mijailovic, Z. (2019). CD4/CD8 ratio as a predictor for the occurrence of metabolic syndrome in HIV / AIDS patients during 6 months of cART therapy. *J. Med. Biochem.* 38, 489–495. doi: 10.2478/jomb-2018-0049

Han, W. M., Apornpong, T., Kerr, S. J., Hiransuthikul, A., Gatechompol, S., Do, T., et al. (2018). CD4/CD8 ratio normalization rates and low ratio as prognostic marker for non-AIDS defining events among long-term virologically suppressed people living with HIV. *AIDS Res. Ther.* 15:13. doi: 10.1186/s12981-018-0200-4

Herrera, S., Fernandez-Felix, B. M., Hunt, P. W., Deeks, S. G., Sainz, T., Heath, S. L., et al. (2020). Impact of first-line antiretroviral therapy regimens on the restoration of the CD4/CD8 ratio in the CNICS cohort. *J Antimicrob Chemother* 75, 1604–1610. doi: 10.1093/jac/dkaa024

Jose, S., Hamzah, L., Jones, R., Williams, D., Winston, A., Burns, F., et al. (2018). Chronic kidney disease risk in African and caribbean populations with HIV. *J. Infect. Dis.* 218, 1767–1772. doi: 10.1093/infdis/jiy397

Kooij, K. W., Vogt, L., Wit, F., van der Valk, M., van Zoest, R. A., Goorhuis, A., et al. (2017). Higher prevalence and faster progression of chronic kidney disease in human immunodeficiency virus-infected middle-aged individuals compared with human immunodeficiency virus-uninfected controls. *J. Infect. Dis.* 216, 622–631. doi: 10.1093/infdis/jix202

Lee, S. S., Wong, N. S., Wong, B. C. K., Wong, K. H., and Chan, K. C. W. (2017). Combining CD4 recovery and CD4: CD8 ratio restoration as an indicator for evaluating the outcome of continued antiretroviral therapy: an observational cohort study. *BMJ Open* 7:e016886. doi: 10.1136/bmjopen-2017-016886

Mallipattu, S. K., Salem, F., and Wyatt, C. M. (2014). The changing epidemiology of HIV-related chronic kidney disease in the era of antiretroviral therapy. *Kidney Int.* 86, 259–265. doi: 10.1038/ki.2014.44

Masia, M., Padilla, S., Barber, X., Sanchis, M., Terol, G., Lidon, F., et al. (2016). Comparative impact of suppressive antiretroviral regimens on the CD4/CD8 T-Cell ratio: a cohort study. *Medicine (Baltimore)* 95:e3108. doi: 10.1097/MD.0000000000003108

Mathabire Rucker, S. C., Tayea, A., Bitilinyu-Bangoh, J., Bermudez-Aza, E. H., Salumu, L., Quiles, I. A., et al. (2018). High rates of hypertension, diabetes, elevated low-density lipoprotein cholesterol, and cardiovascular disease risk factors in HIV-infected patients in Malawi. *AIDS* 32, 253–260. doi: 10.1097/QAD.0000000000001700

Mocroft, A., Lundgren, J. D., Ross, M., Fux, C. A., Reiss, P., Moranne, O., et al. (2016). Cumulative and current exposure to potentially nephrotoxic antiretrovirals and development of chronic kidney disease in HIV-positive individuals with a normal baseline estimated glomerular filtration rate: a prospective international cohort study. *Lancet HIV* 3, e23–e32. doi: 10.1016/S2352-3018(15)00211-8

Mussini, C., Lorenzini, P., Cozzi-Lepri, A., Lapadula, G., Marchetti, G., Nicastri, E., et al. (2015). CD4/CD8 ratio normalisation and non-AIDS-related events in individuals with HIV who achieve viral load suppression with antiretroviral therapy: an observational cohort study. *Lancet HIV* 2, e98–e106. doi: 10.1016/S2352-3018(15)00006-5

Sarfo, F. S., Keegan, R., Appiah, L., Shakoor, S., Phillips, R., Norman, B., et al. (2013). High prevalence of renal dysfunction and association with risk of death amongst HIV-infected Ghanaians. *J. Infect.* 67, 43–50. doi: 10.1016/j.jinf.2013.03.008

Serrano-Villar, S., and Deeks, S. G. (2015). CD4/CD8 ratio: an emerging biomarker for HIV. *Lancet HIV* 2, e76–e77. doi: 10.1016/S2352-3018(15)00018-1

Serrano-Villar, S., Caruana, G., Zlotnik, A., Perez-Molina, J. A., and Moreno, S. (2017). Effects of maraviroc versus efavirenz in combination with zidovudine-lamivudine on the CD4/CD8 ratio in treatment-naive HIV-infected individuals. *Antimicrob. Agents Chemother.* 61, e1763–e1717. doi: 10.1128/AAC.01763-17

Serrano-Villar, S., Martinez-Sanz, J., Ron, R., Talavera-Rodriguez, A., Fernandez-Felix, B. M., Herrera, S., et al. (2020). Effects of first-line antiretroviral therapy on the CD4/CD8 ratio and CD8 cell counts in CoRIS: a prospective multicentre cohort study. *Lancet HIV* 7, e565–e573. doi: 10.1016/S2352-3018(20)30202-2

Sigel, K., Wisnivesky, J., Crothers, K., Gordon, K., Brown, S. T., Rimland, D., et al. (2017). Immunological and infectious risk factors for lung cancer in US veterans with HIV: a longitudinal cohort study. *Lancet HIV* 4, e67–e73. doi: 10.1016/S2352-3018(16)30215-6

Sutton, S. S., Magagnoli, J., Cummings, T. H., Hardin, J. W., Edun, B., and Beaubrun, A. (2019). Chronic kidney disease, cardiovascular disease, and osteoporotic fractures in patients with and without HIV in the US Veteran's affairs administration system. *Curr. Med. Res. Opin* 35, 117–125. doi: 10.1080/03007995.2018.1543183

Trickey, A., May, M. T., Schommers, P., Tate, J., Ingle, S. M., Guest, J. L., et al. (2017). CD4:CD8 ratio and CD8 count as prognostic markers for mortality in human immunodeficiency virus-infected patients on antiretroviral therapy: the antiretroviral therapy cohort collaboration (ART-CC). *Clin. Infect. Dis* 65, 959–966. doi: 10.1093/cid/cix466

Wyatt, C. M., Winston, J. A., Malvestutto, C. D., Fishbein, D. A., Barash, I., Cohen, A. J., et al. (2007). Chronic kidney disease in HIV infection: an urban epidemic. *AIDS* 21, 2101–2103. doi: 10.1097/QAD.0b013e3282ef1bb4

Yanagisawa, N., Ando, M., Ajisawa, A., Imamura, A., Suganuma, A., Tsuchiya, K., et al. (2011). Clinical characteristics of kidney disease in Japanese HIV-infected patients. *Nephron Clin. Pract.* 118, c285–c291. doi: 10.1159/000322278

Yombi, J. C., Pozniak, A., Boffito, M., Jones, R., Khoo, S., Levy, J., et al. (2014). Antiretrovirals and the kidney in current clinical practice: renal pharmacokinetics, alterations of renal function and renal toxicity. *AIDS* 28, 621–632. doi: 10.1097/QAD.0000000000000103

Conflict of Interest: The authors declare that the research was conducted in the absence of any commercial or financial relationships that could be construed as a potential conflict of interest.

frontiers | Frontiers in Immunology

ORIGINAL RESEARCH
published: 04 April 2022
doi: 10.3389/fimmu.2022.869286

Decreased CD73+ Double-Negative T Cells and Elevated Level of Soluble CD73 Correlated With and Predicted Poor Immune Reconstitution in HIV-Infected Patients After Antiretroviral Therapy

Xinyue Wang[1,2,3,4†], Leidan Zhang[1,4,5†], Juan Du[2,3,4†], Yuqing Wei[2,3,4], Di Wang[4,5], Chuan Song[2,3,4], Danying Chen[2,3,4], Bei Li[4,5], Meiqing Jiang[2,3,4], Mengyuan Zhang[2,3,4], Hongxin Zhao[4,5] and Yaxian Kong[1,2,3,4*]*

[1] Peking University Ditan Teaching Hospital, Beijing, China, [2] Beijing Key Laboratory of Emerging Infectious Diseases, Institute of Infectious Diseases, Beijing Ditan Hospital, Capital Medical University, Beijing, China, [3] Beijing Institute of Infectious Diseases, Beijing, China, [4] National Center for Infectious Diseases, Beijing Ditan Hospital, Capital Medical University, Beijing, China, [5] Clinical and Research Center of Infectious Diseases, Beijing Ditan Hospital, Capital Medical University, Beijing, China

Although extensive use of antiretroviral therapy (ART) has made great progress in controlling HIV replication and improving $CD4^+$ T cell recovery, the immune reconstitution remained insufficient in some patients, who were defined as poor immunological responders (PIRs). These PIRs were at a high risk of AIDS-related and non-AIDS complications, resulting in higher morbidity and mortality rate. Thus, it is a major challenge and urgently needed to distinguish PIRs early and improve their immune function in time. Immune activation is a key factor that leads to impaired immune reconstitution in people living with HIV (PLWH) who are receiving effective ART. Double negative T cells (DNT) were reported to associate with the control of immune activation during HIV infection. However, the precise mechanisms by which DNT cells exerted their suppressive capacity during HIV infection remained puzzled. CD73, both a soluble and a membrane-bound form, display immunosuppressive effects through producing adenosine (ADO). Thus, whether DNT cells expressed CD73 and mediated immune suppression through CD73-ADO pathway needs to be investigated. Here, we found a significant downregulation of CD73 expression on DNT cells in treatment-naïve PLWH (TNs) compared to healthy controls, accompanied with increased concentration of sCD73 in plasma. Both the frequency of $CD73^+$ DNT cells and the level of plasma sCD73 recovered after ART treatment. However, PIRs showed decreased percentage of $CD73^+$ DNT cells compared to immunological responders (IRs). The frequency of $CD73^+$ DNT cells was positively correlated with $CD4^+$ T cell count and CD4/CD8 ratio, and negatively correlated with immune activation in PLWH. The level of sCD73 also showed a negative

OPEN ACCESS

Edited by:
Kai Deng,
Sun Yat-sen University, China

Reviewed by:
Selena Vigano,
Lausanne University Hospital (CHUV), Switzerland
Alessandra Noto,
Lausanne University Hospital (CHUV), Switzerland

***Correspondence:**
Yaxian Kong
kongyaxian@ccmu.edu.cn
Hongxin Zhao
Drzhao66@ccmu.edu.cn

†These authors have contributed equally to this work and share first authorship

Specialty section:
This article was submitted to Viral Immunology, a section of the journal Frontiers in Immunology

Received: *04 February 2022*
Accepted: *11 March 2022*
Published: *04 April 2022*

Citation:
Wang X, Zhang L, Du J, Wei Y, Wang D, Song C, Chen D, Li B, Jiang M, Zhang M, Zhao H and Kong Y (2022) Decreased CD73+ Double-Negative T Cells and Elevated Level of Soluble CD73 Correlated With and Predicted Poor Immune Reconstitution in HIV-Infected Patients After Antiretroviral Therapy. Front. Immunol. 13:869286. doi: 10.3389/fimmu.2022.869286

correlation to $CD4^+$ T cell count and CD4/CD8 ratio. More importantly, in the present cohort, a higher level of sCD73 at the time of initiating ART could predict poor immune reconstitution in PLWH after long-term ART. Our findings highlighted the importance of $CD73^+$ DNT cells and sCD73 in the disease progression and immune reconstitution of PLWH, and provided evidences for sCD73 as a potential biomarker of predicting immune recovery.

Keywords: HIV, CD73, double-negative T cell, immune reconstitution, immune activation

INTRODUCTION

In recent decades, extensive use of antiretroviral therapy (ART) in people living with HIV (PLWH) has made continued progress in controlling viral replication and restoring $CD4^+$ T cell count (1). However, part of patients (from 15% to 30%) remained insufficient in immune recovery, leading to a high risk of AIDS-related and non-AIDS complications. These patients were classified as poor immunological responders (PIRs), which had higher rates of morbidity and mortality than immunological responders (IRs) (2–5). Thus, it is a major clinical challenge and urgently needed to identify PIRs early and improve their immune homeostasis in time.

Persistent immune activation played a prominent role in the loss of $CD4^+$ T cells and disease progression during HIV infection (6, 7). High levels of immune activation occurred early in primary HIV infection and still existed in PLWH who were receiving effective ART (8, 9). Indeed, immune activation is a key factor that leads to impaired immune reconstitution (10, 11). The successful control of immune activation could be a target in clinical therapy for improving damaged immune recovery. Double negative T cells (DNT cells) were characterized to express CD3 and TCRαβ, but not NK cell markers (12, 13). Although DNT cells comprised only 1–3% of total T cells in peripheral blood and lymphoid organs of humans and mice, these cells were crucial for maintaining immune homeostasis (14–17). A series of previous studies indicated that DNT cells were predominately memory phenotype in SIV infection, and have a T helper function, secreting CD4-like cytokines (IL-4, IL-17, IFN-γ and TNF-α) in SIV-infected or healthy monkeys such as sooty mangabeys (18–20). However, most studies identified these cells as similar to regulatory T cells (Tregs), which could suppress T cells, B cells, dendritic cells, and NK cells in graft-versus-host disease, autoimmune diseases, and infectious disease (21–23). Elevated DNT cells were reported to associate with the control of immune activation in both primary HIV-1 infection and IRs, suggesting the role of DNT cells in disease progression and immune reconstitution of PLWH (23, 24).

However, the precise mechanisms by which DNT cells exert their suppressive capacity during HIV infection remained puzzled. DNT cells with distinct phenotype and function can mediate inhibition *via* different mechanisms, including secretion of TGF-β, IL-10, perforin, and interaction of CTLA-4, which also involved in Treg-mediated immune suppression (25–28). Nevertheless, extracellular adenosine (ADO), which participated in the suppressive activity of Tregs, has never been noticed in DN T cells (29). ADO is a critical regulator of innate and adaptive immune responses, inhibiting T cell proliferation and the secretion of inflammatory cytokines, including IL-2, TNFα, and IFN-γ (30, 31). The ADO production is generally regulated by two enzymes sequentially, CD39 and CD73, which were expressed by many different cell types including immune cells (32–34). CD39 firstly catalyzes the dephosphorylation of circulating ATP and ADP to 5'-AMP. After that, CD73, an ecto-5'-nucleotidase existing in a soluble or membrane-bound form, converts AMP to ADO (35, 36). Several studies have confirmed the absence of CD73 on Tregs in human despite the key role of CD39 and ADO in immune suppression of Tregs (35). Thus, whether DNT expressed CD73 and mediated immune suppression through CD73- ADO pathway needs to be investigated.

In the present study, we found that $CD73^+$ DNT cells in PLWH were associated with the control of immune activation, disease progression and immune reconstitution after ART. Of interest, soluble CD73 (sCD73) was also involved in immune suppression during HIV infection. Importantly, we provided evidence that elevated baseline levels of sCD73 could predict poor immune recovery in PLWH after long-term ART.

MATERIALS AND METHODS

Study Participants

The study was approved by the Committee of Ethics at Beijing Ditan Hospital, Capital Medical University in Beijing with informed consent acquired from all participants. We conducted a cross-sectional study in 263 PLWH and 25 gender and age-matched healthy control subjects (HCs). These PLWH included 193 treatment-naïve patients (TNs), 49 IRs, and 21 PIRs. IRs were PLWH with $CD4^+$ T cell count≥350 cells/μl who had experienced ART for 5.9 years (IQR 5.1-7.4) with undetectable viral load (<50 copies/ml) according to routine clinical assays. PIRs were PLWH with $CD4^+$ T cell count<350 cells/μl who had experienced ART for 5.5 years (IQR 5.0-6.2) with undetectable viral load. The demographic and clinical characteristics of the participants were shown in **Table 1**.

In the retrospective cohort study, we recruited 171 participants, who were PLWH with baseline $CD4^+$ T cell count<350 cells/μl and had received ART for 4.9 years (IQR 4.5-5.2) with undetectable viral load according to routine clinical assays. These participants were divided into IRs ($CD4^+$ T cell

TABLE 1 | Demographic and clinical characteristics of study participants.

Characteristics	HCs	TNs			IRs	PIRs
		CD4≥350	200≤CD4<350	CD4<200		
N (%)	25	66 (34.20)	71 (36.79)	56 (29.01)	49	21
Sex (M/F)	24/1	64/2	68/3	56/0	48/1	21/0
Age (mean, years)	34 ± 7	32 ± 10	31 ± 7	35 ± 8	36 ± 6	39 ± 7
CD4 count (cells/mm^3), median (IQR)	–	456 (408-529)	281 (244-312)	83 (33-146)	628 (560-743)	271 (229-328)
CD8 count (cells/mm^3), median (IQR)	–	1085 (796-1401)	1017 (727-1267)	729 (547-904)	788 (656-1009)	691 (600-790)
CD4/CD8 ratio, median (IQR)	–	0.43 (0.31-0.61)	0.28 (0.22-0.37)	0.11 (0.05-0.17)	0.77 (0.64-1.06)	0.43 (0.36-0.49)
HIV RNA viral load (copies/mL), median (IQR)	–	11091 (4239-29660)	35908 (10658-119660)	82353 (26229-211286)	<LDL	<LDL

HC, healthy controls; TN, treatment-naive HIV-1-infected patients; IR, immunological responders; PIR, poor immunological responders; M, male; F, female; LDL, lower detection limit. TNs are divided into three subgroups according to blood CD4$^+$ T cell count.

count≥350 cells/μl) and PIRs (CD4$^+$ T cell count<350 cells/μl) according to their CD4$^+$ T cell count at 4.9 years following ART initiation. The demographic and clinical characteristics of the participants were described in **Table S1**.

Separation of Peripheral Blood Mononuclear Cells (PBMCs)

PBMCs were collected from the peripheral blood in EDTA-K_2 tubes using standard Ficoll-Paque gradient centrifugation. All samples were processed and analyzed within 24 hours of collection.

Plasma HIV-1 Viral Load and CD4$^+$ T-Cell Count

The HIV-1-RNA levels in plasma were quantified using a Standard Amplicor HIV Monitor assay, version 1.5 (Roche Diagnostics, Indianapolis, IN, USA), with a limit of detection of 40 copies/ml. The CD4$^+$ T-cell count was measured by a standard flow cytometry technique with a TruCOUNT tube in routinely equipped laboratories (BD Biosciences, San Jose, CA, USA).

Immunofluorescence Staining and Flow Cytometry Analysis

The expression of ectonucleotidases (CD39 and CD73) on αβDNT and activated Treg cells was evaluated by flow cytometry. The gating strategy for activated Treg cells was performed as previously described (5). PBMCs were stained with directly conjugated antibodies for 30 min at 4°C in the dark. The cells were washed before flow cytometry analysis. Antibodies used included anti-human CD3-BV785 (clone SK7), CD4-APC-fire750 (clone SK3), αβTCR-BV421 (clone IP26), CD56-BV510 (clone HCD56), CCR7 (CD197)-PE-cy7 (clone G043H7), HLA-DR-AF700 (clone L243), CD73-PE (clone AD2), CD39-BV605 (clone A1, BioLegend, San Diego, CA, USA), CD45RA-BV711 (clone HI100), CD38-BUV737 (clone HB7), CD25-PE-CF594 (clone M-A251), CD8-FITC (clone SK1), CD8-BUV395 (clone RPA-T8, BD Biosciences, San Diego, CA, USA), and the corresponding isotype controls. Data were acquired on a BD LSR Fortessa flow cytometer (BD Biosciences) and analyzed with FlowJo software (Tree Star, Ashland, OR, USA).

Quantification of Soluble Markers

Plasma samples from healthy controls and patients were assayed for the levels of different cytokines and chemokines (IFN-γ, IFN-α, IL-18, IL-1β, IL-15, TNF-α, IL-2, RANTES, MIP-1β, IP-10, and IL-7) using Luminex multiple kits (Invitrogen, Carlsbad, CA, USA). Plasma levels of sCD73 were analyzed by ELISA (Abcam, ab213761) according to the manufacturer's protocol. Adenosine was detected in plasma by Adenosine Assay Kit (Fluorometric) (Abcam, ab211094).

Statistical Analysis

The data are expressed as the mean (standard deviation, SD), median (interquartile range, IQR), and percentage. SPSS21 (IBM Corporation, New York, NY, USA) and GraphPad8 (GraphPad Software, La Jolla, CA, USA) were used for statistical calculations. The normality of each variable was evaluated using the Kolmogorov-Smirnov test. For normally distributed data, the comparison of two variables was performed using unpaired two-tailed Student's t-tests. When the data were not normally distributed, the comparison of variables was performed with a Mann-Whitney *U* test or a Wilcoxon matched-pairs signed-rank test for unpaired and paired data, respectively. In the case of comparing two more independent samples, the Kruskal-Wallis test followed by Dunn's multiple comparisons test was applied. Correlation coefficients were calculated for nonparametric distributions using Spearman's correlation test. The Chi-square test was used to compare categorical variables.

When performing univariable and multivariable Cox regression analyses, continuous variables of soluble factors were converted into categorical variables according to cutoff value (with the highest Youden index) which was obtained by the receiver operating characteristic (ROC) curve. Significant factors (P<0.05) from univariable Cox proportional regression analysis were included in the multivariable analysis to identify factors independently associated with immune reconstitution expressed as hazard ratios and related 95% confidence intervals (95%CI). Survival analysis was performed using a Kaplan–Meier survival plot, and the log-rank test P value was calculated. The endpoint of Kaplan-Meier and Cox regression analyses was CD4$^+$ T cell recovery or restoration of CD4/CD8 ratio, which was defined by the data of the first values of CD4$^+$ T cell count≥350 cells/μl or CD4/CD8 ratio≥0.7. Receiver operating

characteristic (ROC) was used to evaluate the predicted potential (with 95% confidence intervals), and to calculate the sensitivity and specificity. P<0.05 was considered statistically significant.

RESULTS

Decreased Frequency of CD73$^+$ DNT Cells in PLWH

To investigate the potential role of CD39 and CD73 on DNT cells in HIV infection, we recruited 193 TNs and 25 gender and age-matched HCs. TNs were subdivided into three groups according to their CD4$^+$T cell count (<200 cells/μl, 200-350 cells/μl, and≥350 cells/μl). The demographic and clinical characteristics of these patients were shown in **Table 1**. We examined the expression pattern of CD73 and CD39 on DNT cells by flow cytometry. Representative flow cytometry gating strategy for αβDNT cells was shown in **Figure S1**. DNT cells preferentially expressed CD73 in HCs and TNs compared with CD39 (**Figure 1A**). Despite a significant increase in the absolute number and percentage of DNT cells from TNs (**Figures S2A, B**), the patients showed significantly decreased level of CD73 and comparable expression of CD39 on DNT cells compared to HCs. Accordingly, there was a lower frequency of CD73$^+$CD39$^+$ DNT cells in TNs than in HCs (**Figure 1B**). As previously reported, we also found that activated Tregs (aTregs) expressed high levels of CD39 and almost did not express CD73 in both HCs and TNs (**Figures 1C, D**), implying CD73$^+$ DNT cells as an assistant of

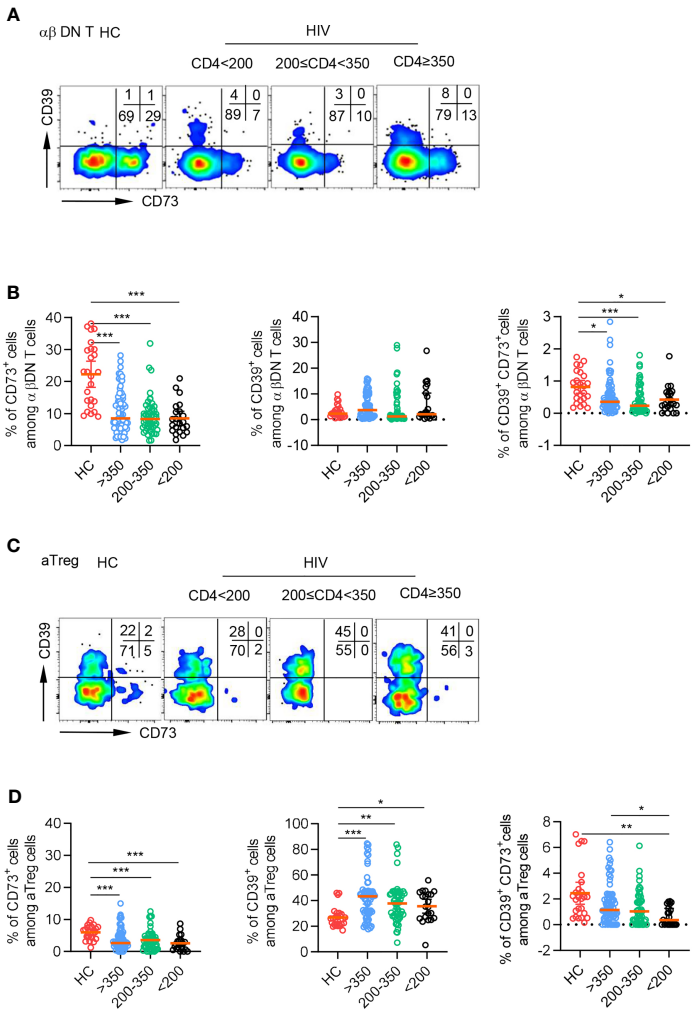

FIGURE 1 | CD73 was downregulated on DNT cells from TNs compared to HCs. Flow cytometry analysis of CD39 and CD73 expression was performed on PBMCs collected from HCs and different TNs groups. **(A)** Representative flow data showed the expression of CD39 and CD73 gated on DN T cells from HCs and different TNs groups. **(B)** Scatter plots of the percentage of CD73$^+$, CD39$^+$ and CD39$^+$ CD73$^+$ DN T cells from HCs and different TNs groups (n=22-66 each group). *P* values were obtained by Kruskal-Wallis test followed by Dunn's multiple comparisons test. **(C)** Representative flow data showed the expression of CD39 and CD73 gated on activated Treg cells from HCs and different TNs groups. **(D)** Scatter plots of the percentage of CD73$^+$, CD39$^+$and CD39$^+$ CD73$^+$ activated Treg cells from HCs and different TNs groups (n=21-66 each group). *P* values were obtained by Kruskal-Wallis test followed by Dunn's multiple comparisons test. **P*<0.05, ***P*<0.01, ****P*<0.001.

aTregs in producing ADO. In all, these data suggested the involvement of CD73$^+$ DNT cells during HIV infection.

Decreased Frequency of CD73$^+$ DNT Cells Was Partly Reversible After ART and Associated With CD4$^+$ T Cell Count and Immune Activation in PLWH

To further investigate the role of CD73$^+$ DNT cells in immune reconstitution after ART, we then assessed the expression of CD73 on DNT cells among patients experiencing 5.7 years of ART. As shown in **Figure 2A**, PLWH who experienced long-term ART displayed elevated frequency of CD73$^+$ DNT cells compared to TNs. Meanwhile, the percentage of DNT cells in PLWH with ART was lower than in TNs (**Figures S2C**). We further divided 70 ART-treated PLWH into two subgroups: 49 IRs with CD4$^+$ T cell count≥350 cells/μl and 21 PIRs with CD4$^+$ T cell count<350 cells/μl after 5.7 years of ART. The percentage of CD73$^+$ DNT cells was significantly higher in IRs than PIRs, despite comparable frequencies of DNT cells between these two groups, implying that the low frequency of CD73$^+$ DNT cells was associated with incomplete restoration of CD4$^+$ T cells (**Figure 2B** and **Figure S2D**).

We next applied correlation analysis in all PLWH, including TNs and ART-treated patients. It was revealed that the frequency

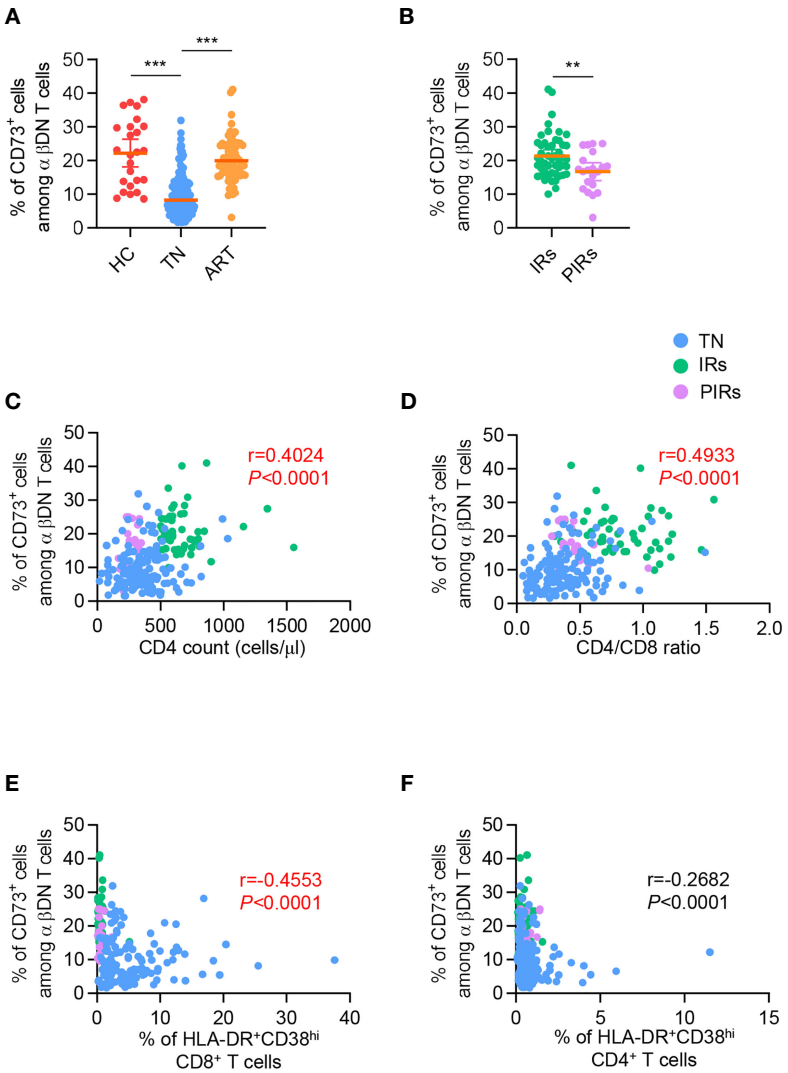

FIGURE 2 | The frequency of CD73$^+$ DN T cells was partly recovered after ART and correlated with CD4 count, CD4/CD8 ratio, and immune activation in PLWH. **(A)** Scatter plots displayed the frequency of CD73$^+$ DN T cells from HCs, TNs, and ART-experienced PLWH (n=25-139 each group). *P* values were obtained by the Kruskal-Wallis test followed by Dunn's multiple comparisons test. **(B)** Comparison of the frequency of CD73$^+$ DN T cells between IRs and PIRs with matched baseline CD4 count (n=21-49 each group). *P* values were obtained by unpaired t-test. **(C–F)** Correlations between percentage of CD73$^+$ DN T cells with CD4 count **(C)**, CD4/CD8 ratio **(D)**, HLA-DR$^+$CD38^{hi} CD8$^+$ T cells **(E)**, HLA-DR$^+$CD38^{hi} CD4$^+$ T cells **(F)**. Spearman's non-parametric test was used to test for correlations. $^{**}P$<0.01, $^{***}P$<0.001.

of CD73$^+$ DNT cells was positively correlated with CD4$^+$ T cell count (r=0.4024, P<0.0001; **Figure 2C**) and CD4/CD8 ratio (r=0.4933, P<0.0001; **Figure 2D**), whereas no significant correlation was observed between the percentage of CD73$^+$ DNT cells and virus load (**Figure S3A**). Of note, CD73$^+$ DNT cells exhibited a significant negative correlation with the percentage of HLA-DR$^+$CD38^{hi} CD8$^+$ T cells instead of the CD4$^+$ T fraction (r=-0.4553, P<0.0001; r=0.2682, P<0.0001, respectively; **Figures 2E, F**). In addition, we also assessed the correlation of DNT cell frequency with CD4$^+$ T cell count, CD4/CD8 ratio, and immune activation and found no correlation among these parameters (**Figures S2E–H**). Collectively, these results suggested that the depletion of CD73$^+$ DNT cells was associated with uncontrolled immune activation and adverse clinical outcomes in PLWH.

Increased Level of sCD73 Was Related to Disease Progression and Clinical Outcomes in PLWH

Considering the low expression of CD73 on DNT cells in TNs, this raises an important question: whether the concentration of sCD73 in plasma has also changed. First, we observed a significant increase of sCD73 in plasma from TNs compared to HCs, whereas the level of sCD73 was downregulated in ART-treated patients (**Figure 3A**). However, there were comparable levels of sCD73 in IRs and PIRs (**Figure 3B**). We next analyzed the longitudinal data of sCD73 from PLWH at the baseline and 5.7 years after ART initiation. The concentration of sCD73 was obviously downregulated after 5.7 years ART (**Figure 3C**). Considering that the membrane-bound form of CD73 expressed by DNT cells was involved in the control of immune

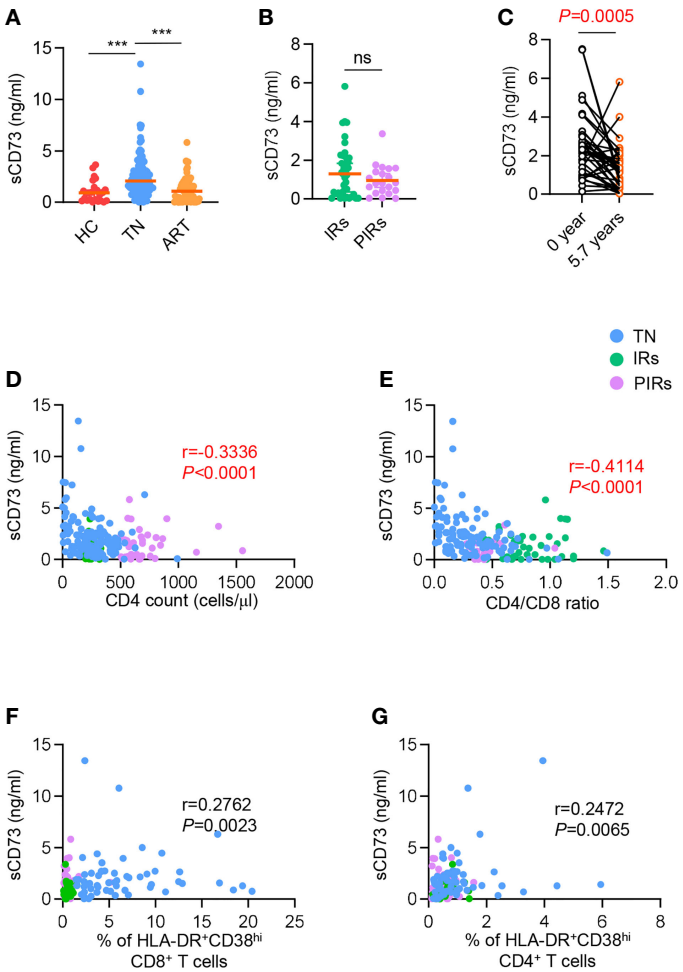

FIGURE 3 | Elevated sCD73 was reversed after ART and associated with clinical outcome. **(A)** Data were shown as scatter plots comparing the concentration of sCD73 in plasma among HCs, TNs, and ART-experienced PLWH (n=25-110 each group). *P* values were obtained by Kruskal-Wallis test followed by Dunn's multiple comparisons test. **(B)** Scatter plots depicting the concentration of sCD73 among IRs and PIRs with matched baseline CD4 count (n=21-41 each group). *P* values were obtained by Mann-Whitney test. **(C)** Longitudinal analysis of sCD73 at baseline and 5.7 years or above following ART (n=38). *P* values were obtained by Wilcoxon matched-pairs signed-rank test. **(D-G)** Correlation analysis of sCD73 level with CD4 count **(D)**, CD4/CD8 ratio **(E)**, HLA-DR$^+$CD38^{hi} CD8$^+$ T cells **(F)**, and HLA-DR$^+$CD38^{hi} CD4$^+$ T cells **(G)**. Spearman's non-parametric test was used to test for correlations. ***P<0.001. ns, not significant.

activation and $CD4^+$ T cell recovery in PLWH, we speculated that sCD73 might play a role in HIV infection. Consistently, the level of sCD73 was inversely correlated with $CD4^+$ T cell count and CD4/CD8 ratio, respectively (r=-0.3336, P<0.0001; r=-0.4114, P<0.0001; **Figures 3D, E**). However, no correlation was found between sCD73 and the percentage of $HLA\text{-}DR^+CD38^{hi}$ cells among $CD8^+$ and $CD4^+$ T cells (r=0.2762, P=0.0023, r=0.2472, P=0.0065, respectively; **Figures 3F, G**). Accordingly, there was no correlation between sCD73 and virus load (**Figure S3B**).

Since CD8 T cells were reported to contribute to ADO-mediated immune suppression by releasing CD73-containing extracellular vesicles, we tested the correlation of sCD73 or ADO with $CD73^+$ CD8 T cells and $CD73^+$ DNT cells, and correlation between ADO and sCD73. Of interest, the concentration of sCD73 was inversely related to the frequency of $CD73^+$ CD8 T cells but not $CD73^+$ DNT cells in TNs (r=-0.3011, P=0.0216; r=-0.04427, P=0.7414, respectively; **Figures S4A, B**). Oppositely, in PLWH who experienced ART, the level of sCD73 showed a negative correlation with $CD73^+$ DNT cells but not CD8 subset (r=-0.3220, P=0.0107; r=-0.1289, P=0.3184, respectively; **Figures S4C, D**). No correlation was observed between ADO and $CD73^+$ DNT, $CD73^+$ $CD8^+$ T cells, and sCD73 (**Figure S5**). These data could provide an explanation for the derivation of sCD73 in different immune status of PLWH.

Plasma sCD73 Was Identified as a Predictive Factor for Immune Reconstitution in PLWH After Long-Term ART

To further identify the potential predictive role of baseline sCD73 in clinical outcomes of ART-treated PLWH, we performed a retrospective cohort study of 171 patients who had a baseline $CD4^+$ T cell count lower than 350 cells/μl and experienced ART for 4.9 years with good viral responses. The detailed demographic and clinical information were shown in **Table S1**. Based on the baseline level of sCD73 at the time of initiating ART, these 171 patients were classified into high-sCD73 (sCD73>4.111 ng/ml) vs. low-sCD73 (sCD73 ≤ 4.111 ng/ml) subgroups. We analyzed the incidence of poor immune reconstitution in these two groups after different duration of ART. It was revealed that patients with high sCD73 exhibited a greater risk of poor immune reconstitution after 1 to 5 years of ART than those with low sCD73 (**Table S2**).

In addition to sCD73, we further detected the baseline concentrations of various cytokines and chemokines, which were reported to associate with disease progression or clinical outcomes during HIV infection, including IFN-γ, IFN-α, IL-18, IL-1β, IL-15, TNF-α, IL-2, RANTES, MIP-1β, IP-10, and IL-7. As shown in **Figure 4A** and **Table S3**, we performed a univariate analysis and found that increased baseline levels of IL-1β (P=0.017), IL-18 (P=0.009), IFN-γ (P=0.007), TNF-α (P<0.0001), and sCD73 (P<0.0001) were significantly associated with a higher risk of poor immune reconstitution in PLWH. We next included these factors in a multivariate Cox regression analysis, and showed that sCD73 (HR 2.057 [95%CI 1.356-3.121]; P=0.001) and TNF-α (HR 1.913 [95%CI 1.241-2.950]; P=0.003) both remained as independent factors affecting $CD4^+$ T cell recovery for ART-treated PLWH.

Furthermore, we sought to utilize sCD73 and TNF-α to predict clinical outcomes. When using optimal cutoff values, patients with high baseline levels of sCD73 or TNF-α demonstrated an elevated incidence of PIRs based on Kaplan-Meier (K-M) curves (P=0.0002, and P=0.0002, respectively; **Figures 4B, C**). More importantly, Receiver operating characteristic (ROC) analysis showed that sCD73 had a higher area under the curve (AUC) (0.7122 [95%CI 0.6291-0.7953]) than TNF-α (AUC 0.6107 [95%CI 0.5202-0.7012]; **Figure 4D**). Additionally, we also defined the clinical outcomes according to CD4/CD8 ratio restoration. Patients were classified into two subgroups: patients with high ratio restoration who achieved CD4/CD8 ratio of 0.7 or above after 4.9 years ART, and patients with low ratio restoration who failed to achieve CD4/8 ratio of 0.7 after 4.9 years ART. Similar results were shown in sCD73 (**Figure 4E**). However, TNF-α may not be a potential predictor for the CD4/CD8 ratio restoration (**Figures 4F, G**).

In summary, sCD73 in plasma represented a potential predictive biomarker of immune reconstitution after ART.

DISCUSSION

Previous studies have identified the crucial role of CD39/ADO pathway in immune suppression of Tregs during chronic HIV infection (37–39). Due to the lack of CD73 in Tregs, the source of CD73 and its essential role in AIDS progression remained puzzled and needed to be well investigated. In the present study, we demonstrated the involvement of $CD73^+$ DNT cells in chronic HIV infection and disease progression. We found that the frequency of $CD73^+$ DNT cells in PLWH, including TNs and those who experienced long-term ART was associated with $CD4^+$ T cell count and immune activation. Additionally, the serum concentration of sCD73 showed a negative correlation with $CD73^+$ DNT cells in PLWH who experienced ART. More importantly, the level of sCD73 at the baseline could predict $CD4^+$ T cell recovery in PLWH. Patients with higher baseline levels of sCD73 had a higher risk of poor immune reconstitution. To our knowledge, this is the first evidence for a predictive role of sCD73 in immune reconstitution after long-term ART.

It is acknowledged that a significant percentage of ART-treated patients, classified as PIRs, failed to achieve optimal $CD4^+$ T cell recovery, despite the HIV RNA being undetectable after several years of ART (4). These PIRs had a higher risk of AIDS-related and non-AIDS complications, such as cardiovascular disease, bone, and renal disease, neurocognitive decline, and premature aging (40–43). Notably, PIRs had higher rates of morbidity and mortality than IRs (5). Thus, there is an urgent need to identify PIRs early and provide effective treatment as soon as possible. Most prior studies indicated that the potential baseline predictors of poor immune reconstitution contained several clinical features (such as age, co-infection, $CD4^+$ T cell count, CD8 count, CD4/CD8 ratio, and viral

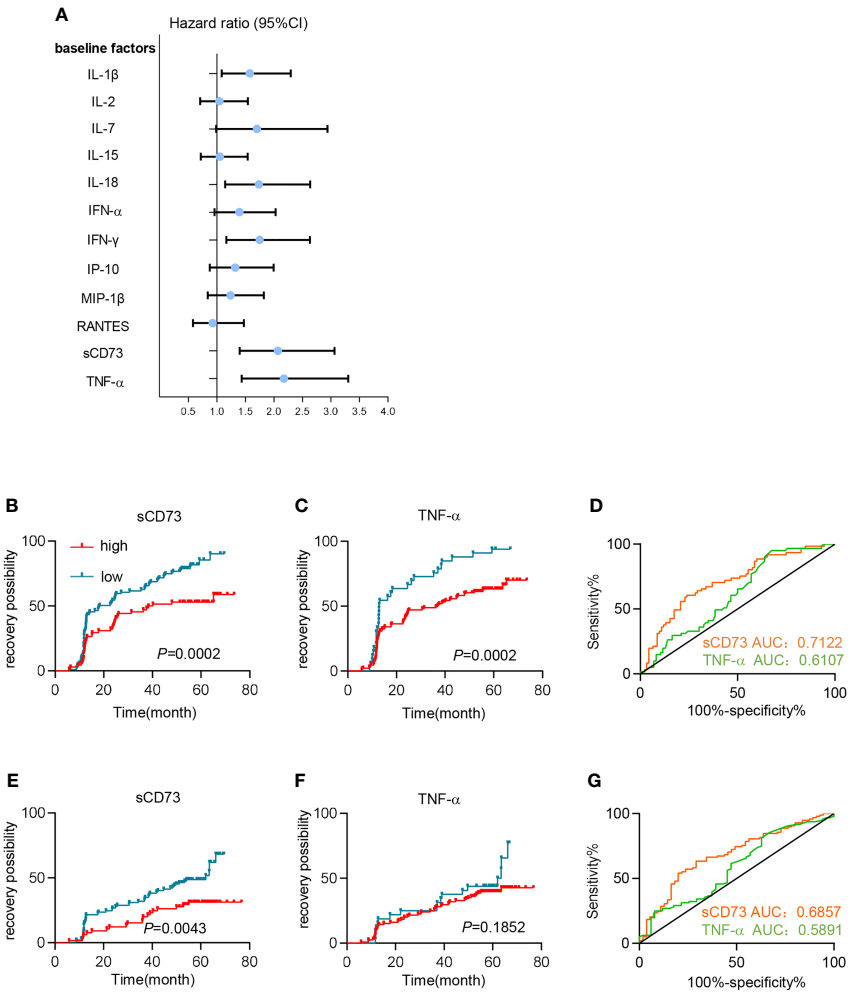

FIGURE 4 | High levels of sCD73 predicted poor immune reconstitution in PLWH. **(A–D)** Patients' clinical outcomes were defined by CD4 cell count. **(A)** Univariate Cox regression analyzed the association between different plasma soluble factors at baseline and immune recovery. Dot and error bars represent the regression coefficients with 95% CI. **(B, C)** Kaplan-Meier curves estimate recovery possibility for patients in high-concentration (red line) and low-concentration groups (blue line) segregated by **(B)** sCD73 (n=68 [high], n=99 [low]) and **(C)** TNF-α (n=129 [high], n=33 [low]). *P* values were obtained by Log-rank test. **(D)** Receiver operating characteristic (ROC) analyses for sCD73 (n=153, yellow line) and TNF-α (n=147, green line). **(E–G)** Patients' clinical outcomes were defined by CD4/CD8 ratio restoration. **(E, F)** Kaplan-Meier curves estimate recovery possibility for patients in high-concentration (red line) and low-concentration groups (blue line) segregated by **(E)** sCD73 (n=65[high], n=97[low]) and **(F)** TNF-α (n=125[high], n=32[low]). *P* values were obtained by Log-rank test. **(G)** Receiver operating characteristic (ROC) analyses for sCD73 (n=153, yellow line) and TNF-α (n=147, green line).

load), immune activation ($CD38^+HLA\text{-}DR^+$), genetic factors (CCR5 polymorphisms, IL7RA polymorphisms and mitochondrial haplogroups), and thymic function (44–52). In fact, the baseline $CD4^+$ T cell count is the most recognized method for predicting the immune recovery after ART, however, it remains a considerable challenge to acquire this data in resource-limiting settings. Additionally, in contrast to stable serological biomarkers, $CD4^+$ T cell count is susceptible to several factors, including physiology, emotion, drugs, age, and even the skill of lab technicians. Indeed, a series of studies indicated that several plasma biomarkers of systemic inflammation after ART initiation are potentially more predictive for future non-AIDS complications or $CD4^+$ T cell recovery than cellular markers of immune activation (53–55).

Here, we took sCD73 and eleven other cytokines, which were indicated to associate with disease progression or clinical outcomes in PLWH, into the present study (56–64). Based on a series of rigorous statistical analysis, only the baseline concentration of sCD73 was identified as the most important predictive biomarker for immune reconstitution after ART. However, Prebensen et al. pointed out that elevated baseline levels of MIP-1β identified long-term PIRs who started ART at $CD4^+$ T cell counts<200 cells/μl, which was not consistent with our study (64). Several possibilities were considered to explain the contradiction. On one hand, our cohort included PLWH with a baseline $CD4^+$ T cell count<350 cells/μl significantly higher than their baseline $CD4^+$ T cell count. Distinct immune characteristics and responses in these two cohorts could

contribute to the heterogeneity of the results. On the other hand, they did not perform accurate predictive analysis, but only binary logistic regression, which was not enough to conclude a predictive biomarker.

More importantly, we evaluated the clinical outcomes not only by $CD4^+$ T cell count but also by using CD4/CD8 ratio, which has been increasingly recognized as a biomarker of immune reconstitution during HIV treatment (65, 66). Indeed, CD4/CD8 ratio has been recommended as a stronger predictor of poor outcomes than the $CD4^+$ T cell count in some clinical guidelines (67). It was gradually recognized that $CD4^+$ T cell count does not reflect immune activation and risk of non-AIDS-defined events, despite its crucial role in monitoring immune recovery (65). Instead, CD4/CD8 ratio was found to independently associate with immune activation and serious non-AIDS events (68–71). In fact, severe immune defects were also identified in some PLWH with virological suppression who had $CD4^+$ T cell count of more than 500 cells/μl but a low CD4/CD8 ratio (65, 72). Therefore, immune reconstitution and prognosis after ART were well monitored by both $CD4^+$ T cell count and CD4/CD8 ratio. In the present study, we found that sCD73 instead of TNF-α could predict $CD4^+$ T cell recovery as well as the restoration of CD4/CD8 ratio, further demonstrating a predictive value of sCD73 for the clinical outcome.

Of surprise, we observed reduced $CD73^+$ DNT cells accompanied with an accumulation of $CD39^+$ Tregs in TNs, despite CD73 being a similar rate-limited enzyme as CD39 in CD39/CD73/ADO pathway (30). In addition, CD73 was also down-regulated in CD8 T cells and B cells during HIV infection (73–75). The distinct dynamics of CD73 and CD39 during HIV infection might be explained by the increased plasma level of sCD73 in PLWH. The notion was further supported by a higher enzymatic activity of CD73 in its soluble form than the membrane-bound variant (76, 77). Thus, we speculated that $CD73^+$ immune cells might release sCD73 in an inflammatory environment, which could cooperate with $CD39^+$ Treg to produce extracellular ADO for immune suppression. Interestingly, the concentration of sCD73 was related to the frequencies of $CD73^+$ CD8 T cells in TNs, while in ART-treated patients, the sCD73 level correlated with $CD73^+$ DNT cells. It was implied that the major source of sCD73 might come from different cells in different immune status, which needed to be further explored. Considering that CD73 was widely expressed on various types of immune cells, further investigation was urgently needed to determine the exact origin of sCD73 in the future.

However, the exact mechanisms of increased sCD73 in plasma during HIV infection still remained in puzzle. To our knowledge, soluble form of CD73 can be cleaved from the cellular membrane or secreted by various tumor cells (78–81). Previous studies showed that the decrease of the membrane-bound CD73 activity on activated $CD8^+$ T cells was accompanied by an increase in the concentration of soluble counterpart, and paralleled by elevated generation of ADO in the cell culture supernatant of activated cells. Similar results were observed on $CD8^+$ T cells when using phosphatidylinositol-specific phospholipase C (PI-PLC) to force shedding of cell surface CD73 (76–78). Thus, considering the inverse trend between cell-bound and soluble forms of CD73 in our study, we preferred to assume that sCD73 were produced by cleavage of membrane-bound counterpart, although the source of secretion could not be completely ruled out.

Given that ADO was a key factor in CD73-mediated immunosuppression, we also detected the concentration of ADO in plasma from PLWH. Unfortunately, no correlation was observed between ADO and sCD73, $CD73^+$ DNT, and $CD73^+$ $CD8^+$ T cells, which could be explained by several possibilities. First, ADO was mainly generated in the local environment of tissue injury, hypoxia, or inflammation where high local concentrations of ATP and ADP would be released and correspondingly exerted its immune effects restricted locally. Thus, the plasma concentration of ADO was hard to reflect their concentration and activity in the local environment owing to dilution and time of circulation (82–84). Second, due to the rapid formation and rapid clearance of ADO in blood, it was challenging to determine accurate concentrations of extracellular ADO in blood samples (84). Finally, the purinergic signaling is a complex network including a number of purinergic ligands, receptors, enzymes, channels, and transporters. In addition to CD73, many other purine-metabolizing enzymes, including adenosine deaminase (ADA), CD38, ATP-degrading enzymes like ENPPs and CD39, as well as ATP-regenerating kinases were also present in human plasma (78, 84–86). Thus, the plasma concentration of ADO could be mediated by multiple pathways, implying a complicated relationship of ADO with CD73-expressing cells or sCD73.

The present study has several limitations. First, due to a minimal number of DNT cells in PLWH, it is difficult to perform *in vitro* functional experiments to verify the role of CD73 in the inhibition mediated by DNT cells and the origin of sCD73. Second, we did not take the frequency of $CD73^+$ DNT cells into the predictive model for clinical outcomes of PLWH, owing to the lack of the baseline flow cytometry data of the retrospective cohort. Third, the confounding factor of therapy initiation was not excluded from the correlation analysis in the present study. Finally, only a single-center cohort study was conducted for the predictive analysis; we need to recruit more cohorts in additional sites to verify our findings.

In summary, our study demonstrated that a higher concentration of sCD73 at the baseline could predict poor $CD4^+$ T cells recovery in PLWH after long-term ART, providing a potential biomarker for detecting immune reconstitution early.

DATA AVAILABILITY STATEMENT

The original contributions presented in the study are included in the article/**Supplementary Material**. Further inquiries can be directed to the corresponding authors.

ETHICS STATEMENT

The studies involving human participants were reviewed and approved by the Committee of Ethics at Beijing Ditan Hospital.

The patients/participants provided their written informed consent to participate in this study.

AUTHOR CONTRIBUTIONS

XW, LZ, and JD performed the experiments and analyzed the data. YW, DW, CS, DC, BL, MJ, and MZ collected samples, and performed the experiments. HZ participated in the critical review of the manuscript and revised the manuscript. YK designed the experiments, analyzed the data and wrote the manuscript. All authors contributed to the article and approved the submitted version.

FUNDING

This work was supported by National Natural Science Foundation of China (82171548, 81971307), Beijing Municipal Natural Science Foundation for Distinguished Young Scholars (JQ21023), Beijing Municipal Administration of Hospitals' Ascent Plan (DFL20191802), and Beijing Municipal Administration of Hospitals Clinical Medicine Development of Special Funding Support (ZYLX202126).

ACKNOWLEDGMENTS

The authors sincerely thank all the patients and healthy donors in this study.

SUPPLEMENTARY MATERIAL

The Supplementary Material for this article can be found online at: https://www.frontiersin.org/articles/10.3389/fimmu.2022.869286/full#supplementary-material

REFERENCES

1. Zhang LX, Jiao YM, Zhang C, Song JW, Fan X, Xu RN, et al. HIV Reservoir Decay and CD4 Recovery Associated With High CD8 Counts in Immune Restored Patients on Long-Term ART. *Front Immunol* (2020) 11:1541. doi: 10.3389/fimmu.2020.01541
2. Gazzola L, Tincati C, Bellistri GM, Monforte A, Marchetti G. The Absence of CD4+ T Cell Count Recovery Despite Receipt of Virologically Suppressive Highly Active Antiretroviral Therapy: Clinical Risk, Immunological Gaps, and Therapeutic Options. *Clin Infect Dis* (2009) 48(3):328–37. doi: 10.1086/595851
3. Corbeau P, Reynes J. Immune Reconstitution Under Antiretroviral Therapy: The New Challenge in HIV-1 Infection. *Blood* (2011) 117(21):5582–90. doi: 10.1182/blood-2010-12-322453
4. Yang X, Su B, Zhang X, Liu Y, Wu H, Zhang T. Incomplete Immune Reconstitution in HIV/AIDS Patients on Antiretroviral Therapy: Challenges of Immunological Non-Responders. *J Leukoc Biol* (2020) 107 (4):597–612. doi: 10.1002/JLB.4MR1019-189R
5. Kong Y, Tian Y, Hao Y, Chong X, Xiao J, Yang D, et al. Two Types of Poor Immunological Responder Showing Distinct Responses to Long-Term HAART. *Int J Infect Dis* (2019) 86:178–87. doi: 10.1016/j.ijid.2019.07.037
6. Paiardini M, Muller-Trutwin M. HIV-Associated Chronic Immune Activation. *Immunol Rev* (2013) 254(1):78–101. doi: 10.1111/imr.12079
7. Vidya Vijayan KK, Karthigeyan KP, Tripathi SP, Hanna LE. Pathophysiology of CD4+ T-Cell Depletion in HIV-1 and HIV-2 Infections. *Front Immunol* (2017) 8:580. doi: 10.3389/fimmu.2017.00580
8. Lv T, Cao W, Li T. HIV-Related Immune Activation and Inflammation: Current Understanding and Strategies. *J Immunol Res* (2021) 2021:7316456. doi: 10.1155/2021/7316456
9. Naidoo KK, Ndumnego OC, Ismail N, Dong KL, Ndung'u T. Antigen Presenting Cells Contribute to Persistent Immune Activation Despite Antiretroviral Therapy Initiation During Hyperacute HIV-1 Infection. *Front Immunol* (2021) 12:738743. doi: 10.3389/fimmu.2021.738743
10. Zhang Y, Jiang T, Li A, Li Z, Hou J, Gao M, et al. Adjunct Therapy for CD4(+) T-Cell Recovery, Inflammation and Immune Activation in People Living With HIV: A Systematic Review and Meta-Analysis. *Front Immunol* (2021) 12:632119. doi: 10.3389/fimmu.2021.632119
11. Bandera A, Masetti M, Fabbiani M, Biasin M, Muscatello A, Squillace N, et al. The NLRP3 Inflammasome Is Upregulated in HIV-Infected Antiretroviral Therapy-Treated Individuals With Defective Immune Recovery. *Front Immunol* (2018) 9:214. doi: 10.3389/fimmu.2018.00214
12. Brandt D, Hedrich CM. TCRalphabeta(+)CD3(+)CD4(-)CD8(-) (Double Negative) T Cells in Autoimmunity. *Autoimmun Rev* (2018) 17(4):422–30. doi: 10.1016/j.autrev.2018.02.001
13. Neyt K, GeurtsvanKessel CH, Lambrecht BN. Double-Negative T Resident Memory Cells of the Lung React to Influenza Virus Infection *via* CD11c(hi) Dendritic Cells. *Mucosal Immunol* (2016) 9(4):999–1014. doi: 10.1038/mi.2015.91
14. Merims S, Li X, Joe B, Dokouhaki P, Han M, Childs RW, et al. Anti-Leukemia Effect of *Ex Vivo* Expanded DNT Cells From AML Patients: A Potential Novel Autologous T-Cell Adoptive Immunotherapy. *Leukemia* (2011) 25(9):1415–22. doi: 10.1038/leu.2011.99
15. Hillhouse EE, Lesage S. A Comprehensive Review of the Phenotype and Function of Antigen-Specific Immunoregulatory Double Negative T Cells. *J Autoimmun* (2013) 40:58–65. doi: 10.1016/j.jaut.2012.07.010
16. Juvet SC, Zhang L. Double Negative Regulatory T Cells in Transplantation and Autoimmunity: Recent Progress and Future Directions. *J Mol Cell Biol* (2012) 4(1):48–58. doi: 10.1093/jmcb/mjr043
17. Hillhouse EE, Delisle JS, Lesage S. Immunoregulatory CD4(-)CD8(-) T Cells as a Potential Therapeutic Tool for Transplantation, Autoimmunity, and Cancer. *Front Immunol* (2013) 4:6. doi: 10.3389/fimmu.2013.00006
18. Sundaravaradan V, Saleem R, Micci L, Gasper MA, Ortiz AM, Else J, et al. Multifunctional Double-Negative T Cells in Sooty Mangabeys Mediate T-Helper Functions Irrespective of SIV Infection. *PloS Pathog* (2013) 9(6): e1003441. doi: 10.1371/journal.ppat.1003441
19. Milush JM, Mir KD, Sundaravaradan V, Gordon SN, Engram J, Cano CA, et al. Lack of Clinical AIDS in SIV-Infected Sooty Mangabeys With Significant CD4+ T Cell Loss Is Associated With Double-Negative T Cells. *J Clin Invest* (2011) 121(3):1102–10. doi: 10.1172/JCI44876
20. Vinton C, Klatt NR, Harris LD, Briant JA, Sanders-Beer BE, Herbert R, et al. CD4-Like Immunological Function by CD4- T Cells in Multiple Natural Hosts of Simian Immunodeficiency Virus. *J Virol* (2011) 85(17):8702–8. doi: 10.1128/JVI.00332-11
21. Li Y, Dong K, Fan X, Xie J, Wang M, Fu S, et al. DNT Cell-Based Immunotherapy: Progress and Applications. *J Cancer* (2020) 11(13):3717–24. doi: 10.7150/jca.39717
22. Ford McIntyre MS, Gao JF, Li X, Naeini BM, Zhang L. Consequences of Double Negative Regulatory T Cell and Antigen Presenting Cell Interaction on Immune Response Suppression. *Int Immunopharmacol* (2011) 11(5):597–603. doi: 10.1016/j.intimp.2010.11.015
23. Lu X, Su B, Xia H, Zhang X, Liu Z, Ji Y, et al. Low Double-Negative CD3(+) CD4(-)CD8(-) T Cells Are Associated With Incomplete Restoration of CD4 (+) T Cells and Higher Immune Activation in HIV-1 Immunological Non-Responders. *Front Immunol* (2016) 7:579. doi: 10.3389/fimmu.2016.00579
24. Meziane O, Salahuddin S, Pham TNQ, Farnos O, Pagliuzza A, Olivenstein R, et al. HIV Infection and Persistence in Pulmonary Mucosal Double Negative T Cells *In Vivo*. *J Virol* (2020) 94(24):e01788–20. doi: 10.1128/JVI.01788-20

25. Petitjean G, Chevalier MF, Tibaoui F, Didier C, Manea ME, Liovat AS, et al. Level of Double Negative T Cells, Which Produce TGF-Beta and IL-10, Predicts CD8 T-Cell Activation in Primary HIV-1 Infection. *AIDS* (2012) 26 (2):139–48. doi: 10.1097/QAD.0b013e32834e1484
26. Zhang D, Yang W, Degauque N, Tian Y, Mikita A, Zheng XX. New Differentiation Pathway for Double-Negative Regulatory T Cells That Regulates the Magnitude of Immune Responses. *Blood* (2007) 109(9):4071–9. doi: 10.1182/blood-2006-10-050625
27. Zhang ZX, Ma Y, Wang H, Arp J, Jiang J, Huang X, et al. Double-Negative T Cells, Activated by Xenoantigen, Lyse Autologous B and T Cells Using a Perforin/Granzyme-Dependent, Fas-Fas Ligand-Independent Pathway. *J Immunol* (2006) 177(10):6920–9. doi: 10.4049/jimmunol.177.10.6920
28. Gao JF, McIntyre MS, Juvet SC, Diao J, Li X, Vanama RB, et al. Regulation of Antigen-Expressing Dendritic Cells by Double Negative Regulatory T Cells. *Eur J Immunol* (2011) 41(9):2699–708. doi: 10.1002/eji.201141428
29. Ohta A, Sitkovsky M. Extracellular Adenosine-Mediated Modulation of Regulatory T Cells. *Front Immunol* (2014) 5:304. doi: 10.3389/fimmu.2014.00304
30. Antonioli L, Pacher P, Vizi ES, Hasko G. CD39 and CD73 in Immunity and Inflammation. *Trends Mol Med* (2013) 19(6):355–67. doi: 10.1016/j.molmed.2013.03.005
31. Meng F, Guo Z, Hu Y, Mai W, Zhang Z, Zhang B, et al. CD73-Derived Adenosine Controls Inflammation and Neurodegeneration by Modulating Dopamine Signalling. *Brain* (2019) 142(3):700–18. doi: 10.1093/brain/awy351
32. Kong Y, Jia B, Zhao C, Claxton DF, Sharma A, Annageldiyev C, et al. Downregulation of CD73 Associates With T Cell Exhaustion in AML Patients. *J Hematol Oncol* (2019) 12(1):40. doi: 10.1186/s13045-019-0728-3
33. Schuler PJ, Macatangay BJ, Saze Z, Jackson EK, Riddler SA, Buchanan WG, et al. CD4(+)CD73(+) T Cells Are Associated With Lower T-Cell Activation and C Reactive Protein Levels and Are Depleted in HIV-1 Infection Regardless of Viral Suppression. *AIDS* (2013) 27(10):1545–55. doi: 10.1097/QAD.0b013e328360c7f3
34. Neo SY, Yang Y, Record J, Ma R, Chen X, Chen Z, et al. CD73 Immune Checkpoint Defines Regulatory NK Cells Within the Tumor Microenvironment. *J Clin Invest* (2020) 130(3):1185–98. doi: 10.1172/JCI128895
35. Beavis PA, Stagg J, Darcy PK, Smyth MJ. CD73: A Potent Suppressor of Antitumor Immune Responses. *Trends Immunol* (2012) 33(5):231–7. doi: 10.1016/j.it.2012.02.009
36. Chang W-X, Huang H-H, Huang L, Shi J-J, Jiao Y-M, Zhang C, et al. Skewed CD39/CD73/adenosine Pathway in B Cells Is Associated With Innate Immune Hyperactivation in Chronic HIV-1 Infection. *Trans Med Commun* (2019) 4(1):4. doi: 10.1186/s41231-019-0033-8
37. Jenabian MA, Seddiki N, Yatim A, Carriere M, Hulin A, Younas M, et al. Regulatory T Cells Negatively Affect IL-2 Production of Effector T Cells Through CD39/adenosine Pathway in HIV Infection. *PloS Pathog* (2013) 9(4):e1003319. doi: 10.1371/journal.ppat.1003319
38. Nikolova M, Carriere M, Jenabian MA, Limou S, Younas M, Kok A, et al. CD39/adenosine Pathway Is Involved in AIDS Progression. *PloS Pathog* (2011) 7(7):e1002110. doi: 10.1371/journal.ppat.1002110
39. Lopez-Abente J, Correa-Rocha R, Pion M. Functional Mechanisms of Treg in the Context of HIV Infection and the Janus Face of Immune Suppression. *Front Immunol* (2016) 7:192. doi: 10.3389/fimmu.2016.00192
40. Deeks SG. HIV Infection, Inflammation, Immunosenescence, and Aging. *Annu Rev Med* (2011) 62:141–55. doi: 10.1146/annurev-med-042909-093756
41. Cohen J, Torres C. HIV-Associated Cellular Senescence: A Contributor to Accelerated Aging. *Ageing Res Rev* (2017) 36:117–24. doi: 10.1016/j.arr.2016.12.004
42. Cotto B, Natarajanseenivasan K, Langford D. HIV-1 Infection Alters Energy Metabolism in the Brain: Contributions to HIV-Associated Neurocognitive Disorders. *Prog Neurobiol* (2019) 181:101616. doi: 10.1016/j.pneurobio.2019.101616
43. Serrao R, Pinero C, Velez J, Coutinho D, Maltez F, Lino S, et al. Non-AIDS-Related Comorbidities in People Living With HIV-1 Aged 50 Years and Older: The AGING POSITIVE Study. *Int J Infect Dis* (2019) 79:94–100. doi: 10.1016/j.ijid.2018.10.011
44. Torti C, Prosperi M, Motta D, Digiambenedetto S, Maggiolo F, Paraninfo G, et al. Factors Influencing the Normalization of CD4+ T-Cell Count, Percentage and CD4+/CD8+ T-Cell Ratio in HIV-Infected Patients on Long-Term Suppressive Antiretroviral Therapy. *Clin Microbiol Infect* (2012) 18(5):449–58. doi: 10.1111/j.1469-0691.2011.03650.x
45. Li CX, Li YY, He LP, Kou J, Bai JS, Liu J, et al. The Predictive Role of CD4(+) Cell Count and CD4/CD8 Ratio in Immune Reconstitution Outcome Among HIV/AIDS Patients Receiving Antiretroviral Therapy: An Eight-Year Observation in China. *BMC Immunol* (2019) 20(1):31. doi: 10.1186/s12865-019-0311-2
46. Hunt PW, Cao HL, Muzoora C, Ssewanyana I, Bennett J, Emenyonu N, et al. Impact of CD8+ T-Cell Activation on CD4+ T-Cell Recovery and Mortality in HIV-Infected Ugandans Initiating Antiretroviral Therapy. *AIDS* (2011) 25 (17):2123–31. doi: 10.1097/QAD.0b013e32834c4ac1
47. Greenblatt R, Bacchetti P, Boylan R, Kober K, Springer G, Anastos K, et al. Genetic and Clinical Predictors of CD4 Lymphocyte Recovery During Suppressive Antiretroviral Therapy: Whole Exome Sequencing and Antiretroviral Therapy Response Phenotypes. *PloS One* (2019) 14(8):e0219201. doi: 10.1371/journal.pone.0219201
48. Rajasuriar R, Gouillou M, Spelman T, Read T, Hoy J, Law M, et al. Clinical Predictors of Immune Reconstitution Following Combination Antiretroviral Therapy in Patients From the Australian HIV Observational Database. *PloS One* (2011) 6(6):e20713. doi: 10.1371/journal.pone.0020713
49. Rb-Silva R, Nobrega C, Azevedo C, Athayde E, Canto-Gomes J, Ferreira I, et al. Thymic Function as a Predictor of Immune Recovery in Chronically HIV-Infected Patients Initiating Antiretroviral Therapy. *Front Immunol* (2019) 10:25. doi: 10.3389/fimmu.2019.00025
50. Sauter R, Huang R, Ledergerber B, Battegay M, Bernasconi E, Cavassini M, et al. CD4/CD8 Ratio and CD8 Counts Predict CD4 Response in HIV-1-Infected Drug Naive and in Patients on cART. *Medicine (Baltimore)* (2016) 95 (42):e5094. doi: 10.1097/MD.0000000000005094
51. Guzman-Fulgencio M, Berenguer J, Jimenez-Sousa MA, Micheloud D, Garcia-Alvarez M, Bellon JM, et al. IL7RA Polymorphisms Predict the CD4 + Recovery in HIV Patients on cART. *Eur J Clin Invest* (2015) 45(11):1192–9. doi: 10.1111/eci.12539
52. Guzman-Fulgencio M, Berenguer J, Micheloud D, Fernandez-Rodriguez A, Garcia-Alvarez M, Jimenez-Sousa MA, et al. European Mitochondrial Haplogroups Are Associated With CD4+ T Cell Recovery in HIV-Infected Patients on Combination Antiretroviral Therapy. *J Antimicrob Chemother* (2013) 68(10):2349–57. doi: 10.1093/jac/dkt206
53. Kroeze S, Rossouw TM, Steel HC, Wit FW, Kityo CM, Siwale M, et al. Plasma Inflammatory Biomarkers Predict CD4+ T-Cell Recovery and Viral Rebound in HIV-1 Infected Africans on Suppressive Antiretroviral Therapy. *J Infect Dis* (2021) 224(4):673–8. doi: 10.1093/infdis/jiaa787
54. Hernandez-Walias F, Ruiz-de-Leon MJ, Rosado-Sanchez I, Vazquez E, Leal M, Moreno S, et al. New Signatures of Poor CD4 Cell Recovery After Suppressive Antiretroviral Therapy in HIV-1-Infected Individuals: Involvement of miR-192, IL-6, Scd14 and miR-144. *Sci Rep* (2020) 10 (1):2937. doi: 10.1038/s41598-020-60073-8
55. Chen X, Liu X, Duan S, Tang R, Zhou S, Ye R, et al. Plasma Inflammatory Biomarkers Associated With Advanced Liver Fibrosis in HIV–HCV-Coinfected Individuals. *Int J Environ Res Public Health* (2020) 17(24):9474. doi: 10.1097/QAD.0000000000002231
56. Watanabe D, Uehira T, Suzuki S, Matsumoto E, Ueji T, Hirota K, et al. Clinical Characteristics of HIV-1-Infected Patients With High Levels of Plasma Interferon-Gamma: A Multicenter Observational Study. *BMC Infect Dis* (2019) 19(1):11. doi: 10.1186/s12879-018-3643-2
57. Nguyen TP, Shukla S, Asaad R, Freeman ML, Lederman MM, Harding CV, et al. Responsiveness to IL-7 But Not to IFN-Alpha Is Diminished in CD4+ T Cells From Treated HIV Infected Patients Who Experience Poor CD4+ T-Cell Recovery. *AIDS* (2016) 30(13):2033–42. doi: 10.1097/QAD.0000000000001161
58. Fernandez S, Tanaskovic S, Helbig K, Rajasuriar R, Kramski M, Murray JM, et al. CD4+ T-Cell Deficiency in HIV Patients Responding to Antiretroviral Therapy Is Associated With Increased Expression of Interferon-Stimulated Genes in CD4+ T Cells. *J Infect Dis* (2011) 204(12):1927–35. doi: 10.1093/infdis/jir659
59. Pino M, Pereira Ribeiro S, Pagliuzza A, Ghneim K, Khan A, Ryan E, et al. Increased Homeostatic Cytokines and Stability of HIV-Infected Memory CD4 T-Cells Identify Individuals With Suboptimal CD4 T-Cell Recovery on-ART. *PloS Pathog* (2021) 17(8):e1009825. doi: 10.1371/journal.ppat.1009825
60. Vaidya SA, Korner C, Sirignano MN, Amero M, Bazner S, Rychert J, et al. Tumor Necrosis Factor Alpha Is Associated With Viral Control and Early

Disease Progression in Patients With HIV Type 1 Infection. *J Infect Dis* (2014) 210(7):1042–6. doi: 10.1093/infdis/jiu206
61. Reis EC, Leal VNC, da Silva LT, Dos Reis MML, Arganaraz ER, Oshiro TM, et al. Antagonistic Role of IL-1ss and NLRP3/IL-18 Genetics in Chronic HIV-1 Infection. *Clin Immunol* (2019) 209:108266. doi: 10.1016/j.clim.2019.108266
62. Stiksrud B, Lorvik KB, Kvale D, Mollnes TE, Ueland PM, Trseid M, et al. Plasma IP-10 Is Increased in Immunological NonResponders and Associated With Activated Regulatory T Cells and Persisting Low CD4 Counts. *J Acquir Immune Defic Syndr* (2016) 73(2):138. doi: 10.1097/QAI.0000000000001080
63. Erikstrup C, Kronborg G, Lohse N, Rye OS, Gerstoft J, Ullum HJJ. T-Cell Dysfunction in HIV-1-Infected Patients With Impaired Recovery of CD4 Cells Despite Suppression of Viral Replication. *J Acquir Immune Defic Syndr* (2010) 53(3):303–10. doi: 10.1097/QAI.0b013e3181ca3f7c
64. Prebensen C, Ueland T, Michelsen AE, Lind A, Pettersen FO, Mollnes TE, et al. High MIP-1β Levels in Plasma Predict Long-Term Immunological Nonresponse to Suppressive Antiretroviral Therapy in HIV Infection. (2015) 69(4):395–402. doi: 10.1097/QAI.0000000000000617
65. Mussini C, Lorenzini P, Cozzi-Lepri A, Lapadula G, Marchetti G, Nicastri E, et al. CD4/CD8 Ratio Normalisation and Non-AIDS-Related Events in Individuals With HIV Who Achieve Viral Load Suppression With Antiretroviral Therapy: An Observational Cohort Study. *Lancet HIV* (2015) 2(3):e98–e106. doi: 10.1016/s2352-3018(15)00006-5
66. Li B, Zhang L, Liu Y, Xiao J, Li C, Fan L, et al. A Novel Prediction Model to Evaluate the Probability of CD4/CD8 Ratio Restoration in HIV-Infected Individuals. *AIDS* (2022). doi: 10.1097/QAD.0000000000003167
67. Serrano-Villar S, Martínez-Sanz J, Ron R, Talavera-Rodríguez A, Fernández-Felix BM, Herrera S, et al. Effects of First-Line Antiretroviral Therapy on the CD4/CD8 Ratio and CD8 Cell Counts in CoRIS: A Prospective Multicentre Cohort Study. *Lancet HIV* (2020) 7(8):e565–e73. doi: 10.1016/s2352-3018(20)30202-2
68. Lu W, Mehraj V, Vyboh K, Cao W, Li T, Routy JP. CD4:CD8 Ratio as a Frontier Marker for Clinical Outcome, Immune Dysfunction and Viral Reservoir Size in Virologically Suppressed HIV-Positive Patients. *J Int AIDS Soc* (2015) 18:20052. doi: 10.7448/IAS.18.1.20052
69. Roca-Bayerri C, Robertson F, Pyle A, Hudson G, Payne BAI. Mitochondrial DNA Damage and Brain Aging in Human Immunodeficiency Virus. *Clin Infect Dis* (2021) 73(2):e466–e73. doi: 10.1093/cid/ciaa984
70. Caby F, Guiguet M, Weiss L, Winston A, Miro JM, Konopnicki D, et al. CD4/CD8 Ratio and the Risk of Kaposi Sarcoma or Non-Hodgkin Lymphoma in the Context of Efficiently Treated Human Immunodeficiency Virus (HIV) Infection: A Collaborative Analysis of 20 European Cohort Studies. *Clin Infect Dis* (2021) 73(1):50–9. doi: 10.1093/cid/ciaa1137
71. Mahapatra S, Shearer WT, Minard CG, Mace E, Paul M, Orange JS. NK Cells in Treated HIV-Infected Children Display Altered Phenotype and Function. *J Allergy Clin Immunol* (2019) 144(1):294–303.e13. doi: 10.1016/j.jaci.2018.11.052
72. Serrano-Villar S, Perez-Elias MJ, Dronda F, Casado JL, Moreno A, Royuela A, et al. Increased Risk of Serious Non-AIDS-Related Events in HIV-Infected Subjects on Antiretroviral Therapy Associated With a Low CD4/CD8 Ratio. *PloS One* (2014) 9(1):e85798. doi: 10.1371/journal.pone.0085798
73. Kim ES, Ackermann C, Toth I, Dierks P, Eberhard JM, Wroblewski R, et al. Down-Regulation of CD73 on B Cells of Patients With Viremic HIV Correlates With B Cell Activation and Disease Progression. *J Leukoc Biol* (2017) 101(5):1263–71. doi: 10.1189/jlb.5A0816-346R
74. Toth I, Le AQ, Hartjen P, Thomssen A, Matzat V, Lehmann C, et al. Decreased Frequency of CD73+CD8+ T Cells of HIV-Infected Patients Correlates With Immune Activation and T Cell Exhaustion. *J Leukoc Biol* (2013) 94(4):551–61. doi: 10.1189/jlb.0113018
75. Carriere M, Lacabaratz C, Kok A, Benne C, Jenabian MA, Casartelli N, et al. HIV "Elite Controllers" Are Characterized by a High Frequency of Memory CD8+ CD73+ T Cells Involved in the Antigen-Specific CD8+ T-Cell Response. *J Infect Dis* (2014) 209(9):1321–30. doi: 10.1093/infdis/jit643
76. Schneider E, Winzer R, Rissiek A, Ricklefs I, Meyer-Schwesinger C, Ricklefs FL, et al. CD73-Mediated Adenosine Production by CD8 T Cell-Derived Extracellular Vesicles Constitutes an Intrinsic Mechanism of Immune Suppression. *Nat Commun* (2021) 12(1):5911. doi: 10.1038/s41467-021-26134-w
77. Lehto MT, Sharom FJ. Release of the Glycosylphosphatidylinositol-Anchored Enzyme Ecto-5'-Nucleotidase by Phospholipase C: Catalytic Activation and Modulation by the Lipid Bilayer. *Biochem J* (1998) 332(Pt 1):101. doi: 10.1042/bj3320101
78. Schneider E, Rissiek A, Winzer R, Puig B, Rissiek B, Haag F, et al. Generation and Function of Non-Cell-Bound CD73 in Inflammation. *Front Immunol* (2019) 10:1729. doi: 10.3389/fimmu.2019.01729
79. Wang M, Jia J, Cui Y, Peng Y, Jiang Y. CD73-Positive Extracellular Vesicles Promote Glioblastoma Immunosuppression by Inhibiting T-Cell Clonal Expansion. *Cell Death Dis* (2021) 12(11):1065. doi: 10.1038/s41419-021-04359-3
80. Botta Gordon-Smith S, Ursu S, Eaton S, Moncrieffe H, Wedderburn LR. Correlation of Low CD73 Expression on Synovial Lymphocytes With Reduced Adenosine Generation and Higher Disease Severity in Juvenile Idiopathic Arthritis. *Arthritis Rheumatol* (2015) 67(2):545–54. doi: 10.1002/art.38959
81. Clayton A, Al-Taei S, Webber J, Mason MD, Tabi Z. Cancer Exosomes Express CD39 and CD73, Which Suppress T Cells Through Adenosine Production. *J Immunol* (2011) 187(2):676–83. doi: 10.4049/jimmunol.1003884
82. Hixson EA, Borker PV, Jackson EK, Macatangay BJ. The Adenosine Pathway and Human Immunodeficiency Virus-Associated Inflammation. *Open Forum Infect Dis* (2021) 8(9):ofab396. doi: 10.1093/ofid/ofab396
83. Hasko G, Cronstein B. Regulation of Inflammation by Adenosine. *Front Immunol* (2013) 4:85. doi: 10.3389/fimmu.2013.00085
84. Lofgren L, Pehrsson S, Hagglund G, Tjellstrom H, Nylander S. Accurate Measurement of Endogenous Adenosine in Human Blood. *PloS One* (2018) 13 (10):e0205707. doi: 10.1371/journal.pone.0205707
85. Goding JW, Grobben B, Slegers H. Physiological and Pathophysiological Functions of the Ecto-Nucleotide Pyrophosphatase/Phosphodiesterase Family. *Biochim Biophys Acta (BBA) - Mol Basis Dis* (2003) 1638(1):1–19. doi: 10.1016/s0925-4439(03)00058-9
86. Alcedo KP, Bowser JL, Snider NT. The Elegant Complexity of Mammalian Ecto-5′-Nucleotidase (CD73). *Trends Cell Biol* (2021) 31(10):829–42. doi: 10.1016/j.tcb.2021.05.008

Conflict of Interest: The authors declare that the research was conducted in the absence of any commercial or financial relationships that could be construed as a potential conflict of interest.

Publisher's Note: All claims expressed in this article are solely those of the authors and do not necessarily represent those of their affiliated organizations, or those of the publisher, the editors and the reviewers. Any product that may be evaluated in this article, or claim that may be made by its manufacturer, is not guaranteed or endorsed by the publisher.

frontiers | Frontiers in Immunology

ORIGINAL RESEARCH
published: 05 April 2022
doi: 10.3389/fimmu.2022.850719

Comparison of the Immunogenicity of HIV-1 CRF07_BC Gag Antigen With or Without a Seven Amino Acid Deletion in p6 Region

Minchao Li[1†], Yue Yuan[1†], Pingchao Li[2†], Zhaomin Deng[1], Ziyu Wen[1], Haiying Wang[3], Fengling Feng[1], Huachun Zou[1], Ling Chen[2], Shixing Tang[3] and Caijun Sun[1,4*]*

[1] School of Public Health (Shenzhen), Shenzhen Campus of Sun Yat-sen University, Shenzhen, China, [2] State Key Laboratory of Respiratory Disease, Guangzhou Institutes of Biomedicine and Health (GIBH), Chinese Academy of Sciences, Guangzhou, China, [3] Guangdong Provincial Key Laboratory of Tropical Disease Research, School of Public Health, Southern Medical University, Guangzhou, China, [4] Key Laboratory of Tropical Disease Control (Sun Yat-Sen University), Ministry of Education, Guangzhou, China

OPEN ACCESS

Edited by:
Tongqing Zhou,
National Institutes of Health (NIH),
United States

Reviewed by:
Maria Issagouliantis,
Riga Stradiņš University,
Latvia
Jue Hou,
Virginia Mason Medical Center,
United States

***Correspondence:**
Caijun Sun
suncaijun@mail.sysu.edu.cn
Shixing Tang
tamgshixing@smu.edu.cn

[†]These authors have contributed equally to this work

Specialty section:
This article was submitted to Vaccines and Molecular Therapeutics, a section of the journal Frontiers in Immunology

Received: 08 January 2022
Accepted: 03 March 2022
Published: 05 April 2022

Citation:
Li M, Yuan Y, Li P, Deng Z, Wen Z, Wang H, Feng F, Zou H, Chen L, Tang S and Sun C (2022) Comparison of the Immunogenicity of HIV-1 CRF07_BC Gag Antigen With or Without a Seven Amino Acid Deletion in p6 Region. Front. Immunol. 13:850719. doi: 10.3389/fimmu.2022.850719

HIV-1 CRF07_BC-p6Δ7, a strain with a seven amino acid deletion in the p6 region of the Gag protein, is becoming the dominant strain of HIV transmission among men who have sex with men (MSM) in China. Previous studies demonstrated that HIV-1 patients infected by CRF07_BC-p6Δ7 strain had lower viral load and slower disease progression than those patients infected with CRF07_BC wild-type strain. However, the underlying mechanism for this observation is not fully clarified yet. In this study, we constructed the recombinant DNA plasmid and adenovirus type 2 (Ad2) vector-based constructs to express the HIV-1 CRF07_BC Gag antigen with or without p6Δ7 mutation and then investigated their immunogenicity in mice. Our results showed that HIV-1 CRF07_BC Gag antigen with p6Δ7 mutation induced a comparable level of Gag-specific antibodies but stronger $CD4^+$ and $CD8^+$ T-cell immune responses than that of CRF07_BC Gag (07_BC-wt). Furthermore, we identified a series of T-cell epitopes, which induced strong T-cell immune response and cross-immunity with CRF01_AE Gag. These findings implied that the $p6^{Gag}$ protein with a seven amino acid deletion might enhance the Gag immunogenicity in particular cellular immunity, which provides valuable information to clarify the pathogenic mechanism of HIV-1 CRF07_BC-p6Δ7 and to develop precise vaccine strategies against HIV-1 infection.

Keywords: HIV-1, CRF07_BC, p6Δ7, Gag, immunogenicity

INTRODUCTION

The epidemic of HIV-1 infection remains a global health crisis. According to the report issued by the Joint United Nations Program on HIV/AIDS (UNAIDS), 37.7 million people were living with HIV-1 including 10.2 million untreated, 1.5 million new HIV-1 infections, and 680,000 AIDS-related deaths at the end of 2020. Although antiretroviral therapy (ART) can effectively control viral replication in AIDS patients, the withdrawal of ART will inevitably lead to a rapid rebound of plasma viremia because of the

stable and long-lived latent virus reservoirs (1, 2). Thus, HIV-1 patients have to receive life-long ART therapy. An effective HIV-1 vaccine is therefore considered the most cost-effective intervention to eventually terminate the HIV-1 spread. However, the extraordinary genetic diversity, latent viral reservoirs, and lack of the immune correlates of protection against HIV-1 infection are the major challenges for developing an effective HIV-1 vaccine. So far, hundreds of HIV-1 vaccine trials have been studied, including the AIDSVAX trial (protein subunit vaccine, aimed to produce the neutralizing antibodies), STEP trial (viral vectored-HIV vaccine, aimed to elicit T-cell immune responses), and RV144 trial (combined immunization with ALVAC-HIV/AIDSVAX, aimed to induce a balanced immunity with both humoral and cellular responses) (3, 4). Among them, the RV144 trial remains the only one to demonstrate a positive signal with an estimated efficacy of 31.2% (5). Therefore, it is of great significance to develop the next generation of HIV-1 prophylactic vaccine to confer better immune protection or therapeutic vaccines to achieve a functional cure.

Circulating recombinant form 07_BC strain (CRF07_BC) is a genotype of HIV-1 with a clade C backbone in which several Thailand variant fragments of clade B into structural and accessory genes were inserted (6). CRF07_BC originated in Yunnan and spread rapidly in Western China and then nationwide (7). Subsequently, HIV-1 CRF07_BC had caused an epidemic among Taiwan injection drug users in 2004 (8, 9). Full-length genomic analysis of CRF07_BC revealed that there were some deletions (7–11 amino acids) in the p6 (Gag) and p6 (Pol) proteins (10). Our previous study showed that the prevalence of 07_BC-p6Δ7 strain constantly increased and exceeded 90% in the men who have sex with men (MSM) population infected by HIV-1 CRF07_BC in China (11), indicating that 07_BC-p6Δ7 is becoming the dominant strain among MSM in China. Notably, the deletion sequences YPX(n)L in the Gag p6 region mediated the interaction with ALG-2 interacting protein X (Alix) protein, which functions not only in multivesicular body (MVB) biogenesis but also in apoptosis, endocytosis, and cytokinesis pathways (12). In addition, p6Δ7 mutation reduced the protease-mediated processing of Gag/Gag-Pol polyproteins and decreased the incorporation of Vpr protein in the virus particle, leading to a reduced viral load and replication, slower viral maturation processes, and an increased proportion of immature virus particles (13, 14). These characteristics of CRF07_BC-p6Δ7 might be the consequence of co-adaption between the host and the virus. The lower viral load and slower disease progression seem to be beneficial to the host survival, but they also prolong the virus survival time, and the unapparent symptom before clinical diagnosis might also provide more opportunity to spread this strain among the population and thus poses a serious public health threat.

It is of note that the Gag protein is a well-known antigen to stimulate cellular responses to control HIV-1 replication and has thus been extensively studied as an ideal target for developing the HIV-1 vaccine. HIV-1-specific T cell responses play pivotal roles in controlling viral infection (15, 16). The strong cellular response not only protected acute HIV-1 infection by reducing initial peak viremia to viral set point (17, 18) but also existed in long-term non-progressors with chronic HIV-1 infection (19, 20). Moreover, HIV-1-specific T-cell immune responses induced by different HIV-1 proteins, especially the specific cytotoxic T lymphocyte (CTL) response against the Gag protein, could control HIV-1 replication to maintain a low steady-state viremia in several independent cohort studies (21–24). Considering that the Gag-specific T-cell immune responses can contribute to controlling the viral load and disease progression, we therefore speculate whether the p6Δ7 mutation in the Gag protein might change the Gag-specific immune responses and then affect the disease progression. We therefore address this critical issue in this study using 15-mer overlapping peptides spanning the entire sequence of the Gag protein to identify the specific T-cell epitopes through ELISpot as well as intracellular cytokine staining (ICS) assay.

MATERIALS AND METHODS

Vaccine and Peptide Preparation

The HIV-1 Gag protein sequences were obtained from the National Center for Biotechnology Information (NCBI) including HIV-1 CRF07_BC-p6Δ7 (GenBank: AHA50525.1) and CRF01_AE (GenBank: AFV34153.1). The Gag sequence was optimized according to the preferred codon usage of mammalian cells as previously described (25) and chemically synthesized by Invitrogen (Carlsbad, CA, USA). Subsequently, the CRF07_BC gag full length with the supplemental deletion of seven amino acids in the p6 region (07_BC-wt) was obtained using overlap extension PCR with two pairs of specific primers designed based on the CRF07_BC-p6Δ7 sequence (Primer: A1:5′ CTTAAGCTTACCATGGGCGCC, B1:5′CCCTCTAGATTTAGGGCAGCAGGGG, A2:5′GTACAGCTCCTTGTCAATGGGCTCCTGCTTCTGGGATGGGG, B2:5′ CCCATTGACAAGGAGCTGTACCCCATCAC CTCCCTGAAGTC). The codon-optimized Gag gene was then cloned into the pVAX-1 expression vector (Invitrogen) and adenovirus type 2 (Ad2) vector. Recombinant adenoviruses were generated using homologous recombination methods as our previous study described (26).

In this study, a total of 121 of 15-mer peptides overlapping by 11 amino acid residues and spanning the gene sequence of 07_BC-wt were designed using the software PeptGen (http://www.hiv.lanl.gov/content/sequence/PEPTGEN/peptgen.html) and synthesized (purity: >85%, GeneScript, China). The peptide pool was divided into 12 pools, each of which contained 10 peptides, and the last peptide pool contained 11 peptides (**Supplementary Table 1**). All of the peptides were dissolved in dimethyl sulfoxide (DMSO) at 0.4 mg/ml.

Western Blotting Analysis

To confirm the expression of the target protein, human embryonic kidney (HEK) 293 cells in 6-well plates were transfected with pVAX-01AEgag, pVAX-07BCgag-p6Δ7, pVAX-07BCgag-wt, or pVAX-empty at 2 μg per well or infected with rAd2-01AEgag, rAd2-07BCgag-p6Δ7, rAd2-07BCgag-wt, or rAd2-empty at 0.2 TCID50 per well for 48 h

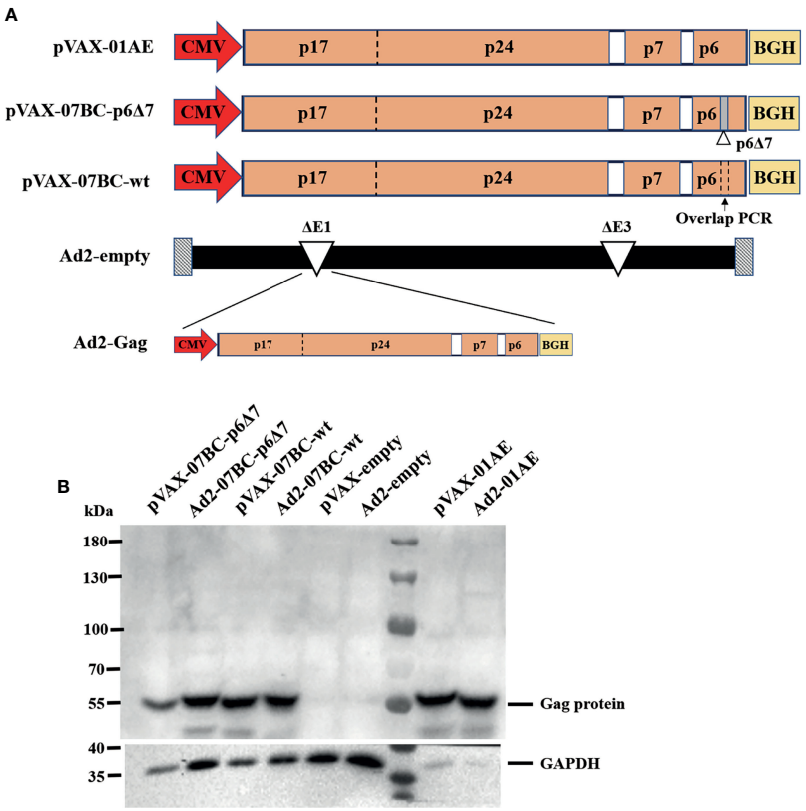

FIGURE 1 | Construction and characteristic of the DNA vectors and Ad2-based vectors carrying the Gag protein of different HIV-1 subtypes. **(A)** Diagrammatic sketch of constructing pVAX-1 and Ad2 vectors carrying various Gag genes under CMV promoter and the gene structure of Gag. There are seven amino acid deletions in Gag protein encoded by 07BC-p6Δ7, while the deletions were supplemented in 07BC-wt through overlap PCR. **(B)** Western blotting analysis of the expression of various Gag proteins in HEK293 cells in 6-well plates transfected with plasmids encoding a codon-modified Gag sequence (pVAX-01AE, pVAX-07BC-p6Δ7, or pVAX-07BC-wt, 2 μg per well) or infected with recombinant Ad2 virus (Ad2-01AE, Ad2-07BC-p6Δ7, or Ad2-07BC-wt, 0.2 TCID50 per well). pVAX-empty plasmid and Ad2-empty virus were used as the negative control. The GAPDH blot examined in parallel served as an internal control.

at 37°C. Subsequently, cells were lysed, and the proteins were separated by sodium dodecyl sulfate–polyacrylamide gel electrophoresis (SDS-PAGE) under denaturing and reducing conditions. Proteins were transferred to the polyvinylidene difluoride (PVDF) membrane (Bio-Rad, Hercules, CA, USA). After being blocked for 1 h with 5% skim milk in Tris buffered saline with Tween-20 (TBST) the membrane was incubated overnight with a rabbit monoclonal anti-Gag antibody (Abcam, Cambridge, UK) and a mouse monoclonal anti-GAPDH antibody (Abcam) at 4°C. The membrane was washed and then incubated with horseradish peroxidase-conjugated anti-rabbit IgG antibody or anti-mouse IgG antibody at a 1:5,000 dilution (Abcam) for 2 h. Finally, the membranes were developed with a chemiluminescent horseradish peroxidase (HRP) substrate (Invitrogen). The expression of GAPDH was also examined in parallel as an internal control.

Animal Experiments

Female BALB/c mice aged 6–8 weeks were randomly allocated into five groups (n = 10 per group). Group 1 received 100 μl of PBS per mouse served as the negative control. Each mouse of groups 2 to 5 was intramuscularly injected with 50 μg of the DNA plasmid dissolved in 100 μl of PBS in the right quadriceps of the leg at weeks 0 and 2 and then boosted intramuscularly with 1×10^9 vp of the corresponding adenoviral vector vaccine in the right quadriceps of the leg at weeks 4. At weeks 3 and 6, five mice in each group were anesthetized with inhaled isoflurane and sacrificed by cervical dislocation. Then, the splenocytes were obtained and subjected to subsequent immunological analyses.

IFN-γ ELISpot Assay

IFN-γ ELISpot assay was performed to detect cellular immune response using freshly isolated mouse splenic lymphocytes as previously described (25). Briefly, 96-well plates (Merck Millipore, Burlington, MA, USA) were washed and coated with purified rat anti-mouse IFN-γ monoclonal antibody U-CyTech, Netherlands at 4°C overnight. Mouse splenic lymphocytes were isolated using mouse lymphocyte separation solution (Dakewe Biotech Co., Ltd., Shenzhen, China) and seeded in the plates at 3×10^5 per well. Then each group was incubated with the peptide pool at 4 μg/ml, while DMSO served as a negative control. After incubation for 24 h, the plates were incubated with biotinylated

detection antibodies (U-CyTech) and developed with alkaline phosphatase-conjugated streptavidin (BD Biosciences, San Jose, CA, USA) and NBT/BCIP reagent (Thermo Fisher Scientific, Waltham, MA, USA). Finally, the spots were counted with an ELISpot reader (Bioreader 4000, BIO-SYS, Karben, Germany).

Intracellular Cytokine Staining

The antigen-specific cytokine secreted by lymphocytes was also detected by ICS assay as previously described (27). Briefly, mouse splenic lymphocytes were seeded in the 96-well plates at 2×10^6 per well and incubated with the peptide pool at 4 μg/ml for 2 h at 37°C. Then brefeldin A (BD Biosciences) was added and incubated for 16 h at 37°C. The cells were harvested and stained with CD3-PerCP-Cy-5.5, CD4-APC, and CD8-PE (BD Biosciences) for 30 min protected from light; then added with cytofix/cytoperm (BD Biosciences) to permeabilize for 30 min protected from light; and stained with IFN-γ-FITC, IL-2-APC-Cy7, and TNF-α-PE-Cy7 (BD Biosciences) for 1 h protected from light at 4°C. Samples were analyzed using the FACSAria instrument with FlowJo software (version 7.6).

Identification of Potential T-Cell Epitope

To identify the potential CTL epitopes, the single 15-mer peptide in the peptide pools of the 07BC Gag protein was analyzed using the NetMHCpan-4.0 EL 4.0 algorithm with a size range of 8- to 11-mers amino acid (28, 29). The most frequent major histocompatibility complex (MHC) class I alleles in BALB/c mice, including H-2-Dd, H-2-Kd, and H-2-Ld, were selected as a model to analyze the potential CTL epitopes. The epitope was determined based on the Percentile Rank, which was lower than 0.5 (most likely to be considered as high-affinity epitopes). In addition, 01AE was aligned with 07BC-p6Δ7 using NCBI blast software (**Supplementary Figure 1**) and predicted CTL epitope through NetMHCpan-4.0 EL 4.0 algorithm.

Statistical Analysis

Flow cytometric data were analyzed using FlowJo version 7.6. Statistical analyses and graphical presentations were conducted with GraphPad Prism version 8.0. One-way ANOVA was used for the comparison among multiple (>2) groups, and a two-tailed unpaired Student's t-test was used for comparison between two groups (07BC-p6Δ7 and 07BC-wt). Data were expressed as mean ± SEM, and p-values of less than 0.05 were deemed statistically significant. *$p < 0.05$; **$p < 0.01$; ***$p < 0.001$; NS, no significance.

RESULTS

Construction of Recombinant DNA and Ad2 Vectors Carrying Various Gag Genes

As described in the *Materials and Methods*, we successfully obtained the genes of CRF07_BC-p6Δ7, CRF07_BC gag full length (07_BC-wt), and CRF01_AEgag. To assess their immunogenicity, we constructed the recombinant pVAX-1 vector and adenovirus type 2 vector carrying various Gag genes under the control of the CMV promoter (**Figure 1A**). The Ad2 vector with deletion of E1 and E3 genes was replication-defective, and Gag gene was inserted into the E1 region. Then recombinant Ad2 was rescued and propagated in HEK293 cells, which can provide E1 protein to support the replication of this E1-deleted virus. Western blotting results showed that both the DNA constructs and Ad2 constructs appropriately expressed the corresponding Gag protein with expected molecular weight (55 kDa) (**Figure 1B**).

Immunization With Recombinant DNA and Ad2 Vectored Constructs Effectively Elicited Antigen-Specific Immune Responses Targeting Different Regions of Gag Protein

To investigate the immunogenicity of the Gag protein with or without p6Δ7 mutation, 6- to 8-week-old female BALB/c mice were immunized as shown in **Figure 2A**, and then the antigen-specific immune responses were evaluated. Previous studies demonstrated that the Gag-specific T-cell immune response, but not Gag-specific antibody, was associated with lower viremia and better HIV-1 control (21, 22). Since there was a comparable level of Gag-specific antibodies in both the 07BCgag-p6Δ7 group and 07BCgag-wt group, we focused on the Gag-specific T-cell immune response in the following study. In our study, the peptide pool covering the full length of the Gag protein was divided into 12 sub-pools (pool 1–pool 12) to stimulate mouse spleen lymphocytes (**Figure 2B**). After immunization with recombinant DNA and Ad2 vectored constructs, the peptide pools covering different regions of the Gag protein elicited T-cell immune responses with different intensities (**Figure 2C**). There were obvious T-cell immune responses induced by pool 2, pool 4, pool 8, pool 11, and pool 12, but not for the remaining sub-peptide pools. Among them, the immune responses elicited by the stimulation of peptide pool 2, pool 4, and pool 8, which are located at the p17 and p24 regions of the Gag protein, were stronger than those of pool 11 and pool 12, which are located at the p7 and p6 regions of the Gag protein. Of note, there were stronger T-cell immune responses in the 07_BC-p6Δ7 group when compared with the 07_BC-wt group, suggesting that the seven amino acid deletion in the p6 region might mainly affect the immunogenicity of T-cell epitopes in the Gag protein.

Identification of Cross-Reactive Cytotoxic T Lymphocyte Epitopes Between 07_BC and 01_AE

We then mapped the T-cell epitopes in the mice immunized with different vaccine constructs. IFN-γ ELISpot assay was performed to identify the vaccine-induced T-cell response towards each peptide in pool 2, pool 4, and pool 8 by setting the cutoff value of 50 spot-forming cells (SFCs)/10^6 cells as a positive response (30). After the background was subtracted, the median value is shown in **Figure 3A**, and a series of T-cell epitopes were identified (**Table 1**). After the identification of overall T-cell responses, the positive responses against specific peptide pools were then

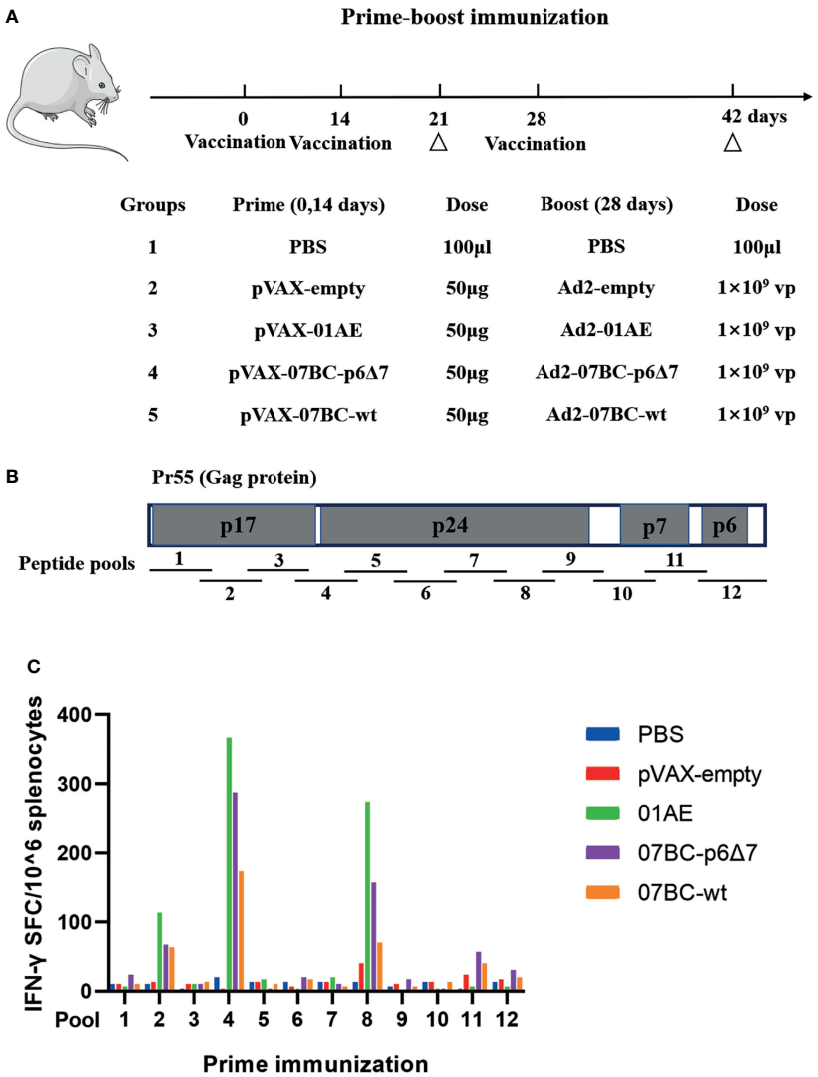

Groups	Prime (0,14 days)	Dose	Boost (28 days)	Dose
1	PBS	100μl	PBS	100μl
2	pVAX-empty	50μg	Ad2-empty	1×10^9 vp
3	pVAX-01AE	50μg	Ad2-01AE	1×10^9 vp
4	pVAX-07BC-p6Δ7	50μg	Ad2-07BC-p6Δ7	1×10^9 vp
5	pVAX-07BC-wt	50μg	Ad2-07BC-wt	1×10^9 vp

FIGURE 2 | Strong antigen-specific IFN-γ response against different regions of Gag protein after primary immunization in mice. **(A)** Vaccination strategy to evaluate the immunogenicity of various Gag proteins. Female BALB/c mice aged 6–8 weeks were randomly allocated into 5 groups (n = 10 per group). Each mouse was intramuscularly injected with 50 μg of the DNA plasmid dissolved in 100 μl of phosphate-buffered saline (PBS) at weeks 0 and 2 and then boosted intramuscularly with 1×10^9 vp of the corresponding adenoviral vector at weeks 4. Group PBS served as the negative control. "Δ" represents the time-point of sacrifice (5 mice per group) and sample collection. **(B)** The structure of Gag protein and the distribution of the peptide pools. Gag gene encodes HIV-1 viral core proteins including p17, p24, and p15. p15 is further cleaved into nucleocapsid proteins p7 and p6. The peptide pool was divided into 12 pools, each of which contained 10 peptides, and the last peptide pool contained 11 peptides. **(C)** Cellular immune responses of different peptide pools after primary immunization with DNA vaccine. The IFN-γ ELISpot assay was used to detect the cellular immune response following stimulation with peptide pools after DNA-based vaccine immunization on day 21. Median responses (n = 5) in BALB/c mice following vaccination are shown by the number of spot-forming cells (SFCs) in one million splenic lymphocytes.

characterized by $CD4^+$ or $CD8^+$ T-cell subsets for ICS assay (**Figure 3B** and **Supplementary Figure 2**). The frequency of IFN-γ-positive $CD4^+$ and $CD8^+$ T cells is shown in **Table 1**. In our study, twelve peptides could stimulate a positive $CD8^+$ T-cell response, and three peptides could stimulate a positive $CD4^+$ T-cell response. Except for peptide 73, the most positive peptides confirmed by IFN-γ ELISpot assay could also be recognized by the ICS assay of $CD4^+$ or $CD8^+$ T-cell subsets.

We further constructed the epitope mapping to analyze the breadth of the cellular response after vaccination (**Figure 3C**). Of note, although the overlapping peptide pool was constructed based on the sequence of the 07BC Gag protein, it also stimulated the splenocytes from 01AE-immunized mice to produce high levels of IFN-γ secretion. Therefore, we aligned 01AE (GenBank: AFV34153.1) and 07BC-p6Δ7 (GenBank: AHA50525.1) sequences using NCBI blast software (**Supplementary Figure 1**) and found that the similarity of amino acid sequences between 01AE and 07BC-p6Δ7 was 82%. To identify the cross-reactive T-cell epitopes, the single 15-mer peptide in the peptide pools of the 07BC Gag protein was analyzed using the

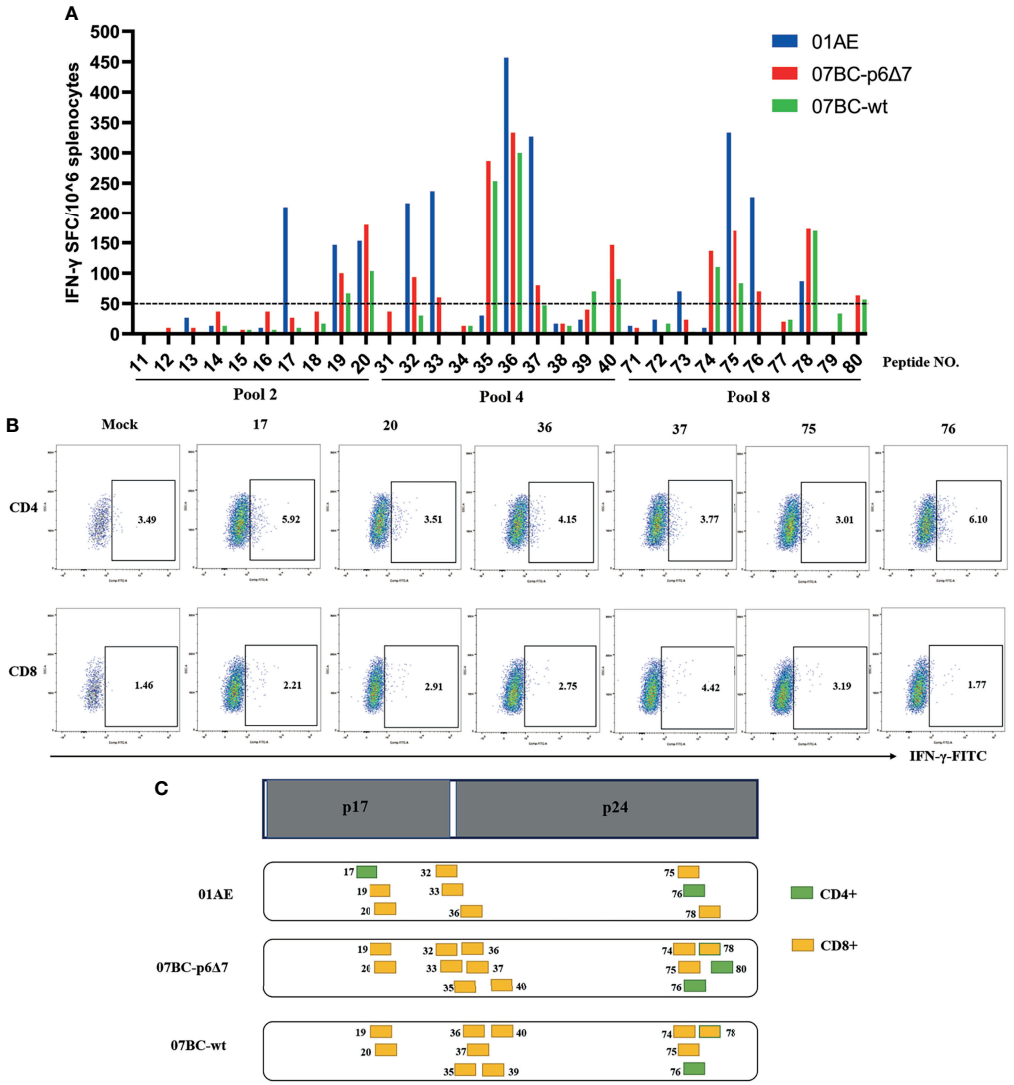

FIGURE 3 | Specific T-cell responses induced by Ad2-based vaccine and identification of the T-cell epitope. After Ad2 boost vaccination, mice were sacrificed, and the splenocytes from mice were restimulated *ex vivo* with peptide pools. The background-subtracted median responses (n = 5) in BALB/c mice following vaccination are shown. **(A)** Mouse splenic lymphocytes isolated after boost vaccination were stimulated with individual overlapping 15-mer peptides (pool 2, pool 4, and pool 8) in IFN-γ ELISpot assay. The dotted line represents the cutoff value. **(B)** Peptides that successfully induced responses above cutoff values in IFN-γ ELISpot assays were then tested for their ability to induce IFN-γ production in T cells by intracellular cytokine staining (ICS) assays. **(C)** Epitope mapping analysis of the $CD8^+$ and $CD4^+$ T-cell epitopes is represented by orange and green boxes, respectively.

NetMHCpan-4.0 EL 4.0 algorithm with a size range of 8- to 11-mer amino acid. As shown in **Table 2**, we predicted 6 cross-reactive CTL epitopes, which were most likely to be high-affinity epitopes. Furthermore, these cross-reactive CTL epitopes were conserved and maintained the recognition of $CD8^+$ T cells restricted by different MHC-I molecules even with a single amino acid substitution. Consistent with our prediction, peptide 36 (HQPISPRTLNAWVKV) contains two epitopes and thus effectively induced more than 300 SFCs/10^6 in IFN-γ ELISpot assay that targets different MHC-I molecules, suggesting that this peptide might induce extensive cross-reactive Gag-specific T-cell responses for effective HIV-1 control.

The Seven Amino Acid Deletion in p6 Region Contributed to the Increased Cellular Immune Response

To further study the poly-functionality of T-cell populations after immunization with various Gag modalities, we performed the multi-parameter ICS assay to assess the Gag-specific cellular immunity. The frequency of $CD4^+$ T-cell subsets producing one cytokine (IFN-γ, TNF-α, and IL-2) or more cytokines (IFN-γ^+/IL-2^+, IFN-γ^+/TNF-α^+, and IL-2^+/TNF-α^+) was analyzed using the exclusive gating strategy (**Figure 4A**). Statistical analysis demonstrated that the frequency of $CD4^+$ T cells secreting one cytokine or dual cytokines in the 07BC-p6Δ7-immunized mice

TABLE 1 | Identification of the T-cell epitope.

Peptide sequence	Peptide no.[a]	SFC/10^{6}[b]	$CD3^+CD4^+$IFN-γ (%)[c]	$CD3^+CD8^+$IFN-γ (%)[d]	Subtype
QPALQTGTEELRSLF	P2-17	210	2.43	0.75	01AE
EELRSLFNTVATLYC	P2-19	147	0.13	1.01	01AE
		100	0.14	0.96	07BC-p6Δ7
		67	N/D	0.33	07BC-wt
SLFNTVATLYCVHTG	P2-20	153	0.02	1.45	01AE
		180	0.39	2.05	07BC-p6Δ7
		103	N/D	0.32	07BC-wt
VSQNYPIVQNIQGQM	P4-32	217	0.58	2.10	01AE
		93	N/D	1.96	07BC-p6Δ7
YPIVQNIQGQMVHQP	P4-33	237	0.34	0.77	01AE
		60	1.05	2.16	07BC-p6Δ7
GQMVHQPISPRTLNA	P4-35	287	N/D	2.07	07BC-p6Δ7
		253	N/D	0.63	07BC-wt
HQPISPRTLNAWVKV	P4-36	457	0.66	1.29	01AE
		333	N/D	1.40	07BC-p6Δ7
		300	N/D	0.98	07BC-wt
SPRTLNAWVKVVEEK	P4-37	327	0.28	2.96	07BC-p6Δ7
		80	N/D	0.58	07BC-wt
VKVVEEKAFSPEVIP	P4-39	70	N/D	1.20	07BC-wt
EEKAFSPEVIPMFSA	P4-40	147	0.45	1.60	07BC-p6Δ7
		90	N/D	0.43	07BC-wt
PFRDYVDRFFKTLRA	P8-73	70	N/D	N/D	01AE
YVDRFFKTLRAEQAT	P8-74	137	0.66	1.83	07BC-p6Δ7
		110	N/D	1.12	07BC-wt
FFKTLRAEQATQDVK	P8-75	333	N/D	1.73	01AE
		170	0.43	1.66	07BC-p6Δ7
		83	N/D	1.02	07BC-wt
LRAEQATQDVKNWMT	P8-76	227	2.61	0.31	01AE
		70	2.82	N/D	07BC-p6Δ7
DVKNWMTDTLLVQNA	P8-78	87	0.10	0.97	01AE
		173	0.16	0.78	07BC-p6Δ7
		170	N/D	0.71	07BC-wt
TLLVQNANPDCKTIL	P8-80	63	1.16	0.68	07BC-p6Δ7
		57	N/D	N/D	07BC-wt

Median responses (n = 5) in BALB/c mice following vaccination are shown.
N/D, not detected; SFC, spot-forming cell.
[a]*The peptide number of the overlapping peptide pool.*
[b]*Background-subtracted IFN-γ SFC/10^{6} splenocytes.*
[c]*Background-subtracted frequency of responding $CD3^+CD4^+$IFN-γ cells as percentage of all $CD3^+CD4^+$ splenocytes.*
[d]*Background-subtracted frequency of responding $CD3^+CD8^+$IFN-γ cells as percentage of all $CD3^+CD8^+$ splenocytes.*

was significantly higher than that of the 07_BC-wt group, especially in response to the stimulation of pool 2 and pool 8 peptides (**Figures 4B, C**). In addition, a similar observation was also found in the $CD8^+$ T cells secreting one cytokine or dual cytokines (**Figures 4D–F**).

DISCUSSION

In this study, we evaluated the immunogenicity of the HIV-1 CRF07_BC Gag antigen with or without a seven amino acid deletion in the p6 region in mice. Our results demonstrated that CRF07_BC-p6Δ7 induced a stronger T-cell immune response than CRF07_BC-wt. The difference between the two sequences is the seven amino acids in the Gag p6 region, which are critical for binding with Alix protein. Mutations at the Alix-binding site of the p6 region led to impaired HIV-1 replication and the decreased efficiency of viral budding in various cell types (12). A previous study revealed that the expression of Galectin-3 was upregulated in response to HIV-1 CRF07_BC infection (31), and the endogenous Galectin-3 facilitated the binding of Alix-Gag p6 complex to promote HIV-1 budding (32). However, this promoting effect could be disrupted because of the seven amino acid deletion in the Gag p6 region (33). Thus, p6Δ7 might play an important role in controlling the lower viral load and slower disease progression. In addition, Galectin-3 negatively regulates the adhesion between T cell and antigen-presenting cells (APCs) by destabilizing the immunological synapse, and the possible mechanism is through modulating Alix's function to downregulate the T-cell function (34). This is consistent with our results that 07BC Gag with a seven amino acid deletion induced higher magnitude IFN-γ in ELISpot assay and higher frequency of Gag-specific (p17 and p24) cytokine including IFN-γ, IL-2, and TNF-α, indicating that the seven amino acid deletion in the p6 region might promote the immunogenicity of Gag antigen by disrupting the interactions between Galectin-3 and Alix-Gag p6 complex. Since it is well known that the enhancement of Gag-specific T-cell immune response can contribute to controlling the

TABLE 2 | Prediction of the T-cell epitopes with cross-reactive T-cell responses between 07BC and 01AE.

Peptide sequence	Peptide no.	Predicted epitope (07BC)[a]	Predicted epitope (01AE)[b]	Predicted MHC subtype[c]	T-cell response[d]
EELRSLFNTVATLYC	P2-19	SLFNTVATL	SLFNTVATL	H-2-Kd	$CD8^+$
SLFNTVATLYCVHTG	P2-20	SLFNTVATL	SLFNTVATL	H-2-Kd	$CD8^+$
VSQNYPIVQNIQGQM	P4-32	YPIVQNIQGQM	YPIVQNAQGQM	H-2-Ld	$CD8^+$
YPIVQNIQGQMVHQP	P4-33	YPIVQNIQGQM	YPIVQNAQGQM	H-2-Ld	$CD8^+$
HQPISPRTLNAWVKV	P4-36	ISPRTLNAW	VSPRTLNAW	H-2-Dd	$CD8^+$
		HQPISPRTL	HQPVSPRTL	H-2-Kd/H-2-Dd	$CD8^+$
SPRTLNAWVKVVEEK	P4-37	SPRTLNAWV	SPRTLNAWV	H-2-Ld	$CD8^+$
DVKNWMTDTLLVQNA	P8-78	NWMTDTLLV	NWMTETLLV	H-2-Kd	$CD8^+$

The epitope was predicted using the NetMHCpan-4.0 EL 4.0 algorithm and a size range of 8- to 11-mers amino acid. The epitope was determined based on the Percentile Rank, which was lower than 0.5.

MHC, major histocompatibility complex; CTL, cytotoxic T lymphocyte.

[a]*Predicted epitope in Gag protein of 07BC.*

[b]*Predicted epitope in Gag protein of 01AE*

[c]*The mice MHC subtype with high binding affinity to CTL epitope.*

[d]*The type of T-cell response.*

viral load and disease progression, our findings provide a new explanation for the abovementioned observation.

The cross-recognition of viral epitopes by $CD8^+$ T cells is related to viral control during HIV-1 infection and is thus vital to develop a vaccine strategy that can elicit cross-reactive T-cell responses to target the conserved regions of the viral antigens, which is an important requirement for an effective vaccine against HIV-1 variants (35, 36). In our study, we also identified seven 15-mer peptides, which can induce a high magnitude of IFN-γ secretion in ELISpot assay, and further predicted six $CD8^+$ T-cell epitopes located at the conserved p17 and p24 region of the 01AE Gag and the 07BC Gag, indicating that there might be a strong cross-reactive immune response between the 01AE Gag antigen and the 07BC Gag antigen. Among them, peptide 36 (HQPISPRTLNAWVKV)

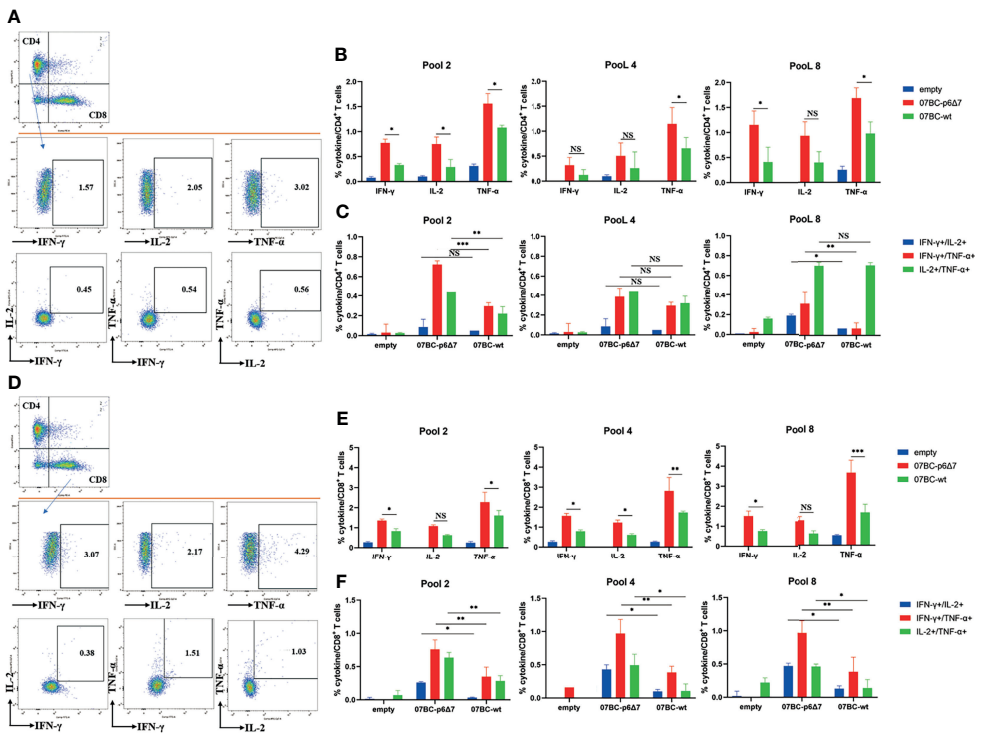

FIGURE 4 | Assessment of Gag-specific cellular immunity elicited by Ad2 vaccine through intracellular cytokine staining (ICS) assay. The ability of polyfunctional $CD4^+$ and $CD8^+$ T-cell populations from immunized mice to secrete IFN-γ, TNF-α, and IL-2 cytokines in response to Gag peptide pools stimulation was assessed. The background-subtracted median responses (n = 5) in BALB/c mice following vaccination are shown. Gating strategy for flow cytometric scatter plots to analyze the frequency of the single or multiple cytokine(s)-positive $CD4^+$ **(A)** or $CD8^+$ **(D)** T cells. Frequencies of $CD4^+$ **(B)** or $CD8^+$ **(E)** T cells secrete IFN-γ, TNF-α, and IL-2 cytokines specific to various Gag antigens after adenoviral-based immunization. Further analysis was performed to show subpopulations of double cytokines-secreting $CD4^+$ T cells **(C)** or $CD8^+$ T cells **(F)**. Data were expressed as mean ± SEM, and p-values of less than 0.05 were deemed statistically significant.*$p < 0.05$; **$p < 0.01$; ***$p < 0.001$; NS, no significance.

induced a robust T-cell immunity, and further analysis demonstrated that it contained two CTL epitopes with the potential to target different MHC-I molecules. HIV-1 CRF07_ BC was a recombinant virus of the B′ and C subtypes, which probably shared 50% CTL epitopes in Gag and reverse transcriptase (RT) with prototype B strain (6). Interestingly, the cross-reactive T-cell responses in HIV CRF01_AE and B′ had been observed (37). This evidence supported that there were cross-reactive T-cell responses between 01AE and 07BC, which is consistent with our findings.

To our best knowledge, this is the first study to investigate the immunogenicity of HIV-1 CRF07_BC with or without seven amino acid deletions in the p6 region of the Gag protein, and we found that the seven amino acid deletion in the p6 region contributed to the increased $CD4^+$ and $CD8^+$ T immune response against Gag antigen. These data should be helpful to clarify the mechanism why HIV-1 CRF07_BC-p6Δ7 patients have a lower viral load and slower disease progression than other patients. However, further study is needed to distinguish the clinical course and immunological response in patients infected with CRF07_BC-p6Δ7 compared to CRF07_BC strains. In addition, our findings will also provide insights for the development of Gag-based vaccine strategies against HIV-1 infection.

DATA AVAILABILITY STATEMENT

The raw data supporting the conclusions of this article will be made available by the authors, without undue reservation.

ETHICS STATEMENT

All animal experiments were conducted in the Animal Experimental Center of the Guangzhou Institutes of Biomedicine and Health, Chinese Academy of Sciences. This experimental protocol was approved by the Institutional Animal Care and Use Committee of Guangzhou Institute of Biomedicine and Health (Aprroved number:2020053; Date of acceptance: April 3, 2020; Duration: Four months).

AUTHOR CONTRIBUTIONS

CS conceived and designed the experiments. ML, YY, PL, ZD, ZW, and HW performed the experiments. ML, ZD, ZW, and CS analyzed the data. ML and CS wrote the manuscript. FF, HZ, LC, and ST contributed to the resource and discussion. All of the authors read the final version of the manuscript.

FUNDING

This work was supported by the National Natural Science Foundation of China (81971927), the Natural Science Foundation of Guangdong Province (2019A1515110458), China Postdoctoral Science Foundation (2020T130150ZX), the National Science and Technology Major Project of China (2018ZX10731101-002), and the Science and Technology Planning Project of Shenzhen City (20190804095916056, JSGG20200225152008136, JCYJ20200109142601702).

ACKNOWLEDGMENTS

We would like to thank all colleagues for their technical assistance in the animal experiments.

SUPPLEMENTARY MATERIAL

The Supplementary Material for this article can be found online at: https://www.frontiersin.org/articles/10.3389/fimmu.2022.850719/full#supplementary-material

REFERENCES

1. Yang Q, Feng F, Li P, Pan E, Wu C, He Y, et al. Arsenic Trioxide Impacts Viral Latency and Delays Viral Rebound After Termination of ART in Chronically SIV-Infected Macaques. *Adv Sci (Weinh)* (2019) 6(13):1900319. doi: 10.1002/advs.201900319
2. Wu C, He Y, Zhao J, Luo K, Wen Z, Zhang Y, et al. Exacerbated AIDS Progression by PD-1 Blockade During Therapeutic Vaccination in Chronically SIV-Infected Rhesus Macaques After ART Treatment Interruption. *J Virol* (2022) 96(3):e0178521. doi: 10.1128/JVI.01785-21
3. Ng'uni T, Chasara C, Ndhlovu ZM. Major Scientific Hurdles in HIV Vaccine Development: Historical Perspective and Future Directions. *Front Immunol* (2020) 11:590780. doi: 10.3389/fimmu.2020.590780
4. Wen Z, Sun C. A Zigzag But Upward Way to Develop an HIV-1 Vaccine. *Vaccines (Basel)* (2020) 8(3):511. doi: 10.3390/vaccines8030511
5. Rerks-Ngarm S, Pitisuttithum P, Nitayaphan S, Kaewkungwal J, Chiu J, Paris R, et al. Vaccination With ALVAC and AIDSVAX to Prevent HIV-1 Infection in Thailand. *N Engl J Med* (2009) 361(23):2209–20. doi: 10.1056/NEJMoa0908492
6. Su L, Graf M, Zhang Y, von Briesen H, Xing H, Kostler J, et al. Characterization of a Virtually Full-Length Human Immunodeficiency Virus Type 1 Genome of a Prevalent Intersubtype (C/B') Recombinant Strain in China. *J Virol* (2000) 74(23):11367–76. doi: 10.1128/jvi.74.23.11367-11376.2000
7. Yang R, Xia X, Kusagawa S, Zhang C, Ben K, Takebe Y. On-Going Generation of Multiple Forms of HIV-1 Intersubtype Recombinants in the Yunnan Province of China. *AIDS* (2002) 16(10):1401–7. doi: 10.1097/00002030-200207050-00012
8. Chang SY, Sheng WH, Lee CN, Sun HY, Kao CL, Chang SF, et al. Molecular Epidemiology of HIV Type 1 Subtypes in Taiwan: Outbreak of HIV Type 1 CRF07_BC Infection in Intravenous Drug Users. *AIDS Res Hum Retroviruses* (2006) 22(11):1055–66. doi: 10.1089/aid.2006.22.1055
9. Lin HH, Shih YL, Liu YC, Lee SS, Huang CK, Chen YL, et al. An Epidemic of HIV Type I CRF07_BC Infection Among Injection Drug Users in Taiwan. *J Acquir Immune Defic Syndr* (2006) 42(2):248–55. doi: 10.1097/01.qai.0000214818.80539.da
10. Lin YT, Lan YC, Chen YJ, Huang YH, Lee CM, Liu TT, et al. Molecular Epidemiology of HIV-1 Infection and Full-Length Genomic Analysis of

Circulating Recombinant Form 07_BC Strains From Injection Drug Users in Taiwan. *J Infect Dis* (2007) 195(9):1283–93. doi: 10.1086/513437
11. Wu Y, Wang H, Ren X, Wan Z, Hu G, Tang S. HIV-1 CRF07_BC With a Seven Amino Acid Deletion in the Gag P6 Region Dominates in HIV-1-Infected Men Who Have Sex With Men in China. *AIDS Res Hum Retroviruses* (2017) 33(9):977–83. doi: 10.1089/aid.2017.0075
12. Fujii K, Munshi UM, Ablan SD, Demirov DG, Soheilian F, Nagashima K, et al. Functional Role of Alix in HIV-1 Replication. *Virology* (2009) 391(2):284–92. doi: 10.1016/j.virol.2009.06.016
13. Lin PH, Lai CC, Yang JL, Huang HL, Huang MS, Tsai MS, et al. Slow Immunological Progression in HIV-1 CRF07_BC-Infected Injecting Drug Users. *Emerg Microbes Infect* (2013) 2(12):e83. doi: 10.1038/emi.2013.83
14. Huang SW, Wang SF, Lin YT, Yen CH, Lee CH, Wong WW, et al. Patients Infected With CRF07_BC Have Significantly Lower Viral Loads Than Patients With HIV-1 Subtype B: Mechanism and Impact on Disease Progression. *PloS One* (2014) 9(12):e114441. doi: 10.1371/journal.pone.0114441
15. Goonetilleke N, Liu MK, Salazar-Gonzalez JF, Ferrari G, Giorgi E, Ganusov VV, et al. The First T Cell Response to Transmitted/Founder Virus Contributes to the Control of Acute Viremia in HIV-1 Infection. *J Exp Med* (2009) 206(6):1253–72. doi: 10.1084/jem.20090365
16. Radebe M, Gounder K, Mokgoro M, Ndhlovu ZM, Mncube Z, Mkhize L, et al. Broad and Persistent Gag-Specific CD8+ T-Cell Responses are Associated With Viral Control But Rarely Drive Viral Escape During Primary HIV-1 Infection. *AIDS* (2015) 29(1):23–33. doi: 10.1097/QAD.0000000000000508
17. Koup RA, Safrit JT, Cao Y, Andrews CA, McLeod G, Borkowsky W, et al. Temporal Association of Cellular Immune Responses With the Initial Control of Viremia in Primary Human Immunodeficiency Virus Type 1 Syndrome. *J Virol* (1994) 68(7):4650–5. doi: 10.1128/JVI.68.7.4650-4655.1994
18. Veenhuis RT, Garliss CC, Bailey JR, Blankson JN. CD8 Effector T Cells Function Synergistically With Broadly Neutralizing Antibodies to Enhance Suppression of HIV Infection. *Front Immunol* (2021) 12:708355. doi: 10.3389/fimmu.2021.708355
19. Betts MR, Nason MC, West SM, De Rosa SC, Migueles SA, Abraham J, et al. HIV Nonprogressors Preferentially Maintain Highly Functional HIV-Specific CD8+ T Cells. *Blood* (2006) 107(12):4781–9. doi: 10.1182/blood-2005-12-4818
20. Ndhlovu ZM, Stampouloglou E, Cesa K, Mavrothalassitis O, Alvino DM, Li JZ, et al. The Breadth of Expandable Memory CD8+ T Cells Inversely Correlates With Residual Viral Loads in HIV Elite Controllers. *J Virol* (2015) 89(21):10735–47. doi: 10.1128/JVI.01527-15
21. Geldmacher C, Currier JR, Herrmann E, Haule A, Kuta E, McCutchan F, et al. CD8 T-Cell Recognition of Multiple Epitopes Within Specific Gag Regions Is Associated With Maintenance of a Low Steady-State Viremia in Human Immunodeficiency Virus Type 1-Seropositive Patients. *J Virol* (2007) 81(5):2440–8. doi: 10.1128/JVI.01847-06
22. Kiepiela P, Ngumbela K, Thobakgale C, Ramduth D, Honeyborne I, Moodley E, et al. CD8+ T-Cell Responses to Different HIV Proteins Have Discordant Associations With Viral Load. *Nat Med* (2007) 13(1):46–53. doi: 10.1038/nm1520
23. Sun C, Chen Z, Tang X, Zhang Y, Feng L, Du Y, et al. Mucosal Priming With a Replicating-Vaccinia Virus-Based Vaccine Elicits Protective Immunity to Simian Immunodeficiency Virus Challenge in Rhesus Monkeys. *J Virol* (2013) 87(10):5669–77. doi: 10.1128/JVI.03247-12
24. Pan E, Feng F, Li P, Yang Q, Ma X, Wu C, et al. Immune Protection of SIV Challenge by PD-1 Blockade During Vaccination in Rhesus Monkeys. *Front Immunol* (2018) 9:2415. doi: 10.3389/fimmu.2018.02415
25. Sun C, Zhang L, Zhang M, Liu Y, Zhong M, Ma X, et al. Induction of Balance and Breadth in the Immune Response Is Beneficial for the Control of SIVmac239 Replication in Rhesus Monkeys. *J Infect* (2010) 60(5):371–81. doi: 10.1016/j.jinf.2010.03.005
26. Sun C, Feng L, Zhang Y, Xiao L, Pan W, Li C, et al. Circumventing Antivector Immunity by Using Adenovirus-Infected Blood Cells for Repeated Application of Adenovirus-Vectored Vaccines: Proof of Concept in Rhesus Macaques. *J Virol* (2012) 86(20):11031–42. doi: 10.1128/JVI.00783-12
27. Wu T, Ma F, Ma X, Jia W, Pan E, Cheng G, et al. Regulating Innate and Adaptive Immunity for Controlling SIV Infection by 25-Hydroxycholesterol. *Front Immunol* (2018) 9:2686. doi: 10.3389/fimmu.2018.02686
28. Jurtz V, Paul S, Andreatta M, Marcatili P, Peters B, Nielsen M. NetMHCpan-4.0: Improved Peptide-MHC Class I Interaction Predictions Integrating Eluted Ligand and Peptide Binding Affinity Data. *J Immunol* (2017) 199(9):3360–8. doi: 10.4049/jimmunol.1700893
29. Li M, Zeng J, Li R, Wen Z, Cai Y, Wallin J, et al. Rational Design of a Pan-Coronavirus Vaccine Based on Conserved CTL Epitopes. *Viruses* (2021) 13(2):333. doi: 10.3390/v13020333
30. Wee EG, Moyo N, Hannoun Z, Giorgi EE, Korber B, Hanke T. Effect of Epitope Variant Co-Delivery on the Depth of CD8 T Cell Responses Induced by HIV-1 Conserved Mosaic Vaccines. *Mol Ther Methods Clin Dev* (2021) 21:741–53. doi: 10.1016/j.omtm.2021.04.018
31. Lin CY, Wang WH, Huang SW, Yeh CS, Yuan RY, Yang ZS, et al. The Examination of Viral Characteristics of HIV-1 CRF07_BC and Its Potential Interaction With Extracellular Galectin-3. *Pathogens* (2020) 9(6):425. doi: 10.3390/pathogens9060425
32. Wang SF, Tsao CH, Lin YT, Hsu DK, Chiang ML, Lo CH, et al. Galectin-3 Promotes HIV-1 Budding *via* Association With Alix and Gag P6. *Glycobiology* (2014) 24(11):1022–35. doi: 10.1093/glycob/cwu064
33. Wang WH, Yeh CS, Lin CY, Yuan RY, Urbina AN, Lu PL, et al. Amino Acid Deletions in P6(Gag) Domain of HIV-1 CRF07_BC Ameliorate Galectin-3 Mediated Enhancement in Viral Budding. *Int J Mol Sci* (2020) 21(8):2910. doi: 10.3390/ijms21082910
34. Chen HY, Fermin A, Vardhana S, Weng IC, Lo KF, Chang EY, et al. Galectin-3 Negatively Regulates TCR-Mediated CD4+ T-Cell Activation at the Immunological Synapse. *Proc Natl Acad Sci USA* (2009) 106(34):14496–501. doi: 10.1073/pnas.0903497106
35. Li F, Finnefrock AC, Dubey SA, Korber BT, Szinger J, Cole S, et al. Mapping HIV-1 Vaccine Induced T-Cell Responses: Bias Towards Less-Conserved Regions and Potential Impact on Vaccine Efficacy in the Step Study. *PloS One* (2011) 6(6):e20479. doi: 10.1371/journal.pone.0020479
36. Boppana S, Fiore-Gartland A, Bansal A, Goepfert P. Cross-Reactive CD8 T-Cell Responses Elicited by Adenovirus Type 5-Based HIV-1 Vaccines Contributed to Early Viral Evolution in Vaccine Recipients Who Became Infected. *J Virol* (2020) 94(2):e01632–19. doi: 10.1128/JVI.01632-19
37. Promadej-Lanier N, Thielen C, Hu DJ, Chaowanachan T, Gvetadze R, Choopanya K, et al. Cross-Reactive T Cell Responses in HIV CRF01_AE and B'-Infected Intravenous Drug Users: Implications for Superinfection and Vaccines. *AIDS Res Hum Retroviruses* (2009) 25(1):73–81. doi: 10.1089/aid.2008.0169

Conflict of Interest: The authors declare that the research was conducted in the absence of any commercial or financial relationships that could be construed as a potential conflict of interest.

frontiers | Frontiers in Microbiology

MINI REVIEW
published: 23 June 2022
doi: 10.3389/fmicb.2022.922887

HIV Pre-exposure Prophylaxis and Its Impact on the Gut Microbiome in Men Having Sex With Men

Nicola Luigi Bragazzi[1], Rola Khamisy-Farah[2,3], Christina Tsigalou[4] and Naim Mahroum[5]*

[1]*Laboratory for Industrial and Applied Mathematics (LIAM), Department of Mathematics and Statistics, York University, Toronto, ON, Canada,* [2]*Clalit Health Services, Akko, Israel,* [3]*Azrieli Faculty of Medicine, Bar-Ilan University, Safed, Israel,* [4]*Laboratory of Microbiology, Department of Medicine, Democritus University of Thrace, Alexandroupolis, Greece,* [5]*International School of Medicine, Istanbul Medipol University, Istanbul, Turkey*

HIV/AIDS still imposes a high epidemiological and societal burden. Together with antiretroviral therapy, pre-exposure prophylaxis (PrEP) represents a fundamental tool in the fight against HIV/AIDS. PrEP is considered effective and safe, even though it may affect organs like the kidney, bone, and liver, as shown by randomized clinical trials (RCTs). These side effects may be mediated by alterations of the gut microbiome. Whilst the impact of the human rectal and vaginal microbiome on HIV prevention has been highly investigated among women, less is known about its effect among men having sex with men (MSM), a vulnerable population at high risk for HIV and disproportionately affected by HIV/AIDS. In the present paper, we will overview the effects of PrEP on the gut microbiota in MSM. Mining PubMed/MEDLINE, we identified three studies that have found significant changes affecting the gut microbiota. However, these shifts in the gut microbiome composition are variable, probably due to methodological differences, even though all studies reviewed in the present overview consistently report aberrations at the level of the gut microbiota. More data are needed, especially concerning the long-term side effects of PrEP: despite the studies included being a high-quality RCT, and two well-designed cross-sectional studies, evidence related to the impact of HIV PrEP on the gut microbiome in MSM is scarce and based on small populations. A better understanding of the interactions between the gut microbiota, sexual orientation/identity, and HIV prevention is expected to improve PrEP adherence and devise strategies to counteract PrEP-related side effects.

Keywords: HIV/AIDS, prevention, prophylaxis, gut microbiome, men having sex with men

OPEN ACCESS

Edited by:
Wenyan Zhang,
First Affiliated Hospital of Jilin University, China

Reviewed by:
Stephanie Dillon,
University of Colorado Anschutz Medical Campus, United States
Shulin Qin,
University of Pittsburgh, United States

****Correspondence:***
Nicola Luigi Bragazzi
bragazzi@yorku.ca

Specialty section:
This article was submitted to Infectious Agents and Disease, a section of the journal Frontiers in Microbiology

Received: *18 April 2022*
Accepted: *09 June 2022*
Published: *23 June 2022*

Citation:
Bragazzi NL, Khamisy-Farah R, Tsigalou C and Mahroum N (2022) HIV Pre-exposure Prophylaxis and Its Impact on the Gut Microbiome in Men Having Sex With Men. Front. Microbiol. 13:922887. doi: 10.3389/fmicb.2022.922887

HIV/AIDS AND ITS BURDEN

Despite tremendous scientific and clinical advancements, HIV/AIDS still imposes a dramatically high epidemiological and societal burden. According to the "Global Burden of Disease" (GBD; GBD HIV Collaborators, 2017) Study, in the period from 1980 to 2017 (GBD HIV Collaborators, 2017; Pandey and Galvani, 2019), global HIV-related mortality peaked in 2006 with 1.95 million deaths and subsequently decreased to 0.95 million deaths, whereas new HIV diagnoses peaked in 1999 (with new 3.16 million cases) and gradually decreased to 1.94 million in 2017. This

trend has been possible thanks to the introduction of effective antiretroviral medications, the scale-up and roll-out of which have significantly curbed HIV-related mortality, while, on the other hand, have increased the prevalence of people living with HIV (PLWH)—approximately, 36.8 million in 2017 [a similar figure in 2019 (GBD HIV Collaborators, 2019), 0.84 males per female, 0.99 male infections for every female infection, and 1.02 male deaths per female death]. HIV prevalence is particularly high in low-resource settings and in southern sub-Saharan Africa, with a highly variable coverage of antiretroviral therapy (ART).

Recently, a new technology has been introduced in the pharmacological armamentarium against HIV/AIDS: the so-called pre-exposure prophylaxis, or PrEP.

HIV PRE-EXPOSURE PROPHYLAXIS AND ITS SIDE EFFECTS

Truvada®, a fixed-dose combination antiretroviral medication for HIV prevention (PrEP), was approved by the United States (US) Food and Drug Administration (FDA) in 2012. Its ingredients are tenofovir disoproxil fumarate (TDF)—a nucleotide analog reverse transcriptase (RT) inhibitor (NARTI/NRTI) – and emtricitabine (FTC)—a nucleoside analog reverse RT inhibitor (NtARTI/NtRTI). Descovy®, approved by the FDA in 2016, is a combination of emtricitabine and tenofovir alafenamide (Spinner et al., 2016).

PrEP, if taken once daily as prescribed, is highly effective in preventing HIV, curbing its risk by more than 90% in men having sex with men (MSM). Together with ART, treatment-as-prevention (TASP), and treat-and-test strategies, PrEP is a fundamental tool in the fight against HIV/AIDS. The roll-out of PrEP has, indeed, contributed to halving new HIV diagnoses in countries like Australia and Scotland (Grulich et al., 2018; Estcourt et al., 2021).

While Truvada® and Descovy® are taken orally, Apretude® represents the third formulation of PrEP, which consists of the long-acting, injectable combination of cabotegravir (an integrase inhibitor) and rilpivirine (a non-nucleoside RT inhibitor, NNRTI), administered every 2 months by a specialized healthcare worker (Kim, 2021). It was recently approved by the FDA, in 2021.

However, despite its high effectiveness, PrEP may have some major side effects, affecting organs like the bone, kidney, and liver. Some randomized clinical trials (RCTs) have shown signs of kidney impairment (with the insurgence of renal tubular toxicity, tubular dysfunction, and phosphaturia; Schaefer et al., 2022), decreased bone mineral density (Spinelli et al., 2019; Baranek et al., 2020), and increased values of hepatic transaminases (Mandala et al., 2014). According to a recently published global PrEP user meta-analysis (Schaefer et al., 2022), pooling together 17 articles and synthesizing 11 RCTs, totaling 13,523 participants, PrEP use was associated with an increased risk of grade 1 and higher kidney adverse events (with an odds-ratio, OR, of 1.49 [95% confidence interval, CI 1.22–1.81]) and grade 2 and higher events (with an OR of 1.75 [95%CI 0.68–4.49]). Changes in bone mineral density are variable in the existing scholarly literature, with a substudy of the international, open-label PrEP demonstration project iPrEx-"open-label extension" (OLE) study estimating a 1.2 and 0.5% decrease in the spine and hip bone mineral density, respectively (Spinelli et al., 2019). A recently published systematic review and meta-analysis (Baranek et al., 2020), pooling together 25 studies, has computed a significant bone mineral density drop at the level of the lumbar spine (with a mean difference, MD, of −0.82% [95% from −1.28% to −0.37%]), and hip (with an MD of −0.81% [95%CI from −1.22% to −0.40%]). On the other hand, the use of PrEP was not associated with an increased risk of fracture. Concerning hepatic toxicity (Mandala et al., 2014), this can be mild to moderate, especially in individuals who are hepatitis B virus (HBV) surface antibody (HBsAb) positive or have underlying liver disease.

The cellular and molecular mechanisms of these adverse events are still poorly understood, and given the increasingly prominent role of PrEP in the fight against HIV/AIDS, it is of paramount importance to better understand them. Some scholars hypothesize that reduced bone mineral density may be due to changes in osteoblast gene expression or could occur *via* osteoprotegerin (OPG)/receptor activator of nuclear factor κB (NFκB; RANK) ligand (RANKL)/RANK system dysregulation (Brown et al., 2011; Delpino and Quarleri, 2020), whereas tubular injury may be mediated by the expression of the organic anion transporter 1 (OAT1) and the multidrug resistance protein 4 (MRP4) transporter (Kohler et al., 2011).

PrEP may result also in gastrointestinal side effects (especially within the first 3 months of treatment, known as "PrEP start-up syndrome"; Mugwanya and Baeten, 2016), and may alter the gut microbiome, which is functionally linked to the kidney, bone, and liver. Whilst the impact of the human (vaginal and rectal) microbiome on HIV prevention has been highly investigated and reviewed among women (Velloza and Heffron, 2017; Farcasanu and Kwon, 2018; Abdool Karim et al., 2019), less is known about its effect among MSM, despite the fact that this population is particularly at high risk for HIV and is disproportionately affected by HIV/AIDS. To the best of our knowledge, there are no comprehensive reviews covering this important topic. In the present paper, we will briefly overview the effects of the use of PrEP on the gut microbiota in MSM. For this purpose, we have mined PubMed/MEDLINE, the major biomedical database, searching for words such as "gut flora," "gut microbial communities," "gut microbiota," "gut microbiome," "intestine," "rectal," "anal," "HIV," "AIDS," "men having sex with men," "sexual identity," "sexual orientation," "tenofovir," "emtricitabine," and "pre-exposure prophylaxis."

THE GUT MICROBIOME AND ITS IMPACT ON HEALTH AND DISEASE

The gut microbiome is extremely heterogeneous and plastic and consists of a highly diverse population of bacteria that can have both beneficial and detrimental impacts on human health (Fan and Pedersen, 2021). It is composed of more than

1,200 species of bacteria (Rinninella et al., 2019), including *Bacteroides*, *Actinomycetes*, *Firmicutes*, *Proteobacteria*, and *Verrucomicrobia*. It plays different functions, ranging from nutrient absorption (in particular, micro-nutrients), and processing to metabolic homeostasis (including favoring insulin sensitivity), and fine-tuning of the immune system, protecting especially newborns from respiratory and intestinal infections and pathogen invasion (Flint et al., 2012). It can also provide the individual with sources of energy, by fermenting and processing short-chain fatty acids (SCFAs), like butyrate, acetate, and propionate (Valdes et al., 2018).

Aberrations at the level of the gut microbiota and enteric dysbiosis have been linked with several disorders, like autoimmune diseases, such as rheumatoid arthritis (RA; Bodkhe et al., 2019), liver disease (like non-alcoholic fatty liver disease or NAFLD; Wang et al., 2021), overweight and obesity, type 1 and 2 diabetes, malnutrition, and other metabolic/nutritional impairments, malignancies (especially colon cancer; Tortora et al., 2022), irritable bowel syndrome (IBS), inflammatory bowel disease (IBD; Glassner et al., 2020), and neurological diseases (Parkinson's disease, transient cerebral ischemia, and ischemic stroke; Pluta et al., 2021; Romano et al., 2021), among others.

Gut microbiome-axes have also been demonstrated for the numerous organs impacted by PreP. The gut microbiota is dynamically interconnected with the kidney. In individuals with chronic kidney disease (CKD), it may be impaired and produce several uremic toxins and solutes, like p-cresyl sulfate (PCS), trimethylamine (TMA) N-oxide (TMAO), and indoxyl sulfate. In turn, increased urea levels result in gut microbiome alterations. The release of uremic toxic metabolites may lead to renal anemia, asthenia, pruritus, impaired mineral bone density, cardiovascular, and neurological disorders, which are commonly observed in CKD patients as well as in subjects with acute kidney injury (AKI), IgA nephropathy, nephrolithiasis, hypertension, or those needing hemodialysis/peritoneal dialysis (Chen et al., 2019; Hobby et al., 2019; Stavropoulou et al., 2021). Gut microbiota overgrowth or change in profile composition may result in alterations in calcium, vitamin K, and vitamin B levels, as well as in vitamin D absorption and metabolism, leading to fractures and osteoporosis (Ding et al., 2020). Cellular and molecular mechanisms include modulation of insulin-like growth factor (IGF)-1-related cascades. IGF-1 is known to fine-tune the bone cells' differentiation into osteoblasts, osteoclasts, and chondrocytes (Pacifici, 2018). The gut microbiota can also affect the concentrations of vitamin D metabolites, steroid hormones, and the parathyroid hormone (PTH; Pacifici, 2018). A new, high interdisciplinary field is emerging, termed "osteomicrobiology," to underline the strong links and connections between bone and microbes (Bhardwaj et al., 2022). The gut microbiome also impacts liver functioning. Gut microbiota overgrowth and, in particular, small intestinal bacterial overgrowth (SIBO) of Gram-negative pathogens contribute to reducing overall microbial diversity and to tissue damage, by the production and release of bacterial 16sDNA, ethanol, toxic metabolites, and endotoxins (like TMAO and LPS), which inhibit cholesterol conversion into bile acids, alter intestinal permeability, promote a pro-inflammatory *milieu*, modulate apoptotic cascades and exacerbate the underlying liver disease (Zhou et al., 2021). Impaired fermentation and processing of SCFAs result in decreased stimulation of gut endocrine cells and reduced secretion of glucagon-like peptide 1 (GLP-1) with a subsequent drop in hepatic fatty acid β-oxidation and lipogenesis. Also, PPARα-mediated β-oxidation of fatty acids is altered, leading to a worsening of hepatosteatosis and liver disease. Moreover, aberrant gut microbiota leads to the activation of hepatic stellate cells (HSCs) *via* the intrahepatic T-cell receptor (TCR) immune repertoire (IR; TCR-IR; Liang et al., 2020). This results in the shift from a quiescent to an active, proliferative, migratory, and fibrogenic phenotype, transforming the cell into a myofibroblast, contributing to liver fibrogenesis.

THE GUT MICROBIOME AND HIV/AIDS

Among the different diseases, changes in the human microbiome composition have been associated with HIV serostatus (Noguera-Julian et al., 2016; Tuddenham et al., 2020; Zhou et al., 2020), with a few exceptions (Li et al., 2019). Shifts in microbial composition have been linked as well with sexual orientation/sexual identity (Noguera-Julian et al., 2016; Li et al., 2019; Tuddenham et al., 2020; Zhou et al., 2020), as shown also by animal models (Li et al., 2019). Li et al. (2019) transplanted feces from HIV-negative men having sex with women (MSW) and MSM, as well as from HIV-positive untreated MSM to gnotobiotic mice. After the transplant, the microbiomes of MSM and MSW conserved distinct compositions in mice. From an immunological standpoint, HIV-negative MSM donors exhibited higher frequencies of blood CD38+ HLA-DR+ and CD103+ T-cells whereas their fecal recipients had higher frequencies of gut CD69+ and CD103+ T-cells. Probably due to the small sample size employed, the authors failed to detect statistically significant differences induced by HIV serostatus both at the level of the microbiome and immunologically. On the other hand, after infecting primary human *lamina propria* cells treated with fecal microbiota, gut flora from MSM caused higher levels of HIV replication. Among humans, HIV-seropositive individuals and MSM consistently report alterations in the gut flora, affecting, for instance, *Bacteroides caccae*, *Bacteroides ovatus*, *Bacteroides uniformis*, and *Prevotella stercorea*, with markedly reduced richness and alpha diversity of the gut microbiota. This can be accompanied by profound metabolic changes involving several functional pathways (such as those regulating carbohydrate, lipid, and amino acid metabolism), according to a recently published systematic review and meta-analysis of 12 studies (Zhou et al., 2020).

Further, the gut microbiome may increase the risk of contracting HIV (Coleman et al., 2020) *via* increased expression of integrin and chemokine receptors on T-cells, especially at the level of the colon. Furthermore, it may influence HIV transmission (Coleman et al., 2020), favoring HIV persistence (Koay et al., 2018) through immune activation and systemic inflammation, and impacting the progression from acute HIV

infection (AHI; Sortino et al., 2019) to AIDS (Sortino et al., 2019), with microbiota diversity correlating with CD4+ T-cell diversity (Koay et al., 2018; Sortino et al., 2019). As the disease progresses, an increase in pathogenic species, including *Proteobacteria*, and a decrease in protective ones (like *Bacteroides*, *Lactobacillus*, and *Bifidobacterium*) are observed (Ling et al., 2016; Ribeiro et al., 2017; Vujkovic-Cvijin et al., 2020). The intestinal microbiome plays a key role also in the pathogenesis of HIV/AIDS- and age-related comorbidities, like cardiovascular disease, stroke, malignancy, long-bone fractures, and renal impairment/dysfunction (Sortino et al., 2019). Moreover, the gut microbiota has effects on HIV drug metabolism, pharmacokinetics, and effectiveness (Imahashi et al., 2021).

THE GUT MICROBIOME AND HIV PRE-EXPOSURE PROPHYLAXIS

Few studies have investigated the impact of HIV PrEP on the gut microbiome, by conducting metagenomic analyses and next-generation sequencing (NGS) of the bacterial 16S/16S-23S ribosomal RNA (rRNA) gene(s) in highly adherent PrEP users to assess the relative abundance of family and genus and potential changes/shifts in the enteric microbiome. Features of these studies are summarized in **Table 1**.

Dubé et al. (2018) were the first to detect and report alterations in the microbiome composition, with *Erysipelotrichaceae* (in particular, *Catenibacterium mitsuokai*, *Holdemanella biformis*, and *Turicibacter sanguinis*) and *Streptococcaceae* (especially, *Streptococcus agalactiae*, *Streptococcus oralis*, and *Streptococcus mitis*) being increased [by a mean $\log_2$ (fold change) of 2.1, from 0.79 to 3.3%] and being decreased [by a mean $\log_2$ (fold change) of −3.3, from 12.0 to 1.2%], respectively, already after 48 weeks of PrEP administration. No correlation with PrEP duration, antiretroviral levels, race, age, drug use, or abuse could be found. The authors hypothesized that changes in the gut microbiome may be linked with serious long-term side events, like colorectal malignancy, metabolic, and cardiovascular disease. However, at the moment, this remains a hypothesis not supported by clinical data, that, anyway, warrants further investigations, according to the same authors.

Different findings were reported by Fulcher et al. (2019), who performed a cross-sectional study, comparing off versus on PrEP users, matched using propensity score 1:1 matching and performing logistic regression based on several covariates. These included age, race/ethnicity, BMI, smoking, alcohol and drug use (methamphetamine, and marijuana), and antibiotic use in the past month (single-dose azithromycin, ceftriaxone, or doxycycline), and sexual practices (recent receptive anal intercourse in the last 7 days and number of acts in the last month). Differently from Dubé et al. (2018) and Fulcher et al. (2019) found that the use of PrEP significantly correlated with an increase in *Streptococcus*. Other pathogens the abundance of which was increased were *Mitsuokella*, and *Fusobacterium*, while a decrease in *Escherichia* and *Shigella* abundance was observed. Of note, increased *Fusobacterium* was associated with increasing exposure to tenofovir, again differently from Dubé et al. (2018), who did not observe any correlation with antiretroviral concentrations. Similarly to Dubé et al. (2018) also Fulcher et al. (2019) warned about the potential long-term side-effects of oral PrEP: indeed, in the literature, increased *Fusobacterium* has been associated with inflammatory conditions, IBD, and colorectal cancer.

Finally, Perler et al. (2021) compared on and off PrEP individuals. In the group of PrEP users, the authors detected a statistically significant decrease in *Pasteurellaceae*, *Corynebacteriaceae*, *Clostridiales* Family XI (at the family level), and *Finegoldia* and *Corynebacterium* 1 (at the genus level), and an increase in *Catenibacterium* and *Prevotella* 2, while no changes were observed at the phylum level. Noteworthy, the increase in *Catenibacterium* had been previously reported by Dubé et al. (2018). *Prevotella* 9 was slightly higher in the PrEP user's group, but not in a statistically significant way. Moreover, this group had a higher number of male receptive anal sex partners, which correlated with the relative abundance of *Prevotella* 2, but not of *Finegoldia* or *Streptococcus*. No changes/shifts in *Streptococcaceae* and *Erysipelotrichaceae* could be observed, differently from previously published studies (Dubé et al., 2018; Fulcher et al., 2019). Of note, no differences could be detected in terms of human behaviors and lifestyles, like drugs/antibiotics exposure, sexual practices (anilingus), hygiene (rectal douching/enema), use of stool softeners, probiotic supplementations, use of lubricants, or use of saliva as a lubricant, and gastrointestinal symptoms, among others. Interestingly, sexually transmitted infections (STIs) were not found to impact the gut microbiome composition. Finally, alpha diversity did not change (as in previous studies; Dubé et al., 2018; Fulcher et al., 2019), differently from beta diversity. In line with the other studies overviewed in the present review (Dubé et al., 2018; Fulcher et al., 2019), the authors concluded that increased pathogens may lead to long-term periodontal disease, RA, insulin resistance, morbid obesity and metabolic impairments, and cardiovascular disease.

While all the studies analyzed consistently report changes and shifts in the gut microbiota, there are differences at the phylum, family, and/or genus level. This could be due to: (i) the different study design (cross-sectional versus longitudinal, case–control versus RCT), (ii) the sample size employed, (iii) the microbiome analysis methods and techniques used for specimen collection (rectal swab versus mucosal biopsy; Araújo-Pérez et al., 2012), and bioinformatics/statistical analysis, and (iv) the period of treatment (from a few months to some years, short- versus long-term). Moreover, further information should be collected about lifestyles, including dietary intake, exercise/physical activity, and sexual practices, which are known to modulate the gut microbiome composition. For example, the use of lubricants could have an effect on gut flora. Haaland et al. (2018) investigated whether the rectal application of a hyperosmolar lubricant impacted tenofovir drug tissue concentration in the rectum and related secretions and the composition of the gut microbiome. The authors found no effects on mucosal PrEP concentration but detected an impact of the use of lubricant on the gut microbiota, with decreased

TABLE 1 | Major features of studies overviewed in the present mini-review.

Study	Sample size	Study design	Specimen	Microbiome profiling technique	Statistical analysis	Age	Race/ ethnicity	Factors potentially affecting the gut microbiota	Sexual behavior	PrEP treatment length	Adherence to PrEP	Increased gut flora	Decreased gut flora	Alpha diversity	Beta diversity	Overall diversity and composition
Dubé et al., 2018	8	Sub-study from the RCT NCT01761643 (cohort "California Collaborative Treatment Group study 595," CCTG-595)	Self-collected rectal swab	Short-read sequencing of bacterial 16S rRNA gene V4 region and long-read sequencing of bacterial 16S–23S rRNA gene V4 region	Permutation tests and PCA clustering analysis	34.8 ± 9.1 (range 22–52) years	Half white, one Asian, one black, and two "of multiple races"	6/8 reporting rectal douching 6/8 reporting any drug use 3/8 reporting drug abuse	NA	48–72 weeks (72 weeks in 5 participants, 48 weeks in 2 subjects, and 60 weeks in 1 participant)	Very good or excellent in 100% of the participants	*Erysipelotrichaceae* (*Catenibacterium mitsuokai*, *Holdemanella biformis*, and *Turicibacter sanguinis*)	*Streptococcaceae* (*Streptococcus agalactiae*, *Streptococcus oralis*, and *S. mitis*)	No changes	β diversity between each participant's pre and post-PrEP specimens was smaller than the β diversity of pre-PrEP specimen pairs of different individuals	No changes
Fulcher et al., 2019	74 (37 on PrEP versus 37 off PrEP)	Cross-sectional, matched case–control study, with participants selected from the ongoing cohort mSTUDY	Rectal swabs collected under direct mucosal visualization *via* anoscopy without preparatory enema	Sequencing of the V4 region of the 16S rRNA gene	Zero-inflated negative binomial models, multinomial LASSO as confirmatory analysis	30.1 ± 6.7 (median 29) years for the control and 29.8 ± 6.5 (median 28) years for the PrEP users' group	56.8% black non-Hispanic, 32.4% Hispanic, 10.8% other non-Hispanic	26/37 reporting marjuana use 7/37 reporting methamphetamine use 10/37 reporting tobacco use 28/37 reporting binge alcohol use 4/37 reporting antibiotic use in the past month 35.1% obese	45.9% recent receptive anal intercourse (2.2 ± 4.5) *per* month)	41 weeks (IQR 14–59 weeks)	Very good or excellent in 78% of the participants	*Streptococcus*, *Mitsuokella*, and *Fusobacterium*	*Escherichia* and *Shigella*	No changes	NA	No changes
Perler et al., 2021	27: 14 taking PrEP	Cross-sectional, case–control study	Self-collected rectal swabs	Sequencing of the V4 region of the 16S rRNA gene	Linear regressions, linear discriminant analysis, Bray–Curtis dissimilarity analysis	36 years (on PrEP), 29 years off PrEP	NA	NA	8.43 partners *per* month	171 weeks (3.3 years)	NA	*Catenibacterium* and *Prevotella* 2	*Pasteurellaceae*, *Corynebacteriaceae*, *Clostridiales* Family XI (at the family level), and *Finegoldia* and *Corynebacterium* 1 (at the genus level)	No changes	Significant changes in the PrEP group	No changes

Bacteroides, increased concentrations of *Prevotella* (statistically borderline significant), and increased microbial diversity. A statistically significant interaction between the use of PrEP and lubricant was found for the relative abundance of the genus *Alicyclobacillus*. Of note, not all the studies analyzed, have adjusted for confounding factors.

CONCLUSION AND FUTURE PROSPECTS

As stated by Hughes et al. (2020), PrEP represents a unique opportunity to study the effects of Truvada® and Descovy® for PrEP on the gut microbiota without the interference of HIV, other drugs, and/or HIV/AIDS-related co-morbidities, as well as other confounding factors. These drugs are generally considered effective and safe. However, the study by Hughes and collaborators (Hughes et al., 2020) and the studies retained in the current review (Araújo-Pérez et al., 2012; Haaland et al., 2018; Hughes et al., 2020) have shown that they may alter and impair the gut microbiota, and repress the transcription of several nuclear transcription factors, inhibit the anti-inflammatory function of mucosal epithelial cells, by favoring a pro-inflammatory milieu, and promote gene signatures related to increased cell viability and proliferation as well as increase the abundance of pathogenic microbes, potentially linked to serious conditions and diseases. However, more data are urgently needed, especially concerning the long-term side effects of PrEP: despite the fact that the studies included in the present overview are a high-quality RCT, and two well-designed cross-sectional studies, evidence related to the impact of HIV PrEP on the gut microbiome in MSMs is still scarce and based on small populations. A better understanding of the complex, nonlinear interactions between the gut microbiota, sexual orientation/identity, and HIV prevention is expected to significantly improve PrEP adherence and potentially devise interventional strategies to counteract PrEP-related side effects.

AUTHOR CONTRIBUTIONS

All authors listed have made a substantial, direct, and intellectual contribution to the work and approved it for publication.

REFERENCES

Abdool Karim, S. S., Baxter, C., Passmore, J. S., McKinnon, L. R., and Williams, B. L. (2019). The genital tract and rectal microbiomes: their role in HIV susceptibility and prevention in women. *J. Int. AIDS Soc.* 22:e25300. doi: 10.1002/jia2.25300

Araújo-Pérez, F., McCoy, A. N., Okechukwu, C., Carroll, I. M., Smith, K. M., Jeremiah, K., et al. (2012). Differences in microbial signatures between rectal mucosal biopsies and rectal swabs. *Gut Microbes* 3, 530–535. doi: 10.4161/gmic.22157

Baranek, B., Wang, S., Cheung, A. M., Mishra, S., and Tan, D. H. (2020). The effect of tenofovir disoproxil fumarate on bone mineral density: a systematic review and meta-analysis. *Antivir. Ther.* 25, 21–32. doi: 10.3851/IMP3346

Bhardwaj, A., Sapra, L., Tiwari, A., Mishra, P. K., Sharma, S., and Srivastava, R. K. (2022). "Osteomicrobiology": The Nexus Between bone and bugs. *Front. Microbiol.* 12:812466. doi: 10.3389/fmicb.2021.812466

Bodkhe, R., Balakrishnan, B., and Taneja, V. (2019). The role of microbiome in rheumatoid arthritis treatment. *Ther. Adv. Musculoskelet. Dis.* 11:1759720X19844632. doi: 10.1177/1759720X19844632

Brown, T. T., Ross, A. C., Storer, N., Labbato, D., and McComsey, G. A. (2011). Bone turnover, osteoprotegerin/RANKL and inflammation with antiretroviral initiation: tenofovir versus non-tenofovir regimens. *Antivir. Ther.* 16, 1063–1072. doi: 10.3851/IMP1874

Chen, Y. Y., Chen, D. Q., Chen, L., Liu, J. R., Vaziri, N. D., Guo, Y., et al. (2019). Microbiome-metabolome reveals the contribution of gut-kidney axis on kidney disease. *J. Transl. Med.* 17:5. doi: 10.1186/s12967-018-1756-4

Coleman, S. L., Neff, C. P., Li, S. X., Armstrong, A. J. S., Schneider, J. M., Sen, S., et al. (2020). Can gut microbiota of men who have sex with men influence HIV transmission? *Gut Microbes* 11, 610–619. doi: 10.1080/19490976.2019.170075

Delpino, M. V., and Quarleri, J. (2020). Influence of HIV infection and antiretroviral therapy on bone homeostasis. *Front. Endocrinol.* 11:502. doi: 10.3389/fendo.2020.00502

Ding, K., Hua, F., and Ding, W. (2020). Gut microbiome and osteoporosis. *Aging Dis.* 11, 438–447. doi: 10.14336/AD.2019.0523

Dubé, M. P., Park, S. Y., Ross, H., Love, T. M. T., Morris, S. R., and Lee, H. Y. (2018). Daily HIV pre-exposure prophylaxis (PrEP) with tenofovir disoproxil fumarate-emtricitabine reduced Streptococcus and increased Erysipelotrichaceae in rectal microbiota. *Sci. Rep.* 8:15212. doi: 10.1038/s41598-018-33524-6

Estcourt, C., Yeung, A., Nandwani, R., Goldberg, D., Cullen, B., Steedman, N., et al. (2021). Population-level effectiveness of a national HIV preexposure prophylaxis programme in MSM. *AIDS* 35, 665–673. doi: 10.1097/QAD.0000000000002790

Fan, Y., and Pedersen, O. (2021). Gut microbiota in human metabolic health and disease. *Nat. Rev. Microbiol.* 19, 55–71. doi: 10.1038/s41579-020-0433-9

Farcasanu, M., and Kwon, D. S. (2018). The influence of Cervicovaginal microbiota on mucosal immunity and prophylaxis in the Battle against HIV. *Curr. HIV/AIDS Rep.* 15, 30–38. doi: 10.1007/s11904-018-0380-5

Flint, H. J., Scott, K. P., Louis, P., and Duncan, S. H. (2012). The role of the gut microbiota in nutrition and health. *Nat. Rev. Gastroenterol. Hepatol.* 9, 577–589. doi: 10.1038/nrgastro.2012.156

Fulcher, J. A., Li, F., Cook, R. R., Zabih, S., Louie, A., Okochi, H., et al. (2019). Rectal microbiome alterations associated With Oral human immunodeficiency virus pre-exposure prophylaxis. Open forum. *Infect. Dis.* 6:ofz463. doi: 10.1093/ofid/ofz463

GBD HIV Collaborators (2017). Global, regional, and national incidence, prevalence, and mortality of HIV, 1980–2017, and forecasts to 2030, for 195 countries and territories: a systematic analysis for the Global Burden of Diseases, Injuries, and Risk Factors Study 2017. *Lancet HIV* 6, e831–e859. doi: 10.1016/S2352-3018(19)30196-1

GBD HIV Collaborators (2019). Global, regional, and national sex-specific burden and control of the HIV epidemic, 1990-2019, for 204 countries and territories: the global burden of diseases study 2019. *Lancet HIV* 8, e633–e651. doi: 10.1016/S2352-3018(21)00152-1

Glassner, K. L., Abraham, B. P., and Quigley, E. M. M. (2020). The microbiome and inflammatory bowel disease. *J. Allergy Clin. Immunol.* 145, 16–27. doi: 10.1016/j.jaci.2019.11.003

Grulich, A. E., Guy, R., Amin, J., Jin, F., Selvey, C., Holden, J., et al. (2018). Expanded PrEP implementation in communities New South Wales (EPIC-NSW) research group. Population-level effectiveness of rapid, targeted, high-coverage roll-out of HIV pre-exposure prophylaxis in men who have sex with men: the EPIC-NSW prospective cohort study. *Lancet HIV.* 5, e629–e637. doi: 10.1016/S2352-3018(18)30215-7

Haaland, R. E., Fountain, J., Hu, Y., Holder, A., Dinh, C., Hall, L., et al. (2018). Repeated rectal application of a hyperosmolar lubricant is associated with microbiota shifts but does not affect PrEP drug concentrations: results from a randomized trial in men who have sex with men. *J. Int. AIDS Soc.* 21:e25199. doi: 10.1002/jia2.25199

Hobby, G. P., Karaduta, O., Dusio, G. F., Singh, M., Zybailov, B. L., and Arthur, J. M. (2019). Chronic kidney disease and the gut microbiome. *Am. J. Physiol. Renal Physiol.* 316, F1211–F1217. doi: 10.1152/ajprenal.00298.2018

Hughes, S. M., Levy, C. N., Calienes, F. L., Stekler, J. D., Pandey, U., Vojtech, L., et al. (2020). Treatment with commonly used antiretroviral drugs induces a type I/III interferon signature in the gut in the absence of HIV infection. *Cell Rep Med.* 1:100096. doi: 10.1016/j.xcrm.2020.100096

Imahashi, M., Ode, H., Kobayashi, A., Nemoto, M., Matsuda, M., Hashiba, C., et al. (2021). Impact of long-term antiretroviral therapy on gut and oral microbiotas in HIV-1-infected patients. *Sci. Rep.* 11:960. doi: 10.1038/s41598-020-80247-8

Kim, Y. S. (2021). Long-acting injectable antiretroviral agents for HIV treatment and prevention. *Infect Chemother.* 53, 686–695. doi: 10.3947/ic.2021.0136

Koay, W. L. A., Siems, L. V., and Persaud, D. (2018). The microbiome and HIV persistence: implications for viral remission and cure. *Curr. Opin. HIV AIDS* 13, 61–68. doi: 10.1097/COH.0000000000000434

Kohler, J. J., Hosseini, S. H., Green, E., Abuin, A., Ludaway, T., Russ, R., et al. (2011). Tenofovir renal proximal tubular toxicity is regulated by OAT1 and MRP4 transporters. *Lab. Investig.* 91, 852–858. doi: 10.1038/labinvest.2011.48

Li, S. X., Sen, S., Schneider, J. M., Xiong, K. N., Nusbacher, N. M., Moreno-Huizar, N., et al. (2019). Gut microbiota from high-risk men who have sex with men drive immune activation in gnotobiotic mice and in vitro HIV infection. *PLoS Pathog.* 15:e1007611. doi: 10.1371/journal.ppat.1007611

Liang, Q., Zhang, M., Hu, Y., Zhang, W., Zhu, P., Chen, Y., et al. (2020). Gut microbiome contributes to liver fibrosis impact on T cell receptor immune repertoire. *Front. Microbiol.* 11:571847. doi: 10.3389/fmicb.2020.571847

Ling, Z., Jin, C., Xie, T., Cheng, Y., Li, L., and Wu, N. (2016). Alterations in the fecal microbiota of patients with HIV-1 infection: An observational study in A Chinese population. *Sci. Rep.* 6:30673. doi: 10.1038/srep30673

Mandala, J., Nanda, K., Wang, M., De Baetselier, I., Deese, J., Lombaard, J., et al. (2014). Liver and renal safety of tenofovir disoproxil fumarate in combination with emtricitabine among African women in a pre-exposure prophylaxis trial. *BMC Pharmacol. Toxicol.* 15:77. doi: 10.1186/2050-6511-15-77

Mugwanya, K. K., and Baeten, J. M. (2016). Safety of oral tenofovir disoproxil fumarate-based pre-exposure prophylaxis for HIV prevention. *Expert Opin. Drug Saf.* 15, 265–273. doi: 10.1517/14740338.2016.1128412

Noguera-Julian, M., Rocafort, M., Guillén, Y., Rivera, J., Casadellà, M., Nowak, P., et al. (2016). Gut microbiota linked to sexual preference and HIV infection. *EBioMedicine* 5, 135–146. doi: 10.1016/j.ebiom.2016.01.032

Pacifici, R. (2018). Bone remodeling and the microbiome. *Cold Spring Harb. Perspect. Med.* 8:a031203. doi: 10.1101/cshperspect.a031203

Pandey, A., and Galvani, A. P. (2019). The global burden of HIV and prospects for control. *Lancet HIV.* 6, e809–e811. doi: 10.1016/S2352-3018(19)30230-9

Perler, B. K., Reinhart, E. M., Montgomery, M., Maynard, M., Shapiro, J. M., Belenky, P., et al. (2021). Evaluation of the microbiome in men taking pre-exposure prophylaxis for HIV prevention. *AIDS Behav.* 25, 2005–2013. doi: 10.1007/s10461-020-03130-7

Pluta, R., Januszewski, S., and Czuczwar, S. J. (2021). The role of gut microbiota in an ischemic stroke. *Int. J. Mol. Sci.* 22:915. doi: 10.3390/ijms22020915

Ribeiro, A. B. D. T. M., Heimesaat, M. M., and Bereswill, S. (2017). Changes of the intestinal microbiome-host homeostasis in HIV-infected individuals - A focus on the bacterial gut microbiome. *Eur. J. Microbiol. Immunol.* 7, 158–167. doi: 10.1556/1886.2017.00016

Rinninella, E., Raoul, P., Cintoni, M., Franceschi, F., Miggiano, G. A. D., Gasbarrini, A., et al. (2019). What is the healthy gut microbiota composition? A changing ecosystem across age, environment, diet, and diseases. *Microorganisms.* 7:14. doi: 10.3390/microorganisms7010014

Romano, S., Savva, G. M., Bedarf, J. R., Charles, I. G., Hildebrand, F., and Narbad, A. (2021). Meta-analysis of the Parkinson's disease gut microbiome suggests alterations linked to intestinal inflammation. *NPJ Parkinsons. Dis.* 7:27. doi: 10.1038/s41531-021-00156-z

Schaefer, R., da Costa, A., Leite, P. H., Silva, R., Abdool Karim, Q., Akolo, C., et al. (2022). Kidney function in tenofovir disoproxil fumarate-based oral pre-exposure prophylaxis users: a systematic review and meta-analysis of published literature and a multi-country meta-analysis of individual participant data. *Lancet HIV* 9, e242–e253. doi: 10.1016/S2352-3018(22)00004-2

Sortino, O., Phanuphak, N., Schuetz, A., Ortiz, A. M., Chomchey, N., Belkaid, Y., et al. (2019). RV254/SEARCH010 study group. Impact of acute HIV infection and early antiretroviral therapy on the human gut microbiome. Open Forum *Infect. Dis.* 7:ofz367. doi: 10.1093/ofid/ofz367

Spinelli, M. A., Glidden, D. V., Anderson, P. L., Gandhi, M., McMahan, V. M., Defechereux, P., et al. (2019). Impact of estimated pre-exposure prophylaxis (PrEP) adherence patterns on bone mineral density in a large PrEP demonstration project. *AIDS Res. Hum. Retrovir.* 35, 788–793. doi: 10.1089/AID.2018.0297

Spinner, C. D., Boesecke, C., Zink, A., Jessen, H., Stellbrink, H. J., Rockstroh, J. K., et al. (2016). HIV pre-exposure prophylaxis (PrEP): a review of current knowledge of oral systemic HIV PrEP in humans. *Infection* 44, 151–158. doi: 10.1007/s15010-015-0850-2

Stavropoulou, E., Kantartzi, K., Tsigalou, C., Konstantinidis, T., Romanidou, G., Voidarou, C., et al. (2021). Focus on the gut-kidney Axis in health and disease. *Front. Med.* 7:620102. doi: 10.3389/fmed.2020.620102

Tortora, S. C., Bodiwala, V. M., Quinn, A., Martello, L. A., and Vignesh, S. (2022). Microbiome and colorectal carcinogenesis: linked mechanisms and racial differences. *World J. Gastrointest. Oncol.* 14, 375–395. doi: 10.4251/wjgo.v14.i2.375

Tuddenham, S. A., Koay, W. L. A., Zhao, N., White, J. R., Ghanem, K. G., and Sears, C. L. (2020). HIV microbiome re-analysis consortium. The impact of human immunodeficiency virus infection on gut microbiota α-diversity: An individual-level Meta-analysis. *Clin. Infect. Dis.* 70, 615–627. doi: 10.1093/cid/ciz258

Valdes, A. M., Walter, J., Segal, E., and Spector, T. D. (2018). Role of the gut microbiota in nutrition and health. *BMJ* 361:k2179. doi: 10.1136/bmj.k2179

Velloza, J., and Heffron, R. (2017). The vaginal microbiome and its potential to impact efficacy of HIV pre-exposure prophylaxis for women. *Curr. HIV/AIDS Rep.* 14, 153–160. doi: 10.1007/s11904-017-0362-z

Vujkovic-Cvijin, I., Sortino, O., Verheij, E., Sklar, J., Wit, F. W., Kootstra, N. A., et al. (2020). HIV-associated gut dysbiosis is independent of sexual practice and correlates with noncommunicable diseases. *Nat. Commun.* 11:2448. doi: 10.1038/s41467-020-16222-8

Wang, R., Tang, R., Li, B., Ma, X., Schnabl, B., and Tilg, H. (2021). Gut microbiome, liver immunology, and liver diseases. *Cell. Mol. Immunol.* 18, 4–17. doi: 10.1038/s41423-020-00592-6

Zhou, J., Tripathi, M., Sinha, R. A., Singh, B. K., and Yen, P. M. (2021). Gut microbiota and their metabolites in the progression of non-alcoholic fatty liver disease. *Hepatoma Res.* 2021:11. doi: 10.20517/2394-5079.2020.134

Zhou, J., Zhang, Y., Cui, P., Luo, L., Chen, H., Liang, B., et al. (2020). Gut microbiome changes associated With HIV infection and sexual orientation. *Front. Cell. Infect. Microbiol.* 10:434. doi: 10.3389/fcimb.2020.00434

Conflict of Interest: The authors declare that the research was conducted in the absence of any commercial or financial relationships that could be construed as a potential conflict of interest.

frontiers | Frontiers in Microbiology

ORIGINAL RESEARCH
published: 23 June 2022
doi: 10.3389/fmicb.2022.888996

Profile of the Lower Respiratory Tract Microbiome in Human Immunodeficiency Virus/Acquired Immunodeficiency Syndrome and Lung Disease

Zhen Chen[1†], Ya Tian[1†], Yu Wang[2], Hongxin Zhao[2], Chen Chen[3] and Fujie Zhang[2]**

[1] Savaid Medical School, University of Chinese Academy of Sciences, Beijing, China, [2] Affiliated Beijing Ditan Hospital, Capital Medical University, Beijing, China, [3] Affiliated Beijing Shijitan Hospital, Capital Medical University, Beijing, China

OPEN ACCESS

Edited by:
Kai Deng,
Sun Yat-sen University, China

Reviewed by:
Zhang Wang,
South China Normal University, China
Tao Ding,
Sun Yat-sen University, China

***Correspondence:**
Chen Chen
chenchen.bj2008@163.com
Fujie Zhang
treatment@chinaaids.cn

[†] These authors have contributed equally to this work

Specialty section:
This article was submitted to Infectious Agents and Disease, a section of the journal Frontiers in Microbiology

Received: 03 March 2022
Accepted: 23 May 2022
Published: 23 June 2022

Citation:
Chen Z, Tian Y, Wang Y, Zhao H, Chen C and Zhang F (2022) Profile of the Lower Respiratory Tract Microbiome in Human Immunodeficiency Virus/Acquired Immunodeficiency Syndrome and Lung Disease. Front. Microbiol. 13:888996. doi: 10.3389/fmicb.2022.888996

Once an human immunodeficiency virus (HIV)-infected individual enters the onset period, a variety of opportunistic infections may occur, affecting various systems and organs throughout the body, due to the considerable reduction in the body's immune function. The objectives of this study were to explore the relationship between immune status and microbial communities in the lungs of individuals with HIV infection. A total of 88 patients with lung disease [80 (91%) HIV-positive and 8 (9%) HIV-negative] were enrolled in our study between January and July 2018, and 88 bronchoalveolar lavage fluid (BALF) samples were obtained during bronchoscopy. In this cross-sectional study, we investigated differences in the pulmonary microbiome of patients with HIV who had different immune statuses. The diversity of bacteria in the lungs of HIV-positive individuals was lower than that in HIV-negative individuals ($p < 0.05$). There was a significant difference in the composition and distribution of bacteria and fungi between the HIV-positive and HIV-negative groups ($p < 0.01$). The number of fungal species in the BALF of HIV-positive patients was higher than in HIV-negative patients. The diversity of bacteria and fungi in the BALF of HIV-positive patients increased with decreasing CD4 T-cell counts. Linear regression analysis showed that Pneumocystis ($R^2 = 6.4e{-}03$, $p < 0.05$), Cryptosphaeria ($R^2 = 7.2e{-}01$, $p < 0.05$), Candida ($R^2 = 3.9e{-}02$, $p < 0.05$), and Trichosporon ($R^2 = 7.7e{-}01$, $p < 0.05$) were negatively correlated with CD4 counts (F-test, $p < 0.05$). The samples collected from HIV-positive patients exhibited a different pattern relative to those from the HIV-negative group. Differences in host immune status cause differences in the diversity and structure of lower respiratory tract microorganisms.

Keywords: HIV, CD4, next-generation sequencing, lower respiratory tract, bronchoalveolar lavage, microbiota

INTRODUCTION

In the past, based on culture-dependent techniques, it was thought that the lungs of healthy individuals were sterile. The primary tool for identifying pathogens responsible for lung infections was bacteriology-based culture (Muggeo et al., 2021). With advances in next-generation sequencing technology, researchers have found that, even in healthy individuals, the lungs are not as sterile as was once thought. Recent studies have shown that there is a unique microbiome in the lungs, which differs considerably between healthy individuals and those with respiratory diseases (Man et al., 2019; Naidoo et al., 2019). The lung flora is susceptible to environmental influences and has significant individual differences, but the correlation between the number of inflammatory cytokines and the lung flora has been confirmed in healthy mice, and the correlation between inflammatory cytokines and the lung flora is higher than that of intestinal bacteria (Dickson et al., 2018). Interactions between the host or through the immune system and the microbiome reveal potential mechanisms by which microbes affect respiratory health (Pattaroni et al., 2022). Studies have shown that the interaction between the environment and the host plays a certain role in the occurrence and development of idiopathic pulmonary fibrosis (IPF). In particular, microbial infection factors play an important role in the pathogenesis and progression of IPF. Respiratory dysbiosis is closely associated with IPF, but association does not equal causation (Segal and Molyneaux, 2019). In a prospective cohort study, factors such as the composition and function of the lower airway microbiota, and the host's lower airway transcriptome characteristics were associated with clinical outcomes (Sulaiman et al., 2021).

These findings suggest that some lung diseases are related to changes in the lung microbiome. In individuals with chronic human immunodeficiency virus (HIV) infection who are not on treatment with antiretroviral agents, as their CD4+ T-lymphocyte count decreases they become vulnerable to a multitude of infections that rarely occur in an immunocompetent host, hence they are termed "opportunistic infections" (Tan et al., 2012). Among HIV-related pulmonary complications, opportunistic pneumonia is the leading cause of morbidity and mortality and a common reason for referral to a respiratory specialist for diagnostic evaluation and treatment (Shebl et al., 2010; Sigel et al., 2012, 2017). For those with access to antiretroviral therapy (ART), the spectrum of lung disease has shifted from acute opportunistic infections, which can lead to death, to chronic lung disease (Cribbs et al., 2020).

Pathogen identification in opportunistic infections is always difficult and is a critical issue faced by infectious disease clinicians. The low detection rate when using conventional culture methodology, especially for fastidious organisms, makes precision diagnosis challenging in most patients (Li et al., 2018). Culture-independent techniques, such as serologic assays and nucleic acid amplification tests, have proven useful for broadening the scope of detectable pathogens, but prior knowledge is necessary, which is sometimes impractical due to the complicated pathogen spectrum resulting from, for example, the popularity of international travel. Previous reports have suggested that up to 60% of cases are treated with no pathogen detected, despite the comprehensive testing methods available (Rhodes et al., 2010; Özçolpan et al., 2015; Schlaberg et al., 2017; Miao et al., 2018). Failure to obtain a specific and timely diagnosis may delay appropriate antimicrobial therapy, lead to unnecessary broad-spectrum antibiotic use and encourage antimicrobial resistance, and increase healthcare costs (Sartelli et al., 2017; Miao et al., 2018).

Amplicon sequencing is an unbiased method that, in theory, can detect all pathogens in a clinical sample; it is particularly suitable for complex infectious diseases, emerging infectious diseases, and atypical etiologies (Goldberg et al., 2015; Graf et al., 2016; Schlaberg et al., 2017; Zhang et al., 2020; Gu et al., 2021; Wang et al., 2021). As this technology evolves, amplicon sequencing may have the potential to become a routine diagnostic test, partly replacing traditional detection techniques, due to its advantages in sensitivity, speed, and cost.

However, the question of whether there is a relationship between immune status and the pulmonary microbiome has not yet been addressed. In this study, we used amplicon sequencing to explore this question. This study systematically investigated the composition and changes of the respiratory microbiome in HIV-infected individuals with different immune status in a large cohort sample. We found differences in the microbial community structure in the lungs of HIV-infected and non-infected individuals. We found that Pneumocystis, Candida and some other fungal species were significantly increased in a state of immunosuppression. At the same time, with the gradual loss of immune function, the types of microorganisms in the lungs of the human body increase. These findings suggest that there is a certain relationship between the community structure of lung microbes and immune status.

MATERIALS AND METHODS

Patient Recruitment and Sample Collection

We recruited 88 patients infected with HIV, who were admitted to Ditan Hospital, Beijing, China, between January and July 2018, according to strict inclusion and exclusion criteria, and collected clinical data for follow-up analysis. As participants in this study, the patients underwent bronchoscopy, and 10 ml of bronchoalveolar lavage fluid (BALF) was set aside for microbiome analysis. Bronchoalveolar lavage is performed on the most involved lung segments on the chest radiograph. The median time to bronchoscopy following admission was 1 day [interquartile range (IQR), 1–3 days]. This study received approval from the Medical Ethics Committee of our hospital, and all patients signed informed consent forms before undergoing bronchoscopy. All participants provided written informed consent to participate in the survey and biomarker testing. At the

TABLE 1 | Clinical features of participants.

	G1 ($n = 45$)	G2 ($n = 26$)	G3 ($n = 9$)	Non HIV ($n = 8$)	p - value
Age	33.00 (29.00–45.00)	42.50 (31.00–51.25)	39.00 (37.00–49.00)	66.50 (53.50–71.00)	<0.001
Gender = male	43 (95.6%)	22 (84.6%)	7 (77.8%)	6 (75.0%)	0.166
Smoking					0.2
giveup	3 (7.9%)	2 (8.3%)	2 (33.3%)	2 (33.3%)	
no	26 (68.4%)	19 (79.2%)	3 (50.0%)	2 (33.3%)	
yes	9 (23.7%)	3 (12.5%)	1 (16.7%)	2 (33.3%)	
Alcohol	7 (18.4%)	3 (12.5%)	0 (0.0%)	4 (66.7%)	0.012
CD3+/CD45+–%	6.9e+01 (11.50)	78.08 (9.51)	75.11 (12.21)	68.54 (8.92)	0.012
CD3+–cells/uL	4.4e+02 (310.25–716.75)	684.50 (466.75–1,241.75)	1,215.00 (1,061.00–1,261.00)	997.00 (896.00–1,669.50)	<0.001
CD8+/CD45+–%	6.4e+01 (10.40)	64.22 (16.22)	49.93 (13.89)	31.32 (6.55)	<0.001
CD8+–cells/uL	4.2e+02 (287.00–653.75)	576.50 (391.00–1,097.00)	754.00 (598.00–996.00)	364.00 (358.00–855.50)	0.021
CD4+/CD45+ - %	1.6e+00 (0.89–3.23)	8.65 (6.62–12.53)	25.00 (16.55–29.08)	33.51 (31.42–40.46)	<0.001
CD4+ - cells/uL	1.0e+01 (6.00–22.00)	86.00 (64.50–127.25)	364.00 (268.00–440.00)	606.00 (524.00–812.00)	<0.001
CD45+ - cells/uL	6.9e+02 (475.75–894.50)	923.00 (622.25–1,508.75)	1,728.00 (1,186.00–2,092.00)	1,320.00 (1,299.50–2,396.00)	<0.001
CD4+/CD8+ - %	2.0e–02 (0.01–0.05)	0.15 (0.09–0.21)	0.57 (0.22–0.70)	1.01 (0.88–1.14)	<0.001
VL - copies/mL	1.7e+05 (113,417.00–4e+05)	430.00 (40.00–73,112.00)	20.00 (0.00–17,759.25)	–	<0.001
ART					
3TC+TDF+EFV	37 (92.5%)	16 (66.7%)	3 (50.0%)	–	
3TC+TDF+KLC	1 (2.5%)	2 (8.3%)	1 (16.7%)	–	
AZT+3TC+EFV	0	1 (4.2%)	1 (16.7%)	–	
AZT+NVP+3TC	0	1 (4.2%)	0	–	
DTG+FTC+TDF	0	1 (4.2%)	0	–	
KLZ+3TC+DTG	0	1 (4.2%)	0	–	
TDF+3TC+LPV/r	2 (5.0%)	2 (8.3%)	1 (16.7%)	–	
WBC - 109/L	4.6e+00 (2.91–6.51)	4.89 (3.67–6.53)	5.42 (3.80–6.86)	5.44 (5.09–9.99)	0.326
PCT - ng/mL	7.0e–02 (0.05–0.13)	0.05 (0.05–0.07)	0.08 (0.06–0.32)	0.05 (0.05–0.05)	0.36
CRP - mg/L	1.4e+01 (4.20–42.90)	11.40 (5.65–30.70)	6.40 (1.80–41.20)	12.40 (4.00–28.20)	0.909

VL, viral load; ART, antiretroviral therapy; 3TC, (–)-2ı,3ı-dideoxy-3ı-thiacytidine; TDF, tenofovir disoproxil fumarate; KLC, keiva lei cadena; AZT, azidothymidine; EFV, efavirenz; NVP, nevirapine; DTG, dolutegravir; FTC, emtricitabine; LPV/r, lopinavir/ritonavir; WBC, white blood count; PCT, procalcitonin; CRP, C-reactive protein.

same time, we used dd water as negative control, and the taxa results are in **Table 1**.

DNA Extraction, Library Construction, and Sequencing

DNA extraction experiments and amplicon sequencing were performed at the Institute of Infectious Diseases, Beijing Ditan Hospital, affiliated to Capital Medical University. We used full-length 16S rDNA and internal transcribed spacer (ITS) rDNA for sequencing, respectively. DNA was extracted using a MagNA Pure LC 2.0 system and a MagNA Pure LC Total NA Isolation kit (Roche, Mannheim, Baden-Württemberg Land, Germany), in accordance with the manufacturer's instructions, and quantified using a Quant-iT PicoGreen dsDNA assay kit (Invitrogen, Eugene, Oregon, United States). Polymerase chain reaction (PCR) amplification of the full length region was performed with the following primers containing Illumina adapter sequences and dual-index barcodes to tag each sample: 341F 50-CCTACGGGNGGCWGCAG-30 and 805R 50-GACTACHVGGGTATCTAATCC-30. The PCR reaction conditions were as follows: 95°C for 3 min, followed by 25 cycles of denaturation at 95°C for 30 s, annealing at 65°C for 30 s, extension at 72°C for 30 s, and a final extension step at 72°C for 5 min. PCR products were then cleaned using AMPure XP beads (item no. A63882; Beckman Coulter Inc., Fullerton, CA, United States). The amplicon sequencing libraries were constructed in accordance with the 16S Metagenomic Sequencing Library Preparation (Illumina, Inc., San Diego, CA, United States). Paired-end sequencing with a read length of 250 bp × 2 was performed on a MiSeq instrument (Illumina, Inc.) using a MiSeq v2 reagent kit (Illumina, Inc.).

Raw Data Processing and Microbial Taxonomy Assignment

16S OTU Table Generation

Quality control of raw sequencing data was performed using Fastqc (v0.11.9) (FastQC, 2015). For bioinformatic processing of the MiSeq results, raw FASTQ files were de-multiplexed and quality filtered using QIIME (Quantitative Insights Into Microbial Ecology, v1.9.1) (Caporaso et al., 2010). The sequencing data were then quality filtered using USEARCH's fastq filter (v7.0.1001) to remove reads with more than two expected errors. The strategy of open-reference out-picking was used for cluster analysis of the sequencing data. This strategy automates species annotation of OTUs by referring to species taxonomic information in the database. At the same time,

the de novo OTU picking method was used to cluster those sequences without corresponding reference sequences in the database. The Greengenes Database (May 2013) was used to assign classifications to OTUs. The database includes a total of 1,262,986 16S ribosomal RNA (rRNA) sequences. The results were manually organized and classified using the commonly used seven-class classification method for easy understanding and reading. QIIME was used to construct the phylogenetic trees. OTUs were filtered by: (1) removing OTUs with contaminants commonly found in BAL samples using the negative control sample as a reference, (2) removing any OTUs in BAL samples with fewer than 10 reads, (3) OTUs with reads less than 1/5000 of the total reads of all samples were removed (Shenoy et al., 2019).

Internal Transcribed Spacer OTU Table Generation

Internal transcribed spacer OTUs were generated using a similar strategy to that outlined above, with the following modifications and annotations: (1) chimeras were removed and taxa assigned using DADA2 (v1.14) *via* the UNITE database (Callahan et al., 2016; Nilsson et al., 2019); (2) no phylogenetic tree was generated; (3) no NTC samples; (4) OTUs with reads less than 1/1000 of the total reads of all samples were removed.

Statistical Analysis

Diversity indices were calculated using QIIME and DADA2. The Bray–Curtis distance was used to find the principal coordinates, and PERMANOVA was used to check the accuracy of the principal coordinates analysis (PCoA) results. The above calculations were performed using the vegan package (Dixon, 2003) in the R language (v.4.0.2). Relative log expression (RLE): similar to TMM, this normalization method is based on the hypothesis that the most genes are not DE. For a given sample, the RLE scaling factor is calculated as the median of the ratio, for each gene, of its read counts over its geometric mean across all samples. By assuming most genes are not DE, the median of the ratio for a given sample is used as a correction factor to all read counts to fulfill this hypothesis. This normalization method is included in the DESeq and DESeq2 Bioconductor packages (Anders and Huber, 2010; Love et al., 2014).

RESULTS

Between 16 January and 5 July 2018, 80 patients with HIV infection who were admitted to Ditan Hospital were included in our study cohort, based on their CD4+ cell counts. For comparison, we also recruited eight HIV-negative patients diagnosed with pulmonary infectious diseases based on clinical experience by experienced clinicians. The patients' clinical characteristics are shown in **Table 1**. The median CD4 count of the HIV-positive group was 39 cells/μl (IQR 9–94), the median plasma HIV RNA concentration was 5.1 log10 copies/ml (2.5–5.4), and 11/74 (15%) patients had HIV RNA concentrations higher than 500,000 copies/ml. The HIV-positive patients were divided into three groups according to WHO guidelines: group I (G1, CD4 < 50 cells/μl), group II (G2, 50 < CD4 < 200 cells/μl), and group III (G3, CD4 > 200 cells/μl). As the CD4 cell count decreased, CD3, CD8, and CD45 decrease in HIV-positive patients, while the viral load (VL) increased (Wilcoxon, $p < 0.001$, **Table 1**).

Alterations in the Profile of Microbiota in the Lungs of Human Immunodeficiency Virus-Infected Patients

The current paradigm for diagnosing infections relies on the physician formulating a differential diagnosis on the basis of a patient's history, clinical presentation, and imaging findings, followed by serial laboratory testing. The most commonly used method for profiling microbial communities is sequencing of the 16S rRNA gene and ITS regions for bacteria and fungi, respectively (Bukin et al., 2019; Johnson et al., 2019). The universal distribution and conserved nature of the 16S rRNA and ITS genes means they are well-established genetic markers used for bacterial and fungal identification and classification.

The data of 25 samples were randomly selected to draw a dilution curve, and the results showed that the sequencing depth met the analysis requirements (**Supplementary Figure 1**). The top five phylum-level species in the 16S data were Firmicutes, Proteobacteria, Actinobacteriota, Bacteroidota, and Fusobacteriota. The top five phylum-level species in the ITS data are Chytridiomycota, Glomeromycota, Mortierellomycota, Basidiomycota, and Ascomycota. Bacterial microbiota profiles were generated using whole 16S rRNA amplicon sequencing for lower airway samples, while BAL fungal microbiota composition was investigated using whole ITS rRNA sequencing. By 16S rDNA sequencing technology, we detected 1291 OTUs, of which 983 were identified as bacterial species. At the same time, 670 OTUs of fungi were found, and 432 fungus were identified. Alpha diversity based on filtered and normalized reads indicated that HIV-positive patients had less bacterial species diversity at the genus level in their alveolar lavage fluid, based on the Chao1 index (Wilcoxon, $p < 0.05$). However, a similar pattern was not observed in the analysis of fungal alpha diversity (Wilcoxon, $p > 0.05$; **Figure 1A,B**). Comparison of bacterial beta-diversity in BAL at the OTU level between uninfected and HIV-infected individuals treated with ART using principal coordinate analysis (Bray–Curtis) revealed that the HIV-positive population remained significantly different compared to BAL from uninfected individuals even on therapy (**Figure 1C**, PERMANOVA, $p < 0.05$). To describe the fungal variation in the composition of samples between groups, PCoA was also used with the fungal datasets. Similar to the results for bacteria, the fungal colony structure of HIV-positive individuals differed greatly from that of HIV-negative individuals. However, different from the results of bacterial PCoA, even within HIV-infected individuals, the differences were still significant (**Figure 1D**, PERMANOVA, $p < 0.05$).

We observed a very interesting phenomenon, which was that in the 16S rRNA dataset of BALF sample of HIV-positive patients, some common pathogenic bacteria, such as Klebsiella, Bacillus, and Haemophilus, were reduced to varying degrees (**Figure 1E**). Instead, a large number of fungi, such as Pneumocystis, Aureobasidium, Cystobasidium, and

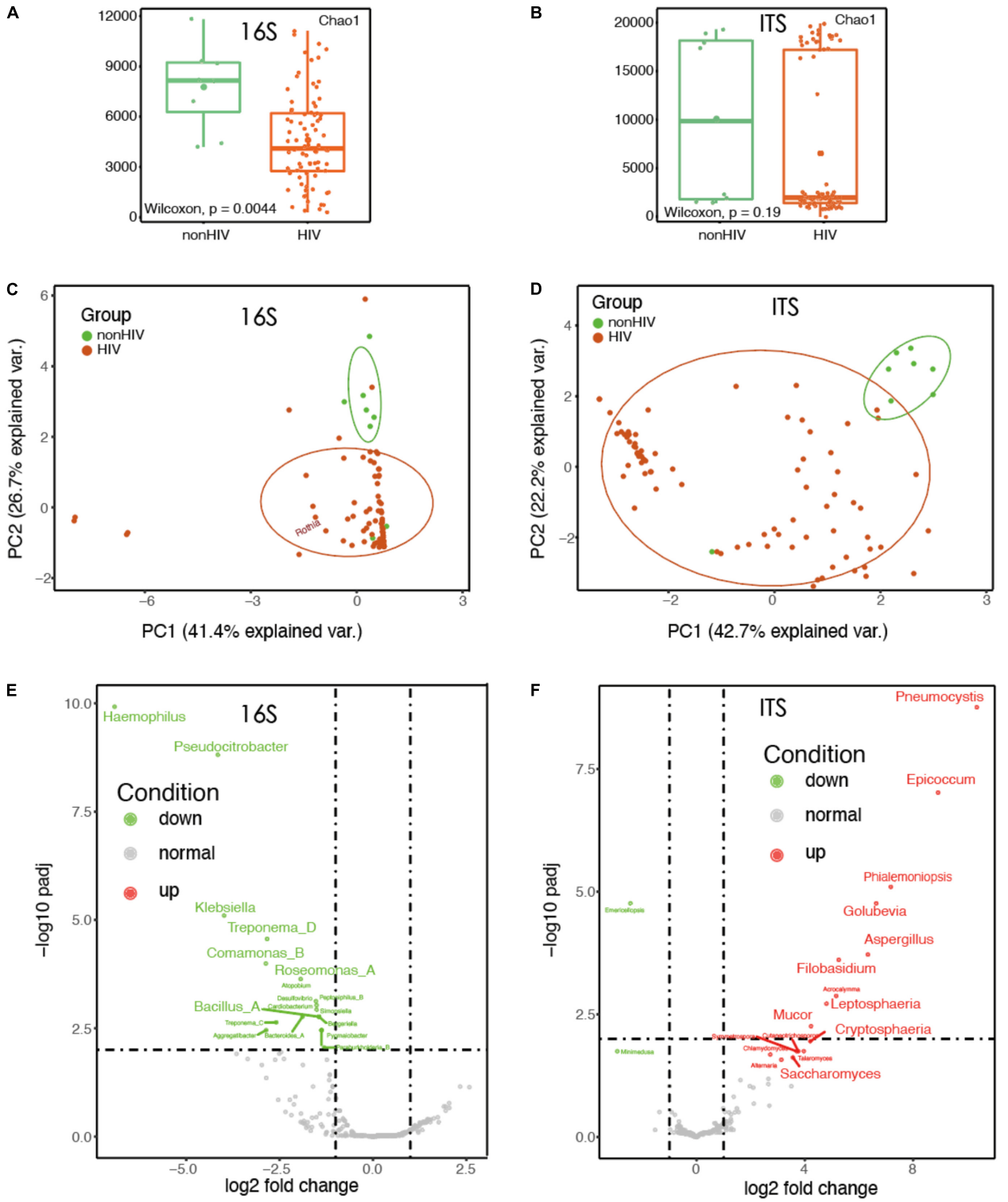

FIGURE 1 | The diversity of HIV-infected microbiota decreased and the structure of the bacteria changed. **(A)** Comparison of bacterial alpha diversity in BALF at the genus level between HIV-negative individuals and HIV-positive individuals treated with HAART. **(B)** Comparison of fungal alpha diversity in BALF fluid at the genus level between HIV-negative individuals and HIV-positive individuals treated with HAART. **(C)** Principal coordinates analysis (PCoA) using a Bray–Curtis dissimilarity of BALF sample (16S rRNA; *n* = 88) bacterial community profiles, representatively rarefied to 38,721 reads/sample. **(D)** Principal coordinates analysis (PCoA) using a Bray–Curtis dissimilarity of BALF sample (ITS rRNA; *n* = 88) fungal community profiles, representatively rarefied to 58,677 reads/sample. **(E)** Volcano plots of genus-level taxonomic bins in the 16S rRNA gene datasets. The *x*-axes display the fold changes in relative abundance (log 2). **(F)** Volcano plots of genus-level taxonomic bins in the ITS rRNA gene datasets. The *x*-axes display the fold changes in relative abundance (log 2).

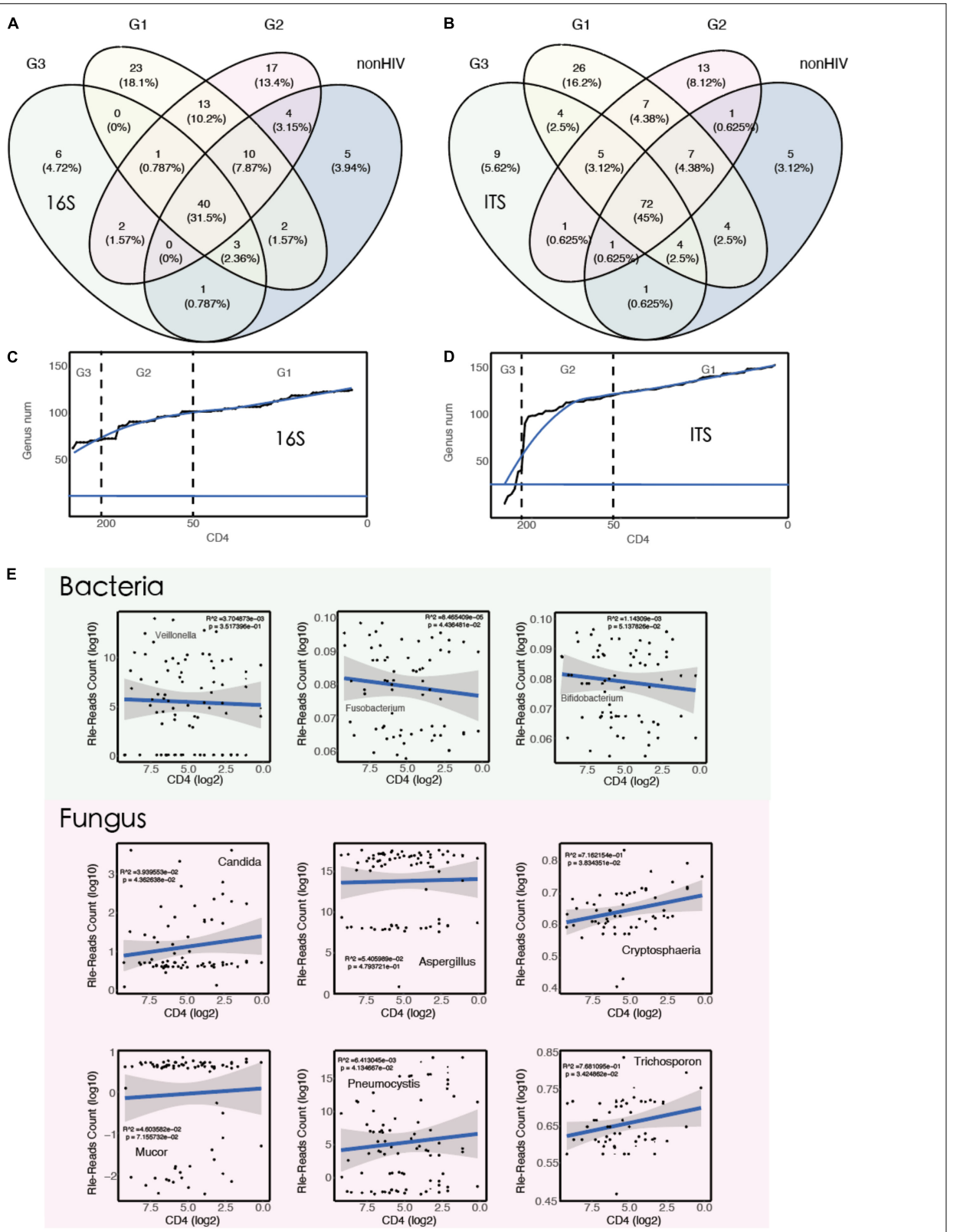

FIGURE 2 | The types of microorganisms in the BALF of HIV-positive individuals increase with decreasing CD4 counts. **(A)** A Venn diagram showing bacterial genus distribution of 16S rRNA for each group (G1 vs. G2 vs. G3 vs. non-HIV). **(B)** A Venn diagram showing fungal genus distribution of ITS rRNA for each group (G1 vs. G2 vs. G3 vs. non-HIV). **(C)** Smooth line diagram of the change in the bacterial count target. **(D)** Smooth line diagram of the change in the fungal count target. **(E)** Linear model used to describe the relationship between species numbers and CD4 counts.

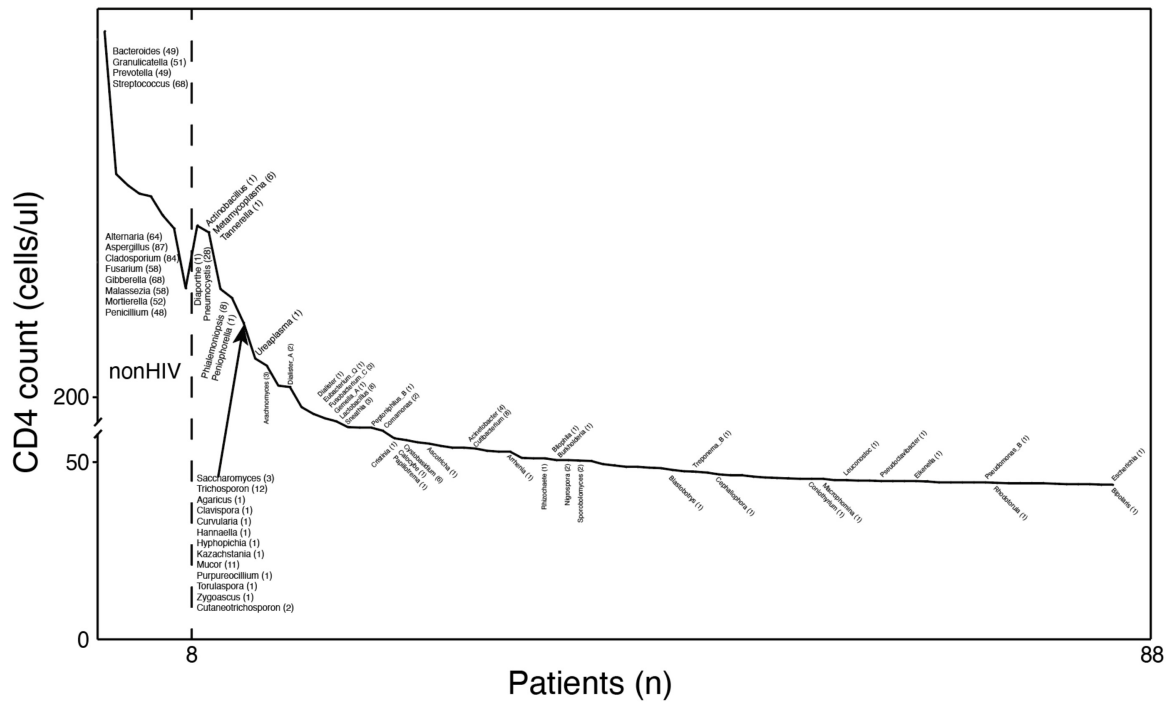

FIGURE 3 | The types of microorganisms in the BALF of HIV-positive individuals increase with decreasing CD4 counts. Profiles of pathogenic microorganisms in HIV/AIDS patients under different immune states. The *y*-axis coordinate is the CD4 cell count. The *x*-axis coordinate is a patient at this CD4 value. The text near the curve indicates newly discovered microorganisms at this CD4 value. The numbers in parentheses are the numbers of samples containing the species.

Saccharomyces, were increased in the samples of HIV-positive patients' BALF; these fungi have mostly been reported to be likely to cause infection (**Figure 1F**).

The Types of Microorganisms in the BAL of Human Immunodeficiency Virus-Positive Individuals Increase With Decreasing CD4 Count

The RLE method was used to standardize the data. For bacteria, 16S rRNA identified a positive microorganism (to genus level) whose coverage rate scored fivefold greater than that of any others. For fungi, ITS identified a microorganism (to genus level) whose coverage rate scored twofold higher than that of any other fungus, because of its low biomass in DNA extraction (Miao et al., 2018). A Venn diagram was plotted and showed that in HIV-positive patients, the types of microorganisms in the BALF increased, including both bacteria and fungi. Moreover, as the immune function of HIV-positive patients continued to decline, more and more microorganisms appeared in the patients' BALF. In addition, it is interesting to note that when CD4 cell counts dropped below 50 cells/μl, the BALF of HIV-positive patients showed a previously unseen pattern of species. There were 23 (18.1%) and 26 (16.2%) specific species of bacteria and fungi in the G1 group, respectively (**Figures 2A,B**).

The patients were ranked by CD4 count decline, and the number of newly emerged species compared with the previous patient was counted. The results showed that the number of species showed an upward trend as CD4 cell counts decreased. This finding also supports the aforementioned results (**Figures 2C,D**). To verify this result from the opposite direction, we randomly calculated 10,000 times, then simulated and counted the changes in the number of species, and the results did not show the increasing trend described above. In other words, the increasing number of microorganisms seen with the decrease in CD4 cell counts is not a common phenomenon. It only occurs when the immune function is suppressed, as in acquired immunodeficiency syndrome (AIDS) patients, as more pathogenic microorganisms appear in various parts of the body. The relationship between the immune system and the microbiota has been reported previously (Weng and Walker, 2013; Mirpuri et al., 2014).

To explore the association between microbiota abundance and immune status, we constructed a linear regression model using CD4 counts and standardized read counts and screened a subset of taxa based on previous studies (Wakefield et al., 1990; Abrahamsson, 2016; Routy et al., 2018; Lam et al., 2022). The results showed that with the decrease in CD4 counts, Fusobacterium (R^2 = 8.5e−05, $p < 0.05$) decreased. At the same time, the abundance of fungi increased with the decrease in CD4 counts, especially some common fungi associated with lung infections, for example, Candida, Cryptosphaeria, Pneumocystis, and Trichosporon (**Figure 2E**). Pneumocystis carinii is a common pathogenic fungus that casuse in lung

infections and has been frequently reported in HIV-positive patients (Balaan, 1990; Thomas and Limper, 2004).

Positive species judged positive by coverage rate were screened according to the aforementioned method and marked at their first occurrence in **Figure 3**. Species that infect humans and have been reported previously were retained in the graph (Bogaert et al., 2004; Kovacs and Masur, 2009; Hampton, 2011; Boussat et al., 2022).

Overall, these results suggest that changes in the flora of HIV-positive patients are associated with changes in immune status and that the loss of normal symbiotic flora may make patients more susceptible to secondary infection by other pathogens.

DISCUSSION

Infection with the human immunodeficiency virus type 1 (HIV-1) results in the progressive loss of immune function, marked by the depletion of CD4+ T-lymphocytes, leading to opportunistic infections and malignancies characteristic of AIDS (Kakuru et al., 2016). Although both host and viral determinants influence the rate of disease progression, the median time from initial HIV infection to the development of AIDS among untreated patients ranges from 8 to 10 years (Hansen et al., 2016). Clinical staging of HIV disease and the relative risk of developing opportunistic infections have historically relied on CD4+ T-lymphocyte counts. Although more recent studies have shown the importance of VL quantitation in determining the rate of disease progression, it is still useful to categorize HIV disease stages based on the degree of immunodeficiency (Eisinger et al., 2019). The host biological factors that determine disease severity and outcome in HIV-positive patients with pneumonia are not fully understood, and previous studies have focused more on the role of gut microbial communities (Ortiz et al., 2018; Wang et al., 2020). Reports suggest that the pulmonary microflora of HIV-positive patients with pneumonia is mainly composed of Prevotellaceae, Streptococcus, and Pseudomonadaceae (Twigg et al., 2017). Our study confirms previous reports that individual bacterial diversity decreases in HIV-positive patients with pneumonia but increases in population bacterial diversity. As we suspected, the lower respiratory tract microbiota was associated with HIV disease severity (CD4 cell count). This is an important finding, as there is increasing evidence that microorganisms play a role in regulating both local and distal mucosal immunity, as well as in responding to inflammatory responses to microbial infections.

A limitation of this study was that all patients in the cohort were given antibiotics, which may have interfered with their microbial community. Despite this limitation, this study is the first to reveal systemic perturbations of the microbiota and the relationship between respiratory microbiota composition and CD4 status in HIV-positive patients with pneumonia. This finding suggests that paying attention to respiratory flora and the development of new treatment strategies may improve the survival rate of HIV-positive patients with respiratory infection.

CONCLUSION

This study systematically examined the respiratory tract mycobiome in a group of patients with lung disease. A strong relationship was observed between an individual's lung microbiome and immune status. As CD4 counts decreased, the variety of bacteria in the lungs increased, but the quantity decreased. At the same time, the number and variety of fungi increased as an individual's immune status worsened.

DATA AVAILABILITY STATEMENT

The datasets presented in this study can be found in online repositories. The names of the repository/repositories and accession number(s) can be found in the article/ **Supplementary Material**.

ETHICS STATEMENT

The studies involving human participants were reviewed and approved by the Ditan Hospital. The patients/participants provided their written informed consent to participate in this study.

AUTHOR CONTRIBUTIONS

FZ and CC conceptualized the survey. YT managed the data collection. ZC conducted the data cleaning, analysis, and manuscript writing. YW and HZ provided the additional analytic support. All authors critically reviewed and approved the final version of the manuscript.

FUNDING

This work was supported by the 13th Five-Year Plan, Ministry of Science and Technology of China (2018ZX103 02-102).

SUPPLEMENTARY MATERIAL

The Supplementary Material for this article can be found online at: https://www.frontiersin.org/articles/10.3389/fmicb.2022.888996/full#supplementary-material

Supplementary Figure 1 | Sparse curve describing sequencing depth. The *x*-axis is richness, the *y*-axis is the number of sequence.

Supplementary Figure 2 | Stacked plot depicting species distribution at the phylum level. The *x*-axis is the grouping information of the samples. The *y*-axis represents the relative abundance of species.

Supplementary Figure 3 | Comparison of alpha diversity in BALF at the genus level between HIV-negative individuals and HIV-positive individuals treated with HAART.

REFERENCES

Abrahamsson, T. R. (2016). Not all probiotic strains prevent necrotising enterocolitis in premature infants. *Lancet* 387, 624–625. doi: 10.1016/S0140-6736(15)01090-9

Anders, S., and Huber, W. (2010). Differential expression analysis for sequence count data. *Genome Biol.* 11, R106–R106.

Balaan, M. R. (1990). Pneumocystis carinii pneumonia. *W V Med J. Dec* 86, 561–565.

Bogaert, D., de Groot, R., and Hermans, P. W. M. (2004). Streptococcus pneumoniae colonisation: the key to pneumococcal disease. *Lancet Infect. Dis.* 4, 144–154. doi: 10.1016/S1473-3099(04)00938-7

Boussat, B., Cazzorla, F., Le Marechal, M., Pavese, P., Mounayar, A.-L., Sellier, E., et al. (2022). Incidence of avoidable 30-Day readmissions following hospitalization for community-acquired pneumonia in france. *JAMA Network Open* 5:e226574. doi: 10.1001/jamanetworkopen.2022.6574

Bukin, Y. S., Galachyants, Y. P., Morozov, I. V., Bukin, S. V., Zakharenko, A. S., and Zemskaya, T. I. (2019). The effect of 16S rRNA region choice on bacterial community metabarcoding results. *Sci. Data* 6:190007.

Callahan, B. J., McMurdie, P. J., Rosen, M. J., Han, A. W., Johnson, A. J. A., and Holmes, S. P. (2016). DADA2: high-resolution sample inference from Illumina amplicon data. *Nat. Methods* 13, 581–583. doi: 10.1038/nmeth.3869

Caporaso, J. G., Kuczynski, J., Stombaugh, J., Bittinger, K., Bushman, F. D., Costello, E. K., et al. (2010). QIIME allows analysis of high-throughput community sequencing data. *Nat. Methods* 7, 335–336. doi: 10.1038/nmeth.f.303

Cribbs, S. K., Crothers, K., and Morris, A. (2020). Pathogenesis of HIV-Related lung disease: immunity, infection, and inflammation. *Physiol Rev.* 1, 603–632. doi: 10.1152/physrev.00039.2018

DeSantis, T. Z., Hugenholtz, P., Larsen, N., Rojas, M., Brodie, E. L., Keller, K., et al. (2006). Greengenes, a chimera-checked 16S rRNA gene database and workbench compatible with ARB. *Appl. Environ. Microbiol.* 72, 5069–5072. doi: 10.1128/AEM.03006-05

Dickson, R. P., Erb-Downward, J. R., Falkowski, N. R., Hunter, E. M., Ashley, S. L., and Huffnagle, G. B. (2018). The lung microbiota of healthy mice are highly variable, cluster by environment, and reflect variation in baseline lung innate immunity. *Am. J. Respir. Crit. Care Med.* 198, 497–508. doi: 10.1164/rccm.201711-2180OC

Dixon, P. (2003). VEGAN, a package of R functions for community ecology. *J. Vegetation Sci.* 14, 927–930.

Edgar, R. C. (2010). Search and clustering orders of magnitude faster than BLAST. *Bioinformatics* 26, 2460–2461. doi: 10.1093/bioinformatics/btq461

Eisinger, R. W., Dieffenbach, C. W., and Fauci, A. S. (2019). HIV viral load and transmissibility of HIV infection: undetectable equals untransmittable. *JAMA* 321, 451–452. doi: 10.1001/jama.2018.21167

FastQC 2015

Goldberg, B., Sichtig, H., Geyer, C., Ledeboer, N., and Weinstock, G. M. (2015). Making the leap from research laboratory to clinic: challenges and opportunities for next-generation sequencing in infectious disease diagnostics. *mBio* 6:e01888-15. doi: 10.1128/mBio.01888-15

Graf, E. H., Simmon, K. E., Tardif, K. D., Hymas, W., Flygare, S., Eilbeck, K., et al. (2016). Unbiased detection of respiratory viruses by use of RNA sequencing-based metagenomics: a systematic comparison to a commercial PCR panel. *J Clin Microbiol.* 54, 1000–1007. doi: 10.1128/JCM.03060-15

Gu, W., Deng, X., Lee, M., Sucu, Y. D., Arevalo, S., Stryke, D., et al. (2021). Rapid pathogen detection by metagenomic next-generation sequencing of infected body fluids. *Nat. Med.* 27, 115–124. doi: 10.1038/s41591-020-1105-z

Hampton, T. (2011). Microbes in the gut. *JAMA* 305, 2162–2162.

Hansen, V., Oren, E., Dennis, L. K., and Brown, H. E. (2016). Infectious disease mortality trends in the United States, 1980-2014. *JAMA* 316, 2149–2151. doi: 10.1001/jama.2016.12423

Johnson, J. S., Spakowicz, D. J., Hong, B.-Y., Petersen, L. M., Demkowicz, P., Chen, L., et al. (2019). Evaluation of 16S rRNA gene sequencing for species and strain-level microbiome analysis. *Nat. Commun.* 10:5029. doi: 10.1038/s41467-019-13036-1

Kakuru, A., Jagannathan, P., Muhindo, M. K., Natureeba, P., Awori, P., Nakalembe, M., et al. (2016). Dihydroartemisinin-Piperaquine for the prevention of malaria in pregnancy. *N Engl J Med.* 374, 928–939.

Kovacs, J. A., and Masur, H. (2009). Evolving health effects of pneumocystis: one hundred years of progress in diagnosis and treatment. *JAMA* 301, 2578–2585. doi: 10.1001/jama.2009.880

Lam, S., Bai, X., Shkoporov, A. N., Park, H., Wu, X., Lan, P., et al. (2022). Roles of the gut virome and mycobiome in faecal microbiota transplantation. *Lancet Gastroenterol. Hepatol.* 7, 472–484. doi: 10.1016/S2468-1253(21)00303-4

Li, L., Zhang, X., Ning, Z., Mayne, J., Moore, J. I., Butcher, J., et al. (2018). Evaluating in vitro culture medium of gut microbiome with orthogonal experimental design and a metaproteomics approach. *J. Proteome Res.* 17, 154–163. doi: 10.1021/acs.jproteome.7b00461

Love, M. I., Huber, W., and Anders, S. (2014). Moderated estimation of fold change and dispersion for RNA-seq data with DESeq2. *Genome Biol.* 15:550. doi: 10.1186/s13059-014-0550-8

Man, W. H., van Houten, M. A., Mérelle, M. E., Vlieger, A. M., Chu, M. L. J. N., Jansen, N. J. G., et al. (2019). Bacterial and viral respiratory tract microbiota and host characteristics in children with lower respiratory tract infections: a matched case-control study. *Lancet Respiratory Med.* 7, 417–426. doi: 10.1016/S2213-2600(18)30449-1

Miao, Q., Ma, Y., Wang, Q., Pan, J., Zhang, Y., Jin, W., et al. (2018). Microbiological diagnostic performance of metagenomic next-generation sequencing when applied to clinical practice. *Clin. Infect. Dis.* 67, S231–S240. doi: 10.1093/cid/ciy693

Mirpuri, J., Raetz, M., Sturge, C. R., Wilhelm, C. L., Benson, A., Savani, R. C., et al. (2014). Proteobacteria-specific IgA regulates maturation of the intestinal microbiota. *Gut Microbes* 5, 28–39. doi: 10.4161/gmic.26489

Muggeo, A., Perotin, J.-M., Brisebarre, A., Dury, S., Dormoy, V., Launois, C., et al. (2021). Extended bacteria culture-based clustering identifies a phenotype associating increased cough and enterobacterales in stable chronic obstructive pulmonary disease. *Front. Microbiol.* 12:781797. doi: 10.3389/fmicb.2021.781797

Naidoo, C. C., Nyawo, G. R., Wu, B. G., Walzl, G., Warren, R. M., Segal, L. N., et al. (2019). The microbiome and tuberculosis: state of the art, potential applications, and defining the clinical research agenda. *Lancet Respiratory Med.* 7, 892–906. doi: 10.1016/S2213-2600(18)30501-0

Nilsson, R. H., Larsson, K. H., Taylor, A. F. S., Bengtsson-Palme, J., Jeppesen, T. S., Schigel, D., et al. (2019). The UNITE database for molecular identification of fungi: handling dark taxa and parallel taxonomic classifications. *Nucl. Acids Res.* 47, D259–D264. doi: 10.1093/nar/gky1022

Ortiz, A. M., Flynn, J. K., DiNapoli, S. R., Vujkovic-Cvijin, I., Starke, C. E., Lai, S. H., et al. (2018). Experimental microbial dysbiosis does not promote disease progression in SIV-infected macaques. *Nat. Med.* 24, 1313–1316. doi: 10.1038/s41591-018-0132-5

Özçolpan, O. O., Sürücüoğlu, S., Özkütük, N., and Çavüoğlu, C. (2015). [Distribution of nontuberculous mycobacteria isolated from clinical specimens and identified with DNA sequence analysis]. *Mikrobiyol. Bul.* 49, 484–493. doi: 10.5578/mb.9698

Pattaroni, C., Macowan, M., Chatzis, R., Daunt, C., Custovic, A., Shields, M. D., et al. (2022). Early life inter-kingdom interactions shape the immunological environment of the airways. *Microbiome* 10, 34–34. doi: 10.1186/s40168-021-01201-y

Rhodes, J., Hyder, J. A., Peruski, L. F., Fisher, C., Jorakate, P., Kaewpan, A., et al. (2010). Antibiotic use in Thailand: quantifying impact on blood culture yield and estimates of pneumococcal bacteremia incidence. *Am. J. Trop. Med. Hyg.* 83, 301–306. doi: 10.4269/ajtmh.2010.09-0584

Routy, B., Gopalakrishnan, V., Daillère, R., Zitvogel, L., Wargo, J. A., and Kroemer, G. (2018). The gut microbiota influences anticancer immunosurveillance and general health. *Nat Rev Clin Oncol.* 15, 382–396. doi: 10.1038/s41571-018-0006-2

Sartelli, M., Catena, F., Abu-Zidan, F. M., Ansaloni, L., Biffl, W. L., Boermeester, M. A., et al. (2017). Management of intra-abdominal infections: recommendations by the WSES 2016 consensus conference. *World J. Emerg. Surg.* 12, 22–22. doi: 10.1186/s13017-017-0132-7

Schlaberg, R., Chiu, C. Y., Miller, S., Procop, G. W., and Weinstock, G. (2017). Validation of metagenomic next-generation sequencing tests for universal pathogen detection. *Arch. Pathol. Lab Med.* 141, 776–786. doi: 10.5858/arpa.2016-0539-RA

Segal, L. N., and Molyneaux, P. L. (2019). The challenging road of moving from association to causation for microbiome research in idiopathic pulmonary fibrosis. *Am. J. Respir. Crit. Care Med.* 199, 1054–1056. doi: 10.1164/rccm.201902-0318ED

Shebl, F. M., Engels, E. A., Goedert, J. J., and Chaturvedi, A. K. (2010). Pulmonary infections and risk of lung cancer among persons with AIDS. *JAIDS J. Acquired Immune Deficiency Syndromes.* 55, 375–379. doi: 10.1097/QAI.0b013e3181eef4f7

Shenoy, M. K., Fadrosh, D. W., Lin, D. L., Worodria, W., Byanyima, P., Musisi, E., et al. (2019). Gut microbiota in HIV–pneumonia patients is related to peripheral CD4 counts, lung microbiota, and in vitro macrophage dysfunction. *Microbiome* 7:37. doi: 10.1186/s40168-019-0651-4

Sigel, K., Wisnivesky, J., Crothers, K., Gordon, K., Brown, S. T., Rimland, D., et al. (2017). Immunological and infectious risk factors for lung cancer in US veterans with HIV: a longitudinal cohort study. *Lancet HIV* 4, e67–e73. doi: 10.1016/S2352-3018(16)30215-6

Sigel, K., Wisnivesky, J., Gordon, K., Dubrow, R., Justice, A., Brown, S. T., et al. (2012). HIV as an independent risk factor for incident lung cancer. *Aids* 26, 1017–1025. doi: 10.1097/QAD.0b013e328352d1ad

Sulaiman, I., Chung, M., Angel, L., Tsay, J. J., Wu, B. G., Yeung, S. T., et al. (2021). Microbial signatures in the lower airways of mechanically ventilated COVID-19 patients associated with poor clinical outcome. *Nat. Microbiol.* 6, 1245–1258. doi: 10.1038/s41564-021-00961-5

Tan, I. L., Smith, B. R., von Geldern, G., Mateen, F. J., and McArthur, J. C. (2012). HIV-associated opportunistic infections of the CNS. *Lancet Neurol.* 11, 605–617.

The Lancet Respiratory Medicine (2019). Harnessing the microbiome for lung health. *Lancet Respiratory Med.* 7:827. doi: 10.1016/S2213-2600(19)30307-8

Thomas, C. F., and Limper, A. H. (2004). Pneumocystis Pneumonia. *New England J. Med.* 350, 2487–2498.

Twigg, H. L. III, Weinstock, G. M., and Knox, K. S. (2017). Lung microbiome in human immunodeficiency virus infection. *Transl. Res.* 179, 97–107. doi: 10.1016/j.trsl.2016.07.008

Wakefield, A. E., Pixley, F. J., Banerji, S., Sinclair, K., Miller, R. F., Moxon, E. R., et al. (1990). Detection of *Pneumocystis carinii* with DNA amplification. *Lancet* 25, 451–453.

Wang, C., Li, A., Shi, Q., and Yu, Z. (2021). Metagenomic next-generation sequencing clinches diagnosis of leishmaniasis. *Lancet* 397:1213. doi: 10.1016/S0140-6736(21)00352-4

Wang, Y., Lifshitz, L., Gellatly, K., Vinton, C. L., Busman-Sahay, K., McCauley, S., et al. (2020). HIV-1-induced cytokines deplete homeostatic innate lymphoid cells and expand TCF7-dependent memory NK cells. *Nat. Immunol.* 21, 274–286. doi: 10.1038/s41590-020-0593-9

Weng, M., and Walker, W. A. (2013). The role of gut microbiota in programming the immune phenotype. *J. Dev. Origins Health Dis.* 4, 203–214. doi: 10.1017/S2040174412000712

Zhang, Y., Cui, P., Zhang, H.-C., Wu, H.-L., Ye, M.-Z., Zhu, Y.-M., et al. (2020). Clinical application and evaluation of metagenomic next-generation sequencing in suspected adult central nervous system infection. *J. Trans. Med.* 18:199. doi: 10.1186/s12967-020-02360-6

Conflict of Interest: The authors declare that the research was conducted in the absence of any commercial or financial relationships that could be construed as a potential conflict of interest.

Publisher's Note: All claims expressed in this article are solely those of the authors and do not necessarily represent those of their affiliated organizations, or those of the publisher, the editors and the reviewers. Any product that may be evaluated in this article, or claim that may be made by its manufacturer, is not guaranteed or endorsed by the publisher.

frontiers | Frontiers in Microbiology

ORIGINAL RESEARCH
published: 06 July 2022
doi: 10.3389/fmicb.2022.880873

Downregulation of TCF1 in HIV Infection Impairs T-cell Proliferative Capacity by Disrupting Mitochondrial Function

Hong-Jiao Cai[1,2,3†], Jue Shi[1,3,4†], Lin-Bo Yin[1,3], Jie-Fu Zheng[1,3], Ya-Jing Fu[1,3], Yong-Jun Jiang[1,3], Hong Shang[1,3‡] and Zi-Ning Zhang[1,3*‡]*

[1]NHC Key Laboratory of AIDS Immunology, National Clinical Research Center for Laboratory Medicine, The First Affiliated Hospital of China Medical University, Shenyang, China, [2]Department of Central Laboratory, Dalian Municipal Central Hospital, Dalian, China, [3]Key Laboratory of AIDS Immunology, Chinese Academy of Medical Sciences, Shenyang, China, [4]Department of Laboratory Medicine, Zhuhai Hospital of Integrated Traditional Chinese and Western Medicine, Zhuhai, China

OPEN ACCESS

Edited by:
Kai Deng,
Sun Yat-sen University, China

Reviewed by:
Lifan Xu,
Army Medical University, China
Huanzhang Zhu,
Fudan University, China

***Correspondence:**
Hong Shang
hongshang100@hotmail.com
Zi-Ning Zhang
zi_ning101@hotmail.com

†These authors have contributed equally to this work and share first authorship

‡These authors have contributed equally to this work and share senior authorship

Specialty section:
This article was submitted to Infectious Agents and Disease, a section of the journal Frontiers in Microbiology

Received: 22 February 2022
Accepted: 13 June 2022
Published: 06 July 2022

Citation:
Cai H-J, Shi J, Yin L-B, Zheng J-F, Fu Y-J, Jiang Y-J, Shang H and Zhang Z-N (2022) Downregulation of TCF1 in HIV Infection Impairs T-cell Proliferative Capacity by Disrupting Mitochondrial Function. Front. Microbiol. 13:880873. doi: 10.3389/fmicb.2022.880873

Background: Despite the benefits of antiretroviral therapy (ART) for people with HIV, T-cell dysfunction cannot be fully restored. Metabolic dysregulation is associated with dysfunction of HIV-1-specific T-cells. Exploration of the factors regulating metabolic fitness can help reverse T-cell dysfunction and provide new insights into the underlying mechanism.

Methods: In this study, HIV-infected individuals and HIV-negative control individuals (NCs) were enrolled. T-cell factor (TCF)1 expression in cells was determined by quantitative reverse-transcriptase polymerase chain reaction and flow cytometry. Relevant microarray data from the GEO database were analyzed to explore the underlying mechanism. The effects of TCF1 on T-cell function and metabolic function were assessed *in vitro*.

Results: *TCF7* mRNA expression in peripheral blood mononuclear cells was downregulated in rapid progressors compared with long-term non-progressors individuals and NCs. TCF1 expression on $CD4^+$ and $CD8^+$ T-cells was downregulated in treatment-naïve HIV-infected individuals compared with NCs. Interleukin (IL)2 production and proliferative capacity were impaired in TCF1 knockdown T-cells. Moreover, glycolytic capacity and mitochondrial respiratory function were decreased in TCF1 knockdown T-cells, and depolarized mitochondria were increased in TCF1 knockdown T-cells.

Conclusion: Downregulation of TCF1 in HIV infection impairs T-cell proliferative capacity by disrupting mitochondrial function. These findings highlight the metabolic regulation as a pivotal mechanism of TCF1 in the regulation of T-cell dysfunction.

Keywords: HIV infection, mitochondrial function, T-cell factor 1, proliferative capacity, metabolism

INTRODUCTION

During chronic viral infections including HIV, T-cell exhaustion occurs due to chronic exposure to antigens, inflammatory signals, lack of $CD4^+$ T-cell helper cells, and/or cell-intrinsic defects (Day et al., 2006; Fenwick et al., 2019). T-cell exhaustion is characterized by progressive loss of cell proliferation and effector functions, metabolic dysregulation, increased inhibitory receptor

expression, and distinct transcriptional signatures (Kurachi, 2019; McLane and Wherry, 2019). Despite the benefits of ART for people with HIV, these deficiencies cannot be fully restored (Rehr et al., 2008; Migueles et al., 2009).

Metabolic dysregulation during chronic HIV infection, including reductions in glucose uptake, progressive mitochondrial damage, and increased reactive oxygen species (ROS) production, likely contributes to accelerated T-cell aging, senescence, and apoptosis (Bengsch et al., 2016; Desdin-Mico et al., 2018; McLane and Wherry, 2019). Accumulating evidence supports the therapeutic potential of targeting exhausted T (Tex) cells, for example *via* inhibitory receptor blockade, thus increasing glucose uptake and mitochondrial fitness and reinvigorating Tex cells (Bengsch et al., 2016; Masao Hashimoto et al., 2018; Saeidi et al., 2018; McLane and Wherry, 2019). Therefore, identifying the mechanism that leads to metabolic dysfunction, which ultimately results in T-cell exhaustion, is essential to explore effective and biologically plausible immunotherapeutic interventions for controlling disease progression.

T-cell factor 1 (TCF1, encoded by *TCF7*) is a key transcription factor that regulates T-cell development and proliferative capacity (Weber et al., 2011; Sharma et al., 2012) by initiating the canonical WNT and NOTCH signaling pathways (Germar et al., 2011; Escobar et al., 2020). In models of chronic viral infection, studies have revealed that $TCF1^+$ T-cells represent a population of stem-like or progenitor exhausted T-cells (Tpex; Snell et al., 2018; Chen et al., 2019). Only $TCF1^+$ T-cells, unlike their $TCF1^-$ counterparts, have the ability to self-renew and give rise to a progeny of terminally exhausted $TCF1^-$ cells with effector potential (Siddiqui et al., 2019). TCF1 overexpression in $CD8^+$ tumor-infiltrating lymphocytes (TILs) enhanced cytokine-producing capacity and suppressed co-inhibitory receptor expression while retaining a heightened response to checkpoint blockade, leading to enhanced tumor control (Kurtulus et al., 2019; Siddiqui et al., 2019; Shan et al., 2020). In clinical trials of individuals with melanoma, an increased frequency of $TCF1^+CD8^+$ T-cells expression was found to be positively correlated with patient survival and responded well to checkpoint-blockade therapy (Miller et al., 2019; Sade-Feldman et al., 2019). HIV-specific $CD8^+$ T-cells expressing TCF1 were highest in "elite controllers" who can naturally control viral load below the detection limit without ART, followed by ART-suppressed and then HIV^+ viremic individuals (Takuya Sekine AP-P, 2020; Rutishauser et al., 2021). Furthermore, TCF1 contributes to the regulation of the expansion capacity of HIV-specific $CD8^+$ T-cells (Rutishauser et al., 2021). Recent research found that Tpex with high TCF1 expression could sustain mitochondrial fitness over time (Gabriel et al., 2021), but the specific role of TCF1 in regulating the metabolic fitness and how TCF1 deletion contributes to metabolic dysfunction or impairs cellular function in chronic HIV infection, is still not entirely clear.

Given that TCF1 plays an important role in regulating T-cell development and proliferative capacity, we hypothesized that TCF1 may act as a protective factor in HIV infection. In this study, we tested our hypothesis by investigating the relationship between TCF1 expression level, viral load, and $CD4^+$ counts. We also studied the effects of TCF1 in T-cell function and metabolic function. Our results demonstrate that lower TCF1 expression with HIV infection could impair T-cell function *via* mitochondrial damage.

Abbreviations: ART, Antiretroviral therapy; ARTs, HIV-infected individuals receiving antiretroviral therapy; AIDS, Acquired immune deficiency Syndrome; DEGs, Differentially expressed genes; ECAR, Extracellular acidification; GEO, Gene expression omnibus; GAPDH, Glyceraldehyde 3-phosphate dehydrogenase; HIV, Human immunodeficiency virus; HIVs, Treatment-naïve HIV-infected individuals; IFN-γ, Interferon-gamma; IL2, Interleukin 2; LTNPs, Long-term non-progressors; MM, Mitochondrial mass; MMP, Mitochondrial membrane potential; NCs, HIV-Negative control individuals; OCR, Oxygen consumption rate; PBMCs, Peripheral blood mononuclear cells; qRT-PCR, Quantitative reverse-transcriptase polymerase chain reaction; ROS, Reactive oxygen species; RPs, Rapid progressors; siRNA, Small interfering RNA; TCF1, T-cell factor 1; Tex, exhausted T-cells; Tpex, Progenitor exhausted T-cells.

MATERIALS AND METHODS

Study Population and Recruitment

A total of 56 HIV-infected individuals and 55 HIV-negative control individuals (NCs) were included in our study. Of these, in our analysis of *TCF7* mRNA expression in peripheral blood mononuclear cells (PBMCs), eight "rapid progressors" (RPs; $CD4^+$ T-cell<350 cells/ul within 1–2 years of HIV infection; 8 males; average age is 48 years), seven "long term non-progressors" (LTNPs; individuals who maintained normal $CD4^+$ T counts and controlled viremia efficiently for prolonged periods after HIV infection; 5 males and 2 females; average age is 51 years), and seven aged- and sex- matched NCs were enrolled. In the analysis of *TCF7* mRNA expression in $CD4^+$ and $CD8^+$ T-cells, seven HIV-infected patients (7 males; average is 45 years) and five aged- and sex- matched NCs were included. To analyze TCF1 expression in T-cells using flow cytometry, 16 HIV-infected individuals receiving ARTs, seven treatment-naïve HIV-infected individuals (HIVs), and 11 NCs were enrolled; to detect interleukin (IL)2 production, we included 18 individuals; and to evaluate the proliferative capacity of T-cells, we included 12 individuals. Finally, we included 13 individuals for a functional and metabolic analysis of TCF1 knockdown by small interfering (siRNA).

All individuals included in our study signed informed consent forms before participating in this research project. The study was approved by the Research and Ethics Committee of the First Affiliated Hospital of China Medical University, Shenyang, China.

Preparation of Cells

Whole blood samples were collected in EDTA vacutainers (BD, New Jersey, United States) to obtain PBMCs by density gradient centrifugation. Human T-cells were isolated from PBMCs using human T-cells negative isolation kit (StemCell Technologies, Vancouver, Canada). Cell purity was >96% confirmed by flow cytometry (**Supplementary Figure 1**).

RNA Reverse Transcription and Quantitative Real-Time Polymerase Chain Reaction

Quantities of *TCF7* mRNA in PBMCs, $CD4^+$ T-cells, and $CD8^+$ T-cells were determined using qRT-PCR. Total RNA was first extracted using the RNeasy RNA isolation kit (Qiagen, Stanford, VA, United States) and was reverse transcribed into complementary DNA (cDNA) using the PrimeScript™ RT reagent kit (TaKaRa Biotechnology) according to the manufacturer's instructions. Expression levels of *TCF7* mRNA were evaluated using TB Green Premix Ex Taq™ II (TaKaRa Biotechnology) on Roche LightCycler®480 Real-Time PCR system with the following primers synthesized by BGI (Beijing, China):

TCF7-F:5′-CCTTGATGCTAGGTTCTGGTGTACC-3′

TCF7-R:5′-CACTCTGCAATGACCTTGGCTCTCA-3′

The housekeeping gene GAPDH was included as an internal standard. *TCF7* mRNA expression was measured in duplicate and calculated *via* the Livak method.

TCF1 Knockdown in T-cells Using siRNA

To investigate the effects of TCF1 on T-cell functions, 200 pmol *TCF7*-siRNA or siRNA Negative Control (Thermo Fisher Scientific, Waltham, MA, United States) was transfected into separate $CD3^+$ T-cells, respectively, using the Human T-cell Nucleofector® Kit (Lonza) according to the manufacturer's protocol. Cells were then incubated for 24 h post Nucleofection. For transfection efficiency detection, quantities of *TCF7* mRNA were performed after transfection for 24 h, as described in the methods section of RNA reverse transcription and qRT-PCR.

Staining and Flow Cytometric Analysis

To investigate TCF1 expression in T-cell subsets, isolated cells were labeled with antibodies against CD3, CD4, CD8, CCR7, CD45RA, PD-1, and TIGIT (Biolegend) for 20 min at 4°C. Subsequently, Fixation/Permeabilization working solution (eBiosciences) was added, and the cells were followed by incubation with anti-TCF1 (BD Biosciences) for 30 min at room temperature. To investigate cytokine production in $TCF1^+$ and $TCF1^-$ T-cell, isolated T-cells or transfected cells were stimulated with Dynabeads™ Human T Activator CD3/CD28 (beads to cell ratio, 1:2; Thermo Fisher) for 24 h. GolgiStop (1 μl/mL, BD Biosciences) was added to the culture for the final 6 h. After that, cells were stained with LIVE/DEAD™ Fixable Aqua Dead Cell Stain kit (Invitrogen) for 30 min at 4°C. The cells were then labeled with antibodies against CD3, CD4, CD8, anti-TCF1, anti-IL-2, and anti-IFN-γ, as described above. To investigate the effects of TCF1 on T-cell proliferation, isolated T-cells or transfected cells were marked with Cell Trace™ Violet (Thermo Fisher) for 30 min at 37°C. After incubation at 37°C for 3 days, cells were incubated with antibodies directed against LIVE/DEAD™ Fixable Aqua Dead Cell Stain kit, CD3, CD4 CD8, and anti-TCF1, as described above. To detect mitochondrial mass (MM) and membrane potential (MMP), the transfected cells were resuspended in prewarmed (37°C) staining solution containing MitoTracker® Green FM (50 nm; Thermo Fisher Scientific) and MitoTracker® Orange CMTMRos (25 nm; Thermo Fisher Scientific) for 30 min, washed the cells with PBS and then stained with LIVE/DEAD™ Fixable Aqua Dead Cell Stain kit.

Cells were detected using the LSR II flow cytometer (BD Biosciences, San Jose, CA, United States) and data were analyzed using FlowJo software (Ashland, OR, United States).

Analysis of Microarray Data

To explore the underlying mechanism of impaired cell function with TCF1, we downloaded microarray data from Gene Expression Omnibus (GEO)[1] with accession number GSE44228. According to the mean expression of TCF1 in the data, we stratified the samples into two groups: $TCF1^{high}$ and $TCF1^{low}$. Using the online GEO2R analysis tool,[2] we identified differentially expressed genes (DEGs) between $TCF1^{high}$ and $TCF1^{low}$ with p-value <0.05 and fold change (FC) >1.2. Functional enrichment of DEGs was conducted using Gene Ontology (GO) and Kyoto Encyclopedia of Genes and Genomes (KEGG) pathway enrichment analyses on the DAVID website,[3] and the results were visualized using the online tool ImageGP.[4]

Seahorse Extracellular Flux Analysis

On the day prior to this assay, we hydrated an Agilent Seahorse XFp Sensor Cartridge with XF Calibrant in a non-CO_2 37°C incubator overnight. Transfected cells were stimulated with ImmunoCult Human CD3/CD28 T-cell Activator (StemCell Technologies, Vancouver, Canada) for 24 h. On the day of the assay, we firstly resuspended cells in a warmed assay medium to the desired concentration (5×10^5 cells in 50 μl/well) before seeding them on Cell-Tak-coated Seahorse Cell Culture Miniplate (wells A and H were background correction wells). Then, we centrifuged the cells at 350 × g (zero braking) for 5 min and added 130 μl assay medium to each well for a final volume of 180 μl. Finally, the Miniplate was transferred to a non-CO_2 37°C incubator for 25–30 min to ensure that the cells were entirely attached. When the above was prepared, basal and maximal respiration (OCR) and extracellular acidification (ECAR) were analyzed using an XFp Cell Mito Stress Test Kit and XFp Glycolysis Stress Test Kit on an Agilent Seahorse XF HS Mini instrument according to the corresponding procedure.

Statistics

All statistical analyses were performed using GraphPad Prism v7.0 (GraphPad, San Diego, CA, United States). Normality tests were performed before analyzing the data. Mann–Whitney U test or Paired t-test were used to evaluate differences between two groups. One-way ANOVA analysis was used to compare *TCF7* mRNA and TCF1 expression levels between

[1]https://www.ncbi.nlm.nih.gov/geo/

[2]https://www.ncbi.nlm.nih.gov/geo/geo2r/

[3]https://david.ncifcrf.gov/tools.jsp

[4]http://www.ehbio.com/ImageGP

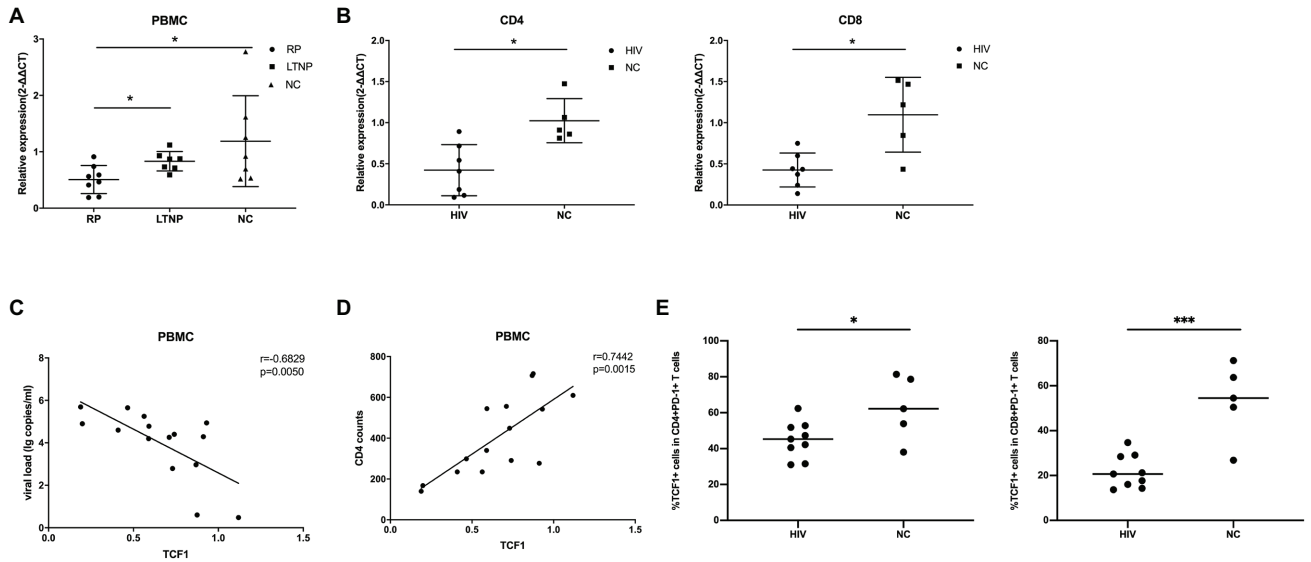

FIGURE 1 | *TCF7* mRNA expression is reduced in HIV-infected individuals and is associated with disease progression. **(A)** *TCF7* mRNA expression in peripheral blood mononuclear cells (PBMCs; from eight "rapid progressors" [RPs], seven long-term non-progressors [LTNPs], and seven HIV-negative control individuals [NCs]) was quantified and normalized to that of glyceraldehyde 3-phosphate dehydrogenase (GAPDH) transcripts, and expressed using the relative quantification method ($2^{-\Delta\Delta Ct}$). *TCF7* mRNA expression levels were compared between three groups by one-way ANOVA analysis. **(B)** *TCF7* mRNA expression in CD4 and $CD8^+$ T cells from HIV-infected individuals ($n = 7$) and NCs ($n = 5$) was quantified and normalized to that of GAPDH transcripts and expressed using the relative quantification method ($2^{-\Delta\Delta Ct}$). The Mann–Whitney U test was used for intergroup comparisons. **(C)** Pearson's correlation analysis of *TCF7* mRNA expression and viral load in PBMCs from RPs and LTNPs ($n = 15$). **(D)** Pearson's correlation analysis of *TCF7* mRNA expression and $CD4^+$ T cell counts in PBMCs from RPs and LTNPs ($n = 15$). **(E)** The percentage of $TCF1^+$ cells in $CD4^+PD1^+$ T cells and $CD8^+PD1^+$ T cells form HIV-infected individuals ($n = 9$) compared with HIV negative control individuals ($n = 5$). $^*p < 0.05$, $^{***}p < 0.001$.

3 groups. Pearson's correlation was used to assess correlations between viral load, $CD4^+$ T-cell counts, and TCF1 expression levels. Data were recorded as mean and standard deviation (SD); p values <0.05 were considered statistically significant.

RESULTS

TCF7 mRNA Expression Is Lower in HIV-Infected Individuals and Is Associated With Disease Progression

To explore the relationship between *TCF7* mRNA and HIV, we first compared the expression of *TCF7* mRNA in three groups (including eight RPs, seven LTNPs, and seven NCs). The qRT-PCR results showed that the level of *TCF7* mRNA was significantly lower in PBMCs from RP individuals than LTNPs ($p = 0.0205$) and NCs ($p = 0.0401$; **Figure 1A**). *TCF7* mRNA expression in PBMCs was negatively correlated with viral load ($p = 0.0050$; **Figure 1C**) and positively correlated with $CD4^+$ counts ($p = 0.0015$; **Figure 1D**). In addition, *TCF7* mRNA expression was substantially lower in HIV-infected patients than in NCs, both in $CD4^+$ T-cells ($p = 0.0101$) and $CD8^+$ T-cells ($p = 0.0177$; **Figure 1B**). The expression of TCF1 on antigen-experienced $CD4^+PD\text{-}1^+$ and $CD8^+PD\text{-}1^+$ T-cells was also significantly lower in HIV-infected patients compared to NCs ($p = 0.0328$, $p = 0.0003$; **Figure 1E**), respectively. These results indicated that TCF1 might prevent disease progression from HIV infection to some extent.

The TCF1 Expression in T-cells Is Significantly Lower in HIV-Infected Patients

To acquire comprehensive and detailed information on TCF1 protein expression, we conducted further analyses using flow cytometry. The percentage of $TCF1^+CD4^+$ T and $TCF1^+CD8^+$ T-cells was significantly lower in the HIVs compared to NCs ($p = 0.0271$, $p = 0.0076$), and the percentage of $TCF1^+CD8^+$ T-cells was significantly higher in ARTs than HIVs ($p = 0.0319$; **Figure 2A**). We subdivided $CD4^+$ and $CD8^+$ T-cells into naïve (Tn), central memory (Tcm), effector memory (Tem), and terminally differentiated effector memory (Temra) cells, based on the cell surface markers CD45RA and CCR7 (**Figure 2B**). We then compared the TCF1 expression on the four T-cell subsets. The results indicated that reduced TCF1 expression on $CD4^+$ T-cells in HIVs predominantly occurred in Tem, and Temra cells ($p = 0.0010$, $p = 0.0079$), and on $CD8^+$ T-cells in HIVs this occurred mainly appeared in Tn, Tcm, Tem, and Temra cells ($p = 0.0265$, $p = 0.0153$, $p = 0.0034$, and $p = 0.0235$; **Figure 2B**). We also observed that TCF1 was expressed to a greater extent on Tn cells and Tcm cells than Tem and Temra cells across all groups (**Figure 2B**). These results together indicate that TCF1 may act as a protective factor in HIV infection, and also that the expression pattern of TCF1 was consistent with the character of $TCF1^+$ stem-like T-cells.

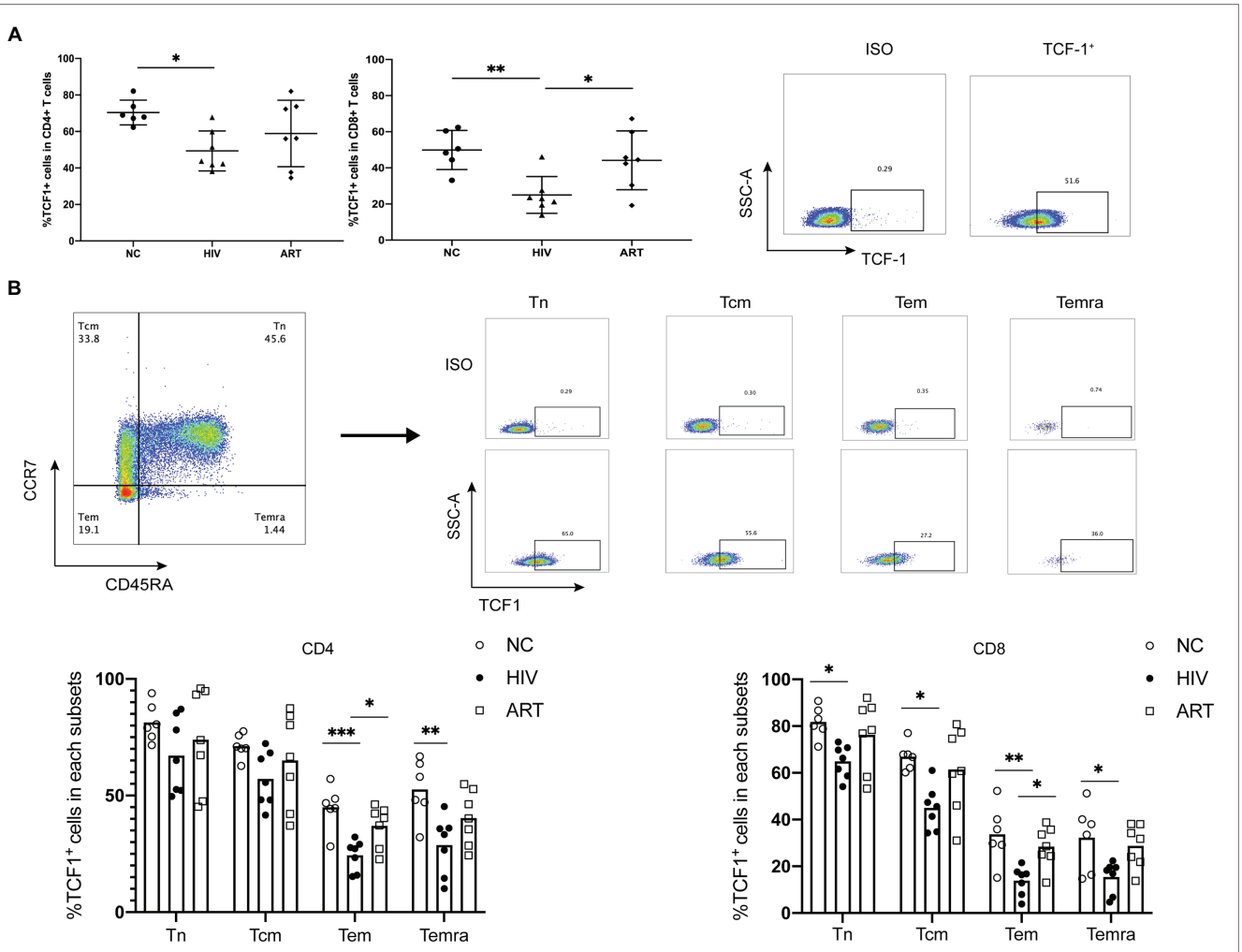

FIGURE 2 | T cell factor (TCF)1 expression is reduced in different CD4⁺ and CD8⁺ T cell subsets from HIV-infected individuals. **(A)** The percentage of TCF1⁺CD4⁺ T cells and TCF1⁺CD8⁺ T cells from treatment-naïve HIV-infected individuals (HIVs, $n = 7$) compared with HIV-negative control individuals (NCs, $n = 6$) and HIV-infected individuals receiving antiretroviral therapy (ARTs, $n = 7$). The TCF1⁺ population was gated based on the ISO from the same individual. **(B)** The percentage of TCF1⁺ cells in naïve (Tn), central memory (Tcm), effector memory (Tem), and terminally differentiated effector memory (Temra) T cell populations from CD4⁺ and CD8⁺ T cells (including HIVs, NCs, and ARTs), distinguished by the level of CCR7 and CD45RA expression. One-way ANOVA analysis was used in **(A,B)**. $^{*}p < 0.05$, $^{**}p < 0.01$, $^{***}p < 0.001$.

Downregulation of TCF1 Impairs the Proliferative Capacity of T-cells

Because TCF1 is downregulated in HIV-infected individuals, we hypothesized that TCF1 may affect T-cell function. To test this, we stimulated T-cells for 24 h with Dynabeads™ Human T Activator CD3/CD28 (Thermo Fisher) and detected the production of IL2 and IFN-γ in TCF1⁺ and TCF1⁻ cell subsets. The results showed that less IL2 was produced by TCF1⁻ compared with TCF1⁺ cells, both in CD4⁺ T-cells ($p = 0.0186$) and CD8⁺ T-cells ($p = 0.0222$; **Figure 3A**). As IL2 can stimulate T-cell entry into the cell cycle and thus induce cell proliferation, we analyzed proliferation capacity in TCF1⁺ and TCF1⁻ cells. The results showed that the new progeny cells mainly originated from TCF1⁺ rather than TCF1⁻ cells, both in CD4⁺ T-cells ($p < 0.0001$) and CD8⁺ T-cells ($p = 0.0018$; **Figure 3C**). And the percentage of new progeny cells in TCF1⁻ after 24 h was less than 10% (**Figure 3C**). To confirm this result, we employed *TCF7*-siRNA to knockdown TCF1 in T-cells. *TCF7* mRNA expression was significantly downregulated in T-cells transfected with siRNA (**Supplementary Figure 2**). The production of IL2 by CD4⁺ ($p = 0.0205$) and CD8⁺ ($p = 0.0261$) T-cells was substantially reduced after TCF1 was knocked down (**Figure 3B**), and the proliferative capacity of CD4⁺ ($p = 0.0076$) and CD8⁺ ($p = 0.0084$). T-cells was also impaired in the TCF1 knockdown cells (**Figure 3D**), confirming the results shown in **Figures 3A,C**. Knockdown of *TCF7* has the tendency to decrease IFN-γ production of the CD8⁺ T-cells, but it did not reach statistical significance ($p = 0.1180$; **Supplementary Figure 3**). These results indicate that TCF1 plays a pivotal role in sustaining the proliferative capacity of T-cells. We also detected immune checkpoints and found that the percentage of PD-1 and TIGIT was significantly lower in the TCF1⁺ cells compared with

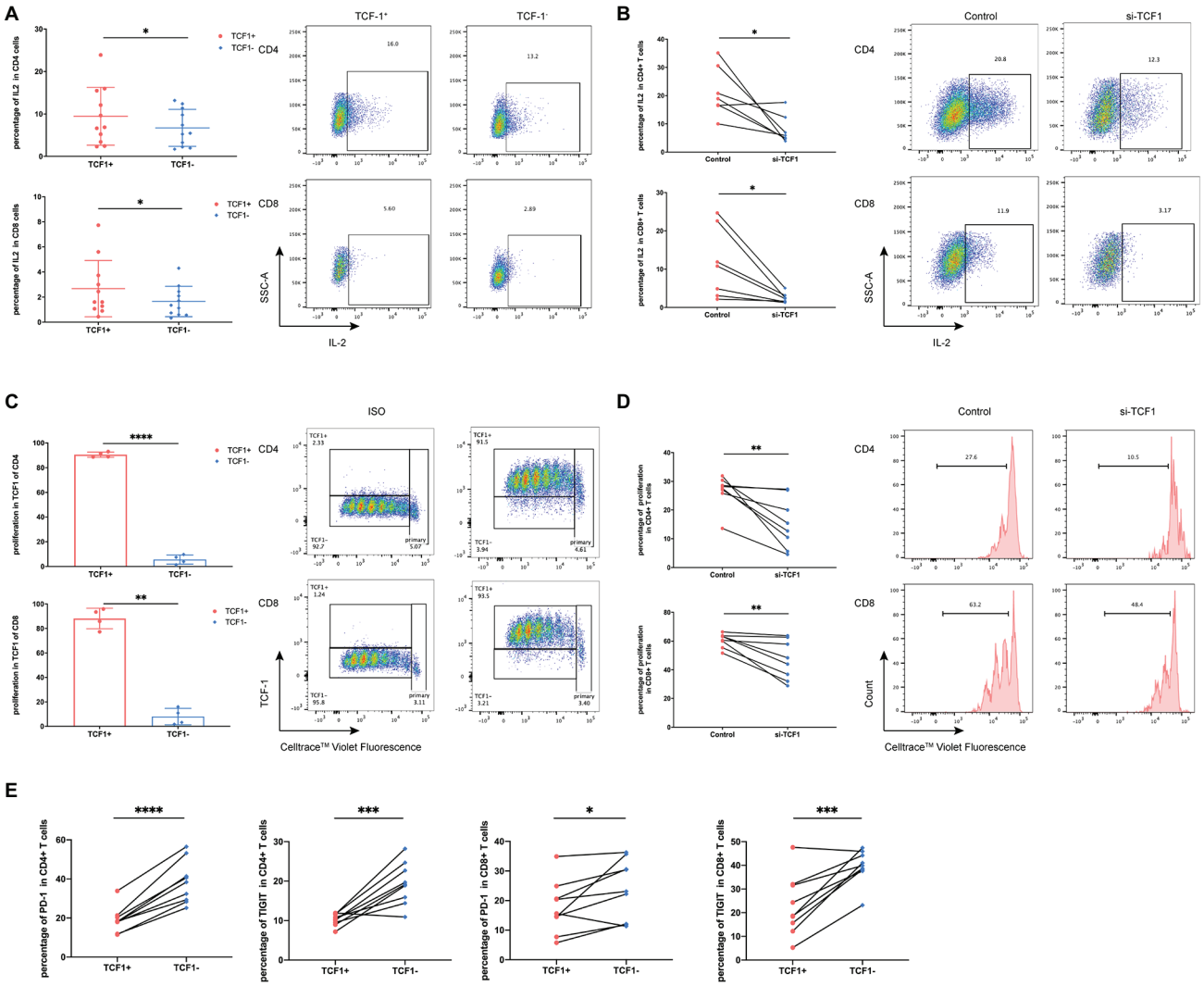

FIGURE 3 | Downregulation of T cell factor (TCF)1 impairs T cell proliferation. **(A)** To investigate whether TCF1 affects T cell function, primary CD3$^+$ T cells ($n = 11$) were stimulated with anti-αCD3/CD28 Dynabeads for 24 h, and GolgiStop (1 μl/ml) was added to the culture for the final 6 h. Interleukin (IL)2 expression in TCF1$^+$ T cells was compared with TCF1$^-$ T cells. **(B)** After 24 h transfection with siTCF1, primary T cells ($n = 7$) were stimulated using anti-αCD3/CD28 Dynabeads for 24 h and intracellular expression of IL2 was determined. **(C)** Primary CD3$^+$ T cells ($n = 4$) were labeled with Cell Trace™ Violet and stimulated using anti-αCD3/CD28 Dynabeads for 72 h. The proliferation of TCF1$^+$CD4$^+$ and TCF1$^+$CD8$^+$ T cells increased significantly compared with TCF1$^-$CD4$^+$ and TCF1$^-$CD8$^+$ T cells. **(D)** After knockdown with siTCF1 for 24 h, primary CD3$^+$ T cells ($n = 8$) were labeled with Cell Trace™ Violet and stimulated using anti-αCD3/CD28 Dynabeads for 72 h. The proliferation of CD4$^+$ and CD8$^+$ T cells decreased significantly in the absence of TCF1 expression. **(E)** PD-1 and TIGIT expression in TCF1$^+$ T cells was compared with TCF1$^-$ T cells ($n = 9$). Paired *t*-tests were used for analysis. $^*p < 0.05$, $^{**}p < 0.01$, $^{***}p < 0.001$.

TCF1$^-$ cells, both in CD4$^+$ T-cells ($p < 0.0001$, $p = 0.0009$) and CD8$^+$ T-cells ($p = 0.0319$, $p = 0.0010$), indicating the relationship between TCF1 expression and T-cell exhaustion (**Figure 3E**).

The Glycolytic Function Was Decreased in TCF1 Knockdown Cells

To further explore the underlying mechanism of impaired cell function with TCF1, we analyzed relevant microarray data from the GEO database. According to the mean expression of TCF1 in the data, the samples were divided into two groups: TCF1^{high} and TCF1^{low}. We found 693 differentially expressed genes (DEGs) with a value of $p < 0.05$ and folder change >1.2, which were used as the cutoff criteria (**Figure 4A**). DEGs were found to be enriched in the "glucose metabolic process" in the GO analysis (**Figure 4B**) and the "FoxO signaling pathway" in the KEGG analysis (**Figure 4C**). The FoxO signaling pathway is involved in many cellular physiological events such as glucose metabolism, so extracellular acidification rate (ECAR) assays were performed to detect changes in glycolytic function in TCF1 knockdown cells. The results showed that, compared with the control, the glycolytic function was decreased in TCF1 knockdown cells, as reflected by lower basal glycolysis ($p = 0.0083$) and maximal glycolytic capacity ($p < 0.0001$; **Figure 4D**). We also measured

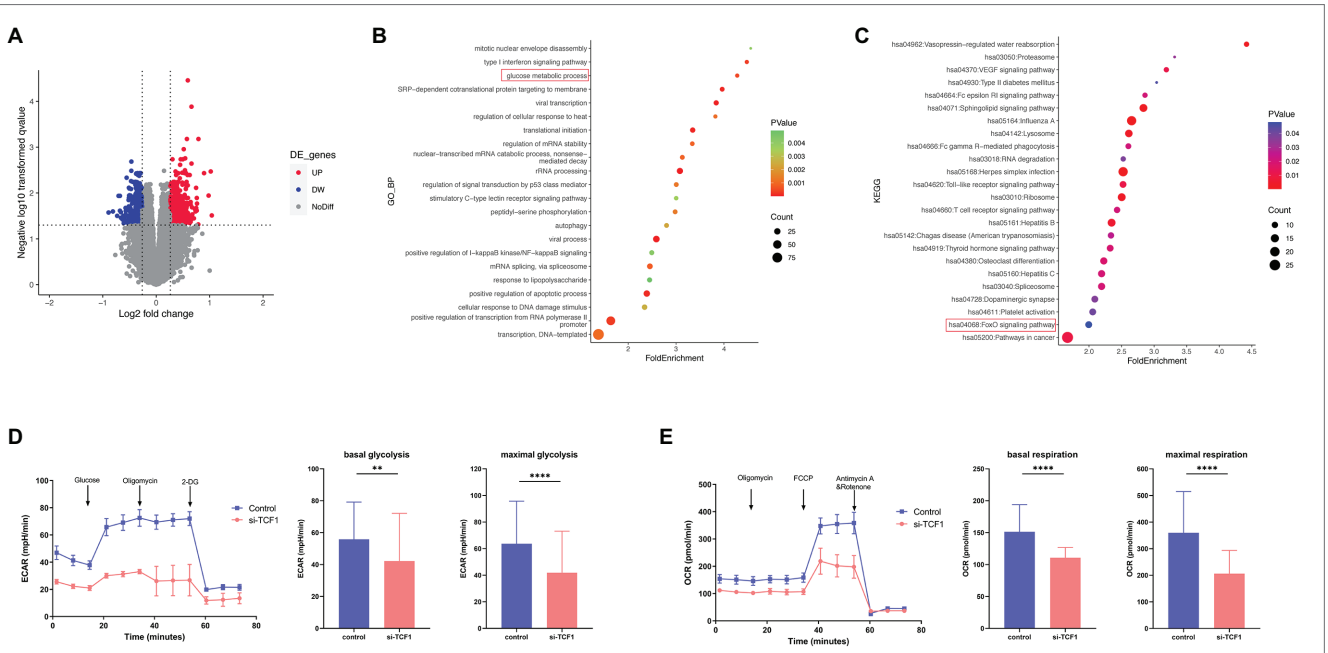

FIGURE 4 | T cell factor (TCF)1 regulates the glycolytic function of T cells. **(A)** The differentially expressed genes (DEGs) in the TCF1^{high} and TCF1^{low} groups. Red points mean upregulated, and blue points mean downregulated in TCF1^{high} groups. **(B)** Gene Ontology (GO) classification of DEGs from TCF1^{high} and TCF1^{low} groups. **(C)** KEGG pathways of DEGs from TCF1^{high} and TCF1^{low} groups. **(D)** ECAR of control or TCF1 knockdown T cells were subjected using Seahorse analysis. (2-deoxyglucose = 2-DG). Basal glycolysis and maximum glycolysis capacity were calculated and compared between control and si-TCF1 group by Paired *t*-tests. **(E)** Oxygen consumption rate (OCR) at baseline and administration of oligomycin (oligo), FCCP, and Rotenone+Antimycin. Basal respiration and maximal respiration were calculated and compared between control and si-TCF1 group by Paired *t*-tests. $^{**}p < 0.01$, $^{****}p < 0.0001$

the mitochondrial respiratory function using an oxygen consumption rate (OCR) assay, and the results showed that both basal respiration ($p < 0.0001$) and maximal respiration ($p < 0.0001$) were decreased in TCF1 knockdown cells (**Figure 4E**). The decreases in ECAR and OCR in TCF1 knockdown cells imply that TCF1 may play a role in sustaining normal cell metabolism.

TCF1 Knockdown Impairs Mitochondrial Function

As mitochondria play a key role in sustaining cell function and cell metabolism, we investigated whether TCF1 downregulation impaired T-cell proliferation *via* mitochondrial dysfunction. We performed mitochondrial mass and membrane potential assays using flow cytometry in transfected T-cells. The results showed that after TCF1 knockdown, there was no change in MM ($p = 0.7446$; **Figure 5A**), but MMP significantly decreased compared with the control ($p = 0.0482$; **Figure 5B**), indicating impaired respiratory chain activity and mitochondrial function.

We observed an accumulation of depolarized mitochondria in TCF1 knockdown T-cells, characterized by increased MM but reduced MMP signals (MMP^{lo}/MM^{hi}; $p = 0.0110$; **Figure 5C**). Previously published work indicated that the MMP^{lo}/MM^{hi} population usually indicates mitochondrial disruption with fewer cristae and decreased crista length, along with reductions in respiratory activity. Cells with a greater number of depolarized mitochondria had impaired effector functions (Scharping et al., 2016; Siska et al., 2017) and higher levels of PD-1 expression (Yu et al., 2020).

The above results indicate that TCF1 plays a key role in sustaining mitochondrial fitness, and the deletion of TCF1 may impair cell function *via* mitochondrial dysfunction.

DISCUSSION

T-cells play a pivotal role in HIV infection, affecting disease progression and therapeutic efficacy. The loss in T-cell number and dysfunction in these cells are usually accompanied by disease progression and poor clinical outcomes (Klein et al., 1995; Soghoian et al., 2012). Owing to the key role of T-cells in HIV infections, exploration of the factors affecting T-cell number and function is of great importance to reverse T-cell dysfunction for controlling HIV infections.

The change in metabolic features of T-cells during chronic infections has been explored in recent years (Bengsch et al., 2016). The consensus among researchers is that metabolism can affect T-cell development (Sun et al., 2021), proliferation (Sabharwal et al., 2018; Fultang et al., 2020), effector function (Barili et al., 2021), and exhaustion (Martins et al., 2021). Moreover, as the energy centers of cell activities, mitochondria are also critical for maintaining T-cell function (Vardhana et al., 2020; Yu et al., 2020). Mitochondria interact with the P2X1, P2X4, and P2Y11 receptors to regulate T-cell metabolism, cell migration, and antigen recognition (Ledderose and Junger, 2020). T-cell mitochondrial dysfunction can lead to premature aging (Lenaers et al., 2020), and distorted mitochondrial metabolism has a role in driving

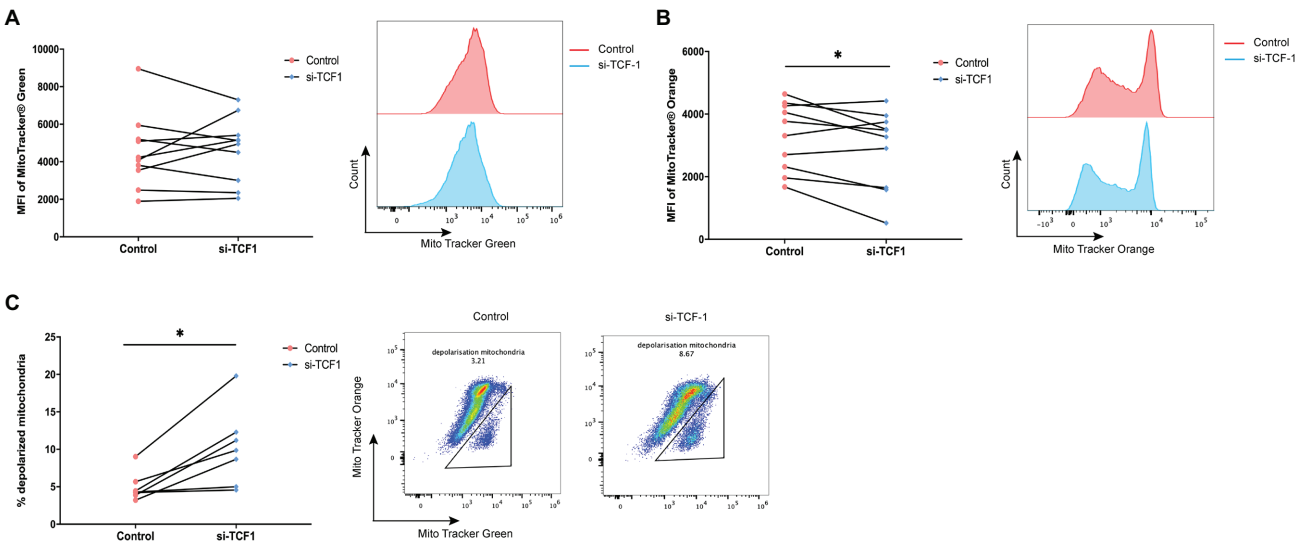

FIGURE 5 | T cell factor (TCF)1 knockdown impairs mitochondrial function. After knockdown with siTCF1 for 24 h, **(A)** mitochondrial mass was analyzed in primary CD3$^+$ T cells ($n = 10$) labeled with Mito Tracker Green and **(B)** mitochondrial membrane potential was analyzed in primary CD3$^+$ T cells ($n = 10$) labeled with Mito Tracker Red. **(C)** The percentage of depolarized mitochondria (defined by low mitochondrial membrane potential and high mitochondrial mass [MMP^{lo}/MM^{hi}]) in TCF1 knockdown T cells ($n = 7$) was increased which were labeled with Mito Tracker Green and Mito Tracker Orange. Paired *t*-tests were used in **(A-C)**. $^*p < 0.05$.

dysfunctional CD8$^+$ T-cells in chronic viral infections and tumors (Leavy, 2016). TCF1, described as a stem cell-like factor in Tpex, is critical for T-cells development and effector functions and plays a crucial role in anti-tumor and antivirus activity. In our study, we analyzed the differential expression of TCF1 in HIV, ART, and NC individuals and found that lower expression of TCF1 with HIV infection may impair T-cell proliferative capacity by disrupting mitochondrial function.

In previous studies on TCF1, researchers have typically focused on CD8$^+$ T-cells (Chen et al., 2021; Rutishauser et al., 2021; Zhao et al., 2021), with scant literature on the role of TCF1 in CD4$^+$ T-cells. In our study, we firstly observed downregulation of TCF1 in individuals with HIV compared with NC and ART individuals, in both CD8$^+$ and CD4$^+$ T-cells, and confirmed a positive correlation between TCF1 downregulation and disease progression. These results indicate that TCF1 may participate in the progression of HIV infection and affect treatment outcomes. As previously reported, TCF1 is essential for memory T-cell formation, especially central memory T-cells (Jeannet et al., 2010; Zhou et al., 2010). In our study, the decline of TCF1 with HIV infection mainly occurred in memory T-cells. This result further supported the key role of TCF1 in cell differentiation. Through siRNA technology, we validated that TCF1 knockdown could impair the proliferative capacity and the production of IL2.

HIV infection is characterized by the persistence activation and inflammation (Zicari et al., 2019). Danilo et al. (2018) found that inflammatory cytokines IL-12 could downregulate TCF1 *via* IL-12R/STAT4 signaling in CD8$^+$ T-cells. And increased level of the proinflammatory cytokine IL-12 was observed in HIV-infected patients (Xia et al., 2022). We speculated that a high level of proinflammation in HIV infection could contribute to the down-expression of TCF1 in T-cells. Is the downregulation of TCF1 in CD4$^+$ cells a physiological process that occurs in all CD4$^+$ T-cells, or is TCF1 down-regulation only in HIV-infected cells? The relationship between the HIV integration and TCF1 expression has been studied by Rutishauser et al. (2021) who did not observe a significant relationship between HIV cell-associated DNA levels in PBMCs and TCF1 expression in HIV-infected patients. Henderson et al. (2012) found that another molecule in TCF/LEF family, TCF4, represses basal HIV LTR transcription. Based on these studies, we postulated that TCF1 may not preferentially be downregulated in HIV-infected cells. It might be a decrease in both HIV-infected and non-infected cells.

Energy metabolism is required for cells to perform their functions and survive. Glycolysis and oxidative phosphorylation are two main sources of adenosine triphosphate (ATP) in cells. Lymphocyte differentiation, proliferation, and effector functions are also linked to cellular energy metabolism (Buck et al., 2017). In our results, reduced metabolism was observed in TCF1 knockdown cells, reflected by decreased OCR and ECAR; this may be caused by mitochondrial dysfunction. Owing to their ability to generate ATP for cell metabolism, mitochondria are critical for sustaining normal cellular function. Recently, Dong et al. (2021) dissected the roles of mitochondrial fusion and fission in mitochondrial function and cell proliferation, highlighting the role of mitochondria in maintaining normal cellular function and proliferative capacity. In this study, we found that the MMP significantly decreased in TCF1 knockdown T-cells and depolarized mitochondria, indicating mitochondrial dysfunction also occurred in TCF1 knockdown T-cells. Recently, Shan et al. (2022) also found the requirement for TCF1 to activate glycolysis in recall-stimulated CD8$^+$ TCM cells in LCMV-infected mice. Their study showed that TCF1 activated glycolysis through the induce glycolytic

enzymes by transcriptional regulation and chromatin opening in recall-stimulated CD8$^+$ TCM cells, but not the canonical Wnt or NOTCH signaling pathway. We postulated that TCF1 may affect mitochondrial function and metabolism in T-cells of HIV-infected patients through signaling pathways other than Wnt or NOTCH signaling pathway, which needs further study. Our results indicate that TCF1 plays a key role in sustaining mitochondrial function, and imply that TCF1 knockdown may impair T-cell function *via* mitochondrial damage.

CONCLUSION

We report that the TCF1 expression is decreased with HIV infection and TCF1 knockdown impairs T-cell function and proliferation capacity. We also validated that mitochondrial damage is caused by TCF1 knockdown, indicating that lower TCF1 expression with HIV infection could impair T-cell function *via* mitochondrial damage.

DATA AVAILABILITY STATEMENT

The original contributions presented in the study are included in the article/**Supplementary Material**, further inquiries can be directed to the corresponding authors.

ETHICS STATEMENT

The studies involving human participants were reviewed and approved by the Research and Ethics Committee of the First Affiliated Hospital of China Medical University, Shenyang, China. The patients/participants provided their written informed consent to participate in this study.

AUTHOR CONTRIBUTIONS

HS and ZN-Z conceived and designed the experiments. HJ-C and JS carried out experiments and analyzed the data. LB-Y, JF-Z, YJ-F, and YJ-J collected the samples and contributed reagents. HS, ZN-Z, HJ-C, and JS prepared the manuscript. All authors contributed to the article and approved the submitted version.

FUNDING

This work was supported by grants from the National Natural Science Foundation of China (81871708) and the Mega-Projects of National Science Research for the 13th Five-Year Plan (2017ZX10201101).

ACKNOWLEDGMENTS

The authors express our gratitude to the generosity of patients who participated in this study.

SUPPLEMENTARY MATERIAL

The Supplementary Material for this article can be found online at: https://www.frontiersin.org/articles/10.3389/fmicb.2022.880873/full#supplementary-material

REFERENCES

Barili, V., Boni, C., Rossi, M., Vecchi, A., Zecca, A., Penna, A., et al. (2021). Metabolic regulation of the HBV-specific T cell function. *Antivir. Res.* 185:104989. doi: 10.1016/j.antiviral.2020.104989

Bengsch, B., Johnson, A. L., Kurachi, M., Odorizzi, P. M., Pauken, K. E., Attanasio, J., et al. (2016). Bioenergetic insufficiencies due to metabolic alterations regulated by the inhibitory receptor PD-1 are an early driver of CD8 + T cell exhaustion. *Immunity* 45, 358–373. doi: 10.1016/j.immuni.2016.07.008

Buck, M. D., Sowell, R. T., Kaech, S. M., and Pearce, E. L. (2017). Metabolic instruction of immunity. *Cell* 169, 570–586. doi: 10.1016/j.cell.2017.04.004

Chen, Z., Ji, Z., Ngiow, S. F., Manne, S., Cai, Z., Huang, A. C., et al. (2019). TCF-1-centered transcriptional network drives an effector versus exhausted CD8 T cell-fate decision. *Immunity* 51, 55.e5–840.e5. doi: 10.1016/j.immuni.2019.09.013

Chen, Y., Zander, R. A., Wu, X., Schauder, D. M., Kasmani, M. Y., Shen, J., et al. (2021). BATF regulates progenitor to cytolytic effector CD8(+) T cell transition during chronic viral infection. *Nat. Immunol.* 22, 996–1007. doi: 10.1038/s41590-021-00965-7

Danilo, M., Chennupati, V., Silva, J. G., Siegert, S., and Held, W. (2018). Suppression of Tcf1 by inflammatory cytokines facilitates effector CD8 T cell differentiation. *Cell Rep.* 22, 2107–2117. doi: 10.1016/j.celrep.2018.01.072

Day, C. L., Kaufmann, D. E., Kiepiela, P., Brown, J. A., Moodley, E. S., Reddy, S., et al. (2006). PD-1 expression on HIV-specific T cells is associated with T-cell exhaustion and disease progression. *Nature* 443, 350–354. doi: 10.1038/nature05115

Desdin-Mico, G., Soto-Heredero, G., and Mittelbrunn, M. (2018). Mitochondrial activity in T cells. *Mitochondrion* 41, 51–57. doi: 10.1016/j.mito.2017.10.006

Dong, F., Zhu, M., Zheng, F., and Fu, C. (2021). Mitochondrial fusion and fission are required for proper mitochondrial function and cell proliferation in fission yeast. *FEBS J.* 289, 262–278. doi: 10.1111/febs.16138

Escobar, G., Mangani, D., and Anderson, A. C. (2020). T cell factor 1: a master regulator of the T cell response in disease. *Sci. Immunol.* 5:9726. doi: 10.1126/sciimmunol.abb9726

Fenwick, C., Joo, V., Jacquier, P., Noto, A., Banga, R., Perreau, M., et al. (2019). T-cell exhaustion in HIV infection. *Immunol. Rev.* 292, 149–163. doi: 10.1111/imr.12823

Fultang, L., Booth, S., Yogev, O., Martins da Costa, B., Tubb, V., Panetti, S., et al. (2020). Metabolic engineering against the arginine microenvironment enhances CAR-T cell proliferation and therapeutic activity. *Blood* 136, 1155–1160. doi: 10.1182/blood.2019004500

Gabriel, S. S., Tsui, C., Chisanga, D., Weber, F., Llano-León, M., Gubser, P. M., et al. (2021). Transforming growth factor-β-regulated mTOR activity preserves cellular metabolism to maintain long-term T cell responses in chronic infection. *Immunity* 54, 1698–1714.e5. doi: 10.1016/j.immuni.2021.06.007

Germar, K., Dose, M., Konstantinou, T., Zhang, J., Wang, H., Lobry, C., et al. (2011). T-cell factor 1 is a gatekeeper for T-cell specification in response to Notch signaling. *Proc. Natl. Acad. Sci. U. S. A.* 108, 20060–20065. doi: 10.1073/pnas.1110230108

Henderson, L. J., Narasipura, S. D., Adarichev, V., Kashanchi, F., and Al-Harthi, L. (2012). Identification of novel T cell factor 4 (TCF-4) binding sites on the HIV long terminal repeat which associate with TCF-4, beta-catenin, and

SMAR1 to repress HIV transcription. *J. Virol.* 86, 9495–9503. doi: 10.1128/JVI.00486-12

Jeannet, G., Boudousquié, C., Gardiol, N., Kang, J., Huelsken, J., and Held, W. (2010). Essential role of the Wnt pathway effector Tcf-1 for the establishment of functional CD8 T cell memory. *Proc. Natl. Acad. Sci. U. S. A.* 107, 9777–9782. doi: 10.1073/pnas.0914127107

Klein, M. R., van Baalen, C. A., Holwerda, A. M., Kerkhof Garde, S. R., Bende, R. J., Keet, I. P., et al. (1995). Kinetics of gag-specific cytotoxic T lymphocyte responses during the clinical course of HIV-1 infection: a longitudinal analysis of rapid progressors and long-term asymptomatics. *J. Exp. Med.* 181, 1365–1372. doi: 10.1084/jem.181.4.1365

Kurachi, M. (2019). CD8+ T cell exhaustion. *Semin. Immunopathol.* 41, 327–337. doi: 10.1007/s00281-019-00744-5

Kurtulus, S., Madi, A., Escobar, G., Klapholz, M., Nyman, J., Christian, E., et al. (2019). Checkpoint blockade immunotherapy induces dynamic changes in PD-1–CD8+ tumor-infiltrating T cells. *Immunity* 50, 94.e6–181.e6. doi: 10.1016/j.immuni.2018.11.014

Leavy, O. (2016). T cell responses: defective mitochondria disrupt CD8(+) T cells. *Nat. Rev. Immunol.* 16, 534–535. doi: 10.1038/nri.2016.98

Ledderose, C., and Junger, W. G. (2020). Mitochondria synergize With P2 receptors to regulate human T cell function. *Front. Immunol.* 11:549889. doi: 10.3389/fimmu.2020.549889

Lenaers, G., Bonneau, D., Delneste, Y., and Papon, N. (2020). Dysfunctional T cell mitochondria Lead to premature aging. *Trends Mol. Med.* 26, 799–800. doi: 10.1016/j.molmed.2020.07.001

Martins, C. P., New, L. A., O'Connor, E. C., Previte, D. M., Cargill, K. R., Tse, I. L., et al. (2021). Glycolysis inhibition induces functional and metabolic exhaustion of CD4(+) T cells in type 1 diabetes. *Front. Immunol.* 12:669456. doi: 10.3389/fimmu.2021.669456

Masao Hashimoto, A. O. K., Se Jin Im, H. T. K., Pillai, R. N., Ramalingam, S. S., Araki, K., and Ahmedl, R. (2018). CD8 T cell exhaustion in chronic infection and Cancer: opportunities for interventions. *Annu. Rev. Med.* 69, 301–318. doi: 10.1146/annurev-med-012017-043208

McLane, L. M., and Wherry, E. J. (2019). CD8 T cell exhaustion During chronic viral infection and Cancer. *Annu. Rev. Immunol.* 37, 457–495. doi: 10.1146/annurev-immunol-041015-

Migueles, S. A., Weeks, K. A., Nou, E., Berkley, A. M., Rood, J. E., Osborne, C. M., et al. (2009). Defective human immunodeficiency virus-specific CD8+ T-cell polyfunctionality, proliferation, and cytotoxicity are not restored by antiretroviral therapy. *J. Virol.* 83, 11876–11889. doi: 10.1128/JVI.01153-09

Miller, B. C., Sen, D. R., Al Abosy, R., Bi, K., Virkud, Y. V., LaFleur, M. W., et al. (2019). Subsets of exhausted CD8+ T cells differentially mediate tumor control and respond to checkpoint blockade. *Nat. Immunol.* 20, 326–336. doi: 10.1038/s41590-019-0312-6

Rehr, M., Cahenzli, J., Haas, A., Price, D. A., Gostick, E., Huber, M., et al. (2008). Emergence of polyfunctional CD8+ T cells after prolonged suppression of human immunodeficiency virus replication by antiretroviral therapy. *J. Virol.* 82, 3391–3404. doi: 10.1128/JVI.02383-07

Rutishauser, R. L., Deguit, C. D. T., Hiatt, J., Blaeschke, F., Roth, T. L., Wang, L., et al. (2021). TCF-1 regulates HIV-specific CD8+ T cell expansion capacity. JCI. *Insight* 6:6648. doi: 10.1172/jci.insight.136648

Sabharwal, S. S., Rosen, D. B., Grein, J., Tedesco, D., Joyce-Shaikh, B., Ueda, R., et al. (2018). GITR Agonism enhances cellular metabolism to support CD8(+) T-cell proliferation and effector cytokine production in a mouse tumor model. *Cancer Immunol. Res.* 6, 1199–1211. doi: 10.1158/2326-6066.Cir-17-0632

Sade-Feldman, M., Yizhak, K., Bjorgaard, S. L., Ray, J. P., de Boer, C. G., Jenkins, R. W., et al. (2019). Defining T cell states associated with response to checkpoint immunotherapy in melanoma. *Cell* 176:404. doi: 10.1016/j.cell.2018.12.034

Saeidi, A., Zandi, K., Cheok, Y. Y., Saeidi, H., Wong, W. F., Lee, C. Y. Q., et al. (2018). T-cell exhaustion in chronic infections: reversing the state of exhaustion and reinvigorating optimal protective immune responses. *Front. Immunol.* 9:2569. doi: 10.3389/fimmu.2018.02569

Scharping, N. E., Menk, A. V., Moreci, R. S., Whetstone, R. D., Dadey, R. E., Watkins, S. C., et al. (2016). The tumor microenvironment represses T cell mitochondrial biogenesis to drive Intratumoral T cell metabolic insufficiency and dysfunction. *Immunity* 45, 701–703. doi: 10.1016/j.immuni.2016.08.009

Shan, Q., Hu, S. S., Zhu, S., Chen, X., Badovinac, V. P., Peng, W., et al. (2022). Tcf1 preprograms the mobilization of glycolysis in central memory CD8+ T cells during recall responses. *Nat. Immunol.* 23, 386–398. doi: 10.1038/s41590-022-01131-3

Shan, Q., Se, H., Chen, X., Danahy, D. B., Badovinac, V. P., Zang, C., et al. (2020). Ectopic Tcf1 expression instills a stem-like program in exhausted CD8+ T cells to enhance viral and tumor immunity. *Cell. Mol. Immunol.* 18, 1262–1277. doi: 10.1038/s41423-020-0436-5

Sharma, A., Chen, Q., Nguyen, T., Yu, Q., and Sen, J. M. (2012). T cell factor-1 and beta-catenin control the development of memory-like CD8 thymocytes. *J. Immunol.* 188, 3859–3868. doi: 10.4049/jimmunol.1103729

Siddiqui, I., Schaeuble, K., Chennupati, V., Fuertes Marraco, S. A., Calderon-Copete, S., Pais Ferreira, D., et al. (2019). Intratumoral Tcf1+PD-1+CD8+ T cells with stem-like properties promote tumor control in response to vaccination and checkpoint blockade immunotherapy. *Immunity* 50, 195–211.e10. doi: 10.1016/j.immuni.2018.12.021

Siska, P. J., Beckermann, K. E., Mason, F. M., Andrejeva, G., Greenplate, A. R., Sendor, A. B., et al. (2017). Mitochondrial dysregulation and glycolytic insufficiency functionally impair CD8 T cells infiltrating human renal cell carcinoma. JCI. *Insight* 2:3411. doi: 10.1172/jci.insight.93411

Snell, L. M., MacLeod, B. L., Law, J. C., Osokine, I., Elsaesser, H. J., Hezaveh, K., et al. (2018). CD8+ T cell priming in established chronic viral infection preferentially directs differentiation of memory-like cells for sustained immunity. *Immunity* 49, 94.e5–678.e5. doi: 10.1016/j.immuni.2018.08.002

Soghoian, D. Z., Jessen, H., Flanders, M., Sierra-Davidson, K., Cutler, S., Pertel, T., et al. (2012). HIV-specific cytolytic CD4 T cell responses during acute HIV infection predict disease outcome. *Sci. Transl. Med.* 4:123ra25. doi: 10.1126/scitranslmed.3003165

Sun, V., Sharpley, M., Kaczor-Urbanowicz, K. E., Chang, P., Montel-Hagen, A., Lopez, S., et al. (2021). The metabolic landscape of Thymic T cell development In vivo and In vitro. *Front. Immunol.* 12:716661. doi: 10.3389/fimmu.2021.716661

Takuya Sekine AP-P (2020). TOX is expressed by exhausted and polyfunctional human effector memory CD8+ T cells. *Sci Immunol.* 5:7918. doi: 10.1126/sciimmunol.aba7918

Vardhana, S. A., Hwee, M. A., Berisa, M., Wells, D. K., Yost, K. E., King, B., et al. (2020). Impaired mitochondrial oxidative phosphorylation limits the self-renewal of T cells exposed to persistent antigen. *Nat. Immunol.* 21, 1022–1033. doi: 10.1038/s41590-020-0725-2

Weber, B. N., Chi, A. W., Chavez, A., Yashiro-Ohtani, Y., Yang, Q., Shestova, O., et al. (2011). A critical role for TCF-1 in T-lineage specification and differentiation. *Nature* 476, 63–68. doi: 10.1038/nature10279

Xia, P., Xing, X. D., Yang, C. X., Liao, X. J., Liu, F. H., Huang, H. H., et al. (2022). Activation-induced pyroptosis contributes to the loss of MAIT cells in chronic HIV-1 infected patients. *Mil. Med. Res.* 9:24. doi: 10.1186/s40779-022-00384-1

Yu, Y. R., Imrichova, H., Wang, H., Chao, T., Xiao, Z., Gao, M., et al. (2020). Disturbed mitochondrial dynamics in CD8(+) TILs reinforce T cell exhaustion. *Nat. Immunol.* 21, 1540–1551. doi: 10.1038/s41590-020-0793-3

Zhao, X., Shan, Q., and Xue, H. H. (2021). TCF1 in T cell immunity: a broadened frontier. *Nat. Rev. Immunol.* 22, 147–157. doi: 10.1038/s41577-021-00563-6

Zhou, X., Yu, S., Zhao, D. M., Harty, J. T., Badovinac, V. P., and Xue, H. H. (2010). Differentiation and persistence of memory CD8(+) T cells depend on T cell factor 1. *Immunity* 33, 229–240. doi: 10.1016/j.immuni.2010.08.002

Zicari, S., Sessa, L., Cotugno, N., Ruggiero, A., Morrocchi, E., Concato, C., et al. (2019). Immune activation, inflammation, and non-AIDS co-morbidities in HIV-infected patients under long-term ART. *Viruses* 11:200. doi: 10.3390/v11030200

Conflict of Interest: The authors declare that the research was conducted in the absence of any commercial or financial relationships that could be construed as a potential conflict of interest.

Publisher's Note: All claims expressed in this article are solely those of the authors and do not necessarily represent those of their affiliated organizations, or those of the publisher, the editors and the reviewers. Any product that may be evaluated in this article, or claim that may be made by its manufacturer, is not guaranteed or endorsed by the publisher.

frontiers | Frontiers in Immunology

TYPE Original Research
PUBLISHED 28 July 2022
DOI 10.3389/fimmu.2022.947647

OPEN ACCESS

EDITED BY
Jiang Shibo,
Fudan University, China

REVIEWED BY
Li Ye,
Guangxi Medical University, China
Kehmia Titanji,
Emory University, United States

*CORRESPONDENCE
Yaxian Kong
kongyaxian@ccmu.edu.cn
Hongxin Zhao
Drzhao66@ccmu.edu.cn

†These authors have contributed equally to this work and share first authorship

SPECIALTY SECTION
This article was submitted to Viral Immunology, a section of the journal Frontiers in Immunology

RECEIVED 19 May 2022
ACCEPTED 29 June 2022
PUBLISHED 28 July 2022

CITATION
Zhang L, Wei Y, Wang D, Du J, Wang X, Li B, Jiang M, Zhang M, Chen N, Deng M, Song C, Chen D, Wu L, Xiao J, Liang H, Zhao H and Kong Y (2022) Elevated Foxp3$^+$ double-negative T cells are associated with disease progression during HIV infection.
Front. Immunol. 13:947647.
doi: 10.3389/fimmu.2022.947647

Elevated Foxp3$^+$ double-negative T cells are associated with disease progression during HIV infection

Leidan Zhang[1,2,3,4,5†], Yuqing Wei[2,3,4†], Di Wang[4,5†], Juan Du[2,3,4], Xinyue Wang[1,2,3,4], Bei Li[4,5], Meiqing Jiang[2,3,4], Mengyuan Zhang[2,3,4], Na Chen[1,4,5], Meiju Deng[2,3,4,5], Chuan Song[2,3,4], Danying Chen[2,3,4], Liang Wu[4,5], Jiang Xiao[4,5], Hongyuan Liang[4,5], Hongxin Zhao[1,4,5*] and Yaxian Kong[1,2,3,4*]

[1]Peking University Ditan Teaching Hospital, Beijing, China, [2]Beijing Key Laboratory of Emerging Infectious Diseases, Institute of Infectious Diseases, Beijing Ditan Hospital, Capital Medical University, Beijing, China, [3]Beijing Institute of Infectious Diseases, Beijing, China, [4]National Center for Infectious Diseases, Beijing Ditan Hospital, Capital Medical University, Beijing, China, [5]Clinical and Research Center of Infectious Diseases, Beijing Ditan Hospital, Capital Medical University, Beijing, China

Persistent immune activation, which occurs during the whole course of HIV infection, plays a pivotal role in CD4$^+$ T cells depletion and AIDS progression. Furthermore, immune activation is a key factor that leads to impaired immune reconstitution after long-term effective antiretroviral therapy (ART), and is even responsible for the increased risk of developing non-AIDS co-morbidities. Therefore, it's imperative to identify an effective intervention targeting HIV-associated immune activation to improve disease management. Double negative T cells (DNT) were reported to provide immunosuppression during HIV infection, but the related mechanisms remained puzzled. Foxp3 endows Tregs with potent suppressive function to maintain immune homeostasis. However, whether DNT cells expressed Foxp3 and the accurate function of these cells urgently needed to be investigated. Here, we found that Foxp3$^+$ DNT cells accumulated in untreated people living with HIV (PLWH) with CD4$^+$ T cell count less than 200 cells/μl. Moreover, the frequency of Foxp3$^+$ DNT cells was negatively correlated with CD4$^+$ T cell count and CD4/CD8 ratio, and positively correlated with immune activation and systemic inflammation in PLWH. Of note, Foxp3$^+$ DNT cells might exert suppressive regulation by increased expression of CD39, CD25, or vigorous proliferation (high levels of GITR and ki67) in ART-naive PLWH. Our study underlined the importance of Foxp3$^+$ DNT cells in the HIV disease progression, and suggest that Foxp3$^+$ DNT may be a potential target for clinical intervention for the control of immune activation during HIV infection.

KEYWORDS

HIV, Foxp3, double-negative T cell, immune activation, immune regulation

Introduction

Persistent immune activation, which occurs at the onset of HIV infection and persists in people living with HIV (PLWH) receiving effective antiretroviral therapy (ART) (1, 2), plays a key role in CD4 depletion and AIDS progression (3, 4). This condition may be associated with several factors including persistent antigen stimulation, microbial translocation, co-infections of other viruses, and cumulative ART toxicity (5). Indeed, immune activation is one of the strongest predictors of disease progression, is related to an increased risk of developing non-AIDS co-morbidities (6, 7), and is a key factor that leads to impaired immune reconstitution after long-term ART (8, 9). More importantly, the successful control of immune activation could be a target in the clinical therapy of PLWH.

Double negative T cells (DNT cells), which were acknowledged to express CD3 and TCRαβ, but not CD4, CD8 and CD56 surface markers (10, 11), constituted approximately 1-3% T lymphocytes in mice, as well as in humans, and an even higher percentage of T cells in some monkey species (12, 13). DNT cells derive either from the thymus by escaping negative selection or from peripheral T cells through downregulation of CD4 and CD8 and can be found in the peripheral blood, lymph nodes, and gut-associated lymphoid tissue (10, 11, 14–17). Previous studies identified the crucial role of DNT cells in graft-versus-host disease, autoimmune disease and infectious diseases, which were capable of limiting immune over-activation and maintaining immune system homeostasis (18–20). These cells exert immunosuppressive effects *via* various mechanisms, including high-level expression of CTLA-4 to downregulate the costimulatory molecules CD80 and CD86 on antigen-presenting mature DCs (21), production of anti-inflammatory cytokines such as IL-10, TGF-β (22), and induction of apoptosis *via* Fas/FasL pathway (23). Recently, accumulating evidence figured out a potential role of DNT cells to provide immunosuppression during HIV/SIV infection (15, 20, 22, 24), but the related mechanism needs to be further explored.

Foxp3, a 431 amino acid forkhead/winged-helix family transcriptional factor, predominantly expressed by a subset of $CD4^+$ T cells, commonly referred as $CD4^+CD25^+$ regulatory T cells (25). It acts as a transcriptional repressor inhibiting the genes encoding synthesis of proinflammatory cytokines, while as an activator promoting the expression of canonical Treg cell components such as CD25, GITR, CD73, CD39 and CTLA-4, which endows the cell with powerful suppressive functions (26). Thus, Foxp3 plays a requisite role in humans for maintaining immunological self-tolerance state, thereby preventing the development of autoimmune diseases (27). Recent studies showed that the impact of Foxp3 on immune regulation was extended to non-CD4 immune cells such as CD8, γδT cells, and iNKT cells (28–30). Additionally, ectopic expression of Foxp3 mediated by retroviral gene transfer or cytokines induction in human non-Tregs was reported to yield a series of new cells with potent immune suppress function (31, 32). More importantly, several studies found a parallel elevation of Foxp3 expression in both $CD4^+$ and $CD8^+$ T cells from untreated PLWH as negative feedback of immune activation, which indicated a role of $Foxp3^+$ T cells in HIV disease progression and the control of immune activation (33, 34). Nevertheless, there are limited data on the presence of $Foxp3^+$ DNT cells in HIV infection. Vinton et al. found that there were a considerable number of $Foxp3^+$ $CD3^+CD4^-CD8^-$ T cells accumulating in most SIV-infected natural hosts with low peripheral immune activation (13). However, $CD3^+CD4^-CD8^-$ T cells were acknowledged to be highly heterogeneous including not only DNT cells but also γδ T cells and iNKT cells (12), both of which definitely expressed Foxp3 (29, 30). Until now, previous studies have not provided sufficient evidence to support the expression of Foxp3 in DNT cells. Further investigations were urgently needed.

Here, we found that $Foxp3^+$ DNT cells accumulated in untreated PLWH with low $CD4^+$ T cells count in a persistent hyperinflammatory state and associated with disease progression. Furthermore, $Foxp3^+$ DNT cells were also involved in the control of immune activation and inflammation during HIV infection. Finally, our data implied that these $Foxp3^+$ DNT cells might exert suppressive regulation by elevated expression of CD39, CD25, or vigorous proliferation (high levels of GITR and ki67) as reported in $Foxp3^+$ $CD4^+$ Tregs in ART-naive PLWH.

Materials and methods

Study participants

We conducted a cross-sectional study, which was approved by the Committee of Ethics at Beijing Ditan Hospital, Capital Medical University in Beijing, and written informed consent was provided by each participant in accordance with the Declaration of Helsinki. In this study, we enrolled a cohort of 25 age-matched healthy controls (HCs), 121 treatment-naïve patients (TNs) and 32 HIV–infected patients receiving successful ART (ARTs). The precise infection time in these PLWH is unknown. At the time of specimen collection, ART-experienced PLWH were treated for a median of 5.2 years (IQR 4.1-6.4) with baseline $CD4^+$ T cells count < 200 cells/μl and had plasma HIV RNA levels that were below detection according to routine clinical assays. TNs with $CD4^+$ T cell count less than 200/μl are highly susceptible to opportunistic infections including tuberculosis and fungal infections. The clinical details of all the PLWH are shown in Table 1.

TABLE 1 Demographic and clinical characteristics of study participants.

Characteristics	HCs	TNs			ARTs	*P*-value*
		CD4 ≥ 350	200 ≤ CD4 < 350	CD4 < 200		
N (%)	25	42 (34.71)	30 (24.79)	49 (40.5)	32	–
Sex (M/F)	24/1	41/1	28/2	46/3	30/2	0.9252
Age (mean, years)	34 ± 7	29 ± 8	35 ± 8	40 ± 13	39 ± 7	0.1183
CD4 count (cells/mm^3), median (IQR)	728 (546-840)	493 (387-572)	268 (249-310)	70 (18-126)	271 (229-328)	P<0.0001
CD8 count (cells/mm^3), median (IQR)	555 (442-867)	1165 (974-1424)	961 (689-1161)	732 (364-1012)	691 (600-790)	P<0.0001
CD4/CD8 ratio, median (IQR)	1.09 (0.87-1.56)	0.42 (0.29-0.55)	0.28 (0.21-0.39)	0.08 (0.03-0.18)	0.43 (0.36-0.49)	P<0.0001
HIV RNA viral load (log copies/mL), median (IQR)	–	4.16 (3.64-4.85)	4.19 (3.74-4.79)	5.15 (4.63-5.56)	<LDL	P<0.0001

HC, healthy controls; TN, treatment-naive HIV-infected patients; ART, PLWH with treatment over 4 years; M, male; F, female; LDL, lower detection limit. TNs are divided into three subgroups according to blood CD4$^+$ T cell count.
*P-value: the difference among HCs, total TNs and ARTs using a Kruskal–Wallis test or Chi-square test.

Sample collection and processing

The peripheral blood samples were centrifuged (2000rpm/15min) to isolate the plasma. The plasma was then stored at - 80° C for later luminex experiment. PBMCs were collected using standard Ficoll-Paque gradient centrifugation according to the manufacturer's instructions (Amersham Pharmacia Biotech, Sweden). All samples were processed and analyzed within 24 hours of collection for Flow cytometry and ICS staining.

Plasma HIV-1 viral load and CD4$^+$ T-cell count

The plasma HIV-1-RNA levels were measured using a Standard Amplicor HIV Monitor assay, version 1.5 (Roche Diagnostics, Indianapolis, IN, USA), with a lower detection limit of 40 copies/mL. The CD4$^+$ T-cell count was determined with a standard flow cytometry technique with a TruCOUNT tube in routinely equipped laboratories (BD Biosciences, San Jose, CA, USA). Both measurements were determined twice per year in a single laboratory using standard methodologies that are included in the National Quality Assurance Programs.

Immunofluorescence staining and flow cytometric analysis

For surface staining, PBMCs were incubated with directly conjugated antibodies for 30 min at 4°C. Antibodies used included anti-human CD3-BUV737 (clone VCHT1), CD3-BV786 (clone SK7), CD4-BUV395 (clone RPA-T4), CD8-BUV395 (clone RPA-T8), GITR-BV605 (clone V27-580), CD38-BUV737 (clone HB7), CD25-PE-CF594 (clone M-A251, BD Biosciences, San Diego, CA, USA), CD4-APC-fire750 (clone SK3), CD8-BV421 (clone RPA-T8), αβTCR-BV421 (clone IP26), CD56-AF700 (clone 5.1H11), CD56-APC (clone 5.1H11), FasL-PE-Cy7 (clone NDK-1), CTLA-4-BV786 (clone BNI3), CD73-BV711 (clone AD2), HLA-DR-AF700 (clone L243, BioLegend, San Diego, CA, USA), LAG3-APC (clone 3DS223H, Invitrogen, Carlsbad, CA, USA) and the corresponding isotype controls. For intracellular staining of Foxp3 (clone 25901C7, BD Biosciences), Granzyme A-PE-cy7 (clone CB9), granzyme B-APC-fire750 (clone A16A02), perforin-PE-CF594 (clone dG9), Ki-67-BV711 (clone Ki-67, BioLegend) and IDO-APC (clone eyedio, Invitrogen) cells were fixed and permeabilized using Foxp3 Staining Buffer Set (BD Biosciences) according to the manufacturer's recommendations. A fixable viability dye eFluor 506 (Ebioscience, San Diego, CA, USA) was used to assess cell viability. Data were acquired on a BD LSR Fortessa flow cytometer (BD Biosciences) and analyzed with FlowJo software (Tree Star, Ashland, OR, USA).

In vitro stimulation and intracellular cytokine staining

PBMCs, isolated as described above, were resuspended to 2×10^6 cells/mL in RPMI 1640 medium plus 10% FBS (R10). Cells were then incubated for 5h at 37°C in a medium with 1 × Cell Stimulation Cocktail (containing 81 nM PMA and 1.34 nM ionomycin plus protein transport inhibitors, Ebioscience). Following incubation, the cells were washed and surface-stained with CD3-BV786 (clone SK7), CD8-BUV395 (clone RPA-T8, BD Biosciences), CD4-APC-fire750 (clone SK3, BioLegend) for 30 minutes in the dark at room temperature, followed by fixation and permeabilization. After permeabilization, cells were stained with IL-10-PE-cy7 (clone JES3-9D7, Ebioscience) antibodies for 50 minutes in the dark at room temperature. A fixable viability dye eFluor 506 (Ebioscience) was used to assess cell viability. Following staining, cells were washed and acquired on an LSRFortessa.

Quantification of soluble markers

Plasma samples from patients were assayed for the levels of different cytokines and chemokines (G-CSF, GM-CSF, I-TAC, IFN-α, IL1-β, IL-15, IL-6, IL-8, IP-10, MCP-1, MIG and MIP-β) using Luminex multiple kits (Invitrogen, Carlsbad, CA, USA).

Statistical analysis

The data are expressed as the mean [standard deviation (SD)], median [interquartile range (IQR)], and percentage [frequency]. The normality of each variable was evaluated using the Kolmogorov–Smirnov test. When the data were not normally distributed, the comparison of variables was performed with a Mann–Whitney U-test or a Wilcoxon matched-pairs signed-rank test for unpaired and paired data. A Kruskal–Wallis test followed by Dunn's multiple comparisons test was applied for comparing two more independent samples. Comparisons of participant characteristics were analyzed using Fisher's exact test (categorical variables) or the Kruskal–Wallis test (continuous variables). Pearson's or Spearman correlation coefficients were used to evaluate correlations for normally or non-normally distributed data, respectively. All analyses were performed using GraphPad8 (GraphPad Software, La Jolla, CA, USA). $P < 0.05$ was considered significant. Heatmaps and the radar map were generated using R version 3.6.3 software (Institute for Statistics and Mathematics, Vienna, Austria; www.r-project.org).

Results

Elevated frequency of Foxp3$^+$ DN T cells associated with HIV disease progression

We recruited 121 TNs and gender and age-matched 25 healthy donors. TNs were divided into three groups according to their baseline CD4 levels (< 200 cells/μl, 200-350 cells/μl, and ≥ 350 cells/μl). The demographic and clinical characteristics were illustrated in Table 1.

In line with previous studies, we also found that DNT cells increased with disease progression of HIV infection (Figure S1A) (24). To further investigate the potential role of Foxp3 in DNT cells during HIV infection, we performed intracellular flow cytometric analysis of Foxp3 in DNT cells. Representative flow cytometry gating strategy for Foxp3$^+$ αβDNT cells was shown in Figure 1A. In line with data concluded from a France cohort, we also found comparable frequency and the absolute number of Foxp3$^+$ DNT cells among HCs and different groups of PLWH with CD4$^+$ T cell count ≥ 200 cells/μl (22). However, PLWH with CD4$^+$ T cell count less than 200 cells/μl displayed significantly higher frequency and the absolute number of Foxp3$^+$ DNT cells than HCs and patients with CD4$^+$ T cell count ≥ 200 cells/μl (Figure 1B). Moreover, correlation analysis revealed that the frequency of Foxp3$^+$ DNT cells negatively correlated with CD4$^+$ T cell count and CD4/CD8 ratio ($r = -0.5862$, $P < 0.0001$; $r = -0.5341$, $P < 0.0001$, respectively; Figures 1C, D). Only a slight positive correlation was observed between the percentage of Foxp3$^+$ DNT cells and virus loads ($r = 0.27$, $P = 0.0025$; Figure 1E). In addition, we also assessed the correlation of DNT cell frequency with CD4$^+$ T cell count, CD4/CD8 ratio, and virus load and found no correlation among these parameters (Figures S1B–D). Collectively, these results suggested that Foxp3$^+$ DNT cells were associated with HIV disease progression, and might be a sign of the severe stage of HIV infection.

Foxp3$^+$ DNT cells correlated with immune activation and systemic inflammation in TNs

To further identify the role of Foxp3$^+$ DNT cells in controlling immune activation during HIV infection, we then applied correlation analysis between the frequency of Foxp3$^+$ DNT cells and immune activation. It was revealed that the percentage of Foxp3$^+$ DNT cells was positively correlated to both CD38^{hi}HLA-DR$^+$CD4$^+$ T cells and CD38^{hi}HLA-DR$^+$CD8$^+$ T cells ($r = 0.6338$, $P < 0.0001$; $r = 0.4577$, $P < 0.0001$, respectively; Figures 2A, B).

Considering a positive feedback loop between pro-inflammatory cytokines and activation of immune cells, we next detected the concentrations of various cytokines and chemokines including G-CSF, GM-CSF, I-TAC, IFN-α, IL1-β, IL-15, IL-6, IL-8, IP-10, MCP-1, MIG and MIP-β in plasma from TNs. As shown in the heatmap, TNs with higher Foxp3 expression on DNT cells displayed higher levels of inflammatory factors in plasma (Figure 2C). In addition, we performed a subgroup analysis, dividing TNs into Foxp3-high group (n=40) and Foxp3-low group (n=40) based on the median of Foxp3 expression. The median value 2.26 of Foxp3 expression on DNT cells of the 80 TNs evaluated was used as the cutoff in the present study. Compared to the Foxp3-low group, Foxp3-high patients showed significantly increased levels of inflammatory factors including I-TAC, IFN-α, IL-6, IL-8, IP-10, MCP-1, and MIG (Figure 2D). More importantly, levels of I-TAC, IL-6, IL-8, and MCP-1 were positively correlated with the frequency of Foxp3$^+$ DNT cells in TNs (Table 2 and Figure S2). Furthermore, we identified overall differences between these two groups using a radar map. Consistently, Foxp3-high patients displayed comprehensively higher levels of pro-inflammatory factors than Foxp3-low patients (Figure 2E). Collectively, these data strongly indicated that Foxp3$^+$ DNT cells in TNs associated with uncontrolled immune activation and systemic inflammation.

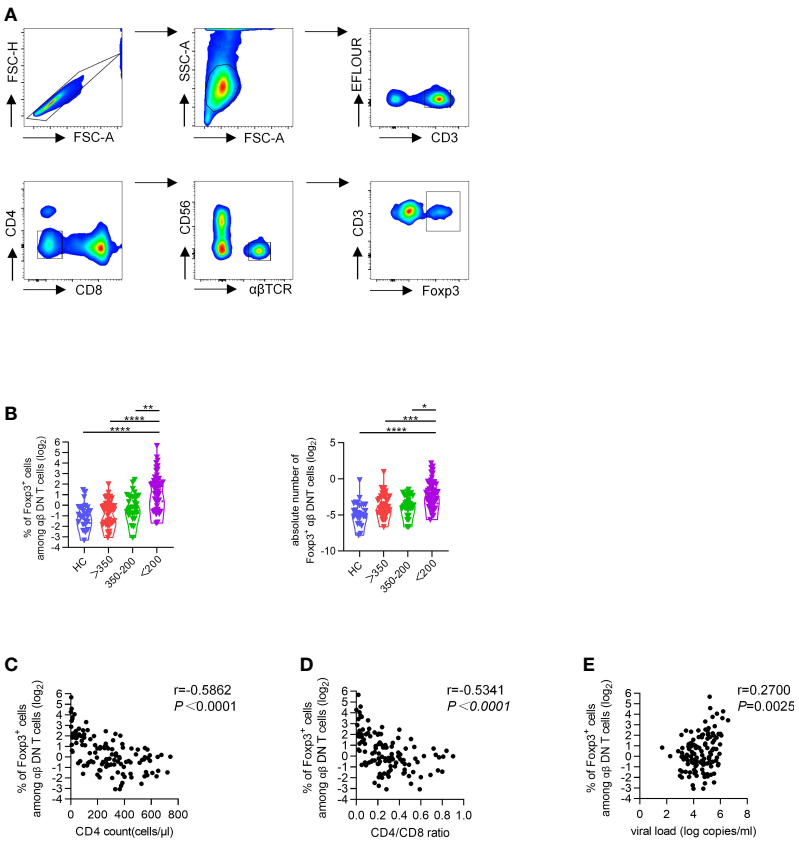

FIGURE 1
Increased proportions of Foxp3$^+$ DNT cells associated with progressive HIV disease. Flow cytometry analysis of Foxp3 expression was performed on PBMCs collected from HCs and different TNs groups. **(A)** Representative flow data showed the expression of Foxp3 on DNT cells from TNs. **(B)** Violin plots of the percentage of Foxp3$^+$ DNT cells from HCs and different TNs groups (n=20-66 each group). P values were obtained by Kruskal-Wallis test followed by Dunn's multiple comparisons test. **(C–E)** Correlation analysis of the percentages of Foxp3$^+$ DNT cells with CD4$^+$ T cell count **(C)**, CD4/CD8 ratio **(D)**, HIV viral load **(E)** in PHIV infected patients without treatment. The percentage of Foxp3$^+$ DNT cells was represented on a log2 scale. The correlation was calculated using Spearman's non-parametric test. *P < 0.05, **P < 0.01, ***P < 0.001, ****P < 0.0001.

Foxp3$^+$ DNT cells exhibited a unique characteristic compared with their circulating Foxp3$^-$ counterpart in TNs

Given that Foxp3 was indispensable to sustaining CD4$^+$ Tregs phenotypic stability, metabolic fitness, and regulatory function (27), we wondered the regulatory role of Foxp3 in DNT cells. Accordingly, we compared several membrane-bound or intracellular biomarkers associated with suppressive effects of CD4$^+$ Tregs between Foxp3$^-$ and Foxp3$^+$ DNT cells. Foxp3$^+$ DNT cells showed higher expression of CD39 as well as lower expression of CD73 than Foxp3$^-$ subset, implying the involvement of ATP/adenosine in Foxp3$^+$ DNT-mediated immune suppression (Figures 3A, B) (35). Additionally, we found elevated levels of GITR and Ki-67 in Foxp3$^+$ DNT cells compared with Foxp3$^-$ population, which suggested an enhanced stimulation and proliferation of Foxp3$^+$ DNT cells (Figures 3C, D) (36). What's more, Foxp3$^+$ DNT cells also preferentially expressed CD25, which was a crucial Treg surface marker implicated in the suppressive function (Figure 3E) (27). However, no significant differences were observed in the expression of LAG-3, CTLA-4, and FasL between Foxp3$^+$ and Foxp3$^-$ DNT cells (Figures 3F–H).

To further determine the function of Foxp3$^+$ DNT cells, we next detected the ability of DNT cells to secrete cytokines and intracellular proteins. Foxp3$^+$ DNT cells produced decreased levels of Granzyme A, Granzyme B and perforin, suggesting an impaired cytolytic capacity (Figures 4A–C). In addition, Foxp3$^+$ DNT cells secreted extremely few levels of IDO and IL-10, two key factors in regulation of immune suppression (Figures 4D, E). Taken together, these data indicated a unique phenotypic and intrinsic characteristic of Foxp3$^+$ DNT cells, which might exert immune modulatory effects through elevated signaling of CD39, CD25, or vigorous proliferation (high levels of GITR and ki67).

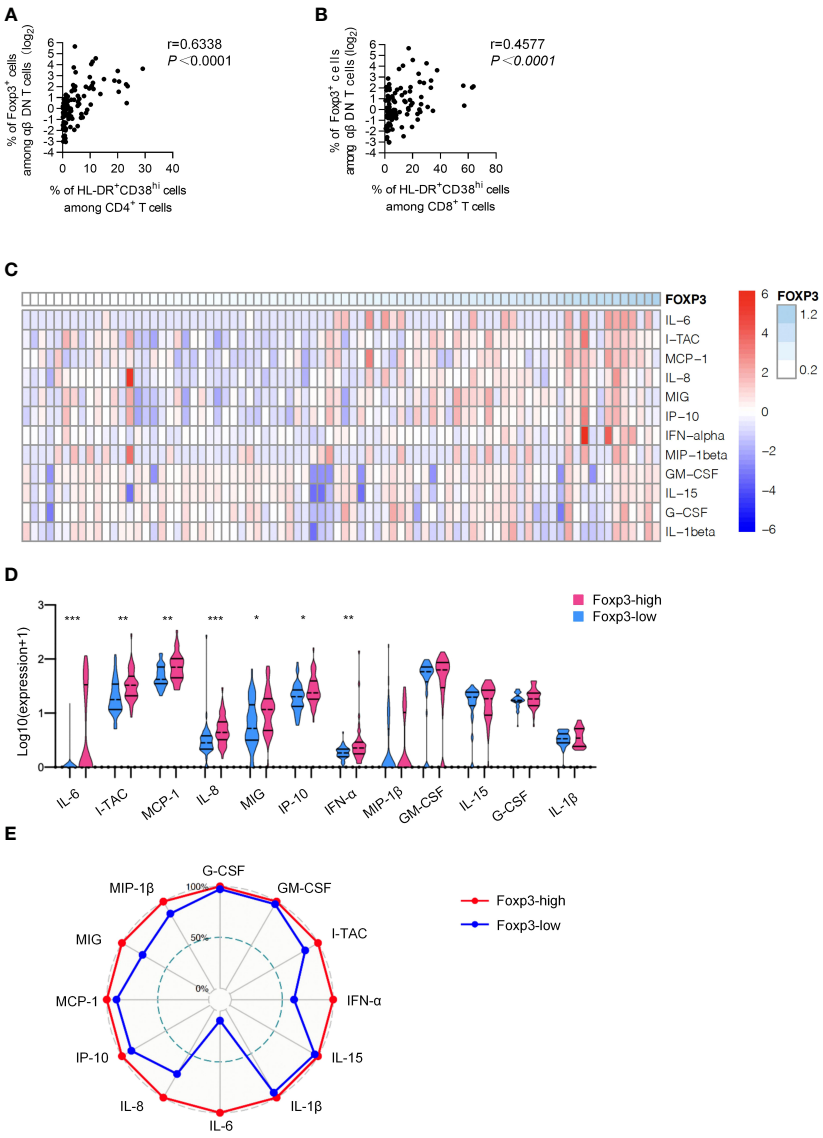

FIGURE 2
Foxp^{3+} DNT cells correlated with the phenotypic profile of activation and systematic inflammation. **(A, B)** Correlation analysis between the percentage of Foxp3$^+$ DNT cells and (HLA-DR$^+$CD38^{hi}CD4$^+$ T cells **(A)** and HLA-DR$^+$CD38^{hi}CD8$^+$ T cells **(B)** from TNs. Spearman's non-parametric test was used to test for correlations. **(C)** Heatmap depicting the relative concentrations of 12 differentially expressed serum proteins in TNs. Each column of the heatmap indicated a sample, while the rows represented different serum proteins. The color scale in the heatmap represented scores standardized across rows.(blue represented low levels; red, high levels) **(D)** Violin plots of the concentration of twelve differentially expressed serum proteins in the Foxp3-low group (n = 40) and Foxp3-high group (n = 40). The concentration of different serum was shown on a log10 scale. P values were obtained by Kruskal-Wallis test followed by Dunn's multiple comparisons test. **(E)** Radar map of 12 differentially expressed serum proteins in Foxp3-low group (n = 40) and Foxp3-high group (n = 40). The radius is the percentage of expression. *P < 0.05, **P < 0.01, ***P < 0.001.

Increased frequency of Foxp3$^+$ DNT cells was partially reversible after ART

In HIV-infected patients, ART can effectively reduce the overall immune activation and improve CD4$^+$ T cell recovery (37). To investigate the impact of ART on Foxp3$^+$ DNT cells, we then assessed the expression of Foxp3 on DNT cells among patients experiencing 5.2 years of ART with baseline CD4$^+$ T cells count < 200 cells/μl. As shown in Figure 5A, the elevated proportion and absolute numbers of Foxp3$^+$ DNT cells were significantly decreased in ART-experienced patients compared with that in TN patients. Consistently, the proportion of Foxp3$^+$

TABLE 2 Correlation Between plasma cytokines and chemokines and the percent of Foxp3$^+$ DNT cells in TNs.

Variable	Foxp3	
	r	P-value
G-CSF	0.01753	0.8773
GM-CSF	0.07337	0.5178
I-TAC	**0.3848**	**0.0004**
IFN-α	0.2767	0.0130
IL1-β	-0.0001876	0.9987
IL-15	0.03419	0.7633
IL-6	**0.3999**	**0.0002**
IL-8	**0.3707**	**0.0007**
IP-10	0.2799	0.0119
MCP-1	**0.3724**	**0.0007**
MIG	0.2821	0.0112
MIP-β	0.1182	0.2965

P values were obtained by Spearman test (n = 80). Bold fonts indicated strong correlations between the variables and Foxp3.

DNT cells in TNs was downregulated after ART (Figure 5B). These data pointed out that Foxp3$^+$ DNT cells were partially reversible after ART and mainly played a role in viremic patients, highlighting the significance of Foxp3$^+$ DNT cells during HIV infection.

Discussion

Previous studies have demonstrated that DNT cells accumulated and played a regulatory role in the control of immune activation during HIV infection (20, 22, 24); however, the underlying mechanisms need to be thoroughly explored. In this study, we found a subpopulation of DNT cells which shared the key factor "Foxp3" of CD4$^+$ Tregs enriched in PLWH with CD4$^+$ T cell count less than 200 cells/μl. Elevated Foxp3$^+$ DNT cells were associated with disease progression and immune activation in ART-naïve PLWH. Moreover, we further showed that these Foxp3$^+$ DNT cells from PLWH expressed higher levels of CD39, CD25, Ki-67, and GITR, which might play a crucial role in the suppressive regulation mediated by Foxp3$^+$ DNT cells. To our knowledge, this is the first time to identify the presence of Foxp3$^+$ DNT cells with a unique characteristic in PLWH and its role in HIV disease progression.

However, it is definitely controversial whether DNT cells expressed Foxp3 during HIV infection. In 2012, Petitjean et al. exhibited opposite results to ours, which pointed out that there were few Foxp3$^+$ DNT cells in PLWH enrolled in four clinical sites in France (22). The contradiction could be explained by the fact that we used cohorts with distinct characteristics. It is worth noting that we demonstrated the enrichment of Foxp3$^+$ DNT cells mainly in PLWH with baseline CD4$^+$ T cell count fewer than 200 cells/μl. Meanwhile, Petitjean's study was based on patients with significantly higher CD4$^+$ T cell count (> 334 cells/μl). In fact, these two cohorts were enrolled from two different countries (France and China respectively) with great differences in cultural backgrounds, economic and medical conditions. In Europe, national medical funding accelerated progress in earlier diagnoses and treatment for PLWH, which allowed patients to visit the hospital at the early stage of the infection. However, in most developing counties including China, patients were unaware of their status until the late stage due to the limited medical resource and the lack of propagation of HIV/AIDS science. This led to the consequence that a high percentage of patients were in a state with impaired thymic output and extremely low CD4$^+$ T cell count. More importantly, the regulation and maintenance of immune homeostasis might vary depending on different statuses. Our results highlight the importance of Foxp3$^+$ DNT in the regulation of immune homeostasis in PLWH, especially in patients with low CD4$^+$ T cell count.

Although Foxp3 is considered as a specific marker of CD4$^+$ regulatory T cells, it was also reported to express in non-Treg immune cells as well as non-immune cells, including CD8$^+$ T cells, γδ T cells, NKT cells, B cells, macrophages, and cancer cells (28–31, 38, 39). Many studies have revealed suppressive effects of Foxp3$^+$CD8$^+$ Tregs, which showed similar phenotypic features with CD4$^+$ Tregs. In untreated PLWH, the proportion of Foxp3$^+$CD8$^+$ T cells correlated positively with the frequency of HLA-DR^{hi}CD4$^+$ T cells and inversely with CD4$^+$ T cell count, which indicated the involvement of Foxp3$^+$CD8$^+$ T cells in HIV disease progression (40). As for γδ T cells, Foxp3 was majorly expressed in Vδ1 T cells from tumor-infiltrating lymphocytes (TILs) and contributed to their suppressive function (29). In fact, γδ T cells freshly isolated from peripheral blood barely expressed Foxp3, while Foxp3$^+$ γδ T cells could be induced in presence of TGF-β and IL-2/IL-15. The inducible Foxp3$^+$ Vδ1 T cells with higher GITR, CTLA-4, and membrane-bound latent form of TGF-β manifested a more potent suppressive effect on responder cells *via* a cell-to-cell contact mechanism compared with Foxp3$^-$ Vδ1 T cells. What's more, the percentage of infiltrating Foxp3$^+$CD3$^+$CD56$^+$ cells in tumors was found to be inversely correlated with patient survival (41). Additionally, lentiviral transduction of Foxp3 into CD3$^+$CD56$^+$ cells endowed these cells with a potent and cell contact-dependent inhibition on T cell activation. Similarly, apart from being crucial in maintaining food tolerance and tending to decrease RA-associated immunopathology, the high proportion of circulating Foxp3$^+$CD19$^+$ B cells in MS patients during relapse is a compensatory peripheral response to the inflammatory circumstances of disease activity (38). DC expressing transgene Foxp3 severely limited T-cell proliferation and T cell type-1 immune responses *in vitro* (31). Collectively, these results

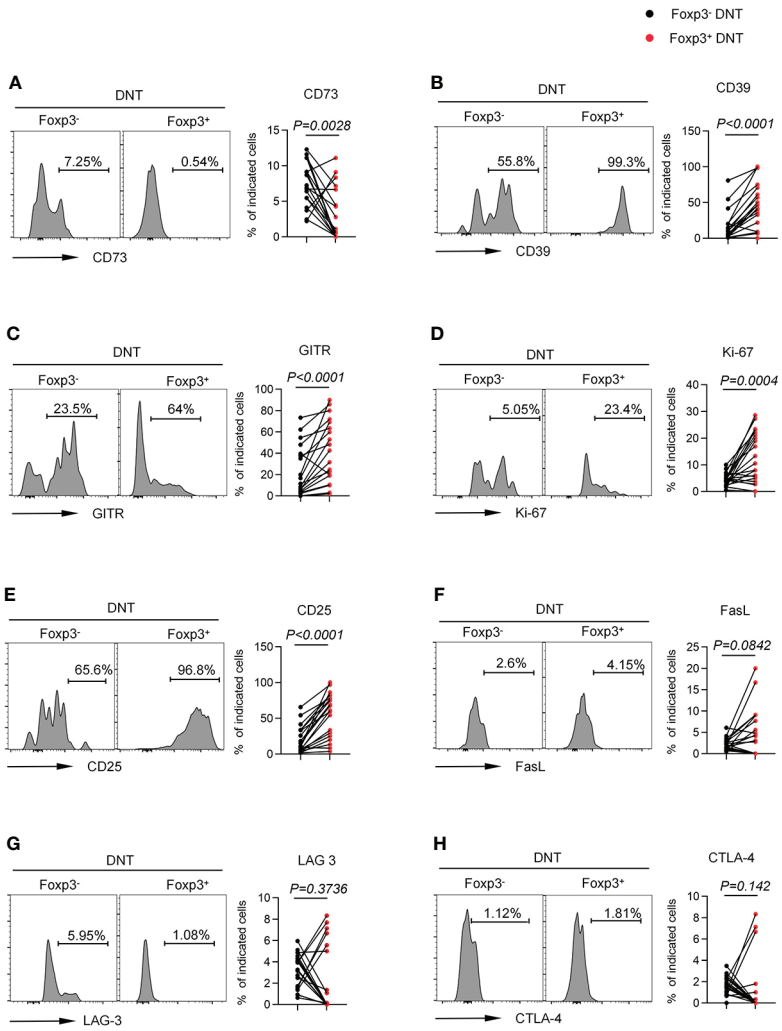

FIGURE 3
Foxp3$^+$ DNT cells showed a unique phenotypic characteristic compared with their circulating Foxp3$^-$ counterpart in TNs. Flow cytometry analysis of expression of CD73 **(A)**, CD39 **(B)**, GITR **(C)**, Ki-67 **(D)**, CD25 **(E)**, FasL **(F)**, LAG-3 **(G)** and CTLA-4 **(H)** on Foxp3$^-$ *vs.* Foxp3$^+$ DNT cells from TNs with baseline CD4$^+$ T cell count ≤ 200 cells/μl. Representative histograms (left) and plots (right) displayed the expression of the above markers on Foxp3$^-$ *vs.* Foxp3$^+$ DNT cells. *P* values were obtained by Wilcoxon matched-pairs signed rank test.

suggested the possibility of Foxp3 being expressed in other cells in addition to CD4$^+$ Treg cells and involved in the regulation of immune response as a complementary mechanism in the presence of pathological immune imbalance.

It is generally recognized that systemic immune activation is a detrimental consequence of HIV infection. On one hand, it is a crucial driving force of the loss of CD4$^+$ T cells, which contributes to the development of AIDS-related events such as opportunistic infections and cancer (3, 4). On the other hand, the enduring immune activation in response to the virus persistence is liable for the growing non-AIDS morbidity and mortality (5, 6). Therefore, it's imperative to identify an effective intervention targeting HIV-associated immune activation to improve disease management. Physiologically, the immune system has protective mechanisms to avoid the aberrant immune activation that in the case of the disease leads to a marked erosion and offset-tune of the entire immune system. However, CD4$^+$ Treg cells, the potent natural regulator which can inhibit T cell activation and proliferation, become draining and dysfunctional during HIV infection, especially in patients with low CD4$^+$ T cell count (42). Of note, we found an accumulation of DNT cells, particularly the Foxp3$^+$ subset with immune suppressive roles in PLWH. Although DNT cells were also identified as target cells of HIV (43), mature DNT cells were reported to be highly resistant to apoptosis (44). In that condition, due to the incapable CD4$^+$ T cells replenishment and

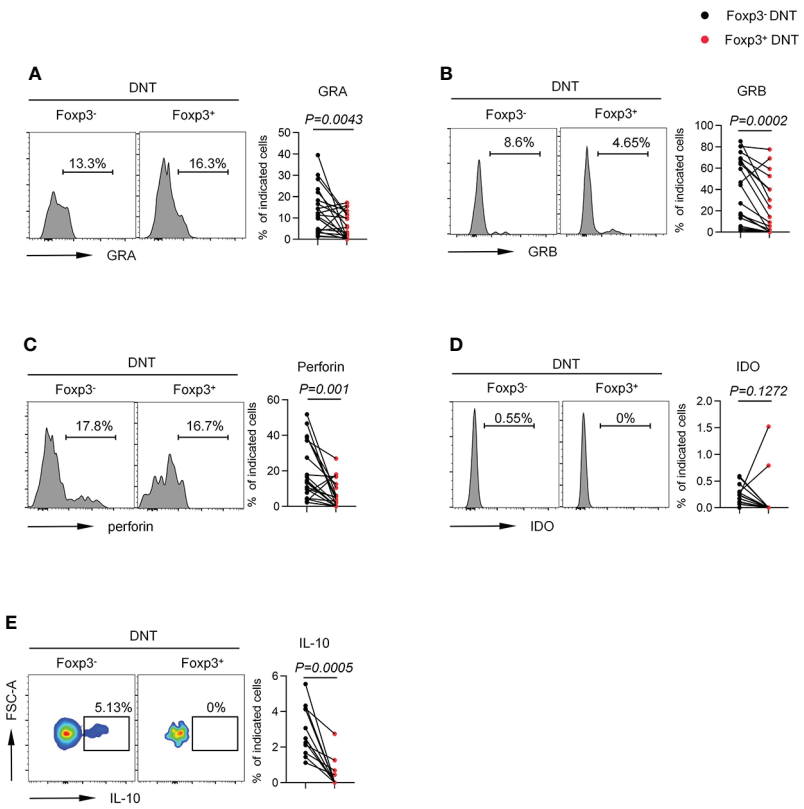

FIGURE 4
Foxp3$^+$ DNT cells secreted different level of cytokine and intracellular proteins compared with their circulating Foxp3$^-$ counterpart in TNs. Flow cytometry analysis of expression of GRA **(A)**, GRB **(B)**, Perforin **(C)**, IDO **(D)** and IL-10 **(E)** on Foxp3$^-$ *vs.* Foxp3$^+$ DNT cells from TNs with baseline CD4$^+$ T cell count ≤ 200 cells/μl. Representative histograms (left) and plots (right) displayed the expression of the above markers on Foxp3$^-$ *vs.* Foxp3$^+$ DNT cells. Statistical tests were performed using the Wilcoxon matched-pairs signed rank test.

impaired thymic output, Foxp3$^+$ DNT cells might act as negative feedback to maintain the immune homeostasis.

A key unresolved issue is the specific origin of these Foxp3$^+$ DNT cells. Previous studies suggested that high levels of immune activation in PLWH might induce and maintain the population of Tregs as negative feedback (34). Here, we revealed a positive correlation between the frequency of Foxp3$^+$ DNT cells and systemic immune activation. Thus, we speculated that these Foxp3$^+$ DNT cells proliferated possibly in response to over-activation of the immune system as similar as the expansion of CD4$^+$ Tregs in peripheral blood of PLWH, which was confirmed by high expression of Ki-67 in Foxp3$^+$ DNT cells. And the elevation of Foxp3$^+$ DNT cells might act as negative feedback to ameliorate pathogenesis in infectious diseases. Of note, peripheral DNT cells were reported to derive from CD8$^+$ or CD4$^+$ T cells in both physiological and pathologic status (10). Due to the serious deficiency of CD4$^+$ T cells during HIV infection, it was extremely possible that Foxp3$^+$ DNT cells come from CD8$^+$ T cells by losing CD8 protein.

An interesting finding in the present study is that Foxp3$^+$ DNT cells also expressed CD25, GITR and CD39, which were verified to contribute to immunoregulatory functions of Foxp3$^+$CD4$^+$ Tregs (27). CD25 rendered Treg cells able to rapidly sense IL-2 produced by self-reactive conventional T cells early in the immune response and compete for growth factors (27). CD39 was an ectoenzyme that converted ATP into adenosine in tandem with CD73, which was reported to involve in the immune regulation mediated by DNT cells in our recent study (24). Additionally, GITR triggering *in vivo* effectively increased the absolute number of cells through enhanced proliferation (36), which was in line with high levels of Ki-67 in Foxp3$^+$ DNT cells. In contrast, Foxp3$^+$ and Foxp3$^-$ DNT cells showed comparable levels of CTLA-4, which prevented costimulation and proliferation of conventional T cells by interacting and downregulating CD80/CD86 on antigen-presenting cells (21). This indicated that the regulatory mechanism of CTLA-4 in DNT cells might be different from that in Tregs, in which foxp3 can form a complex with NFAT to

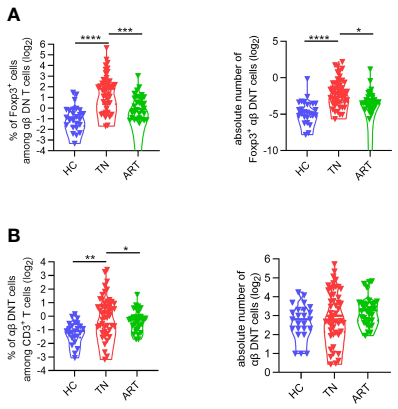

FIGURE 5
The frequency of Foxp3$^+$ DNT cells was partly restored after ART. **(A)**Violin plots of the frequencies (left) and absolute numbers (right) of DNT cells from healthy donors, TNs with baseline CD4$^+$ T cell count < 200 cells/μl, ARTs who have been treated more than 4 years with matched nadir CD4$^+$ T cell count. **(B)** Comparison of Foxp3$^+$ DNT cells frequencies (left) and absolute numbers (right) in healthy donors, TNs, ARTs. *P* values were obtained by the Kruskal–Wallis test, followed by Dunn's multiple comparisons test. **P* < 0.05, ***P* < 0.01, ****P* < 0.001, *****P* < 0.0001.

function as an activator of the Ctla4 gene (45). More importantly, both CD4$^+$ Tregs and DNT were revealed to exert immune regulation *via* cytolytic activity as well as secretion of IL-10. However, in the present study, Foxp3$^+$ DNT cells were found to express lower levels of granzyme A/B and perforin than Foxp3$^-$ DNT cells, suggesting the impaired cytolytic capacity of Foxp3$^+$ DNT cells. Moreover, these Foxp3$^+$ DNT cells even failed to produce IL-10, which was in accordance with limited secretion of IL-10 in Foxp3$^+$ CD8$^+$ T cells (30). Taken together, the expression of Foxp3 conferred Treg-like features to DNT cells (CD25, GITR, and CD39), while it also accompanied with the loss of some intrinsic functions of DNT cells (granzyme B, perforin and IL-10).

Our study has some limitations. First of all, it is difficult to confirm the suppressive role of Foxp3$^+$ DNT cells by performing functional *in vitro* experiments, due to lack of methods to isolate viable Foxp3$^+$ cells. Second, according to the fact that PLWH with low CD4$^+$ T cell count are more susceptible to opportunistic infection, we could not distinguish the effects of HIV itself or opportunistic pathogens responsible for our findings. Finally, a heavily gender-skewed cohort was applied in the present study, which was almost completely made up of men who have sex with men (MSM). It is well acknowledged that women were in a higher immune activation and more inflammatory state during HIV infection (46). Hence, we need to verify our findings in a gender-balanced cohort.

In summary, our study demonstrated that elevated Foxp3$^+$ DNT cells with Treg-like phenotype were associated with systemic immune activation and disease progression during HIV infection, providing a promising clinical intervention for the control of immune activation.

Data availability statement

The original contributions presented in the study are included in the article/Supplementary material. Further inquiries can be directed to the corresponding authors.

Ethics statement

The studies involving human participants were reviewed and approved by the Committee of Ethics at Beijing Ditan Hospital. The patients/participants provided their written informed consent to participate in this study.

Author contributions

LZ performed the experiments, analyzed the data and wrote the manuscript. YW and DW performed the experiments and analyzed the data. XW, BL, MJ, MZ, NC, MD, CS, DC, JX, LW and HL collected samples, and performed the experiments. HZ participated in the critical review of the manuscript and revised the manuscript. YK designed the experiments, analyzed the data and revised the manuscript. All authors contributed to the article and approved the submitted version.

Funding

This work was supported by Beijing Municipal Natural Science Foundation for Distinguished Young Scholars (JQ21023), National Natural Science Foundation of China (82171548, 81971307), Beijing Municipal Administration of Hospitals' Ascent Plan (DFL20191802), and Beijing Municipal Administration of Hospitals Clinical Medicine Development of Special Funding Support (ZYLX202126).

Acknowledgments

The authors sincerely thank all the patients and healthy donors in this study.

Conflict of interest

The authors declare that the research was conducted in the absence of any commercial or financial relationships that could be construed as a potential conflict of interest.

Publisher's note

All claims expressed in this article are solely those of the authors and do not necessarily represent those of their affiliated organizations, or those of the publisher, the editors and the reviewers. Any product that may be evaluated in this article, or claim that may be made by its manufacturer, is not guaranteed or endorsed by the publisher.

Supplementary material

The Supplementary Material for this article can be found online at: https://www.frontiersin.org/articles/10.3389/fimmu.2022.947647/full#supplementary-material

References

1. Lv T, Cao W, Li T. HIV-Related immune activation and inflammation: Current understanding and strategies. *J Immunol Res* (2021) 2021:7316456. doi: 10.1155/2021/7316456

2. Naidoo KK, Ndumnego OC, Ismail N, Dong KL, Ndung'u T. Antigen presenting cells contribute to persistent immune activation despite antiretroviral therapy initiation during hyperacute HIV-1 infection. *Front Immunol* (2021) 12:738743. doi: 10.3389/fimmu.2021.738743

3. Paiardini M, Müller-Trutwin M. HIV-Associated chronic immune activation. *Immunol Rev* (2013) 254(1):78–101. doi: 10.1111/imr.12079

4. Vidya Vijayan KK, Karthigeyan KP, Tripathi SP, Hanna LE. Pathophysiology of CD4+ T-cell depletion in HIV-1 and HIV-2 infections. *Front Immunol* (2017) 8:580. doi: 10.3389/fimmu.2017.00580

5. Zicari S, Sessa L, Cotugno N, Ruggiero A, Morrocchi E, Concato C, et al. Immune activation, inflammation, and non-AIDS Co-morbidities in HIV-infected patients under long-term ART. *Viruses* (2019) 11(3):200. doi: 10.3390/v11030200

6. García F, Fumero E, Gatell JM. Immune modulators and treatment interruption. *Curr Opin HIV AIDS* (2008) 3(2):124–30. doi: 10.1097/COH.0b013e3282f52413

7. Grund B, Neuhaus J, Phillips A. Relative risk of death in the SMART study. *Lancet Infect Dis* (2009) 9(12):724–5. doi: 10.1016/s1473-3099(09)70302-0

8. Zhang Y, Jiang T, Li A, Li Z, Hou J, Gao M, et al. Adjunct therapy for CD4(+) T-cell recovery, inflammation and immune activation in people living with HIV: A systematic review and meta-analysis. *Front Immunol* (2021) 12:632119. doi: 10.3389/fimmu.2021.632119

9. Bandera A, Masetti M, Fabbiani M, Biasin M, Muscatello A, Squillace N, et al. The NLRP3 inflammasome is upregulated in HIV-infected antiretroviral therapy-treated individuals with defective immune recovery. *Front Immunol* (2018) 9:214. doi: 10.3389/fimmu.2018.00214

10. Brandt D, Hedrich CM. TCRalphabeta(+)CD3(+)CD4(-)CD8(-) (double negative) T cells in autoimmunity. *Autoimmun Rev* (2018) 17(4):422–30. doi: 10.1016/j.autrev.2018.02.001

11. Neyt K, GeurtsvanKessel CH, Lambrecht BN. Double-negative T resident memory cells of the lung react to influenza virus infection *via* CD11c(hi) dendritic cells. *Mucosal Immunol* (2016) 9(4):999–1014. doi: 10.1038/mi.2015.91

12. Hillhouse EE, Lesage S. A comprehensive review of the phenotype and function of antigen-specific immunoregulatory double negative T cells. *J Autoimmun* (2013) 40:58–65. doi: 10.1016/j.jaut.2012.07.010

13. Vinton C, Klatt NR, Harris LD, Briant JA, Sanders-Beer BE, Herbert R, et al. CD4-like immunological function by CD4- T cells in multiple natural hosts of simian immunodeficiency virus. *J Virol* (2011) 85(17):8702–8. doi: 10.1128/JVI.00332-11

14. Sundaravaradan V, Mir KD, Sodora DL. Double-negative T cells during HIV/SIV infections: potential pinch hitters in the T-cell lineup. *Curr Opin HIV AIDS* (2012) 7(2):164–71. doi: 10.1097/COH.0b013e3283504a66

15. Milush JM, Mir KD, Sundaravaradan V, Gordon SN, Engram J, Cano CA, et al. Lack of clinical AIDS in SIV-infected sooty mangabeys with significant CD4+ T cell loss is associated with double-negative T cells. *J Clin Invest* (2011) 121(3):1102–10. doi: 10.1172/JCI44876

16. Veazey RS, Rosenzweig M, Shvetz DE, Pauley DR, DeMaria M, Chalifoux LV, et al. Characterization of gut-associated lymphoid tissue (GALT) of normal rhesus macaques. *Clin Immunol Immunopathol* (1997) 82(3):230–42. doi: 10.1006/clin.1996.4318

17. Veazey RS, DeMaria M, Chalifoux LV, Shvetz DE, Pauley DR, Knight HL, et al. Gastrointestinal tract as a major site of CD4+ T cell depletion and viral replication in SIV infection. *Science* (1998) 280(5362):427–31. doi: 10.1126/science.280.5362.427

18. Li Y, Dong K, Fan X, Xie J, Wang M, Fu S, et al. DNT cell-based immunotherapy: Progress and applications. *J Cancer* (2020) 11(13):3717–24. doi: 10.7150/jca.39717

19. Ford McIntyre MS, Gao JF, Li X, Naeini BM, Zhang L. Consequences of double negative regulatory T cell and antigen presenting cell interaction on immune response suppression. *Int Immunopharmacol* (2011) 11(5):597–603. doi: 10.1016/j.intimp.2010.11.015

20. Lu X, Su B, Xia H, Zhang X, Liu Z, Ji Y, et al. Low double-negative CD3(+)CD4(-)CD8(-) T cells are associated with incomplete restoration of CD4(+) T cells and higher immune activation in HIV-1 immunological non-responders. *Front Immunol* (2016) 7:579. doi: 10.3389/fimmu.2016.00579

21. Gao JF, McIntyre MS, Juvet SC, Diao J, Li X, Vanama RB, et al. Regulation of antigen-expressing dendritic cells by double negative regulatory T cells. *Eur J Immunol* (2011) 41(9):2699–708. doi: 10.1002/eji.201141428

22. Petitjean G, Chevalier MF, Tibaoui F, Didier C, Manea ME, Liovat AS, et al. Level of double negative T cells, which produce TGF-beta and IL-10, predicts CD8 T-cell activation in primary HIV-1 infection. *AIDS* (2012) 26(2):139–48. doi: 10.1097/QAD.0b013e32834e1484

23. Zhang ZX, Ma Y, Wang H, Arp J, Jiang J, Huang X, et al. Double-negative T cells, activated by xenoantigen, lyse autologous b and T cells using a perforin/granzyme-dependent, fas-fas ligand-independent pathway. *J Immunol* (2006) 177(10):6920–9. doi: 10.4049/jimmunol.177.10.6920

24. Wang X, Zhang L, Du J, Wei Y, Wang D, Song C, et al. Decreased CD73+ double-negative T cells and elevated level of soluble CD73 correlated with and predicted poor immune reconstitution in HIV-infected patients after antiretroviral therapy. *Front Immunol* (2022) 13:869286. doi: 10.3389/fimmu.2022.869286

25. Fontenot JD, Gavin MA, Rudensky AY. Foxp3 programs the development and function of CD4+CD25+ regulatory T cells. *Nat Immunol* (2003) 4(4):330–6. doi: 10.1038/ni904

26. Piccirillo CA. Transcriptional and translational control of Foxp3(+) regulatory T cell functional adaptation to inflammation. *Curr Opin Immunol* (2020) 67:27–35. doi: 10.1016/j.coi.2020.07.006

27. Georgiev P, Charbonnier LM, Chatila TA. Regulatory T cells: the many faces of Foxp3. *J Clin Immunol* (2019) 39(7):623–40. doi: 10.1007/s10875-019-00684-7

28. Mahic M, Henjum K, Yaqub S, Bjørnbeth BA, Torgersen KM, Taskén K, et al. Generation of highly suppressive adaptive CD8(+)CD25(+)FOXP3(+) regulatory T cells by continuous antigen stimulation. *Eur J Immunol* (2008) 38(3):640–6. doi: 10.1002/eji.200737529

29. Li X, Kang N, Zhang X, Dong X, Wei W, Cui L, et al. Generation of human regulatory gammadelta T cells by TCRgammadelta stimulation in the presence of TGF-beta and their involvement in the pathogenesis of systemic lupus erythematosus. *J Immunol* (2011) 186(12):6693–700. doi: 10.4049/jimmunol.1002776

30. Engelmann P, Farkas K, Kis J, Richman G, Zhang Z, Liew CW, et al. Characterization of human invariant natural killer T cells expressing FoxP3. *Int Immunol* (2011) 23(8):473–84. doi: 10.1093/intimm/dxr040

31. Lipscomb MW, Taylor JL, Goldbach CJ, Watkins SC, Wesa AK, Storkus WJ. DC Expressing transgene Foxp3 are regulatory APC. *Eur J Immunol* (2010) 40 (2):480–93. doi: 10.1002/eji.200939667

32. Kang N, Tang L, Li X, Wu D, Li W, Chen X, et al. Identification and characterization of Foxp3(+) gammadelta T cells in mouse and human. *Immunol Lett* (2009) 125(2):105–13. doi: 10.1016/j.imlet.2009.06.005

33. Oswald-Richter K, Grill SM, Shariat N, Leelawong M, Sundrud MS, Haas DW, et al. HIV Infection of naturally occurring and genetically reprogrammed human regulatory T-cells. *PloS Biol* (2004) 2(7):E198. doi: 10.1371/journal.pbio.0020198

34. Cao W, Jamieson BD, Hultin LE, Hultin PM, Detels R. Regulatory T cell expansion and immune activation during untreated HIV type 1 infection are associated with disease progression. *AIDS Res Hum Retroviruses* (2009) 25(2):183–91. doi: 10.1089/aid.2008.0140

35. Borsellino G, Kleinewietfeld M, Di Mitri D, Sternjak A, Diamantini A, Giometto R, et al. Expression of ectonucleotidase CD39 by Foxp3+ treg cells: hydrolysis of extracellular ATP and immune suppression. *Blood* (2007) 110 (4):1225–32. doi: 10.1182/blood-2006-12-064527

36. van Olffen RW, Koning N, van Gisbergen KP, Wensveen FM, Hoek RM, Boon L, et al. GITR triggering induces expansion of both effector and regulatory CD4+ T cells *in vivo*. *J Immunol* (2009) 182(12):7490–500. doi: 10.4049/jimmunol.0802751

37. Autran B, Carcelain G, Li TS, Blanc C, Mathez D, Tubiana R, et al. Positive effects of combined antiretroviral therapy on CD4+ T cell homeostasis and function in advanced HIV disease. *Science* (1997) 277(5322):112–6. doi: 10.1126/science.277.5322.112

38. Guo Y, Zhang X, Qin M, Wang X. Changes in peripheral CD19(+)Foxp3(+) and CD19(+)TGFβ(+) regulatory b cell populations in rheumatoid arthritis patients with interstitial lung disease. *J Thorac Dis* (2015) 7(3):471–7. doi: 10.3978/j.issn.2072-1439.2015.02.11

39. Vadasz Z, Toubi E. FoxP3 expression in macrophages, cancer, and b cells-is it real? *Clin Rev Allergy Immunol* (2017) 52(3):364–72. doi: 10.1007/s12016-016-8572-5

40. Lim A, French MA, Price P. CD4+ and CD8+ T cells expressing FoxP3 in HIV-infected patients are phenotypically distinct and influenced by disease severity and antiretroviral therapy. *J Acquir Immune Defic Syndr* (2009) 51(3):248–57. doi: 10.1097/QAI.0b013e3181a74fad

41. Li X, Peng J, Pang Y, Yu S, Yu X, Chen P, et al. Identification of a FOXP3(+) CD3(+)CD56(+) population with immunosuppressive function in cancer tissues of human hepatocellular carcinoma. *Sci Rep* (2015) 5:14757. doi: 10.1038/srep14757

42. López-Abente J, Correa-Rocha R, Pion M. Functional mechanisms of treg in the context of HIV infection and the janus face of immune suppression. *Front Immunol* (2016) 7:192. doi: 10.3389/fimmu.2016.00192

43. Marodon G, Warren D, Filomio MC, Posnett DN. Productive infection of double-negative T cells with HIV *in vivo*. *Proc Natl Acad Sci U.S.A.* (1999) 96 (21):11958–63. doi: 10.1073/pnas.96.21.11958

44. Khan Q, Penninger JM, Yang L, Marra LE, Kozieradzki I, Zhang L. Regulation of apoptosis in mature alphabeta+CD4-CD8- antigen-specific suppressor T cell clones. *J Immunol* (1999) 162(10):5860–7.

45. Wu Y, Borde M, Heissmeyer V, Feuerer M, Lapan AD, Stroud JC, et al. FOXP3 controls regulatory T cell function through cooperation with NFAT. *Cell* (2006) 126(2):375–87. doi: 10.1016/j.cell.2006.05.042

46. Griesbeck M, Scully E, Altfeld M. Sex and gender differences in HIV-1 infection. *Clin Sci (Lond)* (2016) 130(16):1435–51. doi: 10.1042/cs20160112

frontiers | Frontiers in Microbiology

TYPE Original Research
PUBLISHED 18 August 2022
DOI 10.3389/fmicb.2022.962477

OPEN ACCESS

EDITED BY
Jiang Shibo,
Fudan University, China

REVIEWED BY
Zhiwei Chen,
The University of Hong Kong,
Hong Kong SAR, China
Chaitanya Kurhade,
University of Texas Medical Branch
at Galveston, United States

*CORRESPONDENCE
Yuhua Ruan
ruanyuhua92@chinaaids.cn
Guanghua Lan
lgh605@163.com

†These authors have contributed
equally to this work

SPECIALTY SECTION
This article was submitted to
Virology,
a section of the journal
Frontiers in Microbiology

RECEIVED 06 June 2022
ACCEPTED 26 July 2022
PUBLISHED 18 August 2022

CITATION
Chen J, Chen H, Li J, Luo L, Kang R, Liang S, Zhu Q, Lu H, Zhu J, Shen Z, Feng Y, Liao L, Xing H, Shao Y, Ruan Y and Lan G (2022) Genetic network analysis of human immunodeficiency virus sexual transmission in rural Southwest China after the expansion of antiretroviral therapy: A population-based study. *Front. Microbiol.* 13:962477. doi: 10.3389/fmicb.2022.962477

Genetic network analysis of human immunodeficiency virus sexual transmission in rural Southwest China after the expansion of antiretroviral therapy: A population-based study

Jin Chen[1†], Huanhuan Chen[2†], Jianjun Li[2], Liuhong Luo[2], Ruihua Kang[1], Shujia Liang[2], Qiuying Zhu[2], Huaxiang Lu[2], Jinhui Zhu[2], Zhiyong Shen[2], Yi Feng[1], Lingjie Liao[1], Hui Xing[1], Yiming Shao[1], Yuhua Ruan[1*] and Guanghua Lan[2*]

[1]State Key Laboratory of Infectious Disease Prevention and Control, National Center for Acquired Immune Deficiency Syndrome (AIDS)/Sexually Transmitted Disease (STD) Control and Prevention, Chinese Center for Disease Control and Prevention, Collaborative Innovation Center for Diagnosis and Treatment of Infectious Diseases, Beijing, China, [2]Guangxi Key Laboratory of Major Infectious Disease Prevention Control and Biosafety Emergency Response, Guangxi Center for Disease Control and Prevention, Nanning, China

Background: This study is used to analyze the genetic network of HIV sexual transmission in rural areas of Southwest China after expanding antiretroviral therapy (ART) and to investigate the factors associated with HIV sexual transmission through the genetic network.

Materials and methods: This was a longitudinal genetic network study in Guangxi, China. The baseline survey and follow-up study were conducted among patients with HIV in 2015, and among those newly diagnosed from 2016 to 2018, respectively. A generalized estimating equation model was employed to explore the factors associated with HIV transmission through the genetic linkage between newly diagnosed patients with HIV (2016–2018) and those at baseline (2015–2017), respectively.

Results: Of 3,259 identified HIV patient sequences, 2,714 patients were at baseline, and 545 were newly diagnosed patients with HIV at follow-up. A total of 8,691 baseline objectives were observed by repeated measurement analysis. The prevention efficacy in HIV transmission for treated HIV patients was 33% [adjusted odds ratio (AOR): 0.67, 95% confidence interval (CI): 0.48–0.93]. Stratified analyses indicated the prevention efficacy in HIV transmission for treated HIV patients with a viral load (VL) of <50 copies/ml and those treated for 4 years with a VL of <50 copies/ml to be 41 [AOR: 0.59, 95% CI: 0.43–0.82] and 65% [AOR: 0.35, 95% CI: 0.24–0.50], respectively. No

significant reduction in HIV transmission occurred among treated HIV patients with VL missing or treated HIV patients on dropout. Some factors were associated with HIV transmission, including over 50 years old, men, Zhuang and other nationalities, with less than secondary schooling, working as a farmer, and heterosexual transmission.

Conclusion: This study reveals the role of ART in reducing HIV transmission, and those older male farmers with less than secondary schooling are at high risk of HIV infection at a population level. Improvements to ART efficacy for patients with HIV and precision intervention on high-risk individuals during the expansion of ART are urgently required.

KEYWORDS

HIV, genetic network, antiretroviral therapy, transmission, prevention

Introduction

The aim of the Acquired Immune Deficiency Syndrome (AIDS) prevention and control strategy 95-95-95 is to help end the AIDS epidemic as a public health threat by 2030 (UNAIDS, 2015; Frank et al., 2019). The first "95" of the Joint United Nations Programme on HIV/AIDS (UNAIDS) 95-95-95 goal is 95% of all people living with HIV will know their HIV status, the second "95" is 95% of people with diagnosed HIV infection will receive sustained antiretroviral therapy (ART), and the final "95" is 95% of all people receiving ART will have viral suppression. ART is among the main means of achieving this goal (Lima et al., 2017; Saag et al., 2020). With the continuous improvement of ART strategies, China's ART standards were adjusted in 2016 to recommend free ART to all HIV-infected persons regardless of their CD4 cell counts, further expanding the scope of treatment. ART has been reported to effectively reduce the viral load (VL) and decline the mortality rate of HIV-infected people (Trickey et al., 2017; Mangal et al., 2019; Zhou et al., 2020). Between 2011 and 2016, the mortality rate of HIV-infected individuals in Western Kenya dropped significantly during the ART scale-up (Otieno et al., 2019). Immediate ART among HIV patients with CD4 cell counts exceeding 500 cells/μl was associated with a 63% reduction in overall mortality (Zhao et al., 2018). ART can improve the quality of the lives of patients with HIV and effectively reduce the spread of HIV by inhibiting its replication (Rodger et al., 2016). HIV Prevention Trials Network (HPTN) 052 programme trial's interim result indicated that early ART prevented over 96% of HIV genetically transmission among serodiscordant couples (Cohen et al., 2016), while the final results of that trial demonstrated that early ART reduced 93% of HIV linkage than that was delayed ART (Cohen et al., 2020). A retrospective observational cohort study in China also exhibited a consistent result, compared with that late-ART initiation, the preventive efficacy of early-ART initiation among serodiscordant couples was 45%, and the preventive efficacy of mid-ART initiation was 39% (Liu et al., 2018). In the two phases of the People on ART-A New Evaluation of the Risks (PARTNER) (partners of PARTNER) study conducted in the European clinical base, ART and viral suppression proved to prevent sexual transmission among serodiscordant couples (Rodger et al., 2016, 2019). The HPTN 071 (PopART) trial, a large randomized population controlled clinical trial established at the community level conducted from 2013 through 2018, showed that ART and universal testing combination intervention can reduce HIV incidence and transmission at a population level (Hayes et al., 2019). There were reductions in HIV-associated mortality and HIV incidence when patients with HIV used ART.

Despite the goal of reaching 95-95-95 of the AIDS prevention and control strategy by 2030, very few studies currently exist on the transmission of HIV and critical factors at a population level globally. At present, most studies on HIV transmission are based on traditional epidemiological methods. Traditional epidemiological methods often require a large HIV cohort, long-term follow-up observation, and high attention. Furthermore, these need substantial financial budgets and human resources to support the follow-up efforts. In recent years, the development and application of genetic transmission network provide new ideas for the evaluation of HIV transmission (Oster et al., 2018). A genetic network refers to a group/s of people infected with HIV whose infectious viruses have a genetic similarity. HIV transmission network refers to the network formed by a group/s of people infected with HIV who have direct or indirect epidemiological links in the transmission process (National Center for HIV/AIDS, Viral Hepatitis, STD, TB Prevention, and Division of HIV/AIDS Prevention, 2018). In the HIV-1 genetic transmission network analysis based in San Mateo County, it was found that African Americans played an important role in community transmission

(Dalai et al., 2018). A genetic network analysis in Guangzhou, China, revealed that undisclosed MSM plays an important role in HIV-1 transmission (Yan et al., 2020). A genomic and spatial epidemiological analysis identified high-risk populations and areas in Sichuan (Yuan et al., 2022). HIV transmission constructed by genetic transmission network analysis can determine the transmission population (Poon et al., 2016; de Oliveira et al., 2017; Dk et al., 2018) and also explore the characteristics and influencing factors of HIV transmission (Su et al., 2018; Wu et al., 2019; Kang et al., 2021). In our previous study, which focused on evaluating the effects of ART on HIV transmission, the longitudinal genetic network method was employed to build a genetic transmission network during 2015–2018 in the rural areas of Guangxi (Kang et al., 2021). However, this study had some limitations. First, this statistical method did not adjust factors, which may overestimate prevention efficacy in HIV transmission for ART, and longitudinal repeated measurement data were not well-utilized. Second, only the ART variable was considered, and this was unable to reveal epidemic characteristics of HIV transmission. Third, genetic linkages between newly diagnosed patients with HIV were not analyzed.

Guangxi Zhuang Autonomous Region (herein "Guangxi") is located in Southwest China. By 2020, Guangxi had accounted for 9.3% of the total number of nationally reported HIV/AIDS cases while representing less than 4% of the national population and had the third highest number of HIV cases reported in China (Jia et al., 2022). Before 2006, the main HIV transmission route was through injected drug abuse. Thereafter, sexual transmission became the primary infection route (Chen et al., 2019a). Heterosexual intercourse became the dominant transmission route for HIV (99.0%), and HIV is now rapidly spreading among the elderly in rural areas of Guangxi (Chen et al., 2019b). Due to the variability of epidemic populations and patterns (Li et al., 2018; Chen et al., 2021), local HIV epidemic prevention and control programmes are challenging. Based on the constructed genetic transmission network from our previous study, genetic linkages between newly diagnosed patients with HIV at follow-up and baseline were calculated, which represents the HIV secondary generation transmission in this study. The generalized estimating equation (GEE) model was used to process longitudinal repeated measurement data. the epidemic characteristics of the HIV sexual transmission in Guangxi were investigated, and the role of factors, including ART for HIV transmission, was evaluated at a population level in the scale-up HIV testing and ART context.

Materials and methods

Study design and participants

Participants living in the Luzhai County and Liujiang District, which are two major HIV epidemic areas in Liuzhou Prefecture, were recruited. Liuzhou is located in the northeast of Central Guangxi. This study was a longitudinal genetic network analysis of patients with HIV in Guangxi from 2015 to 2018. Baseline data of patients with HIV were collected from those diagnosed in Guangxi who received care up until 31 December 2015, while follow-up data encompassed newly diagnosed patients with HIV from 2016 to 2018. Eligibility criteria were as follows: (1) at least 18 years old; (2) living with HIV; and (3) provided written informed consent. The study was approved by the institutional review committee of the Guangxi Center for Disease Control and Prevention.

Data collection

The collected data included sociodemographic information and clinical information. Sociodemographic information included age, sex, ethnicity, education, marital status, occupation, route of HIV transmission, and county. Clinical information included year of HIV diagnoses, CD4 cell count before ART, year of ART initiation, and follow-up data such as follow-up time, VL at follow-up, and follow-up status (e.g., treatment, death, transferred, withdrawal, and loss to follow-up). The dropped out (withdrawal or loss to follow-up) was defined as withdrawal or loss to follow-up for more than 90 days. Individuals were followed up once every 3 months prior to receiving ART. The individuals were followed up at 0.5, 1, 2, and 3 months after receiving ART and then subsequently once every 3 months.

Nucleic acid extraction amplification and sequencing

Whole blood samples were collected from patients with HIV. The plasma components were isolated and sent to the laboratory under cold chain conditions. DNA was extracted from 200 μl of whole blood using the QIAamp DNA Blood Mini Kit (Qiagen, Hilden, Germany), followed by the manufacturer's protocol. RNA was extracted from 200 μl of plasma by using the QIAamp Viral RNA Mini Kit (Qiagen, Hilden, Germany). The HIV pol region was amplified by nested PCR using the extracted DNA and RNA as templates. The amplification and sequencing methods used in this study have been published previously (Liao et al., 2010; Xing et al., 2015).

HIV-1 genetic transmission network

The HIV-1 genetic transmission network refers to a group/s of sequences that are not randomly gathered and have an epidemiological correlation. These sequences were obtained by sequencing and required a series of processes. They were spliced

by BioEdit (Ibis Biosciences, Carlsbad, CA, United States; version 7.0.9.0) and aligned separately by the HIValign tool to obtain the final sequences used for analysis. The MEGA 7 software was used to identify the HIV-1 subtypes, and FastTree (developed by Morgan N. Price; version 1.3.1) constructed the phylogenetic tree. Before constructing the genetic transmission network, the distance between sequences (genetic distance [GD]) was used to represent the distance of patients with HIV. The pairwise Tamura-Nei (TN93) GD of the paired sequences was calculated using Hyphy (version 2.2.4). Finally, the HIV genetic transmission network was visualized by using the Cytoscape software. The genetic distance (GD) with the largest number of linked nodes and clusters was selected as the threshold for analyzing the genetic transmission network. In this study, 0.0075 was used as the GD threshold to calculate pairwise GD and identify linkage sequence pairs, as it had the most genetic networks and linkages.

The patients with early HIV symptoms were defined as those at baseline (e.g., December 31, 2015), and the corresponding newly diagnosed patients with HIV were defined as those diagnosed in the next year (e.g., those newly diagnosed in 2016). First, patients with HIV at baseline on December 31, 2015 were considered to construct genetic transmission network, and then the corresponding newly diagnosed patients with HIV in 2016 were put into the transmission network under the same GD. The genetic linkages between newly diagnosed patients with HIV in 2016 and those at baseline on December 31, 2015 were calculated. Second, based on the genetic transmission network constructed by patients with HIV at baseline on December 31, 2016, those newly diagnosed in 2017 were added into the network according to the same GD. Thereafter, the genetic transmission network between newly diagnosed patients with HIV in 2018 and those at baseline on December 31, 2017 was similarly constructed and the genetic linkages were similarly calculated.

Statistical analysis

After constructing the three genetic transmission networks, the sociodemographic information and clinical information of the baseline characteristics of the three genetic transmission networks were observed repeatedly. Sociodemographic characteristics included age, sex, ethnicity, education, marital status, occupation, route of HIV transmission, and county. Clinical information included year of diagnosis, CD4 cell count before ART, and year of ART initiation. The genetic linkages between newly diagnosed patients with HIV during 2016–2018 and those at baseline during 2015–2017 were calculated. The number of genetic linkages was equal to the number of newly diagnosed patients with HIV linked to those at baseline.

The generalized estimating equation model was used to analyze the factors associated with HIV transmission through the genetic linkage between newly diagnosed patients with HIV during 2016–2018 and those at baseline during 2015–2017, respectively. GEE models could account for repeated and correlated measures within individuals and improve the statistical precision by using information across repeated measures (Ballinger, 2004). Taking the number of genetic linkages to present between newly diagnosed patients with HIV and those at baseline as the dependent variable, the unadjusted and adjusted odds ratio (AORs) were estimated for sociodemographic characteristics and clinical information in the GEE models. Furthermore, stratification analysis was performed to evaluate the impact of ART on the HIV transmission. Patients with HIV at each baseline were divided into treated group and untreated group, and the treated group was further stratified based on VL data available at baseline time point: treated HIV patients with VL of less than 50 copies/ml (ART with VL < 50) and at least 50 copies/ml. For ART without VL information, the follow-up status was used as the basis for further stratification. If withdrawal and loss to follow-up occurred in the follow-up status record, these patients with HIV were defined as treated HIV patients on dropout (ART on dropout); otherwise, patients with HIV were defined as treated HIV patients with VL missing (ART with VL missing). To control potential bias and avoid the influences of other variables, the adjusted baseline characteristics of age, sex, ethnicity, education, occupation, mobility, and route of HIV transmission were included as control variables in the multivariate generalized estimating equation model.

Results

Characteristics of patients with human immunodeficiency virus within the study

Of 3,259 identified HIV patient sequences, 2,714 patients were at baseline, and 545 were newly diagnosed patients with HIV at follow-up. The general characteristics of patients with HIV in this study are shown in **Table 1**. Overall, 51.0% of patients with HIV were 30–49 years old, and 36.0% were 50–69 years old. The majority of patients with HIV were men (61.8%). The proportion of HIV patients with Han ethnicity was 42.8%. More than half of patients with HIV (56.6%) had completed at least secondary education and 62.4% were married; among the married patients with HIV, 23.8% of the spouses of patients with HIV were HIV-positive, 13.6% of the spouses of those were HIV-negative, the remaining 24.8% of those lack spouse information, and 67.0% were farmers. The main route of HIV transmission was heterosexual intercourse (96.1%), and the main HIV-1 genetic subtype was CRF01_AE (93.4%). In addition, 80.2% of patients with HIV had CD4 cell counts of less than 350 cells/mm^3 before receiving ART. Those lived

TABLE 1 General characteristics of patients with HIV between 2015 and 2018 in Guangxi of China.

Variable	2015		2016		2017		2018		Total	
	N	%	N	%	N	%	N	%	N	%
Total	2,714	100.0	175	100.0	199	100.0	171	100.0	3,259	100.0
Age, years										
18∼29	214	7.9	13	7.4	16	8.0	14	8.2	257	7.9
30∼49	1,452	53.5	68	38.9	73	36.3	68	39.8	1,661	51.0
50∼69	914	33.7	87	49.7	93	46.7	81	47.4	1,175	36.0
≥70	134	4.9	7	4.0	17	8.5	8	4.7	166	5.1
Sex										
Male	1,629	60.0	120	68.6	143	71.9	123	71.9	2,015	61.8
Female	1,085	40.0	55	31.4	56	28.1	48	28.1	1,244	38.2
Ethnicity										
Han	1,231	45.4	56	32.0	60	30.2	48	28.1	1,395	42.8
Zhuang and other	1,483	54.7	119	68.0	139	69.8	123	71.9	1,864	57.2
Education										
No school or primary	1,131	41.7	95	54.3	114	57.3	76	44.4	1,416	43.5
Secondary school and above	1,583	58.3	80	45.7	85	42.6	95	55.5	1,843	56.6
Marital status										
Single	358	13.2	43	24.6	43	21.6	36	21.1	480	14.7
Married	1,756	64.7	88	50.3	110	55.3	80	46.8	2,034	62.4
Divorced/widowed	599	22.1	42	24.0	41	20.6	46	26.9	728	22.3
Unknown	1	0.0	2	1.1	5	2.5	9	5.3	17	0.5
Occupation										
Farmer	1,797	66.2	115	65.7	144	72.4	128	74.9	2,184	67.0
Other	917	33.8	60	34.3	55	27.6	43	25.2	1,075	33.0
Route of HIV transmission										
Heterosexual intercourse	2,654	97.8	159	90.9	170	85.4	149	87.1	3,132	96.1
Homosexual intercourse	18	0.7	4	2.3	3	1.5	1	0.6	26	0.8
Unknown	42	1.5	12	6.9	26	13.1	21	12.3	101	3.1
Genetic subtype										
CRF01_AE	2,576	94.9	153	87.4	170	85.5	148	86.5	3,047	93.4
CRF07_BC	71	2.6	8	4.6	10	5.0	11	6.4	100	3.1
CRF08_BC	39	1.4	5	2.9	14	7.0	7	4.1	65	2.0
Other	28	1.0	9	5.1	5	2.5	5	3.0	47	1.4
CD4 count before ART										
<350 cells/mm^3	2,284	84.2	118	67.4	109	54.8	103	60.2	2,614	80.2
≥350 cells/mm^3	287	10.6	17	9.7	17	8.5	19	11.1	340	10.4
Missing	143	5.3	40	22.9	73	36.7	49	28.7	305	9.4
County										
Luzhai	1,794	66.1	98	56.0	69	34.7	67	39.2	2,038	62.5
Liujiang	910	33.5	77	44.0	130	65.3	104	60.8	1,221	37.5
Viral load after 12 months of ART										
<50 copies/mL	814	30.0	61	34.9	43	21.6	1	0.6	919	28.2
≥50 copies/mL	134	4.9	7	4.0	16	8.0	0	0.0	157	4.8
Missing*	1655	61.0	67	38.3	68	34.2	121	70.8	1911	58.6

*Including viral load information of HIV patients with ART time less than 6 months.

in Luzhai County (62.5%) and Liujiang County (37.5%) in Guangxi of China.

HIV-1 genetic transmission network

The genetic transmission networks between newly diagnosed patients with HIV during 2016–2018 and those at baseline during 2015–2017 are shown in Figure 1. There were a total of 8,691 baseline observations in the generalized estimating equation model. Among the patients with HIV at baseline within the networks, 466 and 384 were linked to one newly diagnosed patient with HIV and more than two newly diagnosed HIV patients with a GD threshold of 0.0075, respectively (Table 2). Approximately, 14.1% (98/694) of patients with HIV at baseline did not receive ART linked to the those newly diagnosed. About 13.9% (417/3,009) of patients with HIV at baseline aged 50–60 years were linked

to those newly diagnosed. The proportion of patients with HIV at baseline aged more than 70 years linked to those newly diagnosed was 20.1% (87/433). Approximately, 11.8% (621/5,270) of male patients with HIV at baseline were linked to those newly diagnosed. The proportion of Zhuang and other nationalities linked to newly diagnosed patients with HIV was 12.0% (577/4,826). About 12.8% (473/3,697) of patients with HIV at baseline with primary schooling as their highest level of educational attainment were linked to those newly diagnosed. The proportion of married patients with HIV at baseline linked to those newly diagnosed was 10.2% (567/5,554). Approximately, 11.4% (659/5,765) of patients with HIV at baseline who were farmers were linked to those newly diagnosed. The proportion of patients with HIV at baseline who were infected with HIV through heterosexual intercourse route linked to those newly diagnosed was 10.0% (841/8,450). Finally, the proportions of patients with HIV at baseline with CRF01_AE subtype, CD4 cell counts above 350 cells/mm^3, and living in Liujiang linked to those newly diagnosed were 10.1 (829/8,204), 12.1 (110/912), and 15.8% (476/3,014), respectively.

To determine the factors associated with genetic linkage, the generalized estimating equation model was conducted. According to the univariate generalized estimating equation model, age, sex, ethnicity, education, occupation, route of HIV transmission, ART, genetic subtype, CD4 count before ART, and county factors were significantly associated with

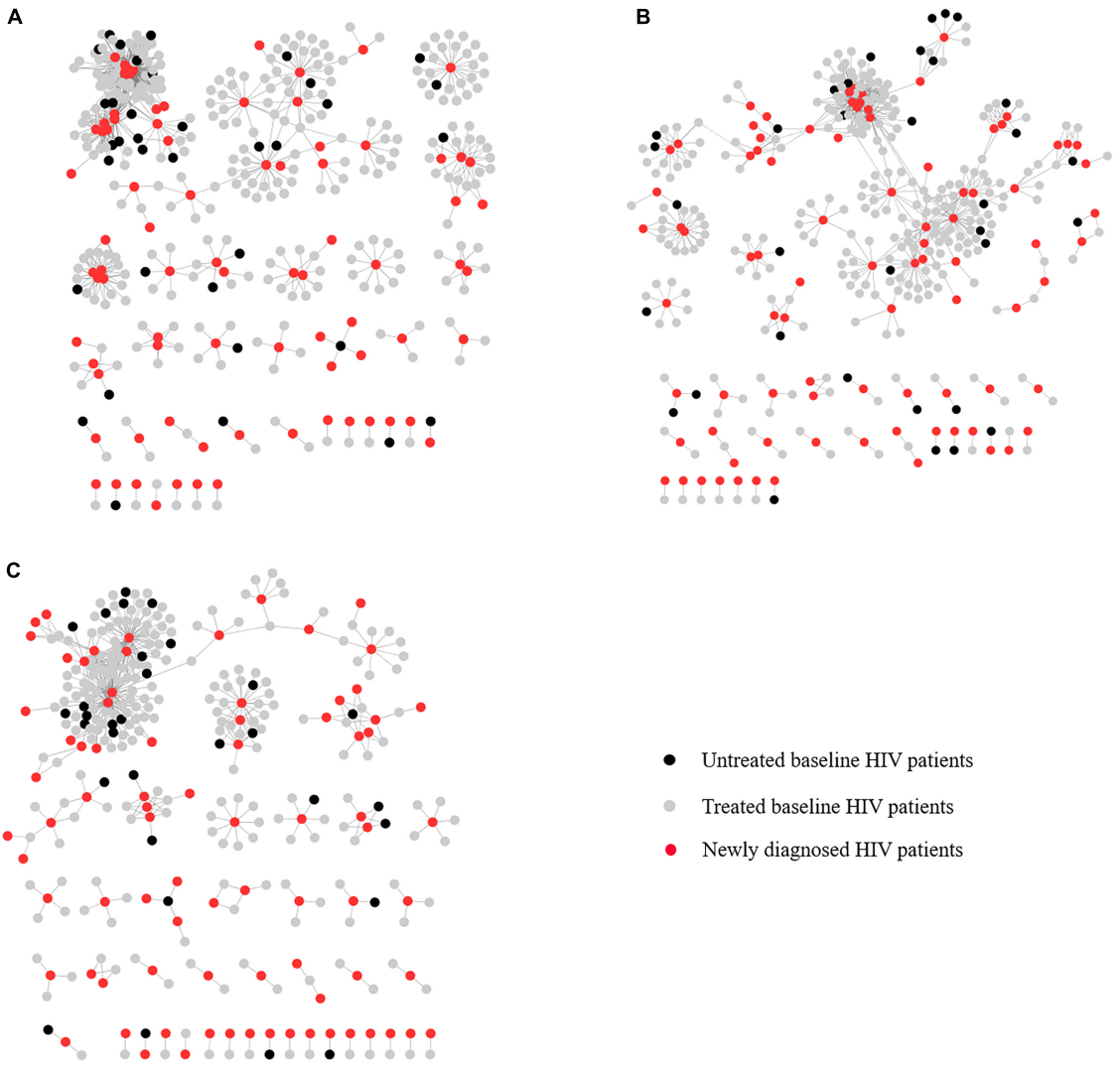

FIGURE 1
Transmission network of genetic linkage between newly diagnosed patients with HIV and those at baseline in Guangxi of China. **(A)** Genetic linkage between newly diagnosed patients with HIV in 2016 and those at baseline in 2015. **(B)** Genetic linkage between newly diagnosed patients with HIV in 2017 and those at baseline in 2016. **(C)** Genetic linkage between newly diagnosed patients with HIV in 2018 and those at baseline in 2017.

HIV transmission through the genetic network between newly diagnosed patients with HIV during 2016–2018 and those at baseline during 2015–2017, respectively. After adjustments in the final generalized estimating equation model, treated HIV patients were significantly associated with less HIV transmission through the genetic network (AOR: 0.67, 95% CI: 0.48–0.93, $P = 0.016$). In contrast, other factors significantly associated with HIV transmission through the genetic network included being aged 50–69 years (AOR: 3.72, 95% CI: 2.16–6.39; reference group: 18–29 years old, $P < 0.001$), over 70 years old (AOR: 5.12, 95% CI: 2.77–9.46; reference group: 18–29 years old, $P < 0.001$), men (AOR: 1.82, 95% CI: 1.46–2.28, $P < 0.001$), Zhuang and other nationalities (AOR: 1.50, 95% CI: 1.22–1.84; reference group: Han, $P < 0.001$), illiteracy or only having

TABLE 2 Genetic linkage between newly diagnosed patients with HIV during 2016–2018 and those at baseline during 2015–2017 in Guangxi of China, respectively.

Variable	Baseline	Number of genetic linkages between newly diagnosed HIV patients and HIV patients at baseline			*OR* (95% CI)	*P*	*AOR* (95% CI)	*P*
		1 person (%)	≥2 person (%)	≥1 person (%)				
Total	8691	466 (5.4)	384 (4.4)	850 (9.8)				
Age, year								
18∼29	684	18 (2.6)	9 (1.3)	27 (3.9)	1.00		1.00	
30∼49	4565	191 (4.2)	128 (2.8)	319 (7.0)	1.83 (1.08–3.10)	0.024	1.75 (1.03–2.98)	0.039
50∼69	3009	210 (7.0)	207 (6.9)	417 (13.9)	3.95 (2.34–6.68)	<0.001	3.72 (2.16–6.39)	<0.001
≥70	433	47 (10.9)	40 (9.2)	87 (20.1)	6.12 (3.37–11.12)	<0.001	5.12 (2.77–9.46)	<0.001
Sex								
Female	3421	137 (4.0)	92 (2.7)	229 (6.7)	1.00		1.00	
Male	5270	329 (6.2)	292 (5.5)	621 (11.8)	1.87 (1.51–2.32)	<0.001	1.82 (1.46–2.28)	<0.001
Ethnicity								
Han	3865	177 (4.6)	96 (2.5)	273 (7.1)	1.00		1.00	
Zhuang and other	4826	289 (6.0)	288 (6.0)	577 (12.0)	1.81 (1.48–2.22)	<0.001	1.50 (1.22–1.84)	<0.001
Education								
Secondary school and above	4994	213 (4.3)	164 (3.3)	377 (7.5)	1.00		1.00	
Illiteracy or primary	3697	253 (6.8)	220 (6.0)	473 (12.8)	1.80 (1.48–2.19)	<0.001	1.43 (1.15–1.77)	<0.001
Marital status								
Single	1203	54 (4.5)	42 (3.5)	96 (8.0)	1.00			
Married	5554	307 (5.5)	260 (4.7)	567 (10.2)	1.31 (0.96–1.79)	0.085		
Divorced/widowed	1922	102 (5.3)	82 (4.3)	184 (9.6)	1.22 (0.86–1.73)	0.264		
Unknown	12	3 (25.0)	0 (0.0)	3 (25.0)	3.31 (0.90–12.22)	0.073		
Occupation								
Other	2926	113 (3.9)	78 (2.7)	191 (6.5)	1.00		1.00	
Farmer	5765	353 (6.1)	306 (5.3)	659 (11.4)	1.85 (1.48–2.32)	<0.001	1.48 (1.17–1.87)	0.001
Route of HIV transmission								
Other or unknown	241	6 (2.5)	3 (1.2)	9 (3.7)	1.00		1.00	
Heterosexual intercourse	8450	460 (5.4)	381 (4.5)	841 (10.0)	2.86 (1.39–5.88)	0.004	3.19 (1.42–7.16)	0.005
Antiretroviral therapy								
Untreated	694	50 (7.2)	48 (6.9)	98 (14.1)	1.00		1.00	
Treated	7997	416 (5.2)	336 (4.2)	752 (9.4)	0.63 (0.46–0.85)	0.003	0.67 (0.48–0.93)	0.016
Genetic subtype								
CRF01_AE	8204	451 (5.5)	378 (4.6)	829 (10.1)	1.00			
Other	487	15 (3.1)	6 (1.2)	21 (4.3)	0.40 (0.25–0.64)	<0.001		
CD4 count before ART, cells/mm^3								
<350	7197	373 (5.2)	289 (4.0)	662 (9.2)	1.00			
≥350	912	55 (6.0)	55 (6.0)	110 (12.1)	1.36 (1.01–1.85)	0.045		
Missing	582	38 (6.5)	40 (6.9)	78 (13.4)	1.54 (1.08–2.20)	0.017		
County								
Luzhai	5677	266 (4.7)	108 (1.9)	374 (6.6)	1.00			
Liujiang	3014	200 (6.6)	276 (9.2)	476 (15.8)	2.75 (2.26–3.34)	<0.001		
Mobility								
Not migrated	4742	226 (4.8)	81 (1.7)	307 (6.5)	1.00			
Migrated	3949	240 (6.1)	303 (7.7)	543 (13.8)	2.37 (1.95–2.87)	<0.001	2.72 (2.21–3.34)	<0.001

primary school educational attainment (AOR: 1.43, 95% CI: 1.15–1.77; reference group: secondary schooling and above, $P < 0.001$), working as a farmer (AOR: 1.48, 95% CI: 1.17–1.87; reference group: others, $P = 0.001$), heterosexual intercourse route (AOR: 3.19, 95% CI: 1.42–7.16; reference group: other or unknown, $P = 0.005$), and migrated (AOR: 2.72, 95% CI: 2.21–3.34; reference group: not migrated, $P < 0.001$).

Genetic linkage between newly diagnosed patients with HIV and those at baseline, stratified by treatment, viral load, and dropout

The treated HIV patients at baseline were divided into subgroups by treatment, VL, and dropout (**Figure 2** and **Table 3**). The proportion of treated HIV patients at baseline with a VL of less than 50 copies/ml linked to those newly diagnosed was 8.2% (583/7,088). Only 4.9% (214/4,395) of patients with HIV who were treated for 4 years and had a VL of less than 50 copies/ml at baseline were linked to those newly diagnosed at baseline. The proportion of treated HIV patients with VL missing at baseline and treated HIV patients on dropout at baseline genetically linked to those newly diagnosed was 27.8 (66/237) and 20.4% (33/162), respectively. The median (IQR) ART duration in treated HIV patients with VL missing was 269 days (192–567). Compared with untreated HIV patients, treated HIV patients with VL of less than 50 copies/ml were associated with less likelihood of HIV transmission (AOR: 0.59, 95% CI: 0.43–0.82; $P = 0.002$). Patients with HIV who were treated for 4 years and had a VL of less than 50 copies/ml at baseline were associated with less likelihood of HIV transmission (AOR: 0.35, 95% CI: 0.24–0. 50; $P < 0.001$). Treated HIV patients with VL missing at baseline were associated with HIV transmission (AOR: 1.64, 95% CI: 1.03–2.60; $P = 0.038$). There was no significant difference in the proportion of genetic linkages between untreated HIV patients at baseline and treated HIV patients on dropout at baseline.

Sensitivity analysis

To avoid the late HIV diagnosis phenomenon, newly infected patients with HIV, diagnosed from 2016 to 2018, with a CD4 count of more than 200 cells/mm^3 at the first visit, were included in this study. Treated patients were significantly associated with less HIV transmission through the genetic network (AOR: 0.62, 95% CI: 0.41–0.95, $P = 0.029$) in the final GEE model.

Patients with HIV undergoing their first infection year are more likely to transmit HIV (Ratmann et al., 2016). Based on linkages between newly diagnosed and baseline patients with HIV, the genetic linkages between newly diagnosed patients themselves were analyzed. Treated patients were significantly associated with less HIV transmission through the genetic network (AOR: 0.65, 95% CI: 0.52–0.82, $P < 0.001$) in the final GEE model.

According to the National Technical Guideline for HIV Transmission Network Monitoring and Intervention in China, the distance threshold (0.0075) resulting in the maximum number of clusters was used as the final GD threshold. The sensitivity of the GD was also analyzed. Furthermore, the prevention efficacy in HIV transmission for patients with HIV was similar when the GD threshold was 0.0065 and 0.0085, respectively (**Supplementary Table 1**).

Discussion

Our longitudinal genetic network study in Guangxi from 2015 to 2018 indicated that ART reduced the risk of HIV transmission by 33% at a population level. Previous studies mainly using traditional epidemiological methods have indicated that ART can reduce the risk of HIV transmission among serodiscordant couples (Eshleman et al., 2017; Ma et al., 2019). The HPTN 071 clinic trial also confirmed the effect of ART in reducing HIV transmission at the population level (Hayes et al., 2019). The previous study, which did not consider the epidemiological factors, has only shown that ART reduced HIV transmission by 53.6% (Kang et al., 2021). Compared with our results in this study, we adjusted the age, sex, ethnicity, education, occupation, mobility, and route of HIV transmission variables, which was more accurately evaluated. In the context of ART scale-up, our study is the first to evaluate the effect of ART on the prevention of HIV transmission at the population level in real-world settings through a longitudinal genetic network analysis. The stratification results showed that the prevention efficacy in HIV transmission for treated HIV patients with a VL of less than 50 copies/ml was 41%. Other studies demonstrated that the virus has been inhibited after ART, and HIV transmission risk can be greatly reduced (Bavinton et al., 2018; LeMessurier et al., 2018). The increased risk of HIV transmission was related to the high VL of patients with HIV (Eshleman et al., 2017; Liu et al., 2018; Eisinger et al., 2019). Our study results also showed that the prevention efficacy in HIV transmission for patients with HIV treated for 4 years and with a VL of less than 50 copies/ml was 65%. The GD threshold of 0.0075 showed that the evolution time of the HIV strain is 4–5 years (National Center for HIV/AIDS, Viral Hepatitis, STD, TB Prevention, and Division of HIV/AIDS Prevention, 2018). Therefore, the time of receiving ART for more than 4 years can abandon irrelevant genetic linkages when building a genetic transmission network, which can show the true effect of ART in preventing HIV transmission. Our study results provide strong evidence to support the World Health Organization's recommendation for treat-all prevention at the population level.

Our study determined that there was no significant reduction in HIV transmission among treated HIV patients with VL missing or those on dropout. Our previous study also found that VL testing was used as a proxy for treatment adherence that was significantly associated with virological failure and death (Shen et al., 2016; Zhang et al., 2021). If patients with HIV stop receiving ART, VL may rebound to a level associated with an increased risk of HIV transmission,

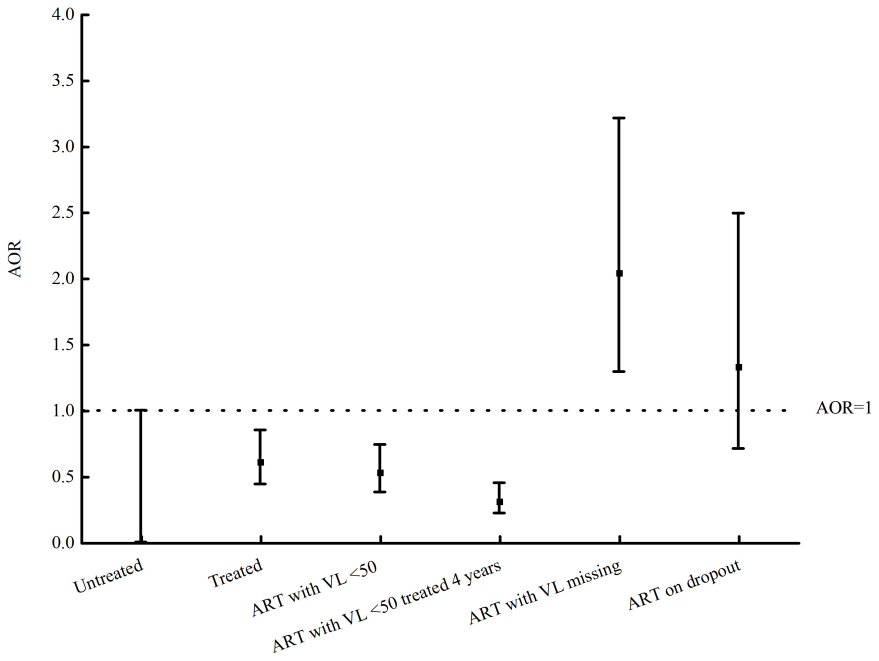

FIGURE 2
AOR values of stratified analysis of genetic transmission network in Guangxi of China.

TABLE 3 Genetic linkage between newly diagnosed patients with HIV and those at baseline in Guangxi of China, stratified by treatment, viral load, and follow-up status.

Variable	Baseline	Number of genetic linkages between newly diagnosed HIV patients and HIV patients at baseline			*OR* (95% CI)	*P*	*AOR* (95% CI)	*P*
		1 person (%)	≥2 person (%)	≥1 person (%)				
Total	8691	466 (5.4)	384 (4.4)	850 (9.8)				
Model 1								
Untreated	694	50 (7.2)	48 (6.9)	98 (14.1)	1.00		1.00	
Treated	7997	416 (5.2)	336 (4.2)	752 (9.4)	0.63 (0.46–0.85)	0.003	0.67 (0.48–0.93)	0.016
Treated HIV patients with VL < 50 copies/mL	7088	337 (4.8)	246 (3.5)	583 (8.2)	0.54 (0.40–0.74)	<0.001	0.59 (0.43–0.82)	0.002
Model 2								
Untreated	694	50 (7.2)	48 (6.9)	98 (14.1)	1.00		1.00	
Treated	7997	416 (5.2)	336 (4.2)	752 (9.4)	0.63 (0.46–0.85)	0.003	0.67 (0.48–0.93)	0.016
Treated HIV patients with VL < 50 copies/mL and treated more than 4 years	4395	155 (3.5)	59 (1.3)	214 (4.9)	0.31 (0.22–0.43)	<0.001	0.35 (0.24–0.50)	<0.001
Model 3								
Untreated	694	50 (7.2)	48 (6.9)	98 (14.1)	1.00		1.00	
Treated	7997	416 (5.2)	336 (4.2)	752 (9.4)	0.63 (0.46–0.85)	0.003	0.67 (0.48–0.93)	0.016
Treated HIV patients with VL missing	237	25 (10.5)	41 (17.3)	66 (27.8)	2.44 (1.59–3.76)	<0.001	1.64 (1.03–2.60)	0.038
Treated HIV patients on dropout	162	12 (7.4)	21 (13.0)	33 (20.4)	1.61 (0.86–3.01)	0.133	1.15 (0.61–2.16)	0.674

Model 1: Stratified by VL; Model 2: Stratified by VL and treatment; Model 3: Stratified by VL and follow-up status.

which will also increase the drug resistance rate of those (Lei et al., 2018). In our previous study, we demonstrated that a high proportion of patients with HIV receiving ART were dropped out in China (Tang et al., 2017; Kang et al., 2019), and the overall attrition rate was 10.86 per 100 person-years in HIV-infected patients who started ART between 2012 and 2015 (Zhu et al., 2021). This study result demonstrates that more attention should be given to ART management and care should be paid on improving the drug adherence of patients with HIV, strengthening the service quality of ART clinics, and conducting VL testing promptly as required. Under the context of ART scale-up, VL monitoring for patients with HIV who received ART can effectively prevent the HIV transmission and reduce death, which provides support for the achievement of the "95-95-95" goal by 2030.

Our study found that migration was significantly associated with HIV transmission, and there are few studies evaluating the impact of migrant population on HIV transmission among heterosexual intercourse at a population level in China. Our study also found that individuals older than 50 years, male, Zhuang and other nationalities, with less than secondary schooling, working as farmers, and heterosexual transmission were at a higher risk of HIV transmission. Older men with low education had a high risk of HIV heterosexual transmission (Wu et al., 2019). By the end of 2021, the proportion of older patients with HIV (more than 50 years of age) reported to be living with HIV/AIDS was 61.4 and 45.7% in Guangxi and China, respectively. HIV is already spreading beyond traditional high-risk individuals, such as injection drug users, female sex workers, and men who have sex with men, to populations that include older heterosexual men in rural areas of China. These new changes in HIV transmission patterns pose greater challenges for new prevention efforts focused on older individuals within the general population. In addition to providing a treat-all prevention strategy, targeted precision prevention and interventions, such as through safe sex education (condom use of sex), HIV testing and counseling, immediate ART, and improve ART adherence, are urgently needed for addressing heterosexual HIV transmission among the older men within the general population.

This study had some limitations. First, a GD of 0.0075 was chosen, which represents the evolution of HIV strains and transmission in 4–5 years. In China, the prevalence of late HIV diagnosis has reached 43% (Sun et al., 2021). We do not have data on those newly infected patients with HIV, which may lead to a reduction in statistical power for the current analysis. Second, the sample size of stratified analysis groups such as treated HIV patients with VL missing may be not large enough. Finally, this study did not adjust the risk tolerance. It seems possible that individuals who do not pay attention to medical care or have a greater tolerance for risk may have a risk of sexual intercourse and have also not been receiving ART.

Conclusion

Understanding the networks of sexually transmitted HIV infections in rural Southwest China at a population level during the expansion of ART is critical. This study reveals the role of ART in reducing HIV transmission in the real world. Ending the HIV epidemic requires a series of comprehensive measures, such as patients with HIV receiving ART immediately after diagnosis, treatment improvements, and focused precision intervention on high-risk individuals during the expansion of ART.

Data availability statement

The data analyzed in this study is subject to the following licenses/restrictions: data not publicly available but could be obtained upon request and approval from Chinese Center for Disease Control and Prevention (China CDC). Requests to access these datasets should be directed to YR, ruanyuhua92@chinaaids.cn.

Ethics statement

The studies involving human participants were reviewed and approved by National Center for AIDS/STD Control and Prevention, Chinese Center for Disease Control and Prevention, China. The patients/participants provided their written informed consent to participate in this study.

Author contributions

JC, LJL, YF, and YR were responsible for study design and planning. HC, JL, LHL, ZS, JZ, HL, GL, QZ, and SL contributed to data collection and management. JC, RK, and YR contributed to data analysis. JC, HX, LJL, YS, and YR contributed to interpretation. JC and YR contributed to writing the report. All authors read and approved the final version of the article.

Funding

This study was supported by the National Natural Science Foundation of China (Grant Nos. 82160636 and 11971479), the Guangxi Natural Science Foundation Project (Grant No. 2020GXNSFAA159020), the Guangxi Key Laboratory of AIDS Prevention Control and Translation (Grant No. ZZH2020010), the Ministry of Science and Technology of China (Grant Nos. 2018ZX10721102-006 and 2018ZX10715008), the Guangxi Bagui Honor Scholarship, the Chinese State Key Laboratory of Infectious Disease Prevention and Control, and the Guangxi Key Laboratory of Major Infectious Disease Prevention and

Control and Biosafety Emergency Response, Guangxi Center for Disease Control and Prevention (21-220-12).

Acknowledgments

Data in this manuscript were collected by the Guangxi Center for Disease Control and Prevention.

Conflict of interest

The authors declare that the research was conducted in the absence of any commercial or financial relationships that could be construed as a potential conflict of interest.

Publisher's note

Supplementary material

The Supplementary Material for this article can be found online at: https://www.frontiersin.org/articles/10.3389/fmicb.2022.962477/full#supplementary-material

References

Ballinger, G. A. (2004). Using generalized estimating equations for longitudinal data analysis. *Organ. Res. Methods* 7, 127–150. doi: 10.1177/1094428104263672

Bavinton, B. R., Pinto, A. N., Phanuphak, N., Grinsztejn, B., Prestage, G. P., Zablotska-Manos, I. B., et al. (2018). Viral suppression and HIV transmission in serodiscordant male couples: an international, prospective, observational, cohort study. *Lancet HIV* 5, e438–e447. doi: 10.1016/s2352-3018(18)30132-2

Chen, H., Luo, L., Pan, S. W., Lan, G., Zhu, Q., Li, J., et al. (2019a). HIV epidemiology and prevention in Southwestern China: trends from 1996-2017. *Curr. HIV Res.* 17, 85–93. doi: 10.2174/1570162X17666190703163838

Chen, H., Wu, X., Chen, L., Lu, H., Tang, Z., Shen, Z., et al. (2019b). Rapidly spreading human immunodeficiency virus epidemic among older males and associated factors: a large-scale prospective cohort study in rural Southwest China. *Sex Transm. Dis.* 46, 234–239. doi: 10.1097/OLQ.0000000000000957

Chen, Y., Shen, Z., Feng, Y., Ruan, Y., Li, J., Tang, S., et al. (2021). HIV-1 subtype diversity and transmission strain source among men who have sex with men in Guangxi, China. *Sci. Rep.* 11, 8319–8391. doi: 10.1038/s41598-021-87745-3

Cohen, M. S., Chen, Y. Q., McCauley, M., Gamble, T., Hosseinipour, M. C., Kumarasamy, N., et al. (2016). Antiretroviral therapy for the prevention of HIV-1 transmission. *N. Engl. J. Med.* 375, 830–839. doi: 10.1056/NEJMoa1600693

Cohen, M. S., Gamble, T., and McCauley, M. (2020). Prevention of HIV transmission and the HPTN 052 study. *Annu. Rev. Med.* 71, 347–360. doi: 10.1146/annurev-med-110918-034551

Dalai, S. C., Junqueira, D. M., Wilkinson, E., Mehra, R., Kosakovsky Pond, S. L., Levy, V., et al. (2018). Combining phylogenetic and network approaches to identify HIV-1 transmission links in San Mateo County, California. *Front. Microbiol.* 9:2799. doi: 10.3389/fmicb.2018.02799

de Oliveira, T., Kharsany, A. B. M., Gräf, T., Cawood, C., Khanyile, D., Grobler, A., et al. (2017). Transmission networks and risk of HIV infection in Kwazulu-Natal, South Africa: a community-wide phylogenetic study. *Lancet HIV* 4, e41–e50. doi: 10.1016/s2352-3018(16)30186-2

Dk, P., Ia, D., La, S. S. H., Leone, P. A., and Sebastian, J. (2018). Leveraging phylogenetic to understand HIV transmission and partner notification networks. *J. Acquir. Immune Defic. Syndr.* 78, 367–375. doi: 10.1097/QAI.0000000000001695

Eisinger, R. W., Dieffenbach, C. W., and Fauci, A. S. (2019). HIV viral load and transmissibility of HIV infection: undetectable equals untransmittable. *JAMA* 321, 451–452. doi: 10.1001/jama.2018.21167

Eshleman, S. H., Hudelson, S. E., Redd, A. D., Swanstrom, R., Ou, S. S., Zhang, X. C., et al. (2017). Treatment as prevention: characterization of partner infections in the HIV prevention trials network 052 trial. *J. Acquir. Immune Defic. Syndr.* 74, 112–116. doi: 10.1097/qai.0000000000001158

Frank, T. D., Carter, A., Jahagirdar, D., Biehl, M. H., Douwes-Schultz, D., Larson, S. L., et al. (2019). Global, regional, and national incidence, prevalence, and mortality of HIV, 1980–2017, and forecasts to 2030, for 195 countries and territories: a systematic analysis for the global burden of diseases, injuries, and risk factors study 2017. *Lancet HIV* 6, e831–e859. doi: 10.1016/s2352-3018(19)30196-1

Hayes, R. J., Donnell, D., Floyd, S., Mandla, N., Bwalya, J., Sabapathy, K., et al. (2019). Effect of universal testing and treatment on HIV incidence - HPTN 071 (Popart). *N. Engl. J. Med.* 381, 207–218. doi: 10.1056/NEJMoa1814556

Jia, J., Zhu, Q., Deng, L., Lan, G., Johnson, A., Chen, H., et al. (2022). Treatment outcomes of HIV patients with hepatitis B and C virus co-infections in Southwest China: an observational cohort study. *Infect. Dis. Poverty* 11:7. doi: 10.1186/s40249-021-00921-5

Kang, R., Li, J., Chen, H., Tang, Z., Pan, S. W., Luo, L., et al. (2021). Using longitudinal genetic-network study to understand HIV treatment-as-prevention. *AIDS* 35, 947–955. doi: 10.1097/QAD.0000000000002812

Kang, R., Luo, L., Chen, H., Zhu, Q., Liao, L., Xing, H., et al. (2019). Treatment outcomes of initial differential 431 antiretroviral regimens among HIV patients in southwest China: comparison from an observational cohort study. *BMJ Open* 9:e025666. doi: 10.1136/bmjopen-2018-025666

Lei, L., Zhongbao, Z., Lingjie, L., Shujia, L., Yanling, M., Guohui, W., et al. (2018). The drug resistance in HIV/AIDS patients who had stopped art in 2016. *J.Trop. Med.* 18, 1613–1618. doi: 10.1093/cid/ciw128

LeMessurier, J., Traversy, G., Varsaneux, O., Weekes, M., Avey, M. T., Niragira, O., et al. (2018). Risk of sexual transmission of human immunodeficiency virus with antiretroviral therapy, suppressed viral load and condom use: a systematic review. *CMAJ* 190, E1350–E1360. doi: 10.1503/cmaj.180311

Li, J., Feng, Y., Shen, Z., Li, Y., Tang, Z., Xiong, R., et al. (2018). HIV-1 transmissions among recently infected individuals in Southwest China are predominantly derived from circulating local strains. *Sci. Rep.* 8:12831. doi: 10.1038/s41598-018-29201-3

Liao, L., Xing, H., Shang, H., Li, J., Zhong, P., Cheng, H., et al. (2010). The prevalence of transmitted antiretroviral drug resistance in treatment-naive HIV-infected individuals in China. *J. Acquir. Immune Defic. Syndr.* 53(Suppl. 1), S10–S14.

Lima, V. D., St-Jean, M., Rozada, I., Shoveller, J. A., Nosyk, B., Hogg, R. S., et al. (2017). Progress towards the United Nations 90-90-90 and 95-95-95 targets: the experience in British Columbia, Canada. *J. Int. AIDS Soc.* 20:e25011. doi: 10.1002/jia2.25011

Liu, P., Tang, Z., Lan, G., Zhu, Q., Chen, H., You, Y., et al. (2018). Early antiretroviral therapy on reducing HIV transmission in China: strengths, weaknesses and next focus of the program. *Sci. Rep.* 8:3431. doi: 10.1038/s41598-018-21791-2

Ma, G., Chen, H., Chen, J., Jiang, Z., and Ma, T. (2019). HIV transmission between spouses living in Lu'an City, Anhui Province, China: a longitudinal study. *Epidemiol. Infect.* 147:e205. doi: 10.1017/s095026881900089x

Mangal, T. D., Meireles, M. V., Pascom, A. R. P., de Almeida Coelho, R., Benzaken, A. S., and Hallett, T. B. (2019). Determinants of survival of people living

with HIV/AIDS on antiretroviral therapy in Brazil 2006-2015. *BMC Infect. Dis.* 19:206. doi: 10.1186/s12879-019-3844-3

National Center for HIV/AIDS, Viral Hepatitis, STD, TB Prevention, and Division of HIV/AIDS Prevention (2018). *Detecting and Responding to HIV Transmission Clusters - a Guide for Health Departments*. Atlanta, GA: CDA.

Oster, A. M., France, A. M., Panneer, N., Bañez Ocfemia, M. C., Campbell, E., Dasgupta, S., et al. (2018). Identifying clusters of recent and rapid HIV transmission through analysis of molecular surveillance data. *J. Acquir. Immune Defic. Syndr.* 79, 543–550. doi: 10.1097/qai.0000000000001856

Otieno, G., Whiteside, Y. O., Achia, T., Kwaro, D., Zielinski-Gutierrez, E., Ojoo, S., et al. (2019). Decreased HIV- associated mortality rates during scale-up of antiretroviral therapy, 2011-2016. *AIDS* 33, 2423–2430.

Poon, A. F. Y., Gustafson, R., Daly, P., Zerr, L., Demlow, S. E., Wong, J., et al. (2016). Near real-time monitoring of HIV transmission hotspots from routine HIV genotyping: an implementation case study. *Lancet HIV* 3, e231–e238. doi: 10.1016/s2352-3018(16)00046-1

Ratmann, O., van Sighem, A., Bezemer, D., Gavryushkina, A., Jurriaans, S., Wensing, A., et al. (2016). Sources of HIV infection among men having sex with men and implications for prevention. *Sci. Transl. Med.* 8:320ra2. doi: 10.1126/scitranslmed.aad1863

Rodger, A. J., Cambiano, V., Bruun, T., Vernazza, P., Collins, S., van Lunzen, J., et al. (2016). Sexual activity without condoms and risk of HIV transmission in serodifferent couples when the HIV-positive partner is using suppressive antiretroviral therapy. *JAMA* 316, 171–181. doi: 10.1001/jama.2016.5148

Rodger, A. J., Cambiano, V., Bruun, T., Vernazza, P., Collins, S., Degen, O., et al. (2019). Risk of HIV transmission through condomless sex in serodifferent gay couples with the hiv-positive partner taking suppressive antiretroviral therapy (partner): final results of a multicentre, prospective, observational study. *Lancet* 393, 2428–2438. 6736(19)30418-0 doi: 10.1016/s0140-350

Saag, M. S., Gandhi, R. T., Hoy, J. F., Landovitz, R. J., Thompson, M. A., Sax, P. E., et al. (2020). Antiretroviral drugs for treatment and prevention of HIV infection in adults: 2020 recommendations of the international antiviral society-USA panel. *JAMA* 324, 1651–1669. doi: 10.1001/jama.2020.17025

Shen, Z., Zhu, Q., Tang, Z., Pan, S. W., Zhang, H., Jiang, H., et al. (2016). Effects of CD4 cell counts and viral load testing on mortality rates in patients with HIV infection receiving antiretroviral treatment: an observational cohort study in rural Southwest China. *Clin. Infect. Dis.* 63, 108–114. doi: 10.1093/cid/ciw146

Su, L., Liang, S., Hou, X., Zhong, P., Wei, D., Fu, Y., et al. (2018). Impact of worker emigration on hiv epidemics in labour export areas: a molecular epidemiology investigation in Guangyuan, China. *Sci. Rep.* 8:16046. doi: 10.1038/s41598-018-33996-6

Sun, C., Li, J., Liu, X., Zhang, Z., Qiu, T., Hu, H., et al. (2021). HIV/AIDS late presentation and its associated factors in China from 2010 to 2020: a systematic review and meta-analysis. *AIDS Res. Ther.* 18:96. doi: 10.1186/s12981-021-00415-2

Tang, Z., Pan, S. W., Ruan, Y., Liu, X., Su, J., Zhu, Q., et al. (2017). Effects of HIgh CD4 cell counts on death and attrition among HIV patients receiving antiretroviral treatment: an observational cohort study. *Sci. Rep.* 7:3129. doi: 10.1038/s41598-017-03384-7

Trickey, A., May, M. T., Vehreschild, J.-J., Obel, N., Gill, M. J., Crane, H. M., et al. (2017). Survival of HIV-positive patients starting antiretroviral therapy between 1996 and 2013: a collaborative analysis of cohort studies. *Lancet HIV* 4, e349–e356. doi: 10.1016/s2352-3018(17)30066-8

UNAIDS (2015). *Understanding Fast-Track: Accelerating Action to End the AIDS Epidemic by 2030*. Available online at: https://www.unaids.org/sites/default/files/media_asset/201506_JC2743_Understanding_FastTrack_en.pdf. (accessed June 6, 2022).

Wu, J., Zhang, Y., Shen, Y., Wang, X., Xing, H., Yang, X., et al. (2019). Phylogenetic analysis highlights the role of older people in the transmission of hiv-1 in Fuyang, Anhui Province, China. *BMC Infect. Dis.* 19:562. doi: 10.1186/s12879-019-4187-9

Xing, H., Ruan, Y., Hsi, J. H., Kan, W., Liao, L., Leng, X., et al. (2015). Reductions in virological failure and drug resistance in Chinese antiretroviral-treated patients due to lamivudine-based regimens, 2003-12. *J. Antimicrob. Chemother.* 70, 2097–2103. doi: 10.1093/jac/dkv078

Yan, H., He, W., Huang, L., Wu, H., Liang, Y., Li, Q., et al. (2020). The central role of nondisclosed men who have sex with men in human immunodeficiency virus-1 transmission networks in Guangzhou, China. *Open Forum Infect. Dis.* 7:ofaa154. doi: 10.1093/ofid/ofaa154

Yuan, D., Yu, B., Liang, S., Fei, T., Tang, H., Kang, R., et al. (2022). HIV-1 genetic transmission networks among people living with HIV/AIDS in Sichuan, China: a genomic and spatial epidemiological analysis. *Lancet Reg. Health West Pac.* 18:100318. doi: 10.1016/j.lanwpc.2021.100318

Zhang, T., Liao, L., Shao, Y., Feng, Y., Ruan, Y., and Xing, H. (2021). Relationship between drug resistance and death in HIV-infected patients receiving antiretroviral therapy - 7 plads, China, 2010-2019. *China CDC Wkly.* 3, 291–297. doi: 10.46234/ccdcw2021.068

Zhao, Y., Wu, Z., McGoogan, J. M., Shi, C. X., Li, A., Dou, Z., et al. (2018). Immediate antiretroviral therapy decreases mortality among patients with high cd4 counts in China: a nationwide retrospective cohort study. *Clin. Infect. Dis.* 66, 727–734. doi: 10.1093/cid/cix878

Zhou, C., Zhang, W., Lu, R. R., Ouyang, L., Xing, H., Shao, Y. M., et al. (2020). Benefits of early and immediate initiation of antiretroviral therapy among HIV patients in Chongqing, China. *Biomed Environ. Sci.* 33, 282–285. doi: 10.3967/bes2020.039

Zhu, J., Yousuf, M., Yang, W., Zhu, Q., Shen, Z., Lan, G., et al. (2021). Mortality and attrition rates within the first year of antiretroviral therapy initiation among people living with HIV in Guangxi, China: an observational cohort study. *BioMed Res. Int.* 2021:6657112. doi: 10.1155/2021/6657112

frontiers | Frontiers in Microbiology

TYPE Original Research
PUBLISHED 22 August 2022
DOI 10.3389/fmicb.2022.895227

OPEN ACCESS

EDITED BY
Kai Deng,
Sun Yat-sen University, China

REVIEWED BY
Li Xing,
Shanxi University,
China
Marcio Roberto Teixeira Nunes,
Evandro Chagas Institute, Brazil

*CORRESPONDENCE
Hanping Li
hanpingline@163.com
Lin Li
dearwood@sina.com

†These authors have contributed equally to this work

SPECIALTY SECTION
This article was submitted to Virology,
a section of the journal Frontiers in Microbiology

RECEIVED 13 March 2022
ACCEPTED 29 July 2022
PUBLISHED 22 August 2022

CITATION
Li Y, Han L, Wang Y, Wang X, Jia L, Li J, Han J, Zhao J, Li H and Li L (2022) Establishment and application of a method of tagged-amplicon deep sequencing for low-abundance drug resistance in HIV-1. *Front. Microbiol.* 13:895227. doi: 10.3389/fmicb.2022.895227

Establishment and application of a method of tagged-amplicon deep sequencing for low-abundance drug resistance in HIV-1

Yang Li[1,2†], Leilei Han[2,3†], Yanglan Wang[2,4], Xiaolin Wang[2], Lei Jia[2], Jingyun Li[2], Jingwan Han[2], Jin Zhao[5], Hanping Li[2*] and Lin Li[1,2*]

[1]School of Basic Medical Sciences, Anhui Medical University, Hefei, Anhui, China, [2]Department of Virology, State Key Laboratory of Pathogen and Biosecurity, Beijing Institute of Microbiology and Epidemiology, Beijing, China, [3]School of Public Health, North China University of Science and Technology, Tangshan, Hebei, China, [4]College of Life Science and Technology, Beijing University of Chemical Technology, Beijing, China, [5]Shenzhen Center for Disease Control and Prevention, Shenzhen, Guangdong, China

In the latest HIV-1 global drug resistance report released by WHO, countries are advised to strengthen pre-treatment monitoring of drug resistance in AIDS patients. In this study, we established an NGS-based segmented amplification HIV-1 drug resistance mutation detection method. The *pol* region of HIV-1 was divided into three short fragments for NGS. The entire amplification and sequencing panel were more cost-effective and batched by using the barcode sequence corresponding to the sample. Each parameter was evaluated using samples with known resistance variants frequencies. The nucleotide sequence error rate, amino acid error rate, and noise value of the NGS-based segmented amplification method were both less than 1%. When the threshold was 2%, the consensus sequences of the HIV-1 NL4-3 strain were completely consistent with the Sanger sequences. This method can detect the minimum viral load of the sample at 10^2 copies/ml, and the input frequency and detection frequency of HIV-1 resistance mutations within the range of 1%–100% had good conformity (R^2=0.9963; R^2=0.9955). This method had no non-specific amplification for Hepatitis B and C. Under the 2% threshold, the incidence of surveillance drug resistance mutations in ART-naive HIV-infected patients was 20.69%, among which NRTIs class resistance mutations were mainly.

KEYWORDS

HIV-1, next-generation sequencing, minority drug resistance variants, assessment, standardization

Introduction

The global HIV-1 drug resistance report released by WHO (2021) pointed out that more and more countries are on the verge of reaching the 10% pre-treatment drug resistance threshold for non-nucleoside reverse transcriptase inhibitors in the WHO releases HIV drug resistance report 2021. As the coverage of antiretroviral drugs

expands and patient treatment experience increases, the prevalence of HIV resistance is expected to increase (Xie et al., 2021). The presence of drug-resistant HIV in the viral population, including the minor frequency drug resistance variants (Palmer et al., 2005), is known to compromise virological response to antiretroviral therapy (ART; Soeria-Atmadja et al., 2020). Minor resistant variants were associated with reduced virologic response and failure of ART (Halvas et al., 2010; Nicot et al., 2012). Low-frequency HIV-1drug resistance variants, particularly NNRTI resistance, were significantly associated with a dose-dependent increase in the risk of first-line ART virological failure (Gupta et al., 2014). If no measures are taken to deal with the problem of drug resistance, this may become a major obstacle to achieving the 90%–90%–90% control target. Once the virus develops drug resistance, the viral load will continue to increase, leading to the failure of ART treatment (Tachbele et al., 2021). If the problem of HIV-1 drug resistance cannot be effectively controlled, it may lead to the widespread of drug-resistant viruses and the emergence of multidrug-resistant (Guglielmetti et al., 2021).

The detection of HIV-1 drug resistance mutations often uses Sanger sequencing (SS) as the "gold standard" (Stranneheim and Lundeberg, 2012). However, SS generally detects variants accounting for greater than 10%–25% of the viral quasispecies (Grant et al., 2003; Chen et al., 2020), which is not sensitive enough to detect low-frequency resistance variants. To assess minor drug resistance mutations of HIV *in vivo*, single genome sequencing (SGS; McKinnon et al., 2011; Wang et al., 2014) and allele-specific real-time PCR (ASPCR; Hauser et al., 2015) were developed, but they cannot be applied to large-scale samples detection due to time-consuming and labor-intensive. In recent years, NGS is becoming a more common sequencing method that is widely used in the current genetic detection field (Gibson et al., 2020; Bendall et al., 2021; Parikh et al., 2021). NGS can detect low-abundance drug resistance mutations by sequencing the HIV-1 quasispecies (Ji et al., 2020). In HIV-1 drug resistance mutation detection, NGS has the advantages of high sensitivity, high data throughput, and parallel detection of large batches of samples. Nevertheless, there is currently no standardized evaluation system for NGS-based HIV drug resistance detection. The Sentosa SQ HIV genotyping assay (Tzou et al., 2018) is currently the only HIV-1 genotyping NGS detection method on the market that has been approved by the U.S. FDA. For the currently widely used NGS-based HIV drug resistance mutation detection method, a standardized evaluation system should be established.

In this study, we established an NGS-based HIV-1 drug resistance mutation detection method that allows surveillance of HIV-1 minor resistant variants in population. HIV strains with known drug resistance variants was used to construct sample to evaluate various parameters of the methods. And this method was used to detect minority drug resistance variants in newly diagnosed HIV-infected patients in Shenzhen from 2014 to 2015.

Materials and methods

Design of tagged-amplicon deep sequencing of fragmented pol region

The segmented tagged-amplicon technology for HIV-1 drug resistance detection was based on the next-generation sequencing platform, and the short sequencing length was the main limitation of the NGS platform. To obtain amplicons suitable for NGS, the HIV-1 *pol* gene region covering the PR and first 226 codons of the RT was amplified in triple fragments with one-step RT-PCR (Takara, RR055A) and nested PCR (Takara, RR901A). The primer sequences used for amplification are shown in Supplementary Table 1. And the effective sequencing length was extended through paired-end sequencing. Each amplicon was approximately 400 bases in length, denoted *pol*-A, *pol*-B, and *pol*-C (nucleotide 2,169~2,583, 2,540~2,944, and 2,834~3,228 by using HXB2 as calibrator). There was a small overlap between the beginning and the end of these three amplicons. There is a small overlap between the start and end of these three amplicons, resulting in an overall amplification length of 1,060 bp. In addition, the barcode sequence was attached to the amplicons to tag different samples (Figure 1). P5/P7 tails were added at both ends of the amplified fragment to construct a high-throughput sequencing library. In a flowcell, amplicon fragment generated clusters by bridge PCR, and hundreds to thousands of amplified fragments were sequenced simultaneously. The amplicon fragments were sequenced on the Illumina sequencing platform using sequencing-by-synthesis sequencing.

Study specimens and population

In order to evaluate and validate the HIV-1 drug resistance detection method, we developed a reference group for this study. Viral load of the wild-type HIV-1 NL4-3 strain (accession number AF003887) and the resistant mutant strains were determined using quantitative real-time PCR and then mixed the wild-type HIV-1 NL4-3 strain and the resistant mutant strains according to the viral load concentration to obtain targeted DRM frequencies of 1%, 2%, 10%, 30%, and 100%. The 187 reference specimens consisted of a known ratio of virus mixtures, HIV-1 NL4-3 strain, Hepatitis B clinical samples, Hepatitis C clinical samples, and HIV-1 positive clinical samples (Supplementary Table 1). The 190 reference samples consisted of known ratios of virus mixtures, HIV-1 NL4-3 strains, Hepatitis B clinical samples, Hepatitis C clinical samples, healthy human plasma samples (HIV-1-/HBV-/HCV-), and HIV-1 positive clinical samples (Supplementary Table 2). Hepatitis B and C plasma samples were provided by clinical patients and these plasma samples were negative after the rapid HIV-1 test.

All newly HIV-1 diagnosed cases in Shenzhen from 2014 to 2015 were enrolled in this study. All patients were antiretroviral-naïve. Blood samples were collected by Shenzhen Center for Disease Prevention and Control. All participants signed written informed consents before sample collection and their background information

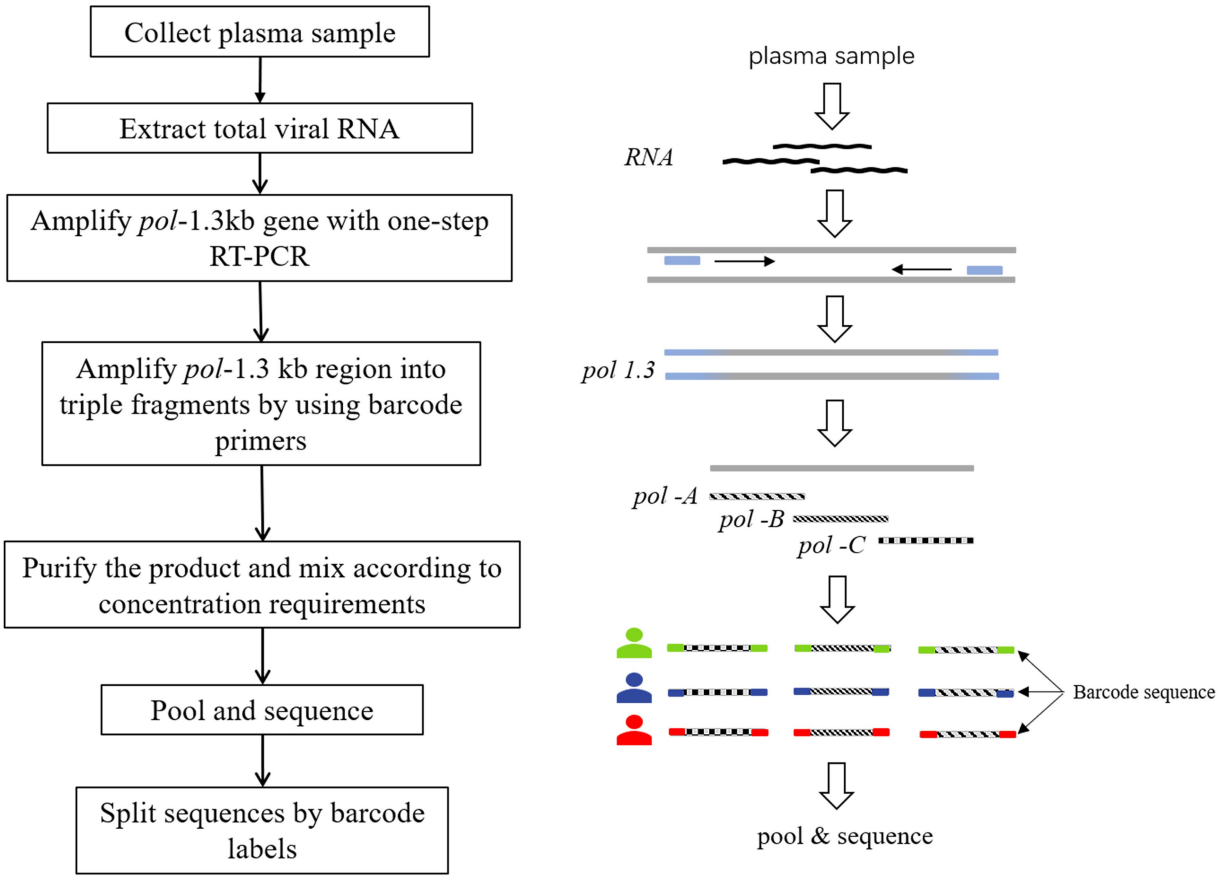

FIGURE 1
Tagged-amplicon deep sequencing strategy. HIV-1 *pol*-1.3kb gene was amplified with one-step RT-PCR. Subsequently, nested PCR was used to amplify pol-1.3kb region into 3 fragments, labeled as *pol*-A, *pol*-B, and *pol*-C. There was a small overlap at the junction of the three amplicons. The molecular barcode was attached to both ends of the amplicons. Barcodes were used to split data to distinguish different samples.

was collected. This study was reviewed and approved by the ethics committees of the Beijing Institute of Microbiology and Epidemiology.

NGS-based HIVDR assay

For the NGS, after the mixed original sequencing results were obtained on the Illumina sequencing platform, the sequencing data of different samples were split by barcode sequence. Quality control is the first step in processing high-throughput sequencing data. FastQC[1] was used for quality control of fastq files obtained from sequencing. Then, the fastq_1 and fastq_2 files obtained by paired-end sequencing were spliced to generate the sequencing data of each sample. Mothur (Schloss et al., 2009) was used to exclude poor-quality sequences from the sequencing data, and mafft (Katoh et al., 2019) was used to align the sequencing results with the reference sequence. HXB2 was used as a ruler to locate the target drug-resistant position. According to the mutations for drug resistance surveillance list of HIV drug resistance database of Stanford University[2], the proportion of the mutations related to drug-resistant at that location was counted.

SS-based HIVDR amplification and assay

The Sanger sequencing amplification process involved in this study was completed according to the following method. Roche High Pure Viral RNA Kit (REF:11858882001) was used to extract total viral RNA from plasma samples. The *pol* gene region (nucleotides positions 2,253–3,555, using HXB2 as the calibrator) spanning the protease gene and partial reverse transcriptase gene was amplified in the first round of nested reverse transcriptase-polymerase chain reaction (RT-PCR) using the One-Step RNA PCR Kit (Takara, RR055A). And the r-Taq kit (Takara, RR901A) was used in the additional PT-PCR. The primer sequences used for Sanger amplification are shown in Supplementary Table 3. Before sequencing, the PCR products were detected by 1% agarose

1 https://www.bioinformatics.babraham.ac.uk/projects/fastqc/

2 https://cms.hivdb.org/prod/downloads/resistance-mutation-handout/resistance-mutation-handout.pdf

gel electrophoresis and then subjected to direct DNA sequencing on an Applied Biosystems 3,730 Sequencer.

Sanger sequences were manually assembled in Contig Express software. The nucleotide where the secondary peak was at least 30% as high as the primary peak was counted as the degenerate bases using the International Union of Pure and Applied Chemistry (IUPAC) designations to obtain the fasta sequences. The fasta sequences were submitted to the HIV drug resistance database of Stanford University[3] to generate a drug resistance report.

NGS SDRMs

Due to the sensitivity of NGS to HIV low-abundance quasispecies populations, the setting of thresholds for deep sequencing data is important for reporting drug resistance variants (Kireev et al., 2018). At present, there is no accurate diagnostic value of minority drug resistance variants of HIV-1 in clinical practice. Studies have shown that the detection of NGS had a good linear relationship in the range of drug resistance mutation frequency from 1% to 100% (Lee et al., 2020). However, compared with the reporting threshold of 1%, the reporting threshold of 2% is not easy to introduce errors caused by PCR amplification and different high-throughput data analysis platforms (Chaillon et al., 2017), and has better robustness and repeatability (Becker et al., 2020; Parkin et al., 2020). Therefore, we chose a reporting threshold of 2% to describe resistance in HIV-infected individuals.

Results

The overall sequence error rate

The NGS sequencing results of the review team are presented in Supplementary Table 4. We wanted to measure the overall sequence error. The overall sequence error was defined as the errors in the entire experimental process of viral nucleic acid extraction, PCR amplification, NGS sequencing, and data processing and analysis. The HIV-1 NL4-3 strain with a known sequence was used for this measurement. We used the segmented amplification method to extract, amplify, and sequence the HIV-1 NL4-3 strain and measured the average frequency of erroneous nucleotide calls. We used the well-established RNA extraction method (Roche High Pure Viral RNA Kit) to improve the RNA recovery and quality of the HIV-1 NL4-3 strain, as well as the tagged amplicon deep sequencing method to amplify and sequence. And measured the average frequency of erroneous nucleotide calls. The error rate of nucleotide sequences we measured using viral RNA ranged from 0.006% to 0.945%, with an average of 0.164%. The consensus sequences generated under the threshold greater than 1% were completely consistent with the SS sequences (Figure 2A). The detection of HIV-1 resistance mutations was the identification of amino acids, so we measured the amino acid sequence error rate of the segmented amplification method. The results showed (Figure 2B) that the average amino acid sequence error rate of *pol*-A gene region was 0.37% (range: 0.11%–0.92%), *pol*-B was 0.36% (range: 0.11%–0.83%), and *pol*-C was 0.61% (range: 0.16%–0.89%). This suggested that the analysis error rate of our HIVDR detection method at the amino acid level was less than 1%.

The lower limit of viral load

To determine the minimum viral load concentration that can be detected by our segmented amplification method, we used HIV-1 NI4-3 mutant strain as a single strain type sample, and wild-type HIV-1 NL4-3 strain and resistance mutant strain were mixed with a DRM frequency of 60% as a mixed strain type sample. Quantitative Real-time PCR was used to detect the viral load level of the samples. Each type of sample was diluted to a different viral load concentration,

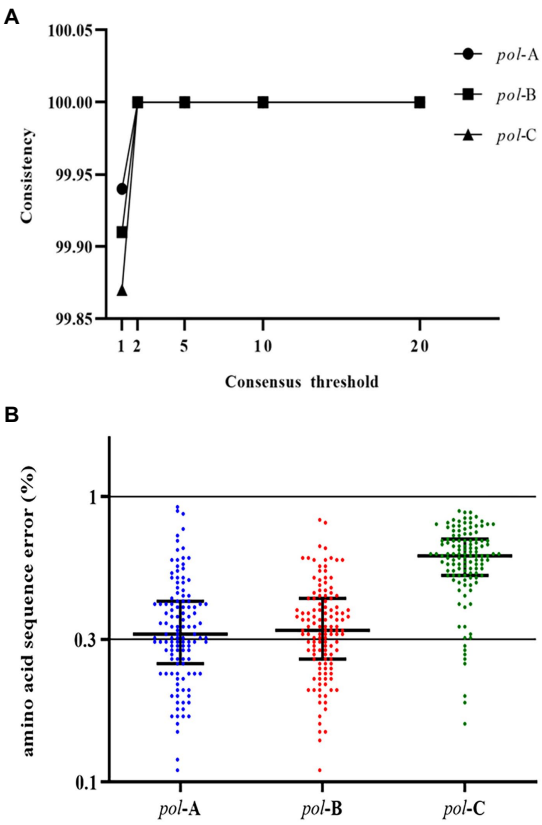

FIGURE 2
(A) Similarity between consensus sequences and SS sequence. Consensus sequences were generated with NGS data under thresholds of 1%, 2%, 5%, 10%, and 20%. Compared with the SS sequence, degenerate bases or incorrectly called bases were regarded as inconsistent bases. **(B)** The amino acid sequence error of the three fragments of the *pol* gene region. Compared with the known sequence, the inconsistent amino acids were all regarded as the wrongly called amino acids. The proportion of error amino acids was defined as the error rate of the amino acid sequence at that position.

3 https://hivdb.stanford.edu/hivdb/by-sequences/

and each sample with a viral load concentration was divided into 5 evenly for viral nucleic acid extraction, amplification, and sequencing. We define a detection rate of less than 80% as a detection failure. It can be seen from the test results that our HIVDR detection method has a minimum viral load of 10^2 copies/ml for samples composed of a single strain or a sample of mixed strains (Supplementary Table 5).

Linear range and accuracy

Next, we were interested in whether the HIVDR detection method was consistent with the input resistance frequency and the detection frequency. Samples with different DRM frequencies were used for viral nucleic acid extraction, amplification, and sequencing. The drug resistance mutations were reported from the high-throughput sequencing data through the above-mentioned analysis process. The detection results at different frequencies were plotted as scatter plots. And we calculated the ratio of the detection frequency to the theoretical frequency. The results of the ratio were distributed around 1, which also showed that the HIVDR detection method had good accuracy (Figure 3). The average of the resistance frequency of three parallel repetitions was calculated as the actual detection frequency, and a fitting curve was made with the input theoretical frequency. From all the tested frequencies, whether it was Y181C or T219Y, the detection frequency and the theoretical frequency had highly relevant. of compliance within the range of 1%–100% ($R^2 > 0.99$), which proved that the segmented amplification method can accurately detect resistance mutations with a frequency of more than 1% (Figure 4).

Precision

The coefficient of variation was used to express the reproducibility between three replicates within a batch. We calculated the intra-batch coefficient of variation based on the results of three replicates on mixed samples with different DRM frequencies. The coefficients of variation of Y181C and T215 were between 0.08%–23.6% and 0.04%–38.22%, respectively, (Supplementary Table 6). The accuracy of this detection method was the worst when the drug resistance mutation frequency was 1%. As the frequency of drug resistance mutation increased, the precision performance was better. It was not surprising that NGS was more stable in the detection of high-frequency resistance mutations due to the sensitivity of NGS detection and the deviations produced by the PCR process.

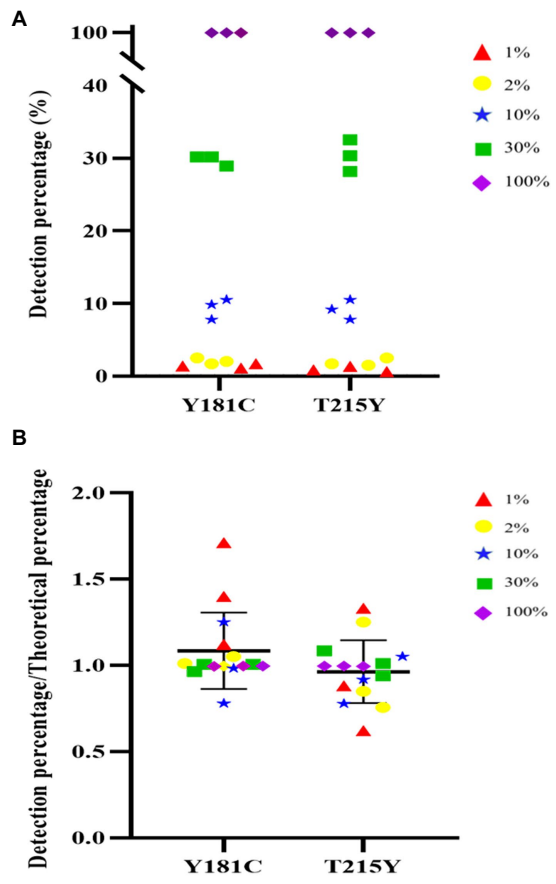

FIGURE 3
(A) Distribution of detect results at different frequencies. **(B)** The distribution of the ratio of the detection frequency to the theoretical frequency.

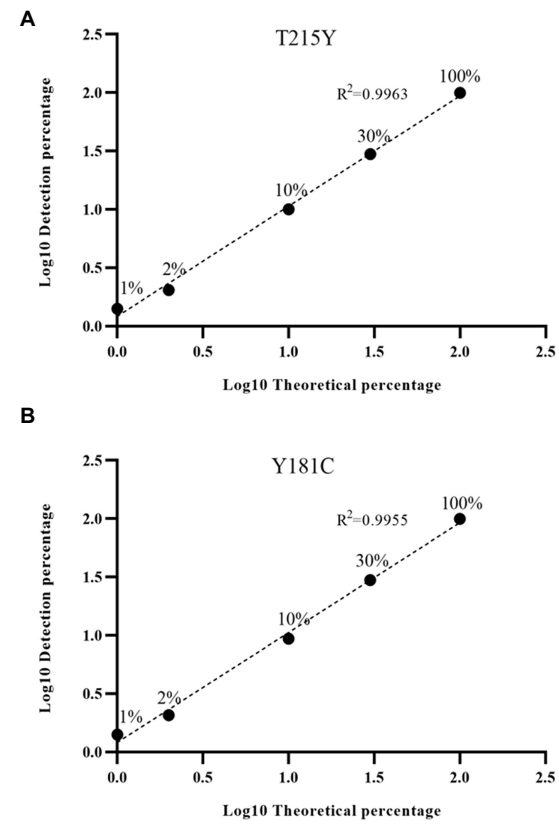

FIGURE 4
(A) Linear detection range of T215Y drug resistance mutation. In our detection range, the input frequency and detection frequency of Y181C and T215Y showed a good correlation. **(B)** Linear detection range of Y181C drug resistance mutation.

Specificity and noise value

To verify the specificity of the segmented amplification method, we selected Hepatitis B and C virus for detection. Hepatitis B and C samples were provided by confirmed clinical patients, and these samples were HIV-1 negative after rapid HIV testing. The Hepatitis B and C samples were amplified using the segmented amplification method, and the results were all negative. It showed that the amplification method had good specificity to the HIV-1 virus, and the possibility of amplifying other virus sequences was low (Supplementary Table 7).

In addition, we also used a well-characterized HIV-1 NL4-3 mutant (K101E + Y181C + T215Y) as input to verify the specificity of the segmented amplification method. The frequency of resistance mutation of three independent replicates was counted, and resistance mutations that only appear once will also be included, and the average of the reported frequency of resistance mutations that appeared multiple times will be taken (Figure 5). Judging from the HIV-1 NL4-3 (K101E + Y181C + T215Y) detection report, some ultra-low-frequency (<1%) false-positive results appeared in the results of the segmented amplification method. The detection specificity of the target mutation can reach 100%.

Method evaluation

One hundred plasma samples of HIV-1 clinical patients were randomly trained and detected using the In-house method and segmented amplification method. The demographic characteristics of HIV-1 clinical samples are shown in Supplementary Table 8. The reads of deep sequencing data after quality control were mostly distributed around 6,000 sequences (Figure 6). A total of 10 subtypes

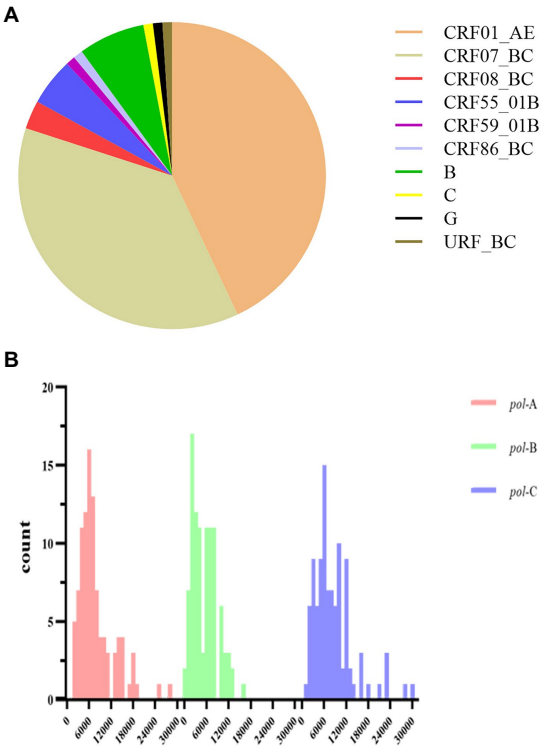

FIGURE 6
(A) Subtype distribution of HIV-1 clinical samples. **(B)** The distribution of reads in the deep sequencing data of HIV-1 clinical samples. After sequence quality control, the poor-quality sequences were filtered. Different colors represented the distribution of reads in the three segments in the *pol* gene region. The reads of *pol*-A, *pol*-B, and *pol*-C were respectively concentrated in 6,000 (range:1,694–28,069), 2,000 (range:389–16,008), and 6,000 (range:1,373–30,018).

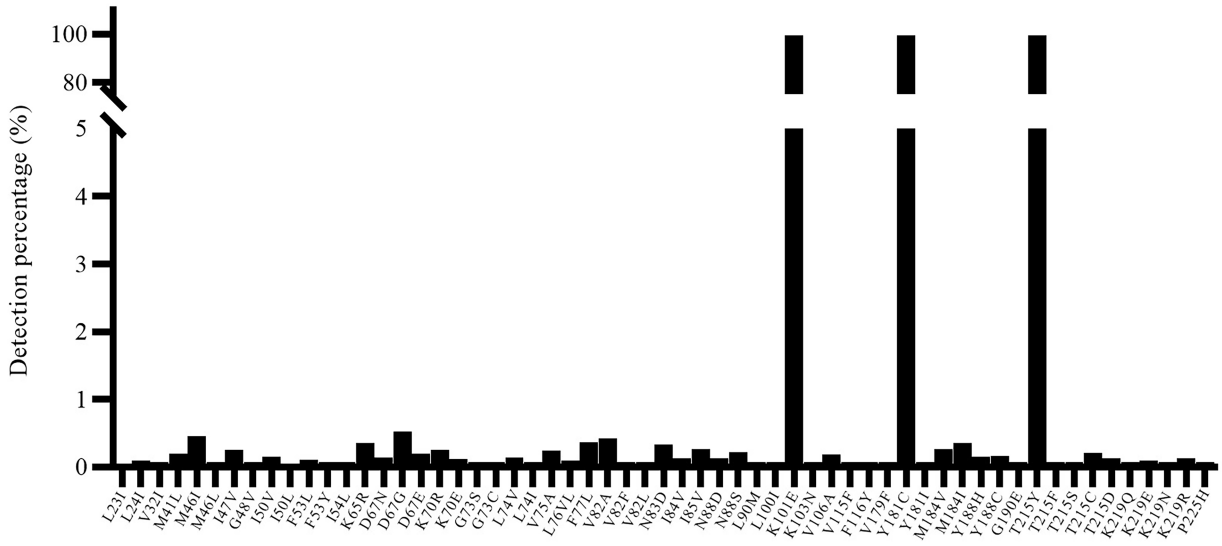

FIGURE 5
The specificity of known resistance mutations and noise value. The HIV-1 NL4-3 with K101E + Y181C + T215Y mutant strain was used for detection, and all three target mutations were detected. At the same time, there were some false positive mutations with a frequency of less than 1% (maybe introduced for PCR amplification).

were included in all samples. According to the detection results of surveillance drug resistance mutations (SDRMs), whether it was analyzed using our NGS-sequence analysis panel or HyDRA, the segmented amplification method can detect all the drug resistance mutations reported by Sanger sequencing. In addition, the NGS method reported an SDRM that had not been detected by SS, which indicated that the segmented amplification method had higher sensitivity than the traditional in-house method (Table 1).

Our NGS-sequence analysis panel and HyDRA were used to detect drug resistance mutations in NGS sequencing data, and the SDRMs with a frequency of more than 1% were counted (Figure 7). Due to the difference in algorithms, it was not surprising that the two methods have slight differences in the number of low-frequency SDRMs. The calculation results of McNemar's test proved the accuracy of our NGS-sequence analysis panel for SDRM detection ($p = 0.972$).

HIV-1 samples detection

All samples were amplified by PT-PCR using a segmented amplification method based on next-generation sequencing methods. Excluding factors such as insufficient plasma samples and failure of viral nucleic acid extraction, a total of 1,755 samples successfully completed the amplification and next-generation sequencing process. Among the samples for which sequencing results were obtained, 15 samples were excluded due to poor sequencing quality, and the remaining 1,740 samples obtained good sequencing results. The proportion of samples with all three segments of *pol*-A, *pol*-B, and *pol*-C positive was 99.15%.

A total of 1,740 participants with demographic data and NGS sequences. General characteristics of the study subjects are shown in Table 2. The age of the patients was mainly distributed between 20 and 50 years old. Most individuals were men (86.03%), single (54.25%), and Han Population (92.13%). The dominant transmission route was heterosexual contact (63.68%). The education level of junior high school and above accounted for 90.52%. CRF01_AE (37.13%) subtype was predominant, followed by CRF07_BC (38.22%) and CRF55_01B (9.54%).

According to the mutations for drug resistance surveillance in the Stanford Drug Resistance Database, a total of 360 out of 1,740 patients contained SDRMs at the 2% threshold (Figure 8). The NRTIs resistance mutations were the most prevalent (48.14%), followed by PIs (39.3%) and NNRTIs (12.56%). Thirty-five strains (2.01%) contain dual-class mutations (PI + NRTI in 24 cases, PI + NNRTI in 8 cases, and NRTI + NNRTI in 3 cases) and 2 cases contain triple-class variants. For NRTIs, the most common mutation was K65R and for PIs there were M46I + N88S. the most frequent mutations related to NNRTIs were G190E.

TABLE 1 Comparison of the detection results of the three detection methods.

Sample number	In-house	NGS-sequence analysis panel[a]	HyDRA[a]
LS10185	Y181C	Y181C-41.16%	Y181C-39.82%
	K219N	K219N-50.51%	K219N-49.94%
LS10202		D67N-62.28%	D67N-59.10%
LS10221	M41L	M41L-23.09%	M41L-29.12%
LS10407	K103N	K103N-98.62%	K103N-98.53%
LS10564	Y181C	Y181C-37.04%	Y181C-27.21%

[a]The percentage indicated the reported frequency of the resistant mutation.

Discussion

Due to the unparalleled advantages of NGS, it is not surprising that NGS is used for HIV drug resistance mutation detection. In this study, a new amplification method based on next-generation sequencing was established to detect the minority resistance variants in HIV-infected patients. This method was based on the Illumina sequencing platform and used PCR amplicons for library construction. Compared with Sanger sequencing, NGS has higher

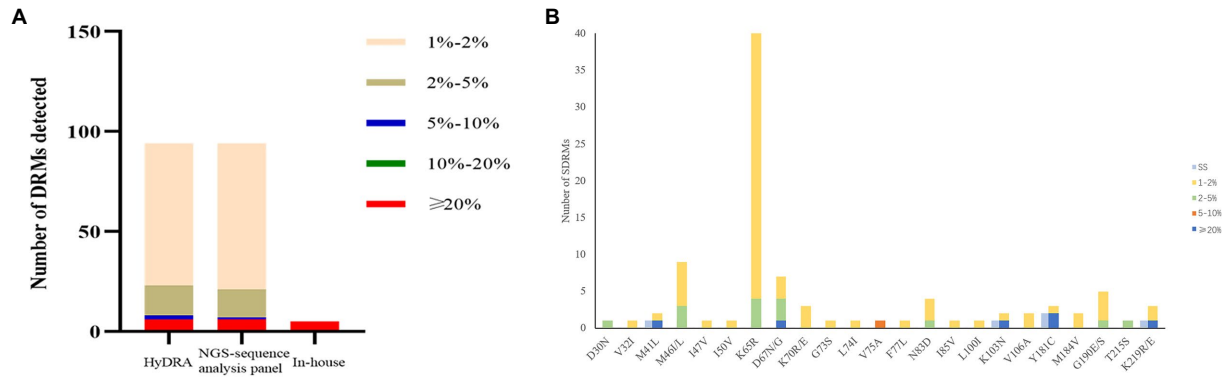

FIGURE 7
(A) The number of DRMs detected by the three detection methods. The range of the interval in the figure was inclusive of the left-side value, and the right-side value was not included. **(B)** Comparison of HIV-1 SDRMs detected by Sanger sequencing and NGS-sequence analysis panel at different detection thresholds.

TABLE 2 Demographic characteristics of HIV-infected persons in Shenzhen, 2014–2015.

Characteristics	Case number and percentage, *n* (%)
Total	1,740
Age (years old)	
≤20	7 (0.4%)
21–30	403 (23.16%)
31–40	676 (38.85%)
41–50	412 (23.68%)
>50	242 (13.91%)
Gender	
Male	1,497 (86.03%)
Female	244 (14.02%)
Route of transmission	
Homosexual	549 (31.55%)
Heterosexual	1,108 (63.68%)
Injecting drug using	55 (3.16%)
Unknown/other	28 (1.61%)
Ethnic group	
Han	1,603 (92.13%)
Others	137 (7.87%)
Marital status	
Single	944 (54.25%)
Married or living with partner	560 (32.18%)
Divorced or widowed	227 (13.05%)
Unknown	9 (0.52%)
Education	
Illiterate	18 (1.03%)
Primary school	147 (8.45%)
Junior middle school	690 (39.66%)
Senior school and technical secondary school	501 (28.79%)
College and above	384 (22.07%)
Subtype	
CRF01_AE	646 (37.13%)
CRF07_BC	665 (38.22%)
CRF55_01B	166 (9.54%)
B	91 (5.23%)
Others	172 (9.89%)

detection sensitivity and automated data flow, and NGS has extremely high sensitivity for less than 20% of minority resistance variants. On the basis of Sanger sequencing to detect the existence of "yes" or "no" drug resistance variants, NGS adds more information about the frequency of variants.

The evaluation of the detection method is an important part of the whole method establishment. Many previous studies often used different data analysis platforms to analyze NGS sequences, and integrated the reports of each platform to finally determine the results of drug resistance detection (Lee et al., 2020). Different from previous studies, we used HIV strains with known resistance variants to complete the evaluation of NGS detection. The introduction of virus strains with known drug-resistant frequencies made the entire detection process completely simulate the amplification and detection process of actual samples, which more truly reflected the accuracy of NGS in detecting species at drug-resistant variants. An overall assessment of the actual errors introduced in the entire workflow from viral nucleic acid extraction to resistance site reporting was completed.

At present, the application of high-throughput sequencing to HIV drug resistance detection is still mainly in the laboratory research stage, and it is rarely used in clinical detecting. The clinical relationship between HIV minority resistance variants and disease is still inconclusive, but it has been documented that minority resistance variants may lead to the failure of HIV virological treatment (Gupta et al., 2014; Hikichi et al., 2021). Population-based studies have proven that NGS can detect a large proportion of low-level variants, while traditional Sanger sequencing cannot detect (Baxter et al., 2021; Tekin et al., 2021). Similarly, the same conclusion was obtained in our study. In the detection of the same samples, NGS outperformed SS in terms of detection accuracy and sensitivity. Compared with SS, NGS can detect more low-frequency resistance mutations. This suggests that the prevalence of resistance in previous reports may be underestimated. Low-frequency resistance mutations could have significant consequences for clinical outcomes (Li et al., 2011; Kyeyune et al., 2016). In our detection of HIV samples in Shenzhen, we found that there were a large number of low-abundance NRTIs resistance variants in the ART-naive HIV population, which may be related to the first-line antiviral drugs used in our country. This suggests that pre-treatment drug resistance testing before initiating ART in newly diagnosed HIV/AIDS patients may be necessary.

Although our evaluation indicators showed that the segmented amplification method can perform reliable quantitative analysis in the range of 1–100%, we do not recommend reporting resistance sites less than 2%. This is also consistent with the recommendations provided by the current research (Avila-Ríos et al., 2016; Lee et al., 2020). When the frequency was lower than 2%, the incidence of false positives increased, as well as the possibility of cross-contamination and PCR reaction deviation (Ávila-Ríos et al., 2020). At present, the optimal threshold for NGS detection of clinical drug resistance mutations is still inconclusive. By strengthening the standardization of NGS operating procedures and data analysis in drug resistance detecting, NGS is expected to become a new standard method for HIV drug resistance genotyping (Noguera-Julian et al., 2020).

It is undeniable that there were still some limitations in this study. The mutations contained in the HIV NL4-3 mutant used in this study were all reverse transcriptase resistance mutations, and no protease mutations were involved. In this method, only one high-throughput sequencing platform was used to establish and evaluate the drug resistance detection method, and the differences in sequencing errors among various high-throughput sequencing platforms were not included in the study. And samples at all frequencies between 1% and 100% were not included in the method evaluation.

In conclusion, we have established a method of tagged-amplicon deep sequencing for low-abundance drug resistance in HIV-1 and had completed the evaluation for the detection of HIV-1

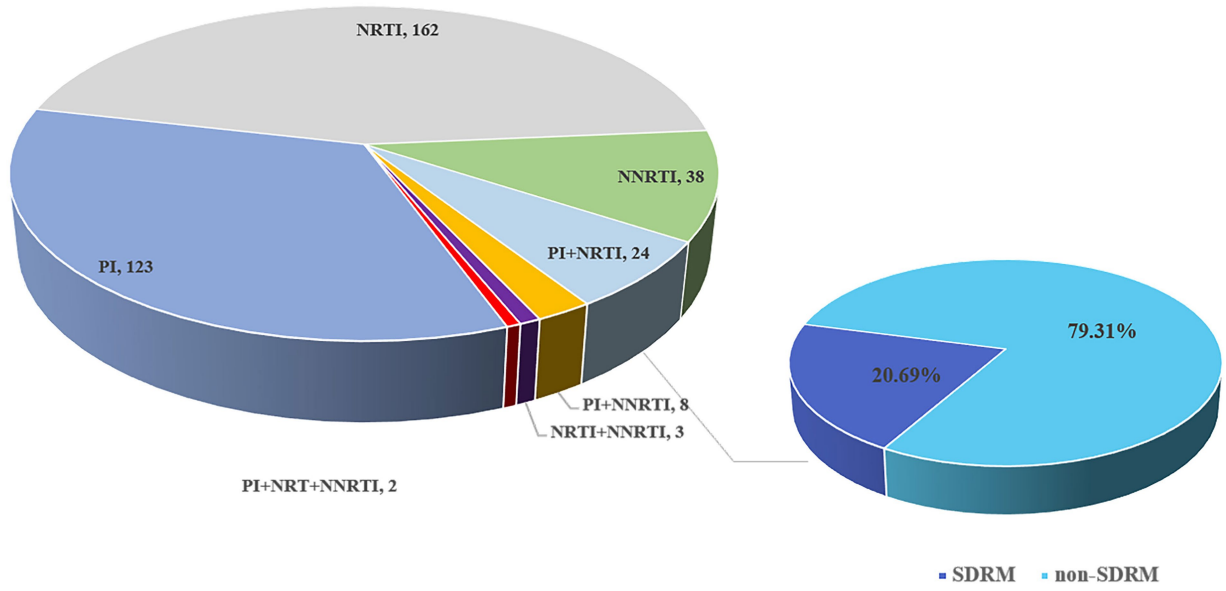

FIGURE 8
Composition and distribution of SDRM in newly diagnosed HIV-1 samples in Shenzhen from 2014 to 2015.

drug resistance mutations. It provided some references for other studies using NGS and provided evaluation criteria for NGS technology to be used in HIV-1 clinical drug resistance detecting.

Data availability statement

The original contributions presented in the study are included in the article/Supplementary material, further inquiries can be directed to the corresponding authors.

Ethics statement

The studies involving human participants were reviewed and approved by the Beijing Institute of Microbial Epidemiology. Written informed consent to participate in this study was provided by the participants' legal guardian/next of kin. Written informed consent was obtained from the individual(s), and minor(s)' legal guardian/next of kin, for the publication of any potentially identifiable images or data included in this article.

Author contributions

LL, HL, and YL conceived the study. YL and LH conducted this study. YW provided help for data analysis. XW, LJ, JL, and JH provided guidance and help for the operation of the experiment. LL and HL provided guidance and reviewed the manuscript. JZ completed the sample collection. All authors contributed to the article and approved the submitted version.

Funding

This study was supported by the National Key Research and Development Program of China (2020YFA0907000), National Natural Science Foundation of China (NSFC; 81773493, 31800149, and 31900157), and the State Key Laboratory of Pathogen and Biosecurity (AMMS; SKLPBS2103 and SKLPBS2118).

Conflict of interest

The authors declare that the research was conducted in the absence of any commercial or financial relationships that could be construed as a potential conflict of interest.

Publisher's note

All claims expressed in this article are solely those of the authors and do not necessarily represent those of their affiliated organizations, or those of the publisher, the editors and the reviewers. Any product that may be evaluated in this article, or claim that may be made by its manufacturer, is not guaranteed or endorsed by the publisher.

Supplementary material

The Supplementary material for this article can be found online at: https://www.frontiersin.org/articles/10.3389/fmicb.2022.895227/full#supplementary-material

References

Avila-Ríos, S., García-Morales, C., Matías-Florentino, M., Tapia-Trejo, D., Hernández-Álvarez, B., Moreira-López, S., et al. (2016). HIV drug resistance in antiretroviral treatment–Naïve individuals in the largest public Hospital in Nicaragua, 2011-2015. *PLoS One* 11:e0164156. doi: 10.1371/journal.pone.0164156

Ávila-Ríos, S., Parkin, N., Swanstrom, R., Paredes, R., Shafer, R., Ji, H., et al. (2020). Next-generation sequencing for HIV drug resistance testing: laboratory, clinical, and implementation considerations. *Viruses* 12:617. doi: 10.3390/v12060617

Baxter, J., Dunn, D., Tostevin, A., Marvig, R., Bennedbaek, M., Cozzi-Lepri, A., et al. (2021). Transmitted HIV-1 drug resistance in a large international cohort using next-generation sequencing: results from the strategic timing of antiretroviral treatment (START) study. *HIV Med.* 22, 360–371. doi: 10.1111/hiv.13038

Becker, M. G., Liang, D., Cooper, B., Le, Y., Taylor, T., Lee, E. R., et al. (2020). Development and application of performance assessment criteria for next-generation sequencing-based HIV drug resistance assays. *Viruses* 10:12. doi: 10.3390/v12060627

Bendall, M., Gibson, K., Steiner, M., Rentia, U., Pérez-Losada, M., and Crandall, K. (2021). HAPHPIPE: haplotype reconstruction and Phylodynamics for deep sequencing of Intrahost viral populations. *Mol. Biol. Evol.* 38, 1677–1690. doi: 10.1093/molbev/msaa315

Chaillon, A., Nakazawa, M., Wertheim, J., Little, S., Smith, D., Mehta, S., et al. (2017). No substantial evidence for sexual transmission of minority HIV drug resistance mutations in men who have sex with men. *J. Virol.* 91. doi: 10.1128/JVI.00769-17

Chen, N., Kao, S., Liu, Z., Wu, T., Tsai, C., Lin, H., et al. (2020). Shall I trust the report? Variable performance of sanger sequencing revealed by deep sequencing on HIV drug resistance mutation detection. *Int. J. Infect. Dis.* 93, 182–191. doi: 10.1016/j.ijid.2020.02.004

Gibson, K., Jair, K., Castel, A., Bendall, M., Wilbourn, B., Jordan, J., et al. (2020). A cross-sectional study to characterize local HIV-1 dynamics in Washington, DC using next-generation sequencing. *Sci. Rep.* 10:1989. doi: 10.1038/s41598-020-58410-y

Grant, R., Kuritzkes, D., Johnson, V., Mellors, J., Sullivan, J., Swanstrom, R., et al. (2003). Accuracy of the TRUGENE HIV-1 genotyping kit. *J. Clin. Microbiol.* 41, 1586–1593. doi: 10.1128/JCM.41.4.1586-1593.2003

Guglielmetti, L., Ardizzoni, E., Atger, M., Baudin, E., Berikova, E., Bonnet, M., et al. (2021). Evaluating newly approved drugs for multidrug-resistant tuberculosis (endTB): study protocol for an adaptive, multi-country randomized controlled trial. *Trials* 22:651. doi: 10.1186/s13063-021-05491-3

Gupta, S., Lataillade, M., Kyriakides, T., Chiarella, J., St John, E., Webb, S., et al. (2014). Low-frequency NNRTI-resistant HIV-1 variants and relationship to mutational load in antiretroviral-naïve subjects. *Viruses* 6, 3428–3437. doi: 10.3390/v6093428

Halvas, E., Wiegand, A., Boltz, V., Kearney, M., Nissley, D., Wantman, M., et al. (2010). Low frequency nonnucleoside reverse-transcriptase inhibitor-resistant variants contribute to failure of efavirenz-containing regimens in treatment-experienced patients. *J. Infect. Dis.* 201, 672–680. doi: 10.1086/650542

Hauser, A., Kuecherer, C., Kunz, A., Dabrowski, P., Radonić, A., Nitsche, A., et al. (2015). Comparison of 454 ultra-deep sequencing and allele-specific real-time PCR with regard to the detection of emerging drug-resistant minor HIV-1 variants after antiretroviral prophylaxis for vertical transmission. *PLoS One* 10:e0140809. doi: 10.1371/journal.pone.0140809

Hikichi, Y., Van Duyne, R., Pham, P., Groebner, J., Wiegand, A., Mellors, J., et al. (2021). Mechanistic analysis of the broad antiretroviral resistance conferred by HIV-1 envelope glycoprotein mutations. *MBio* 12. doi: 10.1128/mBio.03134-20

Ji, H., Sandstrom, P., Paredes, R., Harrigan, P., Brumme, C., Avila Rios, S., et al. (2020). Are we ready for NGS HIV drug resistance testing? The second "Winnipeg consensus" Symposium. *Viruses* 12. doi: 10.3390/v12060586

Katoh, K., Rozewicki, J., and Yamada, K. (2019). MAFFT online service: multiple sequence alignment, interactive sequence choice and visualization. *Brief. Bioinform.* 20, 1160–1166. doi: 10.1093/bib/bbx108

Kireev, D., Lopatukhin, A., Murzakova, A., Pimkina, E., Speranskaya, A., Neverov, A., et al. (2018). Evaluating the accuracy and sensitivity of detecting minority HIV-1 populations by Illumina next-generation sequencing. *J. Virol. Methods* 261, 40–45. doi: 10.1016/j.jviromet.2018.08.001

Kyeyune, F., Gibson, R., Nankya, I., Venner, C., Metha, S., Akao, J., et al. (2016). Low-frequency drug resistance in HIV-infected Ugandans on antiretroviral treatment is associated with regimen failure. *Antimicrob. Agents Chemother.* 60, 3380–3397. doi: 10.1128/AAC.00038-16

Lee, E., Parkin, N., Jennings, C., Brumme, C., Enns, E., Casadellà, M., et al. (2020). Performance comparison of next generation sequencing analysis pipelines for HIV-1 drug resistance testing. *Sci. Rep.* 10:1634. doi: 10.1038/s41598-020-58544-z

Li, J., Paredes, R., Ribaudo, H., Svarovskaia, E., Metzner, K., Kozal, M., et al. (2011). Low-frequency HIV-1 drug resistance mutations and risk of NNRTI-based antiretroviral treatment failure: A systematic review and pooled analysis. *JAMA* 305, 1327–1335. doi: 10.1001/jama.2011.375

McKinnon, J., Delgado, R., Pulido, F., Shao, W., Arribas, J., and Mellors, J. (2011). Single genome sequencing of HIV-1 gag and protease resistance mutations at virologic failure during the OK04 trial of simplified versus standard maintenance therapy. *Antivir. Ther.* 16, 725–732. doi: 10.3851/IMP1812

Nicot, F., Saliou, A., Raymond, S., Sauné, K., Dubois, M., Massip, P., et al. (2012). Minority variants associated with resistance to HIV-1 nonnucleoside reverse transcriptase inhibitors during primary infection. *J. Clin. Virol.* 55, 107–113. doi: 10.1016/j.jcv.2012.06.018

Noguera-Julian, M., Lee, E. R., Shafer, R. W., Kantor, R., and Ji, H. (2020). Dry panels supporting external quality assessment programs for next generation sequencing-based HIV drug resistance testing. *Viruses* 20:12.

Palmer, S., Kearney, M., Maldarelli, F., Halvas, E. K., Bixby, C. J., Bazmi, H., et al. (2005). Multiple, linked human immunodeficiency virus type 1 drug resistance mutations in treatment-experienced patients are missed by standard genotype analysis. *J. Clin. Microbiol.* 43, 406–413. doi: 10.1128/JCM.43.1.406-413.2005

Parikh, U., Penrose, K., Heaps, A., Halvas, E., Goetz, B., Gordon, K., et al. (2021). HIV-1 drug resistance among individuals who seroconverted in the ASPIRE dapivirine ring trial. *J. Int. AIDS Soc.* 24:e25833. doi: 10.1002/jia2.25833

Parkin, N. T., Avila-Rios, S., Bibby, D. F., Brumme, C. J., Eshleman, S. H., Harrigan, P. R., et al. (2020). Multi-laboratory comparison of next-generation to sanger-based sequencing for HIV-1 drug resistance genotyping. *Viruses* 12:12. doi: 10.3390/v12070694

Schloss, P., Westcott, S., Ryabin, T., Hall, J., Hartmann, M., Hollister, E., et al. (2009). Introducing mothur: open-source, platform-independent, community-supported software for describing and comparing microbial communities. *Appl. Environ. Microbiol.* 75, 7537–7541. doi: 10.1128/AEM.01541-09

Soeria-Atmadja, S., Amuge, P., Nanzigu, S., Bbuye, D., Rubin, J., Eriksen, J., et al. (2020). Pretreatment HIV drug resistance predicts accumulation of new mutations in ART-naïve Ugandan children. *Acta Paediatr.* 109, 2706–2716. doi: 10.1111/apa.15320

Stranneheim, H., and Lundeberg, J. (2012). Stepping stones in DNA sequencing. *Biotechnol. J.* 7, 1063–1073. doi: 10.1002/biot.201200153

Tachbele, E., Kyobe, S., Katabazi, F., Kigozi, E., Mwesigwa, S., Joloba, M., et al. (2021). Genetic diversity and acquired drug resistance mutations detected by deep sequencing in Virologic failures among antiretroviral treatment experienced human immunodeficiency Virus-1 patients in a pastoralist region of Ethiopia. *Infect. Drug Resist.* 14, 4833–4847. doi: 10.2147/IDR.S337485

Tekin, D., Gokengin, D., Onay, H., Erensoy, S., and Sertoz, R. (2021). Investigation of drug resistance against protease, reverse transcriptase, and integrase inhibitors by next-generation sequencing in HIV-positive patients. *J. Med. Virol.* 93, 3627–3633. doi: 10.1002/jmv.26582

Tzou, P., Ariyaratne, P., Varghese, V., Lee, C., Rakhmanaliev, E., Villy, C., et al. (2018). In VitroComparison of an diagnostic next-generation sequencing assay with sanger sequencing for HIV-1 genotypic resistance testing. *J. Clin. Microbiol.* 56. doi: 10.1128/JCM.00105-18

Wang, Y., Xing, H., Liao, L., Wang, Z., Su, B., Zhao, Q., et al. (2014). The development of drug resistance mutations K103N Y181C and G190A in long term Nevirapine-containing antiviral therapy. *AIDS Res. Ther.* 11:36. doi: 10.1186/1742-6405-11-36

WHO (2021). *HIV Drug Resistance Report 2021*. Available at: https://www.who.int/news/item/24-11-2021-who-releases-hiv-drug-resistance-report-2021

Xie, Y., Zhu, F., Zhong, Y., Chen, Y., Gao, Q., Lai, X., et al. (2021). Distribution characteristics of drug resistance mutations of HIV CRF01_AE, CRF07_BC and CRF08_BC from patients under ART in Ganzhou, China. *J. Antimicrob. Chemother.* 76, 2975–2982. doi: 10.1093/jac/dkab296

frontiers | Frontiers in Microbiology

TYPE Original Research
PUBLISHED 31 August 2022
DOI 10.3389/fmicb.2022.946787

OPEN ACCESS

EDITED BY
Anna Kramvis,
University of the Witwatersrand,
South Africa

REVIEWED BY
Jose Trinidad Ascencio-Ibáñez,
North Carolina State University,
United States
Xiang He,
Guangdong Provincial Center for Disease Control and Prevention, China

*CORRESPONDENCE
Mariya V. Sivay
mariya.sivay@gmail.com;
sivay_mv@vector.nsc.ru

SPECIALTY SECTION
This article was submitted to Virology, a section of the journal Frontiers in Microbiology

RECEIVED 18 May 2022
ACCEPTED 19 July 2022
PUBLISHED 31 August 2022

CITATION
Sivay MV, Maksimenko LV, Osipova IP, Nefedova AA, Gashnikova MP, Zyryanova DP, Ekushov VE, Totmenin AV, Nalimova TM, Ivlev VV, Kapustin DV, Pozdnyakova LL, Skudarnov SE, Ostapova TS, Yaschenko SV, Nazarova OI, Chernov AS, Ismailova TN, Maksutov RA and Gashnikova NM (2022) Spatiotemporal dynamics of HIV-1 CRF63_02A6 sub-epidemic. *Front. Microbiol.* 13:946787. doi: 10.3389/fmicb.2022.946787

Spatiotemporal dynamics of HIV-1 CRF63_02A6 sub-epidemic

Mariya V. Sivay[1]*, Lada V. Maksimenko[1], Irina P. Osipova[1], Anastasiya A. Nefedova[1], Mariya P. Gashnikova[1], Dariya P. Zyryanova[1], Vasiliy E. Ekushov[1], Alexei V. Totmenin[1], Tatyana M. Nalimova[1], Vladimir V. Ivlev[1], Dmitriy V. Kapustin[2], Larisa L. Pozdnyakova[2], Sergey E. Skudarnov[3], Tatyana S. Ostapova[3], Svetlana V. Yaschenko[3], Olga I. Nazarova[4], Aleksander S. Chernov[5], Tatyana N. Ismailova[5], Rinat A. Maksutov[1] and Natalya M. Gashnikova[1]

[1]Department of Retroviruses, State Research Center of Virology and Biotechnology "Vector", Koltsovo, Russia, [2]City Infectious Clinical Hospital #1, Novosibirsk, Russia, [3]Krasnoyarsk Regional Center for Prevention and Control of AIDS, Krasnoyarsk, Russia, [4]Omsk City Center of Prevention and Control of AIDS and Other Infectious Diseases, Omsk, Russia, [5]Tomsk Regional Center for Prevention and Control of AIDS and Other Infectious Diseases, Tomsk, Russia

HIV-1 epidemic in Russia is one of the fastest growing in the world reaching 1.14 million people living with HIV-1 (PLWH) in 2021. Since mid-1990s, the HIV-1 epidemic in Russia has started to grow substantially due to the multiple HIV-1 outbreaks among persons who inject drugs (PWID) leading to expansion of the HIV-1 sub-subtype A6 (former Soviet Union (FSU) subtype A). In 2006, a local HIV-1 sub-epidemic caused by the distribution of novel genetic lineage CRF63_02A6 was identified in Siberia. In this study, we used a comprehensive dataset of CRF63_02A6 *pol* gene sequences to investigate the spatiotemporal dynamic of the HIV-1 CRF63_02A6 sub-epidemic. This study includes all the available CRF63_02A6 HIV-1 *pol* gene sequences from Los Alamos National Laboratory (LANL) HIV Sequence Database. The HIV-1 subtypes of those sequences were conferred using phylogenetic analysis, and two automated HIV-1 subtyping tools Stanford HIVdb Program and COMET. Ancestral state reconstruction and origin date were estimated using Nextstrain. Evolutionary rate and phylodynamic analysis were estimated using BEAST v 1.10.4. CRF63_02A6 was assigned for 872 *pol* gene sequences using phylogenetic analysis approach. Predominant number (n=832; 95.4%) of those sequences were from Russia; the remaining 40 (4.6%) sequences were from countries of Central Asia. Out of 872 CRF63_02A6 sequences, the corresponding genetic variant was assigned for 75.7 and 79.8% of sequences by Stanford and COMET subtyping tools, respectively. Dated phylogenetic analysis of the CRF63_02A6 sequences showed that the virus most likely originated in Novosibirsk, Russia, in 2005. Over the last two decades CRF63_02A6 has been widely distributed across Russia and has been sporadically detected in countries of Central Asia. Introduction of new genetic variant into mature sub-subtype A6 and CRF02_AG$_{FSU}$ epidemics could promote the increase of viral genetic diversity

and emergence of new recombinant forms. Further HIV-1 studies are needed due to a continuing rapid virus distribution. Also, the implementation of HIV-1 prevention programs is required to reduce HIV-1 transmission. This study also highlights the discrepancies in HIV-1 subtyping approaches. The reference lists of HIV-1 sequences implemented in widely used HIV-1 automated subtyping tools need to be updated to provide reliable results.

KEYWORDS

HIV-1, CRF63_02A6 HIV-1, Russia, Central Asia, spatiotemporal dynamics, phylogenetic analysis, HIV-1 epidemic

Introduction

Russia, as well as other countries of Eastern Europe and Central Asia, has one of the fastest growing HIV-1 epidemics in the world (Frank et al., 2019). In 2021, 1.14 million people are living with HIV-1 (PLWH) in Russia (Central Research Institute of Epidemiology, Federal Service on Customers' Rights Protection and Human Well-being Surveillance, 2021)[1]. Russia has a diverse HIV-1 epidemic with unique patterns shaped by various socio-economical, geographical, and cultural factors influencing the development of local HIV-1 sub-epidemics within the country (Bobkova, 2013). Since mid-1990s, the HIV-1 epidemic in Russia has started to grow explosively due to the multiple HIV-1 outbreaks occurred among PWID leading to expansion of the HIV-1 sub-subtype A6, also known as former Soviet Union (FSU) subtype A (FSU-A). This genetic variant predominates in most of the Russian territories ever since (Bobkov et al., 2004; Thomson et al., 2009; Diez-Fuertes et al., 2015; Aibekova et al., 2018). In late-1990s, HIV-1 sub-epidemic among different high-risk groups was detected on the territories of the Russian Fast East (Kazennova et al., 2014; Kotova et al., 2019) and European part of Russia (Liitsola et al., 2000; Lebedev et al., 2020; Ozhmegova et al., 2020). Currently, along with the predominant sub-subtype A6, subtypes B, C, and CRF03_AB have been constantly identified (Karamov et al., 2018; Pasechnik and Blokh, 2018; Kotova et al., 2019; Safina et al., 2022). In 2006, a local HIV-1 sub-epidemic was caused by the distribution of the novel genetic lineage CRF63_02A6 in Siberia (Baryshev et al., 2012, 2014). The detailed analysis of CRF63_02A6 genome structure revealed that this viral variant originated due to recombination between Russian sub-subtype A6 and CRF02_AG$_{FSU}$ (Central Asian lineage of the CRF02_AG; Carr et al., 2005; Baryshev et al., 2014). Several outbreaks of the CRF63_02A6 were detected in different Siberian regions between 2007 and 2014. This genetic variant has dominated in Siberia since that time (Gashnikova et al., 2015, 2017; Ulyanova et al., 2019; Kazennova et al., 2020; Maksimenko et al., 2020). The number of new HIV-1 cases has been gradually rising in Russia and has peaked in 2014, followed by the decline stage (Figure 1). At the same time, HIV-1 prevalence in Siberia was significantly higher than the country average.

Initial HIV-1 epidemic in Russia occurred mainly among PWID and their sexual partners. But since 2016, the number of people infected through the heterosexual contacts exceeded the PWID cases and the epidemic has transmitted to the general population (Bobkov et al., 1998; Bobkova, 2013; Kazennova et al., 2014; Kotova et al., 2019; Schlösser et al., 2020).

Since 2008, our laboratory has extensively collected HIV-1 sequences in Siberian regions. Beginning in 2016, the HIV-1 surveillance studies have been conducted in the Central Asia countries as a part of the national HIV-1 drug resistance surveillance program. In this study, we used a comprehensive dataset of 872 *pol* gene HIV CRF63_02A6 sequences from Russia and countries of Central Asia to investigate the spatiotemporal dynamic of HIV-1 CRF63_02A6 sub-epidemic.

Materials and methods

Study population and HIV-1 sequence dataset

This study uses HIV-1partial *pol* gene sequences (1,047 base pairs, HXB2 #K03455 positions 2,252–3,299, n = 587) from our previous surveillance studies (Baryshev et al., 2012; Gashnikova et al., 2015, 2017; Ulyanova et al., 2019; Maksimenko et al., 2020; Sivay et al., 2021). Blood samples were collected from 2009 to 2020 from PWLH, both ART-naïve and therapy experienced, and were used for routine antiretroviral drug resistance testing. Samples were collected in six regions of Russia (Novosibirsk, Altai, Tomsk, Omsk, Krasnoyarsk, and Kemerovo). Further manipulations with the RNA/DNA samples as well as the population sequencing procedure were previously described (Sivay et al., 2021). Additional *pol* gene sequences were retrieved from Los Alamos National Laboratory (LANL) HIV Sequence Database (Los Alamos National Laboratory HIV Sequence Database, 2022a)[2]; all sequences classified as CRF63_02A6, CRF63_01A, CRF02A6,

1 http://www.hivrussia.info/wp-content/uploads/2022/03/Spravka-VICH-v-Rossii-na-31.12.2021-g.pdf

2 http://www.hiv.lanl.gov/

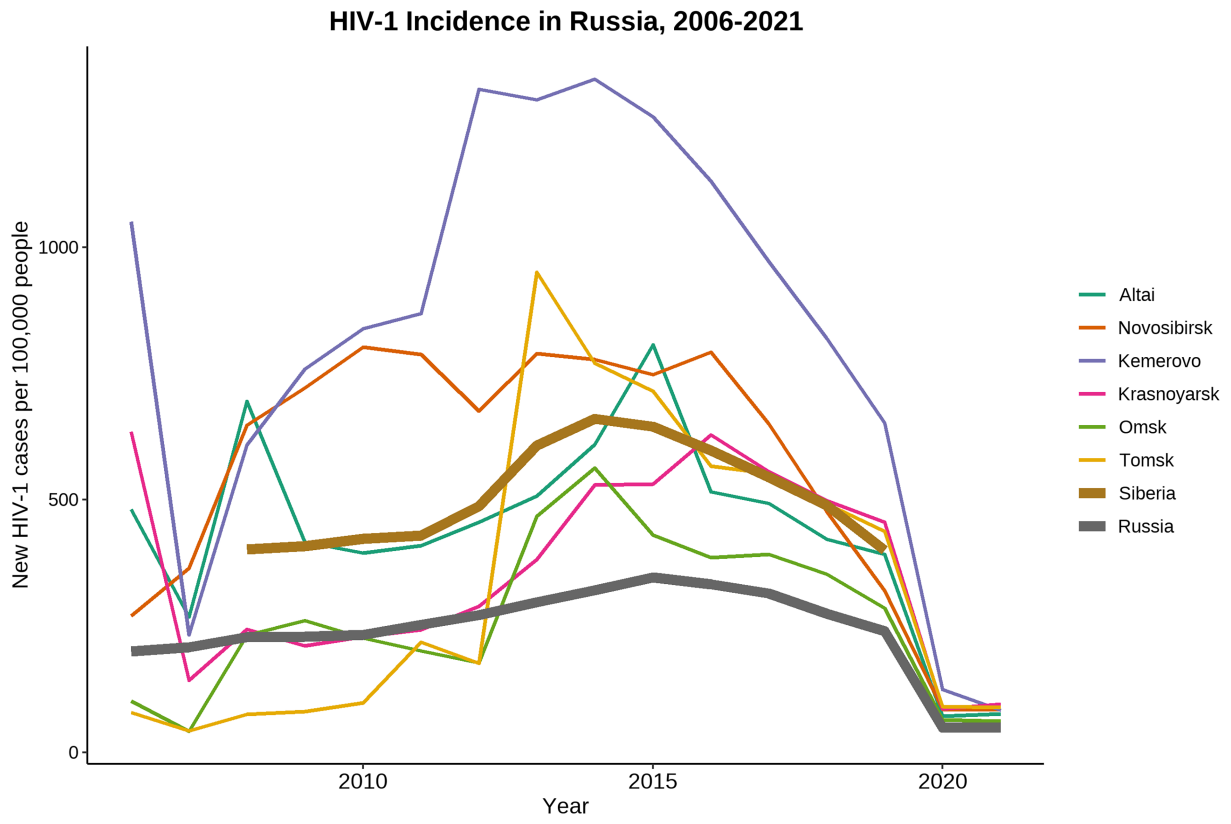

FIGURE 1
Dynamics of HIV-1 incidence in Russia from 2006 to 2021. Data were adopted from the Central Scientific Research Institute of Epidemiology of Rospotrebnadzor, Russian Federal AIDS Center, Moscow, Russia. Incidence data collected in 2019–2021 was most likely biased due to the COVID-19 world pandemic and represented the under-registered new HIV-1 cases.

CRF02_AG, and "other" subtypes from FSU countries were included. A limited number of CRF02_AG sequences from African and European countries were also included in the dataset; those sequences were selected randomly.

HIV-1 subtyping

HIV-1 subtypes were identified by phylogenetic analysis. Study sequences were combined with the 2020 list of LANL HIV-1 subtype reference sequences (including all pure subtypes and CRFs) and the further phylogenetic analysis was performed with IQ-Tree (Nguyen et al., 2015) using maximum likelihood method and GRT+G4+I substitution model and Shimodaira-Hasegawa approximate likelihood-ratio test with 1,000 replicates. HIV-1 subtype was assigned if study sequence falls into monophyletic clade with the corresponding subtype reference sequence with the branch support value ≥90. HIV-1 inter- and intra-subtype recombinants were identified using GARD (Kosakovsky Pond et al., 2006). In addition to the phylogenetic analysis, we applied the two widely used automated HIV-1 subtyping tools -- Stanford HIVdb program (Liu and Shafer, 2006) and COMET (Struck et al., 2014). The other widely used HIV-1 automated subtyping tool – REGA – was not used in this study; list of reference sequences that is used in REGA is outdated and does not include CRF63_02A6 sequences.

HIV-1 phylogenetic and transmission cluster analyses

Maximum likelihood phylogenetic tree was constructed using IQ-Tree under GTR+4G+I substitution model as selected by jModelTest2 (Darriba et al., 2012). Transmission clusters were identified using Cluster Picker v1.2.3 (Ragonnet-Cronin et al., 2013) with the branch support threshold of 90 and maximum genetic distance threshold of 0.03.

Estimation of HIV-1 CRF63_02A6 origin time and location

To estimate ancestral state reconstruction and identify time to the most recent common ancestor (tMRCA) of the CRF63_02A6, a local instance of Nextstrain (Hadfield et al., 2018) was used. This is a recently developed software for real-time tracking of pathogens evolution such as COVID-19. To estimate the

evolutionary rate and examine demographic history of the HIV-1 CRF63_02A6, a Bayesian Markov Chain Monte Carlo (MCMC) approach incorporated into BEAST v1.10.4 (Suchard et al., 2018) was used. To reduce computational complexity, a subsampling step was introduced, so that only a single sequence per transmission cluster was included in the further spatiotemporal analysis. The GTR + 4G substitution model, the lognormal uncorrelated relaxed clock model, and the Bayesian skyline coalescent model were used. Two independent MCMC runs of 15×10^7 simulations were performed. Convergence of the MCMC results was examined in Tracer v1.7.1 (Rambaut et al., 2018) with effective sampling size (ESS) >200 for all parameters considered acceptable. The maximum clade credibility (MCC) tree was generated using TreeAnnotator v1.10.4 and visualized in FigTree v1.4.3 (Rambaut, 2009). We also estimated tMRCA and investigated geographic distribution of the CRF63_02A6 using BEAST v1.10.4 and compared it with the results obtained by the Nextstrain. Migration events of the HIV-1 CRF63_02A6 were reconstructed using the discrete Bayesian phylogeographic approach combined with the Bayesian Stochastic Search Variable Selection (BSSVS). Geographic location of sequences was assigned as a sampling city; if sampling city data was unavailable, then the country's largest city location was used. Viral migration routes were summarized using SPREAD3 v0.9.7.1 (Bielejec et al., 2016).

Results

HIV-1 sequences dataset

A total of 2,637 HIV-1 *pol* gene sequences were included in the initial dataset using the described criteria and were used in phylogenetic analysis. Out of those sequences, 872 sequences were identified as HIV-1 CRF63_02A6, 1,157 sequences were identified as CRF02_AG_{FSU}, 412 sequences were from CRF02_$AG_{AF/EU}$ clade, and 196 sequences were classified as unique recombinant form (URF) (Supplementary Figure S1). We compare HIV-1 subtyping results obtained from the phylogenetic analysis with those from Stanford and COMET automated HIV-1 subtyping tools. Out of the sequences identified as CRF63_02A6 by phylogenetic analysis, subtyping results by Stanford and COMET were concordant for 660 (75.7%) and 696 (79.8%) sequences, respectively. Moreover, out of the full sequence dataset, COMET classified 1,092 (41.4%) sequences as CRF63_02A6; 37.5% (409/1,092) of those sequences were classified as CRF_$02AG_{FSU}$ by phylogenetic analysis. The detailed information about subtyping results is presented in Supplementary Figure S2.

Phylogenetic and transmission cluster analyses

Phylogenetic reconstruction was performed for 872 HIV-1 CRF63_02A6 *pol* gene sequences collected from 2009 to 2020 (Figure 2): 587 sequences were obtained by our research team and additional 285 sequences were retrieved form LANL HIV sequence database. Monophyletic structure of the CRF63_02A6 phylogenetic tree most likely indicates the initiation of the CRF63_02A6 sub-epidemic by a single ancestral virus. Predominant number (n = 832; 95.4%) of those sequences were from 25 regions of Russia; the remaining 40 (4.6%) sequences were from countries of Central Asia. A closer investigation ofHIV-1 CRF63_02A6 tree showed a total intermix of the sequences from different countries and regions across Russia supporting extensive virus distribution between those territories. Three well-supported (branch support value >95) location-specific monophyletic clades were detected: T/K clade was predominantly represented by CRF63_02A6 sequences from Tomsk and Krasnoyarsk regions (82% of the sequences within the clade), T clade was predominantly represented by sequences from Tomsk region (87% of the sequences within the clade), and JA/A clade was presented by sequences from Jewish Autonomous and Amur regions only. Those clades most likely represent separate introductions causing the super-spreading events of the virus. Recombination analysis revealed some evidence of recombination between CRF63_02A6 and sub-subtype A6 among sequences of the JA/A clade (n = 35, sequences dated 2018 and 2019); this could indicate the further local virus evolution.

Out of 872 sequences, 519 (59.5%) sequences were found in 157 transmission clusters (using thresholds of 0.03 of genetic distance and 90 of branch support) of size 2–38 sequences per cluster; Seven large (≥10 sequences) clusters were identified. The remaining 91 clusters were dyads, 38 clusters were triplets, 8 clusters were the size of four, 5 cluster were the size of five, 3 clusters were the size of six, two clusters were the size of seven, one cluster was the size of eight, and two clusters were the size of nine. The detailed information about large transmission clusters is provided in Table 1.

Spatiotemporal dynamics of HIV-1 CRF63_02A6

Phylogenetic and evolutionary analysis of CRF63_02A6 872 *pol* gene sequences using Nextstrain identified that CRF63_02A6 originated in Novosibirsk around February 2005 (confidence interval: December, 2004 – July, 2005; Figure 3). The virus was further transmitted across other Siberian territories (Omsk, Altai, Tomsk, Krasnoyarsk, and Kemerovo). By 2015, CRF63_02A6 was identified in 13 regions of Russia, and by 2020 the virus was also detected in other nine Russian regions and six countries of Central Asia.

Phylodynamic reconstruction of HIV-1 CRF63_02A6

To investigate the evolutionary rate and population dynamics of the CRF63_02A6 using Bayesian phylogenetic

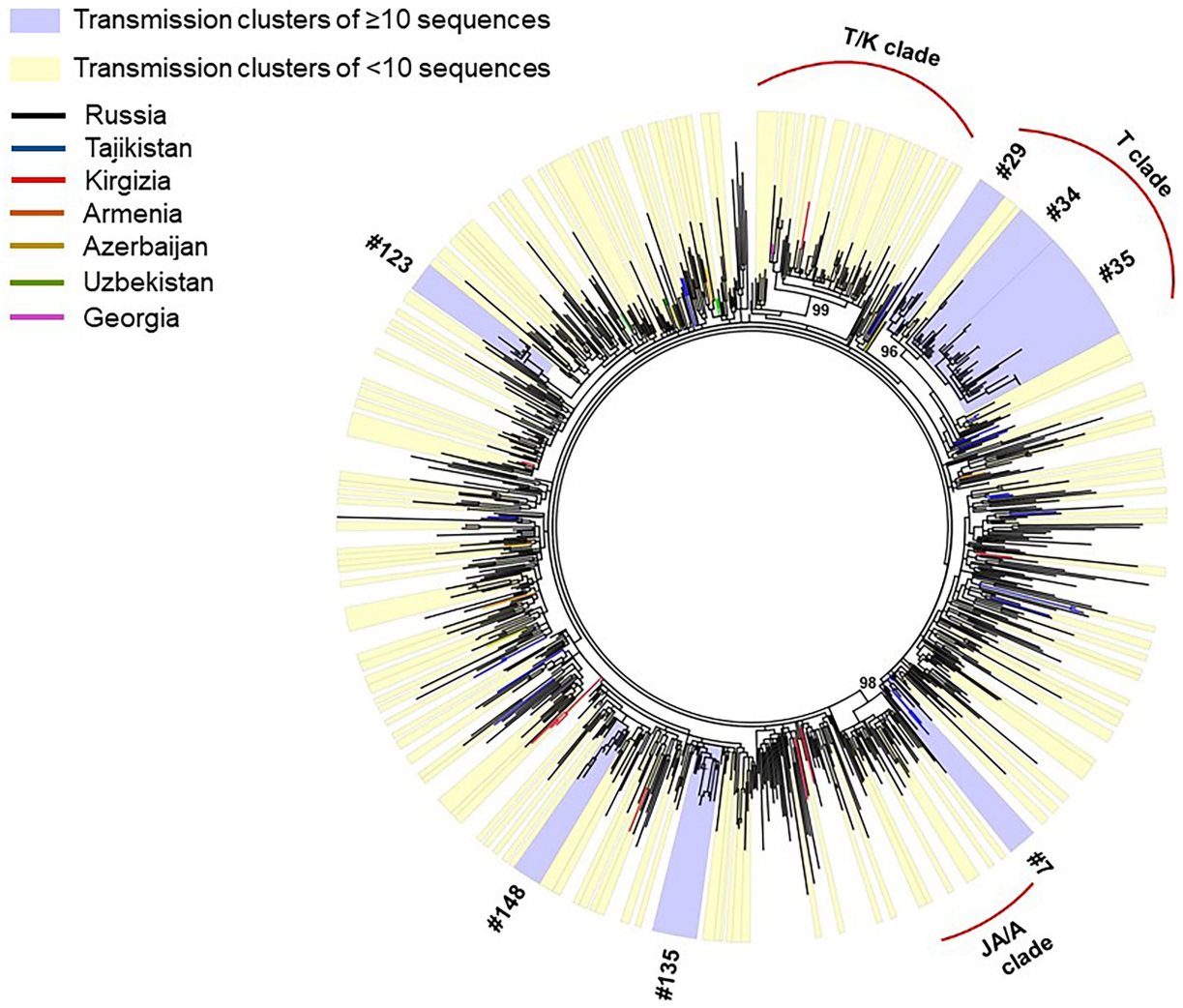

FIGURE 2
IQ-Tree of HIV-1 CRF63_02A 872 *pol* gene sequences. Tree branches color-codded according to the country of isolation (top left chart). Transmission clusters were identified using Cluster Picker v1.2.3 using a branch support value ≥90 and a maximum genetic distance threshold of 0.03. Transmission clusters of ≥10 sequences are colored blue; transmission clusters of <10 sequences are colored yellow.

inference, 510 *pol* gene sequences were included in the analysis. This number of sequences was defined using subsampling strategy described in Methods. The median estimated substitution rate was 2.3×10^{-3} substitutions/year (95% highest posterior density [HPD]: 1.9×10^{-3}-2.7×10^{-3}). The skyline plot shows an exponential growth of the ESS of the HIV-1 CRF63_02A6 from 2005 till 2010 followed by the stable phase (Figure 4). TMRCA was estimated as 2004 (95% highest posterior density: 2002–2006) using BEAST. Both results from the Nextstrain and Bayesian inference agreed and placed Novosibirsk as the most probable ancestral location of the HIV-1 CRF63_02A6 sub-epidemic. The tMRCA obtained by those two methods was also similar (2005 vs. 2004). Bayesian maximum clade credibility (MCC) tree and transmission history of the HIV-1 CRF63_02A6 constructed using SPREAD3 are presented in Supplementary Figure S3.

Discussion

This report represents the characterization of the spatiotemporal dynamics of HIV-1 CRF63_02A6 sub-epidemic. This analysis includes 872 CRF63_02A6 *pol* gene sequences sampled in seven Eurasian countries. By the time the study was conducted, CRF63_02A6 sequences were sampled predominantly in Russia, along with the sporadic cases detected in six countries of Central Asia. The current analysis revealed that the onset date of HIV-1 CRF63_02A6 sub-epidemic was 2005 and the most probable origin location was Novosibirsk; the virus was subsequently transmitted to other regions of Russia and was also detected in Kyrgyzstan, Uzbekistan, Tajikistan, Azerbaijan, Armenia, and Georgia.

The HIV-1 genetic diversity in Russia is broad and characterized by the region-specific sub-epidemics. The first HIV-1 infection outbreak was registered in 1988–1989 among

TABLE 1 Characteristics of the putative CRF63_02A6 transmission clusters.

Cluster ID	Cluster size[1]	Genetic distance	Geographic locations	Years[2]
7	10	0.029	TJ-Altai-NSK-Tomsk	2010–2017
29	10	0.027	Tomsk	2015–2016
34	15	0.03	Tomsk	2014–2016
35	38	0.03	Tomsk-KRS	2015–2018
123	10	0.029	NSK-Oryol	2016–2018
135	15	0.023	NSK-KRS-Omsk	2010–2017
148	10	0.024	NSK-Omsk	2011–2012

The table represents the size of transmission clusters, the maximum genetic distances between the sequences within the cluster, the region where the sequences were collected, and sequences collection dates. Genetic clusters were identified using Cluster Picker v1.2.3 with the maximum genetic distance of 0.03 and the branch support value ≥ 90.
[1]Cluster size indicates the number of sequences in the transmission cluster.
[2]The period when the samples within the cluster were collected.
TJ: Tajikistan; NSK: Novosibirsk region; KRS: Krasnoyarsk region.

nosocomially infected children in the South of Russia and was caused by the HIV-1 subtype G (Thomson and Najera, 2007; Serova et al., 2018), but this subtype is currently rarely detected in the country. In the mid-1990s, the multiple HIV-1 outbreaks among PWID were detected in Central Russia (Kazennova et al., 2014) and gave rise to an extensive expansion of the HIV-1 epidemic in the country caused by the sub-subtype A6. In the following years, the virus was detected in different Russian regions and neighboring countries (Thomson et al., 2009) and currently predominates across all FSU countries. Subtype B was identified among MSM population and presently accounts for up to 2–5% of all HIV-1 cases (Gashnikova et al., 2015; Pasechnik and Blokh, 2018; Lebedev et al., 2019). Recombinant form of subtype B and sub-subtype A6 - CRF03_AB caused several outbreaks among PWID in the Northwestern Russia (Lebedev et al., 2020) and predominates alongside with the sub-subtype A6

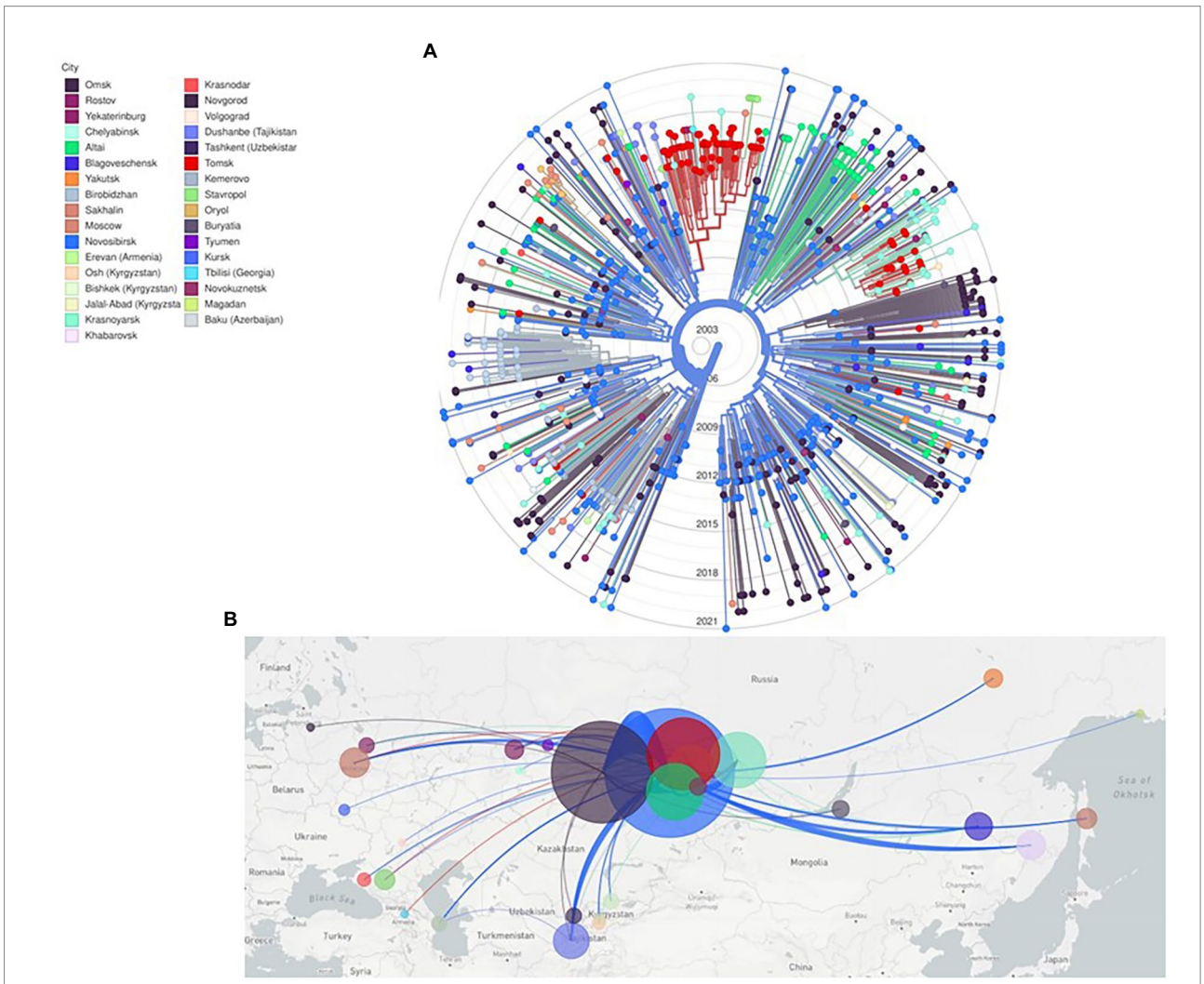

FIGURE 3
Nextstrain maximum likelihood analysis of HIV-1 CRF63_02A6 872 *pol* gene sequences. **(A)** RAx-ML tree was constructed using 832 sequences from Russia and 40 sequences from countries of Central Asia. Tree branches are colored according to the sampling city. **(B)** Geographical representation of CRF63_02A spatial dynamics. Lines between cities represent putative viral transitions; circle sizes are proportional to the square root of the number of sequences from the same location.

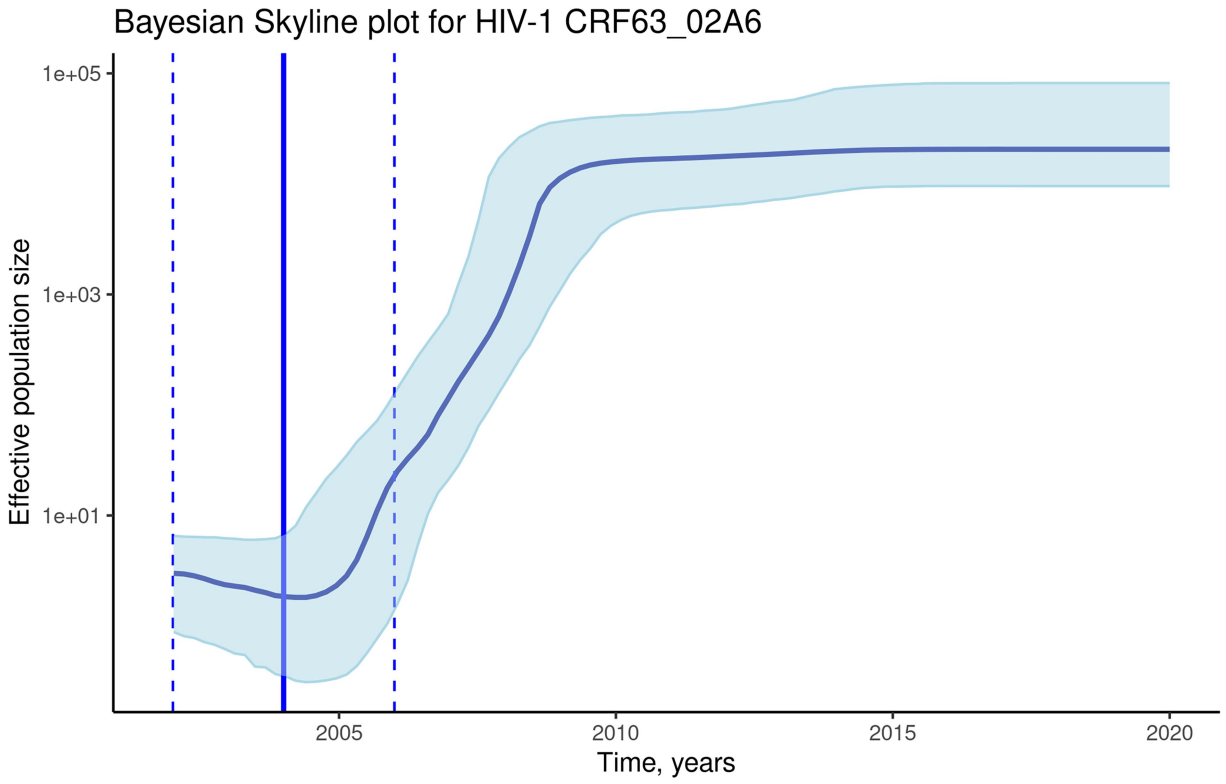

FIGURE 4
The Bayesian skyline plot of the 510 CRF63_02A6 *pol* gene sequences. The solid blue line indicates the median effective population size through time; the shaded blue area indicates the 95% highest posterior density (HPD) interval of the effective population size. The vertical solid black line indicates the median (2004) estimated tMRCA of the HIV-1 CRF63_02A6; the vertical dashed lines indicate the estimated tMRCA 95% HPD interval (2002–2006).

(Ozhmegova et al., 2020). HIV-1 genetic diversity in the Russian Far East is different from the rest of the country. Besides the predominant sub-subtype A6, subtype B and subtype C were found to account for 25% and 10% of the HIV-1 cases, respectively (Kazennova et al., 2008).

Up to mid-2000s, sub-subtype A6 predominated in Siberia. But since 2008, a rapid spread of novel HIV-1 genetic variant was detected in Novosibirsk (Gashnikova et al., 2011). Detailed full genome analysis identified this genetic variant as a recombinant of sub-subtype A6 and CRF02_AG$_{FSU}$; phylogenetic analysis revealed that the new recombinant form (subsequently named as CRF63_02A6) was genetically related to the CRF02_AG$_{FSU}$ from Uzbekistan (Baryshev et al., 2012). A retrospective molecular-epidemiological analysis revealed that some of the PWLH in Novosibirsk were HIV-infected by this recombinant form back in 2004–2006, when the local outbreaks among PWID were registered (Gashnikova et al., 2011). The HIV-1 CRF63_02A6 sub-epidemic distribution in Russia continued and the number of CRF63_02A6 cases started to increase in other regions (Safina et al., 2022). CRF63_02A6 was also detected in the countries of Central Asia, however those cases are sporadic and most likely represent cross-border transmission events (Sivay et al., 2021). In the current study, a large-scale phylogenetic analysis of over 2,500 *pol* gene sequences showed that CRF63_02A6 forms a well-supported distinct monophyletic clade, which most likely indicates the initiation of the CRF63_02A6 epidemic by a single ancestral virus. By now, CRF63_02A6 was detected in over 20 Russian territories and six countries of Central Asia. The current phylogenetic analysis of the CRF63_02A6 revealed three distinct region-specific clades, most likely indicating the local super-spreading events.

Earlier studies (Kostaki et al., 2018) on demographic history and phylodynamic analysis of the CRF02_AG/CRF63_02A6 combined CRF63_02A6 and CRF02_AG$_{FSU}$ lineages. The study identified the origin of the CRF63_02A6 in Kazakhstan and Uzbekistan in 1996; two Russian subclades dated 2003 and 2007 were detected. By the time that study was conducted, a very limited number (n = 136) of the CRF63_02A6 sequences were available. Our study and the study of the global dissemination of the CRF02_AG (Mir et al., 2016) showed that CRF63_02A6 and CRF02_AG$_{FSU}$ represent two distinct HIV-1 genetic variants. Given the results of our previous study and earlier report by Baryshev et al. (2012), CRF63_02A6 most likely descended from CRF02_AG$_{FSU}$ and is characterized by a significant genome change compared to CRF02_AG$_{FSU}$. Both of those CRFs have different geographic characteristics. Thus, CRF_02AG$_{FSU}$ is

endemic in Central Asia (Sivay et al., 2021), while CRF63_02A6 predominantly circulates in Russia. Current report includes all the available HIV-1 CRF63_02A6 and CRF02_AG_{FSU} sequences published in the LANL HIV sequence database from the Eurasian continent (Supplementary Figure S1). Our analysis shows that all the *pol* gene sequences from Kazakhstan available in LANL HIV Sequences Database belong to CRF02_AG_{FSU}. Our analysis also finds only a few CRF63_02A6 sequences from Uzbekistan dated 2015; most of the HIV-1 sequences from Uzbekistan are CRF02_AG_{FSU}.

HIV-1 epidemic in countries of Central Asia was driven by the drug trafficking through the so called "Northern route" from Afghanistan to Russia through Tajikistan, Uzbekistan, Kirgizia, and Kazakhstan (Vorobyev, 2014; Merz, 2018). Since earlier-2000s, the rapid increase of drug use was registered in Russia, and from 2002 to 2014 Siberia was leading by the number of PWID in the country (Andreev and Kokunova, 2017). Also, an intensive labor migration from Central Asian countries to Novosibirsk was registered. Those factors could create favorable conditions for HIV-1 transmission. According to Andreev and Kokunova (2017), a high level of drug use was found among HIV-infected illegal labor migrants. Rapid CRF63_02A6 sub-epidemic expansion in Siberia could also be linked to the high synthetic drug use starting in 2009. Since 2011, the decline in opioid drugs use together with an increase in synthetic drugs use were registered (Vorobyev, 2014; Andreev and Kokunova, 2017). Synthetic drugs induce both stimulant and sexual effects promoting high-risk sexual behavior (Luo et al., 2018). Active synthetic drug use could contribute to dissemination of distinct CRF63_02A6 lineages resulting to a fold-increase of new HIV-1 cases in Siberian regions (Gashnikova et al., 2015, 2017). The well-supported region-specific monophyletic CRF63_02A6 clades identified in the current study most likely indicate these super-spreading events (Figure 2).

Since 2005, the number of new HIV-1 cases in Novosibirsk has started to grow exponentially. The largest increase (from 19.6% in 2003 to 57% in 2007) in new HIV-1 cases in the region was recorded among prisoners (Novosibirsk Region Center on AIDS, 2014).[3] Most likely such increase was driven by the high-risk behavior, such as intravenous drug use (IDU). Most people who entered the Russian penal system in mid-2000s were PWID (Severson, 2011). The penal system had transformed into a unique risk environment for PWID and HIV-1 transmission due to the lack of harm reduction programs. An earlier study among prisoners in Russia showed that almost a half of them had a history of drug injection; that 20% of prisoners had used drugs while imprisoned, 64% of those individuals had injected drugs with previously used injecting equipment, and that 13.5% had started injecting drugs while imprisoned (Jürgens and Betteridge, 2005). Several HIV-1 outbreaks associated with IDU were registered among prisoners in Russia (Bobrik et al., 2005; Severson, 2011). We admit that the emergence of the HIV-1 CRF63_02A6 could have happened within one of the prisons in the Novosibirsk.

In Russia, the guidelines for laboratory testing of HIV-1 infection requires a fourth-generation HIV-EIA test (4th Gen), which detects both antibody and antigen with the following confirmatory Western Blot testing and/or HIV-1 RNA testing (Ministry of Health of Russian Federation, 2020).[4] However, HIV-1 RNA testing is not routinely used and is generally provided to those individuals who have previously confirmed HIV-1 infection, as well as children and pregnant women. Patients with the acute HIV-1 infection can be misdiagnosed during the HIV-1 seronegative window period and can easily transmit the virus. Earlier report described clinical characteristics of patients with acute HIV-1 infection in Novosibirsk. Most of the patients (76%) had CRF63_02A6 infection and 19.4% had sub-subtype A6 infection. Statistically significant differences were found between clinical manifestation in patients with the HIV-1 CRF63_02A6 and sub-subtype A6 infection. Thus, CRF63_02A6 infection is characterized by more severe primary symptoms, such as prolonged fever, generalized lymphadenopathy, higher ($>10^7$) viral load, and lower CD4 cell counts compared to patients with the sub-subtype A6 infection (Ulyanova et al., 2019). These data indicate a faster disease progression and rapid virus transmission among patients with the CRF63_02A6 compared to sub-subtype A6 infection. Symptoms of acute HIV-infection are nonspecific, and the infection often can be misdiagnosed, especially within the ongoing COVID-19 pandemic and COVID-19 mass vaccination. Beginning in 2000, our research team initiated HIV-1 surveillance program in Novosibirsk, which was also launched in other regions of Siberia around 2010. Our studies detected the displacement of sub-subtype A6 by CRF63_02A6, and started in 2009 CRF63_02A6 has been detected in over 80% of new HIV-1 cases in Siberia. Also, various URFs of sub-subtype A6 and CRF63_02A6 has been persistently detected (Gashnikova et al., 2015, 2017; Ulyanova et al., 2019).

Current analysis identified a misclassification of CRF63_02A6 as CRF02_AG by widely used HIV-1 automated subtyping tools. HIV-1 has a high recombination rate promoting viral genetic diversification and escape from the host immune system (Levy et al., 2004). New CRFs are constantly detecting and 118 of them have been described by now (Los Alamos National Laboratory HIV Sequence Database, 2022b).[5] Proper identification of HIV-1 subtypes is challenging due to the frequent recombination. Molecular phylogeny remains the most reliable HIV-1 subtyping approach (Fabeni et al., 2017), however this method requires the data manipulation and interpretation skills. In the clinical settings, HIV-1 subtyping is routinely based on fast and simple HIV-1 automated subtyping tools which have some limitations compared to the phylogenetic approach. Automated subtyping tools often have a very limited number of CRFs in the reference dataset. Most of the automated HIV-1 subtyping algorithms are designed mainly for the

3 https://oblmed.nsk.ru/upload/files/hiv.pdf

4 http://rushiv.ru/category/docs/national-recs/kr-20/

5 https://www.hiv.lanl.gov/content/sequence/HIV/CRFs/CRFs.html

most prevalent viral subtypes such as B and C, and CRFs such as CRF01_AE and CRF02_AG (Fabeni et al., 2017). Also, those tools are not frequently updated. In the current report, we used two automated HIV-1 subtyping tools, Stanford and COMET, and maximum likelihood phylogenetic approach (combined with 2020 LANL HIV-1 subtype reference sequences) to identify CRF63_02A6 sequences. The HIV-1 CRFs were assigned based on high phylogenetic relatedness of the study sequences with the corresponding HIV-1 subtype reference sequences. HIV-1 subtyping results of CRF63_02A6 sequences obtained by Stanford and COMET automated subtyping tools were concordant with the phylogenetic analysis results in approximately 75 and 79% instances, respectively. Moreover, a third of CRF02_AG$_{FSU}$ sequences were classified as CRF63_02A6 by COMET. Our data highlight a rather limited performance of Stanford and COMET subtyping tools in CRF63_02A6 assignment compared to the phylogenetic approach. Although the automated HIV-1 subtyping tools are widely used in clinical settings, the reference datasets of these tools need to be updated to improve reliability of the HIV-1 subtyping results.

This report provides a comprehensive analysis on the origin and dissemination of the recent HIV-1 CRF63_02A sub-epidemic in Russia and countries of Central Asia. The study describes the onset of the CRF63_02A6 in Siberia in the mid-2000s and its following spreading across Russia and the neighboring countries. The CRF63_02A6 distribution simultaneously occurred with the use of injectable and synthetic drugs. Since 2016, the HIV-1 heterosexual transmission in Siberia has prevailed over PWID, however HIV-1 incidence rate among PWID remains high. A high prevalence (from 2 to 30% across the regions) of HIV-1 URFs indicates a substantial level of co-infection with different HIV-1 subtypes. Further surveillance studies of the HIV-1 CRF63_02A6 are needed due to the continuing rapid distribution and high rate of recombination between CRF63_02A6 and other HIV-1 subtypes/CRFs. Studies of epidemiological characteristics and their relationships with the new emerging HIV-1 genetic variants are urgently needed. Also, the introduction of HIV-1 prevention and treatment programs are required to implement further HIV-1 transmission reduction strategies. This study also emphasizes importance of updating of the reference datasets of the widely used automated HIV-1 subtyping tools to provide reliable HIV-1 subtyping results.

Data availability statement

The data presented in this study are deposited in the GenBank repository, accession numbers are listed in Supplementary Data.

Ethics statement

The studies involving human participants were reviewed and approved by Local Ethical Committee of the State Budgetary Healthcare Institution of Novosibirsk Region "City Infectious Clinical Hospital #1". Written informed consent to participate in this study was provided by the participants' legal guardian/next of kin.

Author contributions

MS, AT, and NG planned and designed the study. LM, IO, AN, MG, DZ, VE, TN, and VI performed HIV genotyping and collected sequences. MS performed the analysis of the epidemiological data, performed the phylogenetic and phylodynamic analysis, produced the illustrations, and wrote the manuscript. NG supervised the project and edited the manuscript. DK, LP, SS, TO, SY, ON, AC, and TI collected the epidemiological data and assisted with samples collection at the local study clinics. All authors contributed to the article and approved the submitted version.

Funding

This study was supported by the State Research and Development Program #6–21 State Research Center of Virology and Biotechnology "Vector."

Acknowledgments

The authors want to thank all of the patient for their contributions to the study. We also thank the staff at the study HIV/AIDS clinics for laboratory testing.

Conflict of interest

The authors declare that the research was conducted in the absence of any commercial or financial relationships that could be construed as a potential conflict of interest.

Publisher's note

Supplementary material

The Supplementary material for this article can be found online at: https://www.frontiersin.org/articles/10.3389/fmicb.2022.946787/full#supplementary-material

References

Aibekova, L., Foley, B., Hortelano, G., Raees, M., Abdraimov, S., Toichuev, R., et al. (2018). Molecular epidemiology of HIV-1 subtype A in former Soviet Union countries. *PLoS One* 13:e0191891. doi: 10.1371/journal.pone.0191891

Andreev, A. P., and Kokunova, S. D. (2017). Effect of illegal migration on drug use in Russian Federation. *Counter-Terrorism* 4, 19–27.

Baryshev, P. B., Bogachev, V. V., and Gashnikova, N. M. (2012). Genetic characterization of an isolate of HIV type 1 AG recombinant form circulating in Siberia. *Russia. Arch. Virol.* 157, 2335–2341. doi: 10.1007/s00705-012-1442-4

Baryshev, P. B., Bogachev, V. V., and Gashnikova, N. M. (2014). HIV-1 genetic diversity in Russia: CRF63_02A1, a new HIV type 1 genetic variant spreading in Siberia. *AIDS Res. Hum. Retrovir.* 30, 592–597. doi: 10.1089/aid.2013.0196

Bielejec, F., Baele, G., Vrancken, B., Suchard, M. A., Rambaut, A., and Lemey, P. (2016). SpreaD3: interactive visualization of spatiotemporal history and trait evolutionary processes. *Mol. Biol. Evol.* 33, 2167–2169. doi: 10.1093/molbev/msw082

Bobkov, A., Kazennova, E., Selimova, L., Bobkova, M., Khanina, T., Ladnaya, N., et al. (1998). A sudden epidemic of HIV type 1 among injecting drug users in the former Soviet Union: identification of subtype A, subtype B, and novel gag A/env B recombinants. *AIDS Res. Hum. Retrovir.* 14, 669–676. doi: 10.1089/aid.1998.14.669

Bobkov, A. F., Kazennova, E. V., Selimova, L. M., Khanina, T. A., Ryabov, G. S., Bobkova, M. R., et al. (2004). Temporal trends in the HIV-1 epidemic in Russia: predominance of subtype A. *J. Med. Virol.* 74, 191–196. doi: 10.1002/jmv.20177

Bobkova, M. (2013). Current status of HIV-1 diversity and drug resistance monitoring in the former USSR. *AIDS Rev.* 15, 204–212.

Bobrik, A., Danishevski, K., Eroshina, K., and McKee, M. (2005). Prison health in Russia: the larger picture. *J. Public Health Policy* 26, 30–59. doi: 10.1057/palgrave.jphp.3200002

Carr, J. K., Nadai, Y., Eyzaguirre, L., Saad, M. D., Khakimov, M. M., Yakubov, S. K., et al. (2005). Outbreak of a west African recombinant of HIV-1 in Tashkent, Uzbekistan. *JAIDS J. Acquired Immune Deficiency Syndromes* 39, 570–575.

Central Research Institute of Epidemiology, Federal Service on Customers' Rights Protection and Human Well-being Surveillance (2021). HIV statistics in Russian Federation. http://www.hivrussia.info/wp-content/uploads/2022/03/Spravka-VICH-v-Rossii-na-31.12.2021-g.pdf (Accessed April 5, 2022).

Darriba, D., Taboada, G. L., Doallo, R., and Posada, D. (2012). jModelTest 2: more models, new heuristics and parallel computing. *Nat. Methods* 9:772. doi: 10.1038/nmeth.2109

Diez-Fuertes, F., Cabello, M., and Thomson, M. M. (2015). Bayesian phylogeographic analyses clarify the origin of the HIV-1 subtype A variant circulating in former Soviet Union's countries. *Infect. Genet. Evol.* 33, 197–205. doi: 10.1016/j.meegid.2015.05.003

Fabeni, L., Berno, G., Fokam, J., Bertoli, A., Alteri, C., Gori, C., et al. (2017). Comparative evaluation of subtyping tools for surveillance of newly emerging HIV-1 strains. *J. Clin. Microbiol.* 55, 2827–2837. doi: 10.1128/JCM.00656-17

Frank, T. D., Carter, A., Jahagirdar, D., Biehl, M. H., Douwes-Schultz, D., Larson, S. L., et al. (2019). Global, regional, and national incidence, prevalence, and mortality of HIV, 1980–2017, and forecasts to 2030, for 195 countries and territories: a systematic analysis for the global burden of diseases, injuries, and risk factors study 2017. *Lancet HIV* 6, e831–e859. doi: 10.1016/S2352-3018(19)30196-1

Gashnikova, N. M., Bogachev, V. V., Baryshev, P. B., Totmenin, A. V., Gashnikova, M. P., Kazachinskaya, A. G., et al. (2015). A rapid expansion of HIV-1 CRF63_02A1 among newly diagnosed HIV-infected individuals in the Tomsk region. *Russia. AIDS Res. Hum. Retroviruses* 31, 456–460. doi: 10.1089/aid.2014.0375

Gashnikova, N. M., Zyryanova, D. P., Astakhova, E. M., Ivlev, V. V., Gashnikova, M. P., Moskaleva, N. V., et al. (2017). Predominance of CRF63_02A1 and multiple patterns of unique recombinant forms of CRF63_A1 among individuals with newly diagnosed HIV-1 infection in Kemerovo oblast. *Russia. Arch. Virol.* 162, 379–390. doi: 10.1007/s00705-016-3120-4

Gashnikova, N. M., Safronov, P. F., Nikonorova, Y. V., Unagaeva, N. V., Lapteva, T. A., Bogachev, V. V., et al. (2011). Properties of CRF02_AG HIV-1 isolates circulating in Novosibirsk region. *Zh. Mikrobiol. Epidemiol. Immunobiol.* 3, 38–43.

Hadfield, J., Megill, C., Bell, S. M., Huddleston, J., Potter, B., Callender, C., et al. (2018). Nextstrain: real-time tracking of pathogen evolution. *Bioinformatics* 34, 4121–4123. doi: 10.1093/bioinformatics/bty407

Jürgens, R., and Betteridge, G. (2005). Prisoners who inject drugs: public health and human rights imperatives. *Emerg. Issues in HIV/AIDS* 8, 46–74. doi: 10.2307/4065334

Karamov, E., Epremyan, K., Siniavin, A., Zhernov, Y., Cuevas, M. T., Delgado, E., et al. (2018). HIV-1 genetic diversity in recently diagnosed infections in Moscow: predominance of A_{FSU}, frequent branching in clusters, and circulation of the Iberian subtype G variant. *AIDS Res. Hum. Retrovir.* 34, 629–634. doi: 10.1089/aid.2018.0055

Kazennova, E. V., Bronnikova, A. V., Kuzin, S. N., Kirillova, I. L., Ershova, O. N., Afanaseva, L. R., et al. (2008). Molecular genetic characteristics of HIV-1 variants circulating in Cherepovets, Vologda region: the second case of the epidemic outbreak caused by the recombinant gagAenvB. *Voprosi Virusologii.* 53, 23–27.

Kazennova, E., Laga, V., Lapovok, I., Glushchenko, N., Neshumaev, D., Vasilyev, A., et al. (2014). HIV-1 genetic variants in the Russian Far East. *AIDS Res. Hum. Retrovir.* 30, 742–752. doi: 10.1089/aid.2013.0194

Kazennova, E. V., Antonova, A. A., Ozhmegova, E. N., Demyanenko, E. R., Minakova, M. V., Belousova, O. V., et al. (2020). Genetic analysis of HIV-1 in the Altai Kray: The further spread of the CRF63_02A1 variant in Western Siberia. *HIV Infect. Immunosuppressive Disord.* 12, 47–57. doi: 10.22328/2077-9828-2020-12-1-47-57

Kotova, V. O., Trotsenko, O. E., Balakhontseva, L. A., and Bazykina, E. A. (2019). Molecular genetic characteristics of HIV-1 variants isolated in the subjects of the Russian Far East. *Vopr. Virusol.* 64, 79–89. doi: 10.18821/0507-4088-2019-64-2-79-89

Kosakovsky Pond, S. L., Posada, D., Gravenor, M. B., Woelk, C. H., and Frost, S. D. (2006). GARD: a genetic algorithm for recombination detection. *Bioinformatics* 22, 3096–3098. doi: 10.1093/bioinformatics/btl474

Kostaki, E. G., Karamitros, T., Bobkova, M., Oikonomopoulou, M., Magiorkinis, G., Garcia, F., et al. (2018). Spatiotemporal characteristics of the HIV-1 CRF02_AG/CRF63_02A1 epidemic in Russia and Central Asia. *AIDS Res. Hum. Retrovir.* 34, 415–420. doi: 10.1089/aid.2017.0233

Lebedev, A., Lebedeva, N., Moskaleychik, F., Pronin, A., Kazennova, E., and Bobkova, M. (2019). Human immunodeficiency virus-1 diversity in the Moscow region, Russia: Phylodynamics of the most common subtypes. *Front. Microbiol.* 10:320. doi: 10.3389/fmicb.2019.00320

Lebedev, A., Pasechnik, O., Ozhmegova, E., Antonova, A., Blokh, A., Grezina, L., et al. (2020). Prevalence and spatiotemporal dynamics of HIV-1 circulating recombinant form 03_AB (CRF03_AB) in the former Soviet Union countries. *PLoS One* 15:e0241269. doi: 10.1371/journal.pone.0241269

Levy, D. N., Aldrovandi, G. M., Kutsch, O., and Shaw, G. M. (2004). Dynamics of HIV-1 recombination in its natural target cells. *Proc. Natl. Acad. Sci.* 101, 4204–4209. doi: 10.1073/pnas.0306764101

Liitsola, K., Holm, K., Bobkov, A., Pokrovsky, V., Smolskaya, T., Leinikki, P., et al. (2000). An AB recombinant and its parental HIV type 1 strains in the area of the former Soviet Union: low requirements for sequence identity in recombination. *AIDS Res. Hum. Retrovir.* 16, 1047–1053. doi: 10.1089/08892220050075309

Liu, T. F., and Shafer, R. W. (2006). Web resources for HIV type 1 genotypic-resistance test interpretation. *Clin. Infect. Dis.* 42, 1608–1618. doi: 10.1086/503914

Los Alamos National Laboratory HIV Sequence Database. (2022a). http://www.hiv.lanl.gov/ (Accessed January 15, 2022).

Los Alamos National Laboratory HIV Sequence Database (2022b). https://www.hiv.lanl.gov/content/sequence/HIV/CRFs/CRFs.html (Accessed April 6, 20229).

Luo, W., Hong, H., Wang, X., McGoogan, J. M., Rou, K., and Wu, Z. (2018). Synthetic drug use and HIV infection among men who have sex with men in China: a sixteen-city, cross-sectional survey. *PLoS One* 13:e0200816. doi: 10.1371/journal.pone.0200816

Maksimenko, L. V., Totmenin, A. V., Gashnikova, M. P., Astakhova, E. M., Skudarnov, S. E., Ostapova, T. S., et al. (2020). Genetic diversity of HIV-1 in Krasnoyarsk Krai: area with high levels of HIV-1 recombination in Russia. BioMed Research international, 2020. doi: 10.1155/2020/9057541

Merz, F. (2018). United Nations Office on drugs and crime: world drug report 2017. *SIRIUS-Zeitschrift für Strategische Analysen* 2, 85–86. doi: 10.1515/sirius-2018-0016

Ministry of Health of Russian Federation (2020). Clinical recommendations. HIV infection in adults and children. http://rushiv.ru/category/docs/national-recs/kr-20/

Mir, D., Jung, M., Delatorre, E., Vidal, N., Peeters, M., and Bello, G. (2016). Phylodynamics of the major HIV-1 CRF02_AG African lineages and its global dissemination. *Infect. Genet. Evol.* 46, 190–199. doi: 10.1016/j.meegid.2016.05.017

Nguyen, L. T., Schmidt, H. A., Von Haeseler, A., and Minh, B. Q. (2015). IQ-TREE: a fast and effective stochastic algorithm for estimating maximum-likelihood phylogenies. *Mol. Biol. Evol.* 32, 268–274. doi: 10.1093/molbev/msu300

Novosibirsk Region Center on AIDS (2014). HIV-Infection. Incidence. HIV pre- and post-Testing Counseling. HIV Testing among high risk Groups. https://oblmed.nsk.ru/upload/files/hiv.pdf

Ozhmegova, E. N., Antonova, A. A., Lebedev, A. V., Melnikova, T. N., Krylova, T. V., Kazachek, A. V., et al. (2020). Genetic profile of HIV-1 in the Vologda region: domination of CRF03_AB and rapid distribution of URFs. *HIV Infect. Immunosuppressive Disord. (In Russ.)* 12, 79–88. doi: 10.22328/2077-9828-2020-12-2-79-88

Pasechnik, O. A., and Blokh, A. I. (2018). The prevalence of HIV recombinant forms in Russia and countries of the CIS: systematic review and metaanalysis. *Russ. J. Infect. Immun.* 8, 127–138. doi: 10.15789/2220-7619-2018-2-127-138

Ragonnet-Cronin, M., Hodcroft, E., Hué, S., Fearnhill, E., Delpech, V., Brown, A. J. L., et al. (2013). Automated analysis of phylogenetic clusters. *BMC Bioinform.* 14, 1–10. doi: 10.1186/1471-2105-14-317

Rambaut, A. (2009). FigTree. Tree Figure Drawing tool. http://tree.bio.ed.ac.uk/software/figtree/.

Rambaut, A., Drummond, A. J., Xie, D., Baele, G., and Suchard, M. A. (2018). Posterior summarization in Bayesian phylogenetics using tracer 1.7. *Syst. Biol.* 67, 901–904. doi: 10.1093/sysbio/syy032

Safina, K. R., Sidorina, Y., Efendieva, N., Belonosova, E., Saleeva, D., Kirichenko, A., et al. (2022). Molecular epidemiology of HIV-1 in Oryol oblast, Russia. *Virus Evolution.* 8:1, veac044. doi: 10.1093/ve/veac044

Schlösser, M., Kartashev, V. V., Mikkola, V. H., Shemshura, A., Saukhat, S., Kolpakov, D., et al. (2020). HIV-1 sub-subtype A6: settings for normalised identification and molecular epidemiology in the southern Federal District, Russia. *Viruses* 12:475. doi: 10.3390/v12040475

Serova, E., Murzakova, A., Nossik, M., Shemshura, A., Bazykin, G., and Kireev, D. (2018). The 1988 Elista outbreak and the epidemiology of HIV subtype G in Russia. *Virus Evolution* 4:vey010.010.

Severson, J. L. (2011). *HIV and AIDS in the Russian Federation: Prisons as a case Study of risk Environments and Agency [doctoral dissertation]*. Austin (TX): University of Texas at Austin, 4. doi: 10.1093/ve/vey010.010

Sivay, M. V., Totmenin, A. V., Zyryanova, D. P., Osipova, I. P., Nalimova, T. M., Gashnikova, M. P., et al. (2021). Characterization of HIV-1 epidemic in Kyrgyzstan. *Front. Microbiol.* 2985. doi: 10.3389/fmicb.2021.753675

Struck, D., Lawyer, G., Ternes, A. M., Schmit, J. C., and Bercoff, D. P. (2014). COMET: adaptive context-based modeling for ultrafast HIV-1 subtype identification. *Nucleic Acids Res.* 42:e144. doi: 10.1093/nar/gku739

Suchard, M. A., Lemey, P., Baele, G., Ayres, D. L., Drummond, A. J., and Rambaut, A. (2018). Bayesian phylogenetic and phylodynamic data integration using BEAST 1.10. *Virus Evol.* 4:vey016. doi: 10.1093/ve/vey016

Thomson, M. M., and Nájera, R. (2007). Increasing HIV-1 genetic diversity in Europe. *J. Infect. Dis.* 196, 1120–1124. doi: 10.1086/521683

Thomson, M. M., Vinogradova, A., Delgado, E., Rakhmanova, A., Yakovlev, A., Cuevas, M. T., et al. (2009). Molecular epidemiology of HIV-1 in St Petersburg, Russia: predominance of subtype A, former Soviet Union variant, and identification of intrasubtype subclusters. *JAIDS J. Acquired Immune Deficiency Syndromes* 51, 332–339. doi: 10.1097/QAI.0b013e31819c1757

Ulyanova, Y. S., Gashnikova, N. M., Ivlev, V. V., Krasnova, E. I., Khokhlova, N. I., Totmenin, A. V., et al. (2019). Clinical and laboratory characterictic of acute HIV-infection in adult residents of Novosibirsk region. *J. Infectol.* 11, 40–44. doi: 10.22625/2072-6732-2019-11-2-40-44

Vorobyev, M. V., Injection drug use in Russian Federation, 2005-2013 (2014). Current Problems of Science and Education, 5.

frontiers | Frontiers in Immunology

TYPE Original Research
PUBLISHED 04 October 2022
DOI 10.3389/fimmu.2022.946871

OPEN ACCESS

EDITED BY
Kai Deng,
Sun Yat-sen University, China

REVIEWED BY
Zhizhang Yang,
Mayo Clinic, United States
Vladimir Jurisic,
University of Kragujevac, Serbia

*CORRESPONDENCE
Hong Shang
hongshang100@hotmail.com
Yongjun Jiang
jiangjun55555@163.com

†These authors have contributed equally to this work

SPECIALTY SECTION
This article was submitted to Viral Immunology, a section of the journal Frontiers in Immunology

RECEIVED 18 May 2022
ACCEPTED 13 September 2022
PUBLISHED 04 October 2022

CITATION
Qian S, Xiong C, Wang M, Zhang Z, Fu Y, Hu Q, Ding H, Han X, Shang H and Jiang Y (2022) CD38$^+$CD39$^+$ NK cells associate with HIV disease progression and negatively regulate T cell proliferation.
Front. Immunol. 13:946871.
doi: 10.3389/fimmu.2022.946871

CD38$^+$CD39$^+$ NK cells associate with HIV disease progression and negatively regulate T cell proliferation

Shi Qian[1,2,3†], Chunbin Xiong[1,2†], Meiting Wang[1,2], Zining Zhang[1,2], Yajing Fu[1,2], Qinghai Hu[1,2], Haibo Ding[1,2], Xiaoxu Han[1,2,4], Hong Shang[1,2*] and Yongjun Jiang[1,2*]

[1]National Health Commission (NHC) Key Laboratory of AIDS Immunology (China Medical University), National Clinical Research Center for Laboratory Medicine, The First Hospital of China Medical University, Shenyang, China, [2]Key Laboratory of AIDS Immunology, Chinese Academy of Medical Sciences, Shenyang, China, [3]Department of Clinical Laboratory, Tianjin Medical University General Hospital, Tianjin, China, [4]Units of Medical Laboratory, Chinese Academy of Medical Sciences, Shenyang, China

The ectonucleotidases CD38 and CD39 have a critical regulatory effect on tumors and viral infections *via* the adenosine axis. Natural killer (NK) cells produce cytokines, induce cytotoxic responses against viral infection, and acquire immunoregulatory properties. However, the roles of CD38 and CD39 expressed NK cells in HIV disease require elucidation. Our study showed that the proportions of CD38$^+$CD39$^+$ NK cells in HIV-infected individuals were positively associated with HIV viral loads and negatively associated with the CD4$^+$ T cell count. Furthermore, CD38$^+$CD39$^+$ NK cells expressed additional inhibitory receptors, TIM-3 and LAG-3, and produced more TGF-β. Moreover, autologous NK cells suppressed the proliferation of CD8$^+$ T and CD4$^+$ T cells of HIV-infected individuals, and inhibiting CD38 and CD39 on NK cells restored CD8$^+$ T and CD4$^+$ T cell proliferation *in vitro*. In conclusion, these data support a critical role for CD38 and CD39 on NK cells in HIV infection and targeting CD38 and CD39 on NK cells may be a potential therapeutic strategy against HIV infection.

KEYWORDS
HIV, NK cells, CD38, CD39, negative regulation

Introduction

NK cells are crucial types of immunocytes. They kill cancerous and virus-infected cells (1) while negatively regulating the immune system (2). Previous research has revealed that NK cells can alleviate inflammation during systemic infections by producing interleukin (IL)-10 (3); while one of the NK cell subsets in HIV-infected individuals, CD56–CD16+, negatively regulated IFN-γ release by CD8+ T cells (4).

Extracellular enzymes on immune cells regulate the balance between the proinflammatory extracellular adenosine triphosphate (ATP) and immunosuppressive extracellular adenosine in the tumor microenvironment (5). Ectonucleotidases, such as CD39, CD38, and CD73, are involved in immune modulation (6). Ectoenzyme CD39 hydrolyzes extracellular ATP and adenosine diphosphate (ADP) to generate adenosine monophosphate (AMP) (7). Moreover, CD38 transforms the nicotinamide adenine dinucleotide (NAD+) into ADP-ribose (ADPR), which is converted to AMP by the ectonucleotide pyrophosphatase/phosphodiesterase 1 (ENPP1) (8–10). With the participation of CD73, AMP is converted to adenosine, which inhibits the function of immune cells (9, 11). In the immune system, the cell types that express CD39 include B cells, monocytes, NK cells, and T cells (12). In non-tumor populations, CD38 is generally expressed on NK cells, dendritic cells, B cells, plasma cells, and T cells (10, 13). Previous studies have shown that Tregs expressing CD39 inhibited the antitumor immunity mediated by NK cells (14) and that anti-CD38 antibodies decreased Tregs' suppression and restored CD4+CD25- T cell proliferation in multiple myeloma by decreasing the percentage of CD38 expression (15). Multiple myeloma cells with high CD38 expression reduce the number and activity of NK cells (16). CD56brightCD16− NK cells from blood of juvenile idiopathic arthritis patients highly expressed CD38 molecules, and CD56brightCD16− NK cells inhibited autologous CD4+ T cell proliferation via the CD38-mediated pathway (17).

The CD38 molecule is a marker of activation. The proportion of CD38+ NK cells in HIV infection is increased and positively or negatively associated with the HIV viral load and CD4+ T cell count, respectively (18–20). CD39, an enzyme involved in extracellular nucleotide metabolism, is highly expressed on CD56bright NK cells and is tightly correlated with viral load and to CD4+ T cell count in untreated individuals infected with HIV. However, because CD39 and CD38 are extracellular nucleotide enzymes and produce AMP via different pathways, the correlation between the CD38 and CD39 dual-positive NK cells and disease progression is still unclear. Moreover, the characteristics, cytokine production, and regulation of CD39+CD38+ NK cells need to be elucidated.

Here, we investigated the expression of CD38 and CD39 on NK cells and analyzed the correlation between CD39+CD38+ NK cells and disease progression (HIV viral load and CD4+ T cell count). Furthermore, we explored whether the expression of CD39 and CD38 on NK cells could be related to inhibitory receptors that modulate CD4+ T and CD8+ T cell proliferation. Our findings reveal that the immunosuppression mediated via CD39 and CD38 on NK cells is crucial in modulating CD4+ T and CD8+ T cell proliferation in HIV infection.

Materials and methods

Research participants

Research participants infected with HIV were enrolled in the First Hospital of China Medical University, including 25 untreated individuals infected with HIV (untreated HIV) and 70 individuals infected with HIV receiving antiretroviral therapy (ART). The 20 healthy controls (HC) who were not infected with hepatitis B or C were HIV-negative. Details of the participants in this study are shown in Table 1. Informed consent was collected from study subjects. The study protocol was approved by the Research and Ethics Committee of The First Hospital of China Medical University and was performed in accordance with the Declaration of Helsinki.

Detection of CD38, CD39, and expression of inhibitory receptors

Fresh PBMC were obtained from human blood samples. Human TruStain FcX™ (BioLegend, USA) was added for 5 mins to block Fc receptors. Cell surface staining antibodies included: anti-CD3-fluorescein isothiocyanate (FITC), or Percp, anti-CD56-phycoerythrin (PE)-Cyanin7 (Cy7), anti-CD16-BV786 or BV510, anti-CD14-Percp, anti-CD19-Percp, anti-CD4-Allophycocyanin (APC)-Cy7, anti-CD39-PE or APC, and anti-CD38-BV421 or FITC, anti-TIGIT-BV421, anti-TIM-3-PE, anti-LAG-3-AF647, anti-PD-L1-BV421(BioLegend, USA). 7-AAD was applied to detect dead cells. Cells were measured by

TABLE 1 Clinical characteristics of subjects enrolled in this study.

Characteristics	HC	Untreated HIV	ART	*p*-value
Number	20	25	70	
Gender (male/female)	9/11	24/1	66/4	
Age(years)	38.50(24.00,47.00)	29.00(26.00,31.00)	32.00(28.00,37.00)	> 0.05
$CD4^+$ T cell count (cells/μL)	NA	350.00(272.00,545.00)	611.50(474.00,821.75)	< 0.05
Viral load (Lg copies/mL)	NA	4.44 (3.90,4.58)	undetectable	

Quantitative data are expressed as the median (interquartile range).
NA, not available.

an LSR II Fortessa cytometer (BD Biosciences, USA). For the stimulation experiment of CD38 expression, IL-12 (10 ng/mL, R&D, USA), IL-15 (50 ng/mL, R&D,USA), and IL-18 (100 ng/mL, R&D,USA) were used to stimulate PBMC. The PBMC was cultured for 72 h and stained as indicated above.

Measurement of interleukin-10 and TGF-β production

An isolation kit (Stemcell, CAN) was used to isolate the NK cells, which were activated by Phorbol 12-myristate 13-acetate (PMA)/ionomycin (BioLegend, USA) and protein transport inhibitor GolgiStop (BD Biosciences) in 96-well U-bottomed plates with 5% CO2 at 37 °C for 6 h. First, the NK cells were collected, and Fixable viability stain 620 (BD Pharmingen, USA) was added to exclude dead cells. Antibodies for cell surface staining included anti-CD3-APC-CY7, anti-CD56-PE-Cy7, anti-CD38-PE, anti-CD39-FITC (BioLegend, USA) and were incubated for 20 mins. Next, the cells were fixed and washed by Fixation/Permeabilization solution (BD Biosciences, USA) and intracellularly labeled by anti-IL-10-APC and anti-TGF-β-BV421 (BD Biosciences, USA) at 4 °C for 20 mins. Finally, the cells were measured by LSR II Fortessa cytometer (BD Biosciences, USA).

Detection of the proliferation of T cells suppressed by NK cells

NK, CD4+ T, and CD8+ T cells were collected using negative isolation kits (Stemcell, CAN). The NK cells were cultured with a CD38 inhibitor 1 (78c, 0.5 μM, MCE, USA), ARL67156 trisodium salt (100 μM, MCE, USA), AB-680 (100 nM, MCE, USA), and EHNA hydrochloride (100 μM, MCE,USA) for 30 mins. CD4+ T and CD8+ T cells were stained using CellTrace Violet (Invitrogen, USA) for 30 mins. The NK cells and CD4+ T or CD8+ T cells were activated by Dynabeads™ Human T-Activator CD3/28 (Gibco, USA) and incubated at a ratio of 1:1 for 3 days. The cells were collected, washed, and dyed with anti-CD4-APC-CY7 or anti-CD8-FITC. The dead cells were detected using 7-AAD. The samples were detected by the LSR II Fortessa cytometer (BD Biosciences, USA).

Statistical analysis

Flow cytometry data were analyzed using FlowJo™ 10.5.0. All statistical analyses were conducted using GraphPad Prism v9.0.0. Comparisons of data in multiple groups, unpaired groups, and paired groups were performed using the Kruskal–Wallis test, the Mann–Whitney U test, and the Wilcoxon matched-pairs signed-rank test, respectively. Correlations were analyzed by the Spearman's rank test; a P-value < 0.05 was considered a significant difference.

Results

Higher proportions of CD39 and CD38 on NK cells in HIV infected individuals

The expression of CD39 and CD38 on NK cells and T cells was measured in individuals infected with HIV and healthy donors to investigate the changes in CD39 and CD38 expression after HIV infection. The NK cells were distinguished by CD3- CD14- CD19- CD16+/CD56+, and the subsets of T cells were distinguished by CD3+ CD4+ or CD3+ CD4- (Figure 1A). Compared with a heathy control (HC) group, the proportion of CD39+ NK cells was increased in the untreated HIV group ($P < 0.001$), and the proportion of CD39+ NK cells in the untreated HIV group was higher than that in the ART group ($P < 0.01$; Figure 1B). In the untreated HIV group, CD38 expression on NK cells was higher than HC group ($P < 0.001$; Figure 1C), and the CD38 expressed on the NK cells in the ART group was lower than the untreated HIV group ($P < 0.05$; Figure 1C). As expected, the proportion of CD38+CD39+ NK cells was higher in the untreated HIV group ($P < 0.001$; Figure 1D). HIV infection was conducive to the upregulation of CD38 ($P < 0.001$; Figure 1C), but not to CD39 levels on CD3+ CD4+ and CD3+ CD4- T cells ($P > 0.05$; Figure 1B). The CD39 and CD38 expression on NK cell were of great importance. Furthermore, the proportions of CD73+ NK cells in the untreated HIV group tended to increase compared with the HC group (Supplementary Figure S1A). In lymphocytes, a minimal proportion of CD3+CD4+ and CD3+CD4- T cells express CD39 compared to the NK cells from the individuals infected with HIV ($P < 0.01$ for CD4+ T and $P < 0.01$ for CD4- T; Figure 1E). Similarly, CD38 is expressed less frequently on CD3+CD4+ and CD3+CD4- T cells than on NK cells from the individuals infected with HIV ($P < 0.001$ for CD4+ T and $P < 0.001$ for CD4- T; Figure 1F). The coexpression of CD38 and CD39 was higher on NK cells than on CD3+CD4+ and CD3+CD4- T cells in individuals infected with HIV ($P < 0.001$ for CD4+ T and $P < 0.001$ for CD4- T; Figure 1G). These findings indicated that NK cells expressed more ectonucleotidases than CD3+CD4+ or CD3+CD4- T cells in individuals infected with HIV.

The expression of CD39 and CD38 on NK subsets

Next, we investigated the proportions of CD39 and CD38 in the subpopulation of NK cells. NK cells were classified into three subpopulations according to the level of CD56 and CD16 (Figure 2A). The untreated HIV group had a higher proportion

10.3389/fimmu.2022.946871

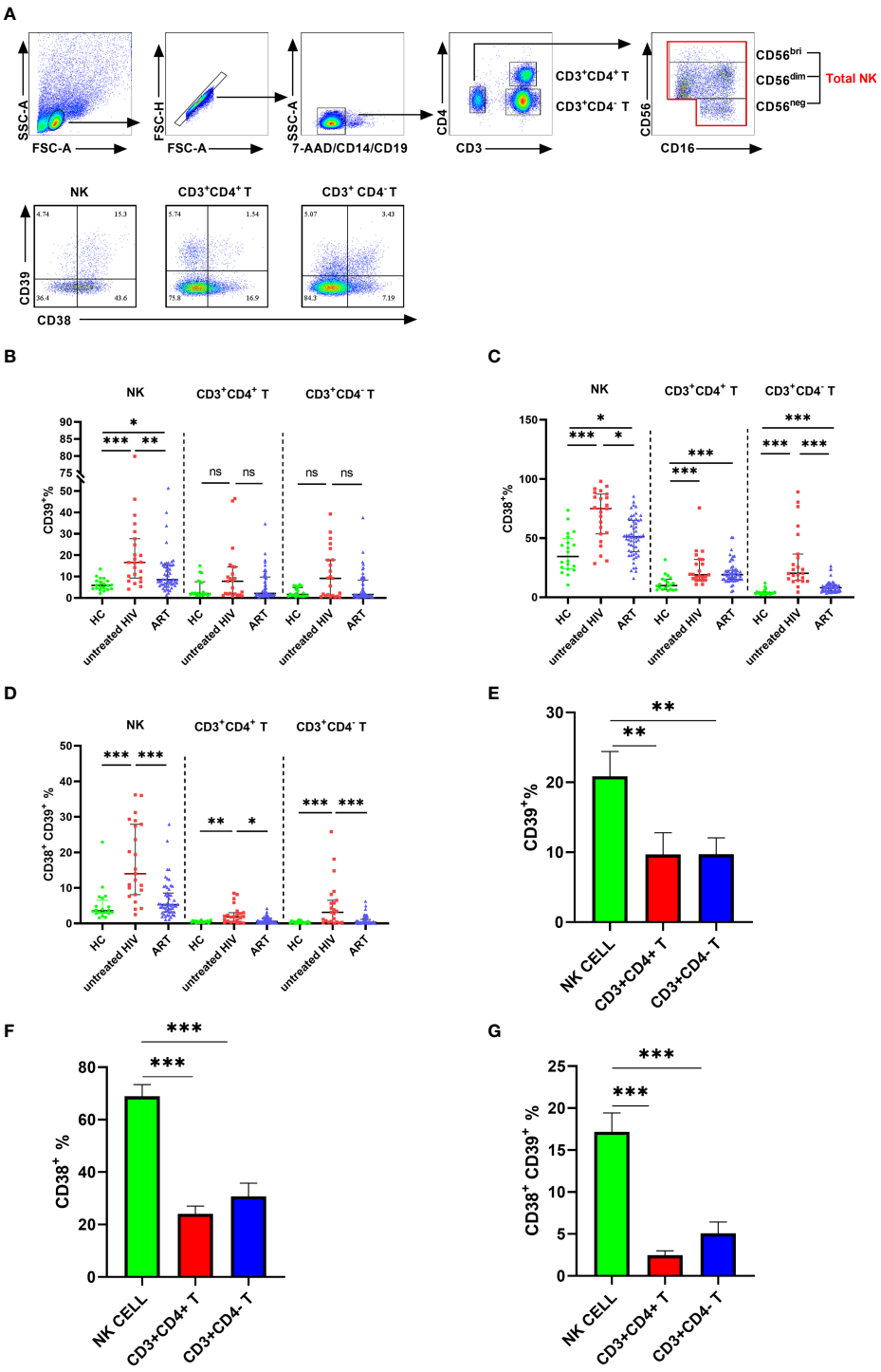

FIGURE 1
The expression of CD38 and CD39 on NK, CD3+CD4- T and CD3+CD4- T cells in HC, untreated HIV, and ART groups. **(A)** Gating strategy from flow cytometry analysis and the representative dot plots showing the expression of CD38 and CD39 on NK, $CD3^+CD4^+$ T cells, and $CD3^+CD4^-$ T cells. **(B)** Comparison of the expression of CD39 on NK, $CD3^+CD4^+$ T, and $CD3^+CD4^-$ T cells in HC, untreated HIV, and ART groups. **(C)** Comparison of the expression of CD38 on NK, $CD3^+CD4^+$ T and $CD3^+CD4^-$ T cells in HC, untreated HIV, and ART groups. **(D)** Comparison of the co-expression of CD38 and CD39 on NK, $CD3^+CD4^+$ T, and $CD3^+CD4^-$ T cells in HC, untreated HIV and ART groups. **(E)** Comparison of the expression of CD39 on NK, $CD3^+CD4^+$ T, and $CD3^+CD4^-$ T cells in HIV. **(F)** Comparison of the expression of CD38 on NK, $CD3^+CD4^+$ T, and $CD3^+CD4^-$ T cells in HIV. **(G)** Comparison of the co-expression of CD38 and CD39 on NK, $CD3^+CD4^+$ T, and $CD3^+CD4^-$ T cells in HIV. The Kruskal–Wallis test was used to compare the three groups. *p < 0.05, **p < 0.01, ***p < 0.001, ns: no significance.

of CD39 on CD56bright and CD56dim NK cells than that of controls ($P < 0.01$ for CD56bright NK and $P < 0.001$ for CD56dim NK). However, CD39 expression was showed no significance differences between the untreated HIV group and the HC group on the CD56neg NK cells (Figure 2B), which indicated that the difference in CD39 expression derived from the CD56bri and CD56dim NK cells. Higher CD38 levels were found in all the NK cell subpopulations in the untreated HIV group compared with controls ($P < 0.001$ for CD56bright NK, $P < 0.001$ for CD56dim NK and $P < 0.001$ for CD56neg NK; Figure 2C). The proportion of the CD38+CD39+ subset in the untreated HIV group was also increased in all subpopulations ($P < 0.001$ for CD56bright NK, $P < 0.001$ for CD56dim NK and $P < 0.001$ for CD56neg NK; Figure 2D). In previous research, the expression of CD39 on CD56bright NK cells was induced by cytokines (21). PBMC from HIV subjects were evaluated after stimulation with IL-12, IL-15, and IL-18 to explore the increased in CD38+ NK cells. The proportion of CD38+ NK cells were markedly increased after stimulation ($P < 0.05$ for IL-12, $P < 0.05$ for IL-15 and $P < 0.05$ for IL-18; Figures 2E, F). Similarly, the mean fluorescence intensity (MFI) of CD38 on the NK cells increased more than the negative control ($P < 0.05$ for IL-12, $P < 0.05$ for IL-15 and $P < 0.05$ for IL-18; Figure 2G).

The proportion of CD38+CD39+ NK cells was positively associated with HIV disease progression

To evaluate whether higher levels of CD38 and CD39 were associated with disease progression, correlation analyses were performed in the untreated HIV group. The results showed that the levels of CD38+, CD39+, and CD38+CD39+ NK cells were negatively correlated with the CD4+ T cell count ($r = -0.498$, $P = 0.02$; $r = -0.575$, $P= 0.004$; $r = -0.569$, $P = 0.005$, respectively; Figure 3A). Furthermore, viral load was positively associated with the frequencies of the CD38+ CD39+ NK cells ($r = 0.470$, $P = 0.02$; Figure 3B), but not the CD38+ and the CD39+ NK cells ($r =0.4$, $P = 0.06$; $r = 0.393$, $P = 0.06$; Figure 3B). Moreover, the proportions of the CD38+, CD39+, and CD38+CD39+ NK cells were negatively correlated with the CD4+/CD8+ T cell count ratio. ($r = -0.546$, $P = 0.007$; $r = -0.531$, $P = 0.009$; $r = -0.556$, $P = 0.006$, respectively; Figure 3C).

The expression of inhibitory receptors increased on CD38+ and/or CD39+ NK cells

The inhibitory receptors (LAG-3, PD-L1, TIGIT, and TIM-3) were detected on the CD38+, CD39+, and CD38+CD39+ NK cells from the untreated HIV group to determine whether the inhibitory receptor increased on CD38+CD39+ NK cells. No obvious differences were found in the expressions of LAG-3, PD-L1, and TIGIT between negative and positive subsets (Figures 4A–D). The proportion of TIM-3 on the CD38+ NK cells was greater than the CD38- NK cells ($P < 0.05$, Figure 4B). Similarly, the CD39+ NK cells expressed higher levels of TIM-3 than the CD39- NK cells ($P < 0.05$, Figure 4D). Moreover, the expression of active receptors (NKG2D and NKG2C) between the CD38+CD39+ and CD38-CD39-NK cells were measured (Figure 4E), but no obvious differences were found ($P > 0.05$ for NKG2D and $P > 0.05$ for NKG2C; Figure 4F). With regard to the inhibitory receptors, the expression of LAG-3 and TIM-3 on the CD38+ CD39+ NK cells was greater than on CD38-CD39- NK cells ($P < 0.01$ for LAG-3 and $P < 0.01$ for TIM-3; Figure 4F). A higher level of inhibitor receptors of the CD38+CD39+ NK cells indicated that these subsets may be associated with negative cell function.

The proportion of TGF-β and interleukin-10 on CD38+ or/and CD39+ NK cells

To evaluate the cell function in producing cytokines, we analyzed the frequencies of TGF-β and IL-10 in NK cells after stimulation (Figure 5A). Interestingly, TGF-β and IL-10 expression was higher in CD39+ NK cells than CD39- NK cells ($P < 0.01$ for TGF-β and $P < 0.05$ for IL-10, Figures 5B, E). CD38+ NK cells did not express more TGF-β and IL-10 than CD38- NK cells ($P < 0.05$ for TGF- β and $P> 0.05$ for IL-10, Figures 5C, F). Furthermore, TGF-β and IL-10 expression was upregulated in CD38+CD39+ NK compared to CD38-CD39- NK cells ($P < 0.05$ for TGF-β and $P < 0.01$ for IL-10, Figures 5D, G).

NK cells suppressed the proliferative ability of CD4+ T and CD8+ T cells in individuals infected with HIV while CD38, CD39, and CD73 inhibitors reverse the effect

To assess the role of CD38 and CD39 on NK cells in T cell proliferation, NK cells from the untreated HIV group were cultured with CD4+ T or CD8+ T cells, considering that the NK cells of the untreated HIV group expressed higher levels of CD38 and CD39. The NK cells decreased the proliferation of CD4+ T and CD8+ T cells ($P < 0.05$ for CD4+ T and $P < 0.05$ for CD8+ T; Figures 6A, B). Consequently, CD38 and CD39 expression on NK cells was inhibited before being cultured with CD4+ T or CD8+ T cells. The CD38 inhibitor, 78c, restored the proliferation of the CD4+ T and CD8+ T cells ($P < 0.05$ for CD4+ T and $P < 0.05$ for CD8+ T, Figures 6C, D). Similarly, the proliferation of CD4+ T and CD8+ T cells was restored by ARL67156, a potent inhibitor of CD39 (22) ($P< 0.05$ for CD4+ T and $P <0.05$ for CD8+ T) (Figures 6C, D). The CD73 inhibitor, AB680, also restored the proliferation of CD8+ T cells

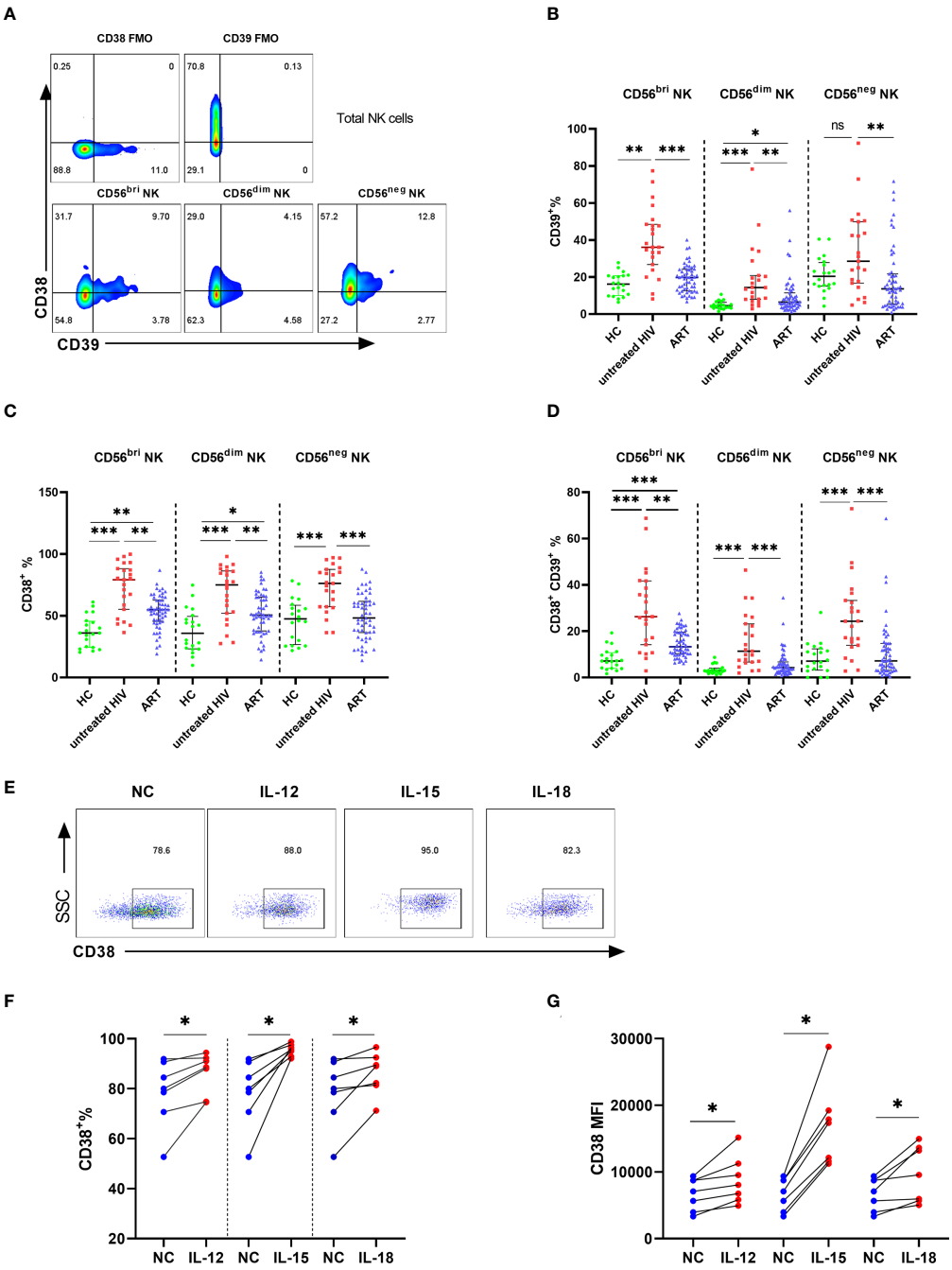

FIGURE 2
The expression of CD39 and CD38 on NK subsets. **(A)** The fluorescence minus one (FMO) control of CD38/CD39 on total NK cells and representative flow cytometry plots showing three subsets of NK cells. **(B)** Comparison of the expression of CD39 on $CD56^{bri}$, $CD56^{dim}$, and $CD56^{neg}$ NK cells in HC, untreated HIV, and ART groups. **(C)** Comparison of the expression of CD38 on $CD56^{bri}$, $CD56^{dim}$ and $CD56^{neg}$ NK cells in HC, untreated HIV and ART groups. **(D)** Comparison of the co-expression of CD38 and CD39 on $CD56^{bri}$, $CD56^{dim}$, and $CD56^{neg}$ NK cells in HC, untreated HIV and ART groups. **(E)** The representative flow cytometry dot plots of CD38 expression on NK cells stimulated by IL-12/15/18. **(F)** Comparison of the percentage of $CD38^+$ NK cells from HIV seropositive individuals in the negative control (NC) group and NK cells stimulated with IL-12, IL-15, and IL-18, respectively. **(G)** The MFI of CD38 on NK cells from HIV infected individuals between negative control (NC) group and the group stimulated with IL-12, IL-15, and IL-18, respectively. *p < 0.05, **p < 0.01, ***p < 0.001, ns: no significance.

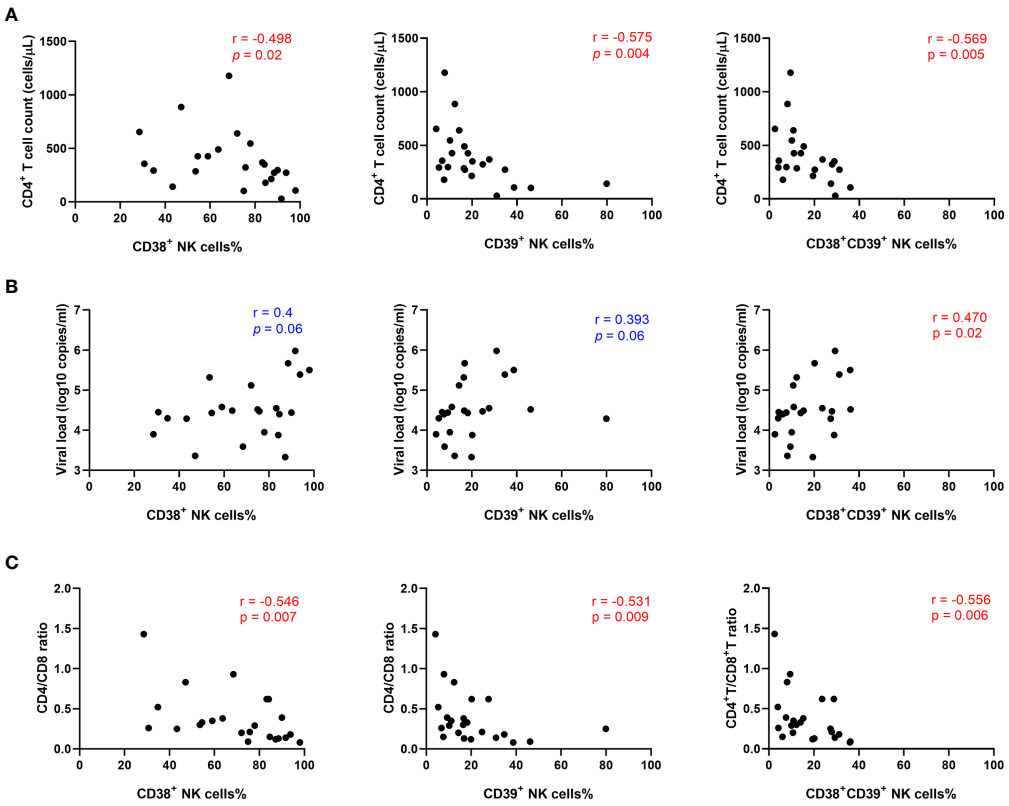

FIGURE 3
The percentage of CD38+CD39+ NK cells was positively associated with HIV disease progression. **(A)** Association between the $CD4^+$ T cell count and the expression of $CD38^+$, $CD39^+$, and $CD38^+39^+$ NK cells in untreated HIV infection individuals. **(B)** Correlations between the viral load and the expression of $CD38^+$, $CD39^+$, and $CD38^+39^+$ NK cells in untreated HIV infection individuals. **(C)** Correlations between the CD4/CD8 ratio and the expression of $CD38^+$, $CD39^+$, and $CD38^+39^+$ NK cells in untreated HIV infection individuals.

and induced CD4+ T cells proliferation (P> 0.05 for CD4+ T and P <0.05 for CD8+ T) (Figures 6C, D). Next, to further support our hypothesis, we inhibited adenosine deaminase (ADA) that converts adenosine to inosine treatment with EHNA (23, 24). Our findings indicated that the proliferation of CD4+ T cells was impaired after inhibiting ADA (P< 0.05, Figure 6C), while the proliferation of CD8+ T cells was not affected (P > 0.05, Figure 6D).

Discussion

Ectonucleotidases, including CD38, CD39, and CD73, have a vital role in the treatment and prognosis of autoimmunity and viral infection (25). In this study, we found that CD38+CD39+ NK cells were more abundant in the untreated HIV group, and that this increase correlated with HIV disease progression. Furthermore, CD38 and CD39 on NK cells in the HIV group reduced the proliferation of the CD4+ T and CD8+ T cells by promoting adenosine production. In addition, in vitro inhibition of CD38 and CD39 expression on NK cells restored autologous CD4+ and CD8+ T cell proliferation.

In this study, we found a higher proportion of CD39 and CD38 on NK cells in the untreated HIV group. Although Dierks et al. (21) also reported higher proportions of CD39+ NK cells in individuals infected with HIV, which may be related to the pathogenesis of HIV, the mechanism was not further explored. To further understand the characteristics of NK cells expressing ectonucleotidases, NK cells expressing CD38 or/and CD39 were detected, and the proportion of CD38+CD39+ NK cells increased in HIV infected subjects. An early study suggested that upregulated levels of CD39 on NK cells were associated with immune activation in HIV infection, while the proinflammatory factors (IL-12, IL-15, and IL-18) upregulated the CD39 expression on NK cells (21). In addition, IL-12 and IL-18 stimulate other activation receptors on NK cells in tumors (26). Based on the earlier study, we found that IL-12, IL-15, and IL-18 upregulated the levels of CD38 on NK cells. The mechanism for this remains unknown; however, it may be associated with the activation of NK cells (27). Swaminathan

10.3389/fimmu.2022.946871

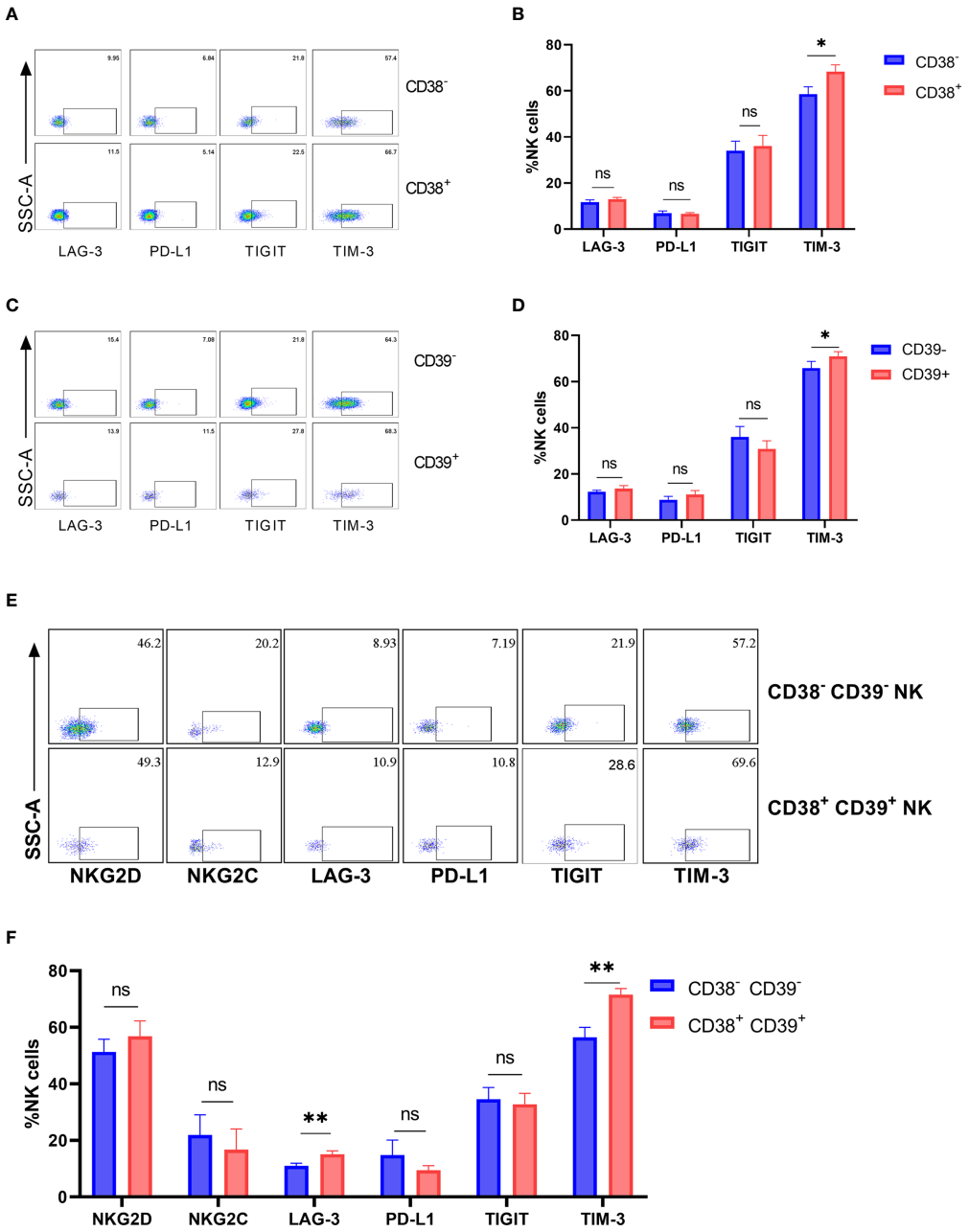

FIGURE 4
The expression of inhibitory receptors increased on CD38+ or/and CD39+ NK cells. **(A)** The representative flow cytometry plots of LAG-3, PD-L1, TIGIT, and TIM-3 on $CD38^-$ and $CD38^+$ NK cells. **(B)** Comparison of the expression of LAG-3, PD-L1, TIGIT, and TIM-3 between $CD38^-$ and $CD38^+$ NK cells. **(C)** The representative flow cytometry plots of LAG-3, PD-L1, TIGIT, and TIM-3 on $CD39^-$ and $CD39^+$ NK cells. **(D)** Comparison of the expression of LAG-3, PD-L1, TIGIT, and TIM-3 between $CD39^-$ and $CD39^+$ NK cells. **(E)** The representative flow cytometry plots of NKG2D, NKG2C, LAG-3, PD-L1, TIGIT, and TIM-3 on $CD38^-CD39^-$ and $CD38^+CD39^+$ NK cells. **(F)** Comparison of the expression of NKG2D, NKG2C, LAG-3, PD-L1, TIGIT, and TIM-3 on $CD38^-CD39^-$ and $CD38^+CD39^+$ NK cells. *p < 0.05, **p < 0.01, ns: no significance.

et al. demonstrated that the concentration of IL-15 and IL-18 were upregulated in individuals infected with HIV (28, 29). Another study found that antiretroviral therapy reduced chronic inflammation in these patients by decreasing IL-12 levels (30). Similarly, CD38 and CD39 expression on NK cells decreased after antiretroviral therapy. The persistent chronic inflammation in individuals infected with HIV induced the expression of CD38 and CD39 on NK cells.

Because the ectonucleotidases on NK cells decreased significantly after antiretroviral treatment, we hypothesized

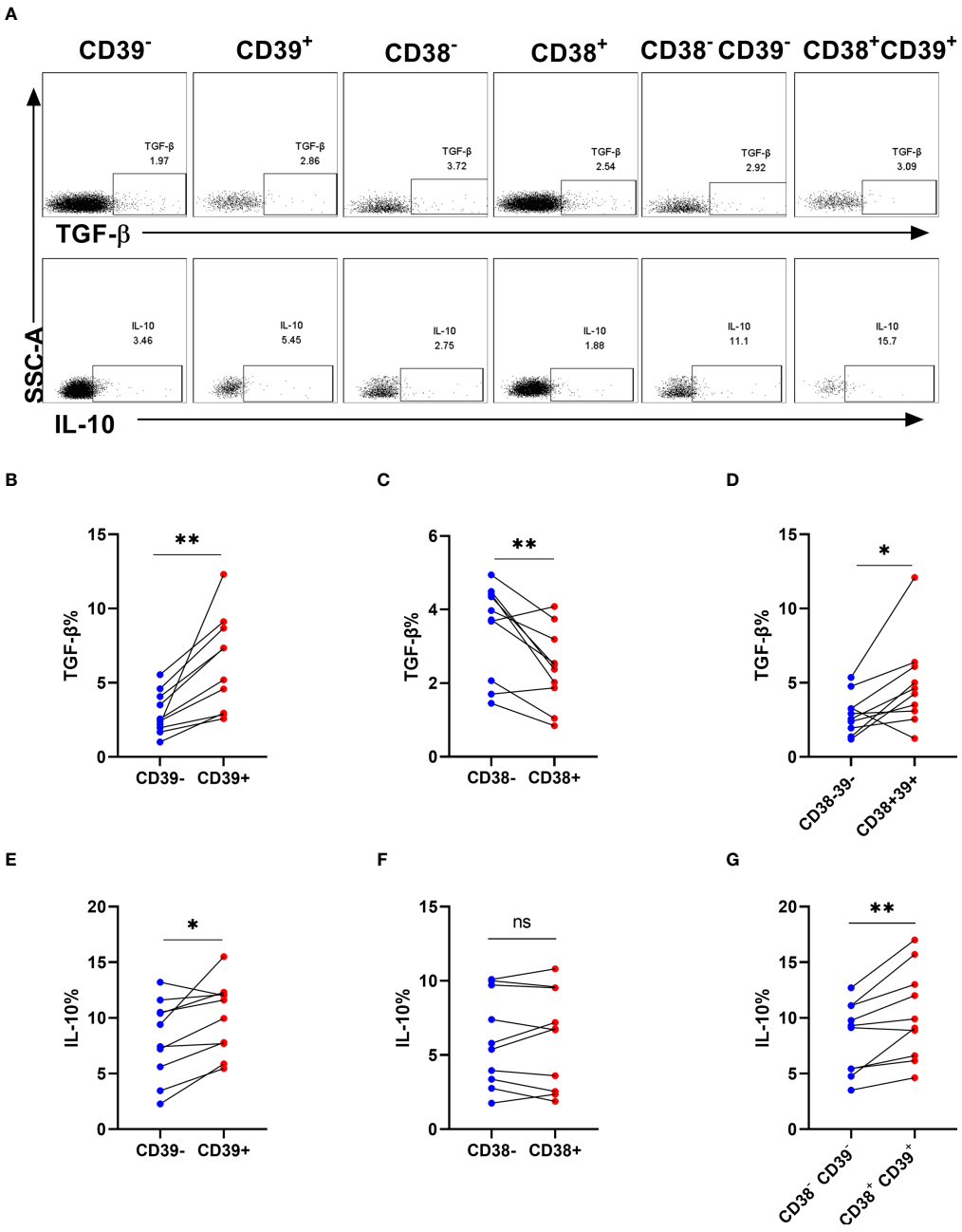

FIGURE 5
The proportion of TGF-β and interleukin-10 on CD38+ or/and CD39+ NK cells. **(A)** The representative flow cytometry spots showing the production of TGF-β and IL-10 in $CD39^-$, $CD39^+$, $CD38^-$, $CD38^+$, $CD38^-CD39^-$, and $CD38^+CD39^+$ NK cells from HIV infected individuals. **(B–D)** Comparison of the production of TGF-β between $CD39^-$ and $CD39^+$ NK cells **(B)**, $CD38^-$ and $CD38^+$ NK cells **(C)**, $CD38^-CD39^-$ and $CD38^+CD39^+$ NK cells **(D)** from HIV infected participants stimulated with PMA/ionomycin for 6 h. **(E–G)** Comparison of the production of IL-10 between $CD39^-$ and $CD39^+$ NK cells **(E)**, $CD38^-$ and $CD38^+$ NK cells **(F)**, $CD38^-CD39^-$ and $CD38^+CD39^+$ NK cells **(G)** from HIV infected participants stimulated with PMA/ionomycin for 6 h. *p < 0.05, **p < 0.01, ns: no significance.

that the NK cell ectonucleotidases had a crucial role in the progression of AIDS. Our data suggest that the CD4+ T cell count and CD4/CD8 ratio were negatively associated with the level of CD38 and CD39 on NK cells. Thus, CD38 and CD39 may be associated with the regulation of T cell counts. Interestingly, our data showed that CD38+CD39+ NK cells were negatively related with the CD4/CD8 ratio count and CD4+ T cell and positively related to the HIV viral load. We

10.3389/fimmu.2022.946871

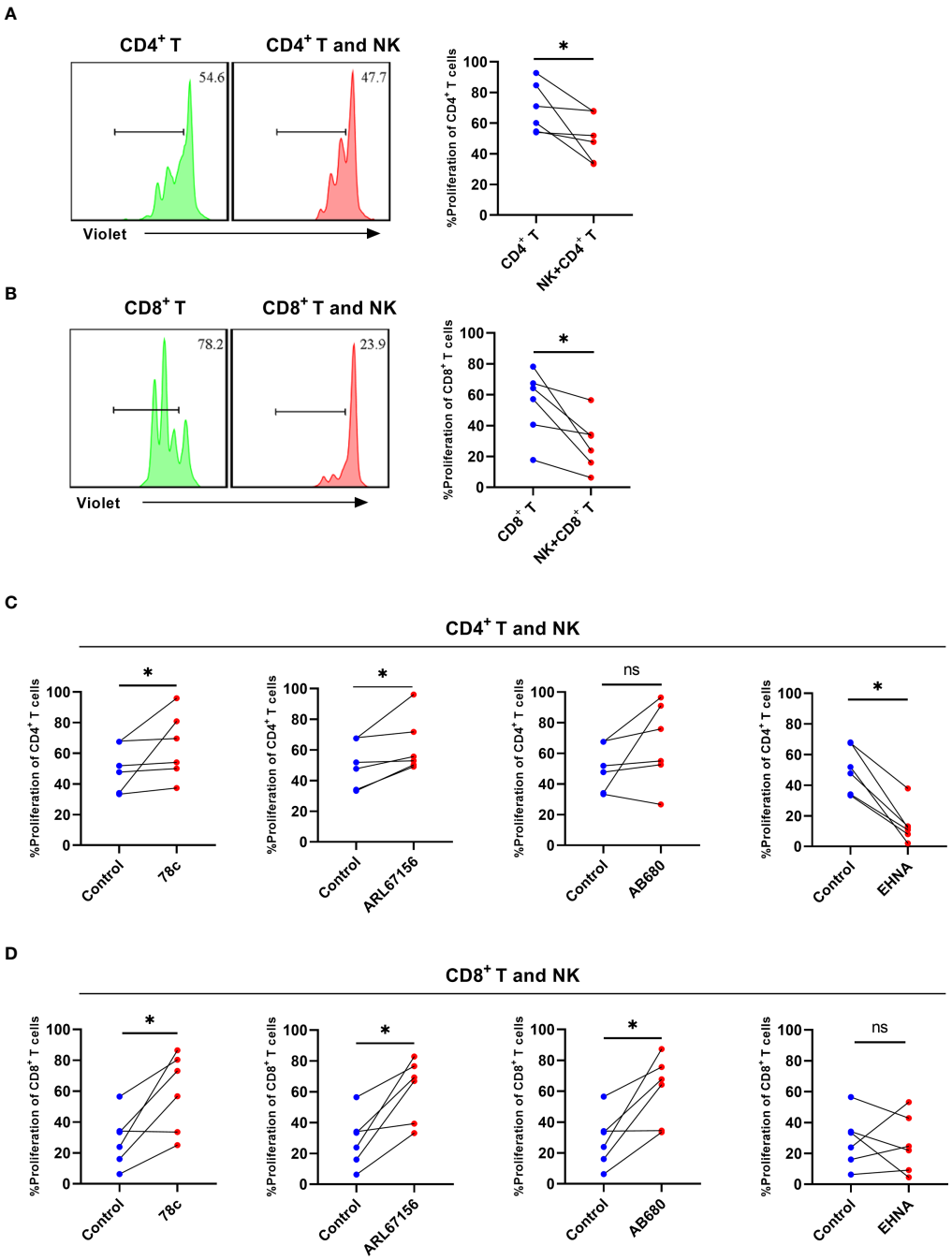

FIGURE 6
NK cells from HIV infected individuals inhibit the proliferation of $CD4^+$ T and $CD8^+$ T cells and CD38, CD39, and CD73 inhibitors reverse the effect. **(A)** A representative histogram and comparison showing the proliferation of $CD4^+$ T cells with or without autologous NK cells for 3 days. **(B)** A representative histogram and comparison showing the proliferation of $CD8^+$ T cells with or without autologous NK cells for 3 days. **(C)** Comparison of the proliferation of $CD4^+$ T cells cultured with NK cells from untreated HIV infected individuals stimulated with 78c, ARL67156, AB680, and EHNA. **(D)** Comparison of the proliferation of $CD8^+$ T cells cultured with NK cells from untreated HIV infected individuals stimulated with 78c, ARL67156, AB680 and EHNA. *$p < 0.05$, ns: no significance.

found that CD38+CD39+ NK cells may negatively regulate antiviral activity. Brauneck et al. (31) suggested that blocking CD39 on NK cells enhanced NK-92 cell-mediated cytotoxicity. Adenosine from the CD39 and CD38 enzymatic cascade is an important immunosuppression pathway in the antiviral function of NK cells (10, 32). Furthermore, CD38+CD39+ NK cells expressed more inhibitory receptors. A possible explanation may be that CD38 and CD39 promoted adenosine production, which had previously been reported to upregulate the level of inhibitory receptors on immune cells (33).

Researchers have found that IL-10 and TGF-β are upregulated in plasma during HIV infection (34, 35). NK cells can secret the cytokines IL-10 and TGF-β, which have been shown to limit the function of T cells (4, 36). Our results showed that CD39+ and CD38+CD39+ NK cells had higher expression of TGF-β. Neo et al. found that NK cells expressing the ectonucleotidases, CD73, produced more IL-10 and TGF-β via STAT3 transcriptional activity (37). In addition, CD39+ Tregs secreted more IL-10 and TGF-β to inhibit inflammation (38). These data indicated that CD38+CD39+ NK cells expressed more IL-10 and TGF-β for immune suppression.

Herein, we showed that autologous NK cells markedly suppressed the proliferation of CD4+ T and CD8+ T cells from untreated individuals with HIV. Morandi et al. demonstrated that adenosine produced by NK cells from inflammatory pleural effusions inhibits the autologous CD4+ T cell proliferation through a CD38-mediated pathway (17). In term of suppressive mechanism, Tomasz et al. found that ATP is released and transformed into adenosine through CD39 and CD73 and play a suppressive role by the adenosine and the A2A receptor, and the activation of A2A receptor reduce the calcium-influx into T cells by inhibiting the tyrosine phosphorylation of the key kinase ZAP-70 (39, 40). In a previous study, CD39 +CD73+ tumor cells reduced the proliferation of CD4+ T and CD8+ T cells by CD39 and the adenosine dependent pathway, and treatment with CD39 inhibitors or blocking antibodies reduced the tumor-induced inhibition (41). Julia et al. demonstrated that degradation of extracellular ATP or AMP by ectonucleotidases lead to the accumulation of deoxyATP, which prevent DNA synthesis by inhibiting ribonucleotide reductase (42). In subsequent experiments, inhibitors of CD39, CD38, and CD73 were added to reduce adenosine production and restore T cell proliferation (43). Damaged and stressed cells release NAD+, which are hydrolyzed in a stepwise manner to synthesize adenosine by CD38 and CD73 (44). Furthermore, TCR stimulation induces ATP release, which allows extracellular ATP to act on the P2X7 receptor to promote T cell activation by mediating Ca2+ influx, while CD39 and CD73 suppressed the proliferation of T cells by decreasing ATP and increasing adenosine production (42, 45). The adenosine axis contains CD38, CD39, and CD73 and is a vital immunosuppression pathway. CD8+ T cell dysfunction in chronic HIV infection can be reversed by blocking the CD39/adenosine pathway (46). In addition, CD8+ T cells participate in immune suppression by CD73-mediated adenosine production (47). For NK cells, CD73 defines a population of NK cells with immune modulation properties in the tumor microenvironment (37).

In conclusion, we demonstrated that CD38+CD39+ NK cells are significantly increased in the untreated HIV group and associated with disease progression. Furthermore, the CD38 +CD39+ NK cells expressed a higher percentage of inhibitory receptors (TIM-3 and LAG-3) and produced more TGF-β. CD38 and CD39 on NK cells impaired the proliferation of CD4+ T and CD8+ T cells by adenosine-mediated immune modulation. Altogether these findings indicate that the inhibition of CD38 and CD39 on NK cells in individuals with HIV can restore T cell proliferation, which represents a potential immunotherapy target for HIV treatment.

Limitations

There are some limitations in our study. We demonstrated CD38 and CD39 on NK cells impaired the proliferation of CD4+ T and CD8+ T cells by adenosine-mediated immune modulation, while we did not carry out further mechanistic experiments. There will be opportunities to explore more mechanism about the suppressive function of CD38 and CD39 on NK cells in our future studies, although the mechanism about the suppressive function of CD38 and CD39 have been reported in previous studies as mentioned above in the discussion (39, 41).

Data availability statement

The original contributions presented in the study are included in the article/Supplementary Material. Further inquiries can be directed to the corresponding authors.

Ethics statement

The studies involving human participants were reviewed and approved by Research and Ethics Committee of The First Hospital of China Medical University. The patients/participants provided their written informed consent to participate in this study.

Author contributions

SQ, CX conducted the study, statistical analysis and wrote the manuscript. YJ and HS designed the experiments and revised the manuscript. MW, ZZ, YF, QH, XH, and HD recruited participants and provided the clinical data. All authors read and approved the final manuscript.

Acknowledgments

We express our gratitude to all participants including patients and blood donors in our study. We are appreciated the support from the CAMS Innovation Fund for Medical Sciences(2019-I2M-5-027) and the Liaoning Provincial Department of Education Basic Scientific Research Project (LJKZ0737), Mega-Projects of National Science Research for the 13th Five-Year Plan (2017ZX10201101 and 2018ZX10732101-001-011).

Conflict of interest

The authors declare that the research was conducted in the absence of any commercial or financial relationships that could be construed as a potential conflict of interest.

Publisher's note

Supplementary material

The Supplementary Material for this article can be found online at: https://www.frontiersin.org/articles/10.3389/fimmu.2022.946871/full#supplementary-material

SUPPLEMENTARY FIGURE 1
The expression of CD73 on NK, $CD3^+CD4^-$ T and $CD3^+CD4^-$ T cells in HC, untreated HIV, and ART-treated patients.

References

1. Mace EM, Orange JS. Emerging insights into human health and NK cell biology from the study of NK cell deficiencies. *Immunol Rev* (2019) 287(1):202–25. doi: 10.1111/imr.12725

2. Fisicaro P, Rossi M, Vecchi A, Acerbi G, Barili V, Laccabue D, et al. The good and the bad of natural killer cells in virus control: Perspective for anti-HBV therapy. *Int J Mol Sci* (2019) 20(20). doi: 10.3390/ijms20205080

3. Perona-Wright G, Mohrs K, Szaba FM, Kummer LW, Madan R, Karp CL, et al. Systemic but not local infections elicit immunosuppressive IL-10 production by natural killer cells. *Cell Host Microbe* (2009) 6(6):503–12. doi: 10.1016/j.chom.2009.11.003

4. Ma M, Yin X, Zhao X, Guo C, Zhu X, Liu T, et al. CD56(-) CD16(+) NK cells from HIV-infected individuals negatively regulate IFN-gamma production by autologous CD8(+) T cells. *J Leukoc Biol* (2019) 106(6):1313–23. doi: 10.1002/JLB.3A0819-171RR

5. Vijayan D, Young A, Teng MWL, Smyt MJ. Targeting immunosuppressive adenosine in cancer. *Nat Rev Cancer* (2017) 17(12):709–24. doi: 10.1038/nrc.2017.86

6. Chambers AM, Wang J, Lupo KB, Yu H, Lanman Atallah NM, Matosevi S, et al. Adenosinergic signaling alters natural killer cell functional responses. *Front Immunol* (2018) 9:2533. doi: 10.3389/fimmu.2018.02533

7. Borsellino G, Kleinewietfeld M, Mitri Di D, Sternjak A, Diamantini A, Giometto R, et al. Expression of ectonucleotidase CD39 by Foxp3+ treg cells: hydrolysis of extracellular ATP and immune suppression. *Blood* (2007) 110 (4):1225–32. doi: 10.1182/blood-2006-12-064527

8. Deterre P, Gelman L, Gary-Gouy H, Arrieumerlou C, Berthelier V, Tixier JM, et al. Coordinated regulation in human T cells of nucleotide-hydrolyzing ecto-enzymatic activities, including CD38 and PC-1. possible role in the recycling of nicotinamide adenine dinucleotide metabolites. *J Immunol* (1996) 157(4):1381–8. doi: 10.1006/cimm.1996.0224

9. Horenstein AL, Chillemi A, Zaccarello G, Bruzzone S, Quarona V, Zito A, et al. A CD38/CD203a/CD73 ectoenzymatic pathway independent of CD39 drives a novel adenosinergic loop in human T lymphocytes. *Oncoimmunology* (2013) 2 (9):e26246. doi: 10.4161/onci.26246

10. Linden J, Koch-Nolte F, Dahl G. Purine release, metabolism, and signaling in the inflammatory response. *Annu Rev Immunol* (2019) 37:325–47. doi: 10.1146/annurev-immunol-051116-052406

11. Yegutkin GG, Henttinen T, Samburski SS, Spychala J, Jalkanen S. The evidence for two opposite, ATP-generating and ATP-consuming, extracellular pathways on endothelial and lymphoid cells. *Biochem J* (2002) 367(Pt 1):121–8. doi: 10.1042/bj20020439

12. Allard B, Longhi MS, Robson SC, Stagg J. The ectonucleotidases CD39 and CD73: Novel checkpoint inhibitor targets. *Immunol Rev* (2017) 276(1):121–44. doi: 10.1111/imr.12528

13. Deaglio S, Zubiaur M, Gregorini A, Bottarel F, Ausiello CM, Dianzani U, et al. Human CD38 and CD16 are functionally dependent and physically associated in natural killer cells. *Blood* (2002) 99(7):2490–8. doi: 10.1182/blood.V99.7.2490

14. Sun X, Wu Y, Gao W, Enjyoji K, Csizmadia E, Muller CE, et al. CD39/ENTPD1 expression by CD4+Foxp3+ regulatory T cells promotes hepatic metastatic tumor growth in mice. *Gastroenterology* (2010) 139(3):1030–40. doi: 10.1053/j.gastro.2010.05.007

15. Feng X, Zhang L, Acharya C, An G, Wen K, Qi L, et al. Targeting CD38 suppresses induction and function of T regulatory cells to mitigate immunosuppression in multiple myeloma. *Clin Cancer Res* (2017) 23(15):4290–300. doi: 10.1158/1078-0432.CCR-16-3192

16. Jurisic V, Colovic N, Konjevic G, Minic I, Colovic M. An aggressive extramedullary cutaneous plasmacytoma associated with extreme alterations in the innate immune system. *Onkologie* (2010) 33(3):113–5. doi: 10.1159/000278713

17. Morandi F, Horenstein AL, Chillemi A, Quarona V, Chiesa S, Imperatori A, et al. CD56brightCD16- NK cells produce adenosine through a CD38-mediated pathway and act as regulatory cells inhibiting autologous CD4+ T cell proliferation. *J Immunol* (2015) 195(3):965–72. doi: 10.4049/jimmunol.1500591

18. Kuri-Cervantes L, Oca GS, Avila-Ríos S, Hernández-Juan R, Reyes-Terán G. Activation of NK cells is associated with HIV-1 disease progression. *J Leukoc Biol* (2014) 96(1):7–16. doi: 10.1189/jlb.0913514

19. Bachle SM, Malone DF, Buggert M, Karlsson AC, Isberg PE, Biague AJ, et al. Elevated levels of invariant natural killer T-cell and natural killer cell activation correlate with disease progression in HIV-1 and HIV-2 infections. *AIDS* (2016) 30 (11):1713–22. doi: 10.1097/QAD.0000000000001147

20. Slyker JA, Lohman-Payne B, John-Stewart GC, Dong T, Mbori-Ngacha D, Tapia K, et al. The impact of HIV-1 infection and exposure on natural killer (NK) cell phenotype in Kenyan infants during the first year of life. *Front Immunol* (2012) 3:399. doi: 10.3389/fimmu.2012.00399

21. Dierks P, Wroblewski R, Eberhard JM, Martrus G, Degen O, Hertling S, et al. Brief report: Increased frequency of CD39+ CD56bright natural killer cells in HIV-1 infection correlates with immune activation and disease progression. *J Acquir Immune Defic Syndr* (2017) 74(4):467–72. doi: 10.1097/QAI.0000000000001266

22. Levesque SA, Lavoie EG, Lecka J, Bigonnesse F, Sevigny J. Specificity of the ecto-ATPase inhibitor ARL 67156 on human and mouse ectonucleotidases. *Br J Pharmacol* (2007) 152(1):141–50. doi: 10.1038/sj.bjp.0707361

23. Lawson KV, Kalisiak J, Lindsey EA, Newcomb ET, Leleti MR, Debien L, et al. Discovery of AB680: A potent and selective inhibitor of CD73. *J Med Chem* (2020) 63(20):11448–68. doi: 10.1021/acs.jmedchem.0c00525

24. Cristalli G, Costanzi S, Lambertucci C, Lupidi G, Vittori S, Volpini R, et al. Adenosine deaminase: functional implications and different classes of inhibitors. *Med Res Rev* (2001) 21(2):105–28. doi: 10.1002/1098-1128(200103)21:2<105::AID-MED1002>3.0.CO;2-U

25. Song JW, Huang HH, Zhang C, Yang HG, Zhang JY, Xu RN, et al. Expression of CD39 is correlated with HIV DNA levels in naive tregs in chronically infected ART naive patients. *Front Immunol* (2019) 10:2465. doi: 10.3389/fimmu.2019.02465

26. Mirjačić Martinović KM, Vuletić AM, Babović Lj N, Džodić RR, Konjevićm GM, Jurišić VB, et al. Attenuated in vitro effects of IFN-α, IL-2 and IL-12 on functional and receptor characteristics of peripheral blood lymphocytes in metastatic melanoma patients. *Cytokine* (2017) 96:30–40. doi: 10.1016/j.cyto.2017.02.024

27. Ewen EM, Pahl JHW, Miller M, Watzl C, Cerwenk A. KIR downregulation by IL-12/15/18 unleashes human NK cells from KIR/HLA-I inhibition and enhances killing of tumor cells. *Eur J Immunol* (2018) 48(2):355–65. doi: 10.1002/eji.201747128

28. Swaminathan S, Qiu J, Rupert AW, Hu Z, Higgins J, Dewa RL, et al. Interleukin-15 (IL-15) strongly correlates with increasing HIV-1 viremia and markers of inflammation. *PLoS One* (2016) 11(11):e0167091. doi: 10.1371/journal.pone.0167091

29. Iannello A, Boulassel MR, Samarani S, Tremblay C, Toma E, Routy JP, et al. HIV-1 causes an imbalance in the production of interleukin-18 and its natural antagonist in HIV-infected individuals: implications for enhanced viral replication. *J Infect Dis* (2010) 201(4):608–17. doi: 10.1086/650314

30. Calza L, Colangeli V, Magistrelli E, Contadini I, Bon I, Re MC, et al. Significant decrease in plasma levels of d-dimer, interleukin-8, and interleukin-12 after a 12-month treatment with rosuvastatin in HIV-infected patients under antiretroviral therapy. *AIDS Res Hum Retroviruses* (2017) 33(2):126–32. doi: 10.1089/aid.2016.0134

31. Brauneck F, Seubert E, Wellbrock J, Wiesch Zur Schulze J, Duan Y, Magnus T, et al. Combined blockade of TIGIT and CD39 or A2AR enhances NK-92 cell-mediated cytotoxicity in AML. *Int J Mol Sci* (2021) 22(23). doi: 10.3390/ijms222312919

32. Wang J, Matosevic S. Adenosinergic signaling as a target for natural killer cell immunotherapy. *J Mol Med (Berl)* (2018) 96(9):903–13. doi: 10.1007/s00109-018-1679-9

33. Leone RD, Sun IM, Oh MH, Sun IH, Wen J, Englert J, et al. Inhibition of the adenosine A2a receptor modulates expression of T cell coinhibitory receptors and improves effector function for enhanced checkpoint blockade and ACT in murine cancer models. *Cancer Immunol Immunother* (2018) 67(8):1271–84. doi: 10.1007/s00262-018-2186-0

34. Brockman MA, Kwon DS, Tighe DP, Pavlik DF, Rosato PC, Sela J, et al. IL-10 is up-regulated in multiple cell types during viremic HIV infection and reversibly inhibits virus-specific T cells. *Blood* (2009) 114(2):346–56. doi: 10.1182/blood-2008-12-191296

35. Poggi A, Zocchi MR. HIV-1 tat triggers TGF-beta production and NK cell apoptosis that is prevented by pertussis toxin b. *Clin Dev Immunol* (2006) 13(2-4):369–72. doi: 10.1080/17402520600645712

36. Vivier E, Ugolini S. Regulatory natural killer cells: new players in the IL-10 anti-inflammatory response. *Cell Host Microbe* (2009) 6(6):493–5. doi: 10.1016/j.chom.2009.12.001

37. Neo SY, Yang Y, Record J, Ma R, Chen X, Chen Z, et al. CD73 immune checkpoint defines regulatory NK cells within the tumor microenvironment. *J Clin Invest* (2020) 130(3):1185–98. doi: 10.1172/JCI128895

38. Jin X, Lin T, Yang G, Cai H, Tang B, Liao X, et al. Use of tregs as a cell-based therapy via CD39 for benign prostate hyperplasia with inflammation. *J Cell Mol Med* (2020) 24(9):5082–96. doi: 10.1111/jcmm.15137

39. Maj T, Wang W, Crespo J, Zhang H, Wang W, Wei S, et al. Oxidative stress controls regulatory T cell apoptosis and suppressor activity and PD-L1-blockade resistance in tumor. *Nat Immunol* (2017) 18(12):1332–41. doi: 10.1038/ni.3868

40. Linnemann C, Schildberg FA, Schurich A, Diehl L, Hegenbarth SI, Endl E, et al. Adenosine regulates CD8 T-cell priming by inhibition of membrane-proximal T-cell receptor signalling. *Immunology* (2009) 128(1 Suppl):e728–37. doi: 10.1111/j.1365-2567.2009.03075.x

41. Bastid J, Regairaz A, Bonnefoy N, Déjou C, Giustiniani J, Laheurte C, et al. Inhibition of CD39 enzymatic function at the surface of tumor cells alleviates their immunosuppressive activity. *Cancer Immunol Res* (2015) 3(3):254–65. doi: 10.1158/2326-6066.CIR-14-0018

42. Festag J, Thelemann T, Schell M, Raith S, Michel S, Jaschinski F, et al. Preventing ATP degradation by ASO-mediated knockdown of CD39 and CD73 results in A2aR-independent rescue of T cell proliferation. *Mol Ther Nucleic Acids* (2020) 21:656–69. doi: 10.1016/j.omtn.2020.06.020

43. Al-Rashida M, Qazi SU, Batool N, Hameed A, Iqbal J. Ectonucleotidase inhibitors: a patent review (2011-2016). *Expert Opin Ther Pat* (2017) 27(12):1291–304. doi: 10.1080/13543776.2017.1369958

44. Scheuplein F, Schwarz N, Adriouch S, Krebs C, Bannas P, Rissiek B, et al. NAD+ and ATP released from injured cells induce P2X7-dependent shedding of CD62L and externalization of phosphatidylserine by murine T cells. *J Immunol* (2009) 182(5):2898–908. doi: 10.4049/jimmunol.0801711

45. Yip L, Woehrle T, Corriden R, Hirsh M, Chen Y, Inoue Y, et al. Autocrine regulation of T-cell activation by ATP release and P2X7 receptors. *FASEB J* (2009) 23(6):1685–93. doi: 10.1096/fj.08-126458

46. Li J, Huang HH, Tu B, Zhou MJ, Hu W, Fu YL, et al. Reversal of the CD8(+) T-cell exhaustion induced by chronic HIV-1 infection through combined blockade of the adenosine and PD-1 pathways. *Front Immunol* (2021) 12:687296. doi: 10.3389/fimmu.2021.687296

47. Schneider E, Winzer R, Rissiek A, Ricklefs I, Meyer-Schwesinger C, Ricklefs FL, et al. CD73-mediated adenosine production by CD8 T cell-derived extracellular vesicles constitutes an intrinsic mechanism of immune suppression. *Nat Commun* (2021) 12(1):5911. doi: 10.1038/s41467-021-26134-w

frontiers | Frontiers in Microbiology

TYPE Original Research
PUBLISHED 02 November 2022
DOI 10.3389/fmicb.2022.968532

OPEN ACCESS

EDITED BY
Axel Cloeckaert,
Institut National de recherche pour l'agriculture, l'alimentation et l'environnement (INRAE), France

REVIEWED BY
Elopy Sibanda,
National University of Science and Technology, Zimbabwe
Shahram Mahmoudi,
Iran University of Medical Sciences, Iran

*CORRESPONDENCE
Xiaoping Tang
tangxiaopinggz@163.com
Linghua Li
llheliza@126.com

†These authors have contributed equally to this work and share first authorship

SPECIALTY SECTION
This article was submitted to Infectious Agents and Disease, a section of the journal Frontiers in Microbiology

RECEIVED 14 June 2022
ACCEPTED 11 October 2022
PUBLISHED 02 November 2022

CITATION
Chen X, Cao Y, Chen M, Wang H, Du P, Li H, Zhong H, Li Q, Zhao S, Yao Z, Chen W, Cai W, Tang X and Li L (2022) HIV-infected patients rarely develop invasive fungal diseases under good immune reconstitution after ART regardless high prevalence of pathogenic filamentous fungi carriage in nasopharynx/oropharynx. *Front. Microbiol.* 13:968532. doi: 10.3389/fmicb.2022.968532

HIV-infected patients rarely develop invasive fungal diseases under good immune reconstitution after ART regardless high prevalence of pathogenic filamentous fungi carriage in nasopharynx/oropharynx

Xiaoman Chen[1†], Yi Cao[1†], Meijun Chen[1†], Haodi Wang[1], Peishan Du[1], Hong Li[1], Huolin Zhong[1], Quanmin Li[1], Santao Zhao[1], Zhenjiang Yao[2], Wanshan Chen[1], Weiping Cai[1], Xiaoping Tang[1*] and Linghua Li[1*]

[1]Infectious Disease Center, Guangzhou Eighth People's Hospital, Guangzhou Medical University, Guangzhou, China, [2]Department of Epidemiology and Health Statistics, School of Public Health, Guangdong Pharmaceutical University, Guangzhou, China

Purpose: We aimed to investigate the prevalence and risk factors of filamentous fungi (FF) carriage in human immunodeficiency virus (HIV)-infected patients in Guangdong province, along with its subsequent incidence of invasive fungal disease (IFD).

Methods: Seven hundred and sixteen HIV-infected individuals from the outpatient clinic and 293 sex-matched healthy controls were recruited prospectively from May 1 to August 31, 2017. Fungi were isolated from oropharyngeal and nasopharyngeal swabs, then identified by morphological and molecular biological techniques. Logistic regression analysis was used to identify risk factors of pathogenic FF carriage. Pathogenic FF carriers were followed up through the end of 2019.

Results: Of the 716 included HIV-infected patients, 602 (84.1%) were male, the median age was 34 (27–42) years, and the median CD4+ count was 385 (254–542) cells/μl. Pathogenic FF were isolated in 119 (16.6%) cases with HIV infection and 40 (13.7%) healthy controls. Mucorales were found in 3 HIV-infected individuals and *Talaromyces marneffei* in 2 HIV-infected individuals, but not in healthy controls. History of cured opportunistic infections (OIs; OR, 1.97; 95% CI, 1.23–3.13, p=0.004), and smoking (OR, 1.55; 95%CI, 1.03–2.32, p=0.035) were independent risk factors of pathogenic FF carriage in HIV-infected individuals. A total of 119 pathogenic FF carriers with HIV infection were followed. During follow-up, 119 (100%) cases received antiretroviral therapy (ART) for at least 28months, 107 (90%) cases had CD4+ counts>200 cells/μl, and none developed IFD.

Discussion: Pathogenic FF carriage is common in HIV-infected individuals but may not develop IFD in those who achieved immune reconstitution. Smoking and cured OIs history increase the risk of pathogenic FF carriage. Smoking abstinence and ART adherence are especially important for these patients.

KEYWORDS

human immunodeficiency virus, pathogenic filamentous fungi, filamentous fungi, invasive fungal disease, immune reconstitution, carrier, smoking, opportunistic infections

Introduction

Invasive fungal disease (IFD) is an opportunistic infection (OI) in immunocompromised patients, with a high mortality rate of more than 50% despite the availability of antifungal drugs (Brown et al., 2012). Individuals with human immunodeficiency virus (HIV) infection are a high-risk population for IFD. It is estimated that up to 1 million patients with HIV infection suffered from IFDs annually, with about 500,000 of them dying each year (Armstrong-James et al., 2014; Chastain et al., 2017). Pathogenic filamentous fungi (FF) have become common in HIV-infected individuals with IFD, mainly including *Talaromyces marneffei*, pathogenic *Aspergillus*, and Mucorales (Marukutira et al., 2014; Moreira et al., 2016; CAO et al., 2021). In Southern China, the prevalence rate of talaromycosis in HIV-positive inpatients was up to 16.0%, with a mortality rate of 50.6% without timely antifungal treatment (Hu et al., 2013; Ying et al., 2020). Aspergillosis occurred in 4.4% of HIV-infected patients with IFD, and the survival possibility was lower than cryptococcosis (Marukutira et al., 2014). Mucormycosis is rare in HIV-infected individuals but may occur in patients with advanced acquired immune deficiency syndrome (AIDS), with a reported mortality rate of 52.2% (Moreira et al., 2016).

IFD in HIV-infected patients has an insidious onset, expresses progress rapidly, and carries a poor prognosis. Early screening, diagnosis, and treatment of IFD are crucial to reducing IFD-related mortality in HIV-infected patients. The nasopharynx and oropharynx are the initial points of entry to the digestive and respiratory tract, colonizing with a wide variety of fungi. Previous studies have focused on *Candida* (Maurya et al., 2013; Hall and Noverr, 2017; Goulart et al., 2018; Aboualigalehdari et al., 2020). *Candida* colonizes about 40–50% of HIV-infected patients and is associated with invasive candidiasis (Maurya et al., 2013; Goulart et al., 2018; Von Lilienfeld-Toal et al., 2019; Aboualigalehdari et al., 2020). However, few studies have explored the asymptomatic carriage of pathogenic FF, such as *Talaromyces marneffei*, pathogenic *Aspergillus*, and Mucorales. This study aimed to investigate the prevalence of asymptomatic FF carriage in nasopharynx and oropharynx of HIV-infected individuals in Guangdong province, and follow their incidence of IFD, thus providing a theoretical basis for the prevention and surveillance of IFD in HIV-infected patients.

Materials and methods

Study design

This was an observational study with participants recruited prospectively, including two parts: (1) A cross-sectional study to investigate the prevalence of fungal carriage in HIV-infected individuals and healthy populations, and risk factors of pathogenic FF carriage in HIV-infected patients; (2) A follow-up study to investigate the occurrence of IFD among pathogenic FF carriers with HIV infection. We randomly enrolled HIV-infected individuals from the outpatient clinic at the Department of Infectious Diseases of the Guangzhou Eighth People's Hospital (GEPH) from May 1, 2017 to August 31, 2017. Meanwhile, healthy controls were recruited from a physical examination center in Guangzhou. All participants were adults ≥18 years of age at enrolment. The exclusion criteria were as follows: (1) the presence of oral fungal infection by clinical examination; (2) received antibiotic or antifungal treatment within the past 2 weeks; (3) received corticosteroids within the past 28 days, or immunosuppressants within the past 3 months; (4) suffered from acute infection at enrolment; (5) skin or mucosa lesions; (6) suffered from OIs, severe underlying or systemic diseases, or tumor at enrolment; (7) pregnancy or lactation. Ethical approval was provided by the Medical Ethics Committee of the GEPH (Approval No. 20150155). All patients signed an informed consent form.

HIV infection was confirmed by positive HIV enzyme-linked immunosorbent assay (ELISA) and a confirmatory Western blot (WB), or RNA Nucleic Acid Amplification Test (NAAT) testing. All participants underwent medical history questionnaires at enrolment. Oropharyngeal and nasopharyngeal swabs were collected at enrolment for fungal culture and strain identification. Risk factors of pathogenic FF carriage were explored. Subsequently, pathogenic FF carriers with HIV infection were followed through the end of 2019 until their first diagnosis of IFD, or their last follow-up.

Data collection

All participants underwent medical history questionnaires at enrolment. The following data were collected. Demographic data:

age and gender; Exposure history within 6 months: rodent exposure, hay or chaff exposure; Lifestyle habits: smoking history, alcoholism; Past medical history within 1 year: cured respiratory tract infections, cured OIs, other infectious diseases, and medication history; HIV-related data: history of antiretroviral therapy (ART). Plasma HIV RNA (viral load) and CD4+ counts were collected from the patient's electronic medical records.

Alcoholism was defined in this study as follows: (1) alcohol abuse for more than 5 years and ethanol consumption ≥40 g/d for men and ≥ 20 g/d for women, or (2) heavy drinking in the most recent 2 weeks equivalent to ethanol ≥80 g/d; OIs were defined as infections caused by conditional pathogens not harmful to healthy populations but to immunodeficient populations, mainly including Pneumocystis pneumonia, cytomegalovirus infection, cryptococcal meningitis, tuberculosis, nontuberculous mycobacterial disease, and bacterial pneumonia.

Swabs collection and fungi culture

Swabs were collected from bilateral nasopharynx and oropharynx. Samples were transferred to Sabouraud broth medium (Guangzhou Detgerm Microbiological Science Ltd. Guangzhou, China) within 2 h and incubated at 25°C for vegetative growth. Examined for fungal growth daily for up to 2 weeks. The presence of white flocs or slag-like sediments was considered positive, otherwise negative. Cultures were plated onto Sabouraud dextrose agar (SDA) plates containing chloramphenicol and incubated in a constant temperature incubator at 25°C. Daily observations were made and recorded. If multiple fungal strains appeared on the plate, isolation and culture were required to obtain monoclonal strains.

Fungal identification

Fungal identification was based on morphological and molecular methods. Fungi were identified according to their phenotypic characteristics, such as color, shape, size, sclerotia, colony surface texture, and hyphal pigmentation.

Molecular biological methods were performed when morphological methods failed to identify filamentous fungal strains. Fungal DNA was extracted using Lysis Buffer for Microorganism. The ITS (internal transcribed spacer) region of each fungus was amplified using the universal primers ITS1 and ITS4. The PCR products were electrophoresed and sent to Invitrogen (Shanghai) for sequencing in both directions. Sequence alignments were performed using NCBI BLAST.[1] Strains showing homology of at least 97% were considered to belong to the same genus, and homology of at least 99% was considered to belong to the same species. The sequences have been submitted to NCBI Genebank database with accession number of OP103924-OP103949, and OP237033-OP237524.

Pathogenic FF included pathogenic *Aspergillus*, Mucorales (*Mucor* spp., *Rhizopus* spp., *Absidia* spp., and *Rhizomucor* spp.), and *Talaromyces marneffei*. Patients with asymptomatic pathogenic FF carriage were named pathogenic FF carriers. Pathogenic *Aspergillus* was defined as *Aspergillus* species that have been reported to cause invasive aspergillosis, including *Aspergillus fumigatus*, *Aspergillus flavus*, *Aspergillus niger*, *Aspergillus terreus*, *Aspergillus versicolor*, *Aspergillus oryzae*, and *Aspergillus sydowii* (Chiu et al., 2005; Perri et al., 2005; Schwetz et al., 2007; Cadena et al., 2021).

Follow-up

Pathogenic FF carriers with HIV infection were followed after initial examination, including ART, plasma HIV RNA (viral load), CD4+ count, and occurrence of IFD. Patients were followed until incident IFD or the last follow-up date (December 31, 2019).

Statistical analysis

EpiData3.1 software was used to input data, and statistical analyses were performed by SPSS 25.5 software. Controls were frequency matched to cases on sex. The chi-squared test was used for categorical variables. Logistic regression analysis was used to determine the risk factors of pathogenic FF carriage in HIV-infected individuals. Odds ratios (OR) are given with their 95% confidence intervals (95% CI). Variables with $p < 0.10$ in the univariate analysis were included in the multivariate analysis. The variance inflation factor (VIF) was used to evaluate collinearity; feature with VIF >10 was excluded. A two-tailed $p < 0.05$ was considered statistically significant.

Results

Baseline characteristics and fungal carriage in HIV-infected and healthy individuals

In this study, 716 HIV-infected patients and 293 healthy individuals were enrolled. No significant differences in sex and age were found between groups. Patients with HIV infection had a higher proportion of history of respiratory tract infection within 1 year (66.1% [472/716] vs. 49.5% [145/293, $p < 0.001$) than healthy individuals. There were no significant differences in environmental exposures, history of smoking or alcoholism between groups (all $p > 0.05$; Table 1). Most HIV-infected patients had received ART, and only 11% had not. Sixteen point three percent of HIV-infected patients had CD4 + T cell counts <200 cells/μl.

1 https://blast.ncbi.nlm.nih.gov/

TABLE 1 Comparison of baseline characteristics and fungal positive rates between the HIV-infected group and the control group.

Variates	Control Group ($n = 293$)	HIV-infected Group ($n = 716$)	p-value
Male	246 [84.0]	602 [84.1]	0.963
Age (Years)	28 (22–45)	34 (27–42)	0.144
18–39	185 [63.1]	493 [(68.9]	–
40–63	106 [36.2]	215 [30.0]	–
>63	2 [0.7]	8 [1.1]	–
Environmental exposures within 6 months			
Rodent exposure	10 [3.4]	36 [5.0]	0.264
Hay or chaff exposure	23 [7.9]	71 [9.9]	0.305
Past medical history within 1 year			
Cured respiratory tract infections	145 [49.5]	472 [66.1]	<0.001
Cured OIs	–	128 [17.9]	–
Other infectious diseases	0 [0.0]	239 [33.4]	–
Smoking History	105 [35.8]	254 [35.5]	0.913
Alcoholism	27 [9.2]	42 [5.9]	0.056
ART	–	–	–
Non-ART	–	79 [11.0]	–
ART <1 year	–	197 [27.5]	–
ART > = 1 year	–	440 [61.5]	–
CD4 + T cell count (cells/μl)	–	385 (254–542)	–
<200	–	117 [16.3]	–
200–500	–	386 [53.9]	–
>500	–	213 [29.7]	–
HIV RNA quantitative <50 copies/ml	–	428 [89.9][a]	–
Fungal culture results[b]			
Fungi (+)	237 [80.9]	646 [90.2]	<0.001
Yeast-like Fungi (+)	89 [30.4] [c]	300 [41.9][d]	0.001
Filamentous Fungi (+)	216 [73.7] [c]	576 [80.5][d]	0.018
Pathogenic Filamentous Fungi (+)	40 [13.7]	119 [16.6]	0.240
Pathogenic *Aspergillus* (+)	40 [13.7]	115 [16.1]	0.335
Mucorales[e] (+)	0 [0.0]	3 [0.4]	–
Talaromyces marneffei (+)	0 [0.0]	2 [0.3]	–

All data are expressed as n [%]; $p < 0.05$ were considered statistically significant. HIV, human immunodeficiency virus; OIs, opportunistic infections; ART, antiretroviral therapy.
[a]Information about HIV RNA quantitative was missing for 240 HIV-infected patients.
[b]Upper respiratory tract samples include nasopharyngeal swabs and oropharyngeal swabs.
[c]Sixty-eight of them carried both yeast-like fungi and filamentous fungi.
[d]Two hundred and thirty of them carried both yeast-like fungi and filamentous fungi.
[e]Mucorales that cause mucormycosis.

All patients underwent oropharyngeal and nasopharyngeal swabs for fungi examinations. In the HIV-infected group, fungi were isolated in 90.2% [646 /716] of patients. Three hundred (41.9%) cases had yeast-like fungi and 576 (80.5%) had FF, higher than those in the control group (all $p < 0.05$; Figure 1). The positive rate of pathogenic FF in the HIV-infected group was similar to that in the control group (16.6% [119 /716] vs. 13.7% [40 /293], $p = 0.24$; Table 1). Mucorales were found in 3 HIV-infected individuals and *Talaromyces marneffei* in 2 HIV-infected individuals, but not in healthy controls.

The identification results of FF were listed in Supplementary Table S1. We identified 623 FF strains in the HIV-infected group and 235 FF strains in the control group, respectively. In HIV-infected group, 125 pathogenic FF strains were identified, including 24.0% [30/125] of *Aspergillus fumigatus*, 14.4% [18/125] of *Aspergillus flavus*, 26.4% [33/125] of *Aspergillus niger*, 4.0% [5/125] of *Aspergillus terreus*, 11.2% [14/125] of *Aspergillus versicolor*, 4.8% [6/125] of *Aspergillus oryzae*, 11.2% [14/125] of *Aspergillus Sydowii*, 1.6% [2/125] of *Talaromyces marneffei*, 0.8% [1/125] of *Rhizomucor variabilis*, 0.8% [1/125] of *Rhizopus microsporus*, and 0.8% [1/125] (Table 2).

Risk factors of pathogenic FF carriage in HIV-infected individuals

Among HIV-infected individuals, proportions of cured OIs history (27.7% [33/119] vs. 15.9% [95/597], $p = 0.002$), and smoking history (44.5% [53/119] vs. 33.7% [201/597], $p = 0.024$)

10.3389/fmicb.2022.968532

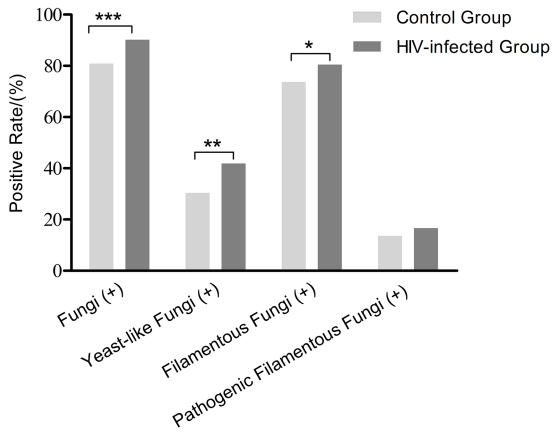

FIGURE 1
Positive rates of fungal carriage in the HIV-infected group and the control group. *p<0.05, **p<0.01, ***p<0.001.

TABLE 2 Identification results of pathogenic filamentous fungi in HIV-infected individuals and healthy controls.

Species	Number of Strains	
	HIV-infected group	Control group
Aspergillus fumigatus	30 [24.0]	11 [26.2]
Aspergillus flavus	18 [14.4]	7 [16.7]
Aspergillus niger	33 [26.4]	9 [21.4]
Aspergillus terreus	5 [4.0]	4 [9.5]
Aspergillus versicolor	14 [11.2]	6 [14.3]
Aspergillus oryzae	6 [4.8]	1 [2.4]
Aspergillus sydowii	14 [11.2]	4 [9.5]
Talaromyces marneffei	2 [1.6]	0 [0.0]
Rhizomucor variabilis	1 [0.8]	0 [0.0]
Rhizopus microsporus	1 [0.8]	0 [0.0]
Rhizopus sp.	1 [0.8]	0 [0.0]
Total	125 [100.0]	42 [100.0]

All data are expressed as *n* [%].

were significantly higher in pathogenic FF carriers than those of non-carriers (Table 3). In univariate analysis, OIs, and smoking history showed strong associations with pathogenic FF carriage in HIV-infected individuals (p<0.05; Table 3). In multivariate analysis, after adjusting for the influence of rodent exposure, hay or chaff exposure, and respiratory tract infections, OIs (OR, 1.97; 95% CI, 1.23–3.13, p=0.004), and smoking history (OR, 1.55; 95%CI, 1.03–2.32, p=0.035) were independent risk factors of pathogenic FF carriage in HIV-infected individuals (Table 4).

IFD in pathogenic FF carriers with HIV infection during follow-up

In this study, all 119 pathogenic FF carriers with HIV infection were followed through the end of 2019, and none developed IFD. As shown in Table 5, 93.3% of the patients have received ART at baseline, and 100% during follow-up. During follow-up, 90% of the patients had CD4+ count >200 cells/μl, 95.4% had sustained virologic suppression (HIV RNA quantitative <50 copies/ml; Table 5).

TABLE 3 Univariate analysis of risk factors for pathogenic filamentous fungi carriage in HIV-infected group.

Variates	Pathogenic filamentous fungi[a]		OR (95% CI)	p-value
	Non-carrier (n=597)	Carrier (n=119)		
Male	500 [83.8]	102 [85.7]	1.16 (0.67–2.03)	0.593
Age groups	–	–	–	0.627
18–39 years	415 [69.5]	78 [65.5]	1 (ref)	–
40–63 years	175 [29.3]	40 [33.6]	1.22 (0.80–1.85)	–
>63 years	7 [1.2]	1 [0.8]	0.76 (0.09–6.26)	–
Environmental exposures within 6 months				
Rodent exposure	26 [4.4]	10 [8.4]	2.02 (0.95–4.30)	0.070
Hay or chaff exposure	54 [9.0]	17 [14.3]	1.68 (0.93–3.01)	0.083
Cured infection within 1 year				
Respiratory tract infections	402 [67.3]	70 [58.8]	0.69 (0.46–1.04)	0.075
Other infectious diseases	201 [33.7]	38 [31.9]	0.92 (0.61–1.41)	0.714
OIs	95 [15.9]	33 [27.7]	2.03 (1.28–3.20)	0.002
Smoking history	201 [33.7]	53 [44.5]	1.58 (1.06–2.36)	0.024
Alcoholism	32 [5.4]	10 [8.4]	1.62 (0.77–3.39)	0.201
ART	–	–	–	0.165
Non-ART	71 [11.9]	8 [6.7]	1 (ref)	–
ART <1 year	167 [28.0]	30 [25.2]	1.59 (0.70–3.65)	–
ART ≥1 year	359 [60.1]	81 [68.1]	2.00 (0.93–4.32)	–
CD4 + T cell count	–	–	–	0.570
<200 cell/μl	95 [15.9]	22 [18.5]	1 (ref)	–
200–500 cells/μl	327 [54.8]	59[49.6]	0.78 (0.45–1.34)	–
>500 cells/μl	175 [29.3]	38 [31.9]	0.94 (0.52–1.68)	–
HIV RNA quantitative <50 copies/ml	347 [89.0] [b]	81 [94.2] [c]	0.50 (0.19–1.30)	0.154

Data were expressed as n [%], or odds ratios (OR) and 95% confidence interval (CI), as appropriate. HIV, human immunodeficiency virus; OR, odds ratio; OIs, opportunistic infections; ART, antiretroviral therapy.
[a]Upper respiratory tract samples include nasopharyngeal swabs and oropharyngeal swabs.
[b]Information about HIV RNA quantitative was missing for 207 non-carriers.
[c]Information about HIV RNA quantitative was missing for 33 carriers; All variables of variance inflation factor (VIF: 1.023–2.683) were less than 5–10; Variables with p<0.10 in the univariate analysis were included in the multivariate analysis.

Discussion

In the present study, we found that asymptomatic fungal carriage in the upper respiratory tract is common in HIV-infected individuals, and both smoking and cured OIs history significantly

TABLE 4 Multivariate analysis of risk factors for pathogenic filamentous fungi carriage in HIV-infected group.

Variates	OR	95% CI		*p*-value
		Lower	Upper	
Rodent exposure	2.08	0.95	4.57	0.068
Hay or chaff exposure	1.56	0.85	2.87	0.154
Respiratory tract infections	0.67	0.44	1.01	0.056
Smoking history	1.55	1.03	2.32	0.035
OIs	1.97	1.23	3.13	0.004
Constant	0.17	–	–	<0.001

HIV, human immunodeficiency virus; OR, odds ratio; OIs, opportunistic infections.

TABLE 5 Baseline characteristics and follow-up of pathogenic filamentous fungi carriers with HIV infection.

	Baseline ($n = 119$)	Follow-up ($n = 119$)
CD4 + T cell count		
<50 cells/μl	3 [2.5]	2 [1.7]
≥50, <200 cells/μl	19 [16.0]	10 [8.4]
200–500 cells/μl	59 [49.6]	56 [47.1]
> 500 cells/μl	38 [31.9]	51 [42.9]
HIV RNA quantitative <50 copies/ml[a]	81 [94.2]	104 [95.4]
ART (n [%])	111 [93.3]	119 [100.0]
Duration of ART (Months)	25 (11–46)	52 (35–73)
Minimum duration of ART (Months)	0	28
Longest duration of ART (Months)	135	163
Invasive fungal infection (n [%])	0 [0.0]	0 [0.0]

Data are expressed as medians (interquartile range), or n [%], as appropriate. HIV, human immunodeficiency virus; ART, antiretroviral therapy.
[a]Information about HIV RNA quantitative was missing for 33 patients at baseline, and 10 patients at follow-up.

increase their risk of pathogenic FF carriage. Besides, asymptomatic carriage of pathogenic FF in HIV-infected individuals does not appear to increase the risk of IFD.

As the access to ART expands, AIDS-relative mortality rates declined year by year. However, IFD remains a fatal threat to patients with advanced AIDS, and its mortality is second only to that of tuberculosis (Hoving et al., 2020). Most occurring cases of IFD begin by inhalation of fungal spores or the colonization of fungi (Von Lilienfeld-Toal et al., 2019; Pathakumari et al., 2020). With the destruction of immunity, FF carried on the mucosal surface can break through the mucosal barrier and cause IFD.

The upper respiratory tract is a major portal for microbial invasion, but few studies had investigated fungal carriage of the upper respiratory tract in patients with HIV infection. We reported the carriage of fungi in HIV-infected and healthy individuals and found that the asymptomatic fungal carrier rate was up to 90.2% in HIV-infected individuals and 80.9% in healthy controls. In our study, 41.9% of the HIV-infected individuals carried yeast-like fungi, which is consistent with previous studies (Maurya et al., 2013; Goulart et al., 2018; Aboualigalehdari et al., 2020). Although FF carrier rate was higher in HIV-infected individuals than that in healthy persons in our report, it was mainly caused by non-pathogenic FF. Pathogenic *Aspergillus* was the most common pathogenic FF, which was present in 16.1% of HIV-infected individuals. The prevalence of pathogenic *Aspergillus* carriers was similar between patients with and without HIV infection, which could be interpreted by host immune response. Human immunity against fungal hyphae is mainly performed by phagocytic cells, especially neutrophils (Rex et al., 1990; Mircescu et al., 2009). The phagocytic cell functions are intact in HIV-infected individuals as HIV primarily infects CD4+ T cells (Singh, 2021). Besides, the majority of participants in our study had relatively preserved immune function with CD4+ counts of more than 200 cells/μl. We reported three asymptomatic Mucorales carriers and two *Talaromyces marneffei* carriers in the HIV-infected group. This suggests that HIV-infected individuals are still at risk of being colonized by the above fungi even if their immune function is relatively preserved. Notably, patients with advanced AIDS are frequently comorbid with neutropenia, and the colonization of pathogenic FF may be a potential threat to IFD (Levine et al., 2006; Shi et al., 2014).

In this study, HIV-infected individuals with smoking history were found to have a 55% increased risk of pathogenic FF carriage (OR, 1.55; 95%CI, 1.03–2.32, $p = 0.035$). Tobacco smoke exerts widespread toxic effects on the immune system (Yamaguchi,

2019). It can inhibit phagocytosis and killing of foreign bodies by macrophages and neutrophils in the mucosa, inhibit the expression of interferon gamma (IFN-γ) gene, and increase regulatory T lymphocyte (Treg) counts, thus impairing the capacity of the body to remove fungi at mucosal surfaces (Yamaguchi, 2019). A study in the United States also found that smoking increased the risk of *Pneumocystis* colonization among HIV-infected men (Morris et al., 2004). Smoking is common among HIV-infected individuals and is associated with adverse outcomes (Helleberg et al., 2013, 2015; Giles et al., 2018). It is necessary to promote health education to reduce the smoking rate of HIV-infected people. The history of cured OIs in HIV-infected individuals was also found to be a risk factor for pathogenic FF carriage, which may be related to low immunity. The occurrence of OIs usually means severe immunodeficiency in patients with HIV infection, and although most patients achieve persistent virological suppression after ART, there is usually incomplete immune reconstitution, resulting in inadequate clearance of mucosal fungi (Yang et al., 2020).

In this study, pathogenic FF carriers with HIV infection were followed up for about 2.5 years, and none developed IFD. All of those patients received ART for at least 28 months, and most achieved sustained virologic suppression and immune reconstitution. This suggests that effective ART is critical for the prevention of IFD in HIV-infected individuals. Pathogenic FF carriage does not increase the risk of IFD in patients with good immune-controlled HIV infection.

This is the first study to investigate asymptomatic fungal carriers among HIV-infected individuals and healthy persons. Previous studies concentrate more on the colonization of bacteria and candida, and the prevalence and risk factors of FF colonization in HIV-infected patients were unknown before this study (Maurya et al., 2013; Goulart et al., 2018; Rossetti et al., 2019; Aboualigalehdari et al., 2020).

Our study had some limitations. Firstly, the definition of pathogenic FF was based on what was reported in the literature, other FF may be pathogenic but have been missed. Secondly, molecular methods were not used in all isolates, but only when identification by morphological methods was not possible. Despite careful identification, some fungal strains without molecular biological identification may have been misidentified. Therefore, further study with complete molecular methods is needed to confirm our findings. Thirdly, most of the participants had received ART and achieved immune reconstitution, so the conclusions from this study may only apply to those who had received effected ART and achieved sustained virologic suppression and immune reconstitution. Notably, once ART is interrupted and the immune deficiency is aggravated, the colonized fungi may invade the host and develop IFD. Further study is needed to explore the mechanism of fungal colonization, the relationship between colonization and infection, and the way to improve the micro-ecological environment in patients with HIV infection.

In summary, asymptomatic fungal carriage is common in HIV-infected individuals but may not develop IFD in those who achieved immune reconstitution. Smoking and cured OIs history increase the risk of pathogenic FF carriage. Smoking abstinence and ART adherence are especially important for these patients.

Data availability statement

The datasets presented in this study can be found in online repositories. The names of the repository/repositories and accession number(s) can be found below: NCBI GenBank database with accession number of OP103924-OP103949 and OP237033-OP237524.

Ethics statement

The studies involving human participants were reviewed and approved by Medical Ethics Committee of the Guangzhou Eighth People's Hospital. The patients/participants provided their written informed consent to participate in this study.

Author contributions

XC: conceptualization (equal), formal analysis (lead), and writing – original draft preparation (lead). YC: conceptualization (equal), methodology (lead), and writing – review and editing (equal). MC: conceptualization (equal), investigation (lead), and writing – review and editing (equal). HW: investigation (equal), methodology (equal), and writing – review and editing (equal). PD, HL, HZ, QL, SZ, and WCh: investigation (equal) and methodology (equal). ZY: methodology (equal) and formal analysis (equal). WCa: supervision (lead) and writing – review and editing (equal). XT and LL: conceptualization (lead), project administration (lead), and writing – review and editing (lead). All authors contributed to the article and approved the submitted version.

Funding

This work was supported by grants from the Guangzhou Basic Research Program on People's Livelihood Science and Technology (grant number: 202002020005) and the National Natural Science Foundation of China (grant number: 82072265).

Acknowledgments

We gratefully acknowledge our study group members for their work.

Conflict of interest

The authors declare that the research was conducted in the absence of any commercial or financial relationships that could be construed as a potential conflict of interest.

Publisher's note

All claims expressed in this article are solely those of the authors and do not necessarily represent those of their affiliated organizations, or those of the publisher, the editors and the reviewers. Any product that may be evaluated in this article, or claim that may be made by its manufacturer, is not guaranteed or endorsed by the publisher.

Supplementary material

The Supplementary material for this article can be found online at: https://www.frontiersin.org/articles/10.3389/fmicb.2022.968532/full#supplementary-material

References

Aboualigalehdari, E., Tahmasebi Birgani, M., Fatahinia, M., and Hosseinzadeh, M. (2020). Oral colonization by Candida species and associated factors in HIV-infected patients in Ahvaz, Southwest Iran. *Epi. Health* 42:e2020033. doi: 10.4178/epih.e2020033

Armstrong-James, D., Meintjes, G., and Brown, G. D. (2014). A neglected epidemic: fungal infections in HIV/AIDS. *Trends Microbiol.* 22, 120–127. doi: 10.1016/j.tim.2014.01.001

Brown, G. D., Denning, D. W., Gow, N. A. R., Levitz, S. M., Netea, M. G., and White, T. C. (2012). Hidden killers: human fungal infections. *Sci. Transl. Med.* 4:165rv13. doi: 10.1126/scitranslmed.3004404

Cadena, J., Thompson, G. R., and Patterson, T. F. (2021). Aspergillosis: epidemiology, diagnosis, and treatment. *Infect. Dis. Clin. N. Am.* 35, 415–434. doi: 10.1016/j.idc.2021.03.008

Cao, Y., Liu, F. L., Gong, D. D., Hu, F. Y., Chen, W. S., Cai, W. P., et al. (2021, 2021). Clinical characteristics and pathogenic spectrum analysis of pulmonary filamentous fungal infection in patients with AIDS in Guangdong Province. *Chin. J. Infect. Dis.* 39:6. doi: 10.3760/cma.j.cn311365-20200525-00623

Chastain, D. B., Henao-Martinez, A. F., and Franco-Paredes, C. (2017). Opportunistic invasive mycoses in AIDS: Cryptococcosis, Histoplasmosis, Coccidiodomycosis, and Talaromycosis. *Curr. Infect. Dis. Rep.* 19:36. doi: 10.1007/s11908-017-0592-7

Chiu, Y.-L., Liaw, S.-J., Wu, V.-C., and Hsueh, P.-R. (2005). Peritonitis caused by *Aspergillus sydowii* in a patient undergoing continuous ambulatory peritoneal dialysis. *J. Inf. Secur.* 51, e159–e161. doi: 10.1016/j.jinf.2004.12.008

Giles, M. L., Gartner, C., and Boyd, M. A. (2018). Smoking and HIV: what are the risks and what harm reduction strategies do we have at our disposal? *AIDS Res. Ther.* 15:26. doi: 10.1186/s12981-018-0213-z

Goulart, L. S., Souza, W. W. R. D., Vieira, C. A., Lima, J. S. D., Olinda, R. A. D., and Araújo, C. D. (2018). Oral colonization by Candida species in HIV-positive patients: association and antifungal susceptibility study. *Einstein* 16:eAO4224. doi: 10.1590/S1679-45082018AO4224

Hall, R. A., and Noverr, M. C. (2017). Fungal interactions with the human host: exploring the spectrum of symbiosis. *Curr. Opin. Microbiol.* 40, 58–64. doi: 10.1016/j.mib.2017.10.020

Helleberg, M., Afzal, S., Kronborg, G., Larsen, C. S., Pedersen, G., Pedersen, C., et al. (2013). Mortality attributable to smoking among HIV-1-infected individuals: a nationwide, population-based cohort study. *Clin. Infect. Dis.* 56, 727–734. doi: 10.1093/cid/cis933

Helleberg, M., May, M. T., Ingle, S. M., Dabis, F., Reiss, P., Fätkenheuer, G., et al. (2015). Smoking and life expectancy among HIV-infected individuals on antiretroviral therapy in Europe and North America. *AIDS* 29, 221–229. doi: 10.1097/QAD.0000000000000540

Hoving, J. C., Brown, G. D., Gómez, B. L., Govender, N. P., Limper, A. H., May, R. C., et al. (2020). AIDS-related mycoses: updated progress and future priorities. *Trends Microbiol.* 28, 425–428. doi: 10.1016/j.tim.2020.01.009

Hu, Y., Zhang, J., Li, X., Yang, Y., Zhang, Y., Ma, J., et al. (2013). Penicillium marneffei infection: an emerging disease in mainland China. *Mycopathologia* 175, 57–67. doi: 10.1007/s11046-012-9577-0

Levine, A. M., Karim, R., Mack, W., Gravink, D. J., Anastos, K., Young, M., et al. (2006). Neutropenia in human immunodeficiency virus infection: data from the Women's interagency HIV study. *Arch. Intern. Med.* 166, 405–410. doi: 10.1001/archinte.166.4.405

Marukutira, T., Huprikar, S., Azie, N., Quan, S.-P., Meier-Kriesche, H.-U., and Horn, D. L. (2014). Clinical characteristics and outcomes in 303 HIV-infected patients with invasive fungal infections: data from the prospective antifungal therapy Alliance registry, a multicenter, observational study. *HIV/AIDS* 6, 39–47. doi: 10.2147/HIV.S53910

Maurya, V., Srivastava, A., Mishra, J., Gaind, R., Marak, R. S. K., Tripathi, A. K., et al. (2013). Oropharyngeal candidiasis and Candida colonization in HIV positive patients in northern India. *J. Infect. Dev. Ctries.* 7, 608–613. doi: 10.3855/jidc.2801

Mircescu, M. M., Lipuma, L, Van Rooijen, N., Pamer, E. G., Pamer, E. G., and Hohl, T. M. (2009). Essential role for neutrophils but not alveolar macrophages at early time points following Aspergillus fumigatus infection. *The Journal of Infectious Diseases* 200, 647–656. doi: 10.1086/600380

Moreira, J., Varon, A., Galhardo, M. C., Santos, F., Lyra, M., Castro, R., et al. (2016). The burden of mucormycosis in HIV-infected patients: a systematic review. *J. Inf. Secur.* 73, 181–188. doi: 10.1016/j.jinf.2016.06.013

Morris, A., Kingsley, L. A., Groner, G., Lebedeva, I. P., Beard, C. B., and Norris, K. A. (2004). Prevalence and clinical predictors of pneumocystis colonization among HIV-infected men. *AIDS* 18, 793–798. doi: 10.1097/00002030-200403260-00011

Pathakumari, B., Liang, G., and Liu, W. (2020). Immune defence to invasive fungal infections: a comprehensive review. *Biomed. Pharm.* 130:110550. doi: 10.1016/j.biopha.2020.110550

Perri, P., Campa, C., Incorvaia, C., Parmeggiani, F., Lamberti, G., Costagliola, C., et al. (2005). Endogenous Aspergillus versicolor endophthalmitis in an immuno-competent HIV-positive patient. *Mycopathologia* 160, 259–261. doi: 10.1007/s11046-005-6871-0

Rex, J. H., Bennett, J. E., Gallin, J. I., Malech, H. L., and Melnick, D. A. (1990). Normal and deficient neutrophils can cooperate to damage Aspergillus fumigatus hyphae. *J. Infect. Dis.* 162, 523–528.

Rossetti, B., Lombardi, F., Belmonti, S., D'andrea, M. M., Tordini, G., D'avino, A., et al. (2019). Nasopharingeal bacterial and fungal colonization in HIV-positive versus HIV-negative adults. *New Microbiol.* 42, 37–42.

Schwetz, I., Horina, J., Buzina, W., Roob, J., Olschewski, H., and Krause, R. (2007). *Aspergillus oryzae* peritonitis in CAPD: case report and review of the literature. *Am. J. Kid. Dis.* 49, 701–704. doi: 10.1053/j.ajkd.2007.02.260

Shi, X., Sims, M. D., Hanna, M. M., Xie, M., Gulick, P. G., Zheng, Y.-H., et al. (2014). Neutropenia during HIV infection: adverse consequences and remedies. *Int. Rev. Immunol.* 33, 511–536. doi: 10.3109/08830185.2014.893301

Singh, R. K. (2021). Chronic pulmonary aspergillosis in a patient with AIDS. *Cureus* 13:e14588. doi: 10.7759/cureus.14588

Von Lilienfeld-Toal, M., Wagener, J., Einsele, H., Cornely, O. A., and Kurzai, O. (2019). Invasive fungal infection. *Deut. Arzteblatt Int.* 116, 271–278. doi: 10.3238/arztebl.2019.0271

Yamaguchi, N. H. (2019). Smoking, immunity, and DNA damage. *Trans. Lung Can. Res.* 8, S3–S6. doi: 10.21037/tlcr.2019.03.02

Yang, X., Su, B., Zhang, X., Liu, Y., Wu, H., and Zhang, T. (2020). Incomplete immune reconstitution in HIV/AIDS patients on antiretroviral therapy: challenges of immunological non-responders. *J. Leukoc. Biol.* 107, 597–612. doi: 10.1002/JLB.4MR1019-189R

Ying, R. S., Le, T., Cai, W. P., Li, Y. R., Luo, C. B., Cao, Y., et al. (2020). Clinical epidemiology and outcome of HIV-associated talaromycosis in Guangdong, China, during 2011-2017. *HIV Med.* 21, 729–738. doi: 10.1111/hiv.13024

frontiers | Frontiers in Immunology

TYPE Review
PUBLISHED 10 November 2022
DOI 10.3389/fimmu.2022.1015775

OPEN ACCESS

EDITED BY
Xia Jin,
Fudan University, China

REVIEWED BY
Julliana Ribeiro Alves Dos Santos,
Universidade Ceuma, Brazil
Charikleia Stefanaki,
National and Kapodistrian University of Athens, Greece

*CORRESPONDENCE
Bin Su
binsu@ccmu.edu.cn
Tong Zhang
zt_doc@ccmu.edu.cn

SPECIALTY SECTION
This article was submitted to Viral Immunology, a section of the journal Frontiers in Immunology

RECEIVED 10 August 2022
ACCEPTED 26 October 2022
PUBLISHED 10 November 2022

CITATION
Li S, Yang X, Moog C, Wu H, Su B and Zhang T (2022) Neglected mycobiome in HIV infection: Alterations, common fungal diseases and antifungal immunity.
Front. Immunol. 13:1015775.
doi: 10.3389/fimmu.2022.1015775

Neglected mycobiome in HIV infection: Alterations, common fungal diseases and antifungal immunity

Shuang Li[1,2], Xiaodong Yang[1,2], Christiane Moog[3,4], Hao Wu[1,2], Bin Su[1,2]* and Tong Zhang[1,2]*

[1]Beijing Key Laboratory for HIV/AIDS Research, Clinical and Research Center for Infectious Diseases, Beijing Youan Hospital, Capital Medical University, Beijing, China, [2]Sino-French Joint Laboratory for Research on Humoral Immune Response to HIV Infection, Clinical and Research Center for Infectious Diseases, Beijing Youan Hospital, Capital Medical University, Beijing, China, [3]Laboratoire d'ImmunoRhumatologie Moléculaire, Institut national de la santé et de la recherche médicale (INSERM) UMR_S 1109, Institut thématique interdisciplinaire (ITI) de Médecine de Précision de Strasbourg, Transplantex NG, Faculté de Médecine, Fédération Hospitalo-Universitaire OMICARE, Fédération de Médecine Translationnelle de Strasbourg (FMTS), Université de Strasbourg, Strasbourg, France, [4]Vaccine Research Institute (VRI), Créteil, France

Human immunodeficiency virus (HIV) infection might have effects on both the human bacteriome and mycobiome. Although many studies have focused on alteration of the bacteriome in HIV infection, only a handful of studies have also characterized the composition of the mycobiome in HIV-infected individuals. Studies have shown that compromised immunity in HIV infection might contribute to the development of opportunistic fungal infections. Despite effective antiretroviral therapy (ART), opportunistic fungal infections continue to be a major cause of HIV-related mortality. Human immune responses are known to play a critical role in controlling fungal infections. However, the effect of HIV infection on innate and adaptive antifungal immunity remains unclear. Here, we review recent advances in understanding of the fungal microbiota composition and common fungal diseases in the setting of HIV. Moreover, we discuss innate and adaptive antifungal immunity in HIV infection.

KEYWORDS

mycobiome, fungal diseases, fungal microbiota, antifungal immunity, HIV

Introduction

The human mycobiome inhabits the skin, respiratory tract, gastrointestinal tract, genitourinary tract, and other mucosal surfaces of the host. It has been shown that over 600 different fungi can cause disease in humans (1). In addition, over 300 million people are affected by serious fungal diseases, causing over 1.6 million deaths each year (2). The

increased incidence of global epidemic mycoses might be attributed to changes in the environment, population growth in endemic areas, and increased human immunodeficiency virus (HIV)-related immunosuppressive status (3).

In HIV infection, differences in bacterial population composition, including the oral microbiome (4, 5), lung microbiome (6, 7) and gut microbiome (8, 9), have been reported in HIV-infected compared to uninfected individuals. In addition, immunity compromised by HIV infection may lead to altered fungal composition, promoting the development of opportunistic fungal infections in HIV-infected individuals (10). It has been shown that opportunistic fungal infections have an unacceptably high toll on people living with HIV (PLWH) and are a major driver of HIV-related death (11). Although ART might decrease the mortality rate, the substantial burden of fungal disease remains high for HIV-infected individuals who are undiagnosed, untreated or fail ART (12). Fungal diseases in HIV infection have also not received sufficient attention from the global community (11).

It has been shown that host innate and adaptive immune responses play an important role in controlling fungal infections (13). Innate antifungal immune responses are triggered when fungal antigens, such as α- and β-glucans, O- and N-linked mannans, and chitin, stimulate pattern recognition receptors (PRRs) expressed on host cells, including C-lectin receptors (CLRs), NOD (nucleotide-binding and oligomerization domain)-like receptors (NLRs), and Toll-like receptors (TLRs), to initiate signal transduction cascades, which promote the production of chemokines and cytokines to eliminate fungal pathogens and activate adaptive responses (14). However, the substantial loss of $CD4^+$ T cells in HIV infection might lead to deficiencies in antifungal immunity, contributing to an increased risk of opportunistic fungal infections. Furthermore, depletion of interleukin (IL)-17 and IL-22-producing T helper (Th) 17 cells might result in impaired integrity of mucosal epithelial barriers, leading to fungal translocation from the gut lumen into the systemic circulation (15, 16). Microbial translocation might contribute to HIV-associated immune activation and inflammation, as well as the development of non-AIDS events (15, 16).

Because appropriate culture conditions remain unclear, most of the human mycobiome is nonculturable by culture-dependent methods (17). However, with the advent of new techniques, next-generation sequencing has been widely used for mycobiome detection in recent years (18). Internal transcribed spacer (ITS) sequencing and 18S rRNA are the most applied techniques to detect the mycobiome (19). In this review, we discuss alterations in the mycobiome and common fungal diseases in HIV infection, as well as the effects of HIV infection on innate and adaptive antifungal immunity.

Alterations of the mycobiome in HIV infection

The oral mycobiome in HIV infection

Alterations in oral bacterial communities and virome in HIV-infected individuals have been reported in many studies (4, 5, 20–22). The possible reasons for oral microbiome dysbiosis might be the disrupted oral immunity caused by HIV infection, including changes in secretory components in saliva, deficiency of innate immune responses and adaptive immune responses (5).

In addition to oral bacterial and virus communities, the oral mycobiome might contribute to understanding host–pathogen interactions that occur in HIV infection (23). For example, Ghannoum et al. characterized the oral mycobiome in healthy individuals using ITS sequencing (24), detecting 74 culturable and 11 nonculturable fungal genera (24). *Candida* species were the most frequent of the oral mycobiome (isolated from 75% of participants), followed by *Cladosporium* (65%), *Aureobasidium* and *Saccharomycetales* (50%, respectively) (24). Previous studies have demonstrated that oral fungal colonization is altered in HIV infection (25–28) (Table 1). In HIV-infected individuals, *Candida* (92%), *Epicoccum* (33%), and *Alternaria* (25%) are the most common genera in the oral mycobiome, whereas the most abundant oral mycobiome genera in HIV-uninfected controls are *Candida*, *Pichia*, and *Fusarium*, present in 58%, 33%, and 33%, respectively (25, 26). A recent study also compared the oral mycobiome between 30 HIV-infected individuals and 30 healthy controls and explored the effect of ART on the oral mycobiome in HIV infection. They found *Candida*, *Mortierella*, *Malassezia*, *Simplicillium*, and *Penicillium* to be significantly increased in HIV-infected individuals and dramatically decreased after ART. In contrast, the abundances of *Verticillium*, *Issatchenkia*, and *Alternaria* were significantly increased in PLWH after ART (27). They found that the composition of the oral mycobiome in the HIV-infected subjects after 6 months of ART was similar to that in the HIV-uninfected individuals. Moreover, *Mortierella*, *Malassezia*, *Simplicillium*, and *Chaetomium* were positively associated with viral load (VL), and *Verticillium*, *Thyrostroma* and *Archaeorhizomyces* were negatively associated with VL and positively correlated with $CD4^+$ T-cell counts. In addition, *Saccharomyces* was positively correlated with VL and negatively associated with $CD4^+$ T-cell counts (27). Therefore, HIV infection and ART administration might impact on the composition of the oral mycobiome, and the dysbiosis of oral mycobiome in HIV infection could be partially restored after ART. Furthermore, some oral fungi were sensitive to the changes in $CD4^+$ T-cell counts and VL in the blood of HIV-infected individuals, thus changes in the oral mycobiome in HIV infection after ART may reflect the immune status of patients.

The respiratory tract mycobiome in HIV infection

Due to incomplete restoration of pulmonary immunity with ART, HIV-infected individuals continue to have high burdens of pulmonary comorbidities, including chronic obstructive pulmonary disease (COPD) (34, 35), lung cancer (36–38), pulmonary fibrosis (39) and pulmonary emphysema (39–41). Overall, the complex respiratory tract microbiome, including the lung mycobiome, may play an important role in lung disease (42).

Previous studies have indicated that the diversity and composition of the lung microbiome in HIV-infected patients are altered compared with HIV-uninfected individuals (43–45) (Table 1). In addition, studies have also reported alterations in the respiratory tract mycobiome in HIV-infected individuals. Bittinger et al. analyzed bronchoalveolar lavage (BAL) samples from 42 lung transplant patients, 19 HIV-positive patients, 13 patients with various pulmonary diseases and 12 healthy controls; only low levels of fungal reads were detected in the healthy individuals, and the fungi detected comprised taxa with little clinical significance, except for *Aspergillus*. Conversely, clinical pathogens such as *Pneumocystis*, *Cryptococcus*, and *Aspergillus* were found in BAL of HIV-infected subjects (30). Another study published by Cui et al. compared fungal communities in the respiratory tract from 24 healthy subjects and 32 HIV-infected subjects: 9 species were overrepresented in the BAL of HIV-infected subjects, including *Pneumocystis jirovecii*, *Junghuhnia nitida*, *Phlebia tremellosa*, *Oxyporus latemarginatus*, *Sebacina incrustans*, *Ceriporia lacerata*, *Pezizella discrete*, *Trametes hirsute*, and *Daedaleopsis confragosa* (29). Of these species, *Pneumocystis jirovecii* and *Ceriporia lacerata* are known to be pulmonary pathogens associated with immunosuppression. In addition, *Pneumocystis jirovecii* pneumonia (PCP) is one of the most common opportunistic infections in PLWH. These data reveal that alterations in the respiratory tract mycobiome might be an important driver of opportunistic infection in HIV-infected individuals.

The gut mycobiome in HIV infection

The gut microbiome is being progressively recognized as playing an important role in promoting immune activation and inflammation in HIV infection. Dysbiosis of the gut microbiome

TABLE 1 The mycobiome in HIV infection.

References	Study cohort	Samples	Design	Mycobiome alterations
The oral mycobiome in HIV infection				
Chang et al. (27)	30 HIV$^+$ subjects prior to and after 6 months of ART and 30 healthy controls	Saliva	Cross-sectional and longitudinal	• Increased *Candida*, *Mortierella*, *Malassezia*, *Simplicillium*, and *Penicillium* in the HIV group, decreasing after ART. • Increased *Verticillium*, *Issatchenkia*, and *Alternaria* in HIV$^+$ subjects after ART.
Fidel et al. (28)	149 HIV$^+$ subjects and 88 HIV$^-$ subjects	Oral rinse	Cross-sectional	• Predominated by four major clusters: *Candida albicans*, *Candida dubliniensis*, *Malassezia restricta*, and *Saccharomyces cerevisiae*. • Several clinical variables affect the oral mycobiome, including HIV positivity and ART.
Mukherjee et al. (25)	12 HIV-infected and 12 uninfected individuals	Oral rinse	Cross-sectional	• Enrichment of *Candida*, *Epicoccum*, and *Alternaria* in HIV-infected individuals (present in 92%, 33%, and 25%, respectively) and *Candida*, *Pichia*, and *Fusarium* in uninfected individuals (58%, 33%, and 33%, respectively).
The respiratory tract mycobiome in HIV infection				
Cui et al. (29)	32 HIV-infected and 24 HIV-uninfected individuals	Oral washes, induced sputa, and BAL	Cross-sectional	• Increased *Pneumocystis jirovecii*, *Junghuhnia nitida*, *Phlebia tremellosa*, *Oxyporus latemarginatus*, *Sebacina incrustans*, *Ceriporia lacerata*, *Pezizella discrete*, *Trametes hirsute*, and *Daedaleopsis confragosa* in HIV-infected individuals.
Bittinger et al. (30)	19 HIV$^+$ subjects and 12 healthy controls	Oropharyngeal wash and BAL	Cross-sectional	• Increased clinical pathogens *Pneumocystis*, *Cryptococcus*, and *Aspergillus* in HIV-infected individuals.
The gut mycobiome in HIV infection				
Hamad et al. (31)	31 HIV-infected individuals and 12 uninfected-HIV individuals	Fecal	Cross-sectional	• Enriched *Ascomycota*, *Pichia*, *Penicillium brevicompactum* and *Penicillium* in healthy controls and enriched *Candida albicans* and *Candida tropicalis* in HIV-infected individuals.
Wu et al. (32)	75 HIV-infected patients and 55 HIV-uninfected participants	Fecal	Cross-sectional	• Nectriaceae, Hypocreales, and Sordariomycetes were the top 3 fungal taxa in HIV-infected individuals. While Basidiomycota, Phallaceae, and Phallales were particularly enriched in HIV-uninfected controls.
Yin et al. (33)	18 HIV-infected patients and 22 healthy controls	Fecal	Cross-sectional	• *Aspergillus* was the most abundant genus (49.92%) in the HIV-infected group, while the most abundant fungal genus was *Candida* (38.31%) in the healthy controls. • Unclassified_Aspergillaceae and Dirkmeia were enriched in the high-CD4$^+$ T-cell group, while *Candida*, Sordariales, Saccharomycetaceae, and *Neocosmospora* were enriched in the low-CD4$^+$ T-cell group.

HIV, human immunodeficiency virus; ART, antiretroviral therapy; BAL, bronchoalveolar lavage.

has been demonstrated in many studies (9, 46, 47), and such alterations of the gut microbiome composition in HIV infection might be attributed to the loss of appropriate innate and adaptive immune responses (48).

In the human gut, the diversity of the fungal community is much lower than that of the bacterial microbiota (49). Fungi in the gastrointestinal tract are often ignored, as fungi comprise a tiny fraction of the gut microbes and most are unculturable. Previous studies have been shown that *Candida*, *Saccharomyces*, *Aspergillus*, *Cryptococcus*, *Malassezia*, *Cladosporium*, *Galactomyces* and *Trichosporon* can grow at 37°C and therefore have the potential to permanently colonize in the gut (50). In addition, although *Histoplasma* spp., *Coccidioides* spp. and *Blastomyces* spp. cannot colonize the mucosal surfaces, they can cause severe lung infections (51) (Figure 1). A recent study investigated the gut mycobiome of the Human Microbiome Project (HMP) cohort and revealed *Saccharomyces*, *Malassezia*, and *Candida* to be the most abundant genera present in this cohort (49). In a study of 96 healthy individuals, the most common genera in fecal samples were *Saccharomyces*, *Candida* and *Cladosporium* (present in 89%, 57% and 42%, respectively) (52). Another study showed that the most prevalent genus in healthy individuals is *Penicillium* (present in 73% of samples), followed by *Candida* and *Saccharomyces* (55% for both), *Mucor* (38%) and *Aspergillus* (35%) (53). Additionally, gut mycobiome alterations in HIV infection have been reported (Table 1). Gouba et al. found decreased fungal species diversity in HIV-infected individuals (54), showing significantly more abundance of *Candida* spp. in HIV-infected patients than in healthy individuals. *Candida albicans* in the gut can affect many processes, such as digestion and immunity (55). *Candida* spp. are more prevalent in HIV-infected individuals with diarrhea and

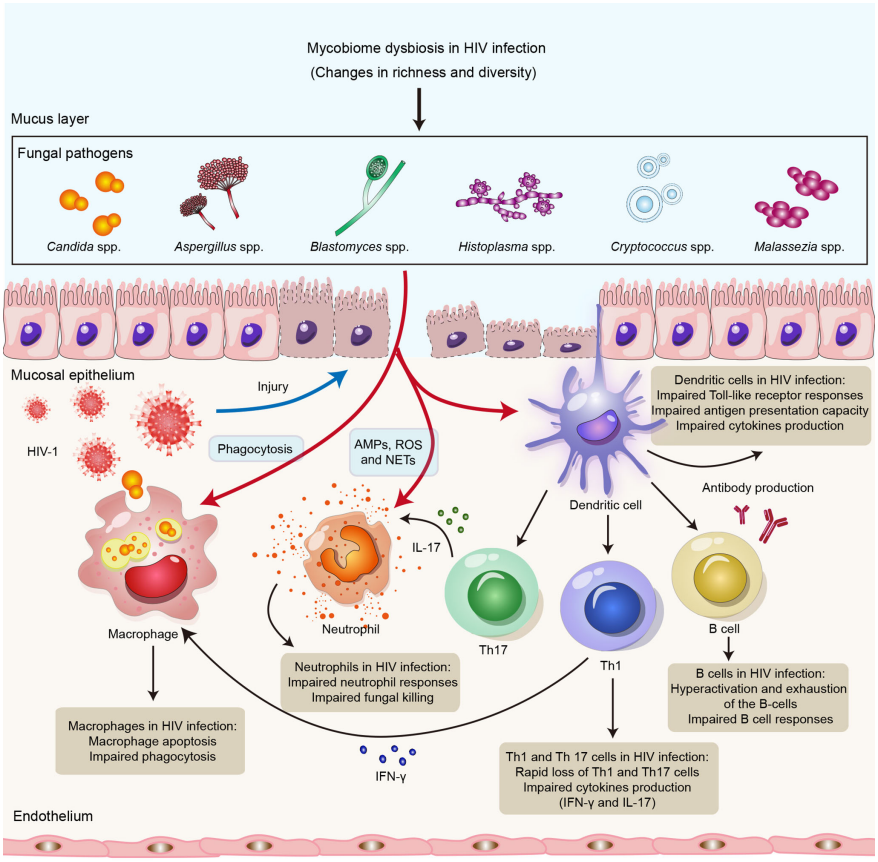

FIGURE 1
Impact of HIV infection on innate and adaptive immune responses to opportunistic fungal pathogens. HIV infection might lead to impairment of the innate and adaptive arms of the immune system, resulting in susceptibility to opportunistic fungal infections. Neutrophils control fungal infections through multiple mechanisms, including AMPs, ROS and NETs. Macrophages directly kill invading fungi through phagocytosis. DCs recognize fungal antigens by PRRs and also promote Th1 and Th17 immunity, as well as antibody production, to clear fungal infections. HIV can not only lead to impairment of neutrophil responses, phagocytosis of macrophages and the antigen presentation capacity of DCs but also cause defects in Th1, Th12 and B-cell responses. Abbreviations: AMPs, antimicrobial peptides; ROS, reactive oxygen species; NETs, neutrophil extracellular traps; DCs, dendritic cells; Th1, T helper 1 cell; Th17, T helper 1 cell; PRR, pattern recognition receptor.

recent antibiotic treatment than in healthy controls (54). Yin et al. showed that *Aspergillus* was the most abundant genus (49.92%) in the HIV-infected group, while the most abundant fungal genus was *Candida* (38.31%) in the healthy controls (33). Wu et al. found that 4 taxa from Ascomycota and 16 taxa from Basidiomycota were differentiated between HIV-infected individuals and HIV-uninfected controls in the fungal linear discriminant analysis (LDA) analysis. *Nectriaceae*, *Hypocreales*, and *Sordariomycetes* were the top 3 fungal taxa in HIV-infected individuals. While *Basidiomycota*, *Phallaceae*, and *Phallales* were particularly enriched in HIV-uninfected controls (32). Another study also compared the fungal populations of fecal samples from HIV-infected individuals and healthy controls; *Ascomycota*, *Pichia*, *Penicillium brevicompactum* and *Penicillium* were more abundant in healthy controls, whereas the abundances of *Candida albicans* and *Candida tropicalis* were enriched in HIV-infected individuals (31). In addition, Yin et al. demonstrated the relationship between $CD4^+$ T-cell counts and the gut mycobiome in the HIV-infected participants (33). They found that patients with low $CD4^+$ T-cell counts and patients with high $CD4^+$ T-cell counts have different fungal community characteristics. *Eurotiomycetes* was significantly decreased and *Saccharomycetes* was significantly increased in the low $CD4^+$ T-cell group compared to the high $CD4^+$ T-cell group. At the genus level, *Candida* was significantly increased in the low $CD4^+$ T-cell group, indicating a high risk of opportunistic infection. Moreover, unclassified *Aspergillaceae* and *Dirkmeia* were enriched in the high $CD4^+$ T-cell group, while *Sordariales*, *Saccharomycetaceae*, and *Neocosmospora* were enriched in the low $CD4^+$ T-cell group. It has been shown that members of the genus *Neocosmospora* can lead to lung infections in liver transplant patients (56) and contain highly prevalent and aggressive fungal pathogens (57), suggesting that the immune T-cell reduction might expose patients to a state of high-risk infection.

Common fungal diseases in HIV infection

Oropharyngeal candidiasis

OPC is the most common opportunistic fungal infection in the early stages of HIV infection (58–60). OPC is caused by various *Candida* species, with *Candida albicans* being the most prevalent species isolated from HIV-infected patients (58, 59, 61, 62). In patients with a new diagnosis of HIV, the prevalence of OPC is reportedly 27% (63). It has also been found that OPC occurs in approximately 80%-90% of HIV-infected individuals in different phases of the disease (64). Although the occurrence of OPC in HIV infection has significantly decreased after the introduction of ART, it remains a common opportunistic infection in HIV (65, 66).

The incidence of OPC in HIV infection is influenced by a multitude of factors (67), including immune status (68), bacteriome–mycobiome interaction (69), anti-fungal therapy and ART (70). Several studies have shown that a lower $CD4^+$ T-cell count, especially below 200 cells/μl, is strongly associated with increased occurrence of OPCs (71–74). A reduction in $CD4^+$ T cells, especially IL-17-producing cells, in the oral mucosa may be associated with susceptibility to OPC (75). In addition, impairment of oral immunity by the reduction of salivary components such as salivary IgA, defensins, and some cytokines might lead to the onset of OPC (76). However, host defense mechanisms executed by keratinocytes, calprotectin, $CD8^+$ T cells, and phagocytes partly compensate for these defects, which may play a key role in controlling *C. albicans* proliferation and preventing systemic dissemination in HIV infection (68).

Pneumocystis jirovecii pneumonia

PCP is one of the most common opportunistic fungal infections in immunocompromised individuals and HIV-infected individuals (77, 78). In the late 1980s, PCP occurred in approximately 75% of HIV-infected individuals (79), though the incidence of HIV-associated PCP has decreased dramatically with the implementation of ART and chemoprophylaxis (80). Nonetheless, PCP continues to be a serious problem in HIV-infected patients who are undiagnosed and untreated or in those with ART failure (81). It is speculated that there are more than 400,000 cases of PCP worldwide each year (82, 83).

As mentioned above, PCP tends to occur most frequently when the $CD4^+$ T-cell count is below 200 cells/μl (84–86), and $CD4^+$ T cells, $CD8^+$ T cells, neutrophils, alveolar macrophages and soluble mediators have been implicated in clearance of PCP (87). Carmona et al. demonstrated that *Pneumocystis*-derived β-glucans activate dendritic cells (DCs) through the Fas ligand (FasL) mechanism and the Dectin-1 receptor, leading to increased expression of costimulatory molecules and T helper 1 (Th1) cell activation (88). Another study found that DCs stimulated by cell-surface β-glucan components of *Pneumocystis* interact with lymphocytes to produce IL-17 and IL-22 (89). Th1, Th2 and Th17 responses are essential in *Pneumocystis* clearance and contribute to host protection against this pathogen (90). However, Th2 and Th17 responses also play a role in *Pneumocystis*-driven pathology (90). In addition, the cytokines produced by $CD4^+$ T cells, such as IFN-γ, also are important for the control of PCP (87, 90).

Cryptococcal meningitis

Cryptococcal meningitis (CM) is one of the most common opportunistic infections in the late stage of AIDS (91), and

Cryptococcus neoformans is the most common cause of death in HIV-infected individuals. An estimated 223,100 cases of CM occur globally each year, resulting in 181,100 deaths; 135,900 occur in sub-Saharan Africa, and CM accounts for 15% of all AIDS-related deaths (91). Despite effective ART and antifungal drugs, the mortality rate of CM in AIDS patients is still as high as 30%-50%, especially in patients in resource-poor areas (92–94).

Evidence suggests that host immune responses to cryptococcosis play a critical role in disease progression (95–97). CM can occur following primary lung infection or by reactivation and dissemination of latent pulmonary infection in the setting of cell-mediated immunodeficiency when $CD4^+$ T-cell counts are <100 cells/μl in the late-stages of HIV-infection (98). Previous studies have shown that $CD4^+$ T cells possibly mediate protective host immunity against cryptococcal *via* production of Th1-type cytokine responses, including IL-2, IL-12, tumor necrosis factor alpha (TNF-α), and IFN-γ, which play an essential role in recruitment of lymphocytes and phagocytes to clear the infection (99, 100). Higher levels of IFN-γ in cerebrospinal fluid (CSF) are associated with a faster rate of fungal clearance and lower fungal burdens (101, 102). Moreover, higher pre-ART levels of IL-4 and IL-17 and lower TNF-α, granulocyte colony-stimulating factor (G-CSF), granulocyte-macrophage colony-stimulating factor (GM-CSF) and vascular endothelial growth factor (VEGF) might predict future immune reconstitution inflammatory syndrome (IRIS) (103).

Talaromyces marneffei infection

Talaromycosis is an invasive fungal disease caused by the opportunistic fungus *Talaromyces marneffei* (TM) and is prevalent mainly in Southeast Asia. Since the HIV pandemic, the prevalence of talaromycosis has rapidly increased, especially in areas of Southeast Asia, including Thailand, Vietnam and Myanmar, and East Asia, including South China, Hong Kong, Taiwan, and northeastern India (104). A recent study showed that the prevalence of TM infection in Asia was 3.6% in HIV-infected individuals (105). The prevalence of TM infection in HIV-infected individuals has been reported to be 6.4% in Vietnam, 3.9% in Thailand, 3.3% in China, 3.2% in India, and 2.1% in Malaysia (105). Furthermore, mortality rate of TM infection is reportedly higher than that of most HIV-related complications in PLWH (106). Although ART has led to a decline in the incidence of TM infection, it remains a major problem in undiagnosed and untreated HIV-infected individuals (81).

Innate and acquired immune responses play a crucial role in controlling TM infection (107). Innate immune cells, including monocytes (108), macrophages (109, 110), polymorphonuclear neutrophils (PMNs) (111), and DCs (112) have been shown to play an essential role in combating TM. These innate immune cells promote clearance of TM infection by producing proinflammatory cytokines such as IL-1β, TNF-α, and IFN-γ and anti-inflammatory cytokines such as IL-10 (107). A recent study also demonstrated that single-nucleotide polymorphisms (SNPs) in TLR2 might contribute to increased susceptibility and severity of TM in Han Chinese populations (113). Moreover, another study found that severe TM infection in Southeast Asia may be related to the high prevalence of anti-IFN-γ autoantibody-associated HLA-DRB1*16:02 and HLA-DQB1*05:02 alleles (114). A previous study found that HIV-infected individuals with $CD4^+$ T-cell counts below 200 cells/μl had a higher risk of TM infection (105). In general, immune deficiencies that reduce $CD4^+$ T cells and IFN-γ, IL-12, and IL-17 functions may be predisposing factors for TM infection, as evidenced by the high infection burden in advanced HIV-infected individuals, highlighting the important roles of Th1 and Th17 responses in host resistance to TM infection (115).

Histoplasmosis

Histoplasmosis is caused by *Histoplasma capsulatum*, which is a common endemic mycosis in PLWH (116). Globally, epidemic distribution of histoplasmosis mainly in regions of the Americas (81). In addition, histoplasmosis is also endemic in many Asia areas, including Southeast Asia, India, and China along the Yangtze River (117, 118). With the spread of HIV, the case-fatality rates of disseminated histoplasmosis increased among culture-positive cases, ranging from 10% to 53% (119). Disseminated histoplasmosis has been neglected due to its nonspecific symptoms, frequent misdiagnosis as tuberculosis, and insensitive diagnostic methods (120).

HIV-infected individuals are at greatly increased risk of developing histoplasmosis, especially those with $CD4^+$ T-cell counts <200 cells/μl (121). *Histoplasma capsulatum* yeasts can infect macrophages and survive within phagocytic cells (122). The strategies of *Histoplasma capsulatum* against macrophages might include immune response evasion on entry, inactivation of nitrogen and oxygen reactive species, hindrance of lysosomal pH reduction, production of siderophore, prevention of phagolysosomal fusion, and induction of apoptosis (123). In addition to the control of *Histoplasma capsulatum* infection by cellular immune response, the roles of antibodies in the serodiagnosis of histoplasmosis have also been proposed. Almeida et al. characterized *Histoplasma capsulatum* proteins specifically recognized by antibodies in serum samples from histoplasmosis patients by an immunoproteomic approach (123).

Aspergillosis

Aspergillosis is a life-threatening fungal disease in immunocompromised individuals, including PLWH. Previous study has been shown that the incidence of aspergillosis was 3.5

cases per 1000 person-years among 35,252 HIV-infected individuals (124). Although aspergillosis occurs uncommonly in HIV-infected individuals, it is associated with a short lifespan after diagnosis.

It has been shown that older people, people with severe immunosuppression or advanced HIV disease, and people with leukopenia and neutropenia are at increased risk of developing aspergillosis (124). Before the advent of ART, invasive aspergillosis in HIV-infected individuals tended to occur when CD4 T-cell counts <100 cells/μl, especially in patients with prior or concomitant opportunistic infections (125). Therefore, modulation of host immunity plays a critical role in the control of aspergillosis. Animal studies in aspergillosis have also demonstrated beneficial effects of G-CSF, GM-CSF, IFN-γ, and monoclonal antibodies (126).

Antifungal immunity in HIV infection

Innate antifungal immunity in HIV infection

The innate immune response is the first line of defense against fungal infections (127). Innate immune cells, such as neutrophils, monocytes, macrophages, and dendritic cells, are known to have a crucial function in recognizing and clearing fungi, inducing protective immune responses, and initiating adaptive immune responses during fungal infections (127, 128). Neutrophils control fungal infections through multiple mechanisms, including production of granule proteins, antimicrobial peptides (AMPs) and reactive oxygen species (ROS) and formation of neutrophil extracellular traps (129, 130). Indeed, neutrophils are critical cells against *Candida* spp. and *Aspergillus* spp (131). Macrophages not only directly kill invading fungi through phagocytosis but also initiate and regulate downstream immune responses to clear fungal infections by releasing cytokines, presenting antigens, and recruiting other immune cells (132). Fungal antigens are also recognized by DCs mediated by CLRs, including dectin-1, dectin-2 and DC-SIGN, as well as TLRs, including TLR2, TLR4 and TLR9 (133). DCs might also collaborate with other immune cells, such as Group 2 innate lymphoid cells (ILC2s), to promote innate antifungal immune responses and regulate adaptive immune responses (130). Nevertheless, the effect of HIV infection on innate antifungal immunity remains unclear.

HIV does not directly infect neutrophils but can cause impaired neutrophil responses, leading to impaired bacterial and fungal killing, which might result in increased susceptibility to bacterial infections and mycoses (134). Enomoto et al. found that anti-cryptococcal activity in HIV-infected patients is enhanced by administration of granulocyte colony stimulating factor (G-CSF) to enhance neutrophil defense (135). Moreover, Kalem et al. showed that HIV-1 infection of THP-1 macrophages increases the rate of *Cryptococcus neoformans* cell phagocytosis (136); these authors revealed that macrophages infected with HIV-1 alone might upregulate production of TNF-α and activate NF-κB signaling but that *Cryptococcus neoformans* coinfection rapidly represses this proinflammatory response (136). In addition, HIV-infected macrophages might contribute to increased susceptibility to opportunistic fungal infections (137). Studies have indicated that HIV infection of macrophages impairs the phagocytosis and killing of *Pneumocystis jirovecii* (138), *Candida albicans* (139) and *Aspergillus fumigatus* (140). A possible reason is that the HIV-1 accessory proteins Nef and Tat downregulate the mannose receptor expressed on the surface of macrophages. It has also been shown that HIV-1 reduces the number of DCs and disrupt their function. In HIV infection, DCs have a reduced ability to present antigens and stimulate T-cell proliferation and show a partially activated phenotype and impaired TLR responses (141, 142). T-cell proliferation in HIV-infected individuals might be inhibited by plasmacytoid DCs (pDCs) *via* induction of indoleamine-2,3-dioxygenase (IDO) (143). IDO expression by pDCs also blocks T-cell differentiation into Th17 cells, which might have a negative effect in adaptive antifungal immunity and predispose patients toward opportunistic infections, such as fungal infections with *C. albicans* and *C. neoformans* (141). Overall, HIV infection might lead to quantitative and qualitative deficiencies in innate antifungal immunity (Figure 1).

Adaptive antifungal immunity in HIV infection

$CD4^+$ T cells are generally considered to play an important role in defense against fungal infections. The importance of Th1 and Th17 responses in antifungal defense mechanisms has been described (144). It is well known that the Th1 response provides protective immunity mainly through production of proinflammatory cytokines, such as IFN-γ, IL-2, IL-12, and TNF-α (144). The IFN-γ produced by Th1 cells activates phagocytes, such as macrophages, and promotes phagocytosis, MHC-II molecule upregulation and antigen presentation by APCs (145). Enhanced protection against *Aspergillosis*, *Cryptococcosis*, and coccidioidomycosis has been demonstrated in patients receiving IFN-γ immunotherapy (146). Th17 cells produce cytokines, including IL-17A, IL-17F, and IL-22, which promote neutrophil recruitment and fungicidal activity and induce production of AMPs from epithelial cells and keratinocytes to prevent fungal overgrowth (145). The Th17 response has been shown to play an essential role in promoting clearance of fungi, such as *Candida albicans* and *Malassezia* spp (147). In addition, antibodies are important in limiting the fungal burden and its clearance (148). Antibodies can defend against fungal pathogens through direct mechanisms, including

inhibition of fungal pathogen growth or fungicidal activity, and indirect mechanisms, including opsonization, complement pathway activation and antibody-directed cell toxicity (ADCC) (146). Antibody responses to *Cryptococcus neoformans* (149) and *Candida albicans* (150) have been reported.

HIV infection leads to a rapid and massive reduction in $CD4^+$ T cells. One recent study showed that levels of Th1 cytokines in CSF, including IL-12 and TNF-α, correlate positively with HIV-associated cryptococcal meningitis (151). Moreover, in HIV-infected individuals, IFN-γ produced by Th1 cells plays an important function in improving the antifungal immune response to cryptococcal infection (102) and oral candidiasis (152). Jarvis et al. found that the Th1 responses of *Cryptococcus*-specific $CD4^+$ T cells play a key role in promoting circulating lymphocyte and monocyte recruitment to the central nervous system (CNS), CNS macrophage and microglial activation and organism clearance (153). In addition to the Th1 response, Th17 cells are critical in defense against bacterial and fungal infections at mucosal sites (154, 155). However, Liu et al. found that Th17-associated functions (IL-22, IL-17 and IL-2) of *Candida albicans*-specific CD4 T cells are disrupted in early HIV infection (156). Early massive loss of Th17 cells in HIV infection has also been shown to be a likely cause of the high prevalence of chronic mucocutaneous candidiasis in people with early HIV infection (157). Therefore, mucosal candidiasis susceptibility in HIV infection may be attributed to Th17-cell depletion.

HIV-1 replication might lead to abnormalities in all major lymphocyte populations as well as hyperactivation and exhaustion of the B-cell compartment (158). Studies have found that impaired B-cell responses due to HIV infection might affect B-cell responses in cryptococcal coinfection (159, 160). Moreover, levels of antibodies, such as plasma IgM, laminarin (Lam)-binding IgM and IgG, are significantly lower in HIV-infected individuals who develop *Cryptococcus*-associated IRIS than in those who do not, supporting the role for antibody immunity in cryptococcosis (161). Immune status is also important in antibody responses to *Pneumocystis jirovecii* (162). A previous study showed that IgM antibody responses to *Pneumocystis jirovecii* major surface glycoprotein (Msg), including MsgC1 (carboxyl terminus), MsgC3, MsgC8 and MsgC9, were significantly lower in HIV-infected individuals than in HIV-uninfected controls (163). Taken together, these findings suggest that competent adaptive immune responses are crucial for defense against fungal infections and that HIV infection might lead to impaired antifungal immunity (Figure 1).

Conclusion

Our review discusses recent findings on alterations in the mycobiome in the setting of HIV infection. The mycobiome contributes greatly to opportunistic infections in individuals with advanced HIV infection. Despite widespread use of ART, fungal opportunistic infections are the leading cause of HIV-related death globally. It is evident that human immune responses play a critical role in defense against fungal infection. We review the impact of HIV infection on host innate and adaptive antifungal immunity, contributing to a better understanding of the underlying immunopathogenesis of fungal infections in HIV infection. In addition, further efforts to develop new diagnostics and global access to antifungal drugs and other effective therapies are needed to enable early diagnosis and treatment of fungal infections.

Author contributions

BS and TZ conceptualized and supervised the whole study, SL, XY, HW, BS, and TZ searched the literature, contributed to the analysis and provided important scientific input. SL, CM and BS wrote the first draft and revised version of the manuscript. All authors contributed to the article and approved the submitted version.

Funding

This project is financially supported by the National Natural Science Foundation of China (NSFC, 82072271 and 81974303), Beijing Natural Science Foundation (Z220018), the High-Level Public Health Specialized Talents Project of Beijing Municipal Health Commission (2022-1-007 and 2022-2-018), the "Climbing the peak (Dengfeng)" Talent Training Program of Beijing Hospitals Authority (DFL20191701), the Beijing Health Technologies Promotion Program (BHTPP2020), and Beijing Key Laboratory for HIV/AIDS Research (BZ0089). The funders had no role in study design, data collection and analysis, decision to publish, or preparation of the manuscript.

Conflict of interest

The authors declare that the research was conducted in the absence of any commercial or financial relationships that could be construed as a potential conflict of interest.

Publisher's note

References

1. Brown GD, Denning DW, Levitz SM. Tackling human fungal infections. *Science* (2012) 336(6082):647. doi: 10.1126/science.1222236

2. Stop neglecting fungi. *Nat Microbiol* (2017) 2:17120. doi: 10.1038/nmicrobiol.2017.120

3. Tirado-Sanchez A, Gonzalez GM, Bonifaz A. Endemic mycoses: epidemiology and diagnostic strategies. *Expert Rev Anti Infect Ther* (2020) 18 (11):1105–17. doi: 10.1080/14787210.2020.1792774

4. Li S, Zhu J, Su B, Wei H, Chen F, Liu H, et al. Alteration in oral microbiome among men who have sex with men with acute and chronic HIV infection on antiretroviral therapy. *Front Cell Infect Microbiol* (2021) 11:695515. doi: 10.3389/fcimb.2021.695515

5. Li S, Su B, He QS, Wu H, Zhang T. Alterations in the oral microbiome in HIV infection: causes, effects and potential interventions. *Chin Med J (Engl)* (2021) 134 (23):2788–98. doi: 10.1097/CM9.0000000000001825

6. Zhou JJ, Zhai J, Zhou H, Chen Y, Guerra S, Robey I, et al. Supraglottic lung microbiome taxa are associated with pulmonary abnormalities in an HIV longitudinal cohort. *Am J Respir Crit Care Med* (2020) 202(12):1727–31. doi: 10.1164/rccm.202004-1086LE

7. Cribbs SK, Crothers K, Morris A. Pathogenesis of HIV-related lung disease: Immunity, infection, and inflammation. *Physiol Rev* (2020) 100(2):603–32. doi: 10.1152/physrev.00039.2018

8. Nganou-Makamdop K, Talla A, Sharma AA, Darko S, Ransier A, Laboune F, et al. Translocated microbiome composition determines immunological outcome in treated HIV infection. *Cell* (2021) 184(15):3899–3914.e3816. doi: 10.1016/j.cell.2021.05.023

9. Rocafort M, Noguera-Julian M, Rivera J, Pastor L, Guillen Y, Langhorst J, et al. Evolution of the gut microbiome following acute HIV-1 infection. *Microbiome* (2019) 7(1):73. doi: 10.1186/s40168-019-0687-5

10. Armstrong-James D, Meintjes G, Brown GD. A neglected epidemic: fungal infections in HIV/AIDS. *Trends Microbiol* (2014) 22(3):120–7. doi: 10.1016/j.tim.2014.01.001

11. Armstrong-James D, Bicanic T, Brown GD, Hoving JC, Meintjes G, Nielsen K, et al. AIDS-related mycoses: Current progress in the field and future priorities. *Trends Microbiol* (2017) 25(6):428–30. doi: 10.1016/j.tim.2017.02.013

12. Hoving JC, Brown GD, Gomez BL, Govender NP, Limper AH, May RC, et al. AIDS-related mycoses: Updated progress and future priorities. *Trends Microbiol* (2020) 28(6):425–8. doi: 10.1016/j.tim.2020.01.009

13. Garcia-Carnero LC, Perez-Garcia LA, Martinez-Alvarez JA, Reyes-Martinez JE, Mora-Montes HM. Current trends to control fungal pathogens: exploiting our knowledge in the host-pathogen interaction. *Infect Drug Resist* (2018) 11:903–13. doi: 10.2147/IDR.S170337

14. Casadevall A. Immunity to invasive fungal diseases. *Annu Rev Immunol* (2022) 40:121–41. doi: 10.1146/annurev-immunol-101220-034306

15. Hoenigl M. Fungal translocation: A driving force behind the occurrence of non-AIDS events? *Clin Infect Dis* (2020) 70(2):242–4. doi: 10.1093/cid/ciz215

16. Ramendra R, Isnard S, Mehraj V, Chen J, Zhang Y, Finkelman M, et al. Circulating LPS and (1–>3)-beta-D-Glucan: A folie a deux contributing to HIV-associated immune activation. *Front Immunol* (2019) 10:465. doi: 10.3389/fimmu.2019.00465

17. Cui L, Morris A, Ghedin E. The human mycobiome in health and disease. *Genome Med* (2013) 5(7):63. doi: 10.1186/gm467

18. Rolling T, Hohl TM, Zhai B. Minority report: the intestinal mycobiota in systemic infections. *Curr Opin Microbiol* (2020) 56:1–6. doi: 10.1016/j.mib.2020.05.004

19. Gu Y, Zhou G, Qin X, Huang S, Wang B, Cao H. The potential role of gut mycobiome in irritable bowel syndrome. *Front Microbiol* (2019) 10:1894. doi: 10.3389/fmicb.2019.01894

20. Guo Y, Xia W, Wei F, Feng W, Duan J, Sun X, et al. Salivary microbial diversity at different stages of human immunodeficiency virus infection. *Microb Pathog* (2021) 155:104913. doi: 10.1016/j.micpath.2021.104913

21. Li J, Chang S, Guo H, Ji Y, Jiang H, Ruan L, et al. Altered salivary microbiome in the early stage of HIV infections among young Chinese men who have sex with men (MSM). *Pathogens* (2020) 9(11):960. doi: 10.3390/pathogens9110960

22. Guo Y, Huang X, Sun X, Yu Y, Wang Y, Zhang B, et al. The underrated salivary virome of men who have sex with men infected with HIV. *Front Immunol* (2021) 12:759253. doi: 10.3389/fimmu.2021.759253

23. Sodre CS, Rodrigues PMG, Vieira MS, Marques Paes da Silva A, Goncalves LS, Ribeiro MG, et al. Oral mycobiome identification in atopic dermatitis, leukemia, and HIV patients - a systematic review. *J Oral Microbiol* (2020) 12 (1):1807179. doi: 10.1080/20002297.2020.1807179

24. Ghannoum MA, Jurevic RJ, Mukherjee PK, Cui F, Sikaroodi M, Naqvi A, et al. Characterization of the oral fungal microbiome (mycobiome) in healthy individuals. *PLos Pathog* (2010) 6(1):e1000713. doi: 10.1371/journal.ppat.1000713

25. Mukherjee PK, Chandra J, Retuerto M, Sikaroodi M, Brown RE, Jurevic R, et al. Oral mycobiome analysis of HIV-infected patients: identification of pichia as an antagonist of opportunistic fungi. *PLos Pathog* (2014) 10(3):e1003996. doi: 10.1371/journal.ppat.1003996

26. Hager CL, Ghannoum MA. The mycobiome in HIV. *Curr Opin HIV AIDS* (2018) 13(1):69–72. doi: 10.1097/COH.0000000000000432

27. Chang S, Guo H, Li J, Ji Y, Jiang H, Ruan L, et al. Comparative analysis of salivary mycobiome diversity in human immunodeficiency virus-infected patients. *Front Cell Infect Microbiol* (2021) 11:781246. doi: 10.3389/fcimb.2021.781246

28. Fidel PLJr., Thompson ZA, Lilly EA, Granada C, Treas K, Dubois KR3rd, et al. Effect of HIV/HAART and other clinical variables on the oral mycobiome using multivariate analyses. *mBio* (2021) 12(2):e00294-21. doi: 10.1128/mBio.00294-21

29. Cui L, Lucht L, Tipton L, Rogers MB, Fitch A, Kessinger C, et al. Topographic diversity of the respiratory tract mycobiome and alteration in HIV and lung disease. *Am J Respir Crit Care Med* (2015) 191(8):932–42. doi: 10.1164/rccm.201409-1583OC

30. Bittinger K, Charlson ES, Loy E, Shirley DJ, Haas AR, Laughlin A, et al. Improved characterization of medically relevant fungi in the human respiratory tract using next-generation sequencing. *Genome Biol* (2014) 15(10):487. doi: 10.1186/s13059-014-0487-y

31. Hamad I, Abou Abdallah R, Ravaux I, Mokhtari S, Tissot-Dupont H, Michelle C, et al. Metabarcoding analysis of eukaryotic microbiota in the gut of HIV-infected patients. *PLos One* (2018) 13(1):e0191913. doi: 10.1371/journal.pone.0191913

32. Wu X, Xu Y, Li Q, Yang F, He S, Li Y, et al. Gut dysbiosis of bacteria and fungi associated with human immunodeficiency virus infection. *Chin Med J (Engl)* (2022) 135(11):1376–8. doi: 10.1097/CM9.0000000000002194

33. Yin Y, Tuohutaerbieke M, Feng C, Li X, Zhang Y, Xu Q, et al. Characterization of the intestinal fungal microbiome in HIV and HCV mono-infected or Co-infected patients. *Viruses* (2022) 14(8):1811. doi: 10.3390/v14081811

34. Lalloo UG, Pillay S, Mngqibisa R, Abdool-Gaffar S, Ambaram A. HIV And COPD: a conspiracy of risk factors. *Respirology* (2016) 21(7):1166–72. doi: 10.1111/resp.12806

35. Bigna JJ, Kenne AM, Asangbeh SL, Sibetcheu AT. Prevalence of chronic obstructive pulmonary disease in the global population with HIV: a systematic review and meta-analysis. *Lancet Glob Health* (2018) 6(2):e193–202. doi: 10.1016/S2214-109X(17)30451-5

36. Sigel K, Wisnivesky J, Gordon K, Dubrow R, Justice A, Brown ST, et al. HIV As an independent risk factor for incident lung cancer. *AIDS* (2012) 26(8):1017–25. doi: 10.1097/QAD.0b013e328352d1ad

37. Sigel K, Makinson A, Thaler J. Lung cancer in persons with HIV. *Curr Opin HIV AIDS* (2017) 12(1):31–8. doi: 10.1097/COH.0000000000000326

38. Sigel K, Wisnivesky J, Crothers K, Gordon K, Brown ST, Rimland D, et al. Immunological and infectious risk factors for lung cancer in US veterans with HIV: a longitudinal cohort study. *Lancet HIV* (2017) 4(2):e67–73. doi: 10.1016/S2352-3018(16)30215-6

39. Leader JK, Crothers K, Huang L, King MA, Morris A, Thompson BW, et al. Risk factors associated with quantitative evidence of lung emphysema and fibrosis in an HIV-infected cohort. *J Acquir Immune Defic Syndr* (2016) 71(4):420–7. doi: 10.1097/QAI.0000000000000894

40. Attia EF, Akgun KM, Wongtrakool C, Goetz MB, Rodriguez-Barradas MC, Rimland D, et al. Increased risk of radiographic emphysema in HIV is associated with elevated soluble CD14 and nadir CD4. *Chest* (2014) 146(6):1543–53. doi: 10.1378/chest.14-0543

41. Petrache I, Diab K, Knox KS, Twigg HL3rd, Stephens RS, Flores S, et al. HIV Associated pulmonary emphysema: a review of the literature and inquiry into its mechanism. *Thorax* (2008) 63(5):463–9. doi: 10.1136/thx.2007.079111

42. Seed PC. The human mycobiome. *Cold Spring Harb Perspect Med* (2014) 5 (5):a019810. doi: 10.1101/cshperspect.a019810

43. Twigg HL3rd, Knox KS, Zhou J, Crothers KA, Nelson DE, Toh E, et al. Effect of advanced HIV infection on the respiratory microbiome. *Am J Respir Crit Care Med* (2016) 194(2):226–35. doi: 10.1164/rccm.201509-1875OC

44. Twigg HL3rd, Weinstock GM, Knox KS. Lung microbiome in human immunodeficiency virus infection. *Transl Res* (2017) 179:97–107. doi: 10.1016/j.trsl.2016.07.008

45. Alexandrova Y, Costiniuk CT, Jenabian MA. Pulmonary immune dysregulation and viral persistence during HIV infection. *Front Immunol* (2021) 12:808722. doi: 10.3389/fimmu.2021.808722

46. Dillon SM, Lee EJ, Kotter CV, Austin GL, Dong Z, Hecht DK, et al. An altered intestinal mucosal microbiome in HIV-1 infection is associated with mucosal and systemic immune activation and endotoxemia. *Mucosal Immunol* (2014) 7(4):983–94. doi: 10.1038/mi.2013.116

47. Armstrong AJS, Shaffer M, Nusbacher NM, Griesmer C, Fiorillo S, Schneider JM, et al. An exploration of prevotella-rich microbiomes in HIV and men who have sex with men. *Microbiome* (2018) 6(1):198. doi: 10.1186/s40168-018-0580-7

48. Crakes KR, Jiang G. Gut microbiome alterations during HIV/SIV infection: Implications for HIV cure. *Front Microbiol* (2019) 10:1104. doi: 10.3389/fmicb.2019.01104

49. Nash AK, Auchtung TA, Wong MC, Smith DP, Gesell JR, Ross MC, et al. The gut mycobiome of the human microbiome project healthy cohort. *Microbiome* (2017) 5(1):153. doi: 10.1186/s40168-017-0373-4

50. Iliev ID, Leonardi I. Fungal dysbiosis: immunity and interactions at mucosal barriers. *Nat Rev Immunol* (2017) 17(10):635–46. doi: 10.1038/nri.2017.55

51. Cutler JE, Deepe GSJr., Klein BS. Advances in combating fungal diseases: vaccines on the threshold. *Nat Rev Microbiol* (2007) 5(1):13–28. doi: 10.1038/nrmicro1537

52. Hoffmann C, Dollive S, Grunberg S, Chen J, Li H, Wu GD, et al. Archaea and fungi of the human gut microbiome: correlations with diet and bacterial residents. *PLos One* (2013) 8(6):e66019. doi: 10.1371/journal.pone.0066019

53. Mar Rodriguez M, Perez D, Javier Chaves F, Esteve E, Marin-Garcia P, Xifra G, et al. Obesity changes the human gut mycobiome. *Sci Rep* (2015) 5:14600. doi: 10.1038/srep14600

54. Gouba N, Drancourt M. Digestive tract mycobiota: a source of infection. *Med Mal Infect* (2015) 45(1-2):9–16. doi: 10.1016/j.medmal.2015.01.007

55. Musumeci S, Coen M, Leidi A, Schrenzel J. The human gut mycobiome and the specific role of candida albicans: where do we stand, as clinicians? *Clin Microbiol Infect* (2022) 28(1):58–63. doi: 10.1016/j.cmi.2021.07.034

56. Yamasmith E, Chongtrakool P, Chayakulkeeree M. Isolated pulmonary fusariosis caused by neocosmospora pseudensiformis in a liver transplant recipient: A case report and review of the literature. *Transpl Infect Dis* (2020) 22(6):e13344. doi: 10.1111/tid.13344

57. Sandoval-Denis M, Crous PW. Removing chaos from confusion: assigning names to common human and animal pathogens in neocosmospora. *Persoonia* (2018) 41:109–29. doi: 10.3767/persoonia.2018.41.06

58. Khedri S, Santos ALS, Roudbary M, Hadighi R, Falahati M, Farahyar S, et al. Iranian HIV/AIDS patients with oropharyngeal candidiasis: identification, prevalence and antifungal susceptibility of candida species. *Lett Appl Microbiol* (2018) 67(4):392–9. doi: 10.1111/lam.13052

59. Hosain Pour A, Salari S, Ghasemi Nejad Almani P. Oropharyngeal candidiasis in HIV/AIDS patients and non-HIV subjects in the southeast of Iran. *Curr Med Mycol* (2018) 4(4):1–6. doi: 10.18502/cmm.4.4.379

60. Pienaar ED, Young T, Holmes H. Interventions for the prevention and management of oropharyngeal candidiasis associated with HIV infection in adults and children. *Cochrane Database Syst Rev* (2010) 11):CD003940. doi: 10.1002/14651858.CD003940.pub3

61. Kwamin F, Nartey NO, Codjoe FS, Newman MJ. Distribution of candida species among HIV-positive patients with oropharyngeal candidiasis in Accra, Ghana. *J Infect Dev Ctries* (2013) 7(1):41–5. doi: 10.3855/jidc.2442

62. Rafat Z, Sasani E, Salimi Y, Hajimohammadi S, Shenagari M, Roostaei D. The prevalence, etiological agents, clinical features, treatment, and diagnosis of HIV-associated oral candidiasis in pediatrics across the world: A systematic review and meta-analysis. *Front Pediatr* (2021) 9:805527. doi: 10.3389/fped.2021.805527

63. Patel PK, Erlandsen JE, Kirkpatrick WR, Berg DK, Westbrook SD, Louden C, et al. The changing epidemiology of oropharyngeal candidiasis in patients with HIV/AIDS in the era of antiretroviral therapy. *AIDS Res Treat* (2012) 2012:262471. doi: 10.1155/2012/262471

64. Vazquez JA. Therapeutic options for the management of oropharyngeal and esophageal candidiasis in HIV/AIDS patients. *HIV Clin Trials* (2000) 1(1):47–59. doi: 10.1310/T7A7-1E63-2KA0-JKWD

65. Thompson GR, Patel PK, Kirkpatrick WR, Westbrook SD, Berg D, Erlandsen J, et al. Oropharyngeal candidiasis in the era of antiretroviral therapy. *Oral Surg Oral Med Oral Pathol Oral Radiol Endod* (2010) 109(4):488–95. doi: 10.1016/j.tripleo.2009.11.026

66. Taverne-Ghadwal L, Kuhns M, Buhl T, Schulze MH, Mbaitolum WJ, Kersch L, et al. Epidemiology and prevalence of oral candidiasis in HIV patients from Chad in the post-HAART era. *Front Microbiol* (2022) 13:844069. doi: 10.3389/fmicb.2022.844069

67. Patil S, Majumdar B, Sarode SC, Sarode GS, Awan KH. Oropharyngeal candidosis in HIV-infected patients-an update. *Front Microbiol* (2018) 9:980. doi: 10.3389/fmicb.2018.00980

68. de Repentigny L, Lewandowski D, Jolicoeur P. Immunopathogenesis of oropharyngeal candidiasis in human immunodeficiency virus infection. *Clin Microbiol Rev* (2004) 17(4):729–59. doi: 10.1128/CMR.17.4.729-759.2004

69. Oever JT, Netea MG. The bacteriome-mycobiome interaction and antifungal host defense. *Eur J Immunol* (2014) 44(11):3182–91. doi: 10.1002/eji.201344405

70. Patton LL. Current strategies for prevention of oral manifestations of human immunodeficiency virus. *Oral Surg Oral Med Oral Pathol Oral Radiol* (2016) 121(1):29–38. doi: 10.1016/j.oooo.2015.09.004

71. Maurya V, Srivastava A, Mishra J, Gaind R, Marak RS, Tripathi AK, et al. Oropharyngeal candidiasis and candida colonization in HIV positive patients in northern India. *J Infect Dev Ctries* (2013) 7(8):608–13. doi: 10.3855/jidc.2801

72. Schoofs AG, Odds FC, Colebunders R, Ieven M, Goossens H. Cross-sectional study of oral candida carriage in a human immunodeficiency virus (HIV)-seropositive population: predisposing factors, epidemiology and antifungal susceptibility. *Mycoses* (1998) 41(5-6):203–11. doi: 10.1111/j.1439-0507.1998.tb00325.x

73. Aboualigalehdari E, Tahmasebi Birgani M, Fatahinia M, Hosseinzadeh M. Oral colonization by candida species and associated factors in HIV-infected patients in ahvaz, southwest Iran. *Epidemiol Health* (2020) 42:e2020033. doi: 10.4178/epih.e2020033

74. Kirti YK. Prevalence of oral candidiasis in Indian HIV sero-positive patients with CD4(+) cell count correlation. *Indian J Otolaryngol Head Neck Surg* (2019) 71 (1):124–7. doi: 10.1007/s12070-018-1342-3

75. Heron SE, Elahi S. HIV Infection and compromised mucosal immunity: Oral manifestations and systemic inflammation. *Front Immunol* (2017) 8:241. doi: 10.3389/fimmu.2017.00241

76. Li Y, Saxena D, Chen Z, Liu G, Abrams WR, Phelan JA, et al. HIV Infection and microbial diversity in saliva. *J Clin Microbiol* (2014) 52(5):1400–11. doi: 10.1128/JCM.02954-13

77. Huang YS, Yang JJ, Lee NY, Chen GJ, Ko WC, Sun HY, et al. Treatment of pneumocystis jirovecii pneumonia in HIV-infected patients: a review. *Expert Rev Anti Infect Ther* (2017) 15(9):873–92. doi: 10.1080/14787210.2017.1364991

78. Hitzenbichler F, Mohr A, Salzberger B. [Pneumocystis jirovecii pneumonia-an opportunistic infection undergoing change]. *Internist (Berl)* (2019) 60(7):669–77. doi: 10.1007/s00108-019-0616-5

79. Shibata S, Kikuchi T. Pneumocystis pneumonia in HIV-1-infected patients. *Respir Investig* (2019) 57(3):213–9. doi: 10.1016/j.resinv.2019.01.009

80. Buchacz K, Baker RK, Palella FJJr., Chmiel JS, Lichtenstein KA, Novak RM, et al. AIDS-defining opportunistic illnesses in US patients, 1994-2007: a cohort study. *AIDS* (2010) 24(10):1549–59. doi: 10.1097/QAD.0b013e32833a3967

81. Limper AH, Adenis A, Le T, Harrison TS. Fungal infections in HIV/AIDS. *Lancet Infect Dis* (2017) 17(11):e334–43. doi: 10.1016/S1473-3099(17)30303-1

82. Brown GD, Denning DW, Gow NA, Levitz SM, Netea MG, White TC. Hidden killers: human fungal infections. *Sci Transl Med* (2012) 4(165):165rv113. doi: 10.1126/scitranslmed.3004404

83. Bongomin F, Gago S, Oladele RO, Denning DW. Global and multi-national prevalence of fungal diseases-estimate precision. *J Fungi (Basel)* (2017) 3(4):57. doi: 10.3390/jof3040057

84. Bozorgomid A, Hamzavi Y, Heidari Khayat S, Mahdavian B, Bashiri H. Pneumocystis jirovecii pneumonia and human immunodeficiency virus Co-infection in Western Iran. *Iran J Public Health* (2019) 48(11):2065–9.

85. Cilloniz C, Dominedo C, Alvarez-Martinez MJ, Moreno A, Garcia F, Torres A, et al. Pneumocystis pneumonia in the twenty-first century: HIV-infected versus HIV-uninfected patients. *Expert Rev Anti Infect Ther* (2019) 17(10):787–801. doi: 10.1080/14787210.2019.1671823

86. Huang L, Cattamanchi A, Davis JL, den Boon S, Kovacs J, Meshnick S, et al. HIV-Associated pneumocystis pneumonia. *Proc Am Thorac Soc* (2011) 8(3):294–300. doi: 10.1513/pats.201009-062WR

87. Kelly MN, Shellito JE. Current understanding of pneumocystis immunology. *Future Microbiol* (2010) 5(1):43–65. doi: 10.2217/fmb.09.116

88. Carmona EM, Vassallo R, Vuk-Pavlovic Z, Standing JE, Kottom TJ, Limper AH. Pneumocystis cell wall beta-glucans induce dendritic cell costimulatory molecule expression and inflammatory activation through a fas-fas ligand mechanism. *J Immunol* (2006) 177(1):459–67. doi: 10.4049/jimmunol.177.1.459

89. Carmona EM, Kottom TJ, Hebrink DM, Moua T, Singh RD, Pagano RE, et al. Glycosphingolipids mediate pneumocystis cell wall beta-glucan activation of the IL-23/IL-17 axis in human dendritic cells. *Am J Respir Cell Mol Biol* (2012) 47 (1):50–9. doi: 10.1165/rcmb.2011-0159OC

90. Otieno-Odhiambo P, Wasserman S, Hoving JC. The contribution of host cells to pneumocystis immunity: An update. *Pathogens* (2019) 8(2):52. doi: 10.3390/pathogens8020052

91. Rajasingham R, Smith RM, Park BJ, Jarvis JN, Govender NP, Chiller TM, et al. Global burden of disease of HIV-associated cryptococcal meningitis: an updated analysis. *Lancet Infect Dis* (2017) 17(8):873–81. doi: 10.1016/S1473-3099(17)30243-8

92. Veltman JA, Bristow CC, Klausner JD. Meningitis in HIV-positive patients in sub-Saharan Africa: a review. *J Int AIDS Soc* (2014) 17:19184. doi: 10.7448/IAS.17.1.19184

93. Loyse A, Thangaraj H, Easterbrook P, Ford N, Roy M, Chiller T, et al. Cryptococcal meningitis: improving access to essential antifungal medicines in resource-poor countries. *Lancet Infect Dis* (2013) 13(7):629–37. doi: 10.1016/S1473-3099(13)70078-1

94. Loyse A, Burry J, Cohn J, Ford N, Chiller T, Ribeiro I, et al. Leave no one behind: response to new evidence and guidelines for the management of cryptococcal meningitis in low-income and middle-income countries. *Lancet Infect Dis* (2019) 19(4):e143–7. doi: 10.1016/S1473-3099(18)30493-6

95. Perfect JR, Dismukes WE, Dromer F, Goldman DL, Graybill JR, Hamill RJ, et al. Clinical practice guidelines for the management of cryptococcal disease: 2010 update by the infectious diseases society of america. *Clin Infect Dis* (2010) 50 (3):291–322. doi: 10.1086/649858

96. Neal LM, Xing E, Xu J, Kolbe JL, Osterholzer JJ, Segal BM, et al. CD4(+) T cells orchestrate lethal immune pathology despite fungal clearance during cryptococcus neoformans meningoencephalitis. *mBio* (2017) 8(6):e01415-17. doi: 10.1128/mBio.01415-17

97. Pirofski LA, Casadevall A. Immune-mediated damage completes the parabola: Cryptococcus neoformans pathogenesis can reflect the outcome of a weak or strong immune response. *mBio* (2017) 8(6):e02063-17. doi: 10.1128/mBio.02063-17

98. Perez-Jacoiste Asin MA, Bisbal O, Iribarren JA, Perez-Rivilla A, Mican R, Dronda F, et al. Cryptococcal infection in HIV-infected patients with CD4(+) T-cell counts under 100/muL diagnosed in a high-income country: a multicentre cohort study. *Clin Microbiol Infect* (2021) 27(8):1171 e1171–1171 e1177. doi: 10.1016/j.cmi.2020.09.053

99. Iyer KR, Revie NM, Fu C, Robbins N, Cowen LE. Treatment strategies for cryptococcal infection: challenges, advances and future outlook. *Nat Rev Microbiol* (2021) 19(7):454–66. doi: 10.1038/s41579-021-00511-0

100. Li A, Zhu W, Yin J, Huang X, Sun L, Hua W, et al. A preliminary study on the characteristics of Th1/Th2 immune response in cerebrospinal fluid of AIDS patients with cryptococcal meningitis. *BMC Infect Dis* (2021) 21(1):500. doi: 10.1186/s12879-021-06138-z

101. Jarvis JN, Bicanic T, Loyse A, Namarika D, Jackson A, Nussbaum JC, et al. Determinants of mortality in a combined cohort of 501 patients with HIV-associated cryptococcal meningitis: implications for improving outcomes. *Clin Infect Dis* (2014) 58(5):736–45. doi: 10.1093/cid/cit794

102. Jarvis JN, Meintjes G, Rebe K, Williams GN, Bicanic T, Williams A, et al. Adjunctive interferon-gamma immunotherapy for the treatment of HIV-associated cryptococcal meningitis: a randomized controlled trial. *AIDS* (2012) 26(9):1105–13. doi: 10.1097/QAD.0b013e3283536a93

103. Boulware DR, Meya DB, Bergemann TL, Wiesner DL, Rhein J, Musubire A, et al. Clinical features and serum biomarkers in HIV immune reconstitution inflammatory syndrome after cryptococcal meningitis: a prospective cohort study. *PLos Med* (2010) 7(12):e1000384. doi: 10.1371/journal.pmed.1000384

104. Narayanasamy S, Dat VQ, Thanh NT, Ly VT, Chan JF, Yuen KY, et al. A global call for talaromycosis to be recognised as a neglected tropical disease. *Lancet Glob Health* (2021) 9(11):e1618–22. doi: 10.1016/S2214-109X(21)00350-8

105. Qin Y, Huang X, Chen H, Liu X, Li Y, Hou J, et al. Burden of talaromyces marneffei infection in people living with HIV/AIDS in Asia during ART era: a systematic review and meta-analysis. *BMC Infect Dis* (2020) 20(1):551. doi: 10.1186/s12879-020-05260-8

106. Jiang J, Meng S, Huang S, Ruan Y, Lu X, Li JZ, et al. Effects of talaromyces marneffei infection on mortality of HIV/AIDS patients in southern China: a retrospective cohort study. *Clin Microbiol Infect* (2019) 25(2):233–41. doi: 10.1016/j.cmi.2018.04.018

107. Pruksaphon K, Nosanchuk JD, Ratanabanangkoon K, Youngchim S. Talaromyces marneffei infection: Virulence, intracellular lifestyle and host defense mechanisms. *J Fungi (Basel)* (2022) 8(2):200. doi: 10.3390/jof8020200

108. Srinoulprasert Y, Pongtanalert P, Chawengkirttikul R, Chaiyaroj SC. Engagement of penicillium marneffei conidia with multiple pattern recognition receptors on human monocytes. *Microbiol Immunol* (2009) 53(3):162–72. doi: 10.1111/j.1348-0421.2008.00102.x

109. Pongpom M, Vanittanakom P, Nimmanee P, Cooper CRJr., Vanittanakom N. Adaptation to macrophage killing by talaromyces marneffei. *Future Sci OA* (2017) 3(3):FSO215. doi: 10.4155/fsoa-2017-0032

110. Lu S, Hu Y, Lu C, Zhang J, Li X, Xi L. Development of *in vitro* macrophage system to evaluate phagocytosis and intracellular fate of penicillium marneffei conidia. *Mycopathologia* (2013) 176(1-2):11–22. doi: 10.1007/s11046-013-9650-3

111. Ellett F, Pazhakh V, Pase L, Benard EL, Weerasinghe H, Azabdaftari D, et al. Macrophages protect talaromyces marneffei conidia from myeloperoxidase-dependent neutrophil fungicidal activity during infection establishment in vivo. *PLos Pathog* (2018) 14(6):e1007063. doi: 10.1371/journal.ppat.1007063

112. Tang Y, Zhang H, Xu H, Zeng W, Qiu Y, Tan C, et al. Dendritic cells promote treg expansion but not Th17 generation in response to talaromyces marneffei yeast cells. *Infect Drug Resist* (2020) 13:805–13. doi: 10.2147/IDR.S239906

113. Wang M, Li L, Xiao S, Chen W, Hu F, Li F, et al. The association of TLR2, TLR3, and TLR9 gene polymorphisms with susceptibility to talaromycosis among han Chinese AIDS patients in guangdong. *Front Cell Infect Microbiol* (2021) 11:625461. doi: 10.3389/fcimb.2021.625461

114. Guo J, Ning XQ, Ding JY, Zheng YQ, Shi NN, Wu FY, et al. Anti-IFN-gamma autoantibodies underlie disseminated talaromyces marneffei infections. *J Exp Med* (2020) 217(12):e20190502. doi: 10.1084/jem.20190502

115. Narayanasamy S, Dougherty J, van Doorn HR, Le T. Pulmonary talaromycosis: A window into the immunopathogenesis of an endemic mycosis. *Mycopathologia* (2021) 186(5):707–15. doi: 10.1007/s11046-021-00570-0

116. Manion M, Boulougoura A, Naqvi N, Lage SL, Richards E, Grivas C, et al. Polyfunctional antigen specific CD4+/- T cell responses in patients with HIV/AIDS and histoplasmosis immune reconstitution inflammatory syndrome. *Clin Infect Dis* (2022) ciac514. doi: 10.1093/cid/ciac514

117. Chen H, Yuan Q, Hu H, Wang J, Yu M, Yang Q, et al. Hemophagocytic lymphohistiocytosis secondary to disseminated histoplasmosis in HIV seronegative patients: A case report and review of the literature. *Front Cell Infect Microbiol* (2022) 12:847950. doi: 10.3389/fcimb.2022.847950

118. Wheat LJ, Azar MM, Bahr NC, Spec A, Relich RF, Hage C. Histoplasmosis. *Infect Dis Clin North Am* (2016) 30(1):207–27. doi: 10.1016/j.idc.2015.10.009

119. Adenis AA, Valdes A, Cropet C, McCotter OZ, Derado G, Couppie P, et al. Burden of HIV-associated histoplasmosis compared with tuberculosis in Latin America: a modelling study. *Lancet Infect Dis* (2018) 18(10):1150–9. doi: 10.1016/S1473-3099(18)30354-2

120. Basso RP, Poester VR, Benelli JL, Stevens DA, Xavier MO. Disseminated histoplasmosis in persons with HIV/AIDS, southern Brazil, 2010-2019. *Emerg Infect Dis* (2022) 28(3):721–4. doi: 10.3201/eid2803.212150

121. Tobon AM, Gomez BL. Pulmonary histoplasmosis. *Mycopathologia* (2021) 186(5):697–705. doi: 10.1007/s11046-021-00588-4

122. Garfoot AL, Rappleye CA. Histoplasma capsulatum surmounts obstacles to intracellular pathogenesis. *FEBS J* (2016) 283(4):619–33. doi: 10.1111/febs.13389

123. Almeida MA, Almeida-Paes R, Guimaraes AJ, Valente RH, Soares CMA, Zancope-Oliveira RM. Immunoproteomics reveals pathogen's antigens involved in homo sapiens-histoplasma capsulatum interaction and specific linear b-cell epitopes in histoplasmosis. *Front Cell Infect Microbiol* (2020) 10:591121. doi: 10.3389/fcimb.2020.591121

124. Holding KJ, Dworkin MS, Wan PC, Hanson DL, Klevens RM, Jones JL, et al. Aspergillosis among people infected with human immunodeficiency virus: incidence and survival. *Adult Adolesc Spectr HIV Dis Project Clin Infect Dis* (2000) 31(5):1253–7. doi: 10.1086/317452

125. Denis B, Guiguet M, de Castro N, Mechai F, Revest M, Melica G, et al. Relevance of EORTC criteria for the diagnosis of invasive aspergillosis in HIV-infected patients, and survival trends over a 20-year period in France. *Clin Infect Dis* (2015) 61(8):1273–80. doi: 10.1093/cid/civ492

126. Scriven JE, Tenforde MW, Levitz SM, Jarvis JN. Modulating host immune responses to fight invasive fungal infections. *Curr Opin Microbiol* (2017) 40:95–103. doi: 10.1016/j.mib.2017.10.018

127. Ward RA, Vyas JM. The first line of defense: effector pathways of anti-fungal innate immunity. *Curr Opin Microbiol* (2020) 58:160–5. doi: 10.1016/j.mib.2020.10.003

128. Kumar V, van de Veerdonk FL, Netea MG. Antifungal immune responses: emerging host-pathogen interactions and translational implications. *Genome Med* (2018) 10(1):39. doi: 10.1186/s13073-018-0553-2

129. Underhill DM, Pearlman E. Immune interactions with pathogenic and commensal fungi: A two-way Street. *Immunity* (2015) 43(5):845–58. doi: 10.1016/j.immuni.2015.10.023

130. Bartemes KR, Kita H. Innate and adaptive immune responses to fungi in the airway. *J Allergy Clin Immunol* (2018) 142(2):353–63. doi: 10.1016/j.jaci.2018.06.015

131. Desai JV, Lionakis MS. The role of neutrophils in host defense against invasive fungal infections. *Curr Clin Microbiol Rep* (2018) 5(3):181–9. doi: 10.1007/s40588-018-0098-6

132. Wang Y, Pawar S, Dutta O, Wang K, Rivera A, Xue C. Macrophage mediated immunomodulation during cryptococcus pulmonary infection. *Front Cell Infect Microbiol* (2022) 12:859049. doi: 10.3389/fcimb.2022.859049

133. Hunniger K, Kurzai O. Phagocytes as central players in the defence against invasive fungal infection. *Semin Cell Dev Biol* (2019) 89:3–15. doi: 10.1016/j.semcdb.2018.03.021

134. Casulli S, Elbim C. Interactions between human immunodeficiency virus type 1 and polymorphonuclear neutrophils. *J Innate Immun* (2014) 6(1):13–20. doi: 10.1159/000353588

135. Musubire AK, Meya DB, Rhein J, Meintjes G, Bohjanen PR, Nuwagira E, et al. Blood neutrophil counts in HIV-infected patients with cryptococcal meningitis: Association with mortality. *PLos One* (2018) 13(12):e0209337. doi: 10.1371/journal.pone.0209337

136. Kalem MC, Humby MS, Wohlfert EA, Jacobs A, Panepinto JC. Cryptococcus neoformans coinfection dampens the TNF-alpha response in HIV-1-Infected human THP-1 macrophages. *mSphere* (2021) 6(2):e00213-21. doi: 10.1128/mSphere.00213-21

137. Lubow J, Collins KL. Vpr is a VIP: HIV vpr and infected macrophages promote viral pathogenesis. *Viruses* (2020) 12(8):809. doi: 10.3390/v12080809

138. Koziel H, Eichbaum Q, Kruskal BA, Pinkston P, Rogers RA, Armstrong MY, et al. Reduced binding and phagocytosis of pneumocystis carinii by alveolar macrophages from persons infected with HIV-1 correlates with mannose receptor downregulation. *J Clin Invest* (1998) 102(7):1332–44. doi: 10.1172/JCI560

139. Crowe SM, Vardaxis NJ, Kent SJ, Maerz AL, Hewish MJ, McGrath MS, et al. HIV Infection of monocyte-derived macrophages *in vitro* reduces phagocytosis of candida albicans. *J Leukoc Biol* (1994) 56(3):318–27. doi: 10.1002/jlb.56.3.318

140. Roilides E, Holmes A, Blake C, Pizzo PA, Walsh TJ. Defective antifungal activity of monocyte-derived macrophages from human immunodeficiency virus-infected children against aspergillus fumigatus. *J Infect Dis* (1993) 168(6):1562–5. doi: 10.1093/infdis/168.6.1562

141. Maldonado S, Fitzgerald-Bocarsly P. Antifungal activity of plasmacytoid dendritic cells and the impact of chronic HIV infection. *Front Immunol* (2017) 8:1705. doi: 10.3389/fimmu.2017.01705

142. Miller E, Bhardwaj N. Dendritic cell dysregulation during HIV-1 infection. *Immunol Rev* (2013) 254(1):170–89. doi: 10.1111/imr.12082

143. Boasso A, Herbeuval JP, Hardy AW, Anderson SA, Dolan MJ, Fuchs D, et al. HIV Inhibits CD4+ T-cell proliferation by inducing indoleamine 2,3-dioxygenase in plasmacytoid dendritic cells. *Blood* (2007) 109(8):3351–9. doi: 10.1182/blood-2006-07-034785

144. Fernandez-Garcia OA, Cuellar-Rodriguez JM. Immunology of fungal infections. *Infect Dis Clin North Am* (2021) 35(2):373–88. doi: 10.1016/j.idc.2021.03.006

145. Speakman EA, Dambuza IM, Salazar F, Brown GD. T Cell antifungal immunity and the role of c-type lectin receptors. *Trends Immunol* (2020) 41(1):61–76. doi: 10.1016/j.it.2019.11.007

146. Verma A, Wuthrich M, Deepe G, Klein B. Adaptive immunity to fungi. *Cold Spring Harb Perspect Med* (2014) 5(3):a019612. doi: 10.1101/cshperspect.a019612

147. Scheffold A, Bacher P, LeibundGut-Landmann S. T Cell immunity to commensal fungi. *Curr Opin Microbiol* (2020) 58:116–23. doi: 10.1016/j.mib.2020.09.008

148. Pathakumari B, Liang G, Liu W. Immune defence to invasive fungal infections: A comprehensive review. *BioMed Pharmacother* (2020) 130:110550. doi: 10.1016/j.biopha.2020.110550

149. Rohatgi S, Pirofski LA. Host immunity to cryptococcus neoformans. *Future Microbiol* (2015) 10(4):565–81. doi: 10.2217/fmb.14.132

150. Wich M, Greim S, Ferreira-Gomes M, Kruger T, Kniemeyer O, Brakhage AA, et al. Functionality of the human antibody response to candida albicans. *Virulence* (2021) 12(1):3137–48. doi: 10.1080/21505594.2021.2015116

151. Xu L, Guo Y, Zhao Y, Xu Y, Peng X, Yang Z, et al. Chemokine and cytokine cascade caused by skewing of the Th1-Th2 balance is associated with high intracranial pressure in HIV-associated cryptococcal meningitis. *Mediators Inflammation* (2019) 2019:2053958. doi: 10.1155/2019/2053958

152. Ayatollahi Mousavi SA, Asadikaram G, Nakhaee N, Izadi A. Plasma levels of IFN-gamma, IL-4, IL-6 and IL-17 in HIV-positive patients with oral candidiasis. *Jundishapur J Microbiol* (2016) 9(2):e32021. doi: 10.5812/jjm.32021

153. Jarvis JN, Meintjes G, Bicanic T, Buffa V, Hogan L, Mo S, et al. Cerebrospinal fluid cytokine profiles predict risk of early mortality and immune reconstitution inflammatory syndrome in HIV-associated cryptococcal meningitis. *PLos Pathog* (2015) 11(4):e1004754. doi: 10.1371/journal.ppat.1004754

154. Renault C, Veyrenche N, Mennechet F, Bedin AS, Routy JP, Van de Perre P, et al. Th17 CD4+ T-cell as a preferential target for HIV reservoirs. *Front Immunol* (2022) 13:822576. doi: 10.3389/fimmu.2022.822576

155. Wacleche VS, Landay A, Routy JP, Ancuta P. The Th17 lineage: From barrier surfaces homeostasis to autoimmunity, cancer, and HIV-1 pathogenesis. *Viruses* (2017) 9(10):303. doi: 10.3390/v9100303

156. Liu F, Fan X, Auclair S, Ferguson M, Sun J, Soong L, et al. Sequential dysfunction and progressive depletion of candida albicans-specific CD4 T cell response in HIV-1 infection. *PLos Pathog* (2016) 12(6):e1005663. doi: 10.1371/journal.ppat.1005663

157. Zhang Q, Frange P, Blanche S, Casanova JL. Pathogenesis of infections in HIV-infected individuals: insights from primary immunodeficiencies. *Curr Opin Immunol* (2017) 48:122–33. doi: 10.1016/j.coi.2017.09.002

158. Ruggiero A, Pascucci GR, Cotugno N, Dominguez-Rodriguez S, Rinaldi S, Tagarro A, et al. Determinants of b-cell compartment hyperactivation in European adolescents living with perinatally acquired HIV-1 after over 10 years of suppressive therapy. *Front Immunol* (2022) 13:860418. doi: 10.3389/fimmu.2022.860418

159. Okurut S, Meya DB, Bwanga F, Olobo J, Eller MA, Cham-Jallow F, et al. B cell compartmentalization in blood and cerebrospinal fluid of HIV-infected ugandans with cryptococcal meningitis. *Infect Immun* (2020) 88(3):e00779-19. doi: 10.1128/IAI.00779-19

160. Rohatgi S, Nakouzi A, Carreno LJ, Slosar-Cheah M, Kuniholm MH, Wang T, et al. Antibody and b cell subset perturbations in human immunodeficiency virus-uninfected patients with cryptococcosis. *Open Forum Infect Dis* (2018) 5(1):ofx255. doi: 10.1093/ofid/ofx255

161. Yoon HA, Nakouzi A, Chang CC, Kuniholm MH, Carreno LJ, Wang T, et al. Association between plasma antibody responses and risk for cryptococcus-associated immune reconstitution inflammatory syndrome. *J Infect Dis* (2019) 219(3):420–8. doi: 10.1093/infdis/jiy447

162. Blount RJ, Daly KR, Fong S, Chang E, Grieco K, Greene M, et al. Effects of clinical and environmental factors on bronchoalveolar antibody responses to pneumocystis jirovecii: A prospective cohort study of HIV+ patients. *PLos One* (2017) 12(7):e0180212. doi: 10.1371/journal.pone.0180212

163. Blount RJ, Jarlsberg LG, Daly KR, Worodria W, Davis JL, Cattamanchi A, et al. Serologic responses to recombinant pneumocystis jirovecii major surface glycoprotein among Ugandan patients with respiratory symptoms. *PLos One* (2012) 7(12):e51545. doi: 10.1371/journal.pone.0051545

frontiers | Frontiers in Microbiology

TYPE Review
PUBLISHED 14 November 2022
DOI 10.3389/fmicb.2022.998058

OPEN ACCESS

EDITED BY
Kai Deng,
Sun Yat-sen University, China

REVIEWED BY
Fengyin Li,
University of Science and Technology of China, China
Federico Perdomo-Celis,
Institut Pasteur, France
Yan-Mei Jiao,
Fifth Medical Center of the PLA General Hospital, China

*CORRESPONDENCE
Lilin Ye
yelilinlcmv@tmmu.edu.cn

SPECIALTY SECTION
This article was submitted to Virology, a section of the journal Frontiers in Microbiology

RECEIVED 19 July 2022
ACCEPTED 24 October 2022
PUBLISHED 14 November 2022

CITATION
Gao L, Zhou J and Ye L (2022) Role of CXCR5$^+$ CD8$^+$ T cells in human immunodeficiency virus-1 infection. *Front. Microbiol.* 13:998058. doi: 10.3389/fmicb.2022.998058

Role of CXCR5$^+$ CD8$^+$ T cells in human immunodeficiency virus-1 infection

Leiqiong Gao[1], Jing Zhou[2] and Lilin Ye[2]*

[1]Microbiome Medicine Center, Department of Laboratory Medicine, Zhujiang Hospital, Southern Medical University, Guangzhou, China, [2]Institute of Immunology, Third Military Medical University, Chongqing, China

Human immunodeficiency virus (HIV) infection can be effectively suppressed by life-long administration of combination antiretroviral therapy (cART). However, the viral rebound can occur upon cART cessation due to the long-term presence of HIV reservoirs, posing a considerable barrier to drug-free viral remission. Memory CD4$^+$ T cell subsets, especially T follicular helper (T_{FH}) cells that reside in B-cell follicles within lymphoid tissues, are regarded as the predominant cellular compartment of the HIV reservoir. Substantial evidence indicates that HIV-specific CD8$^+$ T cell-mediated cellular immunity can sustain long-term disease-free and transmission-free HIV control in elite controllers. However, most HIV cure strategies that rely on expanded HIV-specific CD8$^+$ T cells for virus control are likely to fail due to cellular exhaustion and T_{FH} reservoir-specialized anatomical structures that isolate HIV-specific CD8$^+$ T cell entry into B-cell follicles. Loss of stem-like memory properties is a key feature of exhaustion. Recent studies have found that CXC chemokine receptor type 5 (CXCR5)-expressing HIV-specific CD8$^+$ T cells are memory-like CD8$^+$ T cells that can migrate into B-cell follicles to execute inhibition of viral replication. Furthermore, these unique CD8$^+$ T cells can respond to immune checkpoint blockade (ICB) therapy. In this review, we discuss the functions of these CD8$^+$ T cells as well as the translation of findings into viable HIV treatment and cure strategies.

KEYWORDS
CXCR5$^+$ CD8$^+$ T cell, HIV-1, B-cell follicle, HIV-specific CD8$^+$ T cells, immunotherapy

Introduction

Human immunodeficiency virus type-1 (HIV-1) is the leading cause of acquired immunodeficiency syndrome (AIDS), which remains a global public health concern due to the lack of effective vaccines and treatment strategies (Sharp and Hahn, 2011; Eisinger and Fauci, 2018; Kreider and Bar, 2022).

While combination antiretroviral therapy (cART) potently inhibits HIV replication and dramatically improves life expectancy in HIV-infected individuals, it is not curative and must be administered life-long (Ghosn et al., 2018; Yuan and Kaul, 2021). The main reason is that the virus can rebound from latent long-lived proliferating $CD4^+$ T cells upon cART cessation (Rausch and Le Grice, 2020). Effective and durable control of HIV in the presence or absence of ART is largely mediated by the potent effector function of HIV-specific $CD8^+$ T cells (Walker et al., 1986; Gandhi and Walker, 2002; Jones and Walker, 2016; Rogan and Connors, 2021). The emergence of HIV-specific $CD8^+$ T cells in acute infection is correlated with a rapid decline in viremia (Borrow et al., 1994; Takata et al., 2017; Collins et al., 2021). However, depletion of $CD8^+$ T cells can result in uncontrolled simian immunodeficiency virus (SIV) infection in rhesus macaques (Chowdhury et al., 2015). The emergence of HIV-specific $CD8^+$ T cell epitope mutations enables the virus to escape $CD8^+$ T cell responses (Nowak et al., 1995; Milicic et al., 2005). Moreover, durable control of HIV in elite controllers is not mediated by increased antibodies but by the effector function of HIV-specific $CD8^+$ T cells (Autran et al., 2011; Walker and Yu, 2013). Although HIV-specific $CD8^+$ T cells play important roles in the durable control of HIV, they are not able to eliminate HIV-infected target cells. Many extrinsic and intrinsic factors are required for dampening HIV-specific $CD8^+$ T cell-mediated inhibition of HIV replication. For example, functional exhaustion of HIV-specific $CD8^+$ T cells (Sen et al., 2016; Fenwick et al., 2019; Scharf et al., 2021), which is driven by persistent T cell receptor (TCR) stimulation and inhibitory microenvironments, can occur even during cART, leading to impaired cytolytic activity (Yates and Tonnerre, 2021). Moreover, most HIV cure strategies that rely on HIV-specific $CD8^+$ T cell expansion to control the virus are likely to fail due to $CD8^+$ T cell exhaustion (Kostense et al., 2001; Day et al., 2006; Trautmann et al., 2006; McLane et al., 2019). Furthermore, studies have found that T_{FH} cells in B-cell follicles are major reservoir cells for long-term latent HIV infection and persistently produce infectious viral particles (Perreau et al., 2013; Xu et al., 2013, 2016; Banga et al., 2016; Miles and Connick, 2016; McGary et al., 2017; Aid et al., 2018). Due to the anatomical structure of B-cell follicles, most HIV-specific $CD8^+$ T cells cannot enter B-cell follicles, representing a significant obstacle to HIV-specific $CD8^+$ T cell-mediated clearance of infected T_{FH} reservoirs. Recently, our group and others found that a small population of exhausted HIV-specific $CD8^+$ T cells expressing CXC chemokine receptor type 5 (CXCR5) can migrate into B-cell follicles in HIV infection (He et al., 2016; Leong et al., 2016). These antigen-specific $CXCR5^+$ $CD8^+$ T cells exhibit memory-like properties and are co-expressed with antigen-specific T cell factor 1 ($TCF1^+$) $CD8^+$ T cells in the germinal center during lymphocytic choriomeningitis virus (LCMV) Cl13 infection (He et al., 2016; Im et al., 2016). HIV-specific $TCF1^+$ $CD8^+$ T cells also possess stem-like memory properties with secondary expansion capacity (Rutishauser et al., 2021). Several recent papers have further shown that $TCF1^{high}$-exhausted antigen-specific $CD8^+$ T cells are the major cells responsive to ICB (Burger et al., 2021; Guo et al., 2021). In this review, we focus on the function of HIV-specific CXCR5-expressing follicular cytotoxic cells and propose strategies for the functional cure of HIV infection by combining cART, ICB, and $CXCR5^+$ $CD8^+$ T cells.

Virus-specific $CD8^+$ T cells during chronic human immunodeficiency virus-1 infection

During acute viral infection, native specific $CD8^+$ T cells recognize viral peptide-MHC class I (p-MHCI) complexes presented by antigen-presenting cells and are activated by signals transduced by TCR complexes and co-stimulatory receptors (Badovinac et al., 2007; Zhang and Bevan, 2011). These activated virus-specific $CD8^+$ T cells, also known as cytotoxic T lymphocytes (CTLs), eliminate viruses through both lytic and non-lytic pathways (Lieberman, 2003). In the lytic pathway, $CD8^+$ T cells recognize virus-infected cells in an MHC-I-dependent manner and lyse-infected cells *via* secretion of antiviral cytokines, such as tumor necrosis factor-α (TNF-α) and interferon-γ (INF-γ), and cytotoxic molecules, such as perforin and granzymes (Hudig et al., 1993; Shankar et al., 1999; Trapani et al., 1999). In the non-lytic pathway, CTLs eliminate virus-infected cells *via* engagement with death-inducing ligands expressed on $CD8^+$ T cells that interact with death receptors on the surface of infected cells (McMichael and Rowland-Jones, 2001; Chang et al., 2002; Seich Al Basatena et al., 2013). After virus elimination, more than 90% of effector cells die from apoptosis during the contraction phase. Only a small population of effector cells go through the contraction phase and enter the memory phase (Jameson and Masopust, 2009; Arens and Schoenberger, 2010; Kaech and Cui, 2012). In contrast to acute infection, chronic viral infections, such as HIV-1, exhibit persistent antigen stimulation and loss of viral replication control by virus-specific $CD8^+$ T cells for two main reasons. First, HIV epitope mutations promote escape from functional CTL recognition (Mailliard et al., 2013). Second, although functional HIV-specific exhausted $CD8^+$ T cells can recognize viral epitopes and secrete IFN-γ and TNF-α, they fail to proliferate or kill infected cells due to inhibitory receptors and interactions with ligands, such as PD-1 and PD-L1 (Takata et al., 2017; Fenwick et al., 2019; McLane et al., 2019; Li et al., 2021). Infected cells that evade HIV-specific CTL killing *via* TCR recognition escape and/or CTL functional exhaustion can spread infection and promote further immune dysregulation.

Differentiation and function of virus-specific CXCR5$^+$ CD8$^+$ T cells during chronic human immunodeficiency virus-1 infection

Long-term control of intracellular pathogens mediated by antigen-specific CTLs requires the establishment of a pool of memory CD8$^+$ T cells that proliferate rapidly in response to re-encountering antigens (Jones and Walker, 2016; Mylvaganam et al., 2019). In our previous study, we identified a unique subset of exhausted CD8$^+$ T cells expressing the chemokine receptor CXCR5 during chronic LCMV-cl13 infection (He et al., 2016). These CXCR5$^+$ CD8$^+$ T cells exhibit a memory-like phenotype and show higher surface expression of CD127 [interleukin (IL)-7 receptor] and CD62L, lower expression of most effector and cytotoxic molecules, including granzyme B, and higher proliferation capacity than their CXCR5$^-$ counterparts. Furthermore, the CXCR5$^+$ CD8$^+$ T cells express lower levels of inhibitory receptors, such as PD-1, CTLA-4, and Tim-3, lower levels of CCR7, and more potent cytotoxicity compared to their CXCR5$^-$ counterparts (Walker and Yu, 2013). Higher CXCR5 and lower CCR7 expression initiate CXCR5$^+$ CD8 T cell migration into B-cell follicles but exclusion from the T cell zone, so these cells are also referred to as follicular cytotoxic T (T_{FC}) cells (Yu et al., 2018). These T_{FC} cells also expressed higher tissue resident traits genes CD69 compares with their CXCR5$^-$ counterparts in LCMV cl13-infected mice and HIV patients' lymphoid tissue (Im et al., 2016; Buggert et al., 2018; Yu et al., 2018). It was reported that there are existing a small fraction of CXCR5$^+$CD8$^+$ T cells in the peripheral blood of healthy controls (0.4–5.0% of total CD8$^+$ T cells) (Bai et al., 2017). However, it was still unknown whether GC T_{FC} exits lymphoid tissues and replenishes the circulating T_{FC} pool under certain diseases. The differentiation of T_{FC} cells in mice follows a specific pathway. Both Blimp1 and E2A are upstream transcriptional regulators of *Cxcr5*. Tcf1 and Bcl6 positively regulate CXCR5 expression by inhibiting Blimp1 expression. Id2 is capable of binding to and inhibiting the transcriptional activity of E2A (He et al., 2016; Im et al., 2016; Yu et al., 2018). In addition, Tcf1 and Bcl6 promote CD8$^+$ T cell memory formation (Zhao et al., 2022), and Blimp1 and Id2 enhance effector CD8$^+$ T cell differentiation (Nutt et al., 2007; Johnston et al., 2009; Shaw et al., 2016; Goldrath et al., 2018; Ciucci and Vacchio, 2022). A recent study found that CXCR5$^-$CD8$^+$ T cells have closed chromatin at the *cxcr5* transcriptional start site, *in vitro* culture with recombinant TGF-ß significantly increased CXCR5 expression. However, the detailed mechanism is still unknown (Ogunshola et al., 2022). Thus, Id2, E2A, Tcf1, Bcl6, and Blimp1 form a transcriptional loop to regulate the CXCR5 expression and T_{FC} cell generation in mice.

Follicular cytotoxic T cells play an important role in controlling viral infections, especially LCMV infection in mice, HIV infection in humans, and SIV infection in non-human primates (He et al., 2016; Im et al., 2016; Mylvaganam et al., 2017). First, given the localization of T_{FC} and T_{FH} cells in follicles, T_{FC} cells have the potential to control the infection of T_{FH} cells. Moreover, it is very important for HIV-specific CD8$^+$ T cells to migrate into follicles to kill the virus-production T_{FH} cells during suppressive ART (Baiyegunhi et al., 2022). In LCMV (docile strain) infection, higher viral titers have been reported in T_{FH} cells in mice receiving CXCR5-deficient virus-specific CD8$^+$ T cells than in mice receiving CXCR5-sufficient virus-specific CD8$^+$ T cells, but with no difference in non-T_{FH} cell infections, suggesting that T_{FC} cells play a specific role in controlling T_{FH} infection (He et al., 2016; Im et al., 2016). Second, some studies reported that there are existing higher frequencies/numbers of HIV-specific CXCR5$^+$ CD8$^+$ T cells in the LNs of elite controllers compared with the LNs of chronic progressors (Nguyen et al., 2019; Adams et al., 2020; Rutishauser et al., 2021). Virus-specific CXCR5$^+$ CD8$^+$ T cells have been identified in the blood and lymph nodes of patients with chronic HIV infection, and HIV-specific T_{FC} cells have been shown to exist in the follicular zone of lymph nodes (Sen et al., 2016; Velu et al., 2018; Xiao et al., 2018; Fenwick et al., 2019). Several studies have confirmed that infected T_{FH} cells are major latent HIV reservoirs, which may compromise HIV cure under ART (Miles and Connick, 2016; Vinuesa et al., 2016; Havenar-Daughton et al., 2017; Cirelli et al., 2019; Crotty, 2019). HIV-specific CXCR5$^+$ CD8 T cell number in blood and in lymph node is negatively correlated with plasma viral load (He et al., 2016; Reuter et al., 2017). In Rhesus macaques, also found higher frequencies of polyfunctional SIV-specific T_{FC} cells in lymphoid tissue are associated with low viral loads (Starke et al., 2020). We also found that, upon short-term stimulation with HIV-specific peptides, virus-specific CXCR5$^+$ CD8$^+$ T cells both in blood and in lymph node can rapidly acquire a more polyfunctional effector phenotype (TNF-α^+ and INF-γ^+), with higher expression of perforin and lower expression of granzyme B *ex-vivo* when compared with virus-specific CXCR5$^-$ CD8$^+$ T cells (He et al., 2016; Im et al., 2016; Reuter et al., 2017; Nguyen et al., 2019; Yates and Tonnerre, 2021). Some studies found HIV-specific CD8$^+$ T cells execute non-lytic functions by producing some antiviral factors, such as alpha- and beta-chemokines and interleukin-16 (Vella and Daniels, 2003). Compared with circulating T_{FC} cells, lymph tissue T_{FC} cells express lower perforin, TNF-α^+, and INF-γ^+, and barely express granzyme B, suggesting there are existing non-cytolytic functions of T_{FC} to eradicate HIV-infected cells. These non-cytolytic functions might be of interest and remain to be explored. These results highlight the potential role of virus-specific CXCR5$^+$ CD8$^+$ T cells in immunosurveillance of B-cell follicles for infected cell elimination. Besides, *via* analyzing the T_{FC}, T_{FH}, and T follicular regulatory cells (Tfreg) of SIV-infected rhesus macaques with high viral loads (HVL) and low viral loads (LVL) in lymph node, found that besides

T_{FC} cells, T_{FH} cells and Tfreg cells also play important role in controlling of virus-infected cells in B-cell follicles (Rahman et al., 2018).

Control of chronic viral infection by antigen-specific $CD8^+$ T cells requires a pool of cells with self-renewal capability and effector differentiation ability to continuously replenish the infection site (Speiser et al., 2014; Petrovas et al., 2017; Monel et al., 2019; Rutishauser et al., 2021). The memory-like and self-renewal capabilities of T_{FC} cells are essential to sustain cellular immunity during chronic viral infection (He et al., 2016; Im et al., 2016). Following the isolation of virus-specific $CXCR5^+$ and $CXCR5^-$ $CD8^+$ cells from LCMV cl13-infected mice, then adoptive transfer into matched LCMV cl13-infected recipient mice. $CXCR5^+$ T_{FC} cells proliferated 10–100 times, maintained self-renewal capability, and reduced viral titers (100–1,000 times) compared with $CXCR5^-$ $CD8^+$ T cells (Day et al., 2006; Yates and Tonnerre, 2021). Recent studies have found that human and non-human virus-specific $CD8^+$ T cells that naturally control HIV/SIV infection express higher levels of the TCF1 transcription factor and CXCR5 surface marker than progressors (Rutishauser et al., 2021). In addition, CXCR5 expression in HIV-specific $CD8^+$ T cells is closely related to memory marker (e.g., CD127 and LEF-1) expression and expansion ability and declines with antigenic stimulation (Rutishauser et al., 2021). Thus, $CXCR5^+$ $CD8^+$ T cells can execute long-term antiviral immunity during chronic viral infection (**Figure 1**).

Immune-based strategies for controlling human immunodeficiency virus infection

The goal of many immune-based strategies that aim to control HIV-1 infection long-term is eliciting functional and durable HIV-specific $CD8^+$ T cells that harbor memory-like capacity and can rapidly expand and differentiate into effector cells to eliminate HIV-infected cells (Jones and Walker, 2016; Mylvaganam et al., 2019). Despite tremendous efforts in researching chronic HIV-1 infection, a cure remains elusive. These persistent viruses cannot be eliminated, in part due to the presence of latent HIV reservoirs in T_{FH} cells and the functional exhaustion of HIV-specific $CD8^+$ T cells (Castro-Gonzalez et al., 2018; Ahlenstiel et al., 2020; Chatzidimitriou et al., 2020). Due to the memory-like characteristics, potential expansion capacity, and location of HIV-specific $CXCR5^+$ CD8 T cells (He et al., 2016; Im et al., 2016), the utilization of HIV-1-specific T_{FC} cells represents a promising strategy for reducing chronic infections. Given their proximal location, T_{FC} cells may deplete infected T_{FH} cells (Kostense et al., 2001; Aid et al., 2018), as supported by the ability of T_{FC} cells from HIV-infected humans to kill HIV-infected cells directly (He et al., 2016). Moreover, the up-regulation of CXCR5 expression forces circulating SIV-specific $CD8^+$ T cells back into B-cell follicles with using a human IL-15 superagonist (ALT-803), resulting in

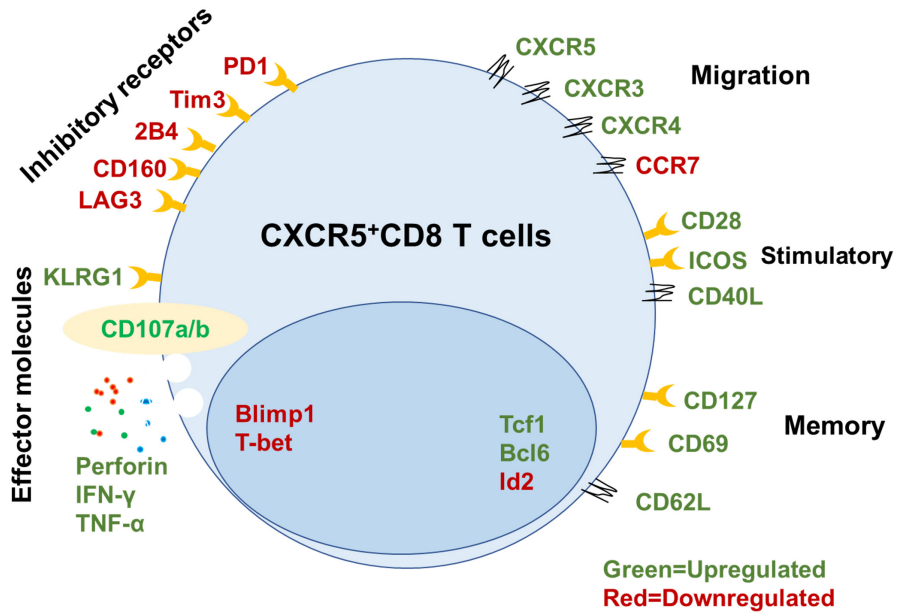

FIGURE 1
Signatures of mouse $CXCR5^+$ $CD8^+$ T cells. Summary of key functional molecules in $CXCR5^+$ $CD8^+$ T cells in lymph tissues (inhibitory receptors, migration, stimulatory, and memory) and peripheral blood compared with $CXCR5^-$ $CD8^+$ T cells based on published data (He et al., 2016; Im et al., 2016; Leong et al., 2016; Nguyen et al., 2019; Adams et al., 2020; Ciucci and Vacchio, 2022).

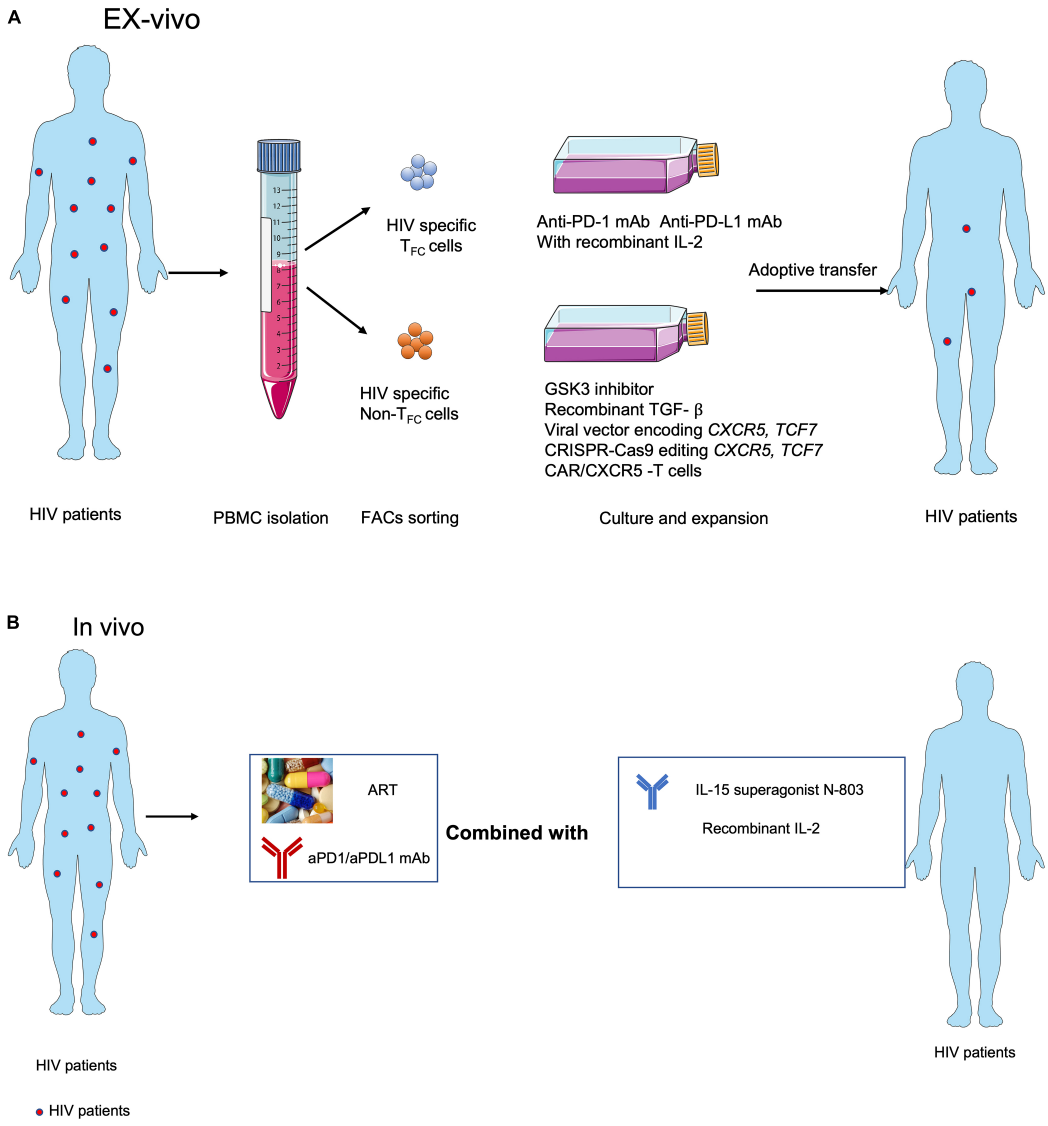

FIGURE 2
Strategies for targeting CXCR5$^+$ CD8$^+$T cells in immunotherapies against HIV infection. **(A)** Adoptive transfer of *ex vivo* expanded endogenous CXCR5$^+$ CD8$^+$ T cells with anti-PD-1 or anti-PD-L1 blocking antibodies or CXCR5$^+$ CD8$^+$ T cell-promoting cytokines, e.g., IL-15 super agonist (Miller et al., 2022), recombinant IL-2 (Codarri Deak et al., 2022; Perdomo-Celis et al., 2022), GSK3 inhibitor (Perdomo-Celis et al., 2022), recombinant TGF- ß (Ogunshola et al., 2022), overexpressed CXCR5 (Ayala et al., 2017) and TCF1 (Rutishauser et al., 2021) and using the CXCR5 expressed CAR-T (Pampusch et al., 2022). **(B)** ART with anti-PD-1 or anti-PDL1 blocking antibodies combined with CXCR5$^+$ CD8$^+$ T cell-promoting cytokines, e.g., IL-15 super agonist (Miller et al., 2022) and IL-2 (Codarri Deak et al., 2022; Perdomo-Celis et al., 2022) *in vivo*.

decreased viral titers in macaques (Webb et al., 2018, 2020). N-803 could not disorder the viral reservoirs in ART-suppressed SHIV-infected rhesus macaques, suggesting N-803 should be coupled with latency reversal agents (Webb et al., 2020). Phase 1 trials of administration of the IL-15 superagonist N-803 in HIV-infected patients resulted in reduced viral reservoirs by activating the virus from latency and enhancing effector function in small population, larger clinical trials are needed to further investigate (Miller et al., 2022). Other methods, which upregulated CXCR5 in PBMC-derived CD8$^+$ T by using murine leukemia virus (MuLV)-based retroviral system also show guide CD8$^+$ T cells migrate to B-cell follicles (Ayala et al., 2017). Recent studies showed that co-expressed CXCR5 in chimeric antigen receptor (CAR) T cells targeting viral-producing (T_{FH}) cells significantly suppressed SIV replication (Haran et al., 2018; Pampusch et al., 2022). Moreover, LCMV cl13-infected recipient mice receiving LCMV-specific CXCR5$^+$ T_{FC} cells showed a significant decrease in viral titers compared to mice receiving CXCR5$^-$ CD8$^+$ T cells (He et al., 2016; Im et al., 2016; Leong et al., 2016). Thus, these results suggest that *ex vivo* expansion

and reinfusion of HIV-specific CXCR5$^+$ CD8$^+$ T cells may be a potential way to execute antiviral immunity against HIV.

Co-inhibitory receptors, such as PD-1, TIM-3, and CTLA-4, play important roles in the maintenance of exhaustion (Das et al., 2017; Hashimoto et al., 2018; Ma et al., 2019; Wolf et al., 2020; Wright et al., 2021). Blockade of these receptors can increase T cell function and viral control in several animal models (Macatangay and Rinaldo, 2009; Ghoneim et al., 2016; Leal et al., 2017; Filaci et al., 2018; Fromentin et al., 2019a; Huang et al., 2019; Spano et al., 2019; Reuss et al., 2020; Lau et al., 2021; Zhen et al., 2021; Uldrick et al., 2022). In HIV infection, high PD-1 expression in CD8$^+$ T cells is associated with increased disease progression and higher viral load (Day et al., 2006). Altogether provided a rationale for trying to use coinhibitory blockade as an immunotherapeutic strategy during HIV infection. Compared with non-treated macaques, PD-1 blockade in SIV-infected macaques before ART can induce rapid expansion of SIV-specific CD8$^+$ T cells, enhance effector function, reduce plasma viral loads, and prolong survival (Bekerman et al., 2019). As T_{FC} cells are the main cell population that responds to ICB therapies that block PD-1 or PD-L1. PD-1/PD-L1 blockade may contribute to enhanced T_{FC} cell survival, proliferation, and differentiation (He et al., 2016; Im et al., 2016; Burger et al., 2021). Indeed, combined PD-L1 blockade and adoptive transfer of virus-specific CXCR5$^+$ CD8$^+$ T cells have been shown to synergistically inhibit LCMV cl13 replication *in vivo* (He et al., 2016). Furthermore, as PD-1 is highly expressed in T_{FH} cells, several studies have found that PD-1 blockade *in vitro* or *ex vivo* can activate latent HIV (Fromentin et al., 2019b; Van der Sluis et al., 2020; Uldrick et al., 2022). Thus, combined adoptive transfer of CXCR5$^+$ CD8$^+$ T cells, PD-1/PD-L1 blockade, and ART should be further explored as a strategy to reverse HIV latency. As for the majority of chronic progressors, there are existing very few T_{FC} cells. So, reprogram the dysfunction of HIV-specific CD8$^+$ T cells to gain the stemness characters, for example, targeting Wnt/transcription TCF-1 (Wnt/TCF-1) and mTORC pathway *via* using small GSK3 inhibitor (Perdomo-Celis et al., 2022). Also, *via* CRISPR-Cas9 to edit the master gene of stemness character, for example, *tcf-7* gene (Rutishauser et al., 2021).

Moreover, other immune-based strategies are aiming to reduce the size of HIV-1 latent reservoir pool. Most studies suggest that HIV-1 specific memory CD4$^+$ T cells are the major cells of HIV latency as described above. Unfortunately, it is remained not fully understood about the characters (e.g., Unique surface makers) of reservoirs. Our recent study found that mTORC2–AKT–GSK3β axis functions as a key signaling hub to promote the longevity of virus-specific memory CD4$^+$ T cells by preventing ferroptosis. This provides a potential strategy that disrupts the mTORC2–AKT–GSK3β axis or induces ferroptosis to minimize the HIV-1 latent pool combine with ART at the beginning of HIV-1 infection (Wang et al., 2022). But experiments are needed to formally test this notion.

Conclusion and future perspectives

Most therapeutic strategies aimed at expanding HIV-specific CD8$^+$ T cells to control viral replication are likely to fail, primarily due to cellular exhaustion and T_{FH} cell reservoirs, particularly anatomical structure that separated largely HIV-specific CD8$^+$ T cells entry into B-cell follicles. Accumulating evidence suggests that T_{FC} cells represent a new subset of cytotoxic T cells with memory-like characteristics and expansion capabilities that can migrate into B-cell follicles and control HIV-1 infection in T_{FH} cell reservoirs. In addition, antigen-specific CXCR5$^+$ CD8$^+$ T cells are positively correlated with prognosis in colorectal, lung, and pancreatic cancers. Although major achievements in PD-1/PD-L1 blockade have been made in the treatment of human tumors, it has not shown success for chronic viral infections. Notably, several remaining hurdles will need to be overcome to successfully harness HIV-specific CXCR5$^+$ CD8$^+$T cells to prevent, treat, and cure viral infection. First, differences in antigen-specific CD8$^+$ T cells in chronic viral infection and tumors need to be elucidated at the transcriptomic, epigenetic, and metabolomic levels to determine why chronic HIV infection responds poorly to PD-1/PD L1 blockade. Second, the origin and early fate commitment of these unique cells need to be clarified. Third, the cytokines and transcription regulators that mediate the differentiation of this subset of cells need to be determined. Recently found IL-2 with PD-1/PDL1 blockade treatment during LCMV cl13 infection epigenetic remodel antigen-specific CD8$^+$ T cells, enforcing them from exhaustion program become effector program (Codarri Deak et al., 2022; Hashimoto et al., 2022). Understanding the features of these cells will not only help to optimize *in vitro* culture conditions for efficient cell expansion but will also facilitate the discovery of the optimal combination of inhibitors, agonists, ART, and ICB for *in vivo* therapy. Based on the evidence from viral infection animal models and analysis of human tumor tissues, we are optimistic that CXCR5$^+$ CD8$^+$ T cells hold promise as putative cellular targets for immunotherapies to treat HIV-1 infection (**Figures 2A,B**).

Author contributions

LG and LY wrote and edited the manuscript. JZ designed the figures. All authors contributed to the article and approved the submitted version.

Funding

This study was supported by grants from the Major National Science and Technology Projects of China (Nos. 2017ZX10202102-006-002 and RCJJ2019-01 to LY) and Classification of Project of China (No. 2021YFC2300602).

Acknowledgments

We thank all members of LY's lab for the discussion of the manuscript.

Conflict of interest

The authors declare that the research was conducted in the absence of any commercial or financial relationships that could be construed as a potential conflict of interest.

The handling editor declared a past co-authorship with the author, LY.

Publisher's note

References

Adams, P., Iserentant, G., Servais, J. Y., Vandekerckhove, L., Vanham, G., and Seguin-Devaux, C. (2020). Cytotoxic CD8+ T Cells Expressing CXCR5 Are detectable in HIV-1 elite controllers after prolonged in vitro peptide stimulation. *Front. Immunol.* 11:622343. doi: 10.3389/fimmu.2020.622343

Ahlenstiel, C. L., Symonds, G., Kent, S. J., and Kelleher, A. D. (2020). Block and lock HIV cure strategies to control the latent reservoir. *Front. Cell. Infect. Microbiol.* 10:424. doi: 10.3389/fcimb.2020.00424

Aid, M., Dupuy, F. P., Moysi, E., Moir, S., Haddad, E. K., Estes, J. D., et al. (2018). Follicular CD4 T helper cells as a major HIV reservoir compartment: A molecular perspective. *Front. Immunol.* 9:895. doi: 10.3389/fimmu.2018.00895

Arens, R., and Schoenberger, S. P. (2010). Plasticity in programming of effector and memory CD8 T-cell formation. *Immunol. Rev.* 235, 190–205. doi: 10.1111/j.0105-2896.2010.00899.x

Autran, B., Descours, B., vettand-Fenoel, V. A., and Rouzioux, C. (2011). Elite controllers as a model of functional cure. *Sci. Transl. Med.* 6, 181–187.

Ayala, V. I., Deleage, C., Trivett, M. T., Jain, S., Coren, L. V., Breed, M. W., et al. (2017). CXCR5-dependent entry of CD8 T cells into rhesus macaque B-cell follicles achieved through T-cell engineering. *J. Virol.* 91, e2507–e2516. doi: 10.1128/JVI.02507-16

Badovinac, V. P., Haring, J. S., and Harty, J. T. (2007). Initial T cell receptor transgenic cell precursor frequency dictates critical aspects of the CD8(+) T cell response to infection. *Immunity* 26, 827–841. doi: 10.1016/j.immuni.2007.04.013

Bai, M., Zheng, Y., Liu, H., Su, B., Zhan, Y., and He, H. (2017). CXCR5(+) CD8(+) T cells potently infiltrate pancreatic tumors and present high functionality. *Exp. Cell Res.* 361, 39–45. doi: 10.1016/j.yexcr.2017.09.039

Baiyegunhi, O. O., Mann, J., Khaba, T., Nkosi, T., Mbatha, A., Ogunshola, F., et al. (2022). CD8 lymphocytes mitigate HIV-1 persistence in lymph node follicular helper T cells during hyperacute-treated infection. *Nat. Commun.* 13:4041. doi: 10.1038/s41467-022-31692-8

Banga, R., Procopio, F. A., Noto, A., Pollakis, G., Cavassini, M., Ohmiti, K., et al. (2016). PD-1(+) and follicular helper T cells are responsible for persistent HIV-1 transcription in treated aviremic individuals. *Nat. Med.* 22, 754–761. doi: 10.1038/nm.4113

Bekerman, E., Hesselgesser, J., Carr, B., Nagel, M., Hung, M., Wang, A., et al. (2019). PD-1 Blockade and TLR7 activation lack therapeutic benefit in chronic simian immunodeficiency virus-infected macaques on antiretroviral therapy. *Antimicrob. Agents Chemother.* 63, e1163–e1119. doi: 10.1128/AAC.01163-19

Borrow, P., Lewicki, H., Hahn, B. H., Shaw, G. M., and Oldstone, M. B. (1994). Virus-specific CD8+ cytotoxic T-lymphocyte activity associated with control of viremia in primary human immunodeficiency virus type 1 infection. *J. Virol.* 68, 6103–6110. doi: 10.1128/JVI.68.9.6103-6110.1994

Buggert, M., Nguyen, S., Salgado-Montes de Oca, G., Bengsch, B., Darko, S., Ransier, A., et al. (2018). Identification and characterization of HIV-specific resident memory CD8(+) T cells in human lymphoid tissue. *Sci. Immunol.* 3:eaar4526. doi: 10.1126/sciimmunol.aar4526

Burger, M. L., Cruz, A. M., Crossland, G. E., Gaglia, G., Ritch, C. C., Blatt, S. E., et al. (2021). Antigen dominance hierarchies shape TCF1(+) progenitor CD8 T cell phenotypes in tumors. *Cell* 184, 4996.e–5014.e. doi: 10.1016/j.cell.2021.08.020

Castro-Gonzalez, S., Colomer-Lluch, M., and Serra-Moreno, R. (2018). Barriers for HIV cure: The latent reservoir. *AIDS Res. Hum. Retroviruses* 34, 739–759.

Chang, T. L., Mosoian, A., Pine, R., Klotman, M. E., and Moore, J. P. (2002). A soluble factor(s) secreted from CD8(+) T lymphocytes inhibits human immunodeficiency virus type 1 replication through STAT1 activation. *J. Virol.* 76, 569–581.

Chatzidimitriou, D., Tsotridou, E., Grigoropoulos, P., and Skoura, L. (2020). HIV-1: Towards understanding the nature and quantifying the latent reservoir. *Acta virol.* 64, 3–9. doi: 10.4149/av_2020_101

Chowdhury, A., Hayes, T. L., Bosinger, S. E., Lawson, B. O., Vanderford, T., Schmitz, J. E., et al. (2015). Differential impact of in vivo CD8+ T lymphocyte depletion in controller versus progressor simian immunodeficiency virus-infected macaques. *J. virol.* 89, 8677–8686. doi: 10.1128/JVI.00869-15

Cirelli, K. M., Carnathan, D. G., Nogal, B., Martin, J. T., Rodriguez, O. L., Upadhyay, A. A., et al. (2019). Slow delivery immunization enhances HIV neutralizing antibody and germinal center responses via modulation of immunodominance. *Immunol. Rev.* 177, 1153.e–1171.e.

Ciucci, T., and Vacchio, M. S. (2022). Dependence on Bcl6 and Blimp1 drive distinct differentiation of murine memory and follicular helper CD4+ T cells. *J. Exp. Med.* 219:e20202343. doi: 10.1084/jem.20202343

Codarri Deak, L., Nicolini, V., Hashimoto, M., Karagianni, M., Schwalie, P. C., Lauener, L., et al. (2022). PD-1-cis IL-2R agonism yields better effectors from stem-like CD8(+) T cells. *Nature* 610, 161–172. doi: 10.1038/s41586-022-05192-0

Collins, U. J. DR, Racenet, Z. J., Arshad, U., Power, K. A., Newman, R. M., Mylvaganam, G. H., et al. (2021). Functional impairment of HIV-specific CD8(+) T cells precedes aborted spontaneous control of viremia. *Immunity* 54, 2372.e–2384.e. doi: 10.1016/j.immuni.2021.08.007

Crotty, S. (2019). T follicular helper cell biology: A decade of discovery and diseases. *Immunity* 50, 1132–1148.

Das, M., Zhu, C., and Kuchroo, V. K. (2017). Tim-3 and its role in regulating anti-tumor immunity. *Nat. Rev. Endocrinol.* 276, 97–111.

Day, C. L., Kaufmann, D. E., Kiepiela, P., Brown, J. A., Moodley, E. S., Reddy, S., et al. (2006). PD-1 expression on HIV-specific T cells is associated with T-cell exhaustion and disease progression. *Nat.* 443, 350–354. doi: 10.1038/nature05115

Eisinger, R. W., and Fauci, A. S. (2018). Ending the HIV/AIDS Pandemic(1). *Emerg. Infect. Dis.* 24, 413–416. doi: 10.3201/eid2403.171797

Fenwick, C., Joo, V., Jacquier, P., Noto, A., Banga, R., Perreau, M., et al. (2019). T-cell exhaustion in HIV infection. *Immunol. Rev.* 292, 149–163.

Filaci, G., Fenoglio, D., Taramasso, L., Indiveri, F., and Di Biagio, A. (2018). Rationale for an association between PD1 checkpoint inhibition and therapeutic vaccination against HIV. *Front. Immunol.* 9:2447. doi: 10.3389/fimmu.2018.02447

Fromentin, R., DaFonseca, S., Costiniuk, C. T., El-Far, M., Procopio, F. A., and Hecht, F. M. (2019a). PD-1 blockade potentiates HIV latency reversal ex vivo in CD4(+) T cells from ART-suppressed individuals. *Sci. Transl. Med.* 10:814. doi: 10.1038s41467-019-08798-7

Fromentin, R., DaFonseca, S., Costiniuk, C. T., El-Far, M., Procopio, F. A., Hecht, F. M. H., et al. (2019b). Chomont, PD-1 blockade potentiates HIV latency reversal ex vivo in CD4(+) T cells from ART-suppressed individuals. *Nat. Commun.* 10:814.

Gandhi, R. T., and Walker, B. D. (2002). Immunologic control of HIV-1. *Curr. HIV/AIDS Rep.* 53, 149–172.

Ghoneim, H. E., Zamora, A. E., Thomas, P. G., and Youngblood, B. A. (2016). Cell-intrinsic barriers of T cell-based immunotherapy. *Trends. Mol. Med.* 22, 1000–1011. doi: 10.1016/j.molmed.2016.10.002

Ghosn, J., Taiwo, B., Seedat, S., Autran, B., Katlama, C. (2018). HIV. *Lancet*. 392, 685–697.

Goldrath, A. W., Omilusik, K. D., and Nadjsombati, M. S. (2018). Sustained Id2 regulation of E proteins is required for terminal differentiation of effector CD8(+) T cells. *Nat. Immunol.* 215, 773–783. doi: 10.1084/jem.20171584

Guo, J., Liang, Y., Xue, D., Shen, J., Cai, Y., Zhu, J., et al. (2021). Tumor-conditional IL-15 pro-cytokine reactivates anti-tumor immunity with limited toxicity. *Cell Res.* 31, 1190–1198. doi: 10.1038/s41422-021-00543-4

Haran, K. P., Hajduczki, A., Pampusch, M. S., Mwakalundwa, G., Vargas-Inchaustegui, D. A., Rakasz, E. G., et al. (2018). Simian immunodeficiency virus (SIV)-specific chimeric antigen receptor-T cells engineered to target B cell follicles and suppress siv replication. *Front. Immunol.* 9:492. doi: 10.3389/fimmu.2018.00492

Hashimoto, M., Araki, K., Cardenas, M. A., Li, P., Jadhav, R. R., Kissick, H. T., et al. (2022). PD-1 combination therapy with IL-2 modifies CD8(+) T cell exhaustion program. *Nature* 610, 173–181. doi: 10.1038/s41586-022-05257-0

Hashimoto, M., Kamphorst, A. O., Im, S. J., Kissick, H. T., Pillai, R. N., Ramalingam, S. S., et al. (2018). CD8 T cell exhaustion in chronic infection and cancer: Opportunities for interventions. *Ann. Rev. Med.* 69, 301–318.

Havenar-Daughton, C., Lee, J. H., and Crotty, S. (2017). Tfh cells and HIV bnAbs, an immunodominance model of the HIV neutralizing antibody generation problem. *Immunol. Rev.* 275, 49–61. doi: 10.1111/imr.12512

He, R., Hou, S., Liu, C., Zhang, A., Bai, Q., Han, M., et al. (2016). Follicular CXCR5- expressing CD8(+) T cells curtail chronic viral infection. *Nature* 537, 412–428.

Huang, Z., Zak, J. P. I, Shaabani, N., Vartabedian, V. F., Nguyen, N., Wu, T., et al. (2019). 27 promotes the expansion of self-renewing CD8(+) T cells in persistent viral infection. *J. Exp. Med.* 216, 1791–1808. doi: 10.1084/jem.20190173

Hudig, D., Ewoldt, G. R., and Woodard, S. L. (1993). Proteases and lymphocyte cytotoxic killing mechanisms. *Curr. Opin. Immunol.* 5, 90–96.

Im, S. J., Hashimoto, M., Gerner, M. Y., Lee, J., Kissick, H. T., Burger, M. C., et al. (2016). Defining CD8+ T cells that provide the proliferative burst after PD-1 therapy. *Nature* 537, 417–421.

Jameson, S. C., and Masopust, D. (2009). Diversity in T cell memory: An embarrassment of riches. *Immunity* 31, 859–871. doi: 10.1016/j.immuni.2009.11.007

Johnston, R. J., Poholek, A. C., DiToro, D. I, Yusuf, D., Eto, B., Barnett, A. L., et al. (2009). Bcl6 and Blimp-1 are reciprocal and antagonistic regulators of T follicular helper cell differentiation. *Science* 325, 1006–1010. doi: 10.1126/science.1175870

Jones, R. B., and Walker, B. D. (2016). HIV-specific CD8? T cells and HIV eradication. *J. Clin. Invest.* 126, 455–463.

Kaech, S. M., and Cui, W. (2012). Transcriptional control of effector and memory CD8+ T cell differentiation. *Nat. Rev. Immunol.* 12, 749–761.

Kostense, S., Ogg, G. S., Manting, E. H., Gillespie, G., Joling, J., Vandenberghe, K., et al. (2001). High viral burden in the presence of major HIV-specific CD8(+) T cell expansions: Evidence for impaired CTL effector function. *Eur. J. Immunol.* 31, 677–686. doi: 10.1002/1521-4141(200103)31:3<677::aid-immu677>3.0.co;2-m

Kreider, E. F., and Bar, K. J. (2022). HIV-1 reservoir persistence and decay: Implications for cure strategies. *Curr. HIV/AIDS Rep.* 19, 194–206. doi: 10.1007/s11904-022-00604-2

Lau, J. S. Y., McMahon, J. H., Gubser, C., Solomon, A., Chiu, C. Y. H., Dantanarayana, A., et al. (2021). The impact of immune checkpoint therapy on the latent reservoir in HIV-infected individuals with cancer on antiretroviral therapy. *AIDS* 35, 1631–1636. doi: 10.1097/QAD.0000000000002919

Leal, L., Lucero, C., Gatell, J. M., Gallart, T., Plana, M., and García, F. (2017). New challenges in therapeutic vaccines against HIV infection. *Exp. Rev. Vaccin.* 16, 587–600.

Leong, Y. A., Chen, Y., Ong, H. S., Wu, D., Man, K., Deleage, C., et al. (2016). CXCR5(+) follicular cytotoxic T cells control viral infection in B cell follicles. *Nat. Immunol.* 17, 1187–1196. doi: 10.1038/ni.3543

Li, J., Huang, H. H., Tu, B., Zhou, M. J., Hu, W., Fu, Y. L., et al. (2021). Reversal of the CD8(+) T-cell exhaustion induced by chronic HIV-1 infection through combined blockade of the adenosine and PD-1 pathways. *Nat. Immunol.* 12:687296. doi: 10.3389/fimmu.2021.687296

Lieberman, J. (2003). The ABCs of granule-mediated cytotoxicity: New weapons in the arsenal. *Nat. Rev. Immunol.* 3, 361–370. doi: 10.1038/nri1083

Ma, J., Zheng, B., Goswami, S., Meng, L., Zhang, D., Cao, C., et al. (2019). PD1(Hi) CD8(+) T cells correlate with exhausted signature and poor clinical outcome in hepatocellular carcinoma. *J. Immunother. Cancer* 7:331. doi: 10.1186/s40425-019-0814-7

Macatangay, B. J., and Rinaldo, C. R. (2009). PD-1 blockade: A promising immunotherapy for HIV? *Cellscience* 5, 61–65.

Mailliard, R. B., Smith, K. N., Fecek, R. J., Rappocciolo, G., Nascimento, E. J., Marques, E. T., et al. (2013). Selective induction of CTL helper rather than killer activity by natural epitope variants promotes dendritic cell-mediated HIV-1 dissemination. *J. Immunol.* 191, 2570–2580. doi: 10.4049/jimmunol.1300373

McGary, C. S., Deleage, C., Harper, J., Micci, L., Ribeiro, S. P., Paganini, S., et al. (2017). CTLA-4(+)PD-1(-) Memory CD4(+) T cells critically contribute to viral persistence in antiretroviral therapy-Suppressed, SIV-infected rhesus macaques. *Immunity* 47, 776.e–788.e. doi: 10.1016/j.immuni.2017.09.018

McLane, L. M., Abdel-Hakeem, M. S., and Wherry, E. J. (2019). CD8 T cell exhaustion during chronic viral infection and cancer. *Ann. Rev. Immunol.* 37, 457–495.

McMichael, A. J., and Rowland-Jones, S. L. (2001). Cellular immune responses to HIV. *Nature* 410, 980–987.

Miles, B., and Connick, E. (2016). TFH in HIV latency and as sources of replication-competent virus. *Trends Microbiol.* 24, 338–344. doi: 10.1016/j.tim.2016.02.006

Milicic, A., Price, D. A., Zimbwa, P., Booth, B. L., Brown, H. L., Easterbrook, P. J., et al. (2005). CD8+ T cell epitope-flanking mutations disrupt proteasomal processing of HIV-1 Nef. *J. Immunol.* 175, 4618–4626. doi: 10.4049/jimmunol.175.7.4618

Miller, J. S., Davis, Z. B., Helgeson, E., Reilly, C., Thorkelson, A., Anderson, J., et al. (2022). Safety and virologic impact of the IL-15 superagonist N-803 in people living with HIV: A phase 1 trial. *Nat. Med.* 28, 392–400. doi: 10.1038/s41591-021-01651-9

Monel, B., McKeon, A., Lamothe-Molina, P., Jani, P., Boucau, J., Pacheco, Y., et al. (2019). Effective CD8(+) T cell recognition of HIV-1-infected non-activated CD4(+) T Cells. *Cell Rep.* 27, 142.e–153.e. doi: 10.1016/j.celrep.2019.03.016

Mylvaganam, G. H., Rios, D., Abdelaal, H. M., Iyer, S., Tharp, G., Mavigner, M., et al. (2017). Dynamics of SIV-specific CXCR5+ CD8 T cells during chronic SIV infection. *Proc. Natl. Acad. Sci. U.S.A.* 114, 1976–1981.

Mylvaganam, G., Yanez, A. G., Maus, M., and Walker, B. D. (2019). Toward T cell-mediated control or elimination of HIV reservoirs: Lessons from cancer immunology. *Front. Immunol.* 10:2109. doi: 10.3389/fimmu.2019.02109

Nguyen, S., Deleage, C., Darko, S., Ransier, A., Truong, D. P., Agarwal, D., et al. (2019). Elite control of HIV is associated with distinct functional and transcriptional signatures in lymphoid tissue CD8(+) T cells. *Sci. Transl. Med.* 11:eaax4077. doi: 10.1126/scitranslmed.aax4077

Nowak, M. A., May, R. M., and Sigmund, K. (1995). Immune responses against multiple epitopes. *J. Theor. Biol.* 175, 325–353.

Nutt, S. L., Fairfax, K. A., and Kallies, A. (2007). BLIMP1 guides the fate of effector B and T cells. *J. Exp. Med.* 7, 923–927. doi: 10.1038/nri2204

Ogunshola, F. J., Smidt, W., Naidoo, A. F., Nkosi, T., Ngubane, T., Khaba, T., et al. (2022). Hypermethylation at the CXCR5 gene locus limits trafficking potential of CD8+ T cells into B-cell follicles during HIV-1 infection. *Blood Adv.* 6, 1904–1916. doi: 10.1182/bloodadvances.2021006001

Pampusch, M. S., Abdelaal, H. M., Cartwright, E. K., Molden, J. S., Davey, B. C., Sauve, J. D., et al. (2022). CAR/CXCR5-T cell immunotherapy is safe and potentially efficacious in promoting sustained remission of SIV infection. *PLoS Pathog.* 18:e1009831. doi: 10.1371/journal.ppat.1009831

Perdomo-Celis, F., Passaes, C., Monceaux, V., Volant, S., Boufassa, F., de Truchis, P., et al. (2022). Reprogramming dysfunctional CD8+ T cells to promote properties associated with natural HIV control. *J. Clin. Invest.* 132:e157549. doi: 10.1172/JCI157549

Perreau, M., Savoye, A. L., De Crignis, E., Corpataux, J. M., Cubas, R., Haddad, E. K., et al. (2013). Follicular helper T cells serve as the major CD4 T cell compartment for HIV-1 infection, replication, and production. *J. Exp. Med.* 210, 143–156.

Petrovas, C., Ferrando-Martinez, S., Gerner, M. Y., Casazza, J. P., Pegu, A., and Deleage, C. (2017). Follicular CD8 T cells accumulate in HIV infection and can kill infected cells in vitro via bispecific antibodies. *Sci. Transl. Med.* 9:eaag2285. doi: 10.1126/scitranslmed.aag2285

Rahman, M. A., McKinnon, K. M., Karpova, T. S., Ball, D. A., Venzon, D. J., Fan, W., et al. (2018). Associations of simian immunodeficiency virus (SIV)-specific follicular CD8(+) T cells with other follicular T cells suggest complex contributions to SIV viremia control. *J. Immunol.* 200, 2714–2726. doi: 10.4049/jimmunol.1701403

Rausch, J. W., and Le Grice, S. F. J. (2020). Characterizing the latent HIV-1 Reservoir in patients with viremia suppressed on cART: Progress, challenges, and opportunities. *Curr. HIV Res.* 18, 99–113. doi: 10.2174/1570162X18666191231105438

Reuss, J. E., Stern, D., Foster, J. C., Ramaswami, R., Lurain, K., Chen, H. X., et al. (2020). Assessment of cancer therapy evaluation program advocacy and inclusion rates of people living With HIV in Anti-PD1/PDL1 Clinical Trials. *JAMA Netw. Open* 3:e2027110. doi: 10.1001/jamanetworkopen.2020.27110

Reuter, M. A., Del Rio Estrada, P. M., Buggert, M., Petrovas, C., Ferrando-Martinez, S., Nguyen, S., et al. (2017). Betts, HIV-specific CD8(+) T cells exhibit reduced and differentially regulated cytolytic activity in lymphoid tissue. *Cell Rep.* 21, 3458–3470. doi: 10.1016/j.celrep.2017.11.075

Rogan, D. C., and Connors, M. (2021). Immunologic control of HIV-1: What have we learned and can we induce it? *Curr. HIV/AIDS Rep.* 18, 211–220.

Rutishauser, R. L., Deguit, C. D. T., Hiatt, J., Blaeschke, F., Roth, T. L., Wang, L., et al. (2021). TCF-1 regulates HIV-specific CD8+ T cell expansion capacity. *JCI Insight* 6:e136648. doi: 10.1172/jci.insight.136648

Scharf, L., Pedersen, C. B., Johansson, E., Lindman, J., Olsen, L. R., and Buggert, M. (2021). Inverted CD8 T-cell exhaustion and Co-stimulation marker balance differentiate aviremic HIV-2-infected from seronegative individuals. *Front. Immunol.* 12:744530. doi: 10.3389/fimmu.2021.744530

Seich Al Basatena, N. K., Chatzimichalis, K., Graw, F., Frost, S. D., Regoes, R. R., and Asquith, B. (2013). Can non-lytic CD8+ T cells drive HIV-1 escape? *PLoS Pathog.* 9:e1003656. doi: 10.1371/journal.ppat.1003656

Sen, D. R., Kaminski, J., Barnitz, R. A., Kurachi, M., Gerdemann, U., Yates, K. B., et al. (2016). The epigenetic landscape of T cell exhaustion. *Immunol. Rev.* 354, 1165–1169.

Shankar, P., Xu, Z., and Lieberman, J. (1999). Viral-specific cytotoxic T lymphocytes lyse human immunodeficiency virus-infected primary T lymphocytes by the granule exocytosis pathway. *Blood* 94, 3084–3093.

Sharp, P. M., and Hahn, B. H. (2011). Origins of HIV and the AIDS pandemic. *Cold Spring Harb. Perspect. Med.* 1:a006841.

Shaw, L. A., Bélanger, S., Omilusik, K. D., Cho, S., Scott-Browne, J. P., Nance, J. P., et al. (2016). Id2 reinforces TH1 differentiation and inhibits E2A to repress TFH differentiation. *Nat. Immunol.* 17, 834–843. doi: 10.1038/ni.3461

Spano, J. P., Veyri, M., Gobert, A., Guihot, A., Perré, P., Kerjouan, M., et al. (2019). Immunotherapy for cancer in people living with HIV: Safety with an efficacy signal from the series in real life experience. *AIDS* 33, F13–F19. doi: 10.1097/QAD.0000000000002298

Speiser, D. E., Utzschneider, D. T., Oberle, S. G., Münz, C., Romero, P., and Zehn, D. (2014). T cell differentiation in chronic infection and cancer: Functional adaptation or exhaustion? Nature reviews. 14, 768–774.

Starke, C. E., Vinton, C. L., Ladell, K., McLaren, J. E., Ortiz, A. M., Mudd, J. C., et al. (2020). SIV-specific CD8+ T cells are clonotypically distinct across lymphoid and mucosal tissues. *J. Clin. Invest.* 130, 789–798. doi: 10.1172/JCI129161

Takata, H., Kessing, C., Fletcher, J. L., Muir, R., Tardif, V., Cartwright, P., et al. (2017). Delayed differentiation of potent effector CD8(+) T cells reducing viremia and reservoir seeding in acute HIV infection. *Sci. Transl. Med.* 9:eaag1809. doi: 10.1126/scitranslmed.aag1809

Trapani, J. A., Sutton, V. R., and Smyth, M. J. (1999). CTL granules: Evolution of vesicles essential for combating virus infections. *Immunol. Today* 20, 351–356. doi: 10.1016/s0167-5699(99)01488-7

Trautmann, L., Janbazian, L., Chomont, N., Said, E. A., Gimmig, S., Bessette, B., et al. (2006). Upregulation of PD-1 expression on HIV-specific CD8+ T cells leads to reversible immune dysfunction. *Nat. Med.* 12, 1198–1202.

Uldrick, T. S., Adams, S. V., Fromentin, R., Roche, M., Fling, S. P., Gonçalves, P. H., et al. (2022). Pembrolizumab induces HIV latency reversal in people living with HIV and cancer on antiretroviral therapy. *Sci. Transl. Med.* 14:eabl3836. doi: 10.1126/scitranslmed.abl3836

Van der Sluis, R. M., Kumar, N. A., Pascoe, R. D., Zerbato, J. M., Evans, V. A., Dantanarayana, A. I., et al. (2020). Combination immune checkpoint blockade to reverse HIV latency. *J. Immunol.* 204, 1242–1254.

Vella, C., and Daniels, R. S. (2003). CD8+ T-cell-mediated non-cytolytic suppression of human immuno-deficiency viruses. *Curr. Drug Targets Infect. Disord.* 3, 97–113. doi: 10.2174/1568005033481196

Velu, V., Mylvaganam, G., Ibegbu, C., and Amara, R. R. (2018). Tfh1 cells in germinal centers during chronic HIV/SIV infection. *Front. Immunol.* 9:1272. doi: 10.3389/fimmu.2018.01272

Vinuesa, C. G., Linterman, M. A., Yu, D., and MacLennan, I. C. (2016). Follicular helper T cells. *Ann. Rev. Immunol.* 34, 335–368.

Walker, B. D., and Yu, X. G. (2013). Unravelling the mechanisms of durable control of HIV-1. *Nat. Rev. Immunol.* 13, 487–498. doi: 10.1038/nri3478

Walker, C. M., Moody, D. J., Stites, D. P., and Levy, J. A. (1986). CD8+ lymphocytes can control HIV infection in vitro by suppressing virus replication. *Science* 234, 1563–1566.

Wang, Y., Tian, Q. H. Y., Yao, W., Lu, J., Chen, C., Chen, X., et al. (2022). The kinase complex mTORC2 promotes the longevity of virus-specific memory CD4(+) T cells by preventing ferroptosis. *Nat. Immunol.* 23, 303–317. doi: 10.1038/s41590-021-01090-1

Webb, G. M., Li, S., Mwakalundwa, G., Folkvord, J. M., Greene, J. M., Reed, J. S., et al. (2018). The human IL-15 superagonist ALT-803 directs SIV-specific CD8(+) T cells into B-cell follicles. *Blood Adv.* 2, 76–84. doi: 10.1182/bloodadvances.2017012971

Webb, G. M., Molden, J., Busman-Sahay, K., Abdulhaqq, S., Wu, H. L., Weber, W. C., et al. (2020). The human IL-15 superagonist N-803 promotes migration of virus-specific CD8+ T and NK cells to B cell follicles but does not reverse latency in ART-suppressed, SHIV-infected macaques. *PLoS Pathog.* 16:e1008339. doi: 10.1371/journal.ppat.1008339

Wolf, Y., Anderson, A. C., and Kuchroo, V. K. (2020). TIM3 comes of age as an inhibitory receptor. *Nat. Rev. Immunol.* 20, 173–185. doi: 10.1038/s41577-019-0224-6

Wright, J. J., Powers, A. C., and Johnson, D. B. (2021). Endocrine toxicities of immune checkpoint inhibitors. *Nat. Rev. Endocrinol.* 17, 389–399.

Xiao, M., Chen, X., He, R., and Ye, L. (2018). Differentiation and function of follicular CD8 T Cells during human immunodeficiency virus infection. *Front. Immunol.* 9:1095. doi: 10.3389/fimmu.2018.01095

Xu, H., Wang, X., Malam, N., Aye, P. P., Alvarez, X., Lackner, A. A., et al. (2016). Persistent simian immunodeficiency virus infection drives differentiation, aberrant accumulation, and latent infection of germinal center follicular T helper cells. *J. Virol.* 90, 1578–1587. doi: 10.1128/JVI.02471-15

Xu, Y., Weatherall, C., Bailey, M., Alcantara, S., De Rose, R., Estaquier, J., et al. (2013). Simian immunodeficiency virus infects follicular helper CD4 T cells in lymphoid tissues during pathogenic infection of pigtail macaques. *J. Virol.* 87, 3760–3773. doi: 10.1128/JVI.02497-12

Yates, K. B., and Tonnerre, P. (2021). Epigenetic scars of CD8(+) T cell exhaustion persist after cure of chronic infection in humans. *Nat. Immunol.* 22, 1020–1029. doi: 10.1038/s41590-021-00979-1

Yu, D., Ye, L., and Portrait, A. (2018). of CXCR5(+) Follicular Cytotoxic CD8(+) T cells. *Trends Immunol.* 39, 965–979.

Yuan, N. Y., and Kaul, M. (2021). Beneficial and adverse effects of cART affect neurocognitive function in HIV-1 infection: Balancing viral suppression against neuronal stress and injury. *J. Neuroimmune Pharmacol.* 16, 90–112. doi: 10.1007/s11481-019-09868-9

Zhang, N., and Bevan, M. J. (2011). CD8(+) T cells: Foot soldiers of the immune system. *Immunity* 35, 161–168. doi: 10.1016/j.immuni.2011.07.010

Zhao, X., Shan, Q., and Xue, H. H. (2022). TCF1 in T cell immunity: A broadened frontier. *Nat. Rev. Immunol.* 22, 147–157. doi: 10.1038/s41577-021-00563-6

Zhen, S., Qiang, R., Lu, J., Tuo, X., Yang, X., and Li, X. (2021). Enhanced antiviral benefit of combination therapy with anti-HBV and anti-PD1 gRNA/cas9 produces a synergistic antiviral effect in HBV infection. *Mol. Immunol.* 130, 7–13. doi: 10.1016/j.molimm.2020.12.004

frontiers | Frontiers in Microbiology

TYPE Original Research
PUBLISHED 22 November 2022
DOI 10.3389/fmicb.2022.1004960

OPEN ACCESS

EDITED BY
Kai Deng,
Sun Yat-sen University, China

REVIEWED BY
Ombretta Turriziani,
Sapienza University of Rome, Italy
Hongbin Song,
Chinese Center For Disease Control and Prevention, China

*CORRESPONDENCE
Jie Peng
pjie138@163.com
Shixing Tang
tamgshixing@smu.edu.cn

†These authors have contributed equally to this work

SPECIALTY SECTION
This article was submitted to Virology, a section of the journal Frontiers in Microbiology

RECEIVED 27 July 2022
ACCEPTED 14 October 2022
PUBLISHED 22 November 2022

CITATION
Zhao J, Chen H, Wan Z, Yu T, Liu Q, Shui J, Wang H, Peng J and Tang S (2022) Evaluation of antiretroviral therapy effect and prognosis between HIV-1 recent and long-term infection based on a rapid recent infection testing algorithm. *Front. Microbiol.* 13:1004960. doi: 10.3389/fmicb.2022.1004960

Evaluation of antiretroviral therapy effect and prognosis between HIV-1 recent and long-term infection based on a rapid recent infection testing algorithm

Jianhui Zhao[1†], Hongjie Chen[2†], Zhengwei Wan[3], Tao Yu[2], Quanxun Liu[1], Jingwei Shui[1], Haiying Wang[1], Jie Peng[2*] and Shixing Tang[1*]

[1]Department of Epidemiology, School of Public Health, Southern Medical University, Guangzhou, China, [2]Department of Infectious Diseases, Nanfang Hospital, Southern Medical University, Guangzhou, Guangdong Province, China, [3]Department of Health Management and Institute of Health Management, Sichuan Provincial People's Hospital, University of Electronic Science and Technology of China, Chengdu, China

Early diagnosis of HIV-1 infection and immediate initiation of combination antiretroviral therapy (cART) are important for achieving better virological suppression and quicker immune reconstitution. However, no serological HIV-1 recency testing assay has been approved for clinical use, and the real-world clinical outcomes remain to be explored for the subjects with HIV-1 recent infection (RI) or long-term infection (LI) when antiretroviral therapy is initiated. In this study, a HIV-1 rapid recent-infection testing strip (RRITS) was developed and incorporated into the recent infection testing algorithms (RITAs) to distinguish HIV-1 RI and LI and to assess their clinical outcomes including virological response, the recovery of $CD4^+$ T-cell count and CD4/CD8 ratio and the probability of survival. We found that the concordance between our RRITS and the commercially available LAg-Avidity EIA was 97.13% and 90.63% when detecting the longitudinal and cross-sectional HIV-1 positive samples, respectively. Among the 200 HIV-1 patients analyzed, 22.5% (45/200) of them were RI patients and 77.5% (155/200) were chronically infected and 30% (60/200) of them were AIDS patients. After cART, 4.1% (5/155) of the LI patients showed virological rebound, but none in the RI group. The proportion of $CD4^+$ T-cell count >500 cells/mm^3 was significantly higher in RI patients than in LI after 2years of cART with a hazard ratio (HR) of 2.6 (95% CI: 1.9, 3.6, p<0.0001) while the probability of CD4/CD8=1 was higher in RI than in LI group with a HR of 3.6 (95% CI: 2.2, 5.7, p<0.0001). Furthermore, the immunological recovery speed was 16 cells/mm^3/month for $CD4^+$ T-cell and 0.043/month for the ratio of CD4/CD8 in the RI group, and was bigger in the RI group than in the LI patients (p<0.05) during the 1st year of cART. The survival probability for LI patients was significantly lower than that for RI patients (p<0.001). Our results indicated that RRITS combined with RITAs could successfully distinguish HIV-1 RI and LI patients whose clinical outcomes were significantly different after

cART. The rapid HIV-1 recency test provides a feasible assay for diagnosing HIV-1 recent infection and a useful tool for predicting the outcomes of HIV-1 patients.

KEYWORDS

HIV-1, recent infection, long-term infection, point-of-care testing, recent infection testing algorithms, clinical prognosis

Introduction

Successful control of HIV-1 epidemics relies on early diagnosis of HIV-1 infection, immediate initiation of combination antiretroviral therapy (cART) and effective suppression of HIV-1 replication during cART, which are the target goals proposed by The Joint United Nations Program on HIV and AIDS (UNAIDS) (2020). It has been well documented that initiation of cART in early HIV-1 infection could result in rapid immunological recovery and better clinical efficacy (Fiebig et al., 2003; Le et al., 2013). In addition, several studies have proved the beneficial effects of starting cART during primary or recent HIV-1 infection on disease progression, such as reducing viremia (Gianella et al., 2011), limiting the size of virus latent pool (Jain et al., 2013), and preserving immune system (Le et al., 2013; Davy-Mendez et al., 2018). Therefore, differentiating HIV-1 recent infection (RI) and long-term infection (LI) may help precisely manage antiretroviral therapy and monitor cART efficacy.

At present, longitudinal sampling and testing of uninfected individuals are the "gold-standard" approach to identify recent HIV-1 infections. However, it is difficult, time-consuming, expensive and technically infeasible (Gable and Lagakos 2008). Several types of serological assays and new biomarkers have recently been developed to differentiate RI and LI of HIV-1, such as less-sensitive enzyme immunoassay (LS-EIA; Rawal et al., 2003), the BED capture enzyme immunoassay (BED-CEIA; Dobbs et al., 2004) and limiting antigen avidity enzyme immunoassay (LAg-Avidity EIA; Duong et al., 2012). Among these assays, BED-CEIA and LAg-Avidity EIA were commercially available and commonly used. Furthermore, HIV-1 recency testing assay has been incorporated into the recent infection testing algorithms (RITAs) and recommended by UNAIDS to differentiate HIV-1 patients with RI and LI (Organization W.H, 2011). However, most serological assays, including LAg-Avidity EIA and BED-CEIA, still depend on the laboratory facility and professional operator, which in turn limit their implementation in point-of-care testing (POCT) and resource-limiting settings.

We have previously identified a 57-mer peptide (gp41-p57) located at the loop region of HIV-1 gp41 protein that could differentiate HIV-1 RI and LI (Li et al., 2016). Our results also confirmed that the recombinant protein MP4 containing HIV-1 gp41 immunodominant epitopes (IDEs) of the major HIV-1 genotype CRF01_AE, CRF07_BC/CRF08_BC and subtype B in China could inhibit the binding of gp41 peptide with anti-HIV antibody of low avidity, and was suitable for distinguishing HIV-1 RI and LI (Cai et al., 2019). The MP4-based enzyme-linked immunosorbent assay showed comparable performance with LAg-Avidity EIA (Cai et al., 2019). In the current study, we reported a HIV-1 rapid recent-infection testing strip (RRITS) assay for distinguishing HIV-1 RI and LI based on the gp41 recombinant antigen MP4 and BE23 and evaluated its clinical utility alone or integrated into the RITAs recommended by UNAIDS to differentiate RI and LI patients. By implementing the rapid HIV-1 recency testing assay in a general hospital in Guangzhou, China, we identified substantial chronically HIV-infected patients whose clinical outcomes after cART were quite different from those with recent HIV-1 infection. Our results confirmed the clinical utility of rapid HIV-1 recency testing assay in precisely identifying and managing HIV-1 patients.

Materials and methods

Specimens for the evaluation of HIV-1 RRITS

The specimens used for the evaluation included three panels (Supplementary Table S1). The optimization of our HIV-1 recency testing RRITS was performed using specimens of Panel 1 that contains 118 samples including 98 anti-HIV positive (11 CRF01_AE, 31 CRF07_BC, 14 CRF08_BC, 3 Subtype B, 39 Unknown) and 20 anti-HIV negative healthy volunteer samples obtained from Beijing Xinchuang Bioengineering Co., Ltd. (Beijing, China) and detected by anti-HIV enzyme-linked immunosorbent assay (ELISA) of WANTAI BioPharm (Beijing, China). HIV-1 positive samples were further classified into HIV-1 RI and LI groups by using the commercial BED-CEIA (Sedia Biosciences, Portland, OR, United States) and LAg-Avidity EIA (Kinghawk Pharmaceutical Co., Ltd., Beijing, China) kits. Panel 2 included 36 archived de-linked serum samples from 9 patients undergoing acute HIV-1 seroconversion. They were prospectively collected and have been previously described (Cai et al., 2019), and were used to calculate the mean duration of recent infection (MDRI) of our RRITS assay. Each patient provided 4 follow-up samples from the last date with anti-HIV

negative result (day 0) up to 602 days after HIV-1 seroconversion. Panel 3 included 110 specimens (40 CRF01_AE, 40 CRF_07BC, 7 Subtype B and 23 CRF55_01B) from the Guangzhou Center for Disease Control and Prevention, 200 from Nanfang Hospital of Guangzhou and 85 from the Guangzhou Eighth People's Hospital. These samples were detected by the recency test of HIV-1 LAg-Avidity EIA Kit and used to further validate the performance of our HIV-1 RRITS.

Patients

To evaluate the impact of HIV-1 recency testing on disease progress and outcome, 200 HIV-1 patients from Nanfang Hospital, a general teaching hospital of Southern Medical University in Guangzhou, China. In our study, 200 HIV-1 patients were selected from 536 HIV-1 infected patients through simple random sampling in Nanfang Hospital during September 2018 and November 2019. Baseline characteristics, including gender, age, mode of infection, marital status and cART regimen were collected from clinical records. The $CD4^+$ and $CD8^+$ T-cell counts, plasma HIV-1 RNA level and other laboratory data were collected. Samples of whole blood and plasma were collected and frozen at −80°C. Virological suppression was defined as a plasma HIV-1 RNA load of <50 copies/mL (CMA and CCDC, 2022). Virological rebound was defined as HIV-1 RNA level ≥ 200 copies/mL after virological suppression (CMA and CCDC, 2022). AIDS patients were defined as HIV-1 patients with $CD4^+$ T-cell counts <200 cells/mm^3 and/or pneumocystis yersini pneumonia (CMA and CCDC, 2022). The clinical study was approved by the Nanfang Hospital Ethics Committee (NFEC-2021-448), and all patients provided informed consent.

Recent infection testing algorithms

The flow chart of RITAs was adapted from the file of UNAIDS/WHO Working Group (Organization W.H, 2011) and shown in Figure 1. The criteria for HIV-1 RI patients included: (1) HIV-1 RRITS line score $T_1 < L3$; Of note, T_1 line was specifically designed to distinguish HIV-1 RI and LI according to its density or score since the coating antigen in T1 line can specifically bind mature anti-gp41 antibody with high avidity, which is usually found in HIV-1 long-term infection, but not in recent infection. (2) HIV-1 diagnosis ≤ 1 year (Rice et al., 2020; de Wit et al., 2021; Teixeira et al., 2021); (3) baseline $CD4^+$ T-cell counts ≥ 200 cells/μl (Chauhan et al., 2020; Karatzas-Delgado et al., 2020; Zhu et al., 2020; Ang et al., 2021; Teixeira et al., 2021); (4) baseline HIV-1 RNA level ≥ 1,000 copies/ml (Rice et al., 2020; Zhu et al., 2020; de Wit et al., 2021; Rwibasira et al., 2021; Voetsch et al., 2021). Otherwise, the HIV-1 patients were considered as long-term infection (LI) of HIV-1. The development, evaluation and testing of RRITS method were presented in the Supplementary methods.

Prediction model of mortality of cART-treated HIV-1 patients

The parameters of HIV-1 mortality risk model (Hou et al., 2019) was obtained from the nomogram with GetData Graph Digitzer (Version 2.5). The prognostic index for each patient (i) was calculated using the following formula:

$$\begin{aligned}\mathrm{PI}_i = &-0.005580907 \times \text{CD4 cell count} - 0.005368102 \times \text{hemoglobin} \\ &+1.019669556\left[\text{if HIV viral load}_i \text{ is within } 200-1000\right] \\ &+2.608969326\left[\text{if HIV viral load}_i \geq 1000\right]\end{aligned}$$

The predicted survival probability at t year ($t = 1$, 2, and 3) after cART initiation for each patient (i) was determined using the following formula:

$$\hat{S}_i(1) = 0.980222074^{\exp(\mathrm{PI}_i)}$$

$$\hat{S}_i(2) = 0.972736744^{\exp(\mathrm{PI}_i)}$$

$$\hat{S}_i(3) = 0.964896148^{\exp(\mathrm{PI}_i)}$$

The risk score for each patient (i) was calculated using the following formula:

$$\text{Risk score}_i = 108.3333333 + 19.90914787 \times \mathrm{PI}_i$$

The adjusted prognostic index by age and gender for each patient (i) was calculated using the following formula (Wang et al., 2020):

$$\begin{aligned}\mathrm{PIadjust}_i = \mathrm{PI}_i &+ 0.2382292\left[\text{if age}_i \text{ is within } 40-60\right] \\ &+ 0.5866749\left[\text{if age}_i \geq 60\right] \\ &-0.3566749\left[\text{if gender}_i = \text{female}\right]\end{aligned}$$

Statistical analysis

The data were analyzed with R software version 3.6.2 and STATA/SE 15.0 (STATA Corp, College Station, TX) and graphed with GraphPad Prism 8.0 (GraphPad Software, California, United States). The Chi-square Test/ANOVA analysis and the independent-sample *T*-Test or Mann–Whitney/Kruskal-Wallis H Test were used for qualitative and quantitative variables, respectively. Polynomial regression was

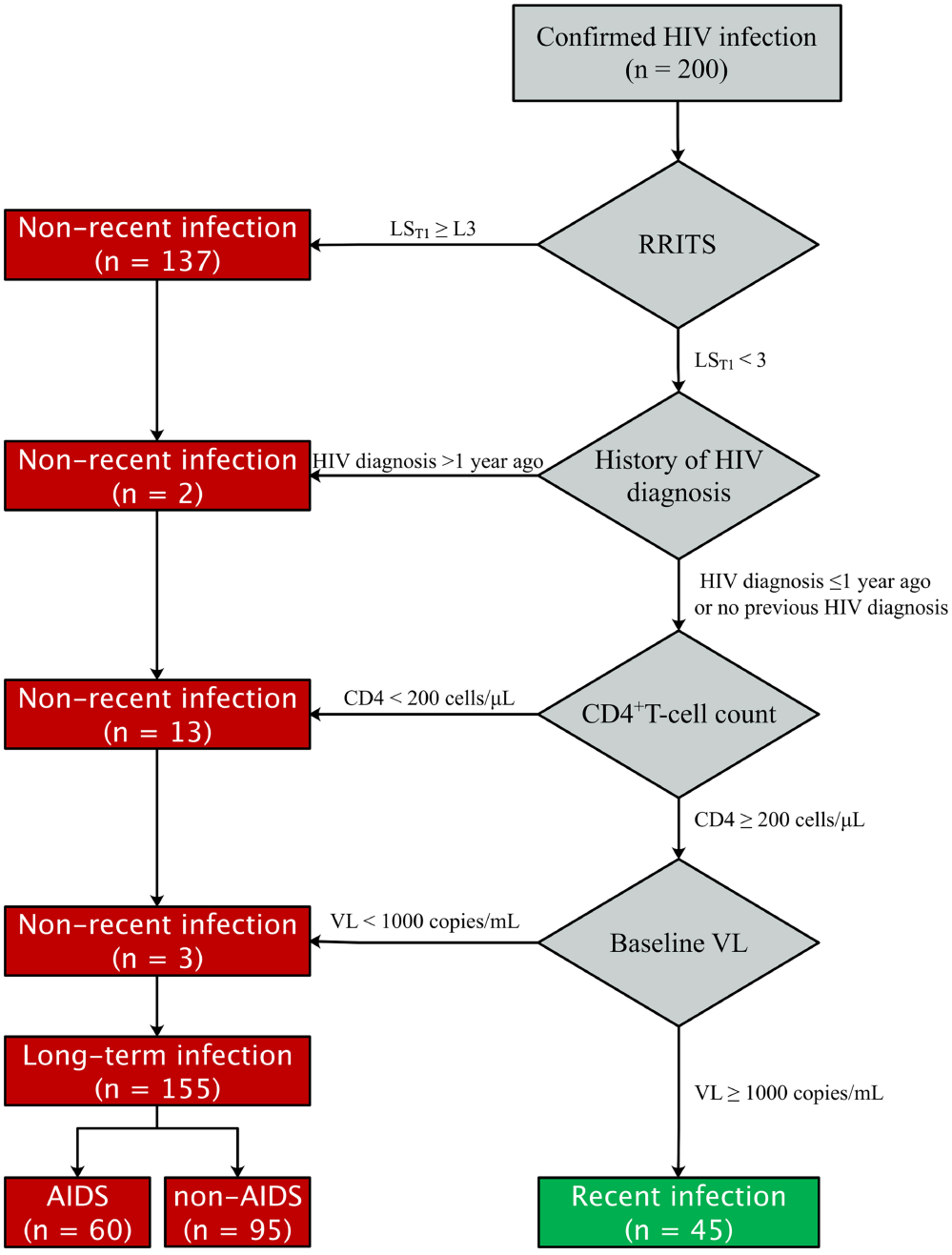

FIGURE 1
Flow chat of HIV-1 recent infection testing algorithms (RITAs) to classify recent and long-term HIV-1 infection. RRITS, rapid recent-infection testing strip; LS$_{T1}$, the T$_1$ line score of RRITS for detection of long-term HIV-1 infection; HIV, human immunodeficiency virus; AIDS, acquired immunodeficiency syndrome; VL, viral load.

used to estimate the mean duration of recent infection (MDRI) of the RRITS, and Spearman correlation was used to analyze the correlation between line score T$_1$ and ODn. The recovery speed of CD4$^+$ T-cell count and CD4/CD8 ratio was compared between the RI and LI groups by using the Log-rank test, and the hazard ratio (HR) was calculated. The dynamics of CD4$^+$ T-cell count and CD4/CD8 ratio for the RI vs. LI groups during cART were compared using generalized estimating equations (GEE). CD4$^+$ T-cell count and CD4/CD8 ratio and 95% pointwise confidence bands were obtained from nonlinear GEE. All tests were two-sided and $p < 0.05$ was set as the significant level. Propensity score matching (PSM) was used to conduct a 1:1 case–control study by controlling age, baseline CD4$^+$ T-cell count, baseline HIV-1 RNA level, gender, mode of infection, marital status, cART regimen and drug therapy adherence.

Results

Development and evaluation of HIV-1 RRITS

We first determined the coating ratio of HIV-1 gp41 recombinant antigen BE23 and MP4, which was 1:3 (Supplementary Figure S1), and the optimal cut-off value of RRITS T1 line as L3 when distinguishing HIV-1 RI and LI (Supplementary Figure S2). Under these conditions, the AUC of the receiver operator characteristic curve was 0.946 (Supplementary Figure S2) and the sensitivity and specificity of RRITS were 98.98% (97/98) and 100.00% (20/20), respectively when compared with anti-HIV ELISA (Supplementary Table S2). Among the 36 seroconversion samples determined to be HIV-1 RI or LI by both Maxim and KingHawk LAg-Avidity EIA, 35 (97.22%) were correctly recognized by the RRITS with a Kappa value of 0.940 (Figure 2A, Table 1). A good correlation between the time of post-infection and the line score of T_1 was obtained by polynomial regression analysis with an R^2 value of 0.872 (Figure 2B). The estimated MDRI of RRITS was 190 days and the false-recent rate (FRR) was 5.88% (2/34). Furthermore, we compared the performance of RRITS and LAg-Avidity EIA assays in 395 cross-sectional specimens. The Kappa value and concordance rate were 0.806% and 90.63%, respectively (Table 1). As shown in Supplementary Figure S3, a good correlation between the line score of T_1 for our RRITS and ODn of LAg-Avidity EIA was observed. The correlation coefficient was 0.843 ($p < 0.001$). Furthermore, our results indicated that HIV-1 RRITS showed a comparable detection capapbility for the predominant HIV-1 genotypes ro subtypes in China (Supplementary Table S3).

Comparison of RITAs and rapid HIV-1 recency testing alone to differentiate HIV-1 recent infection and long-term infection

31.5% (63/200) and 68.5% (137/200) HIV-1 patients were identified as RI and LI, respectively based on RRITS alone while 26.5% (53/200) and 73.5% (147/200) patients were RI and LI, respectively based on the results of RITAs and LAg-Avidity EIA (Supplementary Figure S4). Although the difference of RI and LI identified by RRITS alone or RITAs was statistically significant ($p < 0.01$), the results of the two methods were correlated well (Kappa = 0.774, Supplementary Table S4). Of note, further analysis showed no significant difference in virological response, immune reconstitution and prognostic risk score between HIV-1 RI and LI groups differentiated by RITAs using RRITS or LAg-Avidity EIA and RRITS alone after cART ($p > 0.1$, Table 2).

Differentiation of recent and long-term HIV-1 infection

UNAIDS recommends the combination of RITAs with HIV-1 serological recency testing and routine clinical tests to more accurately distinguish RI and LI (WHO, 2011; accessed January 23, 2022). Thus, we integrated the history of HIV-1 diagnosis, baseline CD4$^+$ T-cell count and HIV-1 RNA level and our RRITS results to determine the infection status of HIV-1 patients (Figure 1). Among the 200 patients analyzed, 45 (22.5%) and 155 (77.5%) patients were identified as RI and LI, respectively while 60 (30%) were AIDS patients. Clinical and demographical characteristics between RI and LI groups were shown in Table 3, and no significant difference was observed between the RI and LI

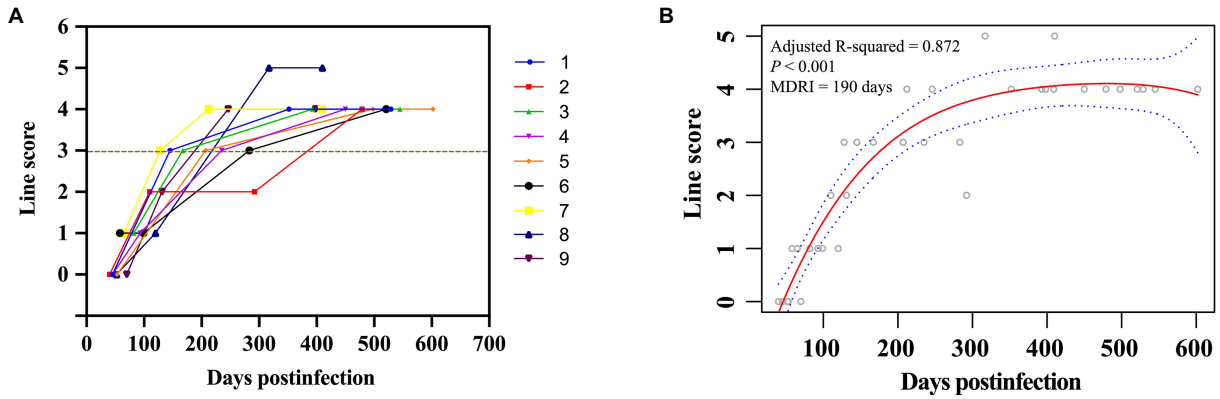

FIGURE 2
Discrimination of HIV-1 recent and long-term infection using rapid recent-infection testing strip in longitudinal cohort samples. **(A)** A total of 36 longitudinal seroconversion samples collected from 9 HIV-1-infected individuals were labeled with different colors and detected by rapid recent-infection testing strip (RRITS) at different time points. Y axis shows T_1 line score of RRITS, which is determined according to the density of T_1 line. The brown dash line represents the cut-off value of T_1 line of RRITS. **(B)** The relationship between the time post-infection and the line score of T_1 through polynomial regression analysis. The polynomial regression values and their 95% confidence intervals are presented in red solid line and blue curves, respectively. MDRI, mean duration of recent infection.

TABLE 1 Comparison of rapid recent-infection testing strip (RRITS) and LAg-Avidity EIA to distinguish HIV-1 recent and long-term infection.

Groups	Methods		LAg-Avidity EIA		Total	Kappa value	Concordance (%)	Predictive Value (%)	
			RI	LI				RI	LI
Longitudinal samples	RRITS	RI	13	1	14	0.940	97.13	92.86	100.00
		LI	0	22	22				
		Total	13	23	36				
Cross-sectional samples[a]		RI	142	11	153	0.806	90.63	92.81	89.26
		LI	26	216	242				
		Total	168	227	395				

[a]395 cross-sectional serum samples from multiple-center studies, including Guangzhou Center for Disease Control and Prevention, The Eighth People's Hospital of Guangzhou and Nanfang Hospital of Guangdong. RI, recent infection; LI, long-term infection.

TABLE 2 Analysis of virological response, immune reconstitution and prognostic risk score in 200 cART-treated HIV-1 patients.

Variable	Differentiation strategies			Value of p^c	Value of p^d	Value of p^e
	RRITS	RITAs1[a]	RITAs2[b]			
HIV-1 patients of recent infection						
Attainment of virological suppression at 6 months after cART	54 (91.5%)	40 (95.2%)	46 (93.9%)	0.744	0.924	>0.999
Attainment of virological suppression at 12 months after cART	56 (96.6%)	40 (97.6%)	46 (95.8%)	>0.999	>0.999	>0.999
Virological rebound at 12 months after cART	0 (0.0%)	0 (0.0%)	1 (2.2%)	-	0.465	>0.999
$CD4^+$ T-cell recovery speed (cells/mm^3/mo) at 1st year of cART	15	16	16	0.384	0.175	0.441
CD4/CD8 recovery speed per month at 1st year of cART	0.036	0.042	0.040	0.152	0.175	0.363
$CD4^+$ T-cell recovery speed (cells/mm^3/mo) at 2nd year of cART	7	8	8	0.257	0.318	0.416
CD4/CD8 recovery speed per month at 2nd year of cART	0.012	0.015	0.015	0.257	0.271	0.465
Prognostic risk score, P_{50} (P_{25}, P_{75})	108 (98, 118)	100 (93, 111)	101 (95, 111)	0.722	0.787	>0.999
HIV-1 patients of long-term infection						
Attainment of virological suppression at 6 months after cART	109 (92.4%)	123 (91.1%)	117 (91.4%)	0.717	0.782	0.933
Attainment of virological suppression at 12 months after cART	107 (93.9%)	123 (93.9%)	117 (94.4%)	0.932	>0.999	0.935
Virological rebound at 12 months after cART	5 (4.6%)	5 (4.1%)	4 (3.5%)	>0.999	0.893	>0.999
$CD4^+$ T-cell recovery speed (cells/mm^3/mo) at 1st year of cART	10	11	10	0.406	0.395	0.492
CD4/CD8 recovery speed per month at 1st year of cART	0.024	0.024	0.024	0.496	0.423	0.446
$CD4^+$ T-cell recovery speed (cells/mm^3/mo) at 2nd year of cART	4	4	4	0.452	0.489	0.443
CD4/CD8 recovery speed per month at 2nd year of cART	0.010	0.009	0.010	0.448	0.395	0.478
Prognostic risk score, P_{50} (P_{25}, P_{75})	119 (100, 128)	116 (102, 127)	121 (102, 128)	>0.999	>0.999	>0.999

[a]RITAs1 was based on HIV-1 rapid recent-infection testing strip (RRITS).
[b]RITAs2 was based on LAg-Avidity EIA.
[c]Value of *p* was calculated for RRITS vs. RITAs1.
[d]Value of *p* was calculated for RRITS vs. RITAs2.
[e]Value of *p* was calculated for RITAs1 vs. RITAs2.

patients in the mode of infection, marital status, cART regimen, cART adherence and baseline HIV-1 RNA level. Only the proportion of female patients was higher in long-term infections than males (95.2% vs. 75.4%).

Difference in virological response and immune-reconstitution between the patients with recent and long-term HIV-1 infection after cART

We then compared RI and LI patients in virological response and immune reconstitution during cART. The results indicated that 95.2% of RI and 91.1% of LI patients reached virological suppression after 6 months of cART while 97.6% of RI and 93.9% of LI patients were virologically suppressed after 12 months of cART (Table 4). Interestingly, 4.1% of LI patients showed virological rebound at 12 months post cART, but no RI patients relapsed although the difference was not statistically significant ($p = 0.336$, Table 4). We further divided LI patients into LI with AIDS (LI AIDS) and without AIDS (LI non-AIDS) according to the Chinese Guidelines for Diagnosis and Treatment of HIV/AIDS (2021) (CMA and CCDC, 2022), and found a lower virological suppression rate in the LI AIDS, i.e., 85.7% at 6 months of cART and 90.6% at 12 months of cART, than LI non-AIDS patients (Table 5). Furthermore, a slightly higher frequency of

10.3389/fmicb.2022.1004960

TABLE 3 Clinical and demographical characteristics of the study cohort.

Variables	RI ($n = 45$)	LI ($n = 155$)	Total ($n = 200$)	Value of p[a]
Age (year), median (IQR)	25.0 (22.0, 34.0)	31.0 (25.0, 41.0)	30.0 (24.0, 39.8)	<0.001
Gender, no. (%)				0.075
Female	1 (2.2)	20 (12.9)	21 (10.5)	
Male	44 (97.8)	135 (87.1)	179 (89.5)	
Mode of infection, no. (%)				0.183
Heterosexual contact	4 (8.9)	31 (20.0)	35 (17.5)	
Homosexual contact	41 (91.1)	122 (78.7)	163 (81.5)	
Unknow	0 (0.0)	2 (1.3)	2 (1.0)	
Marital status, no. (%)				0.223
Married or cohabiting	8 (17.8)	46 (29.7)	54 (27.0)	
Divorced or separated or widowed	5 (11.1)	20 (12.9)	25 (12.5)	
Unmarried	32 (71.1)	89 (57.4)	121 (60.5)	
cART regimen, no. (%)				0.897
TDF + 3TC + EFV	43 (95.6)	144 (92.9)	187 (93.5)	
TDF + 3TC + LPV/r	0 (0.0)	1 (0.7)	1 (0.5)	
TDF + 3TC + DTG	1 (2.2)	7 (4.5)	8 (4.0)	
E + C + T + F	1 (2.2)	3 (1.9)	4 (2.0)	
cART adherence, no. (%)				0.676
Optimal	35 (77.8)	111 (71.6)	146 (73.0)	
Sub-optimal	10 (22.2)	41 (26.5)	51 (25.5)	
Unknow	0 (0.0)	3 (1.9)	3 (1.5)	
Baseline $CD4^+$ T-cell count (cells/mm^3), median (IQR)	391.0 (294.5, 462.0)	155.5 (244.0, 377.5)	284.5 (182.8, 411.3)	<0.001
Baseline HIV-1 RNA level (log_{10} copies/ml), median (IQR)	4.20 (3.77, 4.82)	3.69 (4.20, 4.77)	4.20 (3.73, 4.80)	0.522

RI, recent infection; LI, long-term infection; TDF, tenofovir disoproxil fumarate; 3TC, lamivudine; EFV, efavirenz; LPV/r, lopinavir/ritonavir; E, elvitegravir; C, cobicistat; T, tenofovir; F, emtricitabine; cART, combination antiretroviral therapy; IQR, interquartile range.
[a]Comparison between groups before cART: Mann–Whitney test, or χ^2 test or Fisher exact test.

TABLE 4 Virological suppression and rebound in 200 cART-treated HIV-1 patients of recent or long-term infection.

Variable	No. (%)			Value of p[a]
	Total	RI	LI	
Attainment of virological suppression[b] at 6 months after cART	163 (92.1)	40 (95.2)	123 (91.1)	0.524
Attainment of virological suppression at 12 months after cART	163 (94.8)	40 (97.6)	123 (93.9)	0.688
Virological rebound[c] at 12 months after cART	5 (3.1)	0 (0.0)	5 (4.1)	0.336

cART, combination antiretroviral therapy; RI, recent infection; LI, long-term infection.
[a]Values of p were calculated by chi-square test.
[b]Virological suppression was defined as HIV-1 viral load < 50 copies/ml.
[c]Virological rebound was defined as HIV-1 viral load increased from < 50 copies/ml at 6 months after cART to ≥200 copies/ml at 12 months after cART.

virological rebound was observed in LI AIDS (6.4%) and LI non-AIDS (2.7%) patients during 12 months of cART when compared to the RI group (Table 5).

We selected $CD4^+$ T-cell count ≥500 cells/mm^3 and CD4/CD8 ratio ≥ 1 to represent the primary endpoints of immunological reconstruction (Le et al., 2013), and found that 45.2% patients did not meet the criteria of primary $CD4^+$ T-cell recovery after 2 years of cART, but 95.7% of them were LI patients (Figure 3A). The probability of $CD4^+$ T-cell count recovered to 500 cells/mm^3 was 2.6 times higher in RI patients than LI (95% CI: 1.9, 3.6, $p < 0.0001$, Figure 3A). Meanwhile, 67.4% of RI and 23.8% of LI patients met the criteria for CD4/CD8 ratio recovery after 2 years of cART (Figure 3B). The probability of CD4/CD8 ratio ≥ 1 was 3.6 times higher in RI patients than LI patients (95% CI: 2.2, 5.7, $p < 0.0001$, Figure 3B). In addition, we found that the recovery speed of $CD4^+$ T-cell count was faster in RI patients (16 cells/mm^3 per month) than LI patients (11 cells/mm^3 per month, $p = 0.012$, Figure 4A) while a similar trend was observed for the recovery speed of CD4/CD8 ratio, i.e., 0.042 per month for RI patients and 0.024 per month for LI patients ($p < 0.0001$, Figure 4B). Although the recovery speed of the immune reconstruction of RI patients was slightly quicker than LI patients during 12–24 months of cART, the difference was not statistically significant ($p = 0.061$ for $CD4^+$ T-cell count; $p = 0.197$ for CD4/CD8 ratio). Furthermore, the $CD4^+$ T-cell count recovery speed of RI, LI non-AIDS and LI AIDS patients were 16, 11 and 11 cells/mm^3 per month,

TABLE 5 Virological suppression and rebound in 200 cART-treated HIV-1 patients of recent or long-term infection with or without AIDS.

Variable	No. (%)			Value of p^a	Value of p^b	Value of p^c
	RI	LI (non-AIDS)	LI (AIDS)			
Attainment of virological suppression at 6 months after cART	40 (95.2)	75 (94.9)	48 (85.7)	0.181	>0.999	0.122
Attainment of virological suppression at 12 months after cART	40 (97.6)	75 (96.2)	48 (90.6)	0.227	>0.999	0.268
Virological rebound at 12 months after cART	0 (0.0)	2 (2.7)	3 (6.4)	0.248	0.544	0.375

[a]Value of p was calculated for RI vs LI (AIDS).
[b]Value of p was calculated for RI vs LI (non-AIDS).
[c]Value of p was calculated for LI (AIDS) vs LI (non-AIDS).

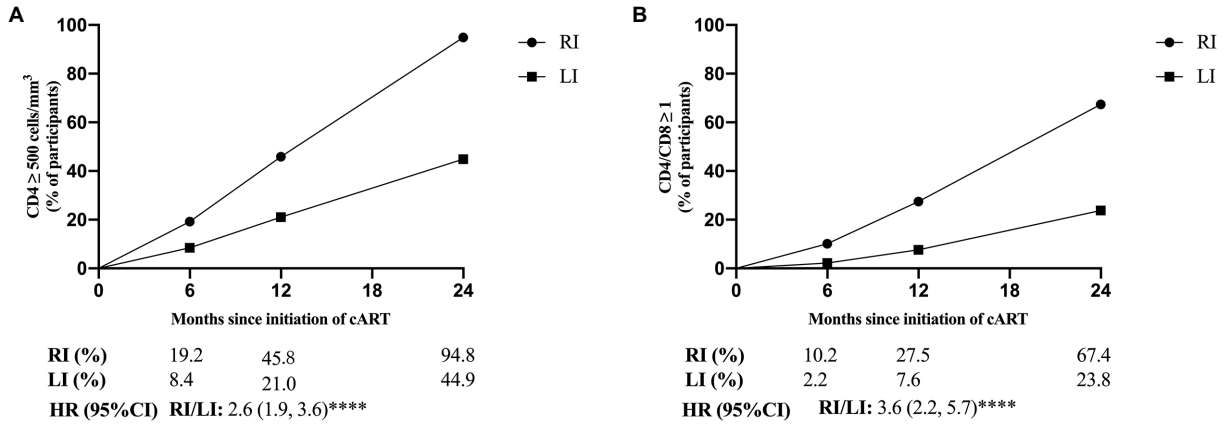

FIGURE 3
The proportion of CD4⁺ T-cell count≥500cells/mm³ and CD4/CD8 ratio≥1 for HIV-1 patients with recent and long-term HIV-1 infections after cART. CD4⁺ and CD8⁺ T-cell counts **(A)** and the ratio of CD4/CD8 **(B)** were detected in 200 cART-treated patients at different time points. RI, recent infection; LI, long-term infection; HR, hazard ratio; *, p<0.05; **, p<0.01; ***, p<0.001; ****, p<0.0001; ns, p>0.05.

respectively (Supplementary Figure S5A) whereas the corresponding CD4/CD8 ratio recovery speed was 0.042, 0.028 and 0.018 per month, respectively (Supplementary Figure S5B). The recovery speed of CD4⁺ T-cell count and CD4/CD8 ratio at the first 6 months, 6–12 and 12–24 months after cART was analyzed separately and was fastest in the first 6 months of cART for both RI and LI patients (Supplementary Figure S6).

To avoid potential variation, we conducted a 1:1 case–control study based on PSM analysis to adjust the factors of age, baseline CD4⁺ T-cell count, baseline HIV-1 RNA level, gender, mode of infection, marital status, cART regimen and cART adherence (Supplementary Table S5). GEE analysis confirmed the difference of CD4⁺ T-cell count recovery speed between RI and LI patients (18 vs. 10 cells/mm³ per month, p = 0.012) and CD4/CD8 ratio recovery speed (0.044 vs. 0.027 per month, p = 0.006) during 12 months of cART (Figures 4C,D). These results indicated better immunological reconstitution in RI patients during 1st year of cART.

Prognosis of cART-treated patients with recent or long-term HIV-1 infection

No mortality event was observed in our study due to the relatively short follow-up time. Thus, the HIV mortality risk model from previous studies (Hou et al., 2019; Wang et al., 2020) was used to predict HIV/AIDS-related mortality of RI and LI patients. The results indicated that the survival probability of the RI group was 98.69%, 98.20%, and 97.68% at the 1st, 2nd and 3rd year after cART, respectively, which were higher than the LI group (96.77% at the 1st year; 95.56% at the 2nd year; 94.30% at the 3rd year, p < 0.001, Figures 5A,B). Meanwhile, similar results were obtained when both age and gender were adjusted. Further analysis suggested that the survival probability of LI AIDS patients was significantly smaller than RI and LI non-AIDS patients (p < 0.001, Figures 5C,D). The prognostic risk scores indicated that 22.22% of RI patients belong to the moderate risk group while 34.41% were in the LI non-AIDS group and 98.33% in the LI AIDS group (p < 0.001, Figure 6). These results showed lower HIV/AIDS-related mortality risk in RI patients than LI patients.

Discussion

In this study, we developed a rapid HIV-1 recency test to distinguish HIV-1 RI or LI patients and further assessed the impact of differentiating HIV-1 RI and LI on virological suppression and rebound, immune reconstitution as well as mortality after cART. We demonstrated the good performance of

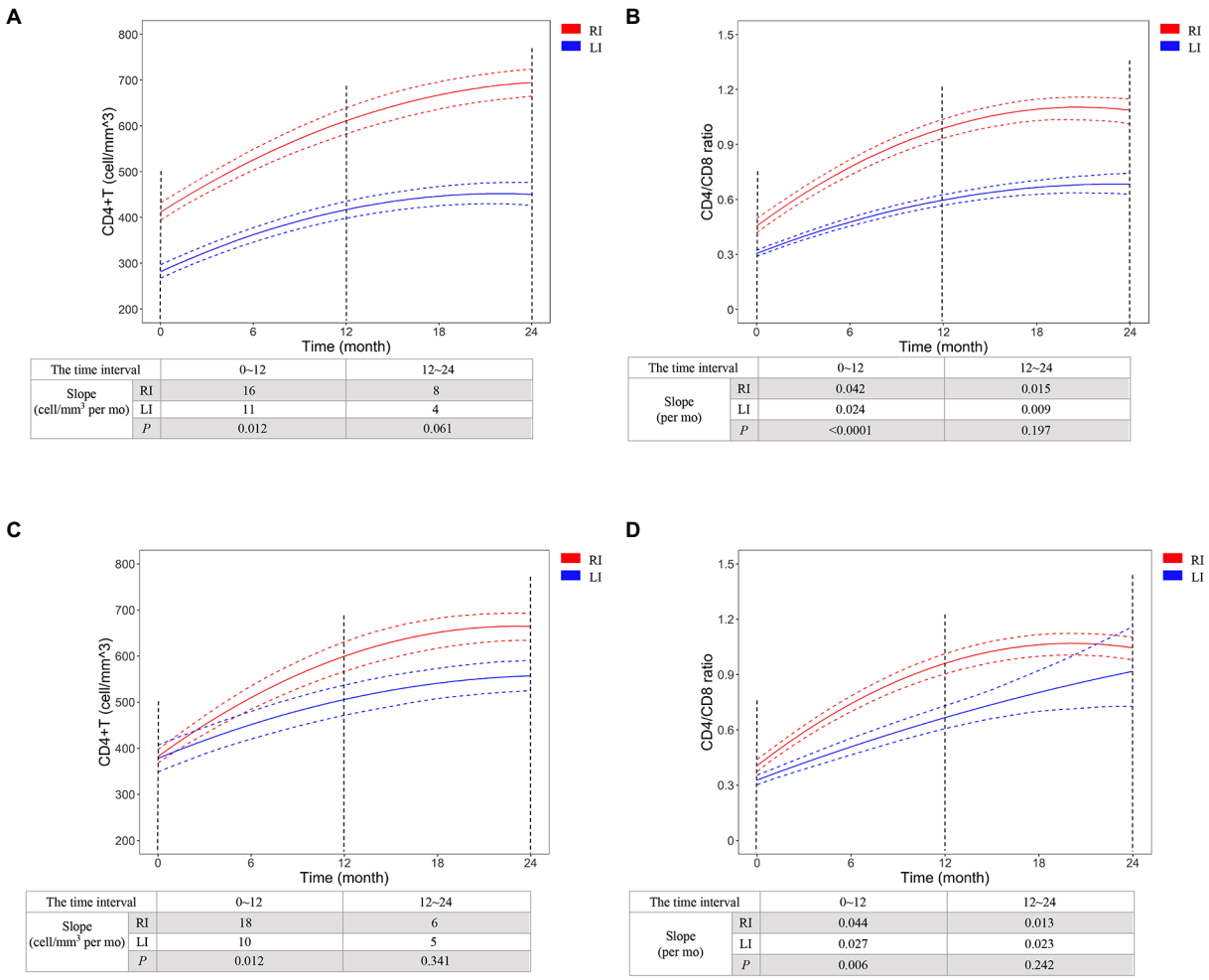

A	The time interval	0~12	12~24
Slope (cell/mm³ per mo)	RI	16	8
	LI	11	4
	P	0.012	0.061

B	The time interval	0~12	12~24
Slope (per mo)	RI	0.042	0.015
	LI	0.024	0.009
	P	<0.0001	0.197

C	The time interval	0~12	12~24
Slope (cell/mm³ per mo)	RI	18	6
	LI	10	5
	P	0.012	0.341

D	The time interval	0~12	12~24
Slope (per mo)	RI	0.044	0.013
	LI	0.027	0.023
	P	0.006	0.242

FIGURE 4
The recovery dynamics of CD4⁺ T-cell count **(A,C)** and CD4/CD8 ratio **(B,D)** after initiation of cART for HIV-1 recent and long-term infection patients. CD4⁺ T-cell count and CD4/CD8 ratio were detected in all 200 cART-treated patients **(A,B)** or the patients of 1:1 case–control analysis using propensity score matching method. The dynamics was predicted by Generalized Estimating Equations (GEE) and compared between HIV-1 recent and long-term infection patients. The red and blue dash lines represent 95% pointwise confidence bands. RI, recent infection; LI, long-term infection. RI, recent infection; LI, long-term infection.

our rapid HIV-1 recency testing RRITS and excellent consistency with the commercial LAg-Avidity EIA assay in detecting both longitudinal and cross-sectional samples. These results proved the feasibility of implementing rapid HIV-1 recency testing assay to determine the status of HIV-1 patients in clinics, hospitals and and in resource-limiting settings.

HIV-1 recency test can be used to estimate HIV-1 incidence in the population since the ordinary anti-HIV immunoassay can only diagnose HIV-1 infection and determine the prevalence of HIV-1. Currently, several assays can distinguish HIV-1 RI and LI and can be used to estimate HIV-1 incidence, such as Western blot and the Fiebig staging method (Fiebig et al., 2003), LAg-Avidity EIA and BED-CEIA method (Le et al., 2013). We have previously described an immunosorbent assay to distinguish HIV-1 RI and LI (Li et al., 2016; Cai et al., 2019). In this study, we further refined the assay format to develop a rapid immunoassay HIV-1 RRITS for POCT. In contrast, the widely used BED-CEIA and LAg-Avidity EIA have stringent criteria for experimental equipment and experimental operators, as well as dozens of testing steps and several hours of experimental time; hence, they are unsuitable for rapid on-site testing. Compared with the current methods, the main advantages of RRITS are as follows: (1) the operation of RRITS is straightforward and does not need experimental equipment; (2) the sample tested does not require dilution; (3) the experiment only takes 30 min; (4) HIV-1 infection diagnosis and differentiation of HIV-1 RI and LI can be performed simultaneously.

When the HIV-1 recency test was used to determine the stage of HIV-infected individuals, the accuracy and reliability are still debated. Therefore, the UNAIDS recommends the RITAs by combining HIV-1 serological recency testing with clinical tests to accurately distinguish RI and LI (WHO, 2011; accessed January

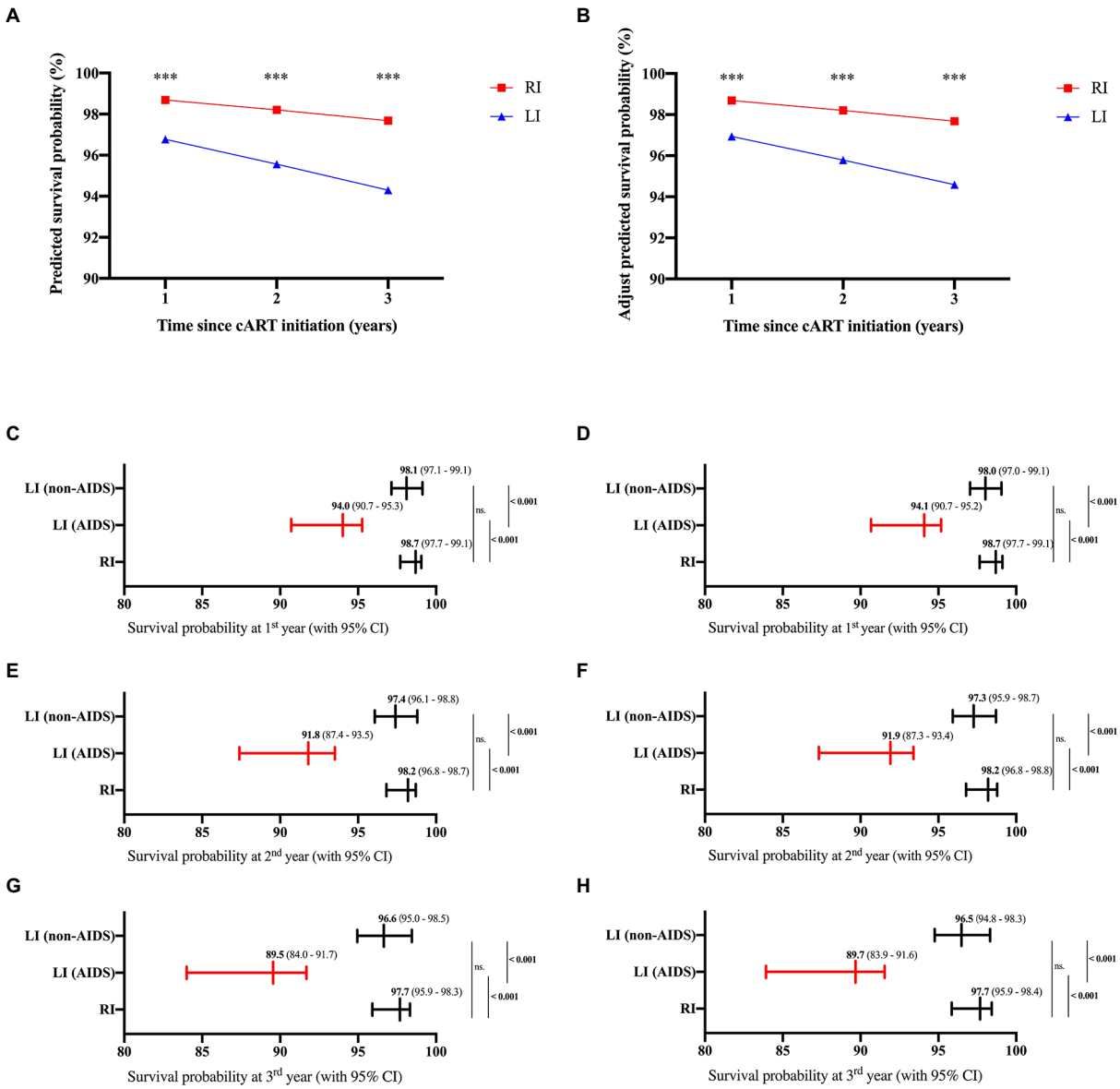

FIGURE 5
Predicted survival probabilities of cART-treated HIV-1 patients. The survival probabilities were predicted based on Wenzhou model (left) and adjusted for age and gender (right) according to the previous studies (Hou et al., 2019; Wang et al., 2020) for HIV-1 patients of recent and long-term infection at 1st, 2nd and 3rd year after cART **(A,B)**, or for HIV-1 patients of recent and long-term infection with or without AIDS at 1st **(C,D)**, 2nd **(E,F)**, and 3rd **(G,H)** year after cART.

23, 2022). It has been reported that excluding cases with CD4$^+$ T-cell count <200 cells/μl and viral load <1,000 copies/ml can reduce FRR from 4.9% to 0 (Karatzas-Delgado et al., 2020). Currently, CD4$^+$ T-cell count test is provided for free to HIV-infected individuals in China, and HIV-1 viral load testing has been used since 2019. Thus, integrating the history of HIV-1 diagnosis, CD4$^+$ T-cell count and HIV-1 RNA level and HIV-1 recency testing results into RITAs for accurate classification of HIV-1 infection status is feasible in China and provides us an opportunity to assess the role of RITAs in managing cART-treated patients. Based on RITAs and our rapid HIV-1 recency test, we found that in our study, only 22.5% of HIV-infected subjects were in the stage of HIV-1 recent infection while 77.5% of them were chronic infection and 30% of them have been AIDS patients when they started cART. Our results indicated that early diagnosis and initiation of cART are still an important but unresolved issue in China.

Furthermore, we found that 4.1% of LI patients experienced virological rebound in the 1st year of cART and none of the RI patients relapsed, suggesting that RI patients were able to achieve and maintain more stable virological suppression after receiving cART, which was consistent with the previous studies (Jain et al.,

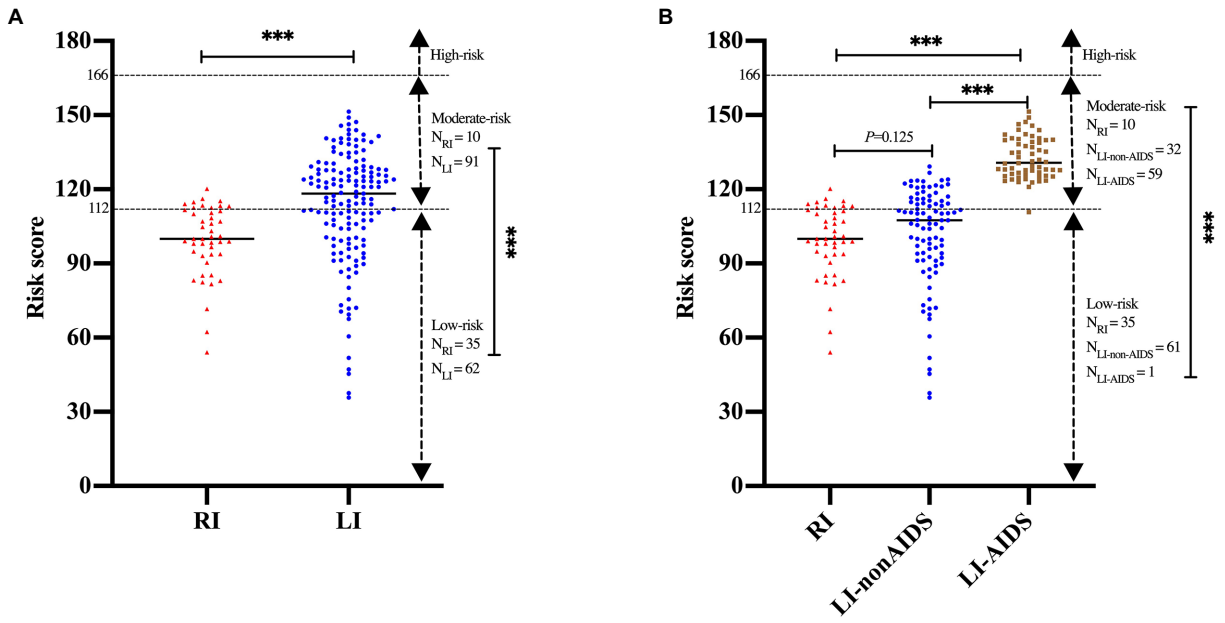

FIGURE 6
Prognostic risk scores of recent and long-term HIV-1 infection patients. The prognostic scores were calculated to predict mortality using Wenzhou model and were categorized into three risk groups: low (<112), moderate (112~) and high (≥166) according to the previous studyies (Hou et al., 2019; Wang et al., 2020). **(A)** The prognostic risk scores for HIV-1 patients of recent and long-term infection. **(B)** The prognostic risk scores for HIV-1 patients of recent and long-term infection with or without AIDS. *, $p<0.05$; **, $p<0.01$; ***, $p<0.001$.

2013; Buzon et al., 2014). The cause of virological rebound is complicated. It is important to effectively control and reduce the viral reservoir to decrease virological rebound (Deeks et al., 2021). Although cART can effectively inhibit viral replication and viral loads, but cannot eradicate HIV-1 since HIV-1 DNA can still be detected in $CD4^+$ T-cell in the blood and lymphoid tissues of cART-treated HIV-1 patients. Previous studies have found that starting cART in the acute phase of HIV-1 infection can accelerate the attenuation of the viral reservoir and maintain a lower and more stable virological suppression (Hocqueloux et al., 2013; Laanani et al., 2015), and also promotes the immune response of HIV-specific T helper cells, and hinders the establishment and expansion of viral reservoirs (Lori et al., 1999; Ananworanich et al., 2012; Archin et al., 2012). Several studies have shown that early cART can reduce microbial translocation, immune activation level and lymphoid tissue damage, and promote immune recovery of HIV-infected patients (Brenchley and Douek, 2008; Buzón et al., 2010; Rajasuriar et al., 2010; Fernandez et al., 2011; Hunt, 2012; Zeng et al., 2012a,b). Previous studies have shown that early cART among the recently HIV-infected patients can quickly eliminate lymphoid tissue damage caused by HIV-1, and enhance the recovery of $CD4^+$ T-cell (Zeng et al., 2012a,b). Even under sustained virological suppression, 30% of cART-treated HIV-infected patients showed abnormal $CD4^+$ T-cell count (Battegay et al., 2006; Gazzola et al., 2009; Handoko et al., 2020). Low $CD4^+$ T-cell count increases the risk of morbidity and mortality of AIDS and non-AIDS-related complications (Baker et al., 2008; Al-Mrabeh et al., 2016) even though these patients have reached virological suppression (Marin et al., 2009; Belloso et al., 2010). One of the reasons for this phenomenon may be that the immune function of LI patients was impaired, which affects the recovery of $CD4^+$ T-cell. Our study also showed that 45.2% of HIV-1 patients did not reach the $CD4^+$ T-cell count of 500 cells/mm^3 after 2 years of cART and 95.7% of them were LI patients. Under cART, $CD4^+$ T-cell count was always higher in the RI group than in the LI group.

It is reported that CD4/CD8 ratio is a reliable marker of systemic immune activation for HIV-infected patients under cART (Buggert et al., 2014; Bruno et al., 2017). Although HIV-infected patients with virological suppression and $CD4^+$ T-cell count ≥500/mm^3, a low CD4/CD8 ratio is also associated with immune failure and abnormal activation, e.g., monocyte activation (Serrano-Villar et al., 2014; Lu et al., 2015). In addition, several studies have shown that CD4/CD8 ratio inversion and high $CD8^+$ T-cell count (≥2,000/mm^3) can increase the risk of all-cause mortality of HIV-1 patients despite receiving effective cART (Mussini et al., 2015; Sigel et al., 2017; Trickey et al., 2017; Caby et al., 2021). The SPARTAC and UK trials indicated that CD4/CD8 ratios recovered to normal (≥1) in 45.1% of recently infected HIV-1 patients after 1 year of cART, but only 11.1% for the patients with delayed cART (Fidler et al., 2013; Thornhill et al., 2016). In our study, we found that the probability of CD4/CD8 ratio recovering to 1 was 3.6 times higher in RI patients than LI patients, which may be caused by the continuous inversion of the CD4/CD8 ratio due to the excessive activation of $CD8^+$ T-cell and the slow recovery speed of $CD4^+$T-cell in LI patients (Caby et al., 2021).

Although the survival of HIV-1 patients has been greatly extended with the widespread use of cART, LI patients may still face greater prognostic risk. In our study, the HIV/AIDS-related mortality risk was lower in RI patients than LI patients. It has been reported that the possibility of HIV/AIDS-related death was 20 times higher in those with moderate prognostic risk than in those with low prognostic risk (Hou et al., 2019). In our study, we found that 22.22% of RI patients had moderate prognostic risk scores, which was lower than 34.41% in the LI non-AIDS patients group and 98.33% in the LI AIDS group. These results also support the higher risk of HIV/AIDS-related death in LI patients even under cART therapy.

Our study has several limitations. First, more HIV-1 infection specimens with seroconversion dates need to be collected to accurately assess FRR and MDRI of the HIV-1 recency test. Second, few clinical endpoints have been observed due to the relatively short observation period. The clinical cohort study is still ongoing. Third, we did not measure HIV-1 DNA levels to evaluate the dynamic of HIV-1 viral reservoir in RI and LI patients after initiation of cART. Finally, we would like to emphasize that HIV-1 recency test may be used as an aid for the management of HIV-1 patients for clinical use, but not for determining the stage of HIV-1 infection for individuals.

In conclusion, we successfully developed a rapid HIV-1 recency test, which can be feasibly implemented in point-of-care settings. Our study supports the incorporation of rapid HIV-1 recency test into RITAs to accurately distinguish HIV-1 RI and LI and to improve the management of HIV-1 patients. Of note, we found that a rapid HIV-1 recency test alone could achieve similar results of differentiating HIV-1 RI and LI as RITAs, suggesting that in the resource-limiting settings, rapid HIV-1 recency test alone may help monitor HIV-1 incidence and predict the prognosis of HIV-1 patients.

Data availability statement

The raw data supporting the conclusions of this article will be made available by the authors, without undue reservation.

Ethics statement

The studies involving human participants were reviewed and approved by Nanfang Hospital Ethics Committee; Nanfang Hospital of Southern Medical University. The patients/participants provided their written informed consent to participate in this study.

Author contributions

JZ: analysis and interpretation of data, conduction of experiment, and drafting of the manuscript. HC and TY: acquisition of data, analysis and interpretation of data. ZW: performed experiment. QL: performed the data analysis, figures plotted. JS and HW: revision of the manuscript. ST and JP: conception, design, and finalizing of the manuscript. All authors contributed to the article and approved the submitted version.

Funding

This work was supported by the National Major Science and Technology Project (grant number 2018ZX10302103-002) and Bureau of Science and Information Technology of Guangzhou Municipality (grant no. 201704020219).

Conflict of interest

The authors declare that the research was conducted in the absence of any commercial or financial relationships that could be construed as a potential conflict of interest.

The handling editor declared a past co-authorship with the author [ST].

Publisher's note

Supplementary material

The Supplementary material for this article can be found online at: https://www.frontiersin.org/articles/10.3389/fmicb.2022.1004960/full#supplementary-material

SUPPLEMENTARY FIGURE S1
Determination of volume ratio of the BE23 and MP4 antigen (Ag) at the T_1 testing line of HIV-1 rapid recent-infection testing strip (RRITS). The concentrations of the BE23 and MP4 were 0.30mg/ml and 0.45mg/ml, respectively.

SUPPLEMENTARY FIGURE S2
Determination of cut-off value of T_1 testing line based on receiver operator characteristic curve (ROC) and maximal Youden index.

SUPPLEMENTARY FIGURE S3
The scatter diagram between the T_1 testing line score of HIV-1 rapid recent-infection testing strip (RRITS) and ODn of LAg-Avidity EIA using specimens, including longitudinal and cross-sectional samples (n=431).

SUPPLEMENTARY FIGURE S4
Rapid recent-infection testing strip (RRITS) alone and recent infection testing algorithms (RITAs) based on LAg-Avidity EIA to distinguish recent and long-term HIV-1 infection. LS_{T1}, the T_1 testing line score of RRITS; HIV-1, human immunodeficiency virus I; AIDS, acquired immunodeficiency syndrome; VL, viral load.

SUPPLEMENTARY FIGURE S5
The recovery speeds of CD4$^+$ T-cell count (A) and CD4/CD8 ratio (B) among HIV-1 recent infection and long-term infection with or without AIDS groups during 12months of cART. *, $p<0.05$; **, $p<0.01$; ***, $p<0.001$; ns, $p>0.05$. RI, recent infection; LI, long-term infection; mo, month.

SUPPLEMENTARY FIGURE S6
The recovery speeds of CD4$^+$ T-cell count (A) and CD4/CD8 ratio (B) in all, recent infection and long-term infection patients during consecutive time intervals after initiation of cART. *, $p<0.05$; **, $p<0.01$; ***, $p<0.001$; ****, $p<0.0001$; ns, $p>0.05$: RI, recent infection; LI, long-term infection; mo, month.

References

Al-Mrabeh, A., Hollingsworth, K. G., Steven, S., and Taylor, R. (2016). Morphology of the pancreas in type 2 diabetes: effect of weight loss with or without normalisation of insulin secretory capacity. *Diabetologia* 59, 1753–1759. doi: 10.1007/s00125-016-3984-6

Ananworanich, J., Schuetz, A., Vandergeeten, C., Sereti, I., de Souza, M., Rerknimitr, R., et al. (2012). Impact of multi-targeted antiretroviral treatment on gut T cell depletion and HIV reservoir seeding during acute HIV infection. *PLoS One* 7:e33948. doi: 10.1371/journal.pone.0033948

Ang, L. W., Low, C., Wong, C. S., Boudville, I. C., Toh, M., Archuleta, S., et al. (2021). Epidemiological factors associated with recent HIV infection among newly-diagnosed cases in Singapore, 2013-2017. *BMC Public Health* 21:430. doi: 10.1186/s12889-021-10478-5

Archin, N. M., Liberty, A. L., Kashuba, A. D., Choudhary, S. K., Kuruc, J. D., Crooks, A. M., et al. (2012). Administration of vorinostat disrupts HIV-1 latency in patients on antiretroviral therapy. *Nature* 487, 482–485. doi: 10.1038/nature11286

Baker, J. V., Peng, G., Rapkin, J., Krason, D., Reilly, C., Cavert, W. P., et al. (2008). Poor initial CD4+ recovery with antiretroviral therapy prolongs immune depletion and increases risk for AIDS and non-AIDS diseases. *J. Acquir. Immune Defic. Syndr.* 48, 541–546. doi: 10.1097/QAI.0b013e31817bebb3

Battegay, M., Nüesch, R., Hirschel, B., and Kaufmann, G. R. (2006). Immunological recovery and antiretroviral therapy in HIV-1 infection. *Lancet Infect. Dis.* 6, 280–287. doi: 10.1016/s1473-3099(06)70463-7

Belloso, W. H., Orellana, L. C., Grinsztejn, B., Madero, J. S., La Rosa, A., Veloso, V. G., et al. (2010). Analysis of serious non-AIDS events among HIV-infected adults at Latin American sites. *HIV Med.* 11, 554–564. doi: 10.1111/j.1468-1293.2010.00824.x

Brenchley, J. M., and Douek, D. C. (2008). HIV infection and the gastrointestinal immune system. *Mucosal Immunol.* 1, 23–30. doi: 10.1038/mi.2007.1

Bruno, G., Saracino, A., Monno, L., and Angarano, G. (2017). The revival of an "old" marker: CD4/CD8 ratio. *AIDS Rev.* 19, 81–88.

Buggert, M., Frederiksen, J., Noyan, K., Svärd, J., Barqasho, B., Sönnerborg, A., et al. (2014). Multiparametric bioinformatics distinguish the CD4/CD8 ratio as a suitable laboratory predictor of combined T cell pathogenesis in HIV infection. *J. Immunol.* 192, 2099–2108. doi: 10.4049/jimmunol.1302596

Buzon, M. J., Martin-Gayo, E., Pereyra, F., Ouyang, Z., Sun, H., Li, J. Z., et al. (2014). Long-term antiretroviral treatment initiated at primary HIV-1 infection affects the size, composition, and decay kinetics of the reservoir of HIV-1-infected CD4 T cells. *J. Virol.* 88, 10056–10065. doi: 10.1128/jvi.01046-14

Buzón, M. J., Massanella, M., Llibre, J. M., Esteve, A., Dahl, V., Puertas, M. C., et al. (2010). HIV-1 replication and immune dynamics are affected by raltegravir intensification of HAART-suppressed subjects. *Nat. Med.* 16, 460–465. doi: 10.1038/nm.2111

Caby, F., Guiguet, M., Weiss, L., Winston, A., Miro, J. M., Konopnicki, D., et al. (2021). CD4/CD8 ratio and the risk of Kaposi sarcoma or non-Hodgkin lymphoma in the context of efficiently treated human immunodeficiency virus (HIV) infection: a collaborative analysis of 20 European cohort studies. *Clin. Infect. Dis.* 73, 50–59. doi: 10.1093/cid/ciaa1137

Cai, Q., Wang, H., Huang, L., Yan, H., Zhu, W., and Tang, S. (2019). Characterization of HIV-1 genotype specific antigens for the detection of recent and long-term HIV-1 infection in China. *Virus Res.* 264, 16–21. doi: 10.1016/j.virusres.2019.02.010

Chauhan, C. K., Lakshmi, P. V. M., Sagar, V., Sharma, A., Arora, S. K., and Kumar, R. (2020). Immunological markers for identifying recent HIV infection in north-West India. *Indian J. Med. Res.* 152, 227–233. doi: 10.4103/ijmr.IJMR_2007_18

CMA and CCDC (2022). Chinese guidelines for diagnosis and treatment of HIV/AIDS (2021 edition). *Med. J. Peking Union Med. Coll. Hosp.* 13, 203–226.

Davy-Mendez, T., Napravnik, S., Zakharova, O., Kuruc, J., Gay, C., Hicks, C. B., et al. (2018). Acute HIV infection and CD4/CD8 ratio normalization after antiretroviral therapy initiation. *J. Acquir. Immune Defic. Syndr.* 79, 510–518. doi: 10.1097/qai.0000000000001843

de Wit, M. M., Rice, B., Risher, K., Welty, S., Waruiru, W., Magutshwa, S., et al. (2021). Experiences and lessons learned from the real-world implementation of an HIV recent infection testing algorithm in three routine service-delivery settings in Kenya and Zimbabwe. *BMC Health Serv. Res.* 21:596. doi: 10.1186/s12913-021-06619-6

Deeks, S. G., Archin, N., Cannon, P., Collins, S., Jones, R. B., de Jong, M., et al. (2021). Research priorities for an HIV cure: international AIDS society global scientific strategy 2021. *Nat. Med.* 27, 2085–2098. doi: 10.1038/s41591-021-01590-5

Dobbs, T., Kennedy, S., Pau, C. P., McDougal, J. S., and Parekh, B. S. (2004). Performance characteristics of the immunoglobulin G-capture BED-enzyme immunoassay, an assay to detect recent human immunodeficiency virus type 1 seroconversion. *J. Clin. Microbiol.* 42, 2623–2628. doi: 10.1128/jcm.42.6.2623-2628.2004

Duong, Y. T., Qiu, M., De, A. K., Jackson, K., Dobbs, T., Kim, A. A., et al. (2012). Detection of recent HIV-1 infection using a new limiting-antigen avidity assay: potential for HIV-1 incidence estimates and avidity maturation studies. *PLoS One* 7:e33328. doi: 10.1371/journal.pone.0033328

Fernandez, S., Tanaskovic, S., Helbig, K., Rajasuriar, R., Kramski, M., Murray, J. M., et al. (2011). CD4+ T-cell deficiency in HIV patients responding to antiretroviral therapy is associated with increased expression of interferon-stimulated genes in CD4+ T cells. *J. Infect. Dis.* 204, 1927–1935. doi: 10.1093/infdis/jir659

Fidler, S., Porter, K., Ewings, F., Frater, J., Ramjee, G., Cooper, D., et al. (2013). Short-course antiretroviral therapy in primary HIV infection. *N. Engl. J. Med.* 368, 207–217. doi: 10.1056/NEJMoa1110039

Fiebig, E. W., Wright, D. J., Rawal, B. D., Garrett, P. E., Schumacher, R. T., Peddada, L., et al. (2003). Dynamics of HIV viremia and antibody seroconversion in plasma donors: implications for diagnosis and staging of primary HIV infection. *AIDS* 17, 1871–1879. doi: 10.1097/00002030-200309050-00005

Gazzola, L., Tincati, C., Bellistrì, G. M., Monforte, A., and Marchetti, G. (2009). The absence of CD4+ T cell count recovery despite receipt of virologically suppressive highly active antiretroviral therapy: clinical risk, immunological gaps, and therapeutic options. *Clin. Infect. Dis.* 48, 328–337. doi: 10.1086/595851

Gianella, S., von Wyl, V., Fischer, M., Niederoest, B., Battegay, M., Bernasconi, E., et al. (2011). Effect of early antiretroviral therapy during primary HIV-1 infection on cell-associated HIV-1 DNA and plasma HIV-1 RNA. *Antivir. Ther.* 16, 535–545. doi: 10.3851/imp1776

Handoko, R., Colby, D. J., Kroon, E., Sacdalan, C., de Souza, M., Pinyakorn, S., et al. (2020). Determinants of suboptimal CD4(+) T cell recovery after antiretroviral therapy initiation in a prospective cohort of acute HIV-1 infection. *J. Int. AIDS Soc.* 23:e25585. doi: 10.1002/jia2.25585

Hocqueloux, L., Avettand-Fènoël, V., Jacquot, S., Prazuck, T., Legac, E., Mélard, A., et al. (2013). Long-term antiretroviral therapy initiated during primary HIV-1 infection is key to achieving both low HIV reservoirs and normal T cell counts. *J. Antimicrob. Chemother.* 68, 1169–1178. doi: 10.1093/jac/dks533

Hou, X., Wang, D., Zuo, J., Li, J., Wang, T., Guo, C., et al. (2019). Development and validation of a prognostic nomogram for HIV/AIDS patients who underwent antiretroviral therapy: data from a China population-based cohort. *EBioMedicine* 48, 414–424. doi: 10.1016/j.ebiom.2019.09.031

Hunt, P. W. (2012). HIV and inflammation: mechanisms and consequences. *Curr. HIV/AIDS Rep.* 9, 139–147. doi: 10.1007/s11904-012-0118-8

Jain, V., Hartogensis, W., Bacchetti, P., Hunt, P. W., Hatano, H., Sinclair, E., et al. (2013). Antiretroviral therapy initiated within 6 months of HIV infection is associated with lower T-cell activation and smaller HIV reservoir size. *J. Infect. Dis.* 208, 1202–1211. doi: 10.1093/infdis/jit311

Karatzas-Delgado, E. F., Ruiz-González, V., García-Cisneros, S., Olamendi-Portugal, M. L., Herrera-Ortiz, A., López-Gatell, H., et al. (2020). Evaluation of an HIV recent infection testing algorithm with serological assays among men who have sex with men in Mexico. *J. Infect. Public Health* 13, 509–513. doi: 10.1016/j.jiph.2019.11.002

Laanani, M., Ghosn, J., Essat, A., Melard, A., Seng, R., Gousset, M., et al. (2015). Impact of the timing of initiation of antiretroviral therapy during primary HIV-1 infection on the decay of cell-associated HIV-DNA. *Clin. Infect. Dis.* 60, 1715–1721. doi: 10.1093/cid/civ171

Le, T., Wright, E., Smith, D., He, W., Catano, G., Okulicz, J., et al. (2013). Enhanced CD4+ T-cell recovery with earlier HIV-1 antiretroviral therapy. *N. Engl. J. Med.* 368, 218–230. doi: 10.1056/NEJMoa1110187

Li, X., Wu, Y., Ren, X., Deng, S., Hu, G., Yu, S., et al. (2016). Characterization of humoral immune responses against capsid protein p24 and transmembrane glycoprotein gp41 of human immunodeficiency virus type 1 in China. *PLoS One* 11:e0165874. doi: 10.1371/journal.pone.0165874

Lori, F., Jessen, H., Lieberman, J., Finzi, D., Rosenberg, E., Tinelli, C., et al. (1999). Treatment of human immunodeficiency virus infection with hydroxyurea, didanosine, and a protease inhibitor before seroconversion is associated with normalized immune parameters and limited viral reservoir. *J. Infect. Dis.* 180, 1827–1832. doi: 10.1086/315113

Lu, W., Mehraj, V., Vyboh, K., Cao, W., Li, T., and Routy, J. P. (2015). CD4:CD8 ratio as a frontier marker for clinical outcome, immune dysfunction and viral reservoir size in virologically suppressed HIV-positive patients. *J. Int. AIDS Soc.* 18:20052. doi: 10.7448/ias.18.1.20052 20052

Marin, B., Thiébaut, R., Bucher, H. C., Rondeau, V., Costagliola, D., Dorrucci, M., et al. (2009). Non-AIDS-defining deaths and immunodeficiency in the era of combination antiretroviral therapy. *AIDS* 23, 1743–1753. doi: 10.1097/QAD.0b013e32832e9b78

Gable, A.R., and Lagakos, S.W. (2008). *Methodological challenges in biomedical HIV prevention trials*. National Academies Press. Available at: https:// books.google.com/books?id=Mw9kAgAAQBAJ&lpg=PP1&ots=GHHLiXBFIK&dq=Medicine%20I.O%20(2008).%20%E2%80%9CMethodological% 20challenges%20in%20biomedical%20hiv%20prevention&lr&hl=zh-CN&pg=PT1#v=onepage&q=Medicine%20I.O%20(2008).%20%E2%80% 9CMethodological%20challenges%20in%20biomedical%20hiv%20prevention&f=false (Accessed October 19, 2022).

Mussini, C., Lorenzini, P., Cozzi-Lepri, A., Lapadula, G., Marchetti, G., Nicastri, E., et al. (2015). CD4/CD8 ratio normalisation and non-AIDS-related events in individuals with HIV who achieve viral load suppression with antiretroviral therapy: an observational cohort study. *Lancet HIV* 2, e98–e106. doi: 10.1016/s2352-3018(15)00006-5

Organization W.H (2011). This document provides guidance on the way in which laboratory tests for recent HIV infection may be used to estimate HIV incidence in populations level. Available at: https://apps.who.int/iris/handle/10665/44612 (Accessed October 19, 2022).

Rajasuriar, R., Booth, D., Solomon, A., Chua, K., Spelman, T., Gouillou, M., et al. (2010). Biological determinants of immune reconstitution in HIV-infected patients receiving antiretroviral therapy: the role of interleukin 7 and interleukin 7 receptor α and microbial translocation. *J. Infect. Dis.* 202, 1254–1264. doi: 10.1086/656369

Rawal, B. D., Degula, A., Lebedeva, L., Janssen, R. S., Hecht, F. M., Sheppard, H. W., et al. (2003). Development of a new less-sensitive enzyme immunoassay for detection of early HIV-1 infection. *J. Acquir. Immune Defic. Syndr.* 33, 349–355. doi: 10.1097/00126334-200307010-00009

Rice, B. D., de Wit, M., Welty, S., Risher, K., Cowan, F. M., Murphy, G., et al. (2020). Can HIV recent infection surveillance help us better understand where primary prevention efforts should be targeted? Results of three pilots integrating a recent infection testing algorithm into routine programme activities in Kenya and Zimbabwe. *J. Int. AIDS Soc.* 23:e25513. doi: 10.1002/jia2.25513

Rwibasira, G. N., Malamba, S. S., Musengimana, G., Nkunda, R. C. M., Omolo, J., Remera, E., et al. (2021). Recent infections among individuals with a new HIV diagnosis in Rwanda, 2018-2020. *PLoS One* 16:e0259708. doi: 10.1371/journal.pone.0259708

Serrano-Villar, S., Sainz, T., Lee, S. A., Hunt, P. W., Sinclair, E., Shacklett, B. L., et al. (2014). HIV-infected individuals with low CD4/CD8 ratio despite effective antiretroviral therapy exhibit altered T cell subsets, heightened CD8+ T cell activation, and increased risk of non-AIDS morbidity and mortality. *PLoS Pathog.* 10:e1004078. doi: 10.1371/journal.ppat.1004078

Sigel, K., Wisnivesky, J., Crothers, K., Gordon, K., Brown, S. T., Rimland, D., et al. (2017). Immunological and infectious risk factors for lung cancer in US veterans with HIV: a longitudinal cohort study. *Lancet HIV* 4, e67–e73. doi: 10.1016/s2352-3018(16)30215-6

Teixeira, S. L., Jalil, C. M., Jalil, E. M., Nazer, S. C., Silva, S., Veloso, V. G., et al. (2021). Evidence of an untamed HIV epidemic among MSM and TGW in Rio de Janeiro, Brazil: a 2018 to 2020 cross-sectional study using recent infection testing. *J. Int. AIDS Soc.* 24:e25743. doi: 10.1002/jia2.25743

The Joint United Nations Program on HIV and AIDS (UNAIDS) (2020). 2020 Progress report on the Global AIDS Response. Available at: https://www.unaids.org/en (Accessed April 22, 2022).

Thornhill, J., Inshaw, J., Kaleebu, P., Cooper, D., Ramjee, G., Schechter, M., et al. (2016). Brief report: enhanced normalization of CD4/CD8 ratio with earlier antiretroviral therapy at primary HIV infection. *J. Acquir. Immune Defic. Syndr.* 73, 69–73. doi: 10.1097/qai.0000000000001013

Trickey, A., May, M. T., Schommers, P., Tate, J., Ingle, S. M., Guest, J. L., et al. (2017). CD4:CD8 ratio and CD8 count as prognostic markers for mortality in human immunodeficiency virus-infected patients on antiretroviral therapy: the antiretroviral therapy cohort collaboration (ART-CC). *Clin. Infect. Dis.* 65, 959–966. doi: 10.1093/cid/cix466

Voetsch, A. C., Duong, Y. T., Stupp, P., Saito, S., McCracken, S., Dobbs, T., et al. (2021). HIV-1 recent infection testing algorithm with antiretroviral drug detection to improve accuracy of incidence estimates. *J. Acquir. Immune Defic. Syndr.* 87, S73–s80. doi: 10.1097/qai.0000000000002707

Wang, J., Yuan, T., Ling, X., Li, Q., Tang, X., Cai, W., et al. (2020). Critical appraisal and external validation of a prognostic model for survival of people living with HIV/AIDS who underwent antiretroviral therapy. *Diagn. Progn. Res.* 4:19. doi: 10.1186/s41512-020-00088-x

WHO (2011). When and how to use assays for recent infection to estimate HIV incidence at a population level. Available at: https://apps.who.int/iris/bitstream/handle/10665/44612/9789241501675_eng.pdf (Accessed January 23, 2022).

Zeng, M., Haase, A. T., and Schacker, T. W. (2012a). Lymphoid tissue structure and HIV-1 infection: life or death for T cells. *Trends Immunol.* 33, 306–314. doi: 10.1016/j.it.2012.04.002

Zeng, M., Southern, P. J., Reilly, C. S., Beilman, G. J., Chipman, J. G., Schacker, T. W., et al. (2012b). Lymphoid tissue damage in HIV-1 infection depletes naïve T cells and limits T cell reconstitution after antiretroviral therapy. *PLoS Pathog.* 8:e1002437. doi: 10.1371/journal.ppat.1002437

Zhu, Q., Wang, Y., Liu, J., Duan, X., Chen, M., Yang, J., et al. (2020). Identifying major drivers of incident HIV infection using recent infection testing algorithms (RITAs) to precisely inform targeted prevention. *Int. J. Infect. Dis.* 101, 131–137. doi: 10.1016/j.ijid.2020.09.1421

frontiers | Frontiers in Microbiology

TYPE Original Research
PUBLISHED 25 November 2022
DOI 10.3389/fmicb.2022.1028383

OPEN ACCESS

EDITED BY
Wenyan Zhang,
First Affiliated Hospital of Jilin University, China

REVIEWED BY
Lingjie Liao,
Chinese Center for Disease Control and Prevention, China
Monick Lindenmeyer Guimarães,
Oswaldo Cruz Foundation (Fiocruz), Brazil

*CORRESPONDENCE
Fu-Xiang Wang
wangfuxiang999@163.com
Xiao-Hong Chen
catherine89034@163.com
Shu-Lin Liu
slliu@hrbmu.edu.cn

†These authors have contributed equally to this work and share first authorship

SPECIALTY SECTION
This article was submitted to Infectious Agents and Disease, a section of the journal Frontiers in Microbiology

RECEIVED 26 August 2022
ACCEPTED 02 November 2022
PUBLISHED 25 November 2022

CITATION
Li Q-H, Wang J-Y, Liu S-Y, Zhang Y-Q, Li E-L, Wang Y-R, Zhang S-L, Zhao W-B, Liu S-L, Chen X-H and Wang F-X (2022) Young MSM changed temporal HIV-1 epidemic pattern in Heilongjiang Province, China.
Front. Microbiol. 13:1028383.
doi: 10.3389/fmicb.2022.1028383

Young MSM changed temporal HIV-1 epidemic pattern in Heilongjiang Province, China

Qing-Hai Li[1†], Jia-Ye Wang[2†], Si-Yu Liu[3], Yun-Qi Zhang[2], En-Long Li[2], Yi-Ru Wang[2], Shu-Lei Zhang[1], Wen-Bo Zhao[1], Shu-Lin Liu[1*], Xiao-Hong Chen[3*] and Fu-Xiang Wang[3,4,5*]

[1]Genomics Research Center, College of Pharmacy, Harbin Medical University, Harbin, China, [2]Department of Microbiology, Harbin Medical University, Harbin, China, [3]Department of Infectious Diseases, The Fourth Affiliated Hospital of Harbin Medical University, Harbin, China, [4]Department of Infectious Diseases, The Second Affiliated Hospital of Southern University of Science and Technology, Shenzhen, China, [5]Department of Infectious Diseases, The Third People's Hospital of Shenzhen, Shenzhen, China

Background: Human immunodeficiency virus type 1 (HIV-1) epidemic in China is featured by geographical diversity of epidemic patterns. Understanding the characteristics of regional HIV-1 epidemic allows carrying out targeted prevention and controlling measures. This seven-year cross-sectional study was conducted in Heilongjiang, one province of Northeast China, where newly diagnosed infection is fast increasing yearly, but temporal HIV-1 epidemic trend is largely unknown.

Methods: Information of 1,006 newly diagnosed HIV-1-infected participants were collected before antiretroviral therapy during 2010–2016 in Heilongjiang province. HIV-1 genotype was identified based on the viral *gag* and *env* gene sequences. Recent infection was determined by Limiting-Antigen Avidity assays. Comparison analyses on the median ages, CD4 counts, proportions of stratified age groups and CD4 count groups, and rates of recent HIV-1 infection among different population and sampling times were performed to understand temporal HIV-1 epidemic features.

Results: Homosexual contact among men who have sex with men (MSM) was the main transmission route and CRF01_AE was the most dominant HIV-1 genotype. During 2010–2016, the HIV-1 epidemic showed three new changes: the median age continued to decline, the cases with a CD4 count more than 500 cells/μl (CD4hi cases) disproportionally expanded, and the recent HIV-1 infection rate steadily increased. MSM cases determined the temporal trend of HIV-1 epidemic here. Increase of young MSM cases (aged <30 years) made the main contribution to the younger age trend of MSM cases. These young MSM exhibited a higher median CD4 count, a higher proportion of CD4hi cases, and a higher rate of recent HIV-1 infection than cases aged 30 years and more. MSM infected by CRF01_AE virus mostly affected HIV-1 epidemic patterns among MSM population.

Conclusion: Young MSM have become a new hotspot and vulnerable group for HIV-1 transmission in Heilongjiang Province, Northeast China. The rapid increase in the number of young MSM cases, mainly those with CRF01_AE

infection, changed temporal HIV-1 epidemic pattern here. Measures for prevention and control of HIV-1 infection among this population are urgently needed in the future.

KEYWORDS

HIV-1 epidemic, young men who have sex with men, CRF01_AE, immune status, recent infection

Introduction

Human immunodeficiency virus/acquired immunodeficiency syndrome (HIV/AIDS) epidemic in China becomes increasingly severe and complicated. By the end of 2018, the reported absolute number of Chinese people living with HIV-1 was approximately 0.89 million, but the real number was estimated at more than 1.25 million (Wu et al., 2021). One big challenge for HIV/AIDS control is the geographical and temporal diversity of epidemic patterns throughout the whole country. In the past 20 years, HIV/AIDS epidemic pattern has obviously changed, including regional distribution, transmission route, age composition, and dominant HIV-1 genotypes (Liu et al., 2018; Ding et al., 2019; Wu et al., 2019). For the regions with high HIV-1 incidence such as southwest provinces Yunnan and Guangxi, the features of HIV/AIDS epidemic have been described extensively (Wu et al., 2019; Chen et al., 2019a, 2019b). However, for the regions where HIV-1 incidence is relatively low but annually reported case number rises rapidly, such as Heilongjiang Province, the data about HIV/AIDS epidemic are limited and sporadic.

Heilongjiang, one province in Northeast China, lies on the border between China and Russia. Since first HIV-1 infection was identified in 1993, annually reported HIV-1 diagnoses in Heilongjiang continued to increase slowly until the year 2008 when an expansion of HIV-1 infection among men who have sex with men (MSM) occurred (Shao et al., 2014). Since then, newly diagnosed HIV/AIDS cases rapidly increased yearly, and homosexual contact among MSM became dominant route of HIV-1 transmission in this province. By the end of 2017, there were 9,495 people living with HIV-1 in Heilongjiang (Ma et al., 2018). MSM accounted for 64.4% of newly reported cases in 2010–2011 and 72.0% in 2012–2017 (Shao et al., 2014; Ma et al., 2018). The predominant HIV-1 genotype circulating in Heilongjiang has also changed, from subtype B to circulating recombinant form 01_AE (CRF01_AE) during 2009–2012 (Wang et al., 2007; Liu et al., 2009; Shao et al., 2013, 2016; Li et al., 2016a). Since being introduced into China in the 1990s, CRF01_AE virus has gradually evolved into several specialized clusters among specialized population in specialized geographical regions. Heilongjiang is one of the hotspots where CRF01_AE infection concentrates on MSM population (Feng et al., 2013; Li et al., 2017). However, the current epidemic trend of HIV-1 infections in this region, especially among MSM or CRF01_AE-infected MSM, is largely unknown.

In this study, we collected clinical information and samples from more than 1,000 new HIV-1 diagnoses in Heilongjiang Province and made a 7-year cross-sectional study. This paper reported that MSM was driving HIV-1 epidemic trend in Heilongjiang Province and highlighted the critical role of young MSM, especially those infected by CRF01_AE virus, on the change of HIV-1 epidemic pattern here.

Materials and methods

The study participants and information collection

All the participants were recruited in the Fourth Affiliated Hospital of Harbin Medical University from January 2010 to December 2016. Peripheral blood samples were collected immediately after diagnosis for HIV-1 genotyping. The information including sex, age, the way to acquire HIV-1, and peripheral blood CD4 positive T cell count (hereinafter referred to as CD4 count) at diagnosis were also collected. The inclusion criteria of the participants included: (1) being newly diagnosed as HIV-1 infection, (2) being before antiretroviral treatment, and (3) having age and CD4 count information recorded at diagnosis. Participants who lacked a peripheral blood sample or for whom HIV-1 genotype information was not available were excluded.

HIV-1 genotyping

For each participant, 5 ml of whole peripheral blood was collected, and then, plasma sample was separated for HIV-1 genotyping. HIV-1 *gag* p17-p24 (HXB2: nt836-1,507) and *env* C2-C4 (HXB2: nt7,002-7,541) genes were amplified from the plasma samples by RT-PCR and subject to sequencing. The genotypes of *gag* and *env* genes were determined by the cluster distribution of genes in neighbor-joining trees constructed using MEGA 6.06 software as previously described (Li et al., 2019a). The *gag* and *env* genotyping information were used together to characterize the viral genotype. For samples with only one *gag* or *env* gene, the viral genotype was determined by the available single-gene genotyping. Considering that the *gag* and *env* regions of CRF07_BC, CRF08_BC, or subtype C virus analyzed in this

study were all subtype C, for the sample with *gag* or *env* gene from CRF07_BC, CRF08_BC, or subtype C, the genotype of the single gene was named as 07&08&C. For the sample with discordant genotypes of *env* and *gag* genes or with an inter-subtype recombinant *gag* gene, the genotype of HIV-1 virus was identified as unique recombinant form (URF).

HIV-1 infection status evaluation

The recent or long-term infection of each participant was determined by the Limiting-Antigen Avidity assays using HIV-1 LAg-Avidity EIA kit (Beijing Kinghawk Pharmaceutical Co., Ltd., Beijing, China) as previously described (Duong et al., 2012; Li et al., 2019a). A normalized optical density (ODn) value of 1.5 was used as the cutoff to determine HIV-1 infection status. Samples with ODn values ranging from 0.4 to 1.5 (including 1.5) were classified as recent infections, and those with values above 1.5 were classified as long-term infections. The recent infection indicated that the individual acquired HIV-1 within a mean time interval of 130 days.

Genbank accession numbers of nucleotide sequences

The nucleotide sequences identified in this study were submitted to GenBank with accession numbers of MK702086-MK702931 for *gag* p17-p24 genes and MK702932-MK703795 for *env* C2-C4 genes.

Statistical analyses

Sampling years were divided into three time phases: 2010–2011, 2012–2014, and 2015–2016. Mann–Whitney test and Kruskal–Wallis test were used for comparison of the quantitative variables across two groups and multiple groups, respectively. Chi-square test was used for comparison of qualitative variables across groups. Nonparametric Spearman correlation test was used to analyze the relationship between variables. Data analyses were performed by GraphPad Prism version 8.3.0 (GraphPad Software, Inc., La Jolla, CA). The *p*-value less than 0.05 was considered as significant unless otherwise specified.

Results

Basic information

From 2010 to 2016, 1,183 newly diagnosed HIV-1 cases were collected. Of them, 177 participants were excluded because of lack of blood samples or unavailability of HIV-1 genotype information. Finally, 1,006 cases were included in our subsequent analyses. In order to ensure the exclusion of participants did not introduce a bias in data analysis, the basic information between the included cases and the excluded cases were compared. There was no significant difference in the median age, CD4 cell count, gender composition, and risk group composition between the two groups (Supplementary Table S1).

Of the 1,006 participants in this study, the majority were male, accounting for 93.7%. Median age was 35 years (interquartile range [IQR] 29–45), and median CD4 count was 384 cells/μl (IQR 214–490). The most important mode of HIV-1 transmission was male-to-male sexual contact among MSM, followed by heterosexual contact. These two modes of sexual contacts together accounted for 85.7% (862/1006) of all cases and 98.6% (862/874) of cases with known transmission routes.

From 1,006 plasma samples, 864 *env* genes (including 543 CRF01_AE, 172 subtype B, 144 07&08&C and 5 subtype A) and 846 *gag* genes (including 567 CRF01_AE, 134 subtype B, 123 07&08&C, 6 subtype A and 16 inter-subtype recombinants) were obtained. That was, 704 samples had both *env* and *gag* genes, 160 samples had *env* gene alone and 142 samples had *gag* gene alone (Supplementary Figure S1). The most prevalent genotype of HIV-1 viruses was CRF01_AE (accounting for 62.5% of all cases), followed by subtype B (16.5%) and 07&08&C (13.0%). In addition, 73 URFs were also identified, including 57 viruses having discordant genotypes of *env* and *gag* genes and 16 viruses having an inter-subtype recombinant *gag* gene (colored in green in Supplementary Figure S1B). Seven subtype A viruses were also found (Table 1).

MSM cases determined the temporal trend of HIV-1 epidemic

During the three sampling times, three main changes in HIV-1 epidemic were found. Firstly, the median age declined from 39 years (IQR 32–46) to 34 years (IQR 28–44) (Figure 1A), suggesting a younger age trend of these cases. Secondly, although the median CD4 counts did not change significantly (Figure 1D), the proportion of cases with CD4 counts more than 500 cells/μl (hereinafter referred to as CD4hi cases) arose gradually from 16.4 to 27.3% (Table 1), indicating the expansion of cases with good immune status. Thirdly, the rate of recent HIV-1 infection gradually increased from 27.1% to 40.9% (Table 1), suggesting the increase of cases who were diagnosed at the early stage of HIV-1 infection.

The changes observed for the entire group were similar among MSM cases: median age decreased from 37 years (IQR 31–45) to 34 years (IQR 27–42) (Figure 1B), the proportion of CD4hi cases increased from 15.9% to 28.8%, and the recent infection rate increased from 32.9% to 43.5% (Table 2; Figure 1E). But such changes were not seen in heterosexual cases (Figures 1C,F; Supplementary Table S2). These data indicated that MSM cases dominated the trend of HIV-1 epidemic among the newly diagnosed infections, and therefore, understanding the

TABLE 1 Basic information of the participants in this study.

	Total ($n = 1,006$)	Sampling year			χ^2	p-value
		2010–2011 ($n = 140$)	2012–2014 ($n = 299$)	2015–2016 ($n = 567$)		
Sex					1.09	0.5794
Male	943 (93.7)	134 (95.7)	279 (93.3)	530 (93.5)	1.09	0.5794
Female	63 (6.3)	6 (4.3)	20 (6.7)	37 (6.5)	1.09	0.5794
Age (years old)					18.04	0.0061
<30	275 (27.3)	23 (16.4)	86 (28.8)	166 (29.3)	9.77	0.0076
30–39	349 (34.7)	52 (37.1)	94 (31.4)	203 (35.8)	2.08	0.3540
40–49	215 (21.4)	37 (26.4)	57 (19.1)	121 (21.3)	3.08	0.2145
>49	167 (16.6)	28 (20.0)	62 (20.7)	77 (13.6)	8.60	0.0136
CD4 count (cells/μl)					12.95	0.0438
<200	227 (22.5)	29 (20.7)	69 (23.1)	129 (22.8)	0.33	0.8477
200–350	194 (19.3)	35 (25.0)	63 (21.1)	96 (16.9)	5.57	0.0618
351–500	345 (34.3)	53 (37.9)	105 (35.1)	187 (33.0)	1.31	0.5187
>500	240 (23.9)	23 (16.4)	62 (20.7)	155 (27.3)	9.64	0.0081
Risk group					39.87	< 0.0001
MSM	667 (66.3)	82 (58.6)	199 (66.6)	386 (68.1)	4.55	0.1026
Heterosexual	195 (19.4)	37 (26.4)	64 (21.4)	94 (16.6)	8.08	0.0176
Other groups	12 (1.2)	8 (5.7)	2 (0.7)	2 (0.4)	28.38	< 0.0001
Unknown	132 (13.1)	13 (9.3)	34 (11.4)	85 (15.0)	4.35	0.1137
HIV-1 genotype (*gag*/*env*)					31.19	0.0001
CRF01_AE	629 (62.5)	75 (53.6)	198 (66.2)	356 (62.8)	6.55	0.0378
Subtype B	166 (16.5)	42 (30.0)	48 (16.1)	76 (13.4)	22.51	< 0.0001
07&08&C	131 (13.0)	18 (12.9)	36 (12.0)	77 (13.6)	0.41	0.8131
Subtype A	7 (0.7)	0 (0.0)	1 (0.3)	6 (1.1)	NA	NA
URF	73 (7.3)	5 (3.6)	16 (5.4)	52 (9.2)	7.53	0.0232
HIV-1 infection status					12.19	0.0023
Recent infection	367 (36.5)	38 (27.1)	97 (32.4)	232 (40.9)	12.19	0.0023
Long-term infection	639 (63.5)	102 (72.9)	202 (67.6)	335 (59.1)	12.19	0.0023

07&08&C, HIV-1 virus that had a genotype of CRF07_BC, CRF08_BC or subtype C; MSM, men who have sex with men; NA: not applicable; other groups, risk groups including former plasma donors (8 cases), injection drug users (3 cases) and mother-to-child infection (1 case); URF, unique recombinant form. Both *gag* and *env* genes were used together to determine HIV-1 genotype of one sample. For the sample with only one gene available, HIV-1 genotype was determined by the known gene. Data were shown as number (%). The comparisons of the proportions among three sampling times were done by Chi-square test with $p < 0.05$ as significant. The Post hoc multiple comparisons were done with $p < 0.0125$ as significant for age groups, CD4 count groups, risk groups, and HIV-1 genotype groups.

contributors to changes in HIV-1 epidemic patterns among MSM cases would be helpful to find out key factors for monitoring and controlling HIV-1 infection in this region.

Increase of young MSM cases made the main contribution to the decline in median age of HIV-1-infected MSM

Median age of all MSM cases was 34 years (IQR 28–44). Cases aged <30 years (hereinafter referred to as young cases), 30–39 years, 40–49 years, and above 49 years accounted for 30.6%, 36.5%, 18.7%, and 14.1% of MSM cases, respectively. From 2010–2011 to 2015–2016, the proportion of young cases increased from 20.7% (17/82) to 32.1% (124/386, $p = 0.0411$), while the proportions of other age groups did not significantly change (Table 2), implying that the increase of young MSM cases was the main cause for the younger age trend of HIV-1-infected MSM.

Young MSM cases exhibited better immune state and a higher rate of recent HIV-1 infection

Compared to MSM cases aged ≥30 years (hereinafter referred to as old cases), young MSM cases had a higher median CD4 count (418 [IQR 307-514] versus 381 [IQR 213–487]) (Figure 2A). Additionally, 28.9% (59/204) of young MSM were CD4hi cases, slightly higher than that of old cases (22.7%, 105/463, $p = 0.0845$), and 15.2% (31/204) of young MSM had a CD4 count less than 200 cells/μl, lower than that of old cases (22.5%, 104/463, $p = 0.0314$).

The recent infection rate of all MSM cases was 38.8% (Table 2). Totally, 44.6% (91/204) of young MSM were identified as recent

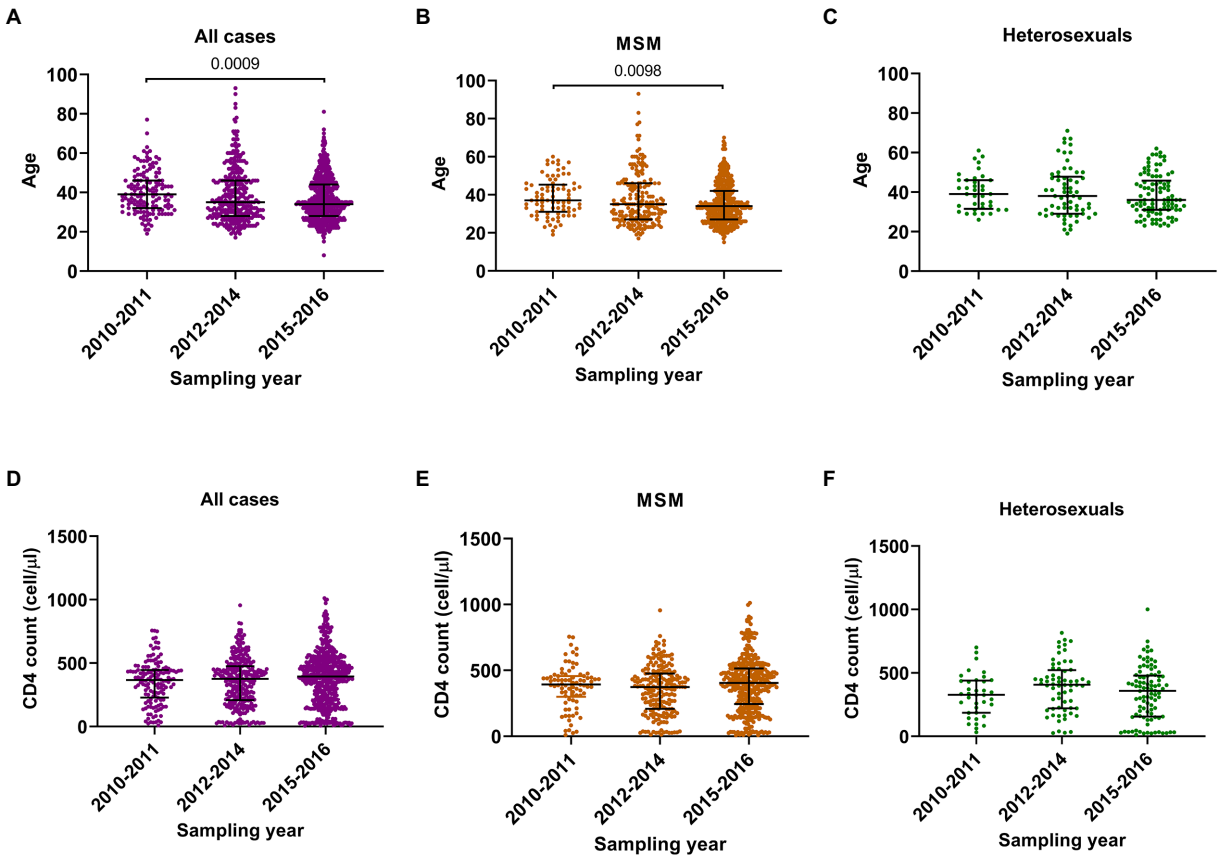

FIGURE 1
Comparison analyses on ages and CD4 cell counts in three sampling times. **(A–C)** The age in all participants, men who have sex with men (MSM) and heterosexuals. **(D–F)** The CD4 cell count in all participants, MSM and heterosexuals. Data were shown as median with interquartile range. Comparison across groups was done by Kruskal–Wallis test.

infections, higher than that of old MSM (36.3%, 168/463, $p = 0.0421$) (Figure 2B). On the other hand, median age of recently infected MSM was lower than that of long-term infected MSM (34 [IQR 27–41] versus 35 [IQR 29–45]), and the proportion of young MSM in recent infections was higher than that in long-term infections (91/259 versus 113/408, $p = 0.0421$) (Figure 2C). As expected, the median CD4 count of recently infected MSM was much higher than that of long-term infected MSM (522 [IQR 448–610] versus 286.5 [IQR 155–386]) (Figure 2D). Of recently infected MSM, 57.5% (149/259) were CD4hi cases, much higher than that of long-term infected MSM (3.7%, 15/408, $p < 0.0001$). Of note, among all CD4hi MSM cases, 90.9% (149/164) were identified as recent infections. Correlation analysis on MSM population showed a negatively correlation between age and CD4 count and a positive correlation between age and the ODn value (Figures 2E,F).

The data above suggested that young MSM seemed to be in better immune state and have a higher recent infection rate, and that the increase of young MSM cases during the study period may be result in increase of diagnoses in early stage of HIV-1 infection and the improvement in the overall immune status of MSM cases.

MSM infected by CRF01_AE virus mostly affected HIV-1 epidemic patterns among MSM population

Next, we wanted to know whether temporal HIV-1 epidemic trend in MSM cases was associated with the infection of a particular viral genotype.

CRF01_AE, subtype B, and 07&08&C were the main genotypes circulating among MSM cases, accounting for 64.3%, 14.7%, and 12.9% of infections, respectively (Table 2). There was no significant difference on the median ages of MSM infected by these HIV-1 genotypes (Figure 3A), but during the three sampling times, MSM cases infected by CRF01_AE virus showed similar changes with total MSM cases in general: median age decreased from 36 years (IQR 32–44) in 2010–2011 to 33 years (IQR 27–41) in 2015–2016 (Figure 3B), and the proportion of young cases increased from 13.6% (6/44) to 34.0% (85/250, $p = 0.0071$).

Median CD4 count in MSM cases infected by CRF01_AE or subtype B virus was lower than that infected by 07&08&C virus (Figure 3C). When compared with the corresponding old cases, the young MSM with CRF01_AE virus showed a higher median

TABLE 2 Basic information of the HIV-1 infected MSM cases.

	Total ($n = 667$)	Sampling year			χ^2	p-value
		2010–2011 ($n = 82$)	2012–2014 ($n = 199$)	2015–2016 ($n = 386$)		
Age (years old)					10.89	0.0919
<30	204 (30.6)	17 (20.7)	63 (31.7)	124 (32.1)		
30–39	244 (36.5)	29 (35.4)	68 (34.2)	147 (38.1)		
40–49	125 (18.7)	21 (25.6)	33 (16.6)	71 (18.4)		
>49	94 (14.1)	15 (18.3)	35 (17.6)	44 (11.4)		
CD4 count (cells/μl)					13.70	0.0332
<200	135 (20.2)	13 (15.9)	45 (22.6)	77 (19.9)	1.69	0.4292
200–350	125 (18.7)	16 (19.5)	43 (21.6)	66 (17.1)	1.79	0.4080
351–500	243 (36.4)	40 (48.8)	71 (35.7)	132 (34.2)	6.28	0.0433
>500	164 (24.6)	13 (15.9)	40 (20.1)	111 (28.8)	9.15	0.0103
HIV-1 genotype (*gag*/*env*)					15.06	0.0198
CRF01_AE	429 (64.3)	44 (53.7)	135 (67.8)	250 (64.8)	5.17	0.0754
Subtype B	98 (14.7)	22 (26.8)	30 (15.1)	46 (11.9)	12.03	0.0024
07&08&C	86 (12.9)	11 (13.4)	21 (10.6)	54 (14.0)	1.40	0.4957
Subtype A & URF	54 (8.1)	5 (6.1)	13 (6.5)	36 (9.3)	1.88	0.3908
HIV-1 infection status					8.51	0.0142
Recent infection	259 (38.8)	27 (32.9)	64 (32.2)	168 (43.5)	8.51	0.0142
Long-term infection	408 (61.2)	55 (67.1)	135 (67.8)	218 (56.5)	8.51	0.0142

07&08&C, HIV-1 virus that had a genotype of CRF07_BC, CRF08_BC or subtype C; MSM, men who have sex with men; URF, unique recombinant form. Both *gag* and *env* genes were used together to determine HIV-1 genotype of one sample. For the sample with only one gene available, HIV-1 genotype was determined by the known gene. Data were shown as number (%). The comparisons of the proportions among three sampling times were done by Chi-square test with $P < 0.05$ as significant. The Post hoc multiple comparisons were done with $p < 0.0125$ as significant for CD4 count groups and HIV-1 genotype groups.

CD4 count (388 [IQR 297–507] versus 359 [180–453]) (Figure 3D). Furthermore, for MSM infected by CRF01_AE virus, 25.6% (34/133) of young cases were CD4hi cases, higher than that of old cases (14.9%, 44/296, $p = 0.0079$), and 15.0% (20/133) of young cases had CD4 counts less than 200 cells/μl, lower than that of old cases (27.4%, 81/296, $p = 0.0054$).

There was no significant difference on the recent infection rates of MSM cases infected by CRF01_AE (37.1%, 159/429), subtype B (33.7%, 33/98), and 07&08&C (44.2%, 38/86) (Figure 3E). But young MSM infected with CRF01_AE virus showed a higher recent infection rate than its corresponding old cases (44.4% [59/133] versus 33.8% [100/296], $p = 0.0359$). Young cases and old cases in subtype B or 07&08&C infected MSM had similar rates of recent infection (Figure 3F).

These data indicated that the increase in number and proportion of young MSM infected by CRF01_AE virus made a substantial contribution to the decline in median age of MSM cases, which may lead to the improvement in the overall immune status and the increase in recent infection rate of the MSM cases. MSM infected by CRF01_AE virus mostly affected HIV-1 epidemic patterns among MSM population.

Discussion

This study was the first cross-sectional molecular epidemiological study based on a large sample size in Heilongjiang of Northeast China. According to our previous report and the report from the Center for Disease Control and Prevention of Heilongjiang Province, during 2010–2016, 8,026 HIV-1 infection cases were newly diagnosed in this province. The participants enrolled in this study represented 12.5% (1,006/8,026) of all newly reported cases and showed representative demographic characteristics (age composition, gender composition, and risk group composition as shown in Table 1) that were seen in the provincial level (Shao et al., 2014; Ma et al., 2018). As the data released by Health Commission of Heilongjiang Province (2017) by the end of October 2017, there were 9,276 people living with HIV (PLWH), of which 51.1% were reported in Harbin City, the capital city of Heilongjiang. Recently, Heilongjiang Provincial People's Government (2021) reported that by the end of October 2021, the cumulative number of HIV-1 infection cases reported in this province was 16,638, including 14,373 PLWH, of which 51.7% was in Harbin City. Based on these data, the participants recruited in this study represented about 25% of newly diagnosed HIV-1 cases during 2010–2016 in Harbin City.

One obvious feature of the participants in our study was that the majority (93.7%) were male, which reflected the epidemiological data from Heilongjiang Province. In the official report from the Center for Disease Control and Prevention of Heilongjiang Province, the ratio of male to female cases during 2012–2017 was 12.3:1, that was, male cases accounted for 92.5% (12.3/13.3) of new HIV-1 diagnoses (Ma et al., 2018). This phenomenon of male case polarization also exists in other

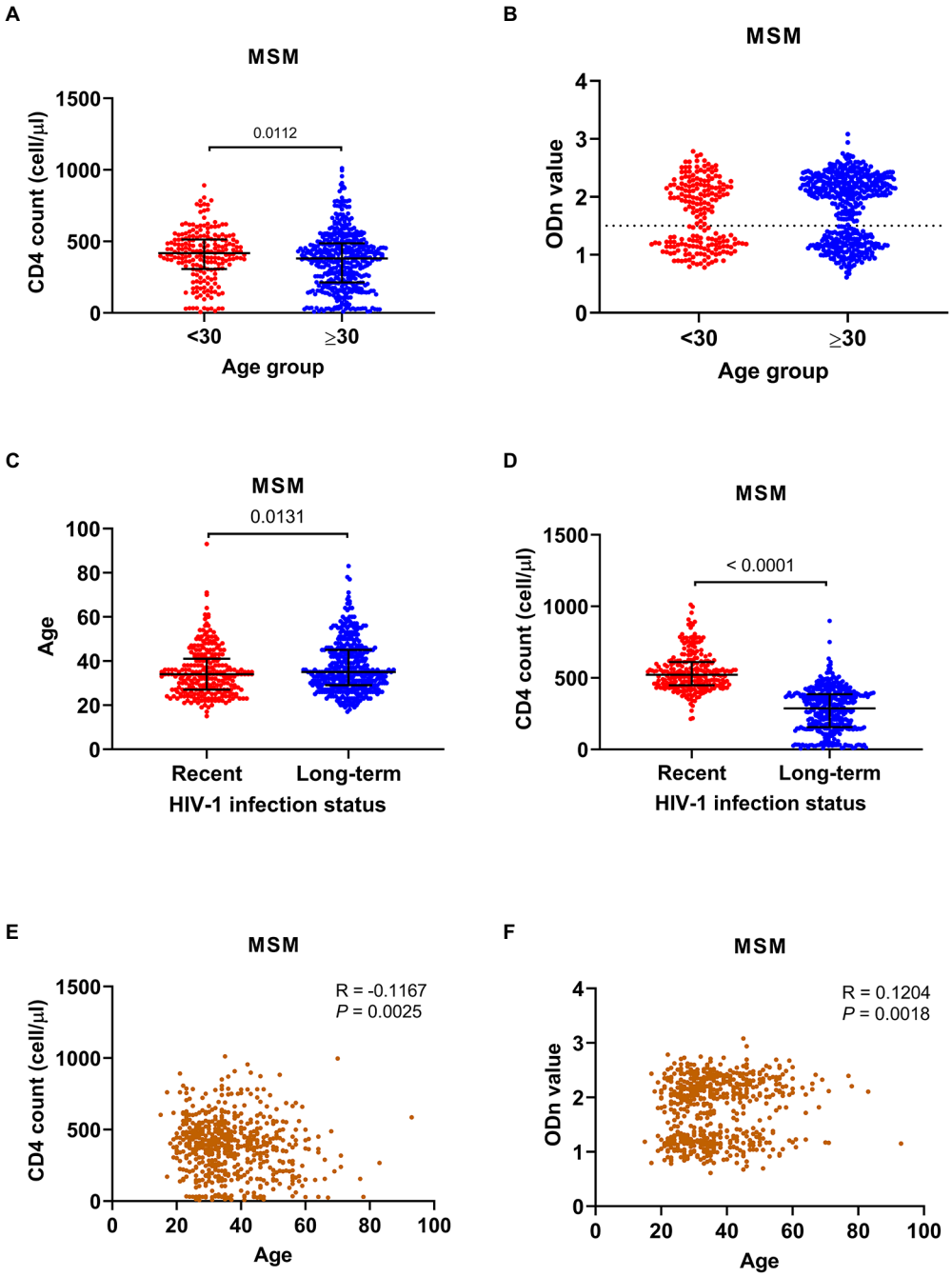

FIGURE 2
Comparison analyses between age groups and HIV-1 infection status groups of men who have sex with men (MSM). **(A)** The CD4 cell count in cases aged <30 years and those aged ≥30 years. **(B)** The normalized optical density (ODn) value of plasma samples from cases aged <30 years and cases aged ≥30 years in Limiting-Antigen Avidity assays. **(C)** The ages of MSM with recent and long-term HIV-1 infections. **(D)** The CD4 cell count of MSM with recent and long-term HIV-1 infections. **(E,F)** Correlation analyses between age and CD4 cell count and ODn value. Data in **(A–D)** were shown as median with interquartile range, and the comparison across groups was done by Kruskal–Wallis test. The correlation analyses in **(E,F)** were done by nonparametric Spearman correlation test.

regions of China where MSM population dominate newly diagnosed HIV-1 infections, such as Beijing (92.9% in 2001–2016) (Ye et al., 2020), Tianjin (96.5% in 2013–2019) (Ge et al., 2021), Nanjing of Jiangsu Province (95.0% in 2015–2017) (Li et al., 2019b), and Anhui Province (95.6% in 2011–2013) (Wu et al., 2015).

In this study, we reported that MSM cases dominated the temporal HIV-1 epidemic trend in this region: the age of

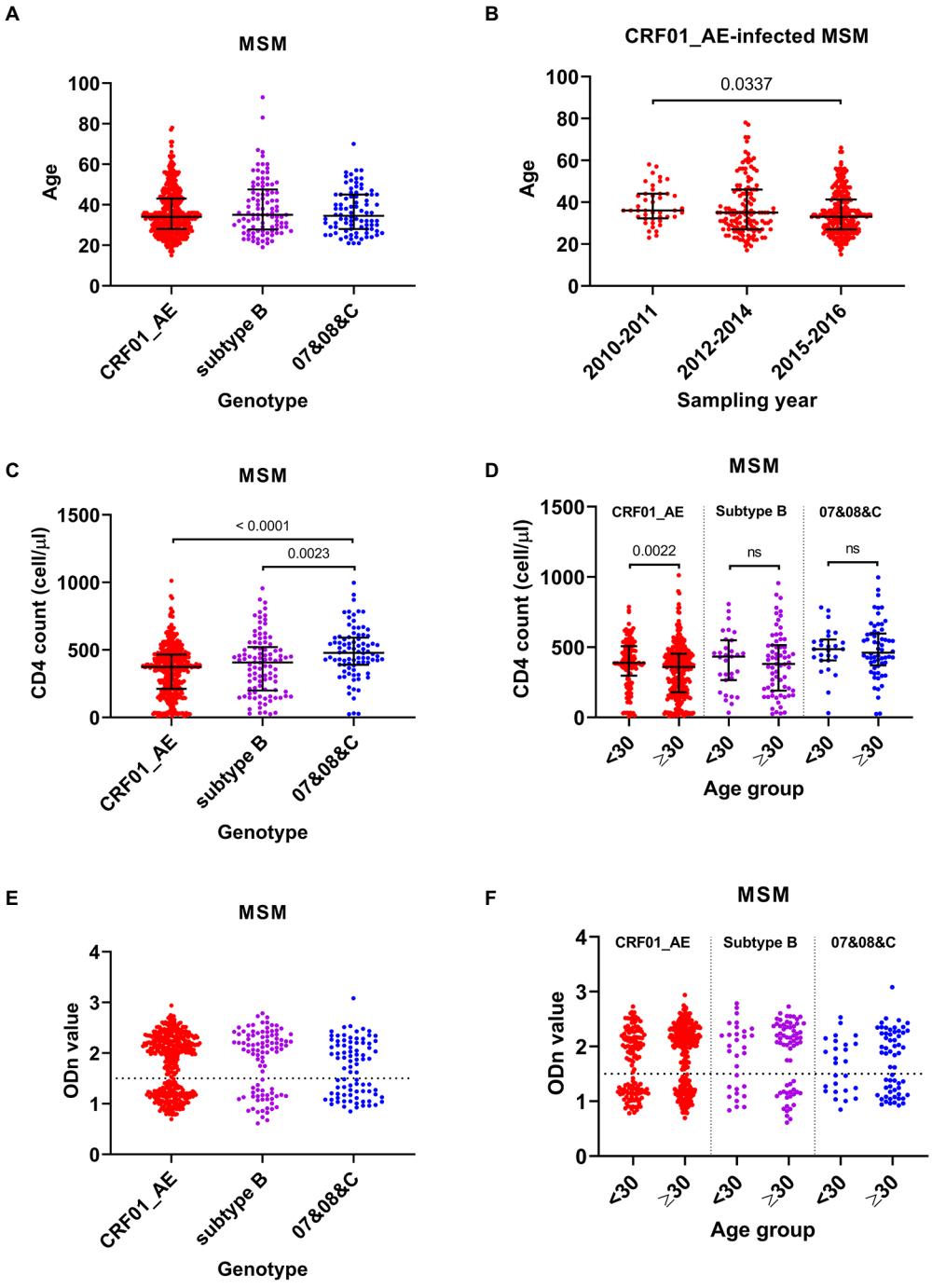

FIGURE 3
Comparison analyses among men who have sex with men (MSM) infected by different HIV-1 genotypes. **(A)** The age of MSM infected by different genotypes. **(B)** The age of CRF01_AE-infected MSM in three sampling times. **(C)** The CD4 cell count of MSM infected by CRF01_AE, subtype B, and 07&08&C viruses. **(D)** The CD4 cell count of cases aged <30 years and aged ≥30 years with different HIV-1 genotype infection. **(E)** The normalized optical density (ODn) value of plasma samples from MSM infected by different genotypes in Limiting-Antigen Avidity assays. **(F)** The ODn value of plasma samples from MSM aged <30 years and aged ≥30 years with different HIV-1 genotype infection. Data in **(A–D)** were shown as median with interquartile range, and the comparison across groups was done by Kruskal–Wallis test. 07&08&C, virus that had a genotype of CRF07_BC, CRF08_BC or subtype C.

cases at diagnosis was getting younger, the proportion of cases with good immune status was increasing, and the rate of recent infection was rising. We also reported that the rapid expansion of young MSM cases, especially the young MSM infected by HIV-1 CRF01_AE virus, was the key contributor to these changes.

Unlike the situation in some European and American countries where HIV-1 epidemic initiated among MSM, few cases were reported among Chinese MSM until the year 2005. Since 2010, MSM population has become the group with the highest risk for HIV-1 transmission in China (Wu et al., 2019). One obvious feature for the HIV-1 epidemic among Chinese MSM is the uneven distribution of cases across provinces and regions, highly concentrating in municipalities, provincial capitals, or cities with large population sizes and fast economic growth, such as Beijing, Shanghai, Guangzhou (Qin et al., 2017).

As the capital of Heilongjiang Province, Harbin City is one of economic centers in Northeast China as well as one of cities that were affected by the first wave of HIV-1 expansion among MSM during 2006–2008 (Qin et al., 2017). HIV-1 prevalence among MSM population in Harbin rapidly increased from 1.0 to 9.5% between 2006 and 2011 (Wang et al., 2012; Zhang et al., 2013). Our previous studies demonstrated that MSM became the highest-risk group for HIV-1 infection in Heilongjiang Province during 2009–2012, accounting for 57.9% and 69.0% of new diagnoses in 2009–2010 and 2011–2012, respectively (Shao et al., 2014). In this study, we reported that MSM cases accounted for 66.3% of all new diagnoses during 2010–2016, consistent with our previous studies (Shao et al., 2014, 2016) and similar with the cities where HIV-1-infected Chinese MSM concentrate, such as Jilin (another northeast province), Beijing (Ye et al., 2020), and Shanghai (Li et al., 2015a). Importantly, although the annual new diagnoses continued to increase, the MSM cases still accounted for a high and stable proportion (ranging from 58.6% to 68.1%) in each sampling time, suggesting a steady increase in the number of HIV-1-infected MSM cases, which could partially explain the dominant role of MSM cases on the overall HIV-1 epidemic in this region.

Young people have been considered as a hot topic in HIV-1/AIDS epidemic in China for many years. But in the initial years (2005–2008), the clustering hotspots of Chinese young people living with HIV/AIDS (aged 15–24 years) mainly distributed within heterosexuals and intravenous drug users in southwest provinces. After 2008, new hotspots among MSM in central and northeast provinces emerged. On the national scale, new HIV-1 cases aged 15–24 years increased by an annual average of 35% during 2011–2015 (Burki, 2018). For Harbin city of Heilongjiang Province, HIV/AIDS cases aged 15–24 years increased about 5-fold between 2005 and 2012 (Zhang et al., 2017). The present study showed the number of newly diagnosed young MSM (aged <30 years) had a 7.2-fold (166/23) increase from 2010–2011 to 2015–2016 and the proportion of young MSM got a 1.5-fold (from 20.7 to 32.1%) increase, implying that young MSM have become a new vulnerable group of HIV-1 infection in Heilongjiang, China. Understanding the changes on HIV-1 epidemic features accompanied by the increasing number of this young population is important and necessary.

Indeed, two interesting changes among MSM cases were also observed: steadily increasing proportion of CD4hi cases (CD4 count >500 cells/μl) and continuously rising rate of recent HIV-1 infections. In China, the overall improvement on immune status of HIV-1-infected persons can be partially explained by the scale-up of HIV testing. It was reported that between 2009 and 2018, the total person-times of HIV testing in China increased from 55.6 million to more than 240 million (Ding et al., 2019), which gives a chance to find more cases at the early stage of the disease. Moreover, young people seem to be more likely to know their HIV-1 status. A cross-sectional survey of HIV-1-infected MSM from seven cities showed that compared with old people, young Chinese MSM had a higher HIV-1 incidence and a higher prevalence of recent HIV-1 infection during 2012–2013 (Mao et al., 2018). Consistent with this finding, in the present study, we reported for first time that young MSM cases (< 30 years) in Heilongjiang Province exhibited better immune state and a higher recent infection rate than the old cases (≥ 30 years). The increase in number of young MSM cases was the positive factor and critical reason for the improved immune status and the elevated recent infection rate of MSM cases.

However, it is worth noting that recently infected HIV-1 cases are usually highly infectious because of their high viral loads, but they mainly remain undetected (Buskin et al., 2014). And, young MSM exhibited a higher prevalence of high-risk behaviors (recreational drug use, unprotected anal intercourse, and concurrent multiple sex partnerships) than old MSM (Mao et al., 2018). Therefore, recently infected young MSM have potential to speed up HIV-1 transmission and secondary infection within MSM population. We speculate that the rapid increase of young MSM cases with high CD4 counts will continue to be an important feature of HIV-1 epidemic in this northeast province of China in the following years.

One more evidence for the overall improvement of immune status of the HIV-1-infected persons was also observed in this study. As shown in Table 1, the proportion of "late diagnoses" (CD4 count <200 cells/μl at diagnosis) in newly diagnosed ART-naïve HIV-1 cases ranged from 20.7% to 23.1% during 2010–2016, much lower than the national level (35.5%–41.8%) in 2010–2014 (Jin et al., 2016), and the Heilongjiang provincial level in 1993–2012 (28.6%–38.4%) (Shao et al., 2014). This may be due to the high availability of HIV testing in China and people's increasing willingness to test.

CRF01_AE genotype which accounts for only approximately 5% of global HIV-1 infections concentrates in Southeast Asia and China (Hemelaar et al., 2011, 2020). In 1990s, CRF01_AE virus was introduced into China and rapidly spread throughout the whole country. Since 2007, CRF01_AE became the most prevalent genotype in China except the northwest region (Feng et al., 2013; Li et al., 2017). Previous studies have reported that in Northeast China, more than half of HIV-1 infections were caused by CRF01_AE genotype (Li et al., 2016b), which is supported by our present findings. Here, we found that CRF01_AE was the main genotype in Heilongjiang in 2010, and continued to dominate HIV-1 genotype during 2010–2016. For HIV-1-infected MSM, CRF01_AE accounted for 64.3% (429/667) of newly diagnosed cases in Heilongjiang, slightly higher than the national level (57.36%) described in a meta-analytic integration of 66 molecular epidemiological studies conducted during 2008–2016 (Yin et al., 2019). That was why CRF01_AE-infected MSM mostly affected HIV-1 epidemic features among MSM cases.

In another study on HIV-1-infected MSM (aged 16–25 years) from 13 provinces in northwest, eastern, and

southwest regions of China, the authors reported that the proportion of CRF01_AE infections decreased from 55.4% to 43.5% between 2009 and 2014 (Li et al., 2015b). In the present study, we added the data in Northeast China. Here the proportion of CRF01_AE infections among young MSM (aged <30 years) obviously increased from 2010–2011 (35.3%, 6/17) to 2012–2014 (66.7%, 42/63, $p = 0.0191$), and 2015–2016 (68.5%, 85/124, $p = 0.0072$). Based on our data, the young MSM infected with CRF01_AE virus increased disproportionately during 2010–2014 in Heilongjiang Province, Northeast China, and the proportion of this population remained stable thereafter. There was no sign that the proportion of this young MSM population would decline. In future, more concerns should be put on the measures of HIV-1 prevention and control targeting the young MSM with CRF01_AE infection.

There were limitations in this study. First, although we had made great efforts to collect samples from the clinical monitoring site, the biggest site in Heilongjiang Province, the sample size in early years (2010–2011) was still small ($n = 140$). Therefore, in some statistical analyses, differences among groups or subgroups may be underestimated. Even so, several important findings were yielded. We believe that using a larger sample size will further confirm our findings. Second, the data from cases that were diagnosed in very recent years lacked. In fact, we had collected the demographical and clinical information of HIV-1-infected persons who were diagnosed in 2017–2019 ($n = 853$). The median age of these cases was 33 years (IQR 27–45) and the proportion of young cases (aged <30 years) was 32.7% (279/853). This seemed that the younger age trend of local new HIV-1 infections was continuing. But because most of them lacked information on CD4 count, transmission route, and HIV-1 genotype, these cases were not included in this study. Third, HIV-1 genotyping based on partial *gag* and *env* gene regions might introduce some bias. Further analyses based on the near full-length genome of HIV-1 will be required in future. Despite these limitations, we still believe that our work could provide several clues for further research and HIV/AIDS control in Northeast China.

In summary, HIV-1 epidemic in Heilongjiang Province of China showed three new changes: the median age continued to decline, the cases with good immune status disproportionally expanded, and the recent infection rate steadily increased. MSM cases drove these changes. Rapid increase in the number of young MSM cases, mainly young MSM with HIV-1 CRF01_AE infection, was the most important contributor to these changes. Young MSM population has become a new hotspot and vulnerable group for HIV-1 transmission in this northeast province of China and development of intervention measures targeting this population is urgently needed.

Data availability statement

The datasets presented in this study can be found in online repository. The name of the repository and accession numbers can be found in the article.

Ethics statement

This study was approved by the Institutional Review Board of the Fourth Affiliated Hospital of Harbin Medical University ([2015] KT003). Written informed consent was obtained from each participant or participant's legal guardian.

Author contributions

F-XW and S-LL conceived the experiments. F-XW and Q-HL designed the experiments. X-HC collected the clinical samples. Q-HL, J-YW, S-YL, S-LZ, and W-BZ performed the experiments. J-YW, Y-QZ, E-LL, and Y-RW analyzed the data. Q-HL and J-YW wrote the original draft of the manuscript. F-XW and S-LL reviewed and edited the manuscript. All authors contributed to the article and approved the submitted version.

Funding

This work was supported by the National Natural Science Foundations of China (grant numbers 81971915 and 81601755) and Natural Science Foundation of Heilongjiang Province (grant number C2017043). The funders had no role in the study design, data collection, analysis, decision to publish, or preparation of the manuscript.

Conflict of interest

The authors declare that the research was conducted in the absence of any commercial or financial relationships that could be construed as a potential conflict of interest.

Publisher's note

Supplementary material

The Supplementary material for this article can be found online at: https://www.frontiersin.org/articles/10.3389/fmicb.2022.1028383/full#supplementary-material

SUPPLEMENTARY FIGURE S1
Genotype identification of HIV-1 isolates from newly diagnosed participants. Phylogenetic trees were constructed with env **(A)**, gag **(B)** sequences and corresponding subtype references, respectively, in Mega 6.06 software using the neighbor-joining method based on Kimura two-parameter model. Bootstrap analysis was conducted with 1000

replications. 07&08&C, virus that had a genotype of CRF07_BC, CRF08_BC or subtype C. The reference sequences on the clusters that contained newly identified sequences were marked as black dots, and the clusters without newly identified sequences were compressed and labeled by the subtype names. The branches colored in green in gag tree indicated sequences that contained an inter-subtype recombinant gag gene.

References

Burki, T. (2018). HIV in China: a changing epidemic. *Lancet Infect. Dis.* 18, 1311–1312. doi: 10.1016/S1473-3099(18)30680-7

Buskin, S. E., Fida, N. G., Bennett, A. B., Golden, M. R., and Stekler, J. D. (2014). Evaluating new definitions of acute and early HIV infection from HIV surveillance data. *Open AIDS J.* 8, 45–49. doi: 10.2174/1874613601408010045

Chen, H., Luo, L., Pan, S. W., Lan, G., Zhu, Q., Li, J., et al. (2019a). HIV epidemiology and prevention in southwestern China: trends from 1996-2017. *Curr. HIV Res.* 17, 85–93. doi: 10.2174/1570162X17666190703163838

Chen, M., Ma, Y., Chen, H., Dai, J., Luo, H., Yang, C., et al. (2019b). Spatial clusters of HIV-1 genotypes in a recently infected population in Yunnan. *China. BMC Infect. Dis.* 19:669. doi: 10.1186/s12879-019-4276-9

Ding, Y., Ma, Z., He, J., Xu, X., Qiao, S., Xu, L., et al. (2019). Evolving HIV epidemiology in mainland China: 2009-2018. *Curr. HIV/AIDS Rep.* 16, 423–430. doi: 10.1007/s11904-019-00468-z

Duong, Y. T., Qiu, M., De, A. K., Jackson, K., Dobbs, T., Kim, A. A., et al. (2012). Detection of recent HIV-1 infection using a new limiting-antigen avidity assay: potential for HIV-1 incidence estimates and avidity maturation studies. *PLoS One* 7:e33328. doi: 10.1371/journal.pone.0033328

Feng, Y., He, X., Hsi, J. H., Li, F., Li, X., Wang, Q., et al. (2013). The rapidly expanding CRF01_AE epidemic in China is driven by multiple lineages of HIV-1 viruses introduced in the 1990s. *AIDS* 27, 1793–1802. doi: 10.1097/QAD.0b013e328360db2d

Ge, Z., Feng, Y., Li, K., Lv, B., Zaongo, S. D., Sun, J., et al. (2021). CRF01_AE and CRF01_AE cluster 4 are associated with poor immune recovery in Chinese patients under combination antiretroviral therapy. *Clin. Infect. Dis.* 72, 1799–1809. doi: 10.1093/cid/ciaa380

Health Commission of Heilongjiang Province (2017). Publicity activities launched at the 30th "World AIDS Day" in Heilongjiang. 2017. http://wsjkw.hlj.gov.cn/pages/5f058063896eb3666cbc065a.

Heilongjiang Provincial People's Government (2021). Progress of AIDS prevention and control in Heilongjiang Province in 2021. 2021. https://www.hlj.gov.cn/n200/2021/1129/c42-11025852.html.

Hemelaar, J., Gouws, E., Ghys, P. D., and Osmanov, S.Isolation, W.-U.N.f.H., and Characterisation (2011). Global trends in molecular epidemiology of HIV-1 during 2000-2007. *AIDS* 25, 679–689. doi: 10.1097/QAD.0b013e328342ff93

Hemelaar, J., Loganathan, S., Elangovan, R., Yun, J., Dickson-Tetteh, L., Kirtley, S., et al. (2020). Country level diversity of the HIV-1 pandemic between 1990 and 2015. *J. Virol.* 95:e01580–20. doi: 10.1128/JVI.01580-20

Jin, X., Xiong, R., Wang, L. Y., and Mao, Y. R. (2016). Analysis on the ' late diagnosis' (LD) phenomena among newly identified HIV/AIDS cases in China, 2010-2014. *Zhonghua Liu Xing Bing Xue Za Zhi* 37, 218–221. doi: 10.3760/cma.j.issn.0254-6450.2016.02.014

Li, W., Chu, J., Wei, F., He, Y., Dong, X., Ge, Y., et al. (2019b). Molecular characteristic of HIV-1 CRF01_AE in Nanjing from 2015 to 2017. *Infect. Genet. Evol.* 75:104038. doi: 10.1016/j.meegid.2019.104038

Li, X., Li, W., Zhong, P., Fang, K., Zhu, K., Musa, T. H., et al. (2016b). Nationwide trends in molecular epidemiology of HIV-1 in China. *AIDS Res. Hum. Retrovir.* 32, 851–859. doi: 10.1089/AID.2016.0029

Li, Z., Liao, L., Feng, Y., Zhang, J., Yan, J., He, C., et al. (2015b). Trends of HIV subtypes and phylogenetic dynamics among young men who have sex with men in China, 2009-2014. *Sci. Rep.* 5:16708. doi: 10.1038/srep16708

Li, X., Liu, H., Liu, L., Feng, Y., Kalish, M. L., Ho, S. Y. W., et al. (2017). Tracing the epidemic history of HIV-1 CRF01_AE clusters using near-complete genome sequences. *Sci. Rep.* 7:4024. doi: 10.1038/s41598-017-03820-8

Li, Q. H., Shao, B., Li, J., Wang, J. Y., Song, B., Lin, Y. L., et al. (2019a). Critical amino acid residues and potential N-linked glycosylation sites contribute to circulating recombinant form 01_AE pathogenesis in Northeast China. *AIDS* 33, 1431–1439. doi: 10.1097/QAD.0000000000002197

Li, Q. H., Wang, F. X., Yue, C., Wang, J. Y., Jin, G., Zhang, C. L., et al. (2016a). Molecular genotyping of HIV-1 strains from newly infected men who have sex with men in Harbin. *China. AIDS Res. Hum. Retrovirus.* 32, 595–600. doi: 10.1089/AID.2016.0028

Li, X., Xue, Y., Cheng, H., Lin, Y., Zhou, L., Ning, Z., et al. (2015a). HIV-1 genetic diversity and its impact on baseline CD4+T cells and viral loads among recently infected men who have sex with men in Shanghai. *China. PLoS One* 10:e0129559. doi: 10.1371/journal.pone.0129559

Liu, Z., Shi, O., Yan, Q., Fang, Q., Zuo, J., Chen, Y., et al. (2018). Changing epidemiological patterns of HIV and AIDS in China in the post-SARS era identified by the nationwide surveillance system. *BMC Infect. Dis.* 18:700. doi: 10.1186/s12879-018-3551-5

Liu, S. Y., Zeng, F. F., Huang, G. F., Zhou, H., Shi, Y. M., Ling, H., et al. (2009). Analysis of human immunodeficiency virus type 1 nef gene sequences among inmates from prisons in China. *AIDS Res. Hum. Retrovir.* 25, 525–529. doi: 10.1089/aid.2008.0271

Ma, J., Tong, X., Hui, S., Yan, H., Yu, L., and Li, Y. (2018). Analysis on HIV/AIDS epidemic situation in HeiLongJiang Province from 2012 to 2017. *Harbin Med. J.* 38:3.

Mao, X., Wang, Z., Hu, Q., Huang, C., Yan, H., Wang, Z., et al. (2018). HIV incidence is rapidly increasing with age among young men who have sex with men in China: a multicentre cross-sectional survey. *HIV Med.* 19, 513–522. doi: 10.1111/hiv.12623

Qin, Q., Guo, W., Tang, W., Mahapatra, T., Wang, L., Zhang, N., et al. (2017). Spatial analysis of the human immunodeficiency virus epidemic among men who have sex with men in China, 2006-2015. *Clin. Infect. Dis.* 64, 956–963. doi: 10.1093/cid/cix031

Shao, B., Li, W. J., Liu, T., Li, Q. H., Li, H., Chang, M. L., et al. (2013). Subtype B was the dominant strain among HIV type 1 infections except for the population of men who have sex with men in Harbin City. *China. AIDS Res. Hum. Retrovirus.* 29, 1260–1264. doi: 10.1089/AID.2013.0135

Shao, B., Li, Y., Yu, L., Wang, K., Chang, M., Wang, B., et al. (2014). The HIV/AIDS epidemic characteristics in a northeast province of China--men who have sex with men have made a tremendous contribution to the growth of the HIV epidemic. *J. Infect.* 68, 273–280. doi: 10.1016/j.jinf.2013.10.014

Shao, B., Song, B., Cao, L., Du, J., Sun, D., Lin, Y., et al. (2016). Molecular epidemiology is becoming complex under the dynamic HIV prevalence: the perspective from Harbin. *China. J. Med. Virol.* 88, 807–814. doi: 10.1002/jmv.24407

Wang, K., Yan, H., Liu, Y., Leng, Z., Wang, B., and Zhao, J. (2012). Increasing prevalence of HIV and syphilis but decreasing rate of self-reported unprotected anal intercourse among men who had sex with men in Harbin, China: results of five consecutive surveys from 2006 to 2010. *Int. J. Epidemiol.* 41, 423–432. doi: 10.1093/ije/dyr182

Wang, F. X., Zhou, H., Ling, H., Zhou, H. Z., Liu, W. H., Shao, Y. M., et al. (2007). Subtype and sequence analysis of HIV-1 strains in Heilongjiang Province. *Chin. Med. J.* 120, 2006–2010. doi: 10.1097/00029330-200711020-00013

Wu, Z., Chen, J., Scott, S. R., and McGoogan, J. M. (2019). History of the HIV epidemic in China. *Curr. HIV/AIDS Rep.* 16, 458–466. doi: 10.1007/s11904-019-00471-4

Wu, Z., McGoogan, J. M., and Detels, R. (2021). The enigma of the human immunodeficiency virus (HIV) epidemic in China. *Clin. Infect. Dis.* 72, 876–881. doi: 10.1093/cid/ciaa835

Wu, J., Shen, Y., Zhong, P., Feng, Y., Xing, H., Jin, L., et al. (2015). The predominant cluster of CRF01_AE circulating among newly diagnosed HIV-1-positive people in Anhui Province. *China. AIDS Res. Hum. Retrovirus.* 31, 926–931. doi: 10.1089/AID.2015.0107

Ye, J., Hao, M., Xing, H., Wang, Y., Wang, J., Feng, Y., et al. (2020). Characterization of subtypes and transmitted drug resistance strains of HIV among Beijing residents between 2001-2016. *PLoS One* 15:e0230779. doi: 10.1371/journal.pone.0230779

Yin, Y., Liu, Y., Zhu, J., Hong, X., Yuan, R., Fu, G., et al. (2019). The prevalence, temporal trends, and geographical distribution of HIV-1 subtypes among men who have sex with men in China: a systematic review and meta-analysis. *Epidemiol. Infect.* 147:e83. doi: 10.1017/S0950268818003400

Zhang, X., Tang, W., Li, Y., Mahapatra, T., Feng, Y., Li, M., et al. (2017). The HIV/AIDS epidemic among young people in China between 2005 and 2012: results of a spatial temporal analysis. *HIV Med.* 18, 141–150. doi: 10.1111/hiv.12408

Zhang, L., Zhang, D., Yu, B., Wang, S., Liu, Y., Wang, J., et al. (2013). Prevalence of HIV infection and associated risk factors among men who have sex with men (MSM) in Harbin. *China. PLoS One* 8:e58440. doi: 10.1371/journal.pone.0058440

frontiers | Frontiers in Microbiology

TYPE Original Research
PUBLISHED 12 December 2022
DOI 10.3389/fmicb.2022.1044676

OPEN ACCESS

EDITED BY
Tongqing Zhou,
National Institutes of Health,
United States

REVIEWED BY
Chandra Nath Roy,
University of Pittsburgh,
United States
Adam Wesley Whisnant,
Julius Maximilian University of Würzburg,
Germany

*CORRESPONDENCE
Lin Li
dearwood@sina.com
Junjun Jiang
jiangjunjun@gxmu.edu.cn

†These authors have contributed equally to this work

SPECIALTY SECTION
This article was submitted to Virology, a section of the journal Frontiers in Microbiology

RECEIVED 14 September 2022
ACCEPTED 11 November 2022
PUBLISHED 12 December 2022

CITATION
Shi Y, Han J, Zhu B, Liu Z, Liang Q, Lan C, Li Z, Li H, Liu Y, Jia L, Li T, Wang X, Li J, Zhang B, Jiang J and Li L (2022) Limited nucleotide changes of HIV-1 subtype B Rev response element in China affect overall Rev-RRE activity and viral replication. *Front. Microbiol.* 13:1044676. doi: 10.3389/fmicb.2022.1044676

Limited nucleotide changes of HIV-1 subtype B Rev response element in China affect overall Rev-RRE activity and viral replication

Yuting Shi[1,2†], Jingwan Han[2†], Bo Zhu[2†], Zhi Liu[2], Qingmiao Liang[3], Chunlin Lan[1,2], Zhengyang Li[2], Hanping Li[2], Yongjian Liu[2], Lei Jia[2], Tianyi Li[2], Xiaolin Wang[2], Jingyun Li[2], Bohan Zhang[2], Junjun Jiang[1]*and Lin Li[2]*

[1]Guangxi Key Laboratory of AIDS Prevention and Treatment, School of Public Health, Guangxi Medical University, Nanning, China, [2]Department of AIDS Research, State Key Laboratory of Pathogen and Biosecurity, Beijing Institute of Microbiology and Epidemiology, Beijing, China, [3]School of Graduate Studies, Guangxi Medical University, Nanning, China

The HIV-1 Rev response element (RRE) is a cis-acting RNA element that facilitates the nuclear export of mRNA-containing introns by binding specifically to the Rev protein, enabling a critical step in the viral replication cycle. This study aims to determine the subtype-specific loci of HIV-1 subtype B RRE circulating in China and to analyze their effects on Rev-RRE function and HIV-1 replication. We amplified 71 HIV-1 subtype B RRE full-length sequences from the HIV patients' blood samples collected in China, analyzed the subtype-specific loci on them by comparing them with subtype B in the United States, and predicted their RNA secondary structures. Rev-RRE activity assay was used to test the binding activity of Rev and different RREs. Infectious clones were mutated to test the effect of the subtype-specific loci on replication capacity. In this study, two sites were determined to be the subtype-specific loci of HIV-1 subtype B RRE circulating in China. Both site 186 and site 56-57insAAC can significantly increase the viral mRNA transcription and Rev-RRE activity, but only the site 186 can significantly improve viral replication ability. Collectively, the subtype-specific loci of subtype B RRE circulating in China have a significant effect on the Rev-RRE activity and viral replication. This study investigates the subtype-specific loci of RRE, which are unique to retroviruses and essential for viral replication, and will help to explore the reasons why subtype B circulating in China is more widespread and persistent than American subtype B in China at the genetic level, and will provide theoretical support for the development of more inclusive detection and treatment methods for subtype B circulating in China. At the same time, it will also provide insight into the impact of different subtype HIV-1 genetic characteristics on viral replication.

KEYWORDS

HIV-1, Rev response element, subtype B, functional activity, virus replication

Introduction

Due to the tremendous genetic variability of HIV-1, there are many different subtypes and prevalent recombinant strains. Among them, subtype B strains were the first to be identified and are widely prevalent in Europe and the United States (US) (Barré-Sinoussi et al., 1983; Gilbert et al., 2007), which accounts for more than 90% of the HIV-1 epidemic in North America (Hemelaar et al., 2011). Additionally, among the main prevalent strains in China are CRF07_BC, CRF01_AE, CRF08_BC, and subtype B (Xu et al., 2013).

HIV-1 RRE is a highly structured RNA sequence with a length of ~350 nt, which is a cis-acting RNA element directly acting in the form of RNA. It is located in the env coding region of the viral genome and exists in all viral mRNA-preserving introns (Fernandes et al., 2012; Wynn et al., 2016). It can bind to the Rev protein, an important regulatory protein of HIV-1, to facilitate the transport of viral mRNA out of the nucleus for expression and play a critical role in the process of HIV-1 replication (Daly et al., 1989; Malim et al., 1990; Jeang et al., 1991; Pollard and Malim, 1998). HIV-1 produces three major classes of mRNA through diversified editing. At the early stage of expression, only ~2 kb fully edited transcripts can be transported out of the nucleus to express the Rev protein through TAP/NXF1-dependent mRNA transport pathways commonly used by host cells, while unedited ~9 kb transcripts and incomplete ~4 kb transcripts remain in the nucleus temporarily (Taniguchi et al., 2014). The RRE sequences of the two transcripts were intact. At the late stage of expression, the Rev protein reaches a threshold outside the nucleus, shuttles back to the nucleus, and carries the viral mRNA into the cytoplasm by binding and polymerization to the RRE, enabling the viral protein to be expressed (Frankel and Young, 1998; Dai et al., 2019; Jackson et al., 2020). See Figure 1.

Early studies on the function of Rev-RRE mainly focused on the Rev protein. With an in-depth understanding of the function of Rev-RRE, people gradually realized that the sequence characteristics of RRE have a much greater impact on the activity of Rev-RRE than the Rev protein (Sloan et al., 2013). The cohort study of Phuphuakrat and Auewarakul (2005) proved that the diversity between RRE sequences of the same subtype has a significant impact on the functional activity of Rev-RRE and the pathogenicity of the virus. Besides, some have demonstrated that the change of a single base in RRE can also significantly change the functional activity of Rev-RRE and the formation of related complexes (Shuck-Lee et al., 2011). Sherpa et al. (2019) observed the activity differences between homologous pairs of Rev-RRE from different patients and different time points of the same patient and found that, compared with early time point RRE, late time point RRE only had 4 nucleotide changes but its functional activity was 2 to 3 times higher. Notably, the major Rev sequences present at early time points persist at late time points, suggesting that limited nucleotide changes in RRE are the primary driver of differential Rev-RRE activity (Sherpa et al., 2019). In addition, the activity of RRE changes with the time of infection, and it has been observed in long-term cohort studies that the rate of decrease of CD4 + T cells is related to the activity of RRE in the late stage of the disease, indicating that the RRE heterogeneity is an important regulatory factor of HIV pathogenesis and disease progression (Phuphuakrat and Auewarakul, 2005). Therefore, further study of the structural and functional evolution of the Rev-RRE system in natural infection is necessary to understand the role of this regulatory axis in the adaptation of HIV-1 to various immune environments, which may be conducive to the development of Rev-RRE-targeted therapy.

The HIV-1 subtype B circulating in China differs significantly from the subtype B in the United States in many aspects, most notably that the American subtype B is rare in China, while the subtype B now prevalent in China is clearly divided into 2 clusters in the evolutionary tree from the American subtype B. The widespread prevalence of this B subcluster in China is significantly associated with changes in transmission and replication capacity due to its genetic characteristics, in addition to the founder effect. This study investigates the subtype-specific loci of RRE, which are unique to retroviruses and essential for viral replication, and will help to explore the reasons why subtype B circulating in China is more widespread and persistent than American subtype B in China at the genetic level, and will provide theoretical support for the development of more inclusive detection and treatment methods for subtype B circulating in China. At the same time, it will also provide insight into the impact of different subtype HIV-1 genetic characteristics on viral replication.

In this study, 71 HIV-1-infected patients from China were collected and identified as subtype B through the Pol region, and the full-length RRE sequence was amplified for analysis. The effects of limited nucleotide changes in RRE on Rev-RRE functional activity and viral replication were analyzed by Rev-RRE function assay, replication kinetics, and qPCR experiments to explore the mechanism behind RRE heterogeneity affecting viral replication.

Materials and methods

Clinical samples and ethics statement

Inclusion criteria for the sample were confirmed HIV-1 antibody positivity, never received antiretroviral therapy (ART), and pol-zone subtype B; exclusion criteria were already on ART and pol-zone subtype non-B. Clinical samples were mainly from Guangdong, Henan, and Hebei provinces in China and were plasma samples. All subjects provided written informed consent.

Viral RNA extraction and cDNA synthesis

Viral RNA was extracted from 1 mL of plasma using the guanidine extraction protocol (Palmer et al., 2003) as described previously. Viral cDNA synthesis was performed immediately

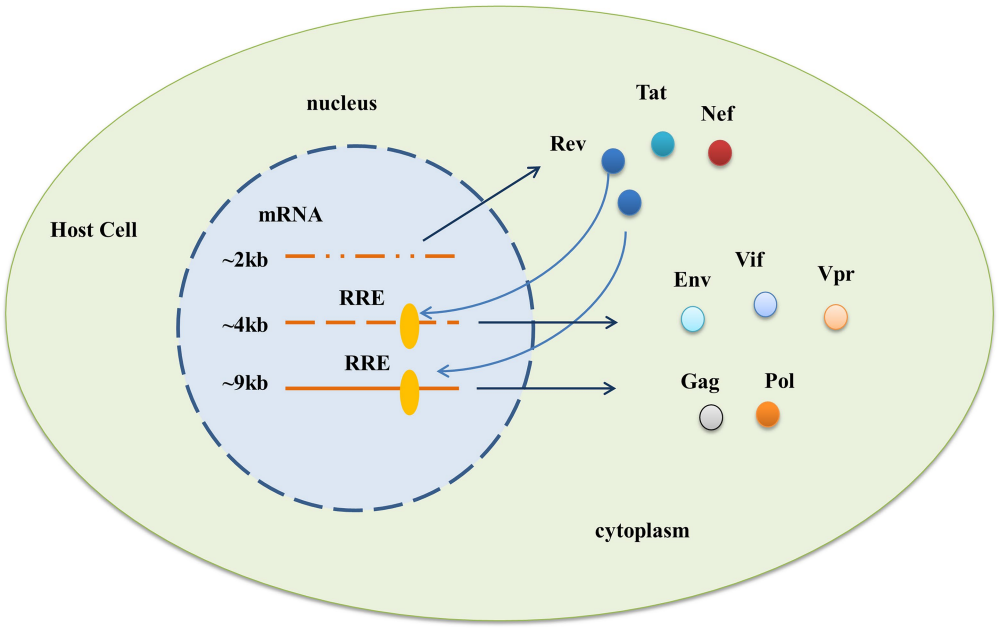

FIGURE 1
Functional requirement of the HIV-1 RRE. After HIV-1 enters the cell, three different mRNAs are produced through diverse editing, and the action of RRE allows the expression of viral proteins in two phases. In the early stage, only ~2kb of fully edited transcripts can be directly transported out of the nucleus to express Rev, Tat, and Nef proteins, while partially edited ~4kb and unedited ~9kb transcripts containing the complete RRE sequence cannot be transported out of the nucleus. At a later stage of expression, the Rev protein reaches a threshold outside the nucleus, shuttles back to the nucleus, and brings both parts of the mRNA into the cytoplasm through binding with the RRE to express viral proteins such as Env, Vif, Vpr, and Gag, Pol, respectively.

after viral RNA extraction. Reverse transcription was performed at 50°C for 32 min to obtain the cDNA product, and then the cDNA product was subjected to PCR amplification to obtain the DNA product. PCR amplification was performed by adding 2 μL of cDNA template to 23 μL of reaction mixture containing high-fidelity polymerase (Takala) (Kearney et al., 2009). Primers for PCR were RRE7355-U (5′-TTGTRGAGGRGAATTTTTCTA CTGTAA-3′) and RRE8262-D (5′-ACAGCCANTTTGTTAT GTYAAACCA-3′). Amplicon size was verified by agarose gel electrophoresis.

Single-genome sequencing and sequence analysis

The PCR products obtained by amplification were sequenced by single gene sequencing technology, and then the full-length RRE sequence was obtained by Contig software. The obtained sequences were compared and edited using BioEdit. The sequences were subtyped using BLAST, a genotyping tool available in the HIV nucleic acid Sequence Library of Los Alamos National Laboratory, United States.

We tested the model on the sequence data using Smart Model Selection (SMS) in the PhyML 3.0 program and calculated GTR + G + I as the optimal nucleotide substitution model (Lefort et al., 2017). Then, we selected this model and constructed the maximum likelihood tree using MEGA v6 (1,000 repetitions), and the final maximum likelihood tree was visualized using the program iTol v6.[1] And the gene dispersion rate was calculated by MEGA v6. Download the HIV-1 subtype B standard strain in China and all RRE reference sequences (629) in the United States from the Los Alamos HIV gene database for RRE phylogenetic analysis [Main Search Interface of HIV Sequence Database (lanl.gov)]. Inclusion criteria for US HIV-1 subtype B RRE sequences were HIV-1 subtype B prevalent in the United States, sequences containing the full length of the RRE sequence, and one sequence for one patient; exclusion criteria were HIV-1 non-subtype B, sequences with missing RRE sequences, and duplicate sequences for the same patient.

Construction of Gag/Pol-RRE reporter gene system

Rev-RRE functional activity was determined by the Gag/Pol-RRE reporter gene system, which consisted of the Gag/Pol-RRE reporter plasmid and the Rev expression plasmid. The Gag/Pol-RRE reporter plasmid was constructed by amplifying the Gag/Pol and RRE coding sequences of HIV-1 subtype B in the

1 https://itol.embl.de/

United States (NL4-3) and concatenating them together into the eukaryotic expression vector pcDNA3.1(+). Meanwhile, the coding sequences of the Rev protein of NL4-3 was amplified and inserted into the eukaryotic expression vector pcDNA3.1(+) to construct the Rev expression plasmid *in vitro*. Subsequently, the subtype B Gag/Pol-RRE reporter plasmid and Rev expression plasmid in China were generated by replacing the RRE and Rev regions of the Gag/Pol-RRE reporter gene system-NL4-3 with the RRE consensus and Rev consensus sequence (base frequency > 60%), respectively (Sherpa et al., 2015; Jackson et al., 2016). Primer information was shown in Table 1.

Rev-RRE activity assays

In this experiment, as mentioned above (Sloan et al., 2013), 1.0×10^5 HeLa cells/well were inoculated into 12-well tissue culture plates in 1 mL cell culture medium 24 h before transfection. HeLa cells were transfected with 1 μg Gag/Pol-RRE reporter gene and 0–64 ng Rev expression plasmids *via* the lipofectamine 2000 transfection reagent. Cell supernatant was collected 48 h after transfection, and the p24 level was measured by ELISA, and the dose–response curve of Rev-RRE activity was plotted. The Rev-RRE activity was measured by quantification of p24 secreted into the cell culture medium, with relative activity measured as the average slope of the best fit line.

Spreading infections

A total of 24 h before transfection, 1.2×10^6 293 T cells/well were inoculated into a 6-well tissue culture plate in 2 mL of cell culture medium. 4 μg of HIV-1 proviral DNA (NL4-3) was transfected into 293 T cells using Lipofectamine 2000 transfection reagent. Supernatants containing infectious virus particles were harvested 48 h after transfection, and p24 was measured by ELISA to quantify the amount of virus present, and these viral reservoirs were used to infect MT2 cells. In 6-well tissue culture plates, 4×10^5 MT2 cells/well were cultured in a volume of 1 mL of the normal growth medium and then infected with infected with an equal amount of p24 (5 ng) of virus supernatant. 6 h later, the cell precipitate was gently washed with phosphate-buffered saline (PBS) to remove the unattached virus, centrifuged (350 g, 5 min), and transferred to 2 mL of a fresh normal medium in a 6-well plate. 300 μL of virus supernatant was taken at day 0 and every 2 days, respectively, and the corresponding volume of fresh culture medium was supplemented to keep the total culture volume at 2 mL. The amount of p24 in the supernatant at each time point was quantified by ELISA and used to map virus growth.

TABLE 1 Primer information for the Gag/Pol-RRE reporter gene system.

Primers	Primer sequence (5′-3′)	Direction
Gag/Pol-F	AGATCTCTCGACGCAGGACTCGGCT	Forward
Gag/Pol-R	CACCCAATTCTGAAATGGATAAACA	Reverse
RRE-F	GTAGCACCCACCAAGGCAAAGAGAA	Forward
RRE-R	TAGCATTCCAAGGCACAGCAGTGGT	Reverse
Rev 1-F	ATGGCAGGAAGAAGCGGAGACAGCG	Forward
Rev 1-R	TGCTTTGATAGAGAAGCTTGATGAG	Reverse
Rev 2-F	ACCCACCTCCCAATCCCGAGGGGAC	Forward
Rev 2-R	CTATTCTTTAGTTCCTGACTCCAAT	Reverse

p24 antigen analysis

The p24 antigen in the supernatant was quantified using the HIV-1 p24 antigen ELISA kit (Biomedical Engineering Center, Hebei Medical University, China) according to the manufacturer's protocol (Li et al., 2021).

Quantification of HIV-1 mRNA transcripts and virus replication in MT2 cells by quantitative PCR

We extracted total RNA using the RNeasy Plus Mini Kit (Qiagen NO. 74134) according to the manufacturer's experimental protocol. All RNA samples were treated with 1 μL gDNA eraser per 1 μg of RNA (Takara, RR047A), to remove genomic DNA. We spiked treated samples or pure water controls with 10^2 and 10^7 DNA standards and compared their CT values, thinking to assess whether these gDNA eraser-treated samples had any residual DNAase activity or might inhibit PCR (Hurst et al., 2016). Subsequently, we reverse-transcribed the mRNA into cDNA using a mixed primer pair containing oligonucleotide dT primers (Takara, RR047A).

Real-time fluorescence quantitative PCR (qPCR) was performed with a Roche LightCycler 480 II System using TB Green® Premix Ex Taq™ (TaKaRa, Cat No. RR420A). Cycling conditions were a denaturation step at 95°C for 10 min, followed by 40 cycles of 10 s at 95°C, 5 s at 60°C, and 10 s at 72°C, followed by melting curve analysis to confirm the specificity of the PCR (Li et al., 2021). Absolute quantification of HIV-1 mRNA-RRE copies was based on available standard curves. RRE-F (5'-GCAGTGGGAATAGGAGCTTTGTTCC-3′) and RRE-R (5′-AGCCCTCAGCAAATTGTTCTGCTGC-3′) primers were used.

Statistical analysis

SPSS 23.0 software was used for the statistical analysis of the data. Where appropriate, the measurement data met the normal distribution as described by ($X \pm S$), and the hypothesis test between groups was adopted by the t-test or one-way ANOVA. All statistical analyses were performed based on a two-sided alpha of 0.05 ($\alpha = 0.05$).

Result

Background information and demographic characteristics of the samples

Among 71 HIV-1-infected patients, 67.6% (48/71) were male, 54.9% (39/71) were over 41 years old, 57.8% (41/71) were heterosexual, and 31.0% (22/71) were homosexual. Guangdong province accounted for 69.0% (49/71), and Hebei province accounted for 15.5% (11/71). In this study, HIV/AIDS patients were mainly middle-aged and elderly men, and heterosexual transmission was the main way of transmission, mainly from Guangdong Province. See Table 2.

TABLE 2 Demographic and epidemiological characteristics of the patients.

Characteristic	Cases (N, %)
Age (year)	
≤20	1 (1.4)
21–40	31 (43.7)
≥41	39 (54.9)
Sex	
Male	48 (67.6)
Female	23 (32.4)
Route of infection	
Blood transmission	1 (1.4)
Intravenous drug use transmission	4 (5.6)
Homosexual transmission	22 (31.0)
Heterosexual transmission	41 (57.8)
Unknown	3 (4.2)
Region	
Hebei	11 (15.5)
Guangdong	49 (69.0)
Henan	11 (15.5)

Subtype specificity of HIV-1 subtype B Rev response element circulating in China

We constructed a phylogenetic tree by combining the RRE sequences obtained by amplification in China with 2 standard strains of subtype B circulating in China (B.CN.2001.CNHN24.AY180905 and B.CN.RL42.U71182), 4 standard strains of subtype B in North America and Europe (B_FR_83_HXB2_LAI_IIIB_BRU_K03455, B_NL_00_671_00T36_AY423387, B_TH_90_BK132_AY173951, and B_US_98_1058_11_AY331295), and some subtype B in the United States downloaded from the United States Los Alamos HIV gene database. As seen from the phylogenetic tree, the 71 cases of HIV-1 subtype B RRE circulating in China sequences obtained by amplification clustered with the subtype B circulating in China standard strains, and the subtype B in the United States is clustered with its standard strain. See Figure 2.

Analysis of subtype-specific loci for Rev response element

MEGA 6 software was used to calculate the gene dispersion rate of the RRE region of HIV-1 subtype B in China and the United States. The results showed that the gene dispersion rate of subtype B in China was (0.062 ± 0.023), and that in the United States was (0.056 ± 0.014). t-test showed that the difference in gene distance between the two subtypes was statistically significant ($p < 0.001$). See Table 3.

In this study, 2 subtype-specific loci in the RRE sequences between HIV-1 subtype B in China and the United States were included, by calculating the base frequencies of both isoforms, sites with base frequencies >60% (site 186), and insertions or deletions (site 56-57insAAC). Among them, the mutation 186 site (G7895A) seems to be of particular interest because it is located in the critical structural domain between 163 and 221 of the RRE sequence, which is the key region where the RRE undergoes adaptive structural changes in the exercise of its function and is essential for maintaining the structure and function of the RRE (Ball et al., 2003). See Table 4.

Structural prediction of Rev response elements containing single-nucleotide mutations

The function of the HIV-1 RNA genome is determined by its sequence and its ability to fold back on itself to form a specific higher-order structure, and the replication and pathogenesis of the virus is closely linked to the structure of its RNA genome (Frankel and Young, 1998). Some investigators invented the high-throughput SHAPE (selective 2′-hydroxyacylation by primer extension analysis) technique, which uses many of the same tools as DNA sequencing to quantify the flexibility of the RNA backbone at single-nucleotide resolution and from which robust structural information can be immediately obtained. Processed SHAPE reactivities reflected the relationship of nucleotide positions, and highly reactive nucleotides (red and orange bars) reported flexible positions in the RNA (Wilkinson et al., 2008). Studies have reported alternative structures containing four or five stem-loops (SL) based on the SHAPE (Watts et al., 2009; Rausch and Le Grice, 2015). It has been suggested that the RRE can regulate HIV-1 replication kinetics by adopting different conformations that alter the nature of the resulting complex and the rate of viral replication (Booth et al., 2014; Jayaraman et al., 2014), and the 5-SL RRE is more active than the 4-SL structures (Sherpa et al., 2015). On the other hand, the Shannon entropy can be used to assess the ability of the RRE to adopt alternative

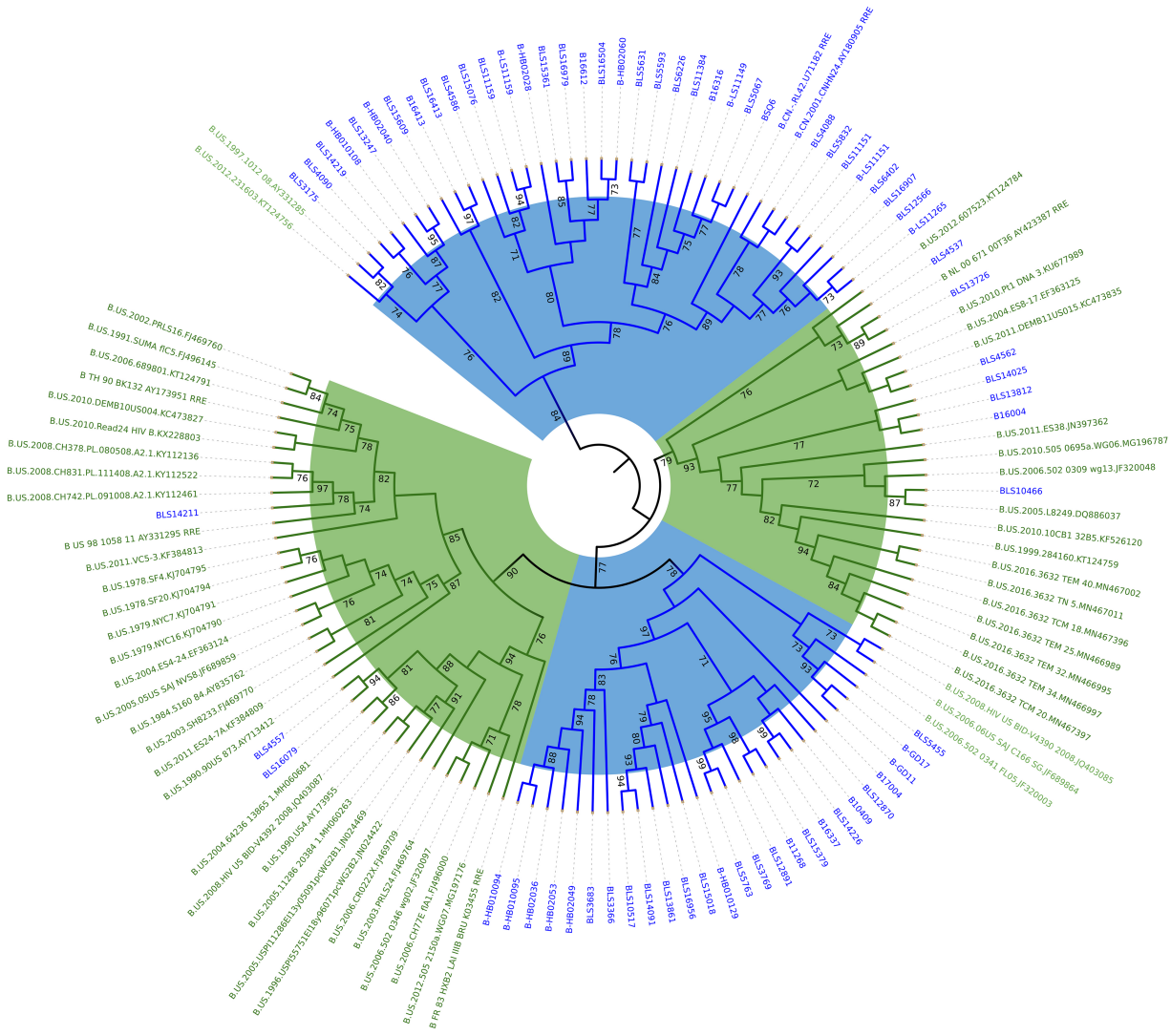

FIGURE 2
Phylogenetic analysis of HIV-1 subtype B RRE in China and the United States. Using the maximum likelihood method to construct the tree, the percentage of replicate trees in which the relevant taxa are clustered together in the bootstrap test (1,000 replicates) is shown next to the branches. The subtype B circulating in China is marked in blue and the American subtype B is marked in green.

TABLE 3 Gene distances of two subtypes of HIV-1 RRE.

HIV-1 subtypes	Cases (N)	Genetic distance (x ± s)	*t* Value	*p* Value
Subtype B in the United States	629	0.056 ± 0.014	23.861	<0.001
Subtype B in China	71	0.062 ± 0.023		

conformations. Shannon entropy is calculated based on the probability of each base pair appearing in all possible structures predicted by the RNA. In general, regions with highly stable RNA structures are characterized by low Shannon entropies. Conversely, regions with high Shannon entropy are likely to form alternative conformations.

Since the RRE structure appears to be the major contributor to the functional activity of Rev-RRE and regulation of viral replication, we next predicted the RNA secondary structure and calculated the Shannon entropy of HIV-1 subtype B RRE in China and the United States at the RNA secondary structure prediction website (RNAfold web server (univie.ac.at)). Meanwhile, the RNA secondary structure of the 186 locus and the 56-57insAAC locus mutant was predicted based on the RNA secondary structure of the American subtype B RRE. We show a mountain plot representation of the Minimum Free Energy (MFE) structure, the thermodynamic ensemble of RNA structures, and the centroid structure in Figures 3, 4. Additionally, we present the positional entropy for each position. The prediction results (Figures 3B–E)

TABLE 4 Analysis and statistics of subtype specific loci of RRE.

Mutation	Sites	Location in RRE	Nucleotide in HXB2	Base frequency (%)[a]		Reason to be selected
				China	United States	
Mut1	56-57insAAC	56–57	7,765 ~ 7,766	A (70.42)	~(64.39)	Insert
				A (71.83)	~(74.88)	
				C (74.65)	~(74.56)	
Mut2	186	Stem IV	7,895	A (61.97)	G (79.01)	Belong to 163–221[b]

[a]Percentage refers to the frequency of this base at this site of the subtype.

[b]The sequence of bits 163–221 of the RRE has been shown to be important in maintaining the structure and function of the RRE.

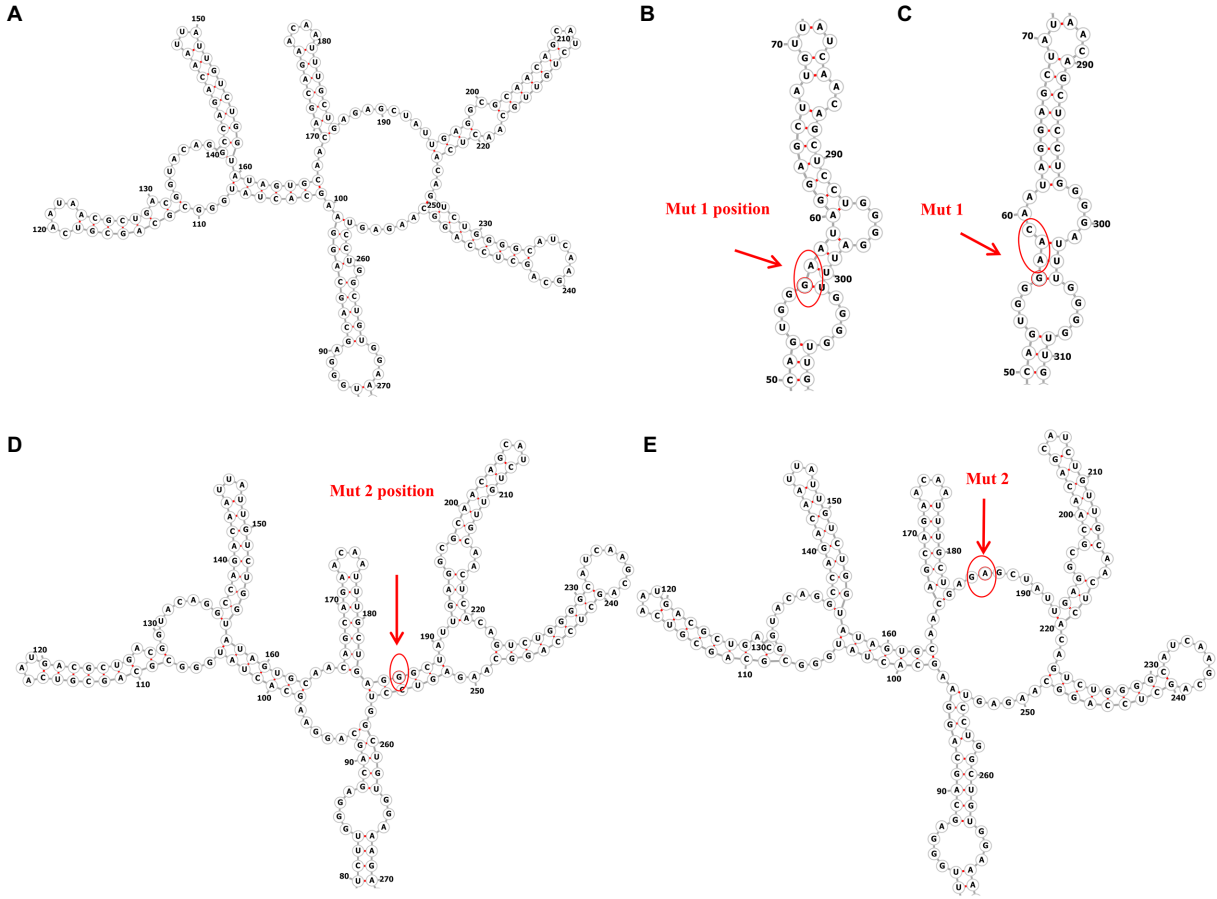

FIGURE 3
Predicted RNA secondary structure of subtype B RRE and each mutation site. **(A)** The RNA secondary structure of subtype B RRE circulating in China. **(B,D)** The RNA secondary structure of subtype B RRE in the United States. **(C,E)** Mutation at site RRE56-57ins AAC and site RRE-G186A accordingly.

showed that the 186 locus mutant was a typical 5-SL structure compared to the RRE secondary structure of the subtype B in the United States, while the 56-57insAAC locus mutant was not significantly changed. Meanwhile, the predicted results showed that both mutant loci could increase the Shannon entropy value (Figures 4C,D).

Analysis of the influence of Rev response element subtype characteristics on the functional activity of Rev-RRE

To test the functional activity of Rev-RRE, we used a transient transfection assay using HIV-1 Gag/Pol reporter

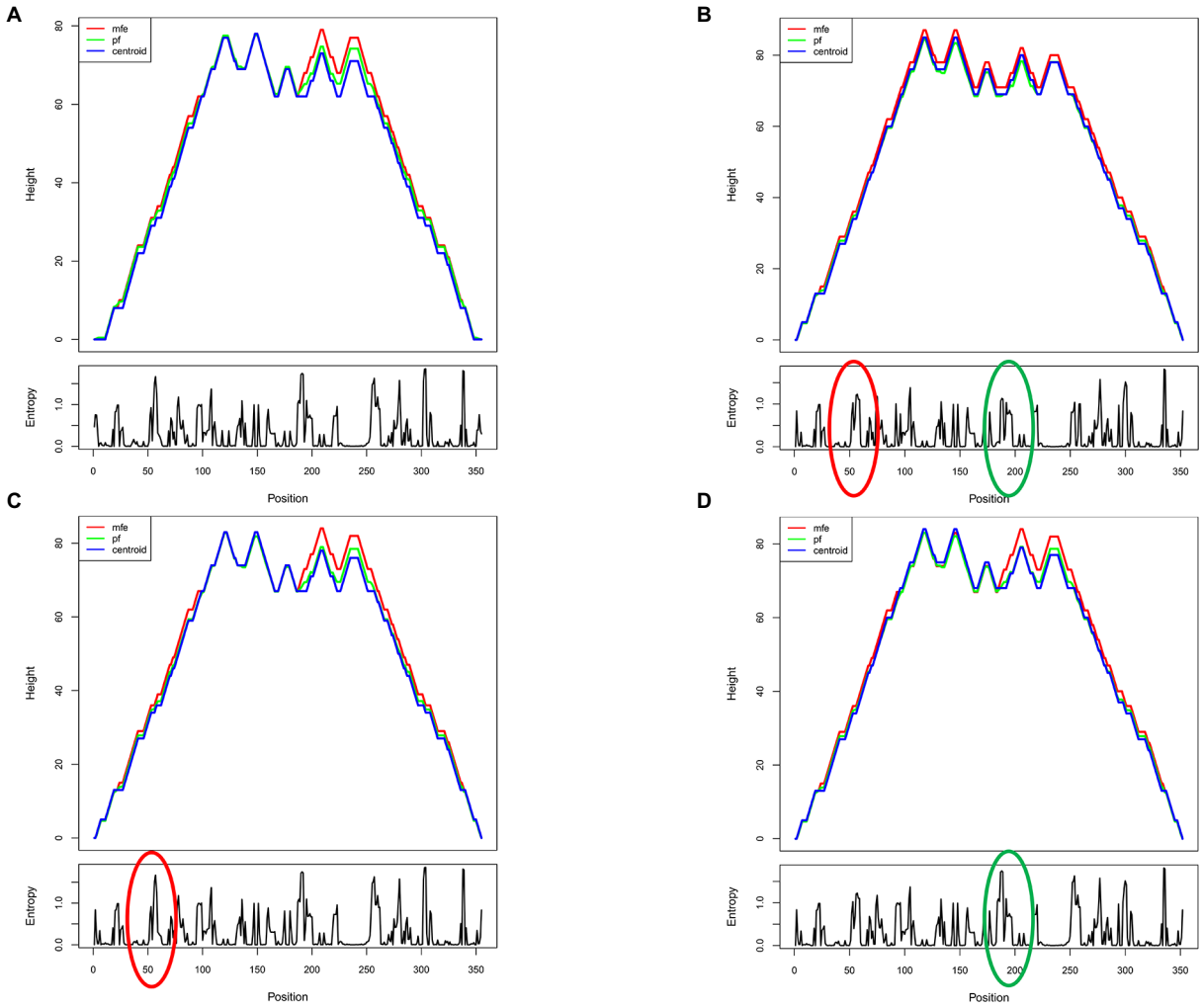

FIGURE 4
Predicted shannon entropy profile of subtype B RRE and each mutation site. **(A)** The Shannon entropy spectrum of subtype B in China. **(B)** The Shannon entropy spectrum of subtype B in the United States. **(C,D)** Mutation at site RRE56-57insAAC and site RRE-G186A, respectively.

plasmids in which Gag-Pol expression is entirely dependent on functional Rev and RRE (Figure 5). American subtype B (NL4-3) and subtype B in China (CN.B) Gag/Pol-RRE reporter plasmids were transfected into HeLa cells with an increase in the number of plasmids expressing the appropriate homologous Rev protein. The results (Figures 6A–F) showed that the relative functional activity sequence of different Rev-RREs was RRE CN.B-Rev CN.B > RRE CN.B-Rev NL4-3 > RRE NL4-3-Rev CN.B > RRE NL4-3-Rev NL4-3. Obviously, the relative activity of Rev-RRE containing subtype B RRE circulating in China was always higher than that containing NL4-3 RRE, regardless of which Rev protein was bound to it, and the difference was statistically significant (all $p < 0.01$), indicating that the functional activity of subtype B RRE circulating in China is greater than that of the United States, and that the functional activity of Rev-RRE is more affected by the subtype characteristics of RRE than the subtype specificity of Rev.

Analysis of single-nucleotide mutations affecting the ability of the Rev response element to mediate HIV Gag/Pol expression

It has been shown that the structure and activity of the RRE are sensitive to minimal nucleotide variation (Shuck-Lee et al., 2011). Therefore, it is of interest to analyze the activity of RREs from different patients to determine the role of RRE sequence variability in mediating the differences in activity between different Rev-RREs. For this purpose, RRE mutant plasmids are generated by point mutation in the RRE region of the Gag/Pol-RRE reporter plasmid-NL4-3, and each RRE in the Gag/Pol-RRE reporter system was tested for activity using the same NL4-3 Rev. Then, each Gag/Pol-RRE reporter plasmid was co-transfected into HeLa cells with varying amounts of NL4-3 Rev-expressing plasmids. These results of this experiment

(Figures 7A,B) show that each RRE variant promoted different levels of Gag/Pol expression in response to the concentration of the Rev plasmid used. Specifically, the following hierarchy of activity was observed in the RRE variants: RRE-G186A > RRE-56-57insAAC > NL4-3.

Effects of single-nucleotide mutations in Rev response element on HIV-1 replication ability *in vitro*

We used the NL4-3 infectious clone as a template, introduced the subtype characteristic sites into the NL4-3 infectious clone, constructed the corresponding mutant strain, and then transfected them into 293 T cells. After 48 h of transfection, the transfection supernatant was collected and the expression level of p24 was measured (Figure 8A). Subsequently, transfected supernatant with the same amount of p24 was used to spread infection in MT2 cells, and replication kinetics curves were plotted to analyze the effect of mutation sites on viral replication capacity (Figure 8B). The results of these experiments (Figures 8A,B) show that the replication capacity of infectious clone mutants corresponding to RRE-G186A was significantly increased compared with the NL4-3 strain ($p < 0.05$ in 293 T cells, $p < 0.0001$ in MT2 cells), while RRE-56-57insAAC had no statistical difference compared with that before mutation ($p > 0.05$).

MT2 cells were infected with the NL4-3 strain and the RRE mutant strain with the same amount of MOI (MOI = 0.1). After 48 h, culture supernatant and cells were collected, and RNA was extracted, respectively. The expression of mRNA in intracellular and viral RNA copies in culture supernatant was detected by qPCR, respectively (Figures 8C,D), and the results showed that RRE-G186A significantly increased the level of mRNA transcription and viral replication compared to NL4-3 ($p < 0.01$). Intriguingly, RRE-56-57insAAC significantly increased the intracellular mRNA transcript levels ($p < 0.01$), while there was no statistical difference in the virus replication ($p > 0.05$).

Discussion

The high variability of HIV-1 makes it produce numerous subtypes with relatively independent gene sequence characteristics in the process of transmission, and form certain regional distribution characteristics in the global epidemic so that we can trace the source of infection according to its

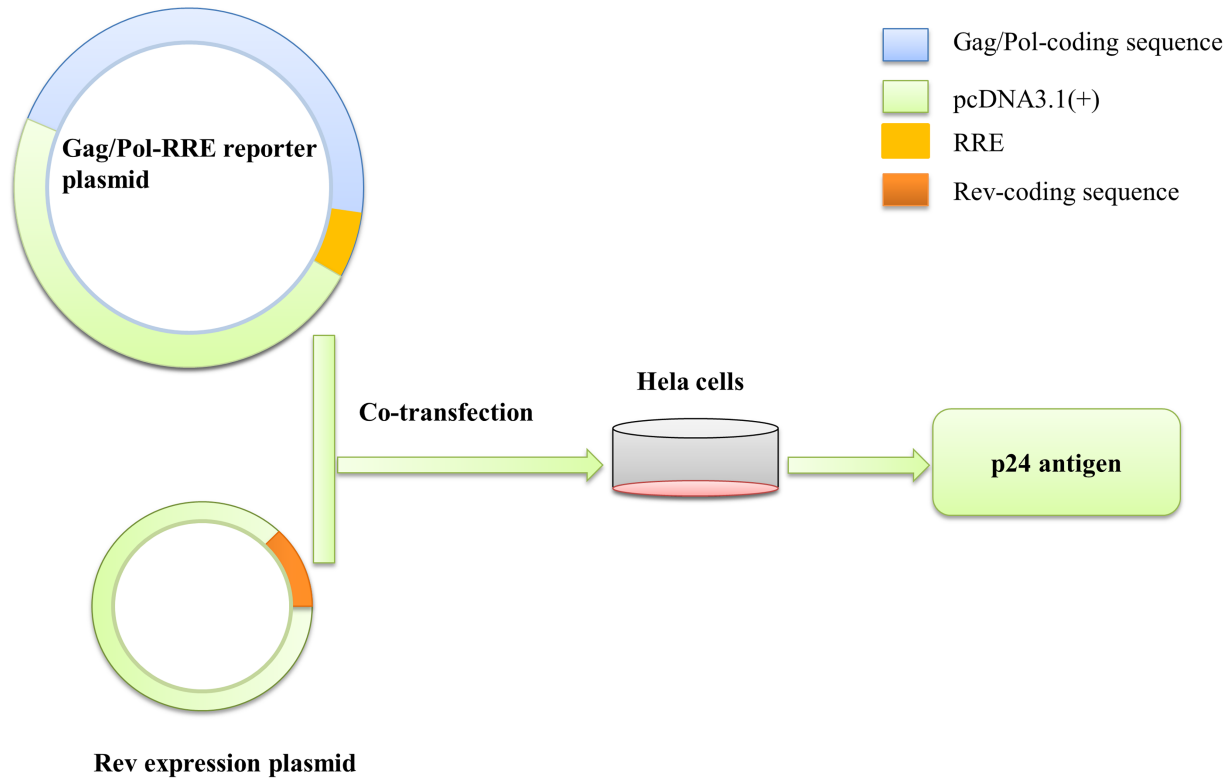

FIGURE 5
Gag/Pol-RRE reporter gene system to assess Rev-RRE functional activity. The Gag/Pol and RRE coding sequences were sequentially linked into the pcDNA3.1(+) vector to construct the Gag/Pol-RRE reporter gene expression plasmid, and the Rev coding sequence was linked into the pcDNA3.1(+) vector to construct the Rev expression plasmid *in vitro*. The two plasmids were co-transfected into HeLa cells, and the Rev-RRE functional activity was assessed by measuring the expression level of p24 antigen in the cell culture supernatant.

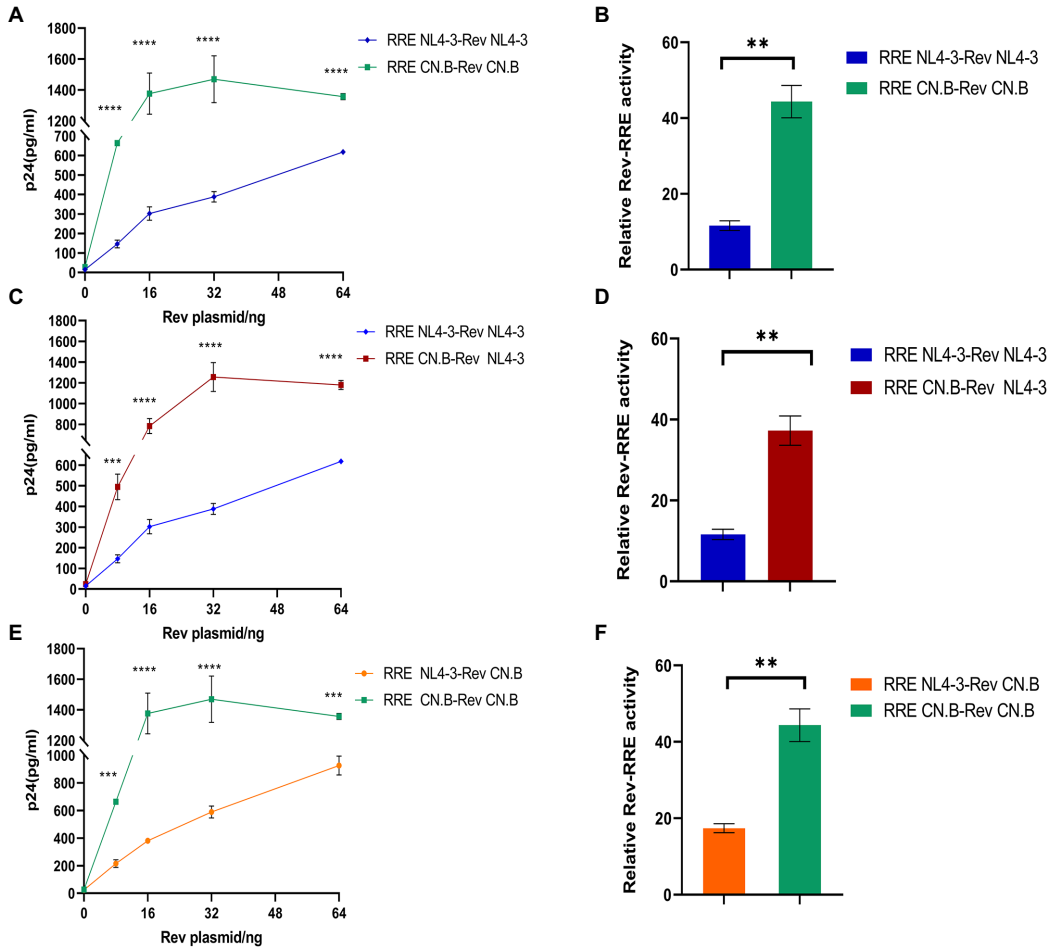

FIGURE 6
Influence of RRE subtype characteristics on functional activity of Rev-RRE. **(A,C,E)** The concentrations of p24 expressed by the reporter gene changed with the changes of Rev expression plasmid concentration when the two subtypes Rev were combined with the two subtypes RRE, respectively. **(B,D,F)** The difference in relative activity of Rev combined with RRE under corresponding conditions. Each experiment was repeated twice, and bars show the standard error of the mean from two replicates. *p<0.05, **p<0.01, ***p<0.001, and ****p<0.0001.

characteristics and study its variation rules. In this study, RRE genotyping combined with phylogenetic tree analysis showed that the samples of HIV-1 subtype B in China were approximately close to the standard strains B.CN.2001. CNHN24.AY180905 in Henan Province and B.CN.RL42. U71182 in Yunnan Province, indicating that the differences between these RRE sequences are minor and homologous. The greater the gene distance, the higher the degree of variation, indicating the earlier the appearance of this subtype and the longer the prevalence. The RRE sequences of subtype B in China and those of the United States have a large in group gene dispersion rate and low homology, and there is a significant difference in the gene dispersion rate between the two subtypes, suggesting that the RRE sequences of subtype B in China were significantly different from those of the United States, with obvious subtype specificity.

Some studies have suggested a potential link between Rev-RRE function and the pathogenesis of HIV-1. Early studies on the function of Rev-RRE mainly focused on the Rev protein. With an in-depth understanding of the function of Rev-RRE, people gradually realize that the sequence characteristics of RRE have a considerably greater impact on the activity of Rev-RRE than Rev (Sloan et al., 2013), which is also confirmed in this study. Clinical studies have confirmed that RRE with different activities can evolve over time (Phuphuakrat and Auewarakul, 2003). It has also been observed in long-term cohort studies that the rate of CD4 + T cell depletion is related to the activity of RRE in advanced diseases (Phuphuakrat and Auewarakul, 2005). Therefore, the evolution of RRE may be an essential regulatory factor for HIV-1 pathogenesis and disease progression.

This study also provides additional support for the hypothesis that the Rev-RRE regulatory axis plays an influential role in the pathogenesis of HIV-1. Early on, a cohort study proved that the diversity between RRE sequences of the same subtype has a significant impact on the functional

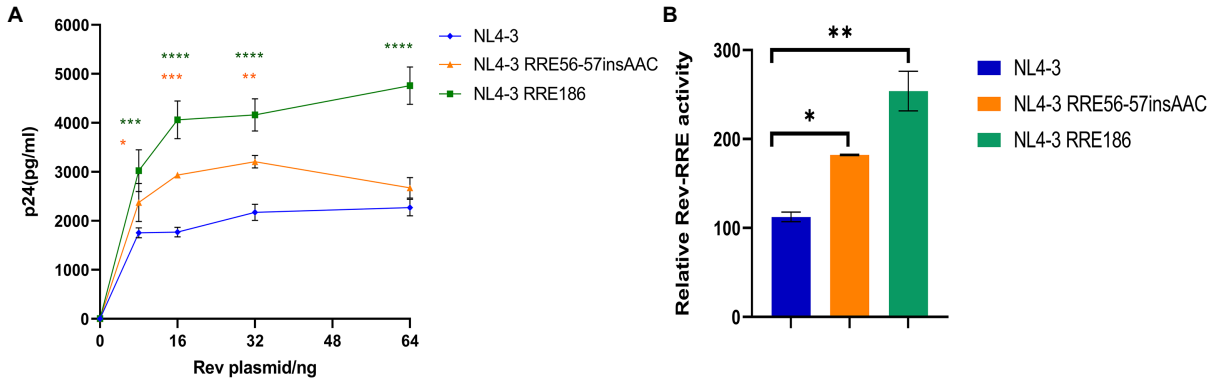

FIGURE 7
Relative function of NL4-3 and mutant RREs. **(A)** Gag/Pol reporter assay and variation of the concentration of p24 expressed by the reporter gene with the change of the concentration of the Rev expressing plasmid when NL4-3 and each mutant RRE were combined with NL4-3-Rev. **(B)** The relative activity of Rev-RRE when NL4-3 and each mutant RRE is combined with NL4-3-Rev. Each experiment was repeated twice, and bars show the standard error of the mean from two replicates. *p<0.05, **p<0.01, ***p<0.001, and ****p<0.0001, compared to NL4-3.

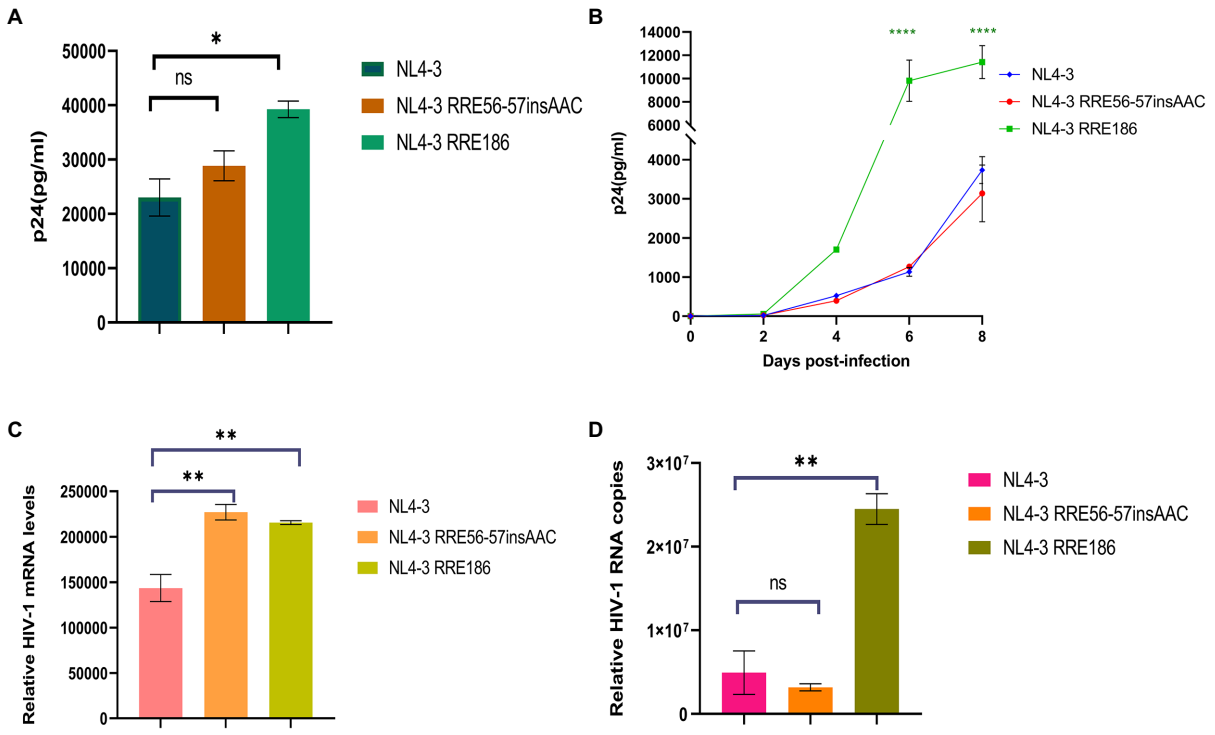

FIGURE 8
Relative viral replication levels of NL4-3 strain and mutant RREs. **(A)** The replication level of the HIV-1 virus after NL4-3 and mutant RREs plasmid transfection into 293T cells. **(B)** The replication level of the corresponding virulent strain in MT2 cells. **(C)** The mRNA transcript levels in intracellular. **(D)** The viral RNA copies in cell culture supernatant. Each experiment was repeated twice, and bars show the standard error of the mean from two replicates. *p<0.05, **p<0.01, ***p<0.001, and ****p<0.0001, compared to NL4-3.

activity of Rev-RRE and the pathogenicity of the virus (Phuphuakrat and Auewarakul, 2005). Subsequently, studies have confirmed that the shift of a single base on RRE can also significantly alter the functional activity of Rev-RRE and the formation of related complexes (Sloan et al., 2013). The two RRE mutants we identified in this study are well worthy of our discussion. Mutation RRE-G186A was able to significantly increase not only the expression level of mRNA in intracellular

but also the functional activity of Rev-RRE and the replication ability of the virus, suggesting that this site may play a key role in the entire replication cycle of HIV-1 subtype B. Notably, mutation RRE-56-57insAAC was able to significantly increase the expression level of intracellular mRNA, as well as significantly increase the functional activity of Rev-RRE. However, there was no significant effect on the replication levels of the virus. These results suggest that this site may increase the transcription level of viral mRNA and enhance the ability of Rev-RRE-mediated mRNA translocation out of the nucleus, but fails to significantly affect the final replication of the virus, the mechanism behind which deserves further exploration. There are also limitations in this study, and further measurements of the relative amounts of nuclear and cytoplasmic RNA of different lengths would help to strengthen the analysis of the nuclear export capacity of each mutant RNA.

The RRE is a 4 or 5-SL structure that can influence the nature of the complex and regulate the rate of viral replication by changing conformation, and the 5-SL structure is more active in promoting viral replication than its 4-SL structure (Sherpa et al., 2015). Notably, limited nucleotide changes in the RRE have the potential to alter its RNA secondary structure and thus regulate the rate of viral replication. Sherpa et al. (2015) demonstrated that the secondary structure of the subtype B RRE at positions 163–221 of the nucleotide sequence composed of secondary structure is essential for the function of the Rev-RRE (Sherpa et al., 2015). In this study, we constructed RRE-G186A (site 186, G-to-A) that induced a 5-SL structure associated with increased activity, which significantly increased the functional activity of Rev-RRE and the replication efficiency of the virus. The data we obtained from this study support the idea that the ability of RRE to adopt different structural conformations that promote different replication activities may allow HIV-1 to modulate its replication rate under different conditions to better survive in the host environment. In addition, both RRE-56-57insAAC and RRE-G186A have some degree of increased Shannon entropy, suggesting that they are structurally dynamic, a feature that confers accessibility to protein-RNA interactions by acting as a landing pad for protein cofactors (Smola et al., 2016). This accessibility may contribute to Rev-RRE binding and subsequent multimerization, which leads to enhanced activity. This may explain why these two RRE mutants have higher Rev-RRE functional activity. While these studies suggest that alterations in RRE RNA conformation may lead to the formation of different Rev/RRE complexes and support different levels of functional activity, further structural studies will be required to understand in detail how 4-SL and 5-SL RREs contribute to different viral replication abilities.

In conclusion, limited nucleotide changes in the subtype B RRE circulating in China can significantly affect Rev-RRE activity and viral replication. Since Rev-RRE binding is a crucial step of viral replication, a clear understanding of RRE evolution will help to realize the possible role of this regulator in key aspects of the viral life cycle, which is also a promising target for drug development.

Data availability statement

Sequences have been uploaded to GenBank (accession numbers: OP512693-OP512763). All data reported in this paper will be shared by the lead contact on request, LL (dearwood@sina.com).

Ethics statement

The studies involving human participants were reviewed and approved by the ethics committees of the Beijing Institute of Microbiology and Epidemiology. The patients/participants provided their written informed consent to participate in this study.

Author contributions

LL and JJ designed the study; HL, YL, LJ, TL, and XW collected sample and the demographic data; BZha, ZhiL, CL, and ZheL performed nucleic acid extraction and amplification; YS, JH, and BZhu performed plasmid construction, functional activity experiments, replication kinetics experiments, qPCR and other experiments. YS, QL, and JL performed sequence analysis and statistical analysis; YS, JH, JJ, and LL participated in the writing process. All authors contributed to the article and approved the submitted version.

Funding

The study was supported by the National Natural Science Foundation of China (NSFC, 31900157 and 3180010279) and State Key Laboratory of Pathogen and Biosecurity (AMMS).

Acknowledgments

We thank Rekosh for the guidance of the construction of the Gag/Pol-RRE reporter gene system, participants, peer workers, and all those who helped during our experiments.

Conflict of interest

The authors declare that the research was conducted in the absence of any commercial or financial relationships that could be construed as a potential conflict of interest.

Publisher's note

References

Ball, S. C., Abraha, A., Collins, K. R., Marozsan, A. J., Baird, H., Quiñones-Mateu, M. E., et al. (2003). Comparing the ex vivo fitness of CCR5-tropic human immunodeficiency virus type 1 isolates of subtypes B and C. *J. Virol.* 77, 1021–1038. doi: 10.1128/jvi.77.2.1021-1038.2003

Barré-Sinoussi, F., Chermann, J. C., Rey, F., Nugeyre, M. T., Chamaret, S., Gruest, J., et al. (1983). Isolation of a T-lymphotropic retrovirus from a patient at risk for acquired immune deficiency syndrome (AIDS). *Science* 220, 868–871. doi: 10.1126/science.6189183

Booth, D. S., Cheng, Y., and Frankel, A. D. (2014). The export receptor Crm 1 forms a dimer to promote nuclear export of HIV RNA. *eLife* 3:e04121. doi: 10.7554/eLife.04121

Dai, Y., Peralta, A. N., Wynn, J. E., Sherpa, C., Li, H., Verma, A., et al. (2019). Molecular recognition of a branched peptide with HIV-1 rev response element (RRE) RNA. *Bioorg. Med. Chem.* 27, 1759–1765. doi: 10.1016/j.bmc.2019.03.016

Daly, T. J., Cook, K. S., Gray, G. S., Maione, T. E., and Rusche, J. R. (1989). Specific binding of HIV-1 recombinant rev protein to the rev-responsive element in vitro. *Nature* 342, 816–819. doi: 10.1038/342816a0

Fernandes, J., Jayaraman, B., and Frankel, A. (2012). The HIV-1 rev response element: an RNA scaffold that directs the cooperative assembly of a homo-oligomeric ribonucleoprotein complex. *RNA Biol.* 9, 6–11. doi: 10.4161/rna.9.1.18178

Frankel, A. D., and Young, J. A. (1998). HIV-1: fifteen proteins and an RNA. *Annu. Rev. Biochem.* 67, 1–25. doi: 10.1146/annurev.biochem.67.1.1

Gilbert, M. T., Rambaut, A., Wlasiuk, G., Spira, T. J., Pitchenik, A. E., and Worobey, M. (2007). The emergence of HIV/AIDS in the Americas and beyond. *Proc. Natl. Acad. Sci. U. S. A.* 104, 18566–18570. doi: 10.1073/pnas.0705329104

Hemelaar, J., Gouws, E., Ghys, P. D., and Osmanov, S. (2011). Global trends in molecular epidemiology of HIV-1 during 2000–2007. *AIDS* 25, 679–689. doi: 10.1097/QAD.0b013e328342ff93

Hurst, T., Pace, M., Katzourakis, A., Phillips, R., Klenerman, P., Frater, J., et al. (2016). Human endogenous retrovirus (HERV) expression is not induced by treatment with the histone deacetylase (HDAC) inhibitors in cellular models of HIV-1 latency. *Retrovirology* 13:10. doi: 10.1186/s12977-016-0242-4

Jackson, P. E. H., Dzhivhuho, G., Rekosh, D., and Hammarskjold, M. L. (2020). Sequence and functional variation in the HIV-1 rev regulatory Axis. *Curr. HIV Res.* 18, 85–98. doi: 10.2174/1570162x18666200106112842

Jackson, P. E., Tebit, D. M., Rekosh, D., and Hammarskjold, M. L. (2016). Rev-RRE functional activity differs substantially among primary HIV-1 isolates. *AIDS Res. Hum. Retrovir.* 32, 923–934. doi: 10.1089/aid.2016.0047

Jayaraman, B., Crosby, D. C., Homer, C., Ribeiro, I., Mavor, D., and Frankel, A. D. (2014). RNA-directed remodeling of the HIV-1 protein rev orchestrates assembly of the rev-rev response element complex. *eLife* 3:e04120. doi: 10.7554/eLife.04120

Jeang, K. T., Chang, Y., Berkhout, B., Hammarskjöld, M. L., and Rekosh, D. (1991). Regulation of HIV expression: mechanisms of action of tat and rev. *AIDS* 5, S3–S14.

Kearney, M., Maldarelli, F., Shao, W., Margolick, J. B., Daar, E. S., Mellors, J. W., et al. (2009). Human immunodeficiency virus type 1 population genetics and adaptation in newly infected individuals. *J. Virol.* 83, 2715–2727. doi: 10.1128/jvi.01960-08

Lefort, V., Longueville, J. E., and Gascuel, O. (2017). SMS: smart model selection in Phy ML. *Mol. Biol. Evol.* 34, 2422–2424. doi: 10.1093/molbev/msx149

Li, X., Guo, Y., Li, H., Huang, X., Pei, Z., Wang, X., et al. (2021). Infection by diverse HIV-1 subtypes leads to different elevations in HERV-K transcriptional levels in human T cell lines. *Front. Microbiol.* 12:662573. doi: 10.3389/fmicb.2021.662573

Malim, M. H., Tiley, L. S., McCarn, D. F., Rusche, J. R., Hauber, J., and Cullen, B. R. (1990). HIV-1 structural gene expression requires binding of the rev trans-activator to its RNA target sequence. *Cells* 60, 675–683. doi: 10.1016/0092-8674(90)90670-a

Palmer, S., Wiegand, A. P., Maldarelli, F., Bazmi, H., Mican, J. M., Polis, M., et al. (2003). New real-time reverse transcriptase-initiated PCR assay with single-copy sensitivity for human immunodeficiency virus type 1 RNA in plasma. *J. Clin. Microbiol.* 41, 4531–4536. doi: 10.1128/jcm.41.10.4531-4536.2003

Phuphuakrat, A., and Auewarakul, P. (2003). Heterogeneity of HIV-1 rev response element. *AIDS Res. Hum. Retrovir.* 19, 569–574. doi: 10.1089/088922203322230932

Phuphuakrat, A., and Auewarakul, P. (2005). Functional variability of rev response element in HIV-1 primary isolates. *Virus Genes* 30, 23–29. doi: 10.1007/s11262-004-4578-9

Pollard, V. W., and Malim, M. H. (1998). The HIV-1 rev protein. *Annu. Rev. Microbiol.* 52, 491–532. doi: 10.1146/annurev.micro.52.1.491

Rausch, J. W., and Le Grice, S. F. (2015). HIV rev assembly on the rev response element (RRE): a structural perspective. *Viruses* 7, 3053–3075. doi: 10.3390/v7062760

Sherpa, C., Jackson, P. E. H., Gray, L. R., Anastos, K., Le Grice, S. F. J., Hammarskjold, M. L., et al. (2019). Evolution of the HIV-1 rev response element during natural infection reveals nucleotide changes that correlate with altered structure and increased activity over time. *J. Virol.* 93:e02102-18. doi: 10.1128/jvi.02102-18

Sherpa, C., Rausch, J. W., Le Grice, S. F., Hammarskjold, M. L., and Rekosh, D. (2015). The HIV-1 rev response element (RRE) adopts alternative conformations that promote different rates of virus replication. *Nucleic Acids Res.* 43, 4676–4686. doi: 10.1093/nar/gkv313

Shuck-Lee, D., Chang, H., Sloan, E. A., Hammarskjold, M. L., and Rekosh, D. (2011). Single-nucleotide changes in the HIV rev-response element mediate resistance to compounds that inhibit rev function. *J. Virol.* 85, 3940–3949. doi: 10.1128/jvi.02683-10

Sloan, E. A., Kearney, M. F., Gray, L. R., Anastos, K., Daar, E. S., Margolick, J., et al. (2013). Limited nucleotide changes in the rev response element (RRE) during HIV-1 infection alter overall rev-RRE activity and rev multimerization. *J. Virol.* 87, 11173–11186. doi: 10.1128/jvi.01392-13

Smola, M. J., Christy, T. W., Inoue, K., Nicholson, C. O., Friedersdorf, M., Keene, J. D., et al. (2016). SHAPE reveals transcript-wide interactions, complex structural domains, and protein interactions across the Xist lncRNA in living cells. *Proc. Natl. Acad. Sci. U. S. A.* 113, 10322–10327. doi: 10.1073/pnas.1600008113

Taniguchi, I., Mabuchi, N., and Ohno, M. (2014). HIV-1 rev protein specifies the viral RNA export pathway by suppressing TAP/NXF1 recruitment. *Nucleic Acids Res.* 42, 6645–6658. doi: 10.1093/nar/gku304

Watts, J. M., Dang, K. K., Gorelick, R. J., Leonard, C. W., Bess, J. W. Jr., Swanstrom, R., et al. (2009). Architecture and secondary structure of an entire HIV-1 RNA genome. *Nature* 460, 711–716. doi: 10.1038/nature08237

Wilkinson, K. A., Gorelick, R. J., Vasa, S. M., Guex, N., Rein, A., Mathews, D. H., et al. (2008). High-throughput SHAPE analysis reveals structures in HIV-1 genomic RNA strongly conserved across distinct biological states. *PLoS Biol.* 6:e96. doi: 10.1371/journal.pbio.0060096

Wynn, J. E., Zhang, W., Tebit, D. M., Gray, L. R., Hammarskjold, M. L., Rekosh, D., et al. (2016). Characterization and in vitro activity of a branched peptide boronic acid that interacts with HIV-1 RRE RNA. *Bioorg. Med. Chem.* 24, 3947–3952. doi: 10.1016/j.bmc.2016.04.009

Xu, H. T., Colby-Germinario, S. P., Asahchop, E. L., Oliveira, M., McCallum, M., Schader, S. M., et al. (2013). Effect of mutations at position E138 in HIV-1 reverse transcriptase and their interactions with the M184I mutation on defining patterns of resistance to nonnucleoside reverse transcriptase inhibitors rilpivirine and etravirine. *Antimicrob. Agents Chemother.* 57, 3100–3109. doi: 10.1128/aac.00348-13

frontiers | Frontiers in Microbiology

TYPE Original Research
PUBLISHED 27 January 2023
DOI 10.3389/fmicb.2023.1033448

OPEN ACCESS

EDITED BY
Francois Villinger,
University of Louisiana at Lafayette,
United States

REVIEWED BY
Guochun Jiang,
University of North Carolina at Chapel Hill,
United States
Lingjie Liao,
Chinese Center for Disease Control and Prevention, China

*CORRESPONDENCE
Xuebin Liao
✉ liaoxuebin@mail.tsinghua.edu.cn
Linqi Zhang
✉ zhanglinqi@tsinghua.edu.cn

†These authors have contributed equally to this work

SPECIALTY SECTION
This article was submitted to Virology, a section of the journal Frontiers in Microbiology

RECEIVED 31 August 2022
ACCEPTED 12 January 2023
PUBLISHED 27 January 2023

CITATION
Li Y, Wang Z, Hou Y, Liu X, Hong J, Shi X, Huang X, Zhang T, Liao X and Zhang L (2023) Novel TLR7/8 agonists promote activation of HIV-1 latent reservoirs and human T and NK cells.
Front. Microbiol. 14:1033448.
doi: 10.3389/fmicb.2023.1033448

Novel TLR7/8 agonists promote activation of HIV-1 latent reservoirs and human T and NK cells

Yangyang Li[1†], Zhisong Wang[2†], Ying Hou[1], Xiaoyu Liu[1], Junxian Hong[1], Xuanling Shi[1], Xiaojie Huang[3], Tong Zhang[3], Xuebin Liao[2*] and Linqi Zhang[1*]

[1]Department of Basic Medical Sciences, School of Medicine, NexVac Research Center, Comprehensive AIDS Research Center, Tsinghua University, Beijing, China, [2]Key Laboratory of Bioorganic Phosphorus Chemistry and Chemical Biology of Ministry of Education, School of Pharmaceutical Sciences, Tsinghua University, Beijing, China, [3]Center for Infectious Diseases, Beijing Youan Hospital, Capital Medical University, Beijing, China

Antiretroviral therapy can successfully suppress HIV-1 replication to undetectable levels but fails to eliminate latent and persistent HIV-1 reservoirs. Recent studies have focused on the immunomodulatory agents such as Toll-like receptor 7 and 8 (TLR7 and TLR8) capable of activating, thereby rendering the reservoir susceptible to antiretroviral inhibition and immune recognition and elimination. In this context, this study focused on generating a diverse repertoire of TLR7/8 agonists to identify more potent candidates for activating latent HIV-1 and immune cells' response. Through combinational strategies of computer-aided design and biological characterization, 159 pyrido [3,2-d] pyrimidine and pyridine-2-amine-based derivatives were synthesized. Of which, two TLR7/8 dual and one TLR8-specific agonists with exceptionally high potency in activating HIV-1 latent reservoirs in cell lines and PBMCs of patients with persistent and durable virologic controls were identified. Particularly, these agonists appeared to enhance NK and T cells activity, which were correlated with the degree of surface activation markers. The outcome of this study highlights the remarkable potential of TLR7/8 agonists in simultaneously activating HIV-1 from the latently infected cells and augmenting immune effector cells.

KEYWORDS

HIV-1, latent reservoir, TLR7 and TLR8 agonists, TNF-α, T cells, NK cells

Introduction

In the past 40 years, the acquired immunodeficiency syndrome (AIDS) caused by human immunodeficiency virus type 1 (HIV-1) has become one of the most deadly infectious diseases in the world, posing a huge threat to global health (Ghosn et al., 2018). Although highly active antiretroviral therapy (HAART) can achieve sustained suppression and reduce transmission of HIV-1, it requires lifelong treatment and fails to cure the patients completely (Finzi et al., 1999; Zhang et al., 1999). The major barrier lies in the existence of a latent virus reservoir that contains replication-competent but transcriptionally dormant HIV DNA proviruses (Finzi et al., 1997; Wong et al., 1997; Bachmann et al., 2019). However, once the HAART is interrupted, the latent proviruses become activated and viral RNA is produced in the plasma up to the pre-treatment levels. Long-lived resting memory CD4+ T cells are the best-characterized cell type harboring the latent HIV-1, although monocytes and macrophages also contribute to the latent pool (Delobel et al., 2005; Gibellini et al., 2008; Clayton et al., 2017; Kruize and Kootstra, 2019). So far, cellular markers specific

for the latently infected cells have not been identified, rendering the cure strategy extremely challenging.

One of the most well-explored strategies to eliminate the latent reservoir is to employ latency-reversing agents (LRAs) to activate, thereby rendering them susceptible to recognition and clearance by immune cells such as NK cells and cytotoxic CD8+ T cells. The LRAs under active investigation include histone deacetylase inhibitors (HDACi), histone methyltransferase inhibitors, bromodomain extra-terminal inhibitors (BETi), protein kinase C (PKC) agonists, as well as cytokines and TLR agonists (Kim et al., 2018). Multiple HDACi, such as vorinostat, romidepsin, and panobinostat, demonstrate capability in activating latency through epigenetic modification of HIV-1 LTR. Their impact in the clinical setting, however, was rather disappointing. While a significant increase in a cell-associated unsliced HIV RNA was noticed, no statistical increase of HIV-1 RNA in plasma and reduction of total HIV DNA was detected in any of the reported studies (Elliott et al., 2014; Rasmussen et al., 2014; McMahon et al., 2020).

Recent studies have focused intensively on the immunomodulatory LRAs, including Toll-like receptor (TLR) agonists, immune-checkpoint inhibitors, and cytokines. These novel LRAs possess the advantage of activating latent reservoirs and enhancing immune cell activity (Del Prete et al., 2019; Harper et al., 2020; McBrien et al., 2020). TLRs are a family of pattern recognition receptors (PRRs) involved in sensing the pathogen-associated molecular patterns by the innate immune system during early infection (Aderem and Ulevitch, 2000; Takeuchi and Akira, 2010). A total of 10 functional TLRs have so far been identified in humans, in which TLR3, TLR7, TLR8, and TLR9 are expressed on the intracellular endosomal membrane and are commonly involved in recognizing nucleic acids (Kanzler et al., 2007; Kawai and Akira, 2010; Fitzgerald and Kagan, 2020). TLR7 and TLR8 have a similar dimer structure but distribute differently on diverse cells. While TLR7 is largely distributed in the plasmacytoid dendritic cells (pDCs) and B cells, TLR8 exists in the monocytes, macrophages, and myeloid dendritic cells (mDCs) (Ito et al., 2002). Activation of TLR7 and TLR8 recruit MyD88, but TLR7 predominantly activates downstream signaling through IRF7 to induce anti-viral type 1 interferon, whereas TLR8, through transcription factor NF-κB, induces the proinflammatory cytokines (Beignon et al., 2005; Kawai and Akira, 2010). Several TLR7/8 agonists have been characterized to reverse HIV-1 latency *in vitro* and *in vivo*. For instance, GS9620 is a potent TLR7-specific agonist synthesized by Gilead Sciences and is in progress in phase 2 clinical trials. GS9620 induced transient viremia and reduced the latent reservoirs in SIV-infected rhesus macaques on ART (Lim et al., 2018). GS9620 combined with HIV-1 broadly-neutralizing antibody (bNAb) PGT121 delayed viral rebound in SHIV-infected monkeys when ART was interrupted (Borducchi et al., 2018). The results of phase 1b illustrate some decrease of intact proviral DNA in patients treated with oral GS9620, and the viral rebound time increased from 4.1 to 5.1 weeks compared with the placebo group (SenGupta et al., 2021). Similarly, a few TLR8 agonists have also been found to activate HIV-1 latency in CD4+ T cell line J-Lat and human peripheral mononuclear cells (Schlaepfer and Speck, 2011; Rochat et al., 2017). More importantly, TLR7/8 agonists enhanced NK and T cells mediated killing, making this class of LRAs promising candidates for achieving a functional cure for HIV-1 infection (Hart et al., 2005).

Capitalizing on the progress made in TLR7/8 as LRAs, this study aims to expand and identify more potent TLR7/8 agonists in activating the HIV-1 reservoir and enhancing cellular immunity against HIV-1 latency. Using combination approaches in computer-aided design and biological characterization, 159 pyrido [3,2-d] pyrimidine and pyridine-2-amine-based derivatives were synthesized. We identified two TLR7/8 dual (D018 and C142) and one TLR8-specific (B-130a) agonists with exceptionally high potency in activating HIV-1 latent reservoirs in cell lines and PBMCs of patients with persistent and durable virologic controls. Moreover, these agonists appear to induce immune effector cell activation, such as NK cells and T cells. Collectively, the results of this study illustrate the promising role of TLR7/8 agonists as potential LRAs in simultaneously increasing HIV-1 expression from the latently infected cells as well as augmenting immune cells' response.

Results

Design and characterization of novel TLR7/8 dual and TLR8-specific agonists

Based on the extensive analysis of the reported crystal structure of TLR7 and TLR8 and the structure–activity relationship (SAR) of the associated small molecule agonists (Tanji et al., 2013; Zhang et al., 2016), a total of 160 compounds were designed, synthesized and characterized to obtain novel and more potent TLR7/8 dual and TLR8-specific agonists, as shown in the flow chart (Figure 1A). Starting with the lead compound, 76 pyrido [3,2-d] pyrimidine derivatives were synthesized and optimized through structural modification from the deep hydrophobic region to the solvent-exposed region. Seventy-six compounds were evaluated for their *in vitro* activity using HEK-Blue hTLR7 or hTLR8 reporter cells, stably expressing the human TLR7 or TLR8 and an NF-κB/AP1-inducible SEAP (secreted embryonic alkaline phosphatase reporter gene). We identified six compounds, D018, C008, 199–1, WA86, C142, and C163, that could induce substantial levels of SEAP in the culture supernatant of both HEK-Blue hTLR7 and hTLR8 cells and therefore classified as TLR7/8 dual agonists. D018 and C142 exhibited the most potent agonistic activity, while the remaining four were rather varied but invariably stronger than the relevant control R848 except C163 (Figures 1B–D). To our knowledge, these molecules are the most potent TLR7/8 dual agonists reported so far.

Following this, using D018, 83 additional pyridine-2-amine-based derivatives were designed and synthesized to achieve high selectivity for TLR8 using the scaffold hopping strategy. By evaluating these compounds using the same *in vitro* activity, two candidate compounds, B-130a and B130b were identified, demonstrating high selectivity for TLR8 over TLR7. The agonistic activity toward TLR8 was 55.22 nM and 67.24 nM, respectively, for B-130a and B130b, while that toward TLR7 was all above 10,000 nM (Figures 1B–D). An attempt was made further to improve TLR8 activity and specificity by generating a series of D018-B-130a hybrids. However, only one compound, WA175, showed moderate activity with an EC50 of 196.7 nM. Nevertheless, two TLR-8-specific compounds, B-130a and B130b, were superior to the control VTX-2337 (Figures 1B–D).

The physicochemical properties of these novel TLR7/8 dual and TLR8-specific agonists were also evaluated through ACD/Percepta platform and Molinspiration software. As shown in Figure 1D, all these compounds demonstrate moderate basicity (cpKa >7.0), consistent with our intended design and SAR analysis, where introducing a basic group was associated with enhancing agonistic activity. Moreover, all these compounds except B-130b and WA175 had acceptable lipophilicity (cLogP) less than 5, obeying Lipinski's rule of five (Figure 1D). Then, the three most potent agonists, two TLR7/8 dual compounds, D018(TLR7/8)

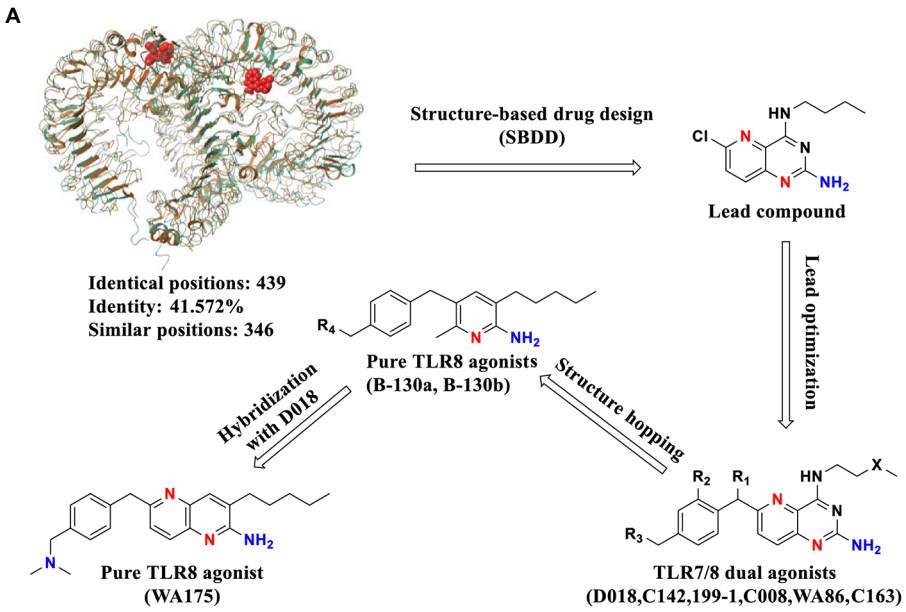

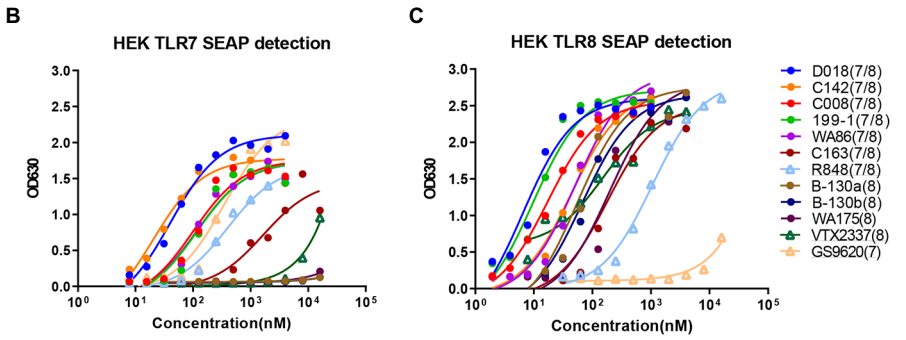

D

Category	Compound	R^1	R^2	R^3	R^4	X	MW	cpKa	cLogP	hTLR7 EC_{50} (nM)	hTLR8 EC_{50} (nM)
Lead	LB06	-	-	-	-	-	-	7.2	4.23	2600	2000
Dual TLR7/8	D018	H	H		-	CH	364	8.5	3.70	40.19	6.457
	C142	H	OMe		-	CH	394	8.5	3.68	20.04	44.06
	C008	H	H		-	CH	390	9.0	4.10	100.8	17.28
	199-1	-	-		-	O	366	8.5	2.24	117.4	9.694
	WA86	H	H		-	CH	406	7.3	3.54	117.8	50.99
	C163	Me	H		-	CH	378	8.5	3.45	1654.00	178.4
	R848	-	-	-	-	-	314	-	-	399.6	1062
TLR8	B-130a	-	-	-		-	325	8.8	4.97	>10000	55.22
	B-130b	-	-	-		-	351	9.7	5.38	>10000	67.24
	WA175	-	-	-	-	-	362	8.0	5.3	>10000	196.7
	VTX-2337	-	-	-	-	-	458	-	-	>10000	150.8
TLR7	GS9620	-	-	-	-	-	410	-	-	352.7	>10000

FIGURE 1
Design, synthesis, and evaluation of novel TLR7/8 agonists through HEK-Blue cell lines expressing either hTLR7 or hTLR8 receptor. **(A)** The design flowchart and chemical structures of novel TLR7/8 agonists with single TLR8 or dual TLR7/8 agonistic activity. Superimposition of MmTLR7-R848 cocrystal (5GMH, brown) and hTLR8-R848 cocrystal (3W3N, bottle green) was performed by Maestro software (v9.1). **(B,C)** Activity evaluation of TLR7/8 agonists through HEK-Blue cell lines expressing either hTLR7 **(B)** or hTLR8 **(C)** receptor, measured by the secreted embryonic alkaline phosphatase (SEAP) in the culture supernatant. Commercially available GS9620 (TLR7 agonist), VTX-2337 (TLR8 agonist), and R848 (TLR7/8 dual agonist) labeled unfilled triangle are reference compounds. **(D)** TLR7/8 agonists were divided into 4 categories, exhibiting the molecular structure (R1,R2,R3,R4,X refer to the functional group in **A**), molecular weight (MW), cpKa, cLogP, as well as EC50 values for hTLR7 and hTLR8. Commercially available GS9620 (TLR7 agonist), VTX-2337 (TLR8 agonist), and R848 (TLR7/8 dual agonist) labeled as underlined are reference compounds.

and C142(TLR7/8) and one TLR8-specific compound, B-130a (TLR8), were selected to analyze their potential in activating HIV-1 latent reservoirs and compared with the commercially available agonists R848 (TLR7/8), VTX-2337 (TLR8), and GS9620 (TLR7) (Supplementary Figure S1).

TLR7/8 agonists activated latent HIV-1 and induced inflammatory cytokines from PBMCs of well-suppressed patients

To study the potential of novel TLR7/8 in activating latent HIV-1 reservoir, TLR7/8 dual agonists D018 and C142 and TLR8-specific agonist B-130a were mixed with PBMCs from six well-suppressed patients whose viral load in the plasma was less than 50 copies/ml, and CD4 counts were more than 350 cells/ml for more than 6 years. After incubation at 37°C for 96 h, the supernatant was collected and analyzed for HIV-1 RNA copies and compared with those stimulated by commercially available agonists, TLR7/8 dual agonist R848, TLR8 specific agonist VTX-2337, and TLR7 specific agonist GS9620, as well as the positive control phorbol myristate acetate (PMA) plus ionomycin and the negative control DMSO was used as a solvent for these agents. As shown in Figure 2A, dual TLR7/8 agonists D018 and C142 and TLR8 specific agonist B-130a activated detectable levels of HIV-1 RNA copies in the supernatant. D018 was the most potent, followed by C142 and then B-130a. The commercially available R848, VTX-2337, and GS9620 showed similar potency as B-130a but substantially lower than D018 and C142. The positive control PMA combined with ionomycin stimulated the highest levels of HIV-1 RNA copies in the supernatant, while the solvent DMSO was the lowest (Figure 2A).

Then, a total of 13 human inflammatory cytokines and chemokines (IL-1β, IFN-α2, IFN-γ, TNF-α, CCL2, IL-6, CXCL8, IL-10, IL-12p70, IL-17A, IL-18, IL-23, and IL-33) were measured in the culture supernatant 48 h after stimulation and compared with two healthy donors. Only 8 out of 13 became detectable and largely fell into the proinflammatory cytokines (IL-1β, IL-6, IL-18, IL-23, and TNF-α), Th1-and Th2-type cytokines (IL-10 and IFN-γ), and type I (IFN-α2) and type II (IFN-γ) interferons (Figures 2B–I). TLR7/8 dual agonists D018 and C142 demonstrated similar potency in triggering the release of these cytokines and were either equivalent (IL-6, IL-10, IL-23, and IFN-γ) or higher (IL-1β, IL-18, and TNF-α) than the commercially available R848. TLR8-specific B-130a and commercially available VTX-2337 exhibited comparable potency but were invariably higher than TLR7-specific GS9620 and negative control DSMO. Compared to DSMO, positive control PMA/ionomycin showed a substantially stronger impact on IFN-γ and TNF-α. At the same time, the differences for the remaining cytokines were minimal, suggesting that DMSO solvent alone could also trigger some release of these cytokines (Figures 2B–I). Interestingly, while no substantial differences were found for most of the cytokines tested, a clear trend of higher levels of IFN-α2 and IFN-γ in healthy individuals than in the HIV-1 infected indicates distinct differences in host innate immune responses between the two groups of individuals toward the tested agonists. These results imply that novel TLR7/8 dual agonists D018 and C142 and TLR8-specific agonist B-130a could activate HIV-1 latent reservoir and cytokine release in a higher capacity than the commercially available R848 and VTX-2337 counterparts.

TLR7/8 agonists activate latent HIV-1 in the U1 monocytic cell lines through the TLR8 pathway

HIV-1 latently infected cell line U1 was used further to study the potential activation mechanism by TLR7/8 agonists. U1 was a promonocyte cell line generated by chronic infection with HIV-1 into U937. A serial dilution of D018, C142, and B-130a agonists and commercially available R848, VTX-2337, and GS9620 were mixed with U1 and monitored for production of HIV-1 antigen p24 in the supernatant by ELISA. As shown in Figure 3A, D018 was the most potent in stimulating p24 production with an EC50 of 70 nM, followed by C142 and then B-130a. Commercially available VTX-2337 and R848 also induced p24 production, albeit at lower efficiency. GS9620, however, failed to trigger detectable levels of p24 even at the highest concentration of 16 μM (Figure 3A).

To gain deeper insight into the mechanisms of activating HIV-1 latency by TLR7/8 agonists, a series of knockdown experiments were conducted in the U1 cell line using a short hairpin RNA (shRNA) lentivirus technology. As GS9620 failed to activate p24 production (Figure 3A), the TLR8 pathway is largely believed to mediate the agonistic effect of TLR7/8. Hence, TLR8-knockdown, MyD88-knockdown, and sham-knockdown U1 cell lines were generated using shRNA lentiviruses, and the silencing effect was verified by qPCR (Supplementary Figures S2A,B) and western-blot analysis (Supplementary Figure S2C). When exposed to D018, B-130a, and GS9620 at a final concentration of 1 μM, knockdown of TLR8 or MyD88 expression essentially abolished the p24 production compared to the sham-knockdown U1 cell line (Figures 3B,C). As shown above, GS9620 could not induce detectable levels of p24 in the supernatant of sham-knockdown or original U1 cell lines. The expression levels of downstream molecules nuclear p65 and phosphorylated p65-s536 in the original U1 cells were further measured through western-blot, as earlier studies indicated that the activation of TLR8 ultimately led to the NF-κB signaling to regulate the expression of a broad range of genes including cytokines (Gringhuis et al., 2010). After incubation at 37°C for 30 min, the U1 cells stimulated by D018 and B-130a exhibited a significant increase in nuclear phos-p65-S536, while that stimulated by GS9620 was similar to the negative control DMSO (Supplementary Figure S2D). These results confirmed the hypothesis that activating latent HIV-1 in the U1 cell line by the novel TLR7/8 agonists were mediated through TLR8 and downstream MyD88 and ultimately regulated through NF-κB signaling.

TLR7/8 agonist effect is mediated through soluble TNF-α in the J-LAT T cell lines

J-LAT is a Jurkat-based CD4 T cell line with an integrated latent HIV-1 provirus in which GFP replaces the nef coding sequence, and the env is non-functional due to a frameshift (Jordan et al., 2003). All the testing agonists failed to induce detectable GFP-positive J-LAT cells through direct stimulation (Supplementary Figure S3A). In contrast, when J-LAT cells were incubated with the supernatant from healthy donor PBMCs stimulated with the testing agonists for 48 h, a substantial proportion of GFP-positive cells became detectable dose-dependently (Figure 4A). Supernatant from D018-stimulated PBMCs was the most potent in activating GFP-positive cells, followed by C142 and B-130a. VTX-2337 demonstrated similar potency to B-130a but was substantially stronger than R848. GS9620 stimulated supernatant did not show any detectable effect on activating GFP expression in J-LAT cells, even at the

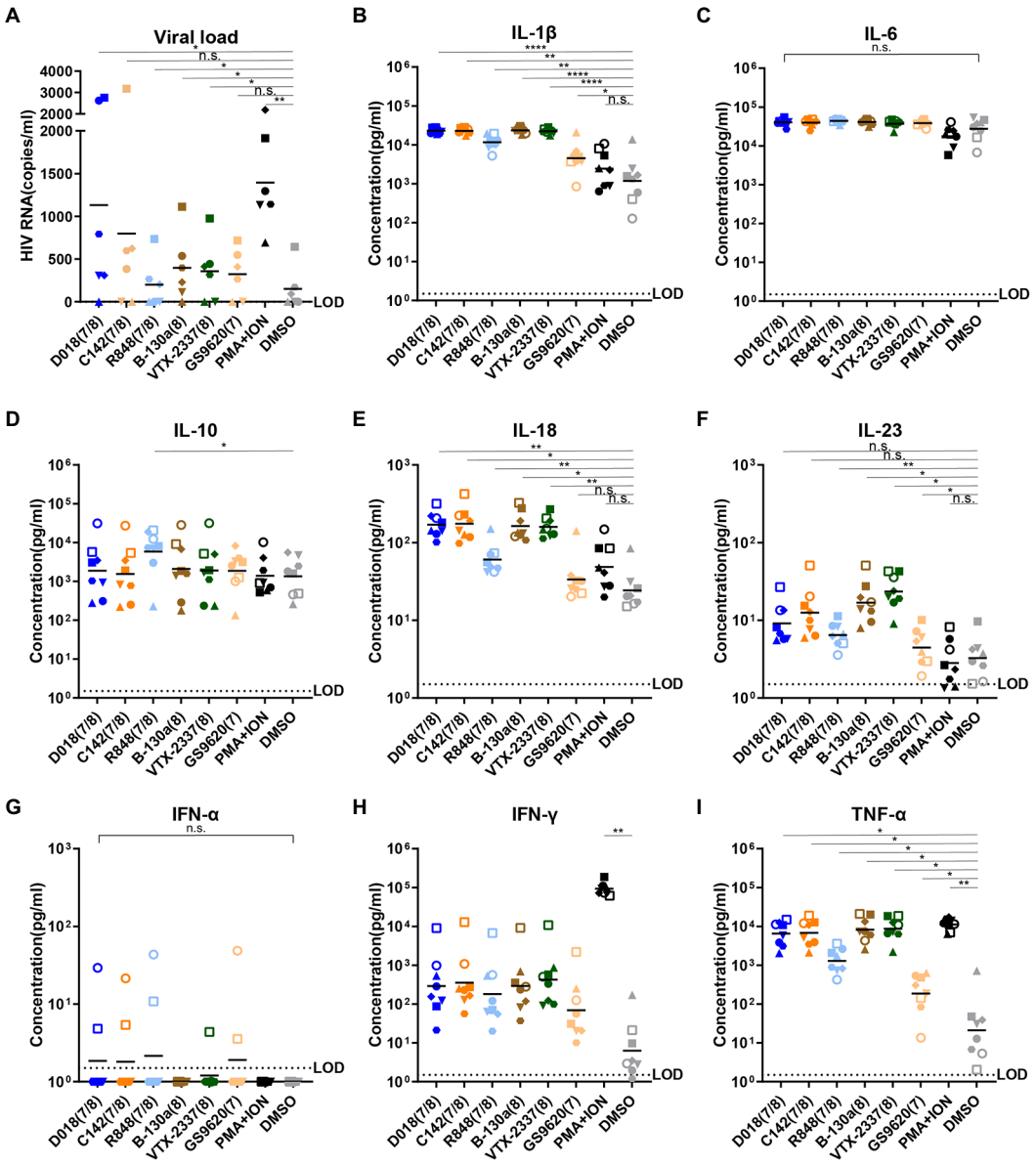

FIGURE 2
TLR7/8 agonists activate latent HIV-1 and inflammatory cytokines from PBMCs of infected individuals. **(A)** HIV-1 RNA copies in the supernatant were measured by RT-qPCR 4 days after stimulation (n =6). **(B–I)** Concentrations of inflammatory cytokines in the culture supernatant 2 days after stimulation by TLR7/8 agonists, including IL-1β **(B)**, IL-6 **(C)**, IL-10 **(D)**, IL-18 **(E)**, IL-23 **(F)**, IFN-α **(G)**, IFN-γ **(H)**, and TNF-α **(I)**. DMSO was negative control whereas PMA plus Ionomycin were positive control. PBMC from each HIV-1 infected patient (n =6) with different shape was filled and PBMC from each normal control (n = 2) with different shape was an open symbol. Data are shown as the mean of two replicates for each donor. Statistical difference between various TLR7/8 agonists and DMSO group analyzed by paired-t-test. ****p <0.0001, ***p <0.001, **p <0.01, *p <0.05, n.s. not significant.

highest concentration of 16 μM. These results indicate that our novel agonists can activate latent HIV-1 in J-LAT T cells, but only indirectly through some soluble molecules in the supernatant of stimulated PBMCs.

Previous experiments demonstrated that the activation of HIV-1 from J-LAT cells was mediated through soluble TNF-α released by the monocyte-derived dendritic cells (MDDCs) (Schlaepfer and Speck, 2011). TLR7/8 dual agonists and TLR8 specific agonists could induce PBMC to express high levels of TNF-α, while TLR7 specific agonist only could induce low levels of TNF-α but high IFN-α (Supplementary Figures 3B,C). Then, J-LAT cells were stimulated with different dilutions of soluble TNF-α and IFN-α. Only TNF-α could activate GFP expression in J-Lat cells in a concentration gradient, while IFN-α failed to activate J-LAT cells even at 10 ng/ml (Supplementary Figure S3D). Therefore, we focused on this possibility to explore the mechanism of activation of latent HIV-1 of our novel TLR7/8 agonists. We sorted CD14+ monocytes from the PBMC of a healthy individual and differentiated them into MDDCs through stimulation with GM-CSF and IL-4. The expression of hTLR7 and hTLR8 was more than 10-fold higher in MDDCs than in the J-LAT cells by qPCR (Supplementary Figure S3E). A serial number of differentiated MDDCs were co-cultured with J-Lat cells in the presence of TLR7/8 agonists at 1 μM for 48 h. As shown in Figure 4B, when D018 and B-130a were added into the co-culture, a marked increase in the percentage of GFP+ J-LAT cells and a concomitant increase in the soluble concentration of TNF-α were observed. In co-cultures with GS9620 or the negative control DMSO, no detectable levels of GFP+ J-LAT cells or soluble TNF-α were found. Furthermore, neutralizing TNF-α with antibodies resulted in a

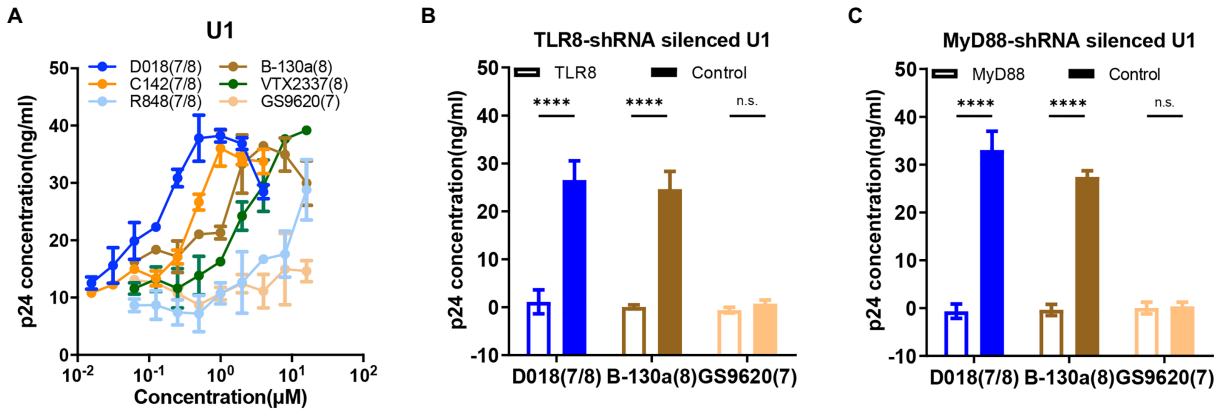

FIGURE 3
TLR7/8 agonists directly activate latent HIV-1 from monocytic U1 cell line. **(A)** Dose–response curves for HIV-1 activation in U1 cell line by the selected novel and control TLR7/8 agonists. Data are shown as mean±SD (n =4). **(B,C)** The p24 concentration in the supernatant of U1 cell line stimulated by D018 (TLR7/8), B-130a (TLR8), or GS9620 (TLR8) before and after **(B)** TLR8-shRNA silencing or **(C)** MyD88-shRNA silencing compared with control shRNA silencing. Data are shown as mean±SD (n =4). Statistical difference between various TLR7/8 agonists was analyzed by two-way ANOVA. ****p <0.0001, ***p <0.001, **p <0.01, *p <0.05, n.s. not significant.

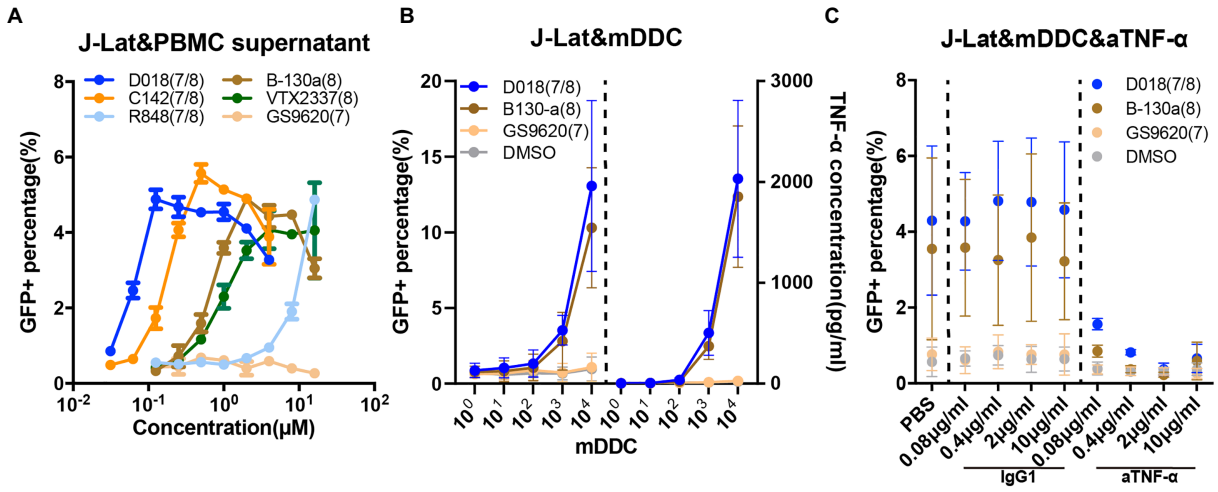

FIGURE 4
TLR7/8 agonists indirectly activate latent HIV-1 from the J-Lat CD4 T cell line through TNF-α. **(A)** Dose–response curves for HIV-1 activation in J-Lat CD4 T cell line by the selected novel and control TLR7/8 agonists. The GFP+ percentage indicated the proportion of J-Lat activated. Data are shown as mean±SD of 2 independent experiments). **(B)** Dose–response curves for HIV-1 activation and TNF-α release in the J-Lat and mDDC co-culture system 48h after stimulation by D018, B130-a, GS9620, and DMSO. Data are shown as mean±SD (n =4). **(C)** Dose–response curves for HIV-1 activation of J-Lat CD4 T cells with varying concentrations of anti-TNF-α monoclonal antibody compared with that of irrelevant IgG1 antibody control, 48h after stimulation by D018, B130-a, GS9620, and DMSO. The GFP+ percentage indicated the proportion of J-Lat activated. Data are shown as mean±SD (n =4).

dose-dependent decrease in GFP+ J-LAT cells, while an irrelevant IgG1 antibody exhibited a minimal effect (Figure 4C). This is consistent with previous reports and confirmed our hypothesis that soluble TNF-α released by the MDDCs largely mediated the activation of latent HIV-1 by TLR7/8 agonists in J-LAT cells. In other words, the activation of TLR7/8 agonists on latent HIV-1 was indirect in the J-LAT cell line, while U1 was direct through the TLR8 pathway.

TLR7/8 agonists activate latently infected PBMCs indirectly through soluble TNF-α

The mechanism of TLR7/8 agonist activation of the latent reservoir in PBMCs derived from HIV-1 chronically infected patients was further investigated. It has been reported that most of the latently infected cell types are resting memory CD4 T cells, with a very small proportion of monocytes and dendritic cells (Finzi et al., 1999; Gibellini et al., 2008). Previous results in HIV-1 latently infected cell lines showed that TLR7/8 agonists alone could not directly stimulate latently infected CD4 T cell lines (Supplementary Figure S3A).

CD4 T cells derived from HIV-1 well-suppressed patients were then stimulated with D018, B-130a, GS9620, positive control PMA + ION, and negative control DMSO. Supplementary Figures S4A,B show that the positive control significantly stimulated the transcriptional expression of HIV-1 RNA copies in the supernatant and p24 in CD4 T compared to the negative control DMSO. However, none of the three TLR7/8 agonists detected the ability to activate HIV-1 latently infected CD4 T cells.

TLR7/8 agonists activated PBMCs from seven well-suppressed patients with the addition of anti-TNF-α monoclonal antibody or IgG1-control monoclonal antibody, respectively. D018, B-130a, and the positive control PMA + ION increased the levels of HIV-1 RNA copies in the supernatant and the concentration of TNF-α concomitantly. In co-cultures with GS9620 or the negative control DMSO, low detectable levels of HIV-1 RNA copies or soluble TNF-α were found. Furthermore, neutralizing TNF-α with antibodies significantly blocked the activity of latent HIV-1 by TLR7/8 agonists, which is consistent with the results of TLR7/8 agonists activating latently infected cell lines. These results confirmed that TNF-α plays a critical role in the indirect stimulation of HIV-1 latently infected PBMC by TLR7/8 agonists (Figures 5A,B).

TLR7/8 agonists preferentially activate NK and T cells

TLR family is essential in connecting innate immunity with acquired immunity in fighting against infection. It was then studied whether the identified TLR7/8 agonists could activate cell populations within PBMC, thereby potentiating their effector functions. PBMCs from healthy donors were stimulated by TLR7/8 agonists for 24 h and analyzed for several activation markers by flow cytometry. The representative diagram of the gating strategy for each immune cell is shown in Supplementary Figure S5. All tested TLR7/8 agonists activated CD69 and NKG2D expression on $CD56^{bright}$ and $CD56^{dim}$ NK cells (Figures 6A–D), as well as CD69 and CD25 expression on CD4+ and CD8+ T cells (Figures 6E–H). However, they failed to have the detectable effect of CD40 and HLA-DR expression on monocytes and CD80 and CD86 expression dendritic cells (Figures 6I–L). In almost all instances, the dual TLR7/8 agonist D018 was the most potent, followed by C142, while the B-130a and other commercially available agonist controls were relatively weaker. These results signify that the dual TLR7/8 agonists D018 and C142 can induce the expression of various activation markers for NK and T cells but not for monocytes and dendritic cells.

Discussion

TLR7 and TLR8 agonists are among the promising agents capable of activating and reversing HIV-1 latent reservoirs in patients treated with antiretroviral therapy and achieving sustained viral suppression. Using combination approaches of computer-aided design and biological characterization, two TLR7/8 dual (D018 and C142) and one TLR8-specific (B-130a) agonists were identified with exceptionally high potency in activating HIV-1 latent reservoirs from U1 and J-LAT6.3 cell lines as well as from PBMCs of patients with persistent and durable virologic controls. The activation mechanism appears to be direct through the TLR8-signaling pathway in the U1 cell line while indirect in the J-LAT6.3 cell line through soluble TNF-α released by the monocyte-derived dendritic cells (MDDCs). The indirect mechanism of soluble TNF-α contributes to the activation in PBMCs of patients, but the exact activation mechanism remains uncertain (Schlaepfer and Speck, 2008; Tsai et al., 2017). This hypothesis is supported by the capacity of these agonists to trigger the expression of various activation markers on NK and T cells and release inflammatory cytokines and chemokines in the supernatant of activated PBMCs. Taken together, these results highlight the remarkable potential of the TLR7/8 agonists in simultaneously increasing the expression of HIV-1 from the latently infected cells and activating the immune cells.

A couple of points need to be highlighted here. The TLR7/8 dual agonists D018 and C142 appeared to be more potent than TLR8-specific B-130a in activating the HIV-1 latent reservoir in PBMC as well as in U1 and J-LAT 6.3 cell lines. The underlying mechanisms accounting for

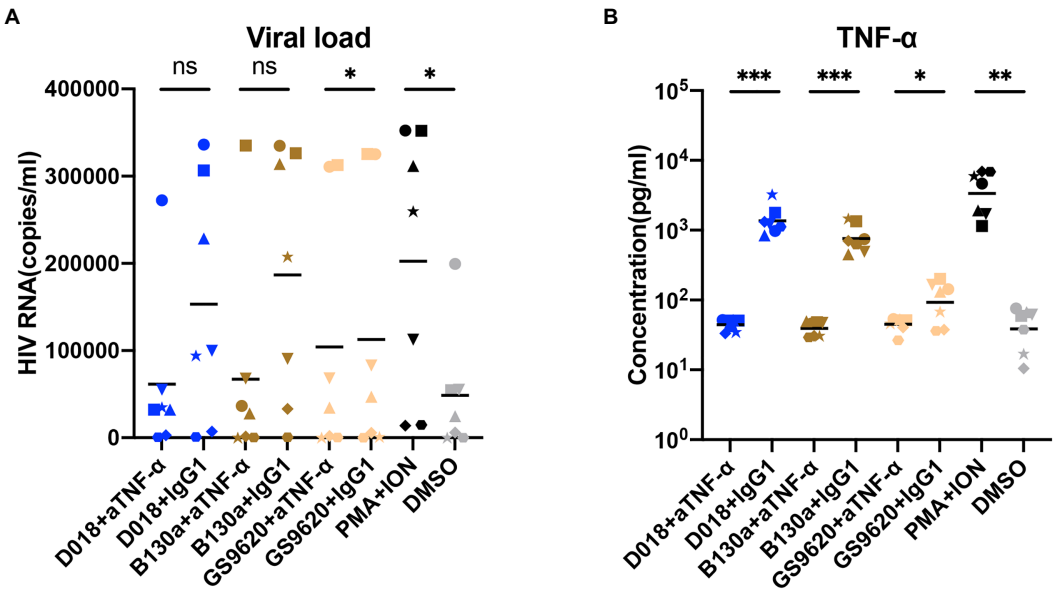

FIGURE 5
TLR7/8 agonists indirectly activate latent-infected cells derived from HIV-1 positive patients through TNF-α. **(A,B)** The PBMCs derived from HIV-1 viremic patients were stimulated by D018 (TLR7/8), B-130a (TLR8), GS9620 (TLR8) with anti-TNF-α monoclonal antibody compared with that of irrelevant IgG1 antibody control. **(A)** The HIV-1 RNA copies and **(B)** TNF-α concentrations in the supernatant were measured after stimulation. Data are shown as mean±SD (n =7). Statistical difference was analyzed by paired t-test. ****p <0.0001, ***p <0.001, **p <0.01, *p <0.05, n.s. not significant.

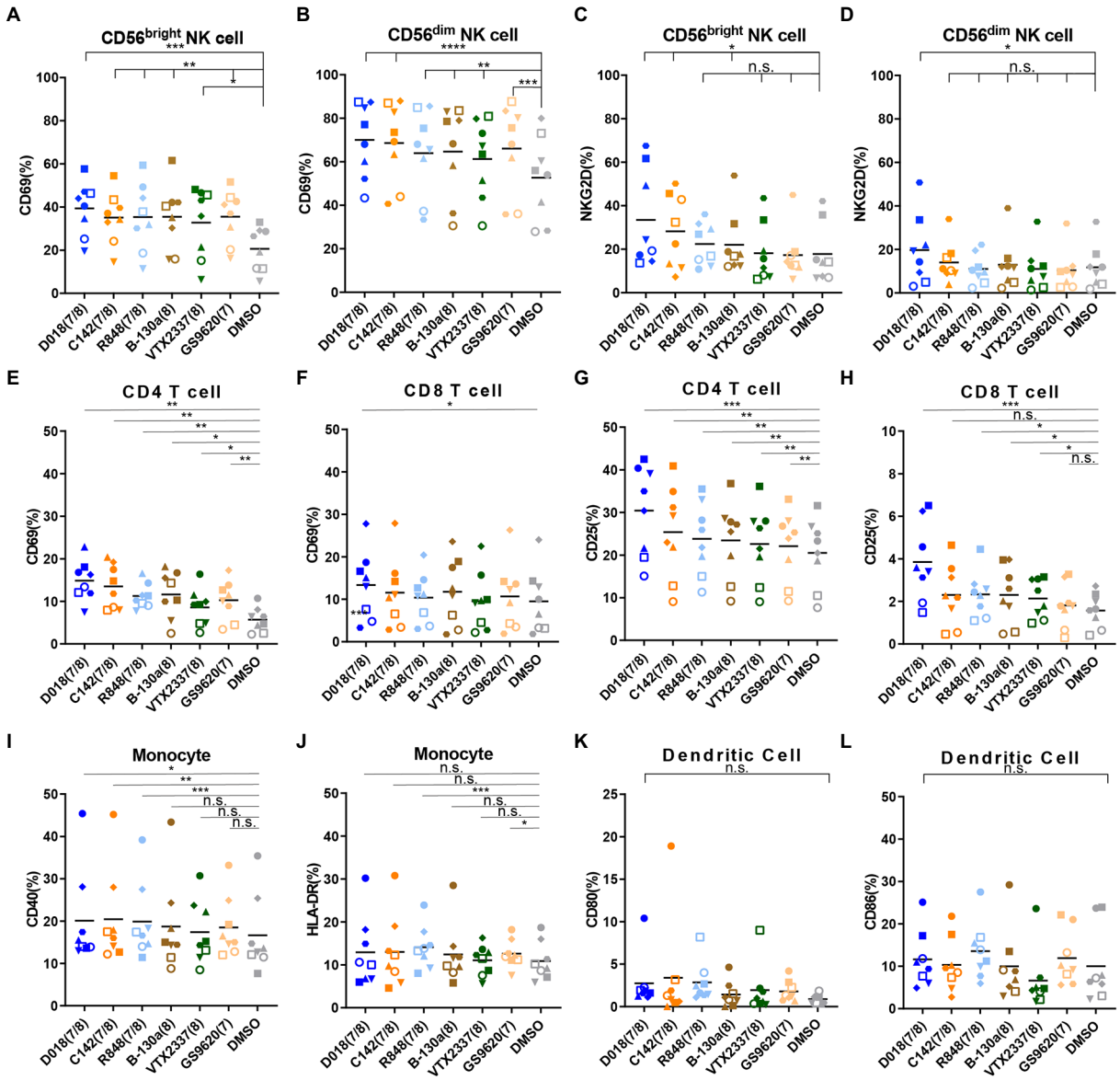

FIGURE 6
TLR7/8 agonists prefer to induce the NK cells and T cells activation and IFN-γ expression. **(A–D)** PBMCs from healthy donors were stimulated by different TLR7/8 agonists or DMSO for 24h, and different activated markers in several immune cells were analyzed by flow cytometry. The percentage of **(A)** CD69 positive $CD56^{bright}$ NK cells and **(B)** $CD56^{dim}$ NK cells, **(C)** NKG2D positive $CD56^{bright}$ NK cells, and **(D)** $CD56^{dim}$ NK cells. **(E–H)** The percentage of **(E)** CD69 positive CD4 T cells and **(F)** CD8 T cells, **(G)** CD25 positive CD4 T cells, and **(H)** CD8 T cells. **(I,J)** The percentage of **(I)** CD40 positive and **(J)** HLA-DR positive monocytes. **(K,L)** The percentage of **(K)** CD80 positive and **(L)** CD86 positive dendritic cells. Each different shaped point represents one donor and data is shown as the mean of 8 donors. Statistical difference between various TLR7/8 agonists and DMSO group was analyzed by paired *t*-test. $^{****}p < 0.0001$, $^{***}p < 0.001$, $^{**}p < 0.01$, $^{*}p < 0.05$, n.s. not significant.

such differences, however, are currently unknown. It is possible that the dual agonists could synergistically act on both TLR7 and TLR8 signal pathways either on the target cells harboring the HIV-1 latent reservoir or on cell types that release more cytokines to promote HIV-1 expression (Schlaepfer et al., 2006). TLR8-specific agonists, on the other hand, could only trigger HIV-1 expression through the TLR8 signal pathway (Rochat et al., 2017). However, this hypothesis does not explain why the control TLR7-specific GS9620 failed to activate HIV-1 expression in U1 and J-LAT6.3 cell lines (Figures 3A, 4A) while exerting some activation levels in PBMCs (Figure 2A). This could be due to the lack of TLR7 expression on U1 cells and relatively lower levels of soluble TNF-α released by the monocyte-derived dendritic cells (MDDCs) after GS9620 stimulation (Figure 2I; Schlaepfer and Speck, 2011; Macedo et al., 2018). In the context of PBMCs, apart from TNF-α, other cytokines, such as IFN-α, may also contribute to the indirect activation of HIV-1 harboring cells, as demonstrated by Tsai and colleagues (Tsai et al., 2017). These results show that TLR7/8 dual and TLR8 specific agonists can induce HIV-1 latency reversal. However, this activity requires sufficient levels of TLR7/8 expression in the targeted cell types, such as HIV-1 latently infected cells or cytokine-releasing cells, to promote HIV-1 activation (Figure 7).

TLR7/8 dual agonist D018 and TLR8-specific agonist B-130a demonstrated higher potency in inducing inflammatory cytokines release than TLR7-specific agonist GS9620. Although the cytokine

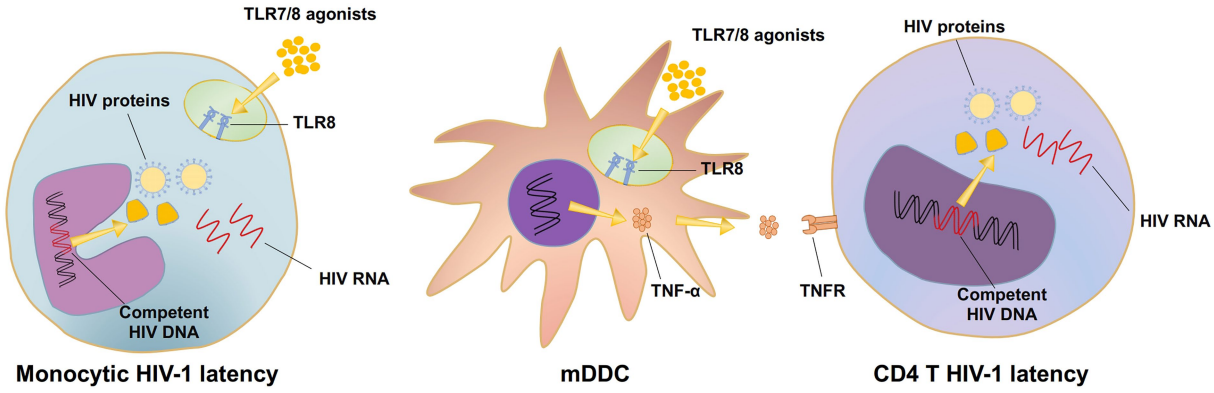

FIGURE 7
The mechanism diagram of TLR7/8 agonists activating HIV latent reservoirs.

release may be important in activating latent reservoirs or stimulating immune effector cells, systemic administration may cause side effects such as inflammatory factor storms. Therefore, their safety should be more strictly evaluated. Currently, TLR7/8 agonists are mainly administered topically or orally. Further modification of novel TLR7/8 dual agonist D018 and TLR8-specific agonist B-130a is urged to broaden the therapeutic index as well as conjugation of monoclonal antibodies so that the target delivery of TLR8 agonists could decrease the continual activation to the immune cells and improve the safety *in vivo* (Comeau et al., 2020). Moreover, TLR7/8 dual agonists and TLR8-specific agonists might be sufficient to stimulate NK cell activation. Compared to NK cells, CD4+ and particularly CD8+ T cells appeared less responsive to stimulation by either TLR7/8 dual or TLR8-specific agonists. However, this does not necessarily contradict the findings by Meas et al., where human primary CD4+ T cells express TLR8 and release inflammatory cytokines upon stimulation by TLR8-specific agonist, favoring HIV-1 replication and reversal of latency (Meas et al., 2020).

Overall, this study identified novel TLR7/8 dual and TLR8-specific agonists capable of reversing HIV-1 latency and activating immune cells *ex vivo*. Further studies are required to understand their mechanism of action and potential application for HIV-1 function cure.

Materials and methods

Reagents

The TLR7/8 agonists, D018, C008, 199–1, WA86, C142, B-130a, B-130b, WA175, C163 were synthesized by Zhisong Wang in Xuebin Liao's Lab. R848, GS9620, and VTX2337 were purchased from MedChemExpress (MCE). IL-2, IL-4, GM-CSF, TNF-α and IFN-α were purchased from Sino Biological. BAY 11–7,082 was purchased from Sigma-Aldrich.

Ethics statement

This study was approved by the Institution Review Board of Tsinghua University. The project number is 20200032. Healthy volunteers over 18 years old who signed the informed consent were recruited to the Tsinghua university hospital for blood donation. Blood sample from HIV-1-infected patients was collected at Beijing YouAn Hospital of Capital Medical University. The project number is EC-B-031-A01-V9.0. All patients were successfully treated by ART (<50 Copies/ml) for more than 6 years, and the CD4 counts were more than 350 cells/ml. Samples from donors were according to protocols approved by the Ethics Committee in Beijing YouAn Hospital of Capital Medical University.

Cell-lines culture

U1 cells were obtained from the NIH AIDS Reagent Program, and J-LAT 6.3 was kindly provided from The First Hospital of Jilin University, Institute of Virology, and AIDS Research. These cells were cultured in RPMI 1640 medium (Gibco) supplemented with 10% FBS (Gibco) and 1% PS (Macgene). HEK-Blue TLR7 and TLR8 overexpressing cells were purchased from InvivoGen and cultured in DMEM (Gibco) supplemented with 10% FBS, 50 μg/ml Normocin (InvivoGen), 30 μg/ml blasticidin (InvivoGen), and 100 μg/ml Zeocin (InvivoGen). HEK293T cells were purchased from ATCC and cultured in DMEM supplemented with 10%FBS and 1% PS.

Primary cells isolation, sorting, and culture

PBMCs were isolated from blood samples by density gradient centrifugation using Ficoll-Paque (GE Healthcare). PBMCs were treated with ACK lysis buffer (Gibco) and washed twice in PBS. Then the cells were resuspended in complete RPMI 1640 (Gibco) medium with the addition of 10% Fetal bovine serum (FBS, Gibco), 1% PS (Macgene),1% Glumax (Gibco),1% NEAA (Gibco),1% Sodium pyruvate (Gibco) and incubated at 37°C in 5% CO2.

Monocytes were isolated by CD14 magnetic beads (Miltenyi) according to the manufacturer's instructions. MDDCs were generated by stimulating monocytes with rhIL-4 and rhGM-CSF (Beyotime) for 5–7 days.

HEK SEAP detection

Add 20 μl various concentrations of TLR agonists (10 dilutions) and in a 96-well plate. Then HEK-Blue hTLR7 and hTLR8 cells were

suspended to 4 × 105 cells/ml in HEK-Blue Detection (InvivoGen) medium and added 180 µl per well. The plates were incubated at 37°C in 5% CO2 for 12 ~ 16 h. Stimulation with a hTLR7or hTLR8 ligand activates NF-κB to induce the production of secreted embryonic alkaline phosphatase (SEAP) in the culture supernatant. SEAP could be measured at OD630nm on an ELISA plate reader.

Viral production and infection

For generating the TLR8, MyD88 silenced U1 cells, we transfected shRNA lentivirus vector pLKO-TLR8/MyD88/Control shRNA, psPAX2, and pM2D.G into HEK293T cells to produce shRNA lentiviral particle. U1 cells were transduced by shRNA lentivirus overnight with 8 µg/ml polybrene. The cells were replaced with the medium supplemented with 8 µg/ml puromycin (Sigma) to select the positive colonies for 7 days, then were changed with 10% FBS 1640 medium containing 2 µg/ml puromycin to keep. All the shRNA lentivirus vectors were purchased from Sigma.

RNA extraction and qPCR

To measure the relative expression of TLR7, TLR8, and MyD88, RNA was extracted from 5×10^5 cells using AxyPrep Multisource RNA Miniprep Kit (Axygen) and measured by Nano-drop. An equal amount of RNA was reverse-transcribed into cDNA through the iScript cDNA Synthesis Kit (Bio-red). Samples were quantified by PCR with SYBR Green (Applied Biosystem). All specific primers used for the analysis were designed by qPrimerDB (Lu et al., 2018), and the sequences were shown as follows:

TLR7-F: TCAGCGTCTAATATCACCAGAC,
TLR7-R: CACTGTCTTTTTGCTAAGCTGT,
TLR8-F: TGGCTCACCATTTGTTTTACTG,
TLR8-R: AAAGGAGAACGTTTTTGTCTCG,
MyD88-F: GCGGGCATCACCACACTT,
MyD88-R: TCCGGCGGCACCTCTTTT,
GADPH-F: CCATGTTCGTCATGGGTGTG,
GADPH-R: GGTGCTAAGCAGTTGGTGGTG.

To measure the HIV viral load, viral RNA from supernatants was extracted by MagaBio Plus Viral DNA / RNA Purification Kit (BIOER). The reverse-transcription and analysis of RNA copies were performed using the HIV-1 Real-time PCR detection kit (BIOER).

HIV p24 antigen ELISA detection

U1 cells or the Patient's PBMC were stimulated by the indicated concentrations of TLR7/8 agonists, and the supernatants were collected for detection. To measure HIV p24 antigen, the supernatants were diluted into an appropriate concentration and analyzed by HIV-1 ELISA kit (Key-Bio Biotech).

Western blot

For measuring TLR8, 2×10^6 U1 cells were centrifuged to remove the supernatant, then were incubated with 200 µl RAPI (Beyotime) and 2 µl PMSF (Beyotime) on ice for 30 min. After centrifuging at 16,000 × g 10 min, whole proteins in the supernatant were obtained for western-blot assay.

For measuring NF-kB p65 and phosphor-p65 S536, 5×10^6 U1 cells were stimulated by 1 µM TLR7/8 agonists D018 (7/8), B-130a (8), GS9620 (7), and DMSO (negative control) for 30 min. Nuclear proteins were extracted by NE-PER Nuclear and Cytoplasmic Extraction Reagents (Pierce) and measured the concentration using BCA protein measure kit (Thermo).

Equal amounts of extracts were loaded on the 10% polyacrylamide gel SDS-PAGE. Then proteins were electro-transferred to nitrocellulose membranes 300 mA for 90 min and incubated with blocking buffer (5% nonfat dry milk and 0.1% Tween 20 in TBS) for 1 h at room temperature. NF-kB p65, phosphorylate p65-s529, and PCNA (as the control of nuclear protein) were separately detected by NF-κB p65 Mouse mAb (CST), Phospho-NF-κB p65 Ser536 Rabbit mAb (CST) and PCNA Rabbit mAb (CST) in blocking buffer overnight at 4°C. After washing 5 times in TBST (1 × TBS + 0.1% Tween), the membranes were incubated with anti-mouse IgG (H + L) HRP (Promega) and anti-rabbit IgG (H + L) HRP (Promega) for 1 h at room temperature. After washing 5 times in TBST, membranes were incubated with ECL detection reagents (Bio-red) and then developed in Bio-red imager.

Cytokine assay

The supernatants from PBMCs culture were collected and stored at-20°C until analysis. For the Multi-cytokines assay, the Legend-plex Human Inflammation Panel 1 kit (Biolegend) was used according to the manual. Thirteen human inflammatory cytokines/chemokines were measured, including IL-1β, IFN-α2, IFN-γ, TNF-α, MCP-1 (CCL2), IL-6, IL-8 (CXCL8), IL-10, IL-12p70, IL-17A, IL-18, IL-23, and IL-33.

For the single-cytokines assay, Human TNF-α, IFN-α, and IFN-γ were separately measured by human TNF-α (1,117,202, DKEWE), IFN-α (1,110,012, DKEWE), IFN-γ (1,110,002, DKEWE) ELISA kit.

J-Lat cells stimulation

5×10^5 PBMCs from health donors were stimulated by TLR7/8 agonists in 96-well plate for 24 h, then cells were transferred to 96-well round plate and spun down at 2000 rpm for 5 min. The supernatants were collected and cultured with 1×10^5 J-Lat cells in 96-well plate. After 48 h, the cell pellets were centrifuged and washed twice with PBS contained 2% FBS and fixed in 2% formaldehyde for FACS analysis using a BD LSR Fortessa flow cytometer (BD Biosciences). GFP positive cells from the live population, defined by forward FSC/SSC gating, were quantified. 10,000 events per treatment condition were analyzed.

For J-Lat and mDDC co-culture assay, 1×10^5 J-Lat cells were cultured with different amount of mDDC in 96-well plate and then stimulated by TLR7/8 agonists for 48 h. The cell pellets were collected for FACS analysis using a BD LSR Fortessa flow cytometer (BD Biosciences).

Immune cells staining

To analyze cell surface activation markers, PBMCs were stimulated by 1 µM TLR7/8 agonists or DMSO (as a negative control) for 24 h at 37°C. Then cells were collected and washed in FACS buffer

(PBS + 2%FBS). Cells were incubated by fluorescence antibodies at 4°C for 30 min. For T cells, CD3-PE-Cy7 (Biolegend), CD4-PE (BD), CD8-FITC (Biolegend), CD25-BV421 (Biolegend), CD69-BV510 (Biolegend). For NK cells, CD16-PE (Biolegend), CD56-APC (Biolegend), CD69-BV510 (Biolegend), NKG2D-BV421 (Biolegend). For monocytes, CD14-PE-Cy7 (Invitrogen), CD40-APC-Cy7 (Biolegend) HLR-DR-BV510 (Biolegend). For dendritic cells, anti-human lineage cocktail-APC (Biolegend), CD11c-PE-Cy7 (Biolegend), CD80-BV510 (Biolegend), CD86-AF488 (Biolegend).

Data analysis

Flow cytometry data were analyzed through the FlowJo version10.1. The statistical analysis was performed with Graphpad Prism version 7 or Microsoft Excel, including two-way ANOVA, paired t-test. The correlation analysis was performed with GraphPad Prism version 7.

Data availability statement

The raw data supporting the conclusions of this article will be made available by the authors, without undue reservation.

Ethics statement

This study was approved by the Institution Review Board of Tsinghua University. The project number is 20200032. Blood sample from HIV-1-infected patients was collected at Beijing YouAn Hospital of Capital Medical University. The project number is EC-B-031-A01-V9.0. The patients/participants provided their written informed consent to participate in this study.

Author contributions

XBL and LZ conceived, designed, and supervised the entire study. YL conceived the study and estimated the *in vitro* activity of reversing the HIV-1 latency of the novel TLR7/8 agonists and studied their activation of immune cells. ZW designed and synthesized all the novel TLR7/8 agonists. XYL and YH analyzed the activity and mechanism of reversing the HIV-1 latency of TLR7/8 agonists in U1 and J-LAT cell-lines. JH analyzed the activity of enhancement of immune cells by TLR7/8 agonists. XS, XH, and TZ were responsible for screening and collecting blood samples from HIV-1 infected patients. YL, LZ, and ZW wrote the main manuscript. All authors reviewed and edited the manuscript.

Funding

The research was supported by grants from the Beijing Municipal Science and Technology Commission (No. D17110700050000) and the National Science and Technology Major Project, Ministry of Science and Technology of China (No. 2018-ZX10302-102).

Acknowledgments

We thank Chen Huan from the First Hospital of Jilin University for kindly providing J-Lat 6.3 cell line. We thank Xiaojie Huang from Beijing You'an Hospital for providing the peripheral blood from HIV viremic patients on ART treatment.

Conflict of interest

The authors declare that the research was conducted in the absence of any commercial or financial relationships that could be construed as a potential conflict of interest.

Publisher's note

Supplementary material

The Supplementary material for this article can be found online at: https://www.frontiersin.org/articles/10.3389/fmicb.2023.1033448/full#supplementary-material

References

Aderem, A., and Ulevitch, R. J. (2000). Toll-like receptors in the induction of the innate immune response. *Nature* 406, 782–787. doi: 10.1038/35021228

Bachmann, N., von Siebenthal, C., Vongrad, V., Turk, T., Neumann, K., Beerenwinkel, N., et al. (2019). Determinants of HIV-1 reservoir size and long-term dynamics during suppressive ART. *Nat. Commun.* 10:3193.

Beignon, A. S., McKenna, K., Skoberne, M., Manches, O., DaSilva, I., Kavanagh, D. G., et al. (2005). Endocytosis of HIV-1 activates plasmacytoid dendritic cells via toll-like receptor-viral RNA interactions. *J. Clin. Invest.* 115, 3265–3275. doi: 10.1172/JCI26032

Borducchi, E. N., Liu, J., Nkolola, J. P., Cadena, A. M., Yu, W. H., Fischinger, S., et al. (2018). Antibody and TLR7 agonist delay viral rebound in SHIV-infected monkeys. *Nature* 563, 360–364. doi: 10.1038/s41586-018-0600-6

Clayton, K. L., Garcia, J. V., Clements, J. E., and Walker, B. D. (2017). HIV infection of macrophages: implications for pathogenesis and cure. *Pathog. Immun.* 2, 179–192. doi: 10.20411/pai.v2i2.204

Comeau, M. R., Brender, T., Childs, M., Brevik, J., Winship, D., Metz, H., et al. (2020). Abstract 4537: SBT6050, a HER2-directed TLR8 ImmunoTAC™therapeutic, is a potent human myeloid cell agonist that provides opportunity for single agent clinical activity. *Cancer Res.* 80:4537. doi: 10.1158/1538-7445.AM2020-4537

Del Prete, G. Q., Alvord, W. G., Li, Y., Deleage, C., Nag, M., Oswald, K., et al. (2019). TLR7 agonist administration to SIV-infected macaques receiving early initiated cART does not induce plasma viremia. *JCI Insight* 4:e127717. doi: 10.1172/jci.insight.127717

Delobel, P., Sandres-Sauné, K., Cazabat, M., L'Faqihi, F. E., Aquilina, C., Obadia, M., et al. (2005). Persistence of distinct HIV-1 populations in blood monocytes and naive and memory CD4 T cells during prolonged suppressive HAART. *AIDS* 19, 1739–1750. doi: 10.1097/01.aids.0000183125.93958.26

Elliott, J. H., Wightman, F., Solomon, A., Ghneim, K., Ahlers, J., Cameron, M. J., et al. (2014). Activation of HIV transcription with short-course vorinostat in HIV-infected patients on suppressive antiretroviral therapy. *PLoS Pathog.* 10:e1004473. doi: 10.1371/journal.ppat.1004473

Finzi, D., Blankson, J., Siliciano, J. D., Margolick, J. B., Chadwick, K., Pierson, T., et al. (1999). Latent infection of CD4+ T cells provides a mechanism for lifelong persistence of HIV-1, even in patients on effective combination therapy. *Nat. Med.* 5, 512–517. doi: 10.1038/8394

Finzi, D., Hermankova, M., Pierson, T., Carruth, L. M., Buck, C., Chaisson, R. E., et al. (1997). Identification of a reservoir for HIV-1 in patients on highly active antiretroviral therapy. *Science* 278, 1295–1300. doi: 10.1126/science.278.5341.1295

Fitzgerald, K. A., and Kagan, J. C. (2020). Toll-like receptors and the control of immunity. *Cells* 180, 1044–1066. doi: 10.1016/j.cell.2020.02.041

Ghosn, J., Taiwo, B., Seedat, S., Autran, B., and Katlama, C. (2018). HIV. *Lancet* 392, 685–697. doi: 10.1016/S0140-6736(18)31311-4

Gibellini, D., Borderi, M., De Crignis, E., Cicola, R., Cimatti, L., et al. (2008). HIV-1 DNA load analysis in peripheral blood lymphocytes and monocytes from naïve and HAART-treated individuals. *J. Infect.* 56, 219–225. doi: 10.1016/j.jinf.2008.01.001

Gringhuis, S. I., van der Vlist, M., van den Berg, L. M., den Dunnen, J., Litjens, M., and Geijtenbeek, T. B. (2010). HIV-1 exploits innate signaling by TLR8 and DC-SIGN for productive infection of dendritic cells. *Nat. Immunol.* 11, 419–426. doi: 10.1038/ni.1858

Harper, J., Gordon, S., Chan, C. N., Wang, H., Lindemuth, E., Galardi, C., et al. (2020). CTLA-4 and PD-1 dual blockade induces SIV reactivation without control of rebound after antiretroviral therapy interruption. *Nat. Med.* 26, 519–528. doi: 10.1038/s41591-020-0782-y

Hart, O. M., Athie-Morales, V., O'Connor, G. M., and Gardiner, C. M. (2005). TLR7/8-mediated activation of human NK cells results in accessory cell-dependent IFN-gamma production. *J. Immunol.* 175, 1636–1642. doi: 10.4049/jimmunol.175.3.1636

Ito, T., Amakawa, R., Kaisho, T., Hemmi, H., Tajima, K., Uehira, K., et al. (2002). Interferon-alpha and interleukin-12 are induced differentially by toll-like receptor 7 ligands in human blood dendritic cell subsets. *J. Exp. Med.* 195, 1507–1512. doi: 10.1084/jem.20020207

Jordan, A., Bisgrove, D., and Verdin, E. (2003). HIV reproducibly establishes a latent infection after acute infection of T cells in vitro. *EMBO J.* 22, 1868–1877. doi: 10.1093/emboj/cdg188

Kanzler, H., Barrat, F. J., Hessel, E. M., and Coffman, R. L. (2007). Therapeutic targeting of innate immunity with toll-like receptor agonists and antagonists. *Nat. Med.* 13, 552–559. doi: 10.1038/nm1589

Kawai, T., and Akira, S. (2010). The role of pattern-recognition receptors in innate immunity: update on toll-like receptors. *Nat. Immunol.* 11, 373–384. doi: 10.1038/ni.1863

Kim, Y., Anderson, J. L., and Lewin, S. R. (2018). Getting the "kill" into "shock and kill": strategies to eliminate latent HIV. *Cell Host Microbe* 23, 14–26. doi: 10.1016/j.chom.2017.12.004

Kruize, Z., and Kootstra, N. A. (2019). The role of macrophages in HIV-1 persistence and pathogenesis. *Front. Microbiol.* 10:2828. doi: 10.3389/fmicb.2019.02828

Lim, S. Y., Osuna, C. E., Hraber, P. T., Hesselgesser, J., Gerold, J. M., Barnes, T. L., et al. (2018). TLR7 agonists induce transient viremia and reduce the viral reservoir in SIV-infected rhesus macaques on antiretroviral therapy. *Sci. Transl. Med.* 10. doi: 10.1126/scitranslmed.aao4521

Lu, K., Li, T., He, J., Chang, W., Zhang, R., Liu, M., et al. (2018). qPrimerDB: a thermodynamics-based gene-specific qPCR primer database for 147 organisms. *Nucleic Acids Res.* 46, D1229–d1236. doi: 10.1093/nar/gkx725

Macedo, A. B., Novis, C. L., De Assis, C. M., Sorensen, E. S., Moszczynski, P., Huang, S. H., et al. (2018). Dual TLR2 and TLR7 agonists as HIV latency-reversing agents. *JCI Insight* 3:e122673. doi: 10.1172/jci.insight.122673

McBrien, J. B., Mavigner, M., Franchitti, L., Smith, S. A., White, E., Tharp, G. K., et al. (2020). Robust and persistent reactivation of SIV and HIV by N-803 and depletion of CD8(+) cells. *Nature* 578, 154–159. doi: 10.1038/s41586-020-1946-0

McMahon, D. K., Zheng, L., Cyktor, J. C., Aga, E., Macatangay, B. J., Godfrey, C., et al. (2020). A phase I/II randomized, placebo-controlled trial of romidepsin in persons with HIV-1 on suppressive antiretroviral therapy to assess safety and activation of HIV-1 expression (A5315). *J. Infect. Dis.* 224, 648–656. doi: 10.1093/infdis/jiaa777

Meas, H. Z., Haug, M., Beckwith, M. S., Louet, C., Ryan, L., Hu, Z., et al. (2020). Sensing of HIV-1 by TLR8 activates human T cells and reverses latency. *Nat. Commun.* 11:147. doi: 10.1038/s41467-019-13837-4

Rasmussen, T. A., Tolstrup, M., Brinkmann, C. R., Olesen, R., Erikstrup, C., Solomon, A., et al. (2014). Panobinostat, a histone deacetylase inhibitor, for latent-virus reactivation in HIV-infected patients on suppressive antiretroviral therapy: a phase 1/2, single group, clinical trial. *Lancet HIV* 1, e13–e21. doi: 10.1016/S2352-3018(14)70014-1

Rochat, M. A., Schlaepfer, E., and Speck, R. F. (2017). Promising role of toll-like receptor 8 agonist in concert with Prostratin for activation of silent HIV. *J. Virol.* 91, e02084–e02016. doi: 10.1128/JVI.02084-16

Schlaepfer, E., Audige, A., Joller, H., and Speck, R. F. (2006). TLR7/8 triggering exerts opposing effects in acute versus latent HIV infection. *J. Immunol.* 176, 2888–2895. doi: 10.4049/jimmunol.176.5.2888

Schlaepfer, E., and Speck, R. F. (2008). Anti-HIV activity mediated by natural killer and CD8+ cells after toll-like receptor 7/8 triggering. *PLoS One* 3:e1999. doi: 10.1371/journal.pone.0001999

Schlaepfer, E., and Speck, R. F. (2011). TLR8 activates HIV from latently infected cells of myeloid-monocytic origin directly via the MAPK pathway and from latently infected CD4+ T cells indirectly via TNF-alpha. *J. Immunol.* 186, 4314–4324. doi: 10.4049/jimmunol.1003174

SenGupta, D., Brinson, C., DeJesus, E., Mills, A., Shalit, P., Guo, S., et al. (2021). The TLR7 agonist vesatolimod induced a modest delay in viral rebound in HIV controllers after cessation of antiretroviral therapy. *Sci. Transl. Med.* 13. doi: 10.1126/scitranslmed.abg3071

Takeuchi, O., and Akira, S. (2010). Pattern recognition receptors and inflammation. *Cells* 140, 805–820. doi: 10.1016/j.cell.2010.01.022

Tanji, H., Ohto, U., Shibata, T., Miyake, K., and Shimizu, T. (2013). Structural reorganization of the toll-like receptor 8 dimer induced by agonistic ligands. *Science* 339, 1426–1429. doi: 10.1126/science.1229159

Tsai, A., Irrinki, A., Kaur, J., Cihlar, T., Kukolj, G., Sloan, D. D., et al. (2017). Toll-like receptor 7 agonist GS-9620 induces HIV expression and HIV-specific immunity in cells from HIV-infected individuals on suppressive antiretroviral therapy. *J. Virol.* 91. doi: 10.1128/JVI.02166-16

Wong, J. K., Hezareh, M., Günthard, H. F., Havlir, D. V., Ignacio, C. C., Spina, C. A., et al. (1997). Recovery of replication-competent HIV despite prolonged suppression of plasma viremia. *Science* 278, 1291–1295. doi: 10.1126/science.278.5341.1291

Zhang, Z., Ohto, U., Shibata, T., Krayukhina, E., Taoka, M., Yamauchi, Y., et al. (2016). Structural analysis reveals that toll-like receptor 7 is a dual receptor for Guanosine and single-stranded RNA. *Immunity* 45, 737–748. doi: 10.1016/j.immuni.2016.09.011

Zhang, L., Ramratnam, B., Tenner-Racz, K., He, Y., Vesanen, M., Lewin, S., et al. (1999). Quantifying residual HIV-1 replication in patients receiving combination antiretroviral therapy. *N. Engl. J. Med.* 340, 1605–1613. doi: 10.1056/NEJM199905273402101

Frontiers in Microbiology

Explores the habitable world and the potential of microbial life

The largest and most cited microbiology journal which advances our understanding of the role microbes play in addressing global challenges such as healthcare, food security, and climate change.

Discover the latest Research Topics

See more →

Frontiers

Avenue du Tribunal-Fédéral 34
1005 Lausanne, Switzerland
frontiersin.org

Contact us

+41 (0)21 510 17 00
frontiersin.org/about/contact